



Laboratory of Virology
Department of Virology, Parasitology and Immunology
Faculty of Veterinary Medicine
Ghent University

**The horse's respiratory mucosa,
airborne pathogens and respirable hazards:
the archetypical trifecta of co-evolution**

Jolien Van Cleemput

Dissertation submitted in fulfilment of the requirements for the degree of
Doctor in Veterinary Sciences (PhD)

2018

Promoter
Prof. dr. Hans Nauwynck

Van Cleemput J. (2018). The horse's respiratory mucosa, airborne pathogens and respirable hazards: the archetypical trifecta of co-evolution. Dissertation, Ghent University, Belgium.

© 2018 Jolien Van Cleemput, Laboratory of Virology, Faculty of Veterinary Medicine, Ghent University, Salisburylaan 133, 9820 Merelbeke, Belgium

The author and the promoter give the authorisation to consult and to copy parts of this work for personal use only. Every other use is subject to the copyright laws. Permission to reproduce any material contained in this work should be obtained from the author.

Jolien Van Cleemput was supported by a doctoral grant (11Y5417N) from the Research Foundation - Flanders (FWO - Vlaanderen).

“There is no elevator to success, you have to take the stairs.”

Zig Ziglar

Table of Contents

Chapter 1: Introduction	13
1 Foreword	15
2 The horse's respiratory tract	16
2.1 Anatomy - morphology	16
2.2 Host barriers	21
2.3 Models to study the respiratory tract.....	30
3 Airborne pathogens of the horse	33
3.1 Equine herpesvirus type 1	34
3.2 Equine herpesvirus type 5	45
3.3 Equine influenza virus.....	49
3.4 Equine arteritis virus	52
3.5 Bacteria.....	55
4 Respirable hazards	60
4.1 Pollens	60
4.2 Mycotoxins.....	61
4.3 Air pollutants.....	61
4.4 Aerosol drugs	62
4.5 Concluding remarks	63
5 References.....	64
Chapter 2: Aims of the thesis	85
Chapter 3: Access to a main alphaherpesvirus receptor, located basolaterally in the respiratory epithelium, is masked by intercellular junctions	89
Chapter 4: Beyond allergy: how pollen proteases destroy respiratory epithelial cell anchors and drive alphaherpesvirus infection	127
Chapter 5: Deoxynivalenol, but not fumonisin B1, aflatoxin B1 or diesel exhaust particles disrupt the horse's respiratory epithelial barrier and predispose the respiratory epithelium for equine herpesvirus type 1 infection.....	161
Chapter 6: Equine β-defensins: active against airborne bacteria and some viruses, but exploited by an ancestral host-specific alphaherpesvirus.....	181
Chapter 7: Unravelling the first key steps in equine herpesvirus type 5 (EHV5) pathogenesis using <i>ex vivo</i> and <i>in vitro</i> equine models.....	229
Chapter 8: General discussion	259
Summary - samenvatting.....	285
Curriculum Vitae	295
Dankwoord.....	299

List of Abbreviations

16 hBE cells	Human bronchial epithelial cells
<i>A. equuli</i>	<i>Actinobacillus equuli</i>
AEBSF	4-(2-Aminoethyl)benzenesulfonyl fluoride hydrochloride
AFB1	Aflatoxin B1
AJ	Adherent junctions
ANOVA	Analysis of variances
ARPE-19	Human retinal pigment cells
ATCC	American Type Culture Collection
<i>B. bronchiseptica</i>	<i>Bordetella bronchiseptica</i>
BALT	Bronchus-associated lymphoid tissue
BD(s)	β -defensin(s)
BoHV	Bovine herpesvirus
BRALT	Bronchioli-associated lymphoid tissue
C3b	Complement factor 3b
Caco-2 cells	Human colonic cells
Calu-3 cells	Human lung adenocarcinoma cells
CD	Cluster of differentiation
CHO-K1 cells	Chinese hamster ovary epithelial cells
CO ₂	Carbon dioxide
COPD	Chronic obstructive pulmonary disease
CPE	Cytopathic effect
CTL	Cytotoxic T lymphocyte
D-MALT	Diffuse mucosa-associated lymphoid tissue
DC	Dendritic cell
DEP	Diesel exhaust particles
Dio	3,3'-Diocetadecyloxacarbocyanine perchlorate
DMEM	Dulbecco's modified eagle medium
DMSO	Dimethyl sulfoxide
DON	Deoxynivalenol
dpi	Days post-inoculation
DTT	Dithiotreitol
E	Early

E-64	Epoxide 64
EAV	Equine arteritis virus
eBD(s)	Equine β -defensin(s)
EBMEC	Equine brain microvascular cells
EBV	Epstein-barr virus
ECC-1 cells	Human endometrial cells
eCG	Equine chorionic gonadotropin
ED cells	Equine dermal cells
EDTA	Ethylene diamine tetra-acetic acid
EEL cells	Equine embryonic lung cells
EGTA	Ethylene glycol tetra-acetic acid
EHM	Equine herpes myeloencephalopathy
EHV	Equine herpesvirus
EIV	Equine influenza virus
ELISA	Enzyme-linked immunosorbent assay
EMA	Ethidium monoazide bromide
EMPF	Equine multinodular pulmonary fibrosis
EREC	Equine respiratory epithelial cells
ERK	Extracellular signal-regulated kinase
ESI-MS	Electrospray ionization mass spectrometry
EVA	Equine viral arteritis
FB1	Fumonisin B1
FCS	Foetal calf serum
FITC	Fluorescein isothiocyanate
g	Glycoprotein
GAG	Glycosaminoglycan
Gan	Ganciclovir
gp	Glycoprotein
H	Hemagglutinin or hazel
HAdV	Human adenovirus
Hep	Heparin
HHV	Human herpesvirus
HIV	Human immunodeficiency virus
hpi	Hours post-inoculation

HPLC	High performance liquid chromatography
HS	Heparan sulphate
HSV	Herpes simplex virus
HVEM	Herpesvirus entry mediator
IAD	Inflammatory airway disease
ICAM	Intercellular adhesion molecule
ICJ	Intercellular junctions
IE	Immediate-early
IEP	Immediate-early protein or polypeptide
IF	Immunofluorescence
IFN	Interferon
Ig	Immunoglobulin
IL	Interleukin
IPMA	Immunoperoxidase monolayer assay
JAM	Junctional adhesion molecule
KBG	Kentucky bluegrass
kbp	Kilobase pairs
KSHV	Kaposi's sarcoma-associated herpesvirus
L	Late
LC	Liquid chromatography
LDV	Lactate dehydrogenase-elevating virus
LPS	Lipopolysaccharide
LTALT	Laryngo-trachea-associated lymphoid tissue
M	Matrix
MACS	Magnetic-activated cell sorting
MALT	Mucosa-associated lymphoid tissue
MAPK	Mitogen-activated protein kinase
MDCK	Madin-Darby canine kidney epithelial cells
MEM	Minimal essential medium
MHC	Major histocompatibility complex
MIC	Minimal inhibitory concentration
MMTS	Methyl methanethiosulfonate
MOI	Multiplicity of infection
MS	Mass spectrometry

MUC	Mucin
MuHV	Murine herpesvirus
MusHV	Mustelid herpesvirus
N	Neuraminidase
NAC	N-acetylcysteine
NALT	Nasal-associated lymphoid tissue
Neu5Ac	N-acetylneuraminic acid
Neu5Gc	N-glycolylneuraminic acid
NGS	Negative goat serum
NK cell	Natural killer cell
NP	Ribonucleoprotein
O-MALT	Organized mucosa-associated lymphoid tissue
ORF	Open reading frame
PB	Polymerase protein
PBMC	Peripheral blood mononuclear cell
PBS	Phosphate-buffered saline
PBST	PBS with 0.01% Tween 20
PCR	Polymerase chain reaction
PFA	Paraformaldehyde
PI	Protease inhibitor
pi	Post-inoculation
PI(3)K	Phosphatidylinositol 3-kinase
PMN cells	Polymorfonuclear cells
PRRSV	Porcine reproductive and respiratory syndrome virus
PRV	Pseudorabies virus
PVDF	Polyvinylidene difluoride
<i>R. equi</i>	<i>Rhodococcus equi</i>
RAO	Recurrent airway obstruction
RITC	Rhodamine B isothiocyanate
RK13 cells	Rabbit kidney epithelial cells
ROCK	Rho-associated coiled-coil kinase
ROI	Region of interest
RPMI	Roswell Park Memorial Institute
RT	Room temperature or retention time

RT-PCR	Reverse transcriptase polymerase chain reaction
<i>S. aureus</i>	<i>Staphylococcus aureus</i>
<i>S. e. equi</i>	<i>Streptococcus equi</i> subspecies <i>equi</i>
<i>S. e. zooepidemicus</i>	<i>Streptococcus equi</i> subspecies <i>zooepidemicus</i>
SA	Sialic acid
SD	Standard deviation
SDS	Sodium dodecyl sulfate
SDS-PAGE	SDS polyacrylamide gel electrophoresis
SHFV	Simian hemorrhagic fever virus
sIgA	Secretory immunoglobulin A
SN	Serum neutralisation
SP-RAO	Summer pasture recurrent airway obstruction
TAP	Transporter associated with antigen processing
TBS	Tris-buffered saline
TCID ₅₀	Tissue culture infectious dose with a 50% endpoint
TEABC	Triethylammonium bicarbonate
TEER	Transepithelial electrical resistance
TFA	Trifluoroacetic acid
Th	T helper
TJ	Tight junction
TK	Thymidine kinase
TLR	Toll-like receptor
TNF- α	Tumor necrosis factor α
TUNEL	Terminal deoxynucleotidyl transferase dUTP nick end labelling
VN	Virus neutralizing
VZV	Varicella-zoster virus
WB	White birch
ZO	Zonula occludens

Chapter 1.

Introduction

1. Foreword

The horse is an extremely athletic mammal with a high relative oxygen uptake, enabling it to cover long distances at high speed. All components of the horse's respiratory tract thus serve a common purpose: providing a potent airflow to exchange oxygen for carbon dioxide. A resting horse breathes out 80 litres of air per minute (L/min) and this volume may add up to 1800 L/min at maximal exertion. The latter increase in minute ventilation is accompanied by a simultaneous increase in tidal volume (i.e. lung volume), breathing frequency and subsequent airflow velocities. In turn, these velocities implicate tremendous air turbulences and pressure fluctuations inside the respiratory system during heavy exercise. When taking into account that breathing is the limiting factor for equine athletic performances, it is not surprising that a small dysfunction in the respiratory tract leads to reduced performance, also known as poor performance syndrome (Lekeux *et al.*, 2014). Problems affecting the respiratory tract can be of infectious (e.g. equine herpesviruses, influenza viruses, strangles, pneumonia), inherent (e.g. dorsal displacement of the soft palate, laryngeal hemiplegia, epiglottic entrapment) and most often multifactorial (inflammatory airway disease, laryngeal lymphoid hyperplasia, [summer pasture-associated] recurrent airway obstruction) origin.

Respiratory problems are often a consequence of domestication and housing of these animals. Horses are usually kept in closed barns or half-open boxes with poor ventilation and trained in dusty arenas accompanied by high levels of dust, moulds, endotoxins, bacteria and ammonia arising from the bedding, manure, hays, cereal foods and arena footing material (Vandenput *et al.*, 1997; Woods *et al.*, 1993). The air breath by pasture-kept horses, although considered healthier, also contains pollutants. Since equestrian enterprises are often located in (sub)urban regions, horses are exposed to the air pollution caused by traffic and industrial activities. In addition, the air is seasonally full of plant pollen allergens, which not only function as a vector for carbon particles from diesel engine fumes and bacteria, but also carry endogenous hazardous proteases (Knox *et al.*, 1997; McKenna *et al.*, 2017). These pollutants might alter mucosal immunology, promote pathogen invasion and predispose horses for the development of airway disease. In addition, the nature of equestrian sports and (international) competitions bring together a considerable amount of horses from different premises in one place, thereby imposing a major risk factor in the spread of infectious diseases. Indeed, most respiratory pathogens spread through direct nose-nose contact or over short distances in the air, either impacted in aerosol droplets or carried on fomites. The horse's respiratory mucosal immunity, airborne pathogens and respirable hazards form an integrated whole. These three main factors

constantly influence one another and should therefore be studied in parallel. A complete understanding of the interplay between these three factors is currently urgently needed to reveal new strategies in respiratory (veterinary) medicine.

2. The horse's respiratory tract

2.1. Anatomy - morphology

The respiratory tract starts at the nostrils, extends through the nasal cavities, the nasopharynx, the larynx to the trachea, which bifurcates into two main bronchi, each leading to one of the two lungs. Within the lungs, bronchi further divide and subdivide into bronchioli, eventually ending in alveoli, microscopic air sacs where gas exchange occurs. A schematic overview of the major organs comprising the respiratory tract is given in Figure 1.

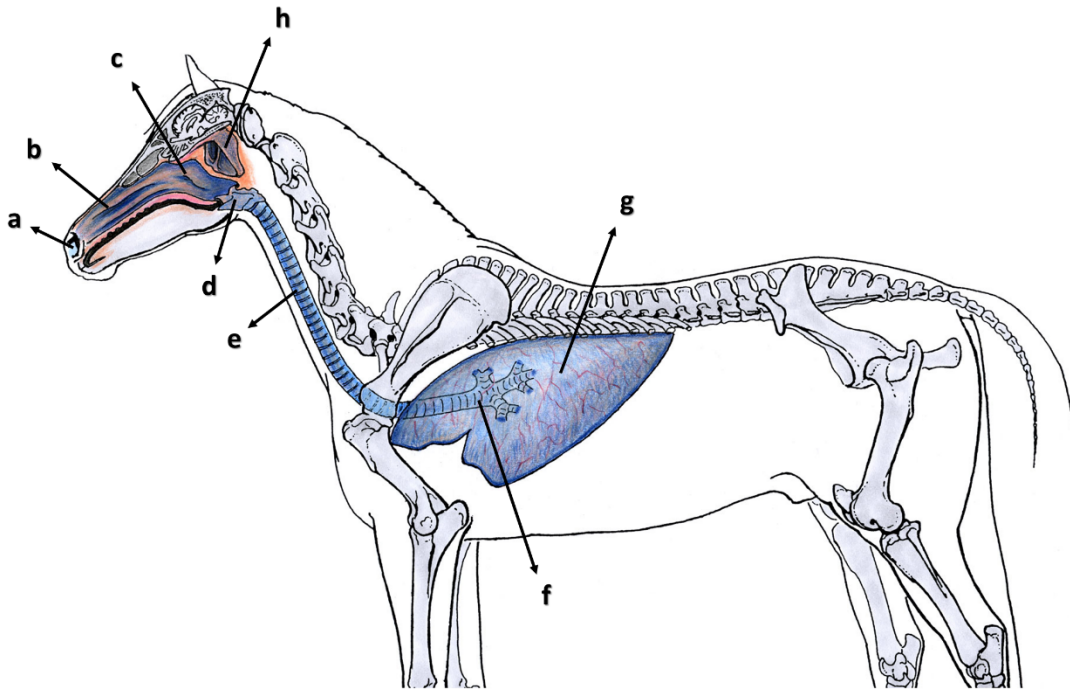


Figure 1. Overview of the horse's respiratory tract. Incoming air passes through the nostrils (a), the nasal cavities divided by a cartilaginous nasal septum (b), the nasopharynx (c), the larynx (d), the trachea (e), the lung hilus (f) and eventually ends in the alveoli, residing deeply within the lungs (g). The guttural pouches are designated by (h). Image courtesy of the Fédération Equestre Internationale (FEI).

2.1.1. The upper airways

The sickle shaped **nostrils**, which become round during intense exercise, allow sufficient air flow into the respiratory tract while simultaneously filtering out the largest debris.

The nasolacrimal duct, draining excessive ocular fluid, ends at the ventromedial part into the ostium nasolacrimale (Budras *et al.*, 2003).

Each nostril leads to a **nasal cavity**, separated from one another by the cartilaginous **nasal septum**. Because of the important vascularisation in the turbinates, the nasal septum and the surrounding walls, the long nasal cavities provide a large area for heat and water exchange to warm up and humidify incoming air (Walker *et al.*, 1961). In addition, the rostral stratified squamous epithelium abruptly shifts to a specialized pseudostratified columnar ciliated epithelium, containing basal progenitor cells, ciliated cells, brush cells and goblet cells. A lamina propria, containing serous, mucous and mixed glands and an underlying submucosa support the epithelium (Bacha Jr and Bacha, 2012). Together with the overlying mucus blanket, the respiratory epithelium efficiently entraps incoming debris. Synchronized beating of the cilia pushes the mucus with entrapped materials distally towards the pharynx, where it is eventually swallowed. Further, specialized lymphoid nodules reside in the respiratory mucosa and local immune cells constantly patrol the respiratory epithelium. The latter common mucosal immune system is denoted nasal-associated lymphoid tissue (NALT) and provides a specific defence system against incoming pathogens (*vide infra*) (Mair *et al.*, 1987, 1988).

The **pharynx** is divided into the dorsal nasopharynx and the ventral oropharynx by the soft palate, which extends from the hard palate to the larynx. The nasopharynx is covered by a respiratory epithelium (i.e. pseudostratified columnar ciliated epithelium), supported by a lamina propria. Inside these mucous walls lining the nasopharynx, a repertoire of lymphoid follicles are gathered together in the ‘nasopharyngeal tonsil’. Together with other more dispersed and diffuse lymphoid deposits, the nasopharyngeal tonsil is part of the NALT.

The nasopharynx communicates with the guttural pouches through fissure-like openings. The guttural pouches, uniquely present in the genus *Equus*, are paired diverticulae of the Eustachian tubes extending between both mandibulae and are covered by a respiratory epithelium (Parillo *et al.*, 2009).

2.1.2. *The lower airways*

The **larynx** is located at the very cranial part of the trachea and serves as the dividing mark between the upper and lower airways. The larynx consists of five different pieces of cartilage, namely the cranial epiglottis, two dorsal corniculate (arytenoid) cartilages, the ventral thyroid and the caudal circular cricoid cartilage, which are connected through a peculiar web of ligaments and muscles. The larynx also resides two vocal cords, allowing horses to vocalize. While adduction of the laryngeal structures prevents food aspiration, full abduction is necessary

during exercise to minimize the resistance against airflow. Since the larynx is the bottleneck of the respiratory tract, it daily encounters high air turbulences and is therefore partly provided with a stratified squamous epithelium, besides another part of respiratory epithelium.

The **trachea** is a flexible but rigid tube of approximately 80 cm that connects the larynx to the lung hilus. Between 68 to 80 C-shaped hyaline cartilage rings, enclosed and connected by fibro-elastic ligaments, provide stability to the trachea's structure. The complete surface of the trachea is lined by the typical respiratory epithelium. A submucosa, containing serous, mucous but mostly mixed glands lies below the epithelium (Bacha Jr and Bacha, 2012). The epithelium is covered by a layer of mucus that is constantly being propelled by the 'mucocilliary escalator' proximally towards the pharynx, clearing the lower airways from foreign materials (Mair and Lane, 2005). In addition, nodular lymphoid tissue and local patrolling immune cells (i.e. laryngo-trachea-associated lymphoid tissue or LTALT) are widely present in the respiratory mucosa of the equine trachea, as well as in that of the larynx (Mair *et al.*, 1987, 1988).

The trachea bifurcates into a left and right **principal bronchus** at the level of the lung hilus, each extensively branching into segmental bronchi, bronchioles and terminal bronchioles, often referred to as the **bronchial tree** (Lekeux *et al.*, 2014). From proximal to distal, the respiratory epithelium gradually shifts to a ciliated cuboidal epithelium, containing more and more Clara cells (Plopper *et al.*, 1980). In horses, lymphoid tissue inside the mucous walls of the bronchi (bronchus-associated lymphoid tissue or BALT) is only poorly developed (Mair *et al.*, 1987, 1988).

Finally, the terminal bronchioles, covered distally by a non-ciliated cuboidal epithelium, divide into alveolar ducts that empty into **alveoli**, which are lined by a thin walled squamous epithelium. This epithelium is exceedingly resided by type I pneumocytes, and to a lesser extent by type II pneumocytes. The former cell type is responsible for gas exchange and upon cell death, is replaced by the latter cell type. In addition, type II pneumocytes produce surfactant, which not only reduces the surface tension of pulmonary fluids, but also neutralizes incoming microbes (Hickman-Davis *et al.*, 2001). Alveoli are wrapped within a bed of thin-walled capillaries, designed for optimal gas exchange through simple diffusion. Foreign material that would find its way to the alveoli is ultimately consumed by alveolar macrophages, controlling the microscopic air sacs. Besides macrophages, lymphoid cells belonging to the bronchioli-associated lymphoid tissue or BRALT, are dispersed across distal bronchioles and across the lung interstitium. Remarkably, the number of lymphocytes within the BRALT showed a marked variation among different horses (Mair *et al.*, 1987).

2.1.3. The respiratory mucosa

As mentioned above, the respiratory mucosa lines the major parts of the respiratory tract, including the nasal cavity, the nasopharynx, part of the larynx, the trachea and the proximal parts of the bronchial tree (Bacha Jr and Bacha, 2012). The respiratory mucosa consists of a luminal ciliated pseudostratified epithelium with an overlying mucus blanket, which is stabilized onto a basement membrane and an underlying lamina propria built out of connective tissue. At least 6 morphologically distinct epithelial cells reside in the equine respiratory epithelium, besides the migrating immune cells (Knight and Holgate, 2003). Mesenchymal cells, glands (mucous, serous or mixed), blood and lymph vessels, neuronal axons, local single immune cells and lymphoid nodules are located within the underlying lamina propria. An illustration of the respiratory mucosa is given in Figure 2.

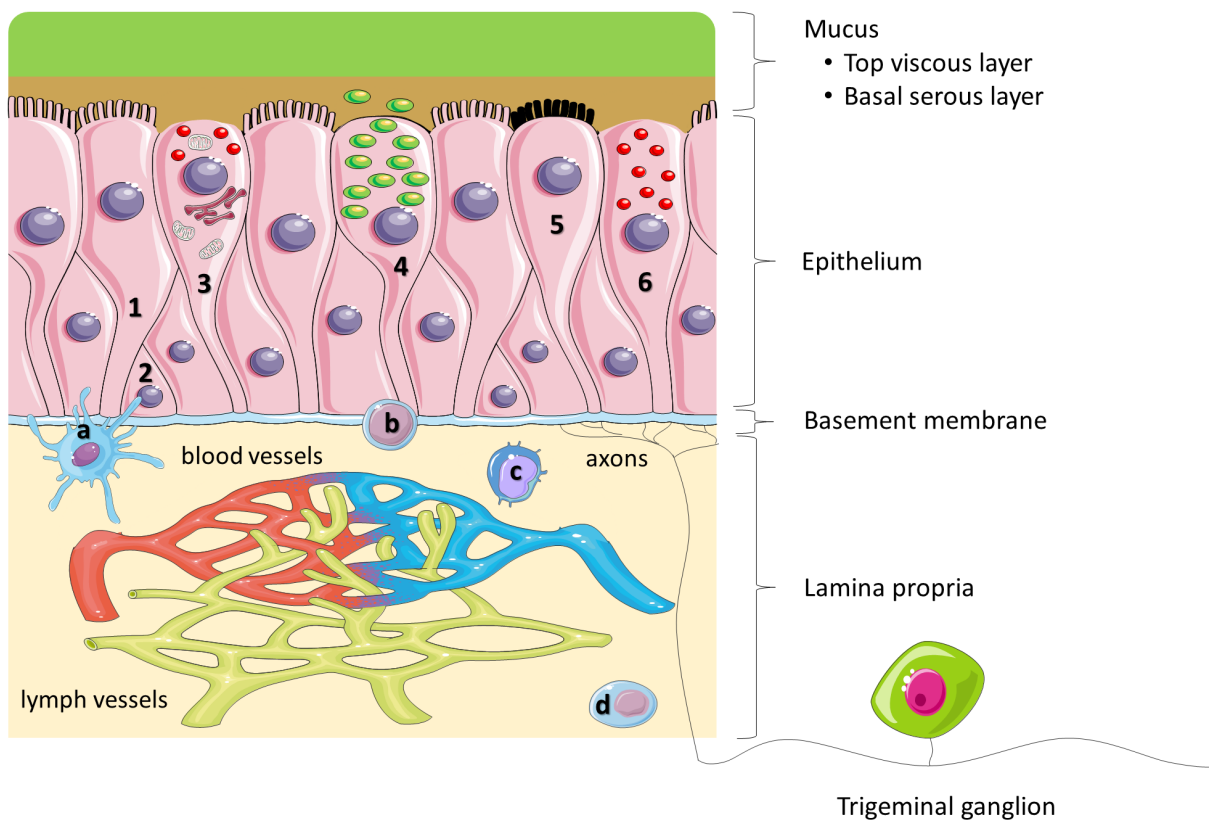


Figure 2. Schematic overview of the respiratory mucosa. A mucus layer, consisting of a top viscous layer (green) and a basal serous layer (brown) forms a blanket on top of the epithelium. Within this luminal pseudo-stratified epithelium, the following cell types reside: ciliated cells (1), basal cells (2), Clara cells (3), Goblet cells with mucoid secretory granules (green) (4), brush cells (5) and serous cells with serous secretory granules (red) (6). A rigid basement membrane supports the epithelium and connects the latter to the connective tissue of the lamina propria. Here, blood and lymph vessels together with neuronal axons are located. In the upper respiratory tract, the majority of axons belong to the trigeminal nerve and end up in the trigeminal ganglion, located at the apex of the petrous part of the temporal bone. Finally, local immune cells, such as dendritic cells (a), lymphocytic cells (b), monocytic cells (c) and plasma cells (d) constantly patrol the respiratory mucosa. Drawings are based on Smart Servier medical art templates.

The epithelial cells can be classified in three major groups, based on ultrastructural, functional and biochemical criteria: basal cells, ciliated cells and secretory cells.

Basal cells - The basal cell most likely functions as a progenitor cell, replacing other damaged or attrited epithelial cells (Boers *et al.*, 1998). In addition, basal cells rapidly flat out and thereby cover the basement membrane upon loss of neighbouring epithelial cells (Erjefalt *et al.*, 1995). Since basal cells are the only cell type within the respiratory epithelium capable of firmly attaching to the basement membrane, they have a major role in fixation of the complete respiratory epithelium. Besides desmosomes, basal cells can express hemidesmosomal complexes, which have the necessary integrins ($\alpha_6\beta_4$) to adhere to the basement membrane (Evans *et al.*, 1990; Evans and Plopper, 1988). Other epithelial cells only express desmosomes, involved in intercellular attachment, but lack hemidesmosomes, rendering them dependent on basal cells for firm attachment to the basement membrane. Basal cells are ubiquitously present in the respiratory tract at the basal side of the respiratory epithelium, although their number decreases more distally in the respiratory tract (Evans and Plopper, 1988).

Columnar ciliated epithelial cells - Ciliated cells are the predominant cell type in the respiratory epithelium. These differentiated cells possess up to 300 motile cilia, together with numerous apically located mitochondria to provide sufficient energy for their primary function: propel the mucus towards the throat (Bacha Jr and Bacha, 2012).

Secretory cells - Brush cells, mucous or Goblet cells, serous cells and Clara cells are four secretory cell types that reside in the respiratory epithelium.

Brush cells - Brush cells, or tuft cells, can easily be distinguished from other epithelial cells by their morphologic appearance. These cells are characterized by the presence of a luminal brush of long, rigid and blunt microvilli, a well-developed cytoplasmic tubulo-vesicular system and by their connection to neuronal axons (Sato, 2007). These axons originate from the trigeminal nerve and are able to trigger the sneeze reflex following certain stimuli, such as a sudden drop in temperature or contact with chemical substances. Besides this chemoreceptive function, brush cells are also presumed to participate in secretion and absorption. Brush cells are found throughout the entire respiratory tract. Recently, studies showed that these cells are also involved in mounting the ‘allergic’ type 2 immunity by producing certain cytokines (IL25), which in turn stimulate specific ‘type two innate lymphoid cells’ (ILC2s) to produce IL13 (Grencis and Worthington, 2016).

Mucous (Goblet) cells - Goblet cells morphologically resemble the shape of a goblet and contain numerous membrane-bound electron-lucent mucous granules (see Figure 2, green dots) (Bacha Jr and Bacha, 2012). They release mucins apically into the lumen, thereby forming the viscous

part of the mucus layer. Secretion of these mucins may be triggered by acute exposure to certain stimuli, such as sulphur dioxide. Mucous cells are found in all parts of the respiratory tract and are capable of self-renewal.

Serous cells - In contrast to mucous cells, serous cells contain electron-dense granules with substances ranging from neutral mucins to peptides and lipids (Jeffery and Li, 1997). Serous cells are the predominant cell type in serous glands of mammals but are rarely found in the luminal epithelium.

Clara cells - Although primarily present in the bronchi and bronchioli, Clara cells are also found in the trachea's epithelium. These peculiar cells lack cilia and harbour numerous secretory vesicles, mitochondria and smooth endoplasmic reticulum inside their cytoplasm. These components allow Clara cells to exert their specific functions: secrete material for the acellular lining of bronchioles, metabolise xenobiotic compounds and serve as the progenitor for both themselves and ciliated cells (Plopper *et al.*, 1980).

2.2. Host barriers

Since the respiratory mucosa is the first line of defence against incoming airborne pathogens and respirable hazards, it is provided with a repertoire of both innate and adaptive barriers (Bosch *et al.*, 2013; Knight and Holgate, 2003). These barriers include the mucus layer, firm intercellular connections between respiratory epithelial cells, the basement membrane, the production of a repertoire of antimicrobial/immunomodulatory peptides and the presence of local immune cells.

2.2.1. Mucus

Mucus is a semi-liquid layer lining the respiratory epithelium and is constantly replenished by the mucous (Goblet) cells and by the subepithelial glands in the lamina propria. It is the first line of defence against incoming hazards, having antioxidant, antiprotease and antimicrobial activities.

Airway mucus typically forms two layers: (i) a top viscous (gel) layer that captures putative pathogens, dust and irritant gasses from the air and (ii) a basal serous (sol) layer that surrounds the cilia (Harkema *et al.*, 2006). Synchronized beating of the cilia within the serous sol layer pushes the overlying mucus with entrapped materials towards the pharynx, where it is then swallowed and cleared through the digestive tract. Besides a normal ciliary beat frequency, an optimal conformation, thickness and ratio of viscosity to elasticity of both the gel and sol layer

are required to facilitate mucus transport. This conformation, thickness and ratio is mainly determined by mucin glycoproteins and by the mucus' hydration state (King, 1980; Randell and Boucher, 2006; Voynow and Rubin, 2009). The periciliary sol layer contains a repertoire of membrane-associated mucins (e.g. MUC1, MUC4, MUC16, MUC20), other glycoproteins and glycolipids. In addition, these membrane-tethered mucins function as receptors and signalling molecules. On the contrary, the luminal gel layer mainly consists of secreted mucins (MUC5AC and MUC5B). These mucins form long strands by interacting with globular proteins and retain a vast amount of water, attending the viscoelastic properties required for particle retention and transport (Voynow and Rubin, 2009). Under normal conditions, there is sufficient water to hydrate both the sol and gel layer of the mucus and clearance proceeds at normal rates. Excess fluid will selectively swell the gel layer, leaving the sol layer unchanged, eventually leading to an increase in clearance due to a reduction of viscoelasticity. Conversely, loss of water will cause both the gel and sol layer to collapse, enforcing the sticky gel layer to interact with membrane-bound glycoproteins, eventually decreasing its clearance (Randell and Boucher, 2006). Alterations in mucus composition favour or impair mucociliary clearance. Acute inflammation typically triggers the release of serous secretions and subsequent swelling of the mucus, resulting in a rapid clearing of invading agents. Similarly, hypertonic saline and mucolytics improve airway clearance by a decrease of the mucus' viscosity (King, 2005). Conversely, chronic inflammations (e.g. asthma, recurrent airway obstruction and cystic fibrosis) are characterized by a relative dehydration and alteration in the macromolecular composition of mucus, affecting its viscoelasticity and thereby hindering normal mucus-clearance. Indeed, most chronic inflammations are accompanied by an overproduction and hypersecretion of mucins or other macromolecules including DNA, filamentous actin, lipids, and proteoglycans (Livraghi and Randell, 2007).

Previous experiments already demonstrated that the mucoprotein network is efficient in entrapping microbes (e.g. *Pseudomonas aeruginosa*, influenza virus, respiratory syncytial virus, pseudorabies virus) by the interaction of opposite charges on the pathogen and mucoproteins (Yang *et al.*, 2012; Zanin *et al.*, 2016). In addition, the mucus layer contains numerous other antimicrobial substances secreted by epithelial cells, submucosal glands and immune cells. These substances include antimicrobial peptides (*vide infra*), hydrogen peroxide, nitric oxide, protease inhibitors and immunoglobulins, especially secretory immunoglobulin A (sIgA) (Ganesan *et al.*, 2013; Marriott, 1990; Zanin *et al.*, 2016). This sIgA is secreted as a dimeric form by plasma cells residing beneath the epithelium. Upon binding to the immunoglobulin receptor, located at the basolateral side of the epithelial cells, sIgA is taken up

through endocytosis and transported to the apical side. Here, the epithelium releases the sIgA into the airway lumen, where it captures specific pathogens before they can invade the host (Marriott, 1990).

2.2.2. Intercellular junctions

The respiratory epithelium is highly polarized and carefully maintains its integrity by the action of cell-cell and cell-matrix contacts. Polarization is characterized by the presence of two distinct regions: the apical domain facing the lumen (i.e. the external environment) and the basolateral domain, which comes in contact with adjacent cells and the basement membrane (Knust and Bossinger, 2002). Consequently, transmembrane proteins are frequently sorted to one of the two domains, resulting in a polarized plasma membrane. In addition, cellular polarization implies that intracellular proteins, organelles and the cytoskeletal network are also unevenly distributed. The connections between adjacent cells, or intercellular junctions (ICJ), form the morphological, functional and impermeable barrier between apical and basolateral cell domains. In addition to extracellular matrix connections, ICJ provide resistance against mechanical forces (Staelin, 1974). Multiple junctional complexes exist including tight junctions, adherent junctions, desmosomes and gap junctions and are schematically represented in Figure 3.

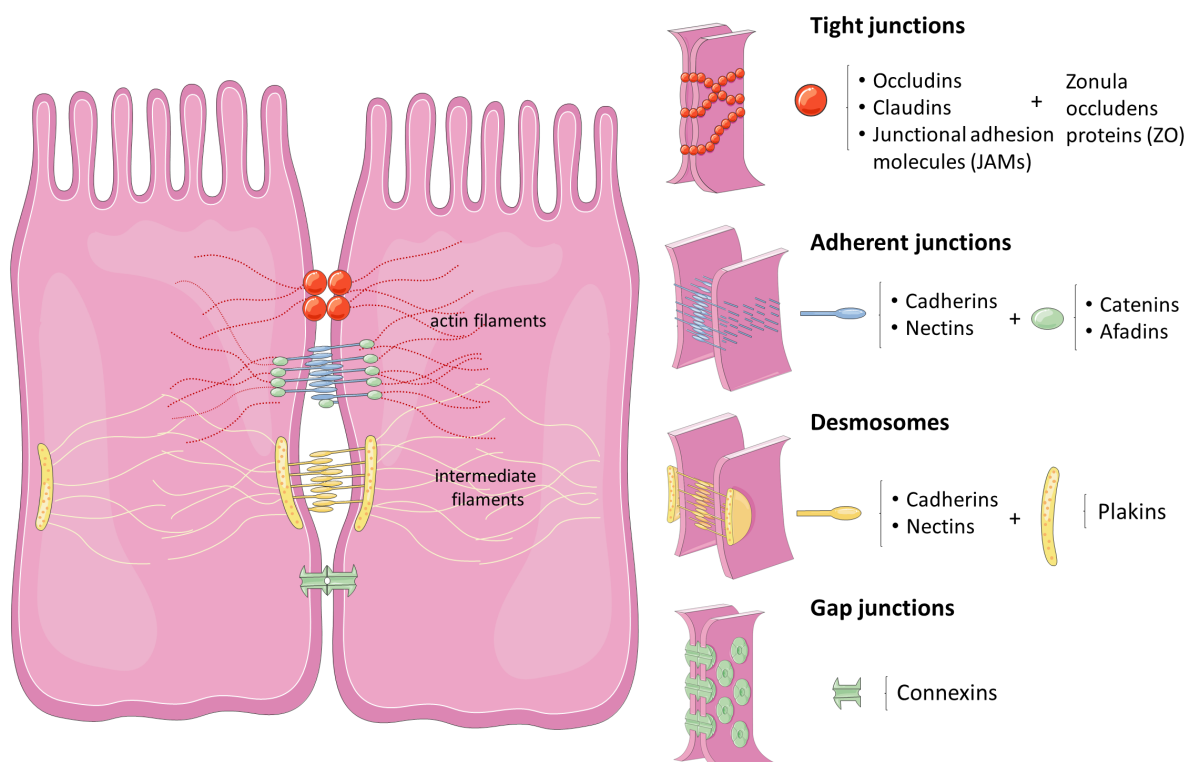


Figure 3. Schematic overview of the different intercellular junctions. Drawings are based on Smart Servier medical art templates.

2.2.2.1 Tight junctions

Tight junctions (TJ) are the most apically located ICJ and function as a size- and ion-selective gate for the passage of molecules in between adjacent cells (Balda and Matter, 2016; Matter and Balda, 2003). In addition, they have a fence-like function, preventing diffusion and mixing of plasma membrane lipids and (glyco)proteins from the apical to the basolateral surface and vice versa.

The TJ complex is composed of both transmembrane proteins and cytoplasmic actin-binding proteins. The former establish cell-cell contacts in the intercellular space, while the latter serve as a link to the actin cytoskeleton. Although more than 40 TJ proteins have been identified, claudins, occludins and junctional adhesion molecules (JAMs) are the primary constituents of the transmembrane proteins and zonula occludens (ZO) proteins are the well-known cytoplasmic actin binding proteins. Claudins form the backbone of TJ and regulate the passage of molecules based on their size (Van Itallie and Anderson, 2006). Occludins, although important for stability of the TJ complex, are dispensable for its formation (Schulzke *et al.*, 2005). Both claudins and occludins span the plasma membrane several times and their C- and N-termini extend in the cytoplasm. On the contrary, JAMs are single membrane-spanning proteins with an extracellular domain, a transmembrane domain and a cytoplasmic tail. By recruiting polarity complex proteins, JAMs are important for maintaining epithelial integrity and polarity (Ebnet *et al.*, 2003). The extracellular domains of these transmembrane TJ proteins typically form homophilic interactions with similar proteins on adjacent cells, while their cytoplasmic tails interact with ZO proteins (Anderson, 2001). ZO proteins finally connect the TJ complex to actin filaments and thus the complete inner cytoskeleton (Fanning and Anderson, 2009).

2.2.2.2 Adherent junctions

Adherent junctions (AJ) are located basally from the TJ and by connecting the cytoskeleton of neighbouring cells, they provide stability and uniformity to the epithelium (Baum and Georgiou, 2011).

Similarly to the TJ, AJ consist of transmembrane proteins, which connect AJ of adjacent cells to cytoplasmic actin-binding proteins. Two major subtypes of AJ complexes exist: the nectin-based adhesions and the cadherin-based adhesions. Both nectins and cadherins typically span the plasma membrane only once, providing them with a cytoplasmic tail, a transmembrane area and an extracellular domain. The cytoplasmic tail of nectin recruits afadin, which in turn binds to actin molecules (Takai and Nakanishi, 2003). In cadherin-based AJ, the function of afadin is

fulfilled by α - and β -catenins (Shapiro and Weis, 2009). The extracellular domain of both nectins and cadherins contains a number of IgG-like loops, which enable them to *trans*-dimerize with homophilic (or heterophilic) proteins on neighbouring cells. Functionally, cadherins are considered to be of major importance in strong cell-cell connections, since nectins alone are unable to support these complexes. On the other hand, nectins facilitate the establishment of cell-cell connections and cell polarity (Campbell *et al.*, 2017).

In the subplasma membrane domain, the cytoplasmic tails of both types of AJ (i.e. cadherin-based and nectin-based complexes) and the TJ are joined to one another. More precisely, α -catenins form the central key element by connecting ZO proteins, β -catenins and afadins (Campbell *et al.*, 2017).

2.2.2.3 Desmosomes

In contrast to AJ, which circumvent each of the interacting cells, desmosomes and hemidesmosomes form button-like points of contact. Desmosomes connect the intracellular intermediate filaments of adjacent cells, thereby creating a network that gives mechanical strength to the epithelium (Garrod and Chidgey, 2008). Desmosomal cadherins span through the intercellular space and connect neighbouring cells. Their cytoplasmic domains are in turn linked to intermediate filaments by plakin family proteins.

While AJ, TJ and desmosomes are present on all different cell types within the respiratory epithelium, hemidesmosomes are limited to basal cells. Hemidesmosomes morphologically resemble desmosomes but rather connect the intermediate cytoskeleton to the underlying basement membrane instead of to adjacent cells (Litjens *et al.*, 2006). This renders the complete respiratory epithelium dependent on basal cells for firm attachment to the subepithelial layers. It is the hemidesmosomal $\alpha_6\beta_4$ integrin that connects the cells to laminin, a major component of the basement membrane, whereas cytoplasmic proteins (e.g. plectin) connect to the intracellular intermediate filament system, thereby creating a stable anchoring complex. Other integrins are also expressed on the rest of the respiratory epithelial cells, where they mainly function in cell signalling pathways (Sheppard, 1998).

2.2.2.4 Gap junctions

Gap junctions serve as the communicating device of the epithelium by forming channels between neighbouring cells. Two hemichannels, each of which is a hexamer composed of connexin proteins, form an aqueous pore in the plasma membrane of two different adjacent cells. Small molecules and ions can pass through these channels, which is essential for epithelial cell synchronisation, differentiation and migration (Hervé *et al.*, 2007).

2.2.3. Basement membrane

Located between the epithelium and the underlying connective tissue, the basement membrane serves as a supportive sheet for epithelial cells. The structural components of the basement membrane comprise collagen (type I, III-VII), laminin, fibronectin, entactin and heparan sulfate proteoglycans, and are secreted by either the above-located epithelial cells or the underlying fibrocyts/fibroblasts (Pozzi *et al.*, 2017). Besides as an anchorage for epithelial cells, the basement membrane also functions as an impermeable barrier to cell migration and pathogen invasion. However, specific proteolytic events allow normal cells to freely traffic the basement membrane during morphogenesis and immune surveillance (Sekiguchi and Yamada, 2018). Some pathogens, such as pseudorabies virus (PRV) in pigs, bovine herpesvirus type 1 (BoHV1) in cows and herpes simplex virus 1 (HSV1) in humans, have evolved specific mechanisms to misuse these proteolytic events, allowing them cross the basement membrane (Glorieux *et al.*, 2011a; Glorieux *et al.*, 2011b; Steukers *et al.*, 2012). In contrast, equine herpesvirus type 1 (EHV1) in horses cleverly hijacks diapeding immune cells as ‘Trojan horses’ to cross the basement membrane (Vandekerckhove *et al.*, 2010).

2.2.4. Antimicrobial peptides

Peptide molecules (< 100 amino-acids) with an antimicrobial activity (i.e. antimicrobial peptides) are a key component of airway mucus and respiratory epithelial cells. These peptides typically contain a large proportion of cationic and hydrophobic residues and comprise several families such as lysozymes, cathelicidins, psoriasins and defensins (Bruhn *et al.*, 2011). Solely defensins will be discussed below, as a detailed description of the complete repertoire of antimicrobial peptides is beyond the scope of this thesis.

2.2.4.1 Defensins

Defensins are small (\pm 20-45 amino-acids) cationic peptides that exhibit a broad-spectrum antimicrobial activity against (myco)bacteria, fungi and viruses, as well immunomodulatory properties (Ganz, 2003; Pazgier *et al.*, 2006; Selsted and Ouellette, 2005; White *et al.*, 1995). The hallmark of all defensins is the presence of three different intramolecular disulphide bonds, pairing three antiparallel β -strands. Based on disulphide-connectivity, the defensin family is divided in two main subtypes: α - and β -defensins. Theta-defensins, originally found in rhesus-macaque monkeys, belong to an additional class of defensins, considering their circular structure. While α -defensins are mainly expressed in mammalian leukocytes and intestinal Paneth cells, β -defensins (BDs) are predominantly found in epithelial tissues lining internal and

external cavities, but can also be synthesized in leukocytes. Since the respiratory epithelium mainly expresses BDs, attention is focussed on this defensin type in this thesis.

The first identified mammalian BD was extracted from bovine tracheal mucosa and was named ‘tracheal antimicrobial peptide’ (Diamond *et al.*, 1991). In the meantime, BDs have been described in several other species including humans, mice, pigs, dogs, sheep and horses (Bals *et al.*, 1999; Bensch *et al.*, 1995; Davis *et al.*, 2004; Huttner *et al.*, 1998; Sang *et al.*, 2005; Zhang *et al.*, 1998). Mammalian (β -)defensins have the capacity to inactivate bacterial and enveloped viral microorganisms by disrupting the microbial membrane (Bals *et al.*, 1998; Harder *et al.*, 2001; Schroeder *et al.*, 2011; Wilson *et al.*, 2013). More precisely, cationic residues on defensins initially interact with negatively charged phospholipids of microbial membranes, followed by insertion of the amphipatic defensin into the bilipid layer which subsequently permeabilizes the membrane, finally resulting in lysis of the pathogen. This electrostatic interaction is diminished in increasing salt concentrations or in the presence of bivalent cations (e.g. Ca^{2+}). However, salt concentrations at mucosal surfaces are relatively low, enabling defensins to exhibit their killing activities (Goldman *et al.*, 1997; Quinones-Mateu *et al.*, 2003).

Besides this direct antimicrobial killing activity, defensins can also mask putative receptors that project through microbial or cellular membranes (Hazrati *et al.*, 2006; Leikina *et al.*, 2005). This lectin-like function is believed to be of major importance in the antiviral activity of defensins and consequently is diminished in the presence of serum (Quinones-Mateu *et al.*, 2003; Wilson *et al.*, 2013). As defensins are known to form multimeric structures, binding of defensins to viral surface proteins can also aggregate virions, facilitating their disposal by the mucocilliary clearance (Dugan *et al.*, 2008). Instead of directly binding to viral or cellular receptors, defensins can also induce changes in intracellular signalling, thereby impacting viral infections. For example, protein kinase C activity is inhibited by defensins *in vitro* and is known to be involved in the replication of several viruses (Charp *et al.*, 1988; Contreras *et al.*, 2012; Leach and Roller, 2010; Siczarski *et al.*, 2003). Furthermore, defensins can inhibit viral replication through even more distinct, yet unknown, mechanisms after viral penetration has been completed (Hazrati *et al.*, 2006; Smith and Nemerow, 2008). An overview of the different known antimicrobial actions of defensins is represented in Figure 4.

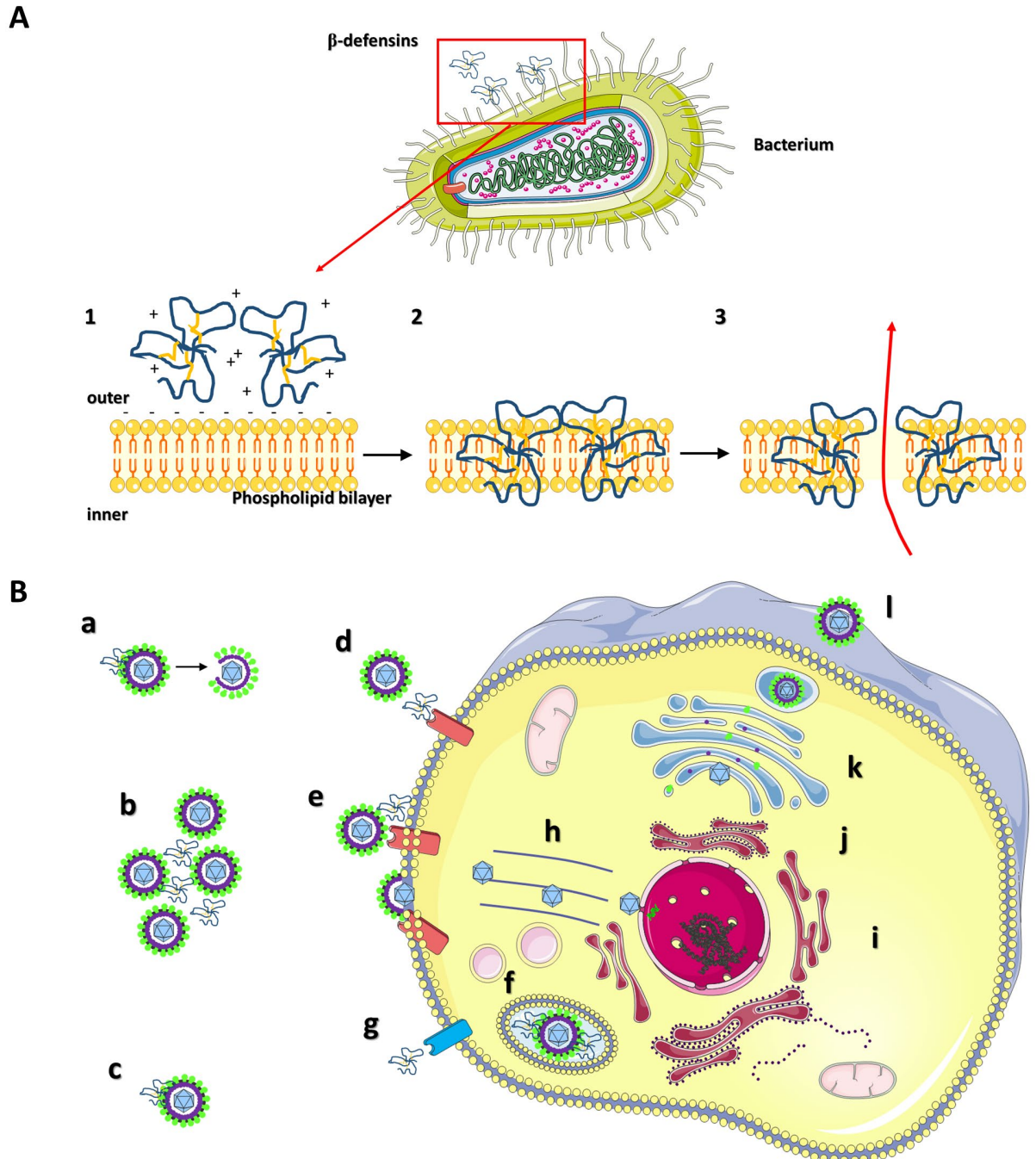


Figure 4. Different modes of action of defensins against (A) bacteria and (B) viruses. (A) Cationic residues on defensins initially interact with negatively charged phospholipids of microbial membranes (1), followed by insertion of the amphipatic defensin into the bilipid layer (2), which subsequently permeabilizes the membrane (3), finally resulting in loss of cytoplasmic material (red arrow) and lysis of the pathogen. (B) Viruses can be inhibited by defensins through permeabilization of the viral envelope (a), aggregation and facilitated disposal of virus particles (b), binding of viral ligands (c), binding of cellular receptors (d), inhibition of fusion (e), facilitating lysis in endosomes (f), activating or inhibiting cellular pathways through cell receptor binding (g), inhibiting viral transport to the nucleus (h), inhibiting viral RNA/DNA transcription (i), preventing of RNA/DNA/protein synthesis, impediment of progeny virus assembly (k) or finally, viral egress (l). Drawings are based on Smart Servier medical art templates.

Finally, defensins bridge the innate and adaptive immune response by recruiting immune cells to sites of infection. It has already been shown that defensins are elicited during viral infections and efficiently attract neutrophils, dendritic cells, monocytes, T lymphocytes and mast cells to

the site of infection (Chong *et al.*, 2008; Niyonsaba *et al.*, 2016; Proud *et al.*, 2004; Quinones-Mateu *et al.*, 2003; Röhrli *et al.*, 2010; Wu *et al.*, 2003; Yang *et al.*, 1999).

The equine variants of BDs are only poorly characterized at present but a detailed description of the limited knowledge on these peptides is given in the introduction of Chapter 6.

2.2.5. Immune cells

Besides the above-mentioned innate immune barriers, the (horse's) respiratory tract is guarded by an ample population of immune cells, including monocytes, macrophages, dendritic cells (DCs), T and B lymphocytes and natural killer cells. These cells are part of a common mucosa-associated lymphoid tissue (MALT) and are located either inside specialized local inductive sites (lymphoid nodules; organized or O-MALT) or patrol the respiratory mucosa individually (diffuse or D-MALT) (Kraehenbuhl and Neutra, 1992). The latter MALT is designated NALT in the nasal cavity together with nasopharynx, LTALT at the level of the larynx and trachea, BALT in the bronchi and finally, BRALT in the bronchioli.

Neutrophils, monocytes, macrophages and DCs belong to the cells of the myeloid lineage (CD172a⁺). **Neutrophils** play a key role in the first defence against (bacterial) pathogens, although they essentially are not a part of the MALT. Neutrophils not only phagocytize invading microbes, but can also kill them by releasing a repertoire of toxic substances. **Monocytes** are mainly phagocytes and play an essential role as cells in the first line of defence against pathogens. They originate from the bone marrow and are released into the peripheral blood, where they circulate for several days before entering tissues to renew tissue macrophage and DC populations (Auffray *et al.*, 2009). **Macrophages** are resident cells in lymphoid and non-lymphoid tissues, where they mainly function as phagocytes and are responsible for the clearance of apoptotic and infected cells. These cells, although of minor importance, can also act as antigen-presenting cells. Finally, they activate the inflammatory pathway by producing tumor necrosis factor alpha (TNF- α), interleukins (IL) type 1 (IL-1) and type 6 (IL-6) (Geissmann *et al.*, 2010). Besides macrophages, **dendritic cells** can also be generated by the differentiation of monocytes. They are specialized antigen-presenting cells and are also known as 'Langerhans cells' in the respiratory mucosa. Upon activation, they migrate from tissues to the draining lymph nodes, where they regulate T cell responses (Auffray *et al.*, 2009; Fokkens *et al.*, 1989). The two predominant **T lymphocyte** populations (CD4⁺ and CD8⁺) reside in the horse's respiratory mucosa. CD8⁺ T lymphocytes are known as cytotoxic T lymphocytes (CTLs) and mainly function to lyse infected cells that present foreign antigens via their MHC I molecules. These T lymphocytes are located within the epithelium, while CD4⁺ T lymphocytes

are mainly found in the lamina propria (Mair *et al.*, 1987). CD4⁺ T lymphocytes provide B lymphocytes, CD8⁺ T lymphocytes and macrophages with the crucial signals for maturation and activation (Reiner, 2007). Once activated by an antigen and a CD4⁺ T lymphocyte, **B lymphocytes** differentiate into plasma cells. Plasma cells embedded in the lamina propria secrete, besides regular IgG and IgM, the most predominant antibody in the respiratory mucosa: sIgA (*vide supra*) (Fallgreen-Gebauer *et al.*, 1993).

Natural killer cells (NK cells) subdue viral infections until the adaptive immunity takes over. More precisely, viruses can hamper the expression of MHC I class molecules at the infected cell surface in order to escape the host's immune system. NK cells, however, are able to recognise these infected cells due to the down regulation of MHC I class molecules. Similarly to CTLs, NK cells release their cytotoxic granules on the target cell upon activation, thereby inducing programmed cell death through effector proteins (Vivier *et al.*, 2008).

Although all of these immune cells are of crucial importance in the host's defence, some airborne pathogens misuse these cells to disseminate within the host. For example, EHV1 and equine arteritis virus (EAV) depend on leukocytes for their spread to target organs (*vide infra*).

2.3. Models to study the respiratory tract

2.3.1. Continuous cell lines

A continuous cell line is the most widely used tool to study (respiratory) epithelial cell biology and pathology. Continuous cell lines originate from specific parts of a multicellular organism (e.g. the human trachea, bronchi or lungs) and can be passaged for prolonged periods *in vitro*, due to genomic mutations (Cozens *et al.*, 1994; Schweppe and Korch, 2018). These mutations enable continuous cell lines to evade normal cellular senescence, thereby making them 'immortal'. Immortalization of cells can occur spontaneously, but is most often experimentally induced by introducing specific (viral) genes that remove biological brakes on proliferative cell control and/or allow cells to extend the DNA sequence of telomeres. Although continuous cell lines are easy to use and allow for the replication of homogeneous results, they exhibit many inherent disadvantages. For instance, genetic mutations may alter cellular phenotypes and mechanisms, leading to inconclusive or erroneous results when using these cells (Schweppe and Korch, 2018). In addition, continuous cell lines cannot fully mimic the *in vivo* 3D architecture.

2.3.2. *Animal models*

Laboratory animals represent a full *in vivo* environment, making them presumably ideal candidates to study the pathogenesis of respiratory diseases and test potential therapeutic interventions (Barrios, 2008). In addition, transgenic mouse technology allows researchers to investigate the role of specific genes and molecular interactions in the development of respiratory diseases. However, animal experiments raise ethical questions and results cannot be blindly extrapolated to other species, including human.

2.3.3. *Explant model*

Explants provide a good alternative to the previously mentioned models, as they maintain the *in vivo* micro-environment, including mucus and normal cell-cell connections. In addition, several explants can be obtained from one animal to test multiple conditions, limiting the number of experimental animals and inter-animal variations. However, it should be taken into account that explants lack a complete MALT-system and a systemic immunity. Therefore, results obtained with explants should be verified in *in vivo* experiments, conducted with representative animals (e.g. horses for equine pathogens).

The first documented airway explant model dates from 1925 and was further developed in the 50's for humans and monkeys (Hoorn, 1964). Over the next years, the culture system of respiratory explants was further optimized and extended to pigs, rats and dogs (Fanucchi *et al.*, 1999; Pol, 1990; Schierhorn *et al.*, 1995; Stahl and Ellis, 1973). Cell viability tests confirmed that these explants were on average viable for up to 4-7 days (Glorieux *et al.*, 2007; Kleinsasser *et al.*, 2004; Park *et al.*, 2007). The majority of these studies agreed on one important feature: respiratory explants should be cultivated at the air-liquid interface for optimal results. This implies that the explants are apically in direct contact with the air and are nourished via the basolateral side with medium. To obtain such a relevant environment, researchers used various explant-supporting materials such as gauzes, gelatine sponges, agar, plastic plates or filter paper (Ali *et al.*, 1996; Glorieux *et al.*, 2007; Jackson *et al.*, 1996; Kleinsasser *et al.*, 2004; Park *et al.*, 2007). In the meantime, respiratory explant models have been developed for a repertoire of domestic mammals (e.g. pigs, cows, horses, cats, dogs and chickens) and used to study pathogen-host interactions for viruses as well as for bacteria (Glorieux *et al.*, 2007; Hamilton *et al.*, 2006; Li *et al.*, 2016; Li *et al.*, 2015; Niesalla *et al.*, 2009; Reddy *et al.*, 2014; Vandekerckhove *et al.*, 2009). A schematic illustration of the mucosal explant model is given in Figure 5A.

2.3.4. Respiratory epithelial cell model

Although respiratory explants represent most optimally the *in vivo* 3D architecture and micro-environment of the respiratory mucosa, collecting and processing them is time-consuming. In addition, explants usually die within a week and it is difficult to study merely epithelial characteristics such as integrity and polarity. Therefore, researchers tried to establish an *in vitro* cell culture model of respiratory epithelial cells through mechanical or enzymatic collection (Harmon *et al.*, 1977; Widdicombe *et al.*, 1985). Again, it became rapidly clear that cultivation at the air-liquid interface, e.g. in transwells, was the most optimal design to maintain epithelial cell differentiation (Clark *et al.*, 1995; Nevo *et al.*, 1975; Whitcutt *et al.*, 1988). This respiratory epithelial cell model appeared to mimic the *in vivo* airway epithelium very well, consisting of a heterogeneous population of ciliated cells, basal cells and (mucus-)secreting cells (Quintana *et al.*, 2011; Rowe *et al.*, 2004; Schwab *et al.*, 2010). The formation of ICJ and thus integrity in this model was also verified by measuring the transepithelial electrical resistance (TEER) (Quintana *et al.*, 2011; Rowe *et al.*, 2004). Measuring the TEER is a generally accepted technique to study integrity and permeability dynamics of epithelial or endothelial cell monolayers, cultured on transwells (Srinivasan *et al.*, 2015). The TEER is measured in ohms (Ω) by an epithelial voltohmmeter using two electrodes, where one electrode is placed in the apical compartment and the other one in the basolateral compartment. Firm intercellular junctions will impair paracellular ionic conductance, resulting in increased resistance measurements. Vice versa, disruption of epithelial integrity will allow the paracellular transport of ions, decreasing the net resistance of the cell monolayer. The TEER method's major advantage is that it can be widely used to monitor live cells during their various stages of growth and differentiation.

In the meantime, the respiratory epithelial cell model has been tested out for several species, including laboratory animals, cows, horses and dogs, and the human model has even been commercialized as MucilAir™ and EpiAirway™ (Coleman *et al.*, 1984; Huang *et al.*, 2008; Kondo *et al.*, 1993; Quintana *et al.*, 2011; Ren and Daines, 2011; Rowe *et al.*, 2004; Schwab *et al.*, 2010). It has already successfully been used to study the replication of airborne pathogens, allergy and immunologic features of the respiratory epithelium (Longphre *et al.*, 1999; Quintana *et al.*, 2011; Sajjan *et al.*, 2008). A schematic illustration of the respiratory epithelial cell model is given in Figure 5B.

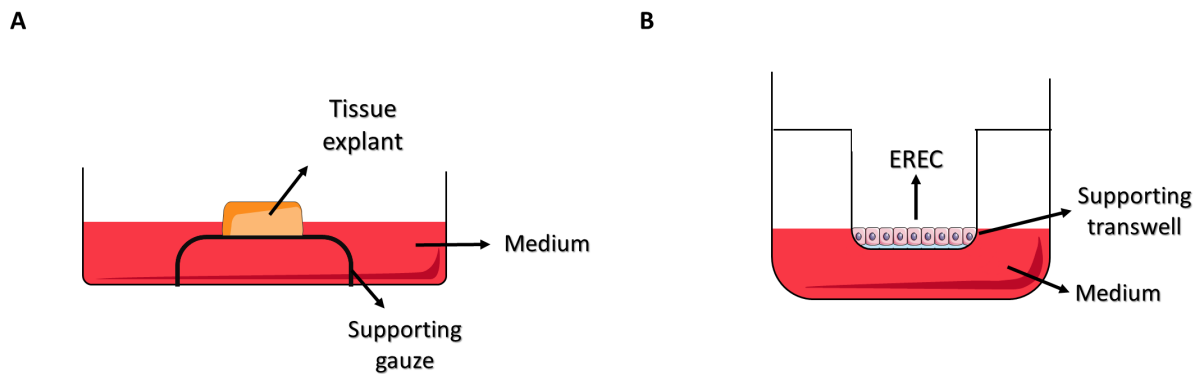


Figure 5. Illustration of (A) the mucosal explant model and (B) the transwell cell culture system. EREC = equine respiratory epithelial cells

3. Airborne pathogens of the horse

Respiratory tract infections are one of the most common illnesses in horses worldwide and are usually initiated by viruses and might be aggravated upon secondary bacterial colonization (Gilkerson *et al.*, 2015; Slater, 2007). Equine herpesviruses (1, 2, 4 and 5), equine influenza virus, picornaviruses (equine rhinitis A virus, equine rhinitis B virus), adenoviruses and equine arteritis virus are the most frequent viral agents of respiratory tract infections in the horse (Gilkerson *et al.*, 2015). Several bacterial species, including *Streptococcus equi* subsp. *equi*, *Rhodococcus equi*, *Bordetella bronchiseptica* and *Mycoplasma felis*, have been isolated from horses with respiratory disease without the presence of viruses (Garcia-Cantu *et al.*, 2000; Hines, 2007; Sweeney *et al.*, 2005; Wood *et al.*, 1997). These organisms can therefore be classified as primary pathogens, capable of causing respiratory disease in the absence of predisposing factors. On the contrary, opportunistic bacteria such as *Streptococcus equi* subsp. *zooepidemicus* and *Staphylococcus aureus* usually do not cause respiratory disease, unless their host is (immuno)compromised (e.g. dysfunction in the innate or adaptive immune system or reduced mucociliary clearance due to long-distance transports where the horse's head is tied in an upright position, poor hygiene conditions, anaesthesia and primary viral infections) (Slater, 2007). This thesis focussed on a limited number of these equine airborne pathogens, thought to be of most importance in global horse industry. These pathogens are further discussed below.

3.1. Equine herpesvirus type 1

3.1.1. Introduction

Equine herpesvirus type 1 (EHV1) is a major and ubiquitous pathogen in the horse population, causing respiratory and neurological disorders, abortion and neonatal foal disease. Although many EHV1 infections occur asymptotically or are accompanied only by signs of mild respiratory disease, severe outbreaks of abortion and neurological disease occur annually. Therefore, the virus has the potential to cause serious economic losses in the horse industry worldwide. EHV1 is one of nine equine herpesviruses (EHV1-9) currently known to infect horses and has also been reported in mules, donkeys, zebras, onagers, giraffes and gazelles (Borchers and Frölich, 1997; Hoenerhoff *et al.*, 2006; Ibrahim *et al.*, 2007). Together with EHV3, EHV4, EHV6 (asinine herpesvirus type 1), EHV8 (asinine herpesvirus 3) and EHV9 (gazelle herpesvirus type 1), EHV1 is taxonomically classified as a member of the family *Herpesviridae*, subfamily *Alphaherpesvirinae*, genus *Varicellovirus* (Roizman and Baines, 1991). The other three equine herpesviruses (EHV2, EHV5 and EHV 7 or asinine herpesvirus type 2) belong to the *Gammaherpesvirinae* subfamily.

Dimonck and Edwards documented the virus for the first time in 1933 during an outbreak of abortion. The virus was first designated ‘equine abortion virus’, was later renamed ‘equine rhinopneumonitis virus’, but is now known as ‘equine herpesvirus type 1’ (Allen and Bryans, 1986). It took another three decades before scientists were able to isolate the virus for the first time (Saxegaard, 1966). EHV1 and EHV4 are antigenically and genetically closely related and were considered as two subtypes of the same virus prior to 1988 (Cullinane *et al.*, 1988; Roizman and Baines, 1991).

Over the next years, it became more and more apparent that two distinct EHV1 subtypes exist in the field, differing in pathogenic capacity (abortion vs neurological) (Allen *et al.*, 1985; Maanen *et al.*, 2001; McCann *et al.*, 1995). In 2006, researchers assigned this distinction to a single nucleotide polymorphism in the catalytic subunit of the viral DNA polymerase (Nugent *et al.*, 2006). Non-neurological/abortigenic strains mostly exhibit amino-acid asparagine at position 752 (N752), whereas neurological strains express amino-acid aspartic acid at the latter position (D752) (Goodman *et al.*, 2007; Nugent *et al.*, 2006; Perkins *et al.*, 2009). However, increasing evidence rises that more differences exist between the two subtypes (Laval *et al.*, 2017; Negussie *et al.*, 2016; Zhao *et al.*, 2017).

3.1.2. Viral structure

EHV1 consists of a double-stranded DNA molecule of approximately 150 kilobase pairs (kbp), an icosahedral capsid built up from 162 capsomers (12 pentons, 150 hexons), a layer of tegument proteins and an outer lipid bilayer envelope, containing 12 different glycoproteins, as shown in Figure 6 (Roizman and Baines, 1991; Roizmann *et al.*, 1992; Telford *et al.*, 1992).

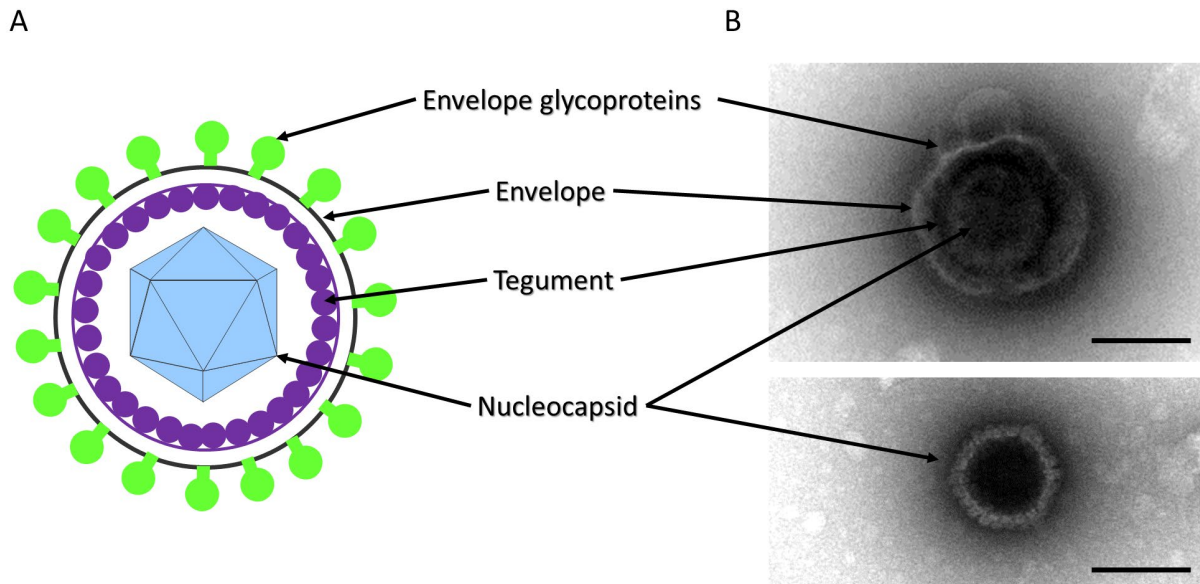


Figure 6. Structure of an EHV1 virion. (A) Schematic representation. Drawing is based on Motifolio art template. (B) Transmission electron microscopic image. The bar represents 100 nm.

The envelope is derived from the trans-Golgi network of the host cell and forms the outer layer of the virus (Granzow *et al.*, 2001). Several glycoproteins are embedded in the envelope and each have a specific role in virus attachment, entry, egress, cell-to-cell spread and/or immune-modulation. All glycoproteins are homologous to other alphaherpesvirus glycoproteins (e.g. of herpes simplex virus (HSV), varicella zoster virus (VZV), pseudorabies virus (PRV) and bovine herpesvirus (BoHV)), except gp2. Briefly, **glycoprotein B (gB)** and **gC** are involved in the initial attachment of EHV1 to host cell surfaces (Neubauer *et al.*, 1997; Osterrieder, 1999). Following initial non-essential binding, **gD** anchors the virus onto a putative cellular receptor (Csellner *et al.*, 2000). Next, glycoproteins **gB**, **gD**, **gM** and **gK** aid the virus in a process called penetration/fusion, which is the release of naked nucleocapsids in the host cell cytoplasm (Csellner *et al.*, 2000; Neubauer *et al.*, 1997; Neubauer and Osterrieder, 2004; Osterrieder *et al.*, 1996). Alternatively, **gH** and **gD** can guide the viral entry towards endocytosis through interaction with $\alpha_4\beta_1$ or α_v integrins (Azab *et al.*, 2013; Van de Walle *et al.*, 2008a). EHV-1 **gB**, **gD**, **gE/gI**, **gK**, **gM** and **gH** assist the virus in an important and characteristic herpetic strategy: cell-to-cell spread (Azab *et al.*, 2012; Csellner *et al.*, 2000; Flowers and O'Callaghan, 1992; Matsumura *et al.*, 1998; Neubauer *et al.*, 1997; Neubauer and Osterrieder, 2004; Osterrieder *et al.*

al., 1996; Wellington *et al.*, 1996). **Glycoprotein K**, **gp2** and **gC** are essential during viral egress and release of progeny virions (Neubauer and Osterrieder, 2004; Osterrieder, 1999; Rudolph and Osterrieder, 2002). **Glycoprotein G** is both a structural component of the virion and secreted by infected cells. Upon secretion, gG binds chemokines such as CCL3, CXCL1 and IL-8 and thereby impedes the recruitment of host immune cells and thus the onset of an inflammatory response (Thormann *et al.*, 2012; Van de Walle *et al.*, 2007; Van de Walle *et al.*, 2008b). On the contrary, **gp2** induces the production of cytokines and chemokines in infected mice (Smith *et al.*, 2005). The exact role that gp2 plays during infection of the horse remains unclear so far. **Glycoprotein N** is necessary for functional processing of gM (Rudolph *et al.*, 2002). In addition, gN contributes to EHV1 immune evasion through inhibition of the antigen transporter TAP and subsequent downregulation of cell surface MHC I (Koppers-Lalic *et al.*, 2008). Until present, the function of EHV1 **gL** remains unclear. In HSV, gL forms a functional entity with gH and is critical for correct folding and trafficking of the latter glycoprotein (Fan *et al.*, 2009).

3.1.3. Replication cycle

A single EHV1 replication cycle generally takes 12 hours (h) and is illustrated in Figure 7. The initial step in EHV1 replication is the attachment of the virus to the cell. EHV1 interacts with sugar moieties (e.g. heparan sulphate, sialic acids and other putative glycans) on the cell surface via gB and gC (Laval *et al.*, 2016; Neubauer *et al.*, 1997; Osterrieder, 1999). Next, EHV1 glycoprotein gD binds to a cellular receptor to stabilise the binding and trigger entry into the cell (Csellner *et al.*, 2000). MHC I has been put forward as a putative receptor for EHV1 gD in equine brain microvascular cells (EBMEC), equine dermal (ED) cells and peripheral blood mononuclear cells (PBMC) (Kurtz *et al.*, 2010; Sasaki *et al.*, 2011). However, MHC I is ubiquitously expressed in all cell types and, therefore, does not correlate with EHV1 tissue tropism. In PBMC, attachment to and subsequent entry is additionally mediated by the binding of EHV1 gD to cellular integrins (Laval *et al.*, 2016; Van de Walle *et al.*, 2008a). Nectin-1, nectin-2 and herpesvirus entry mediator (HVEM) are known to interact with gD homologs of several alphaherpesviruses including HSV1 and 2, PRV and BoHV1 (Geraghty *et al.*, 1998). Nonetheless, EHV1 presumably does not depend on nectins, since Chinese hamster ovary epithelial cells (CHO-K1) lack HVEM, nectin-1 and -2 expression, although they are fully susceptible to EHV1 (Frampton *et al.*, 2005). Until present, the precise equine respiratory epithelial cell (EREC) binding/entry receptor for EHV1 remains unknown.

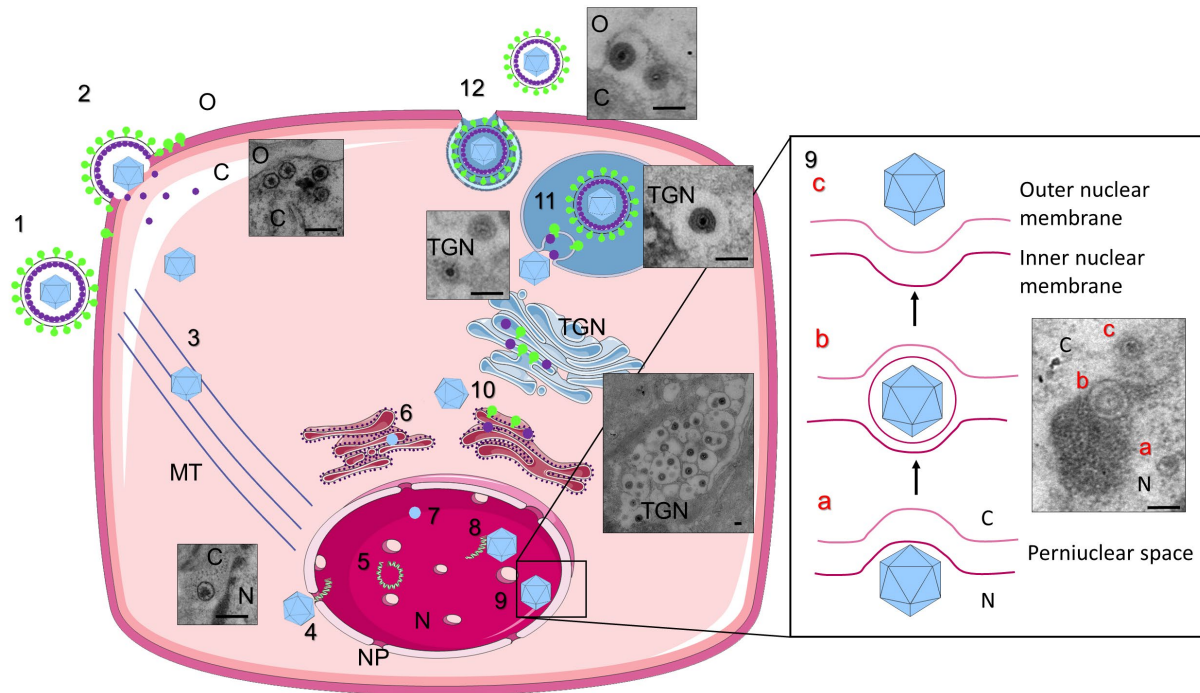


Figure 7. Schematic representation of EHV1's replication cycle, illustrated with transmission electron micrographs of EHV1-infected respiratory epithelial cells in explants. (1) EHV1 particles from the outer environment (O) attach to the host cell. (2) EHV1 penetration into the cytoplasm (C) of the host cell. (3) Transport of EHV1 nucleocapsids to the nucleus (N) via interaction with microtubules (MT). (4) The viral genome is released into the nucleus via a nuclear pore (NP). (5) Viral DNA circularizes and is transcribed and replicated in the nucleus. (6) Viral proteins are synthesized in the cytoplasm and (7) capsid proteins route to the nucleus. (8) Newly synthesized viral DNA is cleaved and packaged into capsids resulting in mature nucleocapsids. (9) Nucleocapsids leave the nucleus by budding into the inner nuclear membrane. Nucleocapsids lose this envelope when passing through the outer nuclear membrane. (10) Naked nucleocapsids travel towards the trans-Golgi network (TGN). (11) Nucleocapsids acquire their secondary (final) envelope by budding into the trans-Golgi network. (12) Mature virus particles are transported to the cell surface within sorting vesicles and released via exocytosis in the extracellular space. Drawings are based on Smart Servier medical art templates. The scale bar measures 150 nm.

After binding, EHV1 has to get into the cell and depending on the cell type, is able to use two distinct pathways for this purpose: fusion and/or endocytosis. EHV1 penetrates equine endothelial cells (EC), ED cells and rabbit kidney (RK13) cells via fusion, while the virus can enter PBMC, EBMEC (but not ECs), RK13 cells, CD172a⁺ cells and CHO-K1 cells via endocytosis (Frampton *et al.*, 2007; Hasebe *et al.*, 2009; Laval *et al.*, 2016; Van de Walle *et al.*, 2008a). Determinants in the choice between fusion and endocytosis are viral gD and gH on the one hand and cellular integrins on the other hand (Azab *et al.*, 2013; Van de Walle *et al.*, 2008a). Both entry pathways require the activation of cell signalling via activation of the Rho-associated coiled-coil kinase (ROCK1) (Frampton *et al.*, 2007)

Irrespective of the entry route into the cell, the virus releases a naked nucleocapsid in the cytoplasm, which travels along the microtubule network towards the nucleus. At the level of nuclear membrane, the virus injects its DNA via the nuclear pore complex into the nucleus (Frampton Jr *et al.*, 2010).

Following circularization of viral DNA, its transcription occurs in a cascade-like manner. The immediate-early (IE) gene is first synthesized and encodes for a major IE polypeptide (IEP),

which functions as a regulatory protein. IEP expression is necessary for the expression of early (E) genes and late (L) genes (Caughman *et al.*, 1985; Gray *et al.*, 1987). The E genes encode proteins required for DNA replication, such as the DNA polymerase and thymidine kinase. Viral DNA replication is then initiated in the nucleus. L genes encode multiple viral structural proteins such as capsid proteins, tegument proteins and envelope glycoproteins.

Viral proteins are synthesized in the cytoplasm and capsid proteins reroute to the nucleus for assembly of the capsids, prior to encapsidation of the viral DNA. The nucleocapsid then travels via the inner and outer nuclear membrane, into the cytoplasm. Naked nucleocapsids, together with structural viral late tegument proteins and glycoproteins enter the trans-Golgi complex. Mature progeny virions receive their final envelope from the Golgi apparatus and exit their host cell through vesicle-mediated exocytosis (Granzow *et al.*, 2001).

3.1.4. Pathogenesis and accompanying clinical symptoms

The pathogenesis of EHV1 is illustrated in Figure 8.

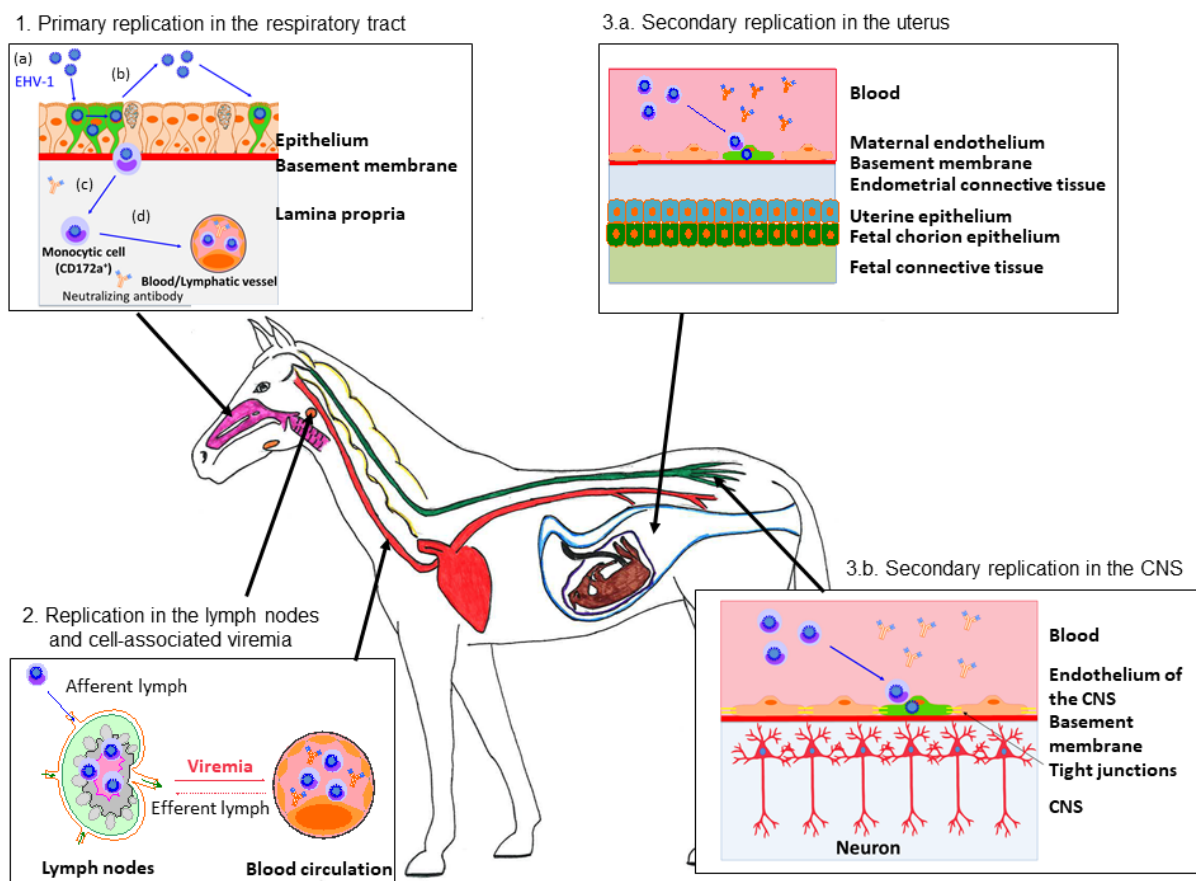


Figure 8. Schematic overview of the pathogenesis of EHV1, adapted from Laval (2016). Pink = respiratory tract; red = blood circulation; orange = lymph nodes; yellow = vertebrae; green = spinal cord; blue = uterus + vagina. (1) EHV1 first replicates in the respiratory epithelium; EHV1 infection (a); viral spread and shedding (b); EHV1 crosses the basement membrane by the use of single immune cells (c); viral dissemination (d). (2) Upon crossing the basement membrane, EHV1 penetrates the connective tissues and reaches the bloodstream and draining lymph nodes. (3) Via a cell-associated viremia in PBMC, EHV1 is transported to target organs such as the pregnant uterus (3.a) and the central nervous system (3.b), where it initiates a secondary replication in the endothelial cells lining the blood vessels of these organs.

3.1.4.1 Entry

Horses become infected with EHV1 via the upper respiratory tract after inhalation of virus-loaded aerosol droplets, originating from infectious secretions such as nasal discharge or from contaminated foetal or placental tissues. Although of minor importance, infectious aerosols can also be transmitted over a short distance through the air (Allen and Bryans, 1986; Patel *et al.*, 1982; Reed and Toribio, 2004). The exact distance EHV1 virions can travel through the air remains unclear so far. The virus gets into contact with the epithelia lining the nasal cavities, the nasal septum, the turbinates, the nasopharynx and the trachea. EHV1 infects these epithelial cells in a plaque-wise manner, thereby causing cell destruction and shed of infectious progeny virus particles into nasal secretions (Gryspeerd *et al.*, 2010; Van Maanen, 2002). EHV1 single infected cells and plaques can be observed starting from 12 hours post-inoculation (pi) and 24 hours pi (hpi), respectively (Gryspeerd *et al.*, 2010; Vandekerckhove *et al.*, 2010). Nasal shedding of EHV1 can be detected starting from 1 day pi up until 14 days pi (Edington *et al.*, 1986; Gibson *et al.*, 1992; Gryspeerd *et al.*, 2010).

Destruction of the epithelial cells and local inflammation results, after an incubation period of 2 to 10 days, in mild clinical symptoms, such as serous nasal discharge, coughing, mild pyrexia, anorexia and depression (Allen and Bryans, 1986; Patel *et al.*, 1982). Most EHV1 infections are self-limiting and accompanying respiratory symptoms disappear 9 to 12 days pi (Gibson *et al.*, 1992). However, epithelial cell destruction might facilitate bacterial colonization. Secondary bacterial infections aggravate and prolong respiratory symptoms, resulting in the shed of mucopurulent discharge, severe coughing and severe pyrexia (McGavin and Zachary, 2007).

3.1.4.2 Viremia

During replication in the respiratory epithelium, EHV1 attracts and infects diapeding leukocytes, enabling the virus to cross the basement membrane (Vandekerckhove *et al.*, 2011; Zhao *et al.*, 2017). This strategy is in contrast with other alphaherpesviruses (e.g. HSV1, PRV, BoHV1), which spread in a plaque-wise manner across the basement membrane by directly infecting the underlying fibroblasts (Glorieux *et al.*, 2011a; Glorieux *et al.*, 2007; Steukers *et al.*, 2012). EHV1-infected leukocytes then carry the virus either directly into the bloodstream or along the lymph vessels towards the draining lymph nodes. EHV1 has been detected in the submandibular, retropharyngeal and bronchial lymph nodes upon experimental inoculation. Here, EHV1 infection is amplified in even more leukocytes, which then take the virus into the blood circulation via the efferent lymph (Kydd *et al.*, 1994).

Viremia can be detected starting from 1 day pi until 14 days pi, and peaks between day 4 and 10 pi (Gryspeerd *et al.*, 2010). *In vivo* infected leukocytes have been mainly identified as CD172a⁺ monocytic cells, followed by T lymphocytes and B lymphocytes (Gryspeerd *et al.*, 2010; Scott *et al.*, 1983). However, all PBMC subpopulations, including DCs, are susceptible to EHV1 *in vitro* (Siedek *et al.*, 1999; van der Meulen *et al.*, 2000). Interestingly, replication is restricted and the majority of these PBMC do not show late viral glycoproteins on their cell surface upon EHV1 infection, suggesting that the virus misuses these cells as ‘Trojan horses’ to disseminate into the host (Gryspeerd *et al.*, 2010; Laval *et al.*, 2015a; van der Meulen *et al.*, 2000).

Spread to the local lymph nodes and in the bloodstream leads to clinical symptoms consisting of lymph node swelling, moderate to severe temperature spiking, anorexia and depression (Allen and Bryans, 1986; Patel *et al.*, 1982).

3.1.4.3 Secondary replication

This cell-associated viremia enables the virus to reach secondary target organs, such as the pregnant uterus, the central nervous system and the conjunctiva (Kydd *et al.*, 1994). At the target organs, EHV1 initiates a secondary replication cycle in endothelial cells lining the blood vessels. Adhesion of EHV1-carrying leukocytes to the endothelium is a key step in transferring the virus from infected leukocytes to endothelial cells. EHV1 then switches its replication cycle back on and infects the target cell (Laval *et al.*, 2015b). Some of these adhesion molecules on CD172a⁺ monocytic cells have been identified as $\alpha_4\beta_1$ (VLA-4), $\alpha_L\beta_2$ (LFA-1), and $\alpha_v\beta_3$ integrins (Laval *et al.*, 2015b). On endothelial cells, intercellular adhesion molecule (ICAM), E-selectin and P-selectin were shown to be involved in the adherence of EHV1 infected leukocytes (Smith *et al.*, 2001). Adhesion of EHV1-infected leukocytes is favoured in the presence of TNF α and is dependent on both cellular kinases (PI(3)K and ERK/MAPK) and viral protein kinases (US3) (Laval *et al.*, 2015b; Spiesschaert *et al.*, 2015). Endothelial cells upregulate specific adhesion molecules in the environment of 17-oestradiol, equine chorionic gonadotropin (eCG), IL-2 or lipopolysaccharides (LPS) (Smith *et al.*, 2002)

Reproductive disorders

EHV1 replication in the endothelial cells of the pregnant uterus causes vasculitis and thrombosis, subsequently leading to avascular necrosis and oedema of the endometrium (Bryans and Prickett, 1970; Edington *et al.*, 1991; Prickett, 1970). Widespread endometrial vascular damage causes detachment of the foetal membranes and the foetus, thus leading to abortion of a virus negative foetus. Less extensive endometrial vascular damage allows EHV1

to invade the foetus through the utero-placental barrier (Edington *et al.*, 1991). Here, EHV1 replicates in the endothelial cells of the umbilical cord and the allantochorion, amongst other organs (Smith *et al.*, 1997; Smith *et al.*, 1993). Aborted EHV1-positive foeti typically show multiple lesions, including multifocal hepatic necrosis, subcutaneous oedema, pleural fluid accumulation, pulmonary oedema and splenic enlargement (Machida *et al.*, 1997).

EHV1-induced abortion typically occurs in the last trimester of pregnancy, although one case of abortion has been reported in the fourth month of gestation (Allen and Bryans, 1986; Prickett, 1970). Following infection or reactivation of EHV1 at late stage of gestation or at full term, a live EHV1-infected foal can be delivered. However, most of these foals show signs of weakness, jaundice and respiratory distress, due to infection of their inner organs. This condition is also known as neonatal foal disease and these foals usually die within 7 days (Murray *et al.*, 1998). This gestation phase-dependent manner of viral transfer has been a subject of investigation for several years. It has been suggested that the above-mentioned endothelial surface adhesion molecules are increasingly expressed at the end of gestation under the influence of cytokines (e.g. IL-2) and hormones (e.g. 17-oestradiol) (Smith *et al.*, 2002). In addition, the immune system of the mare is compromised at that time, due to high concentrations of cortisone, progesterone and oestrogens (Smith *et al.*, 1996).

The incubation period of abortion following viremia, arising from either a primary infection or a reactivation of latent virus, varies between 9 days and 4 months (Allen, 1999, 2002). Mares may experience respiratory symptoms and fever prior to abortion, but can also abort without showing any other clinical symptoms. The reproductive potential of the mare is usually not affected and the virus is rapidly cleared from the reproductive tract.

Central nervous system disorders

EHV1 can also replicate in vessel endothelia at the level of the central nervous system (Edington *et al.*, 1986). Endothelial damage subsequently leads to local inflammation, vasculitis, thrombosis and oedema in a similar manner as in the pregnant uterus. The lack of nutrients and oxygen and the elevated levels of inflammatory cytokines cause neurons to degenerate, eventually leading to equine herpes myeloencephalopathy (EHM) (Jackson and Kendrick, 1971; Wilson, 1997). Neurological symptoms go from ataxia to a complete fore and hind limb paralysis. Other clinical signs comprise faecal and/or urinary incontinence, head tilting, tail paralysis, distal limb oedema, oedema of testes, penis prolapse and even blindness (Borchers *et al.*, 2006; Gryspeerdt *et al.*, 2011; Jackson *et al.*, 1977; Maanen *et al.*, 2001).

Researchers and clinicians have tried to identify risk factors for the development of EHM. They found that the level of CTLs (low), gender (female), age (elder), breed (Standardbred), season

(late autumn, winter, spring) and type of EHV1 strain (neurovirulent) increase the risk of EHM development (Allen, 2008; Goehring *et al.*, 2006; Henninger *et al.*, 2007; Perkins *et al.*, 2009; Pusterla *et al.*, 2016). In fact, neurovirulent strains are more likely to cause central nervous system disorders, not due to the fact that they are neurotropic but because they initiate a higher and longer viremia (Allen and Breathnach, 2006).

The incubation period of EHM varies between 6 to 8 days (Jackson and Kendrick, 1971; Mumford *et al.*, 1994). The prognosis for non-recumbent horses is favourable, although full recovery can last up to several months. Recumbent horses usually develop fatal complications and require euthanasia.

3.1.4.4 Latency and reactivation

The hallmark of all herpesviruses is the establishment of lifelong latency in their host to ensure survival and spread of the virus within the natural host population (Grinde, 2013). Following primary EHV1 replication in the respiratory epithelium, the virus spreads to latency-inducible cells such as leukocytes and neurons. CD8⁺ T lymphocytes and neurons of the trigeminal ganglion were found to be the predominant site of EHV1 latency (Baxi *et al.*, 1995; Chesters *et al.*, 1997; Edington *et al.*, 1994; Slater *et al.*, 1994). Except for transcription of latency-associated transcripts, latent virus shuts down the transcription of its genome, allowing the virus to stay hidden from the host's immune surveillance (Roizmann *et al.*, 1992). During the latent phase, the viral genome is associated with de-acetylated and thus closed heterochromatin. Acetylation results in opening up of the chromatin, which in turn allows transcription of the viral DNA and initiation of the viral lytic cycle (Danaher *et al.*, 2005; Laval *et al.*, 2015a). Upon reactivation, weeks, months or even years after primary infection, EHV1 travels back to the upper respiratory tract. Spread to the upper respiratory tract can occur via infected leukocytes or via infected neurons through anterograde axonal transport. EHV1 initiates a new lytic replication in the respiratory epithelium, causing the horse to shed the virus to new potential hosts. In addition, another cell-associated viremia is initiated upon reactivation, elevating the risk for abortion or development of EHM. Reactivation of herpesviruses is typically associated with periods of stress (e.g. weaning, transport, surgery, heavy training or competitions) or with the administration of corticosteroids (Burrows and Goodridge, 1984; Edington *et al.*, 1985; Slater *et al.*, 1994).

3.1.5. Immune evasion mechanisms

As a herpesvirus, EHV1 is among the most ancient viruses and thus, experienced a long-term co-evolution with its host. As a result, the virus has evolved multiple strategies to overcome the host's immune system (Karlin *et al.*, 1994).

First, the virus **hampers expression of its late glycoproteins** gD, gC and to a lesser extent gB and gM in infected leukocytes (Gryspeerd *et al.*, 2012; Laval *et al.*, 2015a; van der Meulen *et al.*, 2006; van der Meulen *et al.*, 2003). As a result, exposure of viral proteins at the plasma membrane is declined and an infected cell is protected from antibody-dependent cell lysis. Most of the studies addressing this phenomenon were performed with an abortigenic/non-neurovirulent strain (97P70). Although Gryspeerd *et al.* (2012) did not observe a significant difference in glycoprotein suppression in PBMC infected with abortigenic (97P70) or neurovirulent strains (03P37), a clear distinction between the two subtypes was found in infected CD172a⁺ cells a few years later (Laval *et al.*, 2015a; Laval *et al.*, 2017). Interestingly, abortigenic EHV1 (97P70) is able to delay its replication in CD172a⁺ monocytic cells by epigenetic silencing of its gene expression through the activity of histone deacetylases (Laval *et al.*, 2015a). Conversely, neurovirulent strains (95P105 and 03P37) only showed a restriction of infection, but no association with histone deacetylase activity and no subsequent delay in gene and protein expression (Laval *et al.*, 2017). These findings are in line with a previous *in vivo* study, where 3-7 times more PBMC expressing late viral glycoproteins were found in the lamina propria of infected animals upon inoculation with the neurovirulent strain compared to the non-neurovirulent strain (Gryspeerd *et al.*, 2010). These results indicate that besides the single nucleotide polymorphism, more differences exist between neurovirulent and non-neurovirulent strains.

Complement-mediated cell lysis is additionally suppressed by EHV1 **gC binding to C3**, a key component in mounting the alternative complement cascade pathway (van der Meulen *et al.*, 2003).

Next, EHV1 is able to **downregulate MHC I cell surface expression** in equine cells (Ambagala *et al.*, 2004; Rappocciolo *et al.*, 2003). MHC I presents viral peptides, arising from the proteasome and the 'transporter associated with antigen processing' (TAP). This MHC I-mediated antigen presentation is required for CTLs to recognize and lyse infected cells. The latter immune evasion mechanism has been a topic of interest over the past years and studies showed that one of the IEP or EP (e.g. pUL43 and pUL56) is responsible for endocytosis of MHC I molecules (Huang *et al.*, 2014; Ma *et al.*, 2012; Rappocciolo *et al.*, 2003). In addition,

EHV1 glycoprotein N inhibits viral protein loading onto MHC I molecules by preventing ATP binding to TAP (Koppers-Lalic *et al.*, 2008). Cells with reduced MHC I expression at the plasma membrane are normally recognized and cleared by host NK cells. EHV1 may affect MHC I expression in an allele-specific manner, thereby leaving a small amount of MHC I present on the plasma membrane, which may enable the virus to evade NK-activated lysis of infected cells (Rappocciolo *et al.*, 2003).

The onset of a strong immune response is additionally avoided by **inhibition of interferon and a broad range of chemokines** (Sarkar *et al.*, 2015; von Einem *et al.*, 2007). More precisely, EHV1 has been shown to modulate the onset of antiviral type I interferon production in endothelial cells (Sarkar *et al.*, 2015). In addition, EHV1 glycoprotein gG acts as a chemokine-binding protein and effectively blocks chemokines such as CCL3, CXCL1 and IL-8 (Bryant *et al.*, 2003; Van de Walle *et al.*, 2007; Van de Walle *et al.*, 2008b). These chemokines play a crucial role in mounting the inflammatory immune response to clear the infection.

Finally, direct **cell-to-cell spread** is another major strategy for EHV1 to bypass the hostile extracellular environment, containing phagocytes, antibodies and complement (van der Meulen *et al.*, 2002). Cell-to-cell spread in the respiratory epithelium rapidly induces virus plaque formation and ensures the production of virion progeny in nasal secretions. In addition, this mode of transfer is key for the virus to spread from infected leukocytes to local endothelial cells in the presence of neutralizing antibodies (Goehring *et al.*, 2011; Smith *et al.*, 2001).

3.1.6. Concluding remarks

Over years of co-evolution with the horse, EHV1 has mastered various strategies to persist in an immunocompetent host population. The virus is ubiquitous and an important pathogen in the horse population and therefore has raised a lot of interest by owners, veterinarians, as well as researchers. This led to the discovery of a number of immune-evasive, survival and spreading mechanisms of EHV1, as described above. Despite all the knowledge that has been gathered on EHV1, no fully effective vaccine or antiviral therapy could be developed yet. Therefore, further research into the pathogenesis of EHV1 is urgently needed, starting with its primary replication in the respiratory tract.

3.2. Equine herpesvirus type 5

3.2.1. Introduction

Equine herpesvirus type 5 (EHV5) is a ubiquitous, yet obscure pathogen in the horse population. Although probably more than 80% of all horses carry the virus latently, only a slight amount of them develop fatal equine multimodal pulmonary fibrosis (EMPF) (Marenzoni *et al.*, 2010; Williams *et al.*, 2007). So far, the exact pathogenic role played by EHV5 in EMPF is unknown. The virus may be an etiologic agent or cofactor in the development of EMPF (Williams *et al.*, 2013; Wong *et al.*, 2008).

EHV5 is classified as a member of the family *Herpesviridae*, subfamily *Gammaherpesvirinae*, genus *Percavirus*. EHV5 shares this classification with equine herpesvirus type 2 (EHV2) and mustelid herpesvirus type 1 (MusHV1). The virus is closely related to other equine gammaherpesviruses such as EHV2 and EHV7 (asinine herpesvirus type 2), as well as to herpesviruses from other species, such as Epstein-barr virus (EBV), human herpesvirus type 8 (HHV8 or Kaposi's sarcoma-associated herpesvirus), bovine herpesvirus type 4 (BoHV4) and murid herpesvirus type 4 (MuHV4) (Davison *et al.*, 2009). EHV5 and EHV2 have previously been described as one and the same equine cytomegalovirus (subfamily *Betaherpesvirinae*), due to their similar slow cytopathic effect in cell cultures. Only in 1987, a distinction between EHV2 and EHV5 was made and it took another 6 years before they were reclassified to the subfamily *Gammaherpesvirinae* (Browning and Studdert, 1987; Roizman and Baines, 1991; Telford *et al.*, 1993). Consequently, it is unclear whether the findings in most studies before 1988 refer to EHV2 or EHV5.

The initial isolates of EHV5 were obtained in Australia from horses with upper respiratory tract disease (Turner and Studdert, 1970; Wilks and Studdert, 1974). In the meantime, EHV5 has been detected in nasal swabs and PBMC of horses with and without clinical symptoms all over the world (Akkutay *et al.*, 2014; Bell *et al.*, 2006b; Dunowska *et al.*, 1999; Dynon *et al.*, 2001; Hue *et al.*, 2014; Wang *et al.*, 2007). Remarkably, EHV5 isolates from different horses, housed in the same premise or region, showed a vast heterogeneity in their gB genes, showing that multiple genotypes are circulating in the field (Back *et al.*, 2016; Dunowska *et al.*, 2000). Some horses were even infected with two or more strains from different genotypes, suggesting that host-virus interactions influence the viability of different strains.

3.2.2. *Viral structure*

EHV5 is structurally built up from a dsDNA molecule with a length of 179 kbp, surrounded by a capsid, tegument proteins and an outer bilipidic envelope. At least one major and five minor glycoproteins, including glycoproteins B, H, L and M, are embedded in the viral envelope (Agius *et al.*, 1994; Agius *et al.*, 1992).

3.2.3. *Pathogenesis and accompanying clinical symptoms*

Little is known about the pathogenesis of EHV5 and many statements remain speculative. A lot of information is deduced from its sister virus EHV2 but cannot automatically be assumed for EHV5.

Infectious virus is frequently recovered from nasal fluids, suggesting that the virus uses the respiratory tract as a port of exit and entry. Although other gammaherpesviruses, e.g. HHV8, BoHV4 and MuHV4, commonly spread through sexual contact or intrauterine transmission, presence of EHV5 in the equine reproductive tract has not been reported yet (Davison, 2011; Donofrio *et al.*, 2007; François *et al.*, 2013). Upon entry, EHV5 infects leukocytes originating from either the lymphoid nodules or single patrolling cells within the MALT. *In vivo*, viral DNA was predominantly found in equine blood B lymphocytes and T lymphocytes and to a lesser extent in monocytes (Bell *et al.*, 2006a; Mekuria *et al.*, 2017). Alveolar macrophages were also found to harbour the virus. However, whether this observation was due to an actual viral infection or whether it was merely a consequence of phagocytosis is speculative (Williams *et al.*, 2007). The virus presumably uses these PBMC populations to establish latency inside its host and to persist in the horse population (Mekuria *et al.*, 2017).

How exactly the virus escapes from leukocytes and transmits to new potential hosts is currently unknown. As for Epstein Barr virus (EBV), latently infected leukocytes might reroute from the blood circulation or secondary lymphoid tissues, e.g. tonsils, to the respiratory tract and either transfer infectious virus to local epithelial cells, which then amplify the infection, or directly shed new virus into respiratory secretions (Shannon-Lowe and Rowe, 2011).

The most dreadful complication of an EHV5 infection in horses is the development of progressive nodular fibrotic lung disease, also known as equine multinodular pulmonary fibrosis (EMPF). The clinical appearance of an EMPF-affected horse is shown in Figure 9. The precise causes of such condition and the role of EHV5 herein are rarely identified (Williams *et al.*, 2007). EMPF is characterized by the presence of multiple fibrotic nodules throughout the lungs. Histologically, marked interstitial fibrosis with an 'alveolar-like' architecture, lined by cuboidal epithelial cells and thickening of the alveolar walls is visible. In the alveoli, few

intraluminal alveolar macrophages contain intranuclear viral inclusion bodies, positive for EHV5 DNA (Poth *et al.*, 2009; Williams *et al.*, 2007; Wong *et al.*, 2008). Interstitial lesions are most often infiltrated by lymphocytes, plasma cells and neutrophils, and to a lesser extent by mast cells and eosinophils (Poth *et al.*, 2009). The high correlation between the presence of EMPF and EHV5 DNA suggests that the virus is a causative agent of lung fibrosis. This is corroborated with the findings of a study on MuHV4, where the virus induces lung fibrosis in mice with a progressive deposition of interstitial collagen, increased transforming growth factor β and T helper 2 cytokine expression and hyperplasia of type II pneumocytes (Mora *et al.*, 2005). In addition, Williams *et al.* (2013) were able to experimentally induce lung fibrosis in horses upon direct delivery of virulent EHV5 strains into the lungs. However, the choice of viral strain, experimental animals and inoculation route may have favoured the outcome of disease. Moreover, a lot of clinically healthy animals carry the virus their entire life-span and never develop any signs of EMPF. Thus, other predisposing conditions besides EHV5 must be present in order to trigger disease.

The clinical signs associated with EHV5 infection or reactivation are not well defined and include nasal discharge, tachypnea coughing, fever, pharyngitis, enlarged lymph nodes, anorexia, poor body condition and depression (Dunowska *et al.*, 2002; Franchini *et al.*, 1997; Hart *et al.*, 2008; Wong *et al.*, 2008). EMPF progressively worsens as horses age and eventually forces veterinarians to euthanize the horse.

One study reported the presence of EHV5 inclusion bodies in a dermatitis lesion rostrally to the left eye of a horse, which was suggested to resemble herpes-associated erythema multiform in humans (Herder *et al.*, 2012).

3.2.4. Concluding remarks

Severe clinical symptoms of EHV5 infection are only rarely encountered, as EHV5, like many other gammaherpesviruses, is optimally adapted to its natural host. Further investigation of this virus-host relationship during infection should help in elucidating the mechanisms regulating disease and triggering the development of EMPF. Future studies on EHV5 should trace back roots and elucidate the pathogenesis of the virus. Representative *in vitro* and/or *ex vivo* models would be very helpful to study primary infection, induction of latency and reactivation and finally, mimic the onset of EMPF.

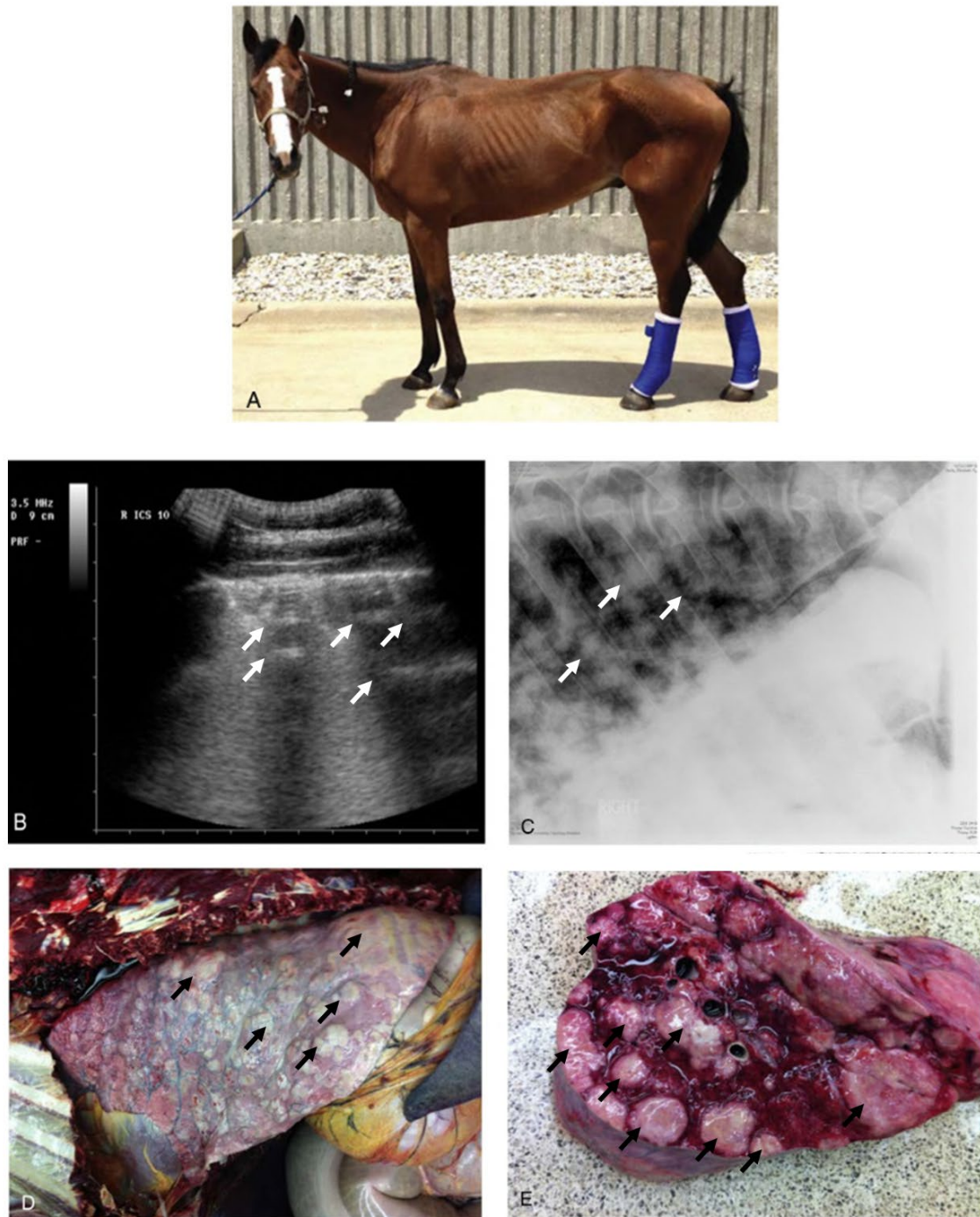


Figure 9. Clinical case of equine multinodular pulmonary fibrosis (EMPF), from Rush and Mair (2008). (A) A 15-year-old Thoroughbred gelding presenting for weight loss and poor appetite was diagnosed with EHV5-associated EMPF. (B) Thoracic ultrasound revealed multiple peripherally located nodular lesions (arrows). (C) Thoracic radiographs confirmed the presence of a diffuse nodular interstitial radiographic pattern (arrows). (D) Failure to respond to therapy necessitated euthanasia, which revealed gross pulmonary changes consistent with EMPF. Arrows point at fibrotic nodules. (E) Cross section of EMPF lesions. Arrows point at fibrotic nodules.

3.3. Equine influenza virus

3.3.1. Introduction

Equine influenza virus (EIV) is a highly contagious virus, capable of causing explosive, yet self-limiting outbreaks of respiratory disease in naive horse populations. The viral capacity to cause epidemics, together with the global transportation of horses has led to the spread of EIV all over the world, except for geographically isolated countries, such as New Zealand and Iceland (Burrows *et al.*, 1982; Cowled *et al.*, 2009; Gerber, 1970; Klingeborn *et al.*, 1980; Powell *et al.*, 1995; Virmani *et al.*, 2010). These outbreaks have a significant economic impact on the equine industry due to loss of performance and time out of work. Despite numerous studies on different mammalian influenza viruses and the development of vaccines, EIV still circulates in the field. Naïve horses infected with EIV typically display a distinctive harsh and dry cough, together with nasal discharge, anorexia, depression and high fever (Gerber, 1970). EIV is a member of the family *Orthomyxoviridae*, genus *Influenza A/B*, species influenza A virus. Influenza A viruses can be further divided into subtypes, differing in hemagglutinin (H1-H14) and/or neuraminidase (N1-N9). Although various combinations of H_xN_x subtypes have been described in birds and other mammals, only H7N7 and H3N8 subtypes have been reported in equine species to date.

EIV was diagnosed and isolated for the first time in 1956 in Prague, during a widespread epidemic of respiratory disease among horses in Eastern Europe (A/equine/1/Prague/56). This EIV strain was characterized as H7N7 and was classified as equine 1 subtype (A/equine 1) (Sovinova *et al.*, 1958). Since the latter subtype has not been isolated since 1979, it is currently of less or even no importance (Webster, 1993). A few years after the first outbreak in Eastern Europe, a second major epidemic occurred in Miami, USA. Here, an EIV of the subtype H3N8 was recovered (A/equine/1Miami/63) and was classified as equine 2 subtype (A/equine 2) (Waddell, 1963). Viruses of the H3N8 subtype evolved into two distinct evolutionary lineages, American and Eurasian. Further genetic divergence of the American lineages resulted in the formation of three American-like sublineages (South American, Kentucky and Florida). Eurasian lineage viruses have not been isolated since 2005 and are therefore considered as unimportant at present (Elton and Cullinane, 2013).

3.3.2. *Viral structure*

The general structure of an EIV virion is represented in Figure 10. The EIV genome has a total size of 13.6 kbp, which is divided over eight negative-sense ssRNA segments and encodes at least 10 polypeptides (Skehel and Schild, 1971). These RNA strands are coated by a ribonucleoprotein (NP), which in turn is associated with three RNA polymerase proteins (PB1, PB2 and PA). All segments are enclosed by a layer of matrix proteins M1 and a lipid bilayer, through which two main viral molecules project: hemagglutinin (H) and neuraminidase (N). H is used by the virus to bind to susceptible host cells and is considered to be the major antigen against which neutralizing antibodies are generated. N exhibits hydrolytic/proteolytic activities and thus enables the virus to detach from sugar residues during virus release from infected cells and viral transport through the mucus (Saito *et al.*, 1993; Yang *et al.*, 2014).

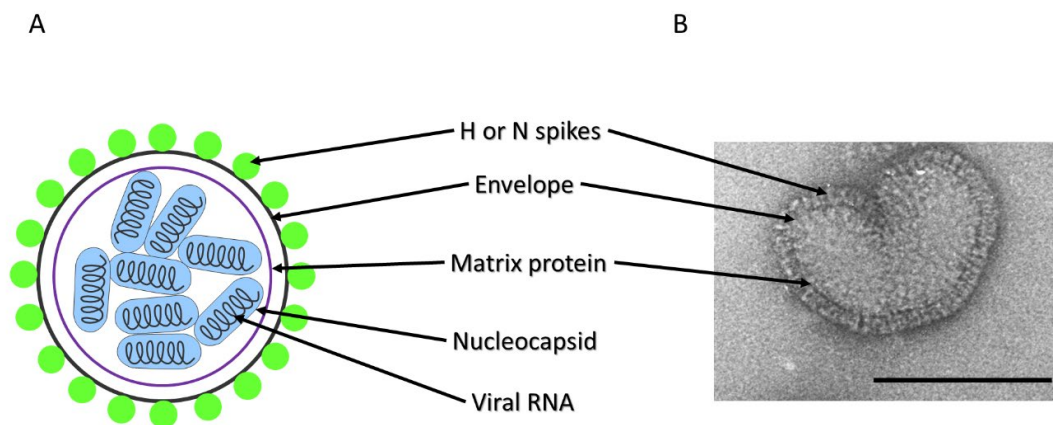


Figure 10. Structure of an EIV virion. (A) Schematic representation. Drawing is based on Motifolio art template. (B) Transmission electron microscopic image. Image courtesy of EMBL-UVHCI. The scale bar represents 50 nm.

The RNA-based genome, present in different segments, confers influenza viruses with the capacity for rapid evolution. As viral RNA-dependent RNA polymerases lack proofreading mechanisms, genetic point mutations often occur and allow a fast antigenic change if they affect surface proteins H and/or N. In addition, genetic recombination of nucleocapsid segments can occur in cells simultaneously infected with different influenza strains. However, to date, there is no evidence that EIV participated in genetic recombination and antigenic changes in EIV are only minor, compared to human and swine influenza viruses (Kawaoka *et al.*, 1989; Landolt, 2014; Webster *et al.*, 1992). Nonetheless, genetic and antigenic change in EIV allowed the virus so far to survive in the horse population.

3.3.3. *Replication cycle*

Infection of the host cell with EIV is initiated when viral H adsorbs to cellular glycoprotein receptors whose oligosaccharide side chains terminate in sialic acid (SA). Equine respiratory epithelial cells predominantly express non-human N-glycolylneuraminic acid (Neu5Gc) α 2,3-galactose linked residues, which are the preferential binding site of EIV (Daly *et al.*, 2008; Suzuki *et al.*, 2000; Yamanaka *et al.*, 2010). The virus enters permissive cells through endocytosis, which allows a conformational change in H to occur at pH 5.0, essential for membrane fusion and subsequent release of the nucleocapsids within the cytoplasm. EIV nucleocapsids migrate to the nucleus, where viral mRNA is transcribed by the use of its own nucleoprotein and viral polymerase proteins. Following viral protein synthesis, the RNA segments are incorporated into new virions, which finally mature by budding from the apical surface of the cell (Studdert, 1996). During virus release, viral H sticks to cellular surface SA and progeny virus particles must cleave this binding by viral N. Remarkably, EIV N substrate specificity (N-acetylneuraminic acid or Neu5Ac) is in disagreement with the virus binding specificity (Neu5Gc) (Takahashi *et al.*, 2016). This suggests that viral N is predominantly of importance during viral transport through the mucus towards the cell. More precisely, viral N cleaves off mucus-associated Neu5Ac SA, allowing fast migration of virus particles and leaves Neu5Gc intact, essential for viral binding and entry. The replication cycle of influenza is usually completed within 6 h (Frensing *et al.*, 2016).

3.3.4. *Pathogenesis and accompanying clinical symptoms*

Horses become infected with EIV through inhalation of aerosolized EIV particles, originating from the air, nose-nose contacts or fomites. The virus is then embedded in the respiratory mucus, but with the help of viral N rapidly drills its way towards susceptible epithelial cells (Myers and Wilson, 2006; Yang *et al.*, 2014). EIV efficiently replicates in the respiratory epithelium (Lin *et al.*, 2002). Progeny virus particles then travel along with the mucociliary escalator and re-infect new epithelial cells. A fast replication cycle and the fact that its binding receptor is readily available on the cell surface allows EIV to replicate in an explosive way within the respiratory tract (Gerber, 1970). Viral replication is accompanied by the loss of respiratory epithelial cells and their associated cilia. Reduced mucociliary clearance enables the virus to disperse towards the bronchial tree, where more virus particles replicate and cause necrosis and desquamation of respiratory epithelial cells. These pathologies cause a distinctive harsh and dry cough, nasal discharge, pyrexia and depression in the infected horse, usually within 48 hpi (Willoughby *et al.*, 1992). At this time point, horses also start to shed new virus

particles in nasal fluids. Symptoms usually last less than a week but might persevere upon secondary bacterial infection. The horse's local and systemic antibody- and cell-mediated immune responses rapidly clear the virus from the respiratory tract and protect them from re-infection with the same strain (Hannant and Mumford, 1989; Kumanomido and Akiyama, 1975). Complete recovery of epithelial damage takes a minimum of three weeks, during which horses should be rested.

Viremia is rare but possible if the virus breaches the basement membrane and disseminates in the bloodstream. Secondary replication potentially causes inflammation of skeletal and cardiac muscles (myositis and myocarditis), encephalitic signs and limb oedema (Wilson, 1993).

3.3.5. Concluding remarks

Despite the availability of (semi-)efficacious vaccines, EIV still cannot be fully controlled and remains an important respiratory pathogen among horses. This can be attributed to the fact that inactivated vaccines only elicit a systemic humoral, but no local or cellular immunity and that influenza viruses continuously evolve (genetically and antigenically). Several recent EIV outbreaks, some of which occurred in vaccinated horses, clearly highlight the need for constant surveillance, periodic updating of vaccines and further research (Beuttemüller *et al.*, 2016; Martella *et al.*, 2007; Yamanaka *et al.*, 2008).

3.4. Equine arteritis virus

3.4.1. Introduction

Equine arteritis virus (EAV) causes equine viral arteritis (EVA), a respiratory and reproductive disease of equids. EAV belongs to the genus *Arterivirus*, family *Arteriviridae* and order *Nidovirales*. The virus shares this taxonomy with porcine reproductive and respiratory syndrome virus (PRRSV), simian hemorrhagic fever virus (SHFV) and lactate dehydrogenase-elevating virus (LDV) of mice (Cavanagh, 1997).

EAV was first isolated from an outbreak of respiratory disease and abortion on a Standardbred breeding farm near Bucyrus, Ohio, USA, in 1953 (Bryans *et al.*, 1957). As the virus was associated with distinctive vascular lesions leading to arteritis, it was designated 'equine arteritis virus'. A decade later, the first important EAV outbreak in Europe was reported in Bern, Switzerland (Burki and Gerber, 1966). Since then, EAV outbreaks were occasionally reported all over the world and recently drastically increased due to globalisation of horse and semen transport (Echeverria *et al.*, 2003; Eichhorn *et al.*, 1995; Gryspeerdt *et al.*, 2009; Holyoak

et al., 2008; Larsen *et al.*, 2001; Monreal *et al.*, 1995; Timoney, 1984; van der Meulen *et al.*, 2001; Wood *et al.*, 1995). Serological surveys confirmed that EAV is distributed worldwide, except for Iceland, Japan and New Zealand. However, the seroprevalence of EAV in horse populations varies markedly among different countries and different horse breeds, ranging from 0.5% to 93% (Holyoak *et al.*, 2008; Hullinger *et al.*, 2001; Newton *et al.*, 1999).

The majority of EAV infections are asymptomatic but occasionally, horses develop clinical signs such as nasal discharge, conjunctivitis, depression, pyrexia, limb and ventral oedema. In addition, pregnant mares may abort due to foetal infection and in-utero or neonatally infected foals most often die of bronchopneumonia or enteritis (Timoney and McCollum, 1987, 1993). The hallmark of EAV is its unique strategy to establish a persistent infection in the reproductive tract of stallions, which in turn functions as a ‘viral reservoir’. Herein, EAV is harboured between breeding seasons and genetic diversification of the virus occurs, enabling the virus to survive in the host population.

3.4.2. Viral structure

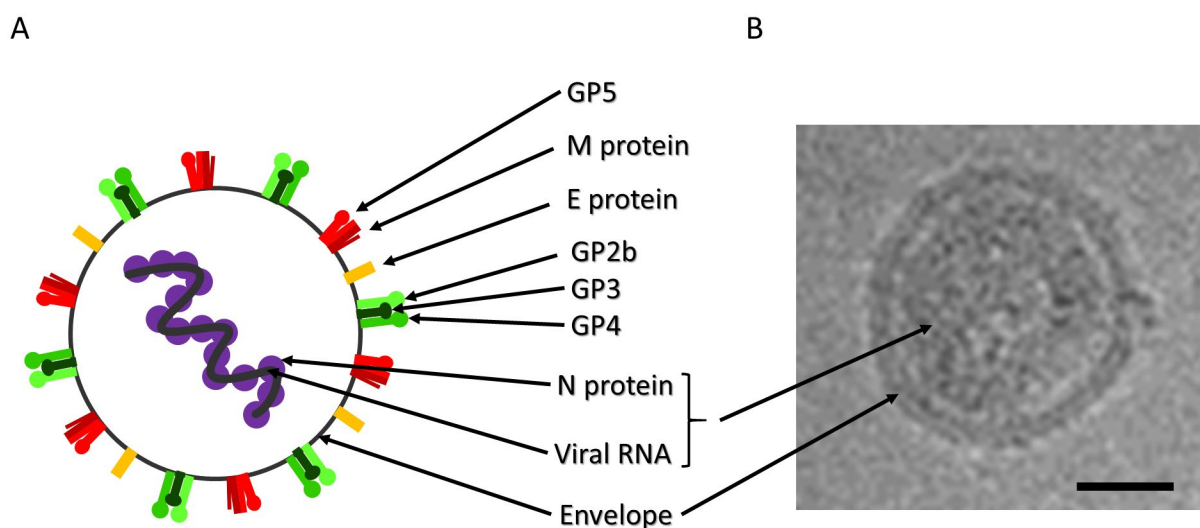


Figure 11. (A) Schematic structure of an EAV virion. (B) Electron microscopy picture of a PRRSV virion, a close relative of EAV, from Spilman *et al.* (2009). The scale bar measures 25 nm.

The general structure of an EAV virion is represented in Figure 11. The genome of EAV consists of a 12.7 kbp positive-sense ssRNA molecule and is surrounded by nucleocapsid proteins. The genome with nucleocapsid proteins is enclosed by a lipid bilayer envelope, embedded with up to six (glyco)proteins, two major envelope proteins that heterodimerize (M and GP5 protein) and four minor envelope proteins (E, GP2b, GP3 and GP4) of which the last three form a heterotrimer (De Vries *et al.*, 1992; Wieringa *et al.*, 2002; Wieringa *et al.*, 2003). *In vitro*, the replication cycle of EAV is usually completed within 6 h (Moore *et al.*, 2002).

3.4.3. Pathogenesis and accompanying clinical symptoms

Horses can become infected with EAV via either aerosol spread (respiratory route), sexual transmission (venereal route) or vertical spread (trans-placental route). Inhalation of EAV particles originating from virus-positive nasal fluids, urine, faeces, placental fluids, aborted foetuses, vaginal fluids or fomites disperses the virus over the respiratory mucosa of the complete respiratory tract, including the tonsils. Copulation or insemination with contaminated semen deposits EAV particles onto the vaginal mucosa or endometrium. In the respiratory or reproductive tract, the virus infects diapeding leukocytes, originating from the local and/or diffuse MALT (Timoney and McCollum, 1993). Susceptible PBMC populations were identified as pulmonary macrophages, CD172a⁺ monocytic cells, CD3⁺ T lymphocytes and to a lesser extent IgM⁺ B lymphocytes (Vairo *et al.*, 2013). Infected leukocytes travel through submucosa-associated capillaries, to which they transfer infectious virus, or through the draining lymph nodes into the bloodstream. Replication in the respiratory tract is accompanied by respiratory symptoms (e.g. nasal discharge), lymph node swelling, depression and fever (Timoney and McCollum, 1993; Vairo *et al.*, 2012).

Cell-free and cell-associated viremia is detectable starting from 1 dpi and the cell-associated viremia can last up to several weeks (MacLachlan *et al.*, 1996; Neu *et al.*, 1988; Vairo *et al.*, 2012). The virus then systemically spreads to the lymphoid tissues and capillaries of various organs, including the subcutis, the liver, the conjunctiva, the respiratory, intestinal, reproductive and urinary tract (McCollum *et al.*, 1971; Timoney and McCollum, 1993; Vairo *et al.*, 2012). In these target organs, EAV infects local leukocytes, endothelial cells and myocytes, which results in vasculitis with local inflammation, fluid exudation, thrombosis and ischemia of local tissues. Subsequently, these pathologies typically lead to oedema, urticaria, lacrimal and nasal discharge, stiffness and fever. Viral spread to the placenta and foetus during the first months of gestation will result in abortion, due to endometrial and placental vascular damage but mostly due to foetal infection (Del Piero, 2000; Timoney and McCollum, 1993). When mares become infected at the end of gestation, foetal infection occurs but does not result in abortion. However, these foals most often die after delivery due to extensive respiratory and/or intestinal damage (Piero *et al.*, 1997).

Spread to and replication in the respiratory, reproductive and urinary tract, which follow a respiratory infection, but also venereal transmission, is key for viral spread to new hosts.

Horses usually recover within 3 weeks pi and by that time, the virus is cleared from all organs, except for the reproductive tract of some stallions. Here, EAV may cause a persistent infection

and thereby induce a carrier state in its host, essential for virus survival over longer periods (Neu *et al.*, 1988; Timoney and McCollum, 1993).

3.4.4. Concluding remarks

Although EAV has no direct epithelial cell tropism in the respiratory tract, it is one of the most important viruses causing respiratory disease in horses. Moreover, the virus's ability to establish a natural reservoir in stallions allowed viral genetic evolution and maintenance within the horse population. Although vaccines are available, they lack the ability to clear these carrier stallions from persistent infection. Therefore, prevention procedures (e.g. serosurveillance and semen testing) and further research are of major importance in the control of EAV.

3.5. Bacteria

3.5.1. *Streptococcus equi*

Streptococci are the most important respiratory bacterial pathogens of the horse and are the major etiological agents of strangles and (broncho)pneumonia, either as single infections or mixed infections with other pathogens.

Streptococcus equi subspecies *equi* (*S. e. equi*) is a virulent Gram-positive, β -haemolytic bacterium belonging to the antigenic Lancefield C group and most likely evolved from the closely related commensal *Streptococcus equi* subspecies *zooepidemicus* (*S. e. zooepidemicus*) (Chanter *et al.*, 1997). Both subtypes belong to the family *Streptococcaceae*, order *Lactobacillales*.

The streptococcal cell wall consists of a lipid bilayer cell membrane, surrounded by a cell wall consisting of peptidoglycan and teichoic acid and an outer capsule of hyaluronic acids. Since hyaluronic acid is a polysaccharide found in mammalian tissues, it is not recognized as foreign by the horse and is thus not opsonized (Anzai *et al.*, 1999). A variety of surface proteins form fibrillary structures that project into the environment and are responsible for adherence, immune evasion and other, yet unknown, functions. In addition, streptococci secrete a variety of proteins, referred to as exotoxins, that are cytolytic to host cells including respiratory epithelial cells and leukocytes (Boyle *et al.*, 2018).

Horses acquire strangles via the oral or nasal uptake of *S. e. equi*-contaminated droplets, originating from other horses or fomites. These bacteria then adhere to the epithelial cells of the upper respiratory tract, including the tonsillar epithelium of the oro- and nasopharynx, before colonizing the draining lymph nodes, including the submandibular, parotid,

retropharyngeal, and cervical lymph nodes (Timoney and Kumar, 2008). As these bacteria are not well recognized by the host's immune system, their continued survival within the lymph nodes drives further recruitment of neutrophils and eventually abscess formation. Strangles is accompanied by unambiguous clinical symptoms: high fever, purulent nasal discharge, lymph node swelling and abscessation, which might drain externally or internally into the respiratory tract or the guttural pouches (Judy *et al.*, 1999; Timoney, 1993).

Release of bacteria from the efferent lymph into the bloodstream results in systemic bacterial dissemination, with potential metastatic abscessation. The presence of bacterial antigens in the systemic circulation might also trigger the development of 'purpura hemorrhagica', a severe immune complex-mediated vasculitis resulting in systemic oedema, petechiae, ecchymotic hemorrhages and skin lesions. The exact pathogenesis of this disease is not fully understood (Pusterla *et al.*, 2003).

Unlike *S. e. equi*, *S. e. zooepidemicus* belongs to the residential microbial community of the horse's upper respiratory tract. This opportunistic bacterium does not usually cause respiratory disease, unless the horse's mucosal immunity and/or mucociliary escalator is suppressed and/or the respiratory epithelium is damaged. Events leading to such conditions are for example stress, long-distance transports where the horse's head is tied in an upright position, poor hygiene conditions, anaesthesia and primary viral infections. These bacteria then colonize the respiratory tract and thereby cause bronchitis and pneumonia. Affected horses show pyrexia, depression, coughing, variable mucopurulent nasal discharge and tachypnea or dyspnea (Slater, 2007). Finally, people should take preventive hygienic measurements when handling *S. e. zooepidemicus*-infected horses, as this zoonotic pathogen can cause severe infections in humans upon transmission (e.g. septicaemia, meningitis, polysynovitis and abscessations) (Pelkonen *et al.*, 2013).

3.5.2. *Rhodococcus equi*

Rhodococcus equi (*R. equi*) normally resides within the environment (soil and faeces) and the intestinal tract of adult horses, but can cause a severe pyogranulomatous pneumonia upon inhalation by foals 3 weeks to 6 months of age.

The ubiquitous Gram-positive bacterium belongs to the genus *Rhodococcus*, family *Nocardiaceae*, order *Actinomycetale* and shares this order with other pathogenic organisms such as *Mycobacterium*, *Corynebacterium* and *Nocardia* (Gürtler and Seviour, 2010). All these bacteria are characterized by a layer of mycolic acids within the inner lipid-rich cell envelope, which anchors to the outer peptidoglycan-arabinogalactan cell wall. This distinct layer is

thought to be of significant clinical importance, because it protects bacteria from external aggressions, either from the environment or from the host (e.g. phagocytosis) (Sutcliffe *et al.*, 2010). In addition, virulent strains carry a large virulence plasmid which confers them the ability to survive and replicate within macrophages (Letek *et al.*, 2008).

Inhalation of dust particles containing virulent *R. equi* is the major route of infection in foals. The bacterium then colonizes the respiratory tract and infects monocytes/macrophages. Due to extensive bacterial replication and the inability to clear infection, host cells die and release a vast amount of cytokines and chemokines. These are not only responsible for pulmonary damage, but also attract more immune cells and induce the formation of pyogranulomas (Hines, 2007; Sutcliffe *et al.*, 2010). Migration of infected cells to the lymph nodes might eventually disseminate the bacteria to the circulation. This pyogranulomatous bronchopneumonia with abscessation and suppurative lymphadenitis results in clinical symptoms such as fever, tachypnea or dyspnea, coughing, depression, anorexia and variable mucopurulent nasal discharge (Chaffin *et al.*, 2011).

Systemic spread of bacteria and subsequent replication of bacteria in extrapulmonary sites or immune-mediated disorders might result in non-septic polysynovitis (immune-mediated), haemolytic anemia or thrombocytopenia (immune-mediated), polyarthritis or osteomyelitis and metastatic abscessations in other organs or the subcutis (Reuss *et al.*, 2009).

Finally, ingestion of environmental or mucociliary-conveyed contaminated sputum delivers the bacteria to the foal's intestinal tract. Although rare, *R. equi* can cause enterocolitis, typhlitis, abdominal abscesses and peritonitis in these foals, which is often accompanied with colic or diarrhea (Zink *et al.*, 1986).

3.5.3. *Staphylococcus aureus*

Another commensal, yet often opportunistic bacterium of the horse is *Staphylococcus aureus* (*S. aureus*). As it accounts for the vast majority of staphylococcal infections and it tends to acquire resistance against antimicrobials, *S. aureus* (e.g. the methicillin-resistant *Staphylococcus aureus* or MRSA) is the most notorious bacterium within the species *Staphylococcus* (Sieber *et al.*, 2011).

S. aureus is a Gram-positive, coagulase-positive bacillus, belonging to the genus *Staphylococcus*, family *Staphylococcaceae* and order Bacillales. Cytoplasmic material is enclosed by a lipid cell membrane and protected by an outer cell wall of peptidoglycans and teichoic acids, embedded with a number of wall-associated surface proteins (Dmitriev *et al.*, 2004). *Staphylococcus aureus* typically produces multiple enzymes (e.g. catalase, coagulase,

hyaluronidase, deoxyribonuclease, lipase, collagenase, staphylokinase and β -lactamase), providing the bacterium with opportunities for immune and antibiotic evasion, survival and spread within its host. In addition, bacterial toxins such as α -, β - and δ -toxins are involved in the alteration of junction integrity, formation of biofilms, hemolysis and cell lysis, thereby contributing to bacterial virulence, survival and spread (Berube and Wardenburg, 2013; Huseby *et al.*, 2010; Kwak *et al.*, 2012; Marshall *et al.*, 2000).

Merely the presence of *S. aureus* in the horse's upper respiratory tract will not cause disease. Similarly to *S. e. zooepidemicus*, *S. aureus* is an opportunist, meaning that one or more risk factors (e.g. stress, anesthesia, surgery, viral infections) must be present before disease can occur. The precise pathogenesis remains unclear, but upon colonization of the upper or lower respiratory tract, the bacterium can cause rhinitis, sinusitis and/or bronchopneumonia with typical accompanying symptoms, as described above (Anderson *et al.*, 2009).

Since *S. aureus* not only resides in the respiratory system, but also on the horse's skin, intestinal tract and conjunctiva, it is often associated with bacterial infections of the latter organs. Lymphatic and/or systemic spread can typically result in a number of immune- and/or bacterial-mediated pathologies, such as toxic shock syndrome, lymphangitis, osteomyelitis, meningitis, etc. (Anderson *et al.*, 2009; Sieber *et al.*, 2011).

3.5.4. *Actinobacillus equuli*

Although characteristically found as commensal organism in the intestinal mucosa of normal horses, *Actinobacillus equuli* (*A. equuli*) is a potential respiratory pathogen, causing pneumonia and septicaemia with accompanying symptoms in foals and occasionally infections in adult horses.

Two subspecies of *A. equuli* exist, i.e. *A. equuli* subspecies *equuli* and *A. equuli* subspecies *haemolyticus*, which can be differentiated based on the disability or ability to induce hemolysis, respectively (Christensen *et al.*, 2002). Both Gram-negative subspecies belong to the genus *Actinobacillus*, family *Pasteurellaceae* and order *Pasteurellales* and harbour in the digestive tract of healthy horses (Ward *et al.*, 1998). In a recent retrospective study of equine actinobacillosis cases, *A. equuli* subspecies *haemolyticus* was most commonly isolated from clinical cases of septicaemia and respiratory disease, suggesting that this subspecies is more virulent than its sister subspecies. (Layman *et al.*, 2014).

The pathogenesis of *A. equuli*-induced respiratory disorders in horses resembles that of other commensal bacteria, e.g. *S. e. zooepidemicus* and *S. aureus*.

3.5.5. *Bordetella bronchiseptica*

Bordetella bronchiseptica (*B. bronchiseptica*) is especially known for its major role in atrophic rhinitis in swine and infectious tracheobronchitis in dogs and guinea pigs, although it is occasionally isolated from horses with respiratory disorders. Whether *B. bronchiseptica* is a commensal or primary pathogen in horses is still speculative, although most studies suggest that it is a non-commensal opportunistic pathogen (Christley *et al.*, 2001; Garcia-Cantu *et al.*, 2000; Saxegaard *et al.*, 1971; Vaid *et al.*, 2018)

The Gram-negative bacterium belongs to the genus *Bordetella*, family *Alcaligenaceae*, order *Burkholderiales* and typically produces a repertoire of attachment factors (e.g. filamentous hemagglutinin, fimbriae and pertactin) and toxins (e.g. dermonecrotic toxin, tracheal toxin).

B. bronchiseptica reaches the ciliated epithelium of the horse's respiratory tract following uptake of contaminated droplets, originating from other mammals or fomites. With the help of attachment factors, the bacteria then firmly adhere to the ciliated epithelium. Attachment of the bacteria to the epithelial cilia rapidly induces ciliostasis and production of toxins (e.g. dermonecrotic toxin and tracheal toxin) eventually destructing the epithelial cells (Bemis *et al.*, 1977). The bacteria then further replicate and colonize the respiratory mucosa, while they circumvent the action of macrophages and neutrophils (e.g. respiratory burst) through the production of cyclolysin (Confer and Eaton, 1982). Further steps in its pathogenesis and elicited clinical symptoms resemble that of other bacterial-induced respiratory disorders, as mentioned above.

3.5.6. *Concluding remarks*

Taken together, bacterial-induced respiratory disorders are often secondary to other environmental factors (e.g. overcrowding in dusty premises with poor hygiene, long distance transports with the horse's head tied in an upright position, anaesthesia, surgery, etc.) or to viral infections (e.g. EHV1, EHV4, EIV). However, a minority of virulent bacteria (e.g. *S. e. equi*, *R. equi* and *B. bronchiseptica*) can cause serious purulent bronchopneumonia or abscesses in the absence of predisposing factors. Bacteria pose a major challenge to horse breeders and veterinarians, due to the limited availability of efficacious vaccines and the rise of antimicrobial resistance against antibiotics. In addition, most bacteria are omnipresent in the horse's environment, making them hard to eradicate. Therefore, a better understanding of the pathogenesis of these bacteria is urgently needed.

4. Respirable hazards

4.1. Pollens

The male gametophytes or pollen grains are seasonally released from anthers and serve to deliver the male gametes to the female partner deeply within the flower pistil. After landing on the top of the pistil, the pollen grain needs to penetrate the pistil's transmission tract through the formation of a pollen tube. The assembly of this peculiar conduit requires participation of a series of (enzymatic) complexes, including proteases (Radlowski, 2005; Swanson *et al.*, 2004). These proteases are localized to the pollen wall, from which they are easily washed, in pollen secretions during hydration and in the germinating pollen tube.

Proteases hydrolyse peptide bonds, either by acting from the ends of the polypeptide chain (exopeptidases) or within them (endopeptidases). Exoproteases are divided in two classes according to their substrate specificity; aminopeptidases, which cleave peptides at the N-terminus and carboxypeptidases, which degrade peptides at the C-terminus. Endoproteases are classified according to their active site (aspartic, cysteine, serine, threonine, metallo, etc.) (González-Rábade *et al.*, 2011; Rawlings and Barrett, 1994).

Plant proteases have mainly been identified as serine, cysteine, threonine and metalloproteases in several plants including maize, white birch, pine, giant ragweed, rye and blue grass, Easter lily and olive tree (González-Rábade *et al.*, 2011; Höllbacher *et al.*, 2017; Runswick *et al.*, 2007; Vinhas *et al.*, 2011; Widmer *et al.*, 2000). They have acquired more attention during the past several years, due to their role in pollen allergy. More precisely, it is believed that pollen allergens are delivered to subepithelial antigen-presenting cells through degradation of epithelial integrity by these proteases (Robinson *et al.*, 1997; Taketomi *et al.*, 2006; Xiao *et al.*, 2011). Mammalian epithelia lack endogenous protease inhibitors, as plant proteases are completely different from their mammalian homologs and are therefore susceptible to degradation. Indeed, several studies already showed that plant proteases are capable of disrupting epithelial integrity (Runswick *et al.*, 2007; Vinhas *et al.*, 2011; Widmer *et al.*, 2000). Nonetheless, additional factors must contribute to the development of allergy, since pollens with 'low allergenicity' also exhibit proteolytic activities and disrupt epithelial integrity (Vinhas *et al.*, 2011). Finally, pollens contribute to allergic disease and asthma by delivering other hazards into the respiratory tract, such as carbon particles from diesel engine fumes and bacteria (Knox *et al.*, 1997; McKenna *et al.*, 2017). In pasture-kept horses, the inhalation of pollens has already been shown to be associated with chronic allergies, also known as 'summer pasture recurrent airway obstruction (SP-RAO)' (Costa *et al.*, 2006).

4.2. Mycoses and mycotoxins

Mycoses are fungal infections in humans and animals and mycotoxins are the toxic secondary metabolites produced by fungi. These fungi mainly belong to the genera *Fusarium*, *Aspergillus* and *Penicillium*. Aflatoxins, ochratoxins, fumonisins, trichothecenes (e.g. deoxynivalenol or DON) and zearalenone are five frequently encountered mycotoxins in equine feeds such as green forages, hays, silages and grains (Liesener *et al.*, 2010; Ogunade *et al.*, 2018). Pathologic effects following ingestion of one or more of these toxins range from liver degeneration to reproductive problems, immunosuppression, central nervous system disorders and even death (Caloni and Cortinovis, 2011; Marasas *et al.*, 2014; Schumann *et al.*, 2016; Zain, 2011).

In horses, inhalation of these toxins or potentially toxin-producing moulds can cause acute respiratory disease, such as guttural pouch mycosis and/or a more chronic asthma-like syndrome, recurrent airway obstruction (RAO) (Laan *et al.*, 2006; Lepage *et al.*, 2004). Consequently, a correlation between mycotoxins and epithelial integrity could be assumed. Indeed, mycotoxins such as deoxynivalenol, ochratoxin and fumonisin have already been shown to alter epithelial integrity in intestinal epithelia *in vivo* and *in vitro* through inhibition of intercellular junction protein neosynthesis (Bracarense *et al.*, 2012; Gao *et al.*, 2017; Gerez *et al.*, 2015; Van De Walle *et al.*, 2010).

4.3. Air pollutants

The majority of air pollution consists of diesel exhaust, a mixture of particulate matter, hydrocarbons (e.g. benzene), gases (e.g. nitrogen oxide), sulfur and particulate matter, produced during the combustion of diesel fuel in engines from vehicles, as well as industrial plants. Over the past two decades, numerous studies have highlighted the hazardous nature of diesel exhaust, as it affects multiple organ functions, including the respiratory, cardiovascular, renal and central nervous system. Especially the particulate matter, mainly comprised of soot, contributes to the toxic effects of diesel exhaust as these small particles (ranging from 0.1 μm to 10 μm) can easily reach the deeper structures of the respiratory tract upon inhalation (Mohankumar and Senthilkumar, 2017; Reis *et al.*, 2018). In addition, these small particles function as vehicles for toxic metals and sulfur, which can be absorbed into the bloodstream, together with diesel exhaust toxic gases, thereby causing systemic effects.

The majority of respiratory and systemic symptoms are a consequence of the toxic gas- and particulate matter-induced oxidative stress and accompanying inflammatory processes. Indeed, most studies find elevated levels of H_2O_2 and pro-inflammatory cytokines (e.g. IL-6, IL-1,

TNF- α) in target organs of laboratory animals upon diesel exhaust exposure (Allen *et al.*, 2017; Ma and Ma, 2002; Salvi *et al.*, 2017; Zhao *et al.*, 2009). Long-term exposure to air pollution also increases the (lung and systemic) carcinogenic risk, which is related to oxidative DNA-damage, as well as direct binding and alteration of DNA by diesel exhaust components (Beland *et al.*, 1994; Grevendonk *et al.*, 2016). Moreover, these compounds have been shown to alter gap junction intercellular communication by decreasing the amount of connexin, which in turn promotes tumorigenesis (Heussen and Alink, 1992; Rivedal and Witz, 2005; Song and Ye, 1997).

At the level of the respiratory tract, diesel exhaust is implicated in the development of allergic diseases and asthma. The oxidative damage and release of specific cytokines and chemokines in the respiratory mucosa initiates a cascade of airway inflammatory reactions, mucus secretion and bronchial smooth muscle contractions (Totlandsdal *et al.*, 2015; Zhao *et al.*, 2009). In addition, diesel exhaust particles promote the expression of Th2 immunologic response, by inhibiting the recruitment of Th1 cells and thereby promote the development of allergies (Meldrum *et al.*, 2017). Most of the above-mentioned data arose from human cell lines or rodent models. To our knowledge, the effect of diesel exhaust on the horse's respiratory epithelium has not been studied so far.

4.4. Aerosol drugs

In humans as well as in animals such as the horse, aerosol therapy is the preferential delivery route in the treatment of pulmonary diseases. The key advantage of inhaled drug administration is that it enables delivery of drugs directly to their site of action, i.e. the respiratory mucosa and the lung alveoli, for a localised effect. This leads to a rapid clinical response and minimizes the undesirable systemic side-effects (Duvivier *et al.*, 1999). Nonetheless, aerosolized drugs should be administered in the correct way in order to reach the deeper structures of the respiratory tract. Inappropriate vaporizers or nebulizers might result in the production of large particles (>10 μm), which are filtered out in the upper respiratory tract and do not effectively reach the lower airways. In addition, horses are obligatory nasal breathers and do not breath on command, necessitating the use of proper spacers to deliver pressurized cartridge dispensers (Cha and Costa, 2017). Nostril masks for horses include the Equine HalerTM, the AeroHippusTM, and the AeroMaskTM. Drug solutions or suspensions might also be delivered to the horse's respiratory tract through nebulisation via a fitted muzzle, e.g. the FlexinebTM Equine Nebulizer.

Aerosol therapy with mucolytic agents (e.g. acetylcysteine together with isotonic saline), bronchodilators (β 2-adrenergic agonists and the muscarinic antagonists) and corticosteroids is commonly used in the treatment of equine asthma, including recurrent airway obstruction (RAO) and inflammatory airway disease (IAD) (Breuer and Becker, 1983; Dauvillier *et al.*, 2011; Mair and Derksen, 2000; Olson *et al.*, 1989). In addition, horses suffering from pneumonia might benefit from direct aerosolic delivery of mucolytic agents and antibiotics, such as gentamicin, ceftiofur and cefquinome (Cha and Costa, 2017). Apart from the beneficial effects of aerosol therapy, veterinarians should be cautious when selecting the drugs and the therapy dose. Some drugs might be harmful if overdosed, not only because of their direct effects but also because of accompanying preservatives or stabilizers.

4.5. Concluding remarks

In modern equestrian society, the air breath by horses is inevitably filled with respirable hazards, ranging from dust and ammonia to mycotoxins, pollens and air pollutants. Despite this daily struggle, the well-equipped respiratory tract of most horses seems to efficiently cope with these constant threats. Nonetheless, today, the number of horses exhibiting asthma or other chronic respiratory diseases is high, pointing out that research on these airborne hazards is urgently needed.

5. References

- Agius, C., Crabb, B., Telford, E., Davison, A., Studdert, M., 1994.** Comparative studies of the structural proteins and glycoproteins of equine herpesviruses 2 and 5. *Journal of general virology* 75, 2707-2717.
- Agius, C.T., Nagesha, H.S., Studdert, M.J., 1992.** Equine herpesvirus 5: comparisons with EHV2 (equine cytomegalovirus), cloning, and mapping of a new equine herpesvirus with a novel genome structure. *Virology* 191, 176-186.
- Akkutay, A.Z., Osterrieder, N., Damiani, A., Tischler, B.K., Borchers, K., Alkan, F., 2014.** Prevalence of equine gammaherpesviruses on breeding farms in Turkey and development of a TaqMan MGB real-time PCR to detect equine herpesvirus 5 (EHV-5). *Archives of virology* 159, 2989-2995.
- Ali, M., Maniscalco, J., Baraniuk, J.N., 1996.** Spontaneous release of submucosal gland serous and mucous cell macromolecules from human nasal explants *in vitro*. *American Journal of Physiology-Lung Cellular and Molecular Physiology* 270, L595-L600.
- Allen, G., 1999.** Advances in understanding of the pathogenesis, epidemiology and immunological control of equine herpesvirus abortion. *Equine infectious diseases*, 129-146.
- Allen, G., 2002.** Epidemic disease caused by Equine herpesvirus-1: recommendations for prevention and control. *Equine Veterinary Education* 14, 136-142.
- Allen, G., Breathnach, C., 2006.** Quantification by real-time PCR of the magnitude and duration of leucocyte-associated viraemia in horses infected with neuropathogenic vs. non-neuropathogenic strains of EHV-1. *Equine veterinary journal* 38, 252-257.
- Allen, G., Yeargan, M., Turtinen, L., Bryans, J., 1985.** A new field strain of equine abortion virus (equine herpesvirus-1) among Kentucky horses. *American journal of veterinary research* 46, 138-140.
- Allen, G.P., 2008.** Risk factors for development of neurologic disease after experimental exposure to equine herpesvirus-1 in horses. *American journal of veterinary research* 69, 1595-1600.
- Allen, G.P., Bryans, J.T., 1986.** Molecular epizootiology, pathogenesis, and prophylaxis of equine herpesvirus-1 infections. *Progress in veterinary microbiology and immunology* 2, 78-144.
- Allen, J., Oberdorster, G., Morris-Schaffer, K., Wong, C., Klocke, C., Sobolewski, M., Conrad, K., Mayer-Proschel, M., Cory-Slechta, D., 2017.** Developmental neurotoxicity of inhaled ambient ultrafine particle air pollution: Parallels with neuropathological and behavioral features of autism and other neurodevelopmental disorders. *Neurotoxicology* 59, 140-154.
- Ambagala, A.P., Gopinath, R.S., Srikumaran, S., 2004.** Peptide transport activity of the transporter associated with antigen processing (TAP) is inhibited by an early protein of equine herpesvirus-1. *Journal of General Virology* 85, 349-353.
- Anderson, J.M., 2001.** Molecular structure of tight junctions and their role in epithelial transport. *Physiology* 16, 126-130.
- Anderson, M., Lefebvre, S., Rankin, S., Aceto, H., Morley, P., Caron, J., Welsh, R., Holbrook, T., Moore, B., Taylor, D., 2009.** Retrospective multicentre study of methicillin-resistant *Staphylococcus aureus* infections in 115 horses. *Equine veterinary journal* 41, 401-405.
- Anzai, T., Timoney, J., Kuwamoto, Y., Fujita, Y., Wada, R., Inoue, T., 1999.** *In vivo* pathogenicity and resistance to phagocytosis of *Streptococcus equi* strains with different levels of capsule expression. *Veterinary microbiology* 67, 277-286.
- Auffray, C., Sieweke, M.H., Geissmann, F., 2009.** Blood monocytes: development, heterogeneity, and relationship with dendritic cells. *Annual review of immunology* 27, 669-692.
- Azab, W., Lehmann, M.J., Osterrieder, N., 2013.** Glycoprotein H and $\alpha 4\beta 1$ integrins determine the entry pathway of alphaherpesviruses. *Journal of virology* 87, 5937-5948.
- Azab, W., Zajic, L., Osterrieder, N., 2012.** The role of glycoprotein H of equine herpesviruses 1 and 4 (EHV-1 and EHV-4) in cellular host range and integrin binding. *Veterinary research* 43, 61.
- Bacha Jr, W.J., Bacha, L.M., 2012.** Chapter 15 - Respiratory System, *Color Atlas of Veterinary Histology* (Second Edition). Blackwell Publishing, pp. 175-190.

- Back, H., Ullman, K., Leijon, M., Soderlund, R., Penell, J., Stahl, K., Pringle, J., Valarcher, J.F., 2016.** Genetic variation and dynamics of infections of equid herpesvirus 5 in individual horses. *The Journal of general virology* 97, 169-178.
- Balda, M.S., Matter, K., 2016.** Tight junctions as regulators of tissue remodelling. *Current Opinion in Cell Biology* 42, 94-101.
- Bals, R., Wang, X., Meegalla, R.L., Wattler, S., Weiner, D.J., Nehls, M.C., Wilson, J.M., 1999.** Mouse beta-defensin 3 is an inducible antimicrobial peptide expressed in the epithelia of multiple organs. *Infect Immun* 67, 3542-3547.
- Bals, R., Wang, X., Wu, Z., Freeman, T., Bafna, V., Zasloff, M., Wilson, J.M., 1998.** Human beta-defensin 2 is a salt-sensitive peptide antibiotic expressed in human lung. *The Journal of clinical investigation* 102, 874-880.
- Barrios, R., 2008.** Animal Models of Lung Disease, in: Zander, D.S., Popper, H.H., Jagirdar, J., Haque, A.K., Cagle, P.T., Barrios, R. (Eds.), *Molecular Pathology of Lung Diseases*. Springer New York, New York, NY, pp. 144-149.
- Baum, B., Georgiou, M., 2011.** Dynamics of adherens junctions in epithelial establishment, maintenance, and remodeling. *The Journal of cell biology* 192, 907-917.
- Baxi, M.K., Efstathiou, S., Lawrence, G., Whalley, J.M., Slater, J.D., Field, H.J., 1995.** The detection of latency-associated transcripts of equine herpesvirus 1 in ganglionic neurons. *The Journal of general virology* 76 (12), 3113-3118.
- Beland, F.A., Fullerton, N.F., Smith, B.A., Heflich, R.H., 1994.** Formation of DNA adducts and induction of mutations in rats treated with tumorigenic doses of 1, 6-dinitropyrene. *Environmental health perspectives* 102, 185.
- Bell, S.A., Balasuriya, U.B., Gardner, I.A., Barry, P.A., Wilson, W.D., Ferraro, G.L., MacLachlan, N.J., 2006a.** Temporal detection of equine herpesvirus infections of a cohort of mares and their foals. *Veterinary microbiology* 116, 249-257.
- Bell, S.A., Balasuriya, U.B., Nordhausen, R.W., MacLachlan, N.J., 2006b.** Isolation of equine herpesvirus-5 from blood mononuclear cells of a gelding. *Journal of veterinary diagnostic investigation* 18, 472-475.
- Bemis, D.A., Greisen, H.A., Appel, M.J., 1977.** Pathogenesis of canine bordetellosis. *Journal of Infectious Diseases* 135, 753-762.
- Bensch, K.W., Raida, M., Magert, H.J., Schulz-Knappe, P., Forssmann, W.G., 1995.** hBD-1: a novel beta-defensin from human plasma. *FEBS letters* 368, 331-335.
- Berube, B.J., Wardenburg, J.B., 2013.** Staphylococcus aureus α -toxin: nearly a century of intrigue. *Toxins* 5, 1140-1166.
- Beutemüller, E.A., Woodward, A., Rash, A., dos Santos Ferraz, L.E., Alfieri, A.F., Alfieri, A.A., Elton, D., 2016.** Characterisation of the epidemic strain of H3N8 equine influenza virus responsible for outbreaks in South America in 2012. *Virology journal* 13, 45.
- Boers, J.E., Ambergen, A.W., Thunnissen, F.B., 1998.** Number and proliferation of basal and parabasal cells in normal human airway epithelium. *American journal of respiratory and critical care medicine* 157, 2000-2006.
- Borchers, K., Frölich, K., 1997.** Antibodies against equine herpesviruses in free-ranging mountain zebras from Namibia. *Journal of Wildlife diseases* 33, 812-817.
- Borchers, K., Thein, P., Sterner-Kock, A., 2006.** Pathogenesis of equine herpesvirus-associated neurological disease: a revised explanation. *Equine veterinary journal* 38, 283-287.
- Bosch, A.A., Biesbroek, G., Trzcinski, K., Sanders, E.A., Bogaert, D., 2013.** Viral and bacterial interactions in the upper respiratory tract. *PLoS pathogens* 9, e1003057.
- Boyle, A., Timoney, J., Newton, J., Hines, M., Waller, A., Buchanan, B., 2018.** Streptococcus equi Infections in Horses: Guidelines for Treatment, Control, and Prevention of Strangles—Revised Consensus Statement. *Journal of veterinary internal medicine* 32, 633-647.
- Bracarense, A.-P.F., Luciola, J., Grenier, B., Pacheco, G.D., Moll, W.-D., Schatzmayr, G., Oswald, I.P., 2012.** Chronic ingestion of deoxynivalenol and fumonisin, alone or in interaction, induces morphological and immunological changes in the intestine of piglets. *British Journal of Nutrition* 107, 1776-1786.
- Breuer, D., Becker, M., 1983.** Acetylcysteine (Fluimucil) in the treatment of COPD of the horse. *Tierärztliche Praxis* 11, 209-212.

- Browning, G., Studdert, M., 1987.** Genomic heterogeneity of equine betaherpesviruses. *Journal of general virology* 68, 1441-1447.
- Bryans, J., Crowe, M., Doll, E., McCollum, W., 1957.** Isolation of a filterable agent causing arteritis of horses and abortion by mares; its differentiation from the equine abortion (influenza) virus. *The Cornell veterinarian* 47, 3.
- Bryans, J., Prickett, M., 1970.** consideration of the pathogenesis of abortigenic disease caused by equine herpesvirus 1, *Int Conf Equine Infec Dis Proc.*
- Bryant, N.A., Davis-Poynter, N., Vanderplasschen, A., Alcami, A., 2003.** Glycoprotein G isoforms from some alpha herpesviruses function as broad-spectrum chemokine binding proteins. *Embo Journal* 22, 833-846.
- Budras, K.-D., Sack, W.O., Rock, S., 2003.** *Anatomy of the horse.* Schlütersche, pp. 44-49.
- Burki, F., Gerber, H., 1966.** Ein virologisch gesicherter Große ausbruch von Equiner Arteritis. *Berl Münch Tierärztl Wochenschr*, 79, 391-395.
- Burrows, R., Goodridge, D., 1984.** Studies of persistent and latent equid herpesvirus 1 and herpesvirus 3 infections in the Pirbright pony herd, *Latent Herpes Virus Infections in Veterinary Medicine.* Springer, pp. 307-319.
- Burrows, R., Goodridge, D., Denyer, M., Hutchings, G., Frank, C., 1982.** Equine influenza infections in Great Britain, 1979. *Veterinary Record* 110, 494-497.
- Caloni, F., Cortinovis, C., 2011.** Toxicological effects of aflatoxins in horses. *The Veterinary Journal* 188, 270-273.
- Campbell, H.K., Maiers, J.L., DeMali, K.A., 2017.** Interplay between tight junctions & adherens junctions. *Experimental cell research* 358, 39-44.
- Caughman, G.B., Staczek, J., O'Callaghan, D.J., 1985.** Equine herpesvirus type 1 infected cell polypeptides: evidence for immediate early/early/late regulation of viral gene expression. *Virology* 145, 49-61.
- Cavanagh, D., 1997.** Nidovirales: a new order comprising Coronaviridae and Arteriviridae. *Arch. Virol.* 142, 629-633.
- Cha, M.L., Costa, L.R., 2017.** Inhalation Therapy in Horses. *Veterinary Clinics: Equine Practice* 33, 29-46.
- Chaffin, M.K., Cohen, N.D., Martens, R.J., O'Connor, M., Bernstein, L.R., 2011.** Evaluation of the efficacy of gallium maltolate for chemoprophylaxis against pneumonia caused by *Rhodococcus equi* infection in foals. *American journal of veterinary research* 72, 945-957.
- Chanter, N., Collin, N., Holmes, N., Binns, M., Mumford, J., 1997.** Characterization of the Lancefield group C streptococcus 16S-23S RNA gene intergenic spacer and its potential for identification and sub-specific typing. *Epidemiology & Infection* 118, 125-135.
- Charp, P.A., Rice, W.G., Raynor, R.L., Reimund, E., Kinkade Jr, J.M., Ganz, T., Selsted, M.E., Lehrer, R.I., Kuo, J., 1988.** Inhibition of protein kinase C by defensins, antibiotic peptides from human neutrophils. *Biochemical pharmacology* 37, 951-956.
- Chesters, P., Allsop, R., Purewal, A., Edington, N., 1997.** Detection of latency-associated transcripts of equid herpesvirus 1 in equine leukocytes but not in trigeminal ganglia. *Journal of virology* 71, 3437-3443.
- Chong, K.T., Thangavel, R.R., Tang, X., 2008.** Enhanced expression of murine beta-defensins (MBD-1, -2, -3, and -4) in upper and lower airway mucosa of influenza virus infected mice. *Virology* 380, 136-143.
- Christensen, H., Bisgaard, M., Olsen, J.E., 2002.** Reclassification of equine isolates previously reported as *Actinobacillus equuli*, variants of *A. equuli*, *Actinobacillus suis* or Bisgaard taxon 11 and proposal of *A. equuli* subsp. *equuli* subsp. nov. and *A. equuli* subsp. *haemolyticus* subsp. nov. *International journal of systematic and evolutionary microbiology* 52, 1569-1576.
- Christley, R.M., Hodgson, D.R., Rose, R.J., Wood, J.L.N., Reid, S.W.J., Whitear, K.G., Hodgson, J.L., 2001.** A case-control study of respiratory disease in Thoroughbred racehorses in Sydney, Australia. *Equine Veterinary Journal* 33, 256-264.
- Clark, A.B., Randell, S.H., Nettesheim, P., Gray, T.E., Bagnell, B., Ostrowski, L.E., 1995.** Regulation of ciliated cell differentiation in cultures of rat tracheal epithelial cells. *American journal of respiratory cell and molecular biology* 12, 329-338.

- Coleman, D., Tuet, I., Widdicombe, J., 1984.** Electrical properties of dog tracheal epithelial cells grown in monolayer culture. *American Journal of Physiology-Cell Physiology* 246, C355-C359.
- Confer, D.L., Eaton, J.W., 1982.** Phagocyte impotence caused by an invasive bacterial adenylate cyclase. *Science (New York, N.Y.)* 217, 948-950.
- Contreras, X., Mzoughi, O., Gaston, F., Peterlin, M.B., Bahraoui, E., 2012.** Protein kinase C-delta regulates HIV-1 replication at an early post-entry step in macrophages. *Retrovirology* 9, 37.
- Costa, L.R., Johnson, J.R., Baur, M.E., Beadle, R.E., 2006.** Temporal clinical exacerbation of summer pasture-associated recurrent airway obstruction and relationship with climate and aeroallergens in horses. *American journal of veterinary research* 67, 1635-1642.
- Cowled, B., Ward, M.P., Hamilton, S., Garner, G., 2009.** The equine influenza epidemic in Australia: spatial and temporal descriptive analyses of a large propagating epidemic. *Preventive veterinary medicine* 92, 60-70.
- Cozens, A.L., Yezzi, M.J., Kunzelmann, K., Ohrui, T., Chin, L., Eng, K., Finkbeiner, W.E., Widdicombe, J.H., Gruenert, D.C., 1994.** CFTR expression and chloride secretion in polarized immortal human bronchial epithelial cells. *American journal of respiratory cell and molecular biology* 10, 38-47.
- Csellner, H., Walker, C., Wellington, J.E., McLure, L.E., Love, D.N., Whalley, J.M., 2000.** EHV-1 glycoprotein D (EHV-1 gD) is required for virus entry and cell-cell fusion, and an EHV-1 gD deletion mutant induces a protective immune response in mice. *Arch Virol* 145, 2371-2385.
- Cullinane, A.A., Rixon, F.J., Davison, A.J., 1988.** Characterization of the genome of equine herpesvirus 1 subtype 2. *Journal of general virology* 69, 1575-1590.
- Daly, J.M., Blunden, A.S., MacRae, S., Miller, J., Bowman, S.J., Kolodziejek, J., Nowotny, N., Smith, K.C., 2008.** Transmission of equine influenza virus to English foxhounds. *Emerging infectious diseases* 14, 461.
- Danaher, R.J., Jacob, R.J., Steiner, M.R., Allen, W.R., Hill, J.M., Miller, C.S., 2005.** Histone deacetylase inhibitors induce reactivation of herpes simplex virus type 1 in a latency-associated transcript-independent manner in neuronal cells. *Journal of neurovirology* 11, 306-317.
- Dauvillier, J., Felipe, M., Lunn, D., Lavoie-Lamoureux, A., Leclere, M., Beauchamp, G., Lavoie, J.P., 2011.** Effect of Long-Term Fluticasone Treatment on Immune Function in Horses with Heaves. *Journal of veterinary internal medicine* 25, 549-557.
- Davis, E.G., Sang, Y., Blecha, F., 2004.** Equine beta-defensin-1: full-length cDNA sequence and tissue expression. *Vet Immunol Immunopathol* 99, 127-132.
- Davison, A.J., 2011.** Evolution of sexually transmitted and sexually transmissible human herpesviruses. *Annals of the New York Academy of Sciences* 1230.
- Davison, A.J., Eberle, R., Ehlers, B., Hayward, G.S., McGeoch, D.J., Minson, A.C., Pellett, P.E., Roizman, B., Studdert, M.J., Thiry, E., 2009.** The order herpesvirales. *Archives of virology* 154, 171-177.
- De Vries, A., Chirnside, E., Horzinek, M., Rottier, P., 1992.** Structural proteins of equine arteritis virus. *Journal of virology* 66, 6294-6303.
- Del Piero, F., 2000.** Equine viral arteritis. *Veterinary Pathology* 37, 287-296.
- Diamond, G., Zasloff, M., Eck, H., Brasseur, M., Maloy, W.L., Bevins, C.L., 1991.** Tracheal antimicrobial peptide, a cysteine-rich peptide from mammalian tracheal mucosa: peptide isolation and cloning of a cDNA. *Proceedings of the National Academy of Sciences of the United States of America* 88, 3952-3956.
- Dmitriev, B.A., Toukach, F.V., Holst, O., Rietschel, E., Ehlers, S., 2004.** Tertiary structure of *Staphylococcus aureus* cell wall murein. *Journal of bacteriology* 186, 7141-7148.
- Donofrio, G., Herath, S., Sartori, C., Cavirani, S., Flammini, C.F., Sheldon, I.M., 2007.** Bovine herpesvirus 4 is tropic for bovine endometrial cells and modulates endocrine function. *Reproduction* 134, 183-197.
- Dugan, A.S., Maginnis, M.S., Jordan, J.A., Gasparovic, M.L., Manley, K., Page, R., Williams, G., Porter, E., O'Hara, B.A., Atwood, W.J., 2008.** Human α -defensins inhibit BK virus infection by aggregating virions and blocking binding to host cells. *Journal of Biological Chemistry* 283, 31125-31132.
- Dunowska, M., Holloway, S.A., Wilks, C.R., Meers, J., 2000.** Genomic variability of equine herpesvirus-5. *Archives of Virology* 145, 1359-1371.

- Dunowska, M., Meers, J., Wilks, C., 1999.** Isolation of equine herpesvirus type 5 in New Zealand. *New Zealand Veterinary Journal* 47, 44-46.
- Dunowska, M., Wilks, C., Studdert, M., Meers, J., 2002.** Equine respiratory viruses in foals in New Zealand. *New Zealand Veterinary Journal* 50, 140-147.
- Duvivier, D.H., Votion, D., Roberts, C., Art, T., Lekeux, P., 1999.** Inhalation therapy of equine respiratory disorders. *Equine Veterinary Education* 11, 124-131.
- Dynon, K., Varrasso, A., Ficorilli, N., Holloway, S., Reubel, G., Li, F., Hartley, C., Studdert, M., Drummer, H., 2001.** Identification of equine herpesvirus 3 (equine coital exanthema virus), equine gammaherpesviruses 2 and 5, equine adenoviruses 1 and 2, equine arteritis virus and equine rhinitis A virus by polymerase chain reaction. *Australian veterinary journal* 79, 695-702.
- Ebnet, K., Aurrand-Lions, M., Kuhn, A., Kiefer, F., Butz, S., Zander, K., zu Brickwedde, M.-K.M., Suzuki, A., Imhof, B.A., Vestweber, D., 2003.** The junctional adhesion molecule (JAM) family members JAM-2 and JAM-3 associate with the cell polarity protein PAR-3: a possible role for JAMs in endothelial cell polarity. *J Cell Sci* 116, 3879-3891.
- Echeverria, M., Pecoraro, M., Galosi, C., Etcheverrigaray, M., Nosetto, E., 2003.** The first isolation of equine arteritis virus in Argentina. *Revue Scientifique et Technique-Office International des Epizooties* 22, 1029-1034.
- Edington, N., Bridges, C., Huckle, A., 1985.** Experimental reactivation of equid herpesvirus 1 (EHV 1) following the administration of corticosteroids. *Equine veterinary journal* 17, 369-372.
- Edington, N., Bridges, C., Patel, J., 1986.** Endothelial cell infection and thrombosis in paralysis caused by equid herpesvirus-1: equine stroke. *Archives of virology* 90, 111-124.
- Edington, N., Smyth, B., Griffiths, L., 1991.** The role of endothelial cell infection in the endometrium, placenta and foetus of equid herpesvirus 1 (EHV-1) abortions. *Journal of comparative pathology* 104, 379-387.
- Edington, N., Welch, H., Griffiths, L., 1994.** The prevalence of latent equid herpesviruses in the tissues of 40 abattoir horses. *Equine veterinary journal* 26, 140-142.
- Eichhorn, W., Heilmann, M., Kaaden, O.R., 1995.** Equine viral arteritis with abortions: serological and virological evidence in Germany. *Zoonoses and Public Health* 42, 573-576.
- Elton, D., Cullinane, A., 2013.** Equine influenza: Antigenic drift and implications for vaccines. *Equine veterinary journal* 45, 768-769.
- Erjefalt, J.S., Erjefalt, I., Sundler, F., Persson, C.G., 1995.** *In vivo* restitution of airway epithelium. *Cell and tissue research* 281, 305-316.
- Evans, M.J., Cox, R.A., Shami, S.G., Plopper, C.G., 1990.** Junctional adhesion mechanisms in airway basal cells. *American journal of respiratory cell and molecular biology* 3, 341-347.
- Evans, M.J., Plopper, C.G., 1988.** The role of basal cells in adhesion of columnar epithelium to airway basement membrane. *The American review of respiratory disease* 138, 481-483.
- Fallgreen-Gebauer, E., Gebauer, W., Bastian, A., Kratzin, H.D., Eiffert, H., Zimmermann, B., Karas, M., Hilschmann, N., 1993.** The covalent linkage of secretory component to IgA. Structure of sIgA. *Biological Chemistry Hoppe-Seyler* 374, 1023-1028.
- Fan, Q., Lin, E., Spear, P.G., 2009.** Insertional mutations in herpes simplex virus type 1 gL identify functional domains for association with gH and for membrane fusion. *Journal of virology* 83, 11607-11615.
- Fanning, A.S., Anderson, J.M., 2009.** Zonula occludens-1 and-2 are cytosolic scaffolds that regulate the assembly of cellular junctions. *Annals of the New York Academy of Sciences* 1165, 113-120.
- Fanucchi, M.V., Harkema, J.R., Plopper, C.G., Hotchkiss, J.A., 1999.** *In vitro* culture of microdissected rat nasal airway tissues. *American journal of respiratory cell and molecular biology* 20, 1274-1285.
- Flowers, C., O'Callaghan, D., 1992.** Equine herpesvirus 1 glycoprotein D: mapping of the transcript and a neutralization epitope. *Journal of virology* 66, 6451-6460.
- Fokkens, W.J., Vroom, T.M., Rijntjes, E., Mulder, P., 1989.** CD-1 (T6), HLA-DR-expressing cells, presumably Langerhans cells, in nasal mucosa. *Allergy* 44, 167-172.
- Frampton, A.R., Goins, W.F., Cohen, J.B., von Einem, J., Osterrieder, N., O'Callaghan, D.J., Glorioso, J.C., 2005.** Equine Herpesvirus 1 Utilizes a Novel Herpesvirus Entry Receptor. *Journal of Virology* 79, 3169-3173.

- Frampton, A.R., Jr., Stolz, D.B., Uchida, H., Goins, W.F., Cohen, J.B., Glorioso, J.C., 2007.** Equine herpesvirus 1 enters cells by two different pathways, and infection requires the activation of the cellular kinase ROCK1. *J Virol* 81, 10879-10889.
- Frampton Jr, A.R., Uchida, H., Von Einem, J., Goins, W.F., Grandi, P., Cohen, J.B., Osterrieder, N., Glorioso, J.C., 2010.** Equine herpesvirus type 1 (EHV-1) utilizes microtubules, dynein, and ROCK1 to productively infect cells. *Veterinary microbiology* 141, 12-21.
- Franchini, M., Akens, M., Bracher, V., v Fellenberg, R., 1997.** Characterisation of gamma herpesviruses in the horse by PCR. *Virology* 238, 8-13.
- François, S., Vidick, S., Sarlet, M., Desmecht, D., Drion, P., Stevenson, P.G., Vanderplasschen, A., Gillet, L., 2013.** Illumination of murine gammaherpesvirus-68 cycle reveals a sexual transmission route from females to males in laboratory mice. *PLoS pathogens* 9, e1003292.
- Frensing, T., Kupke, S.Y., Bachmann, M., Fritzsche, S., Gallo-Ramirez, L.E., Reichl, U., 2016.** Influenza virus intracellular replication dynamics, release kinetics, and particle morphology during propagation in MDCK cells. *Applied Microbiology and Biotechnology* 100, 7181-7192.
- Ganesan, S., Comstock, A.T., Sajjan, U.S., 2013.** Barrier function of airway tract epithelium. *Tissue barriers* 1, e24997.
- Ganz, T., 2003.** Defensins: antimicrobial peptides of innate immunity. *Nature reviews. Immunology* 3, 710-720.
- Gao, Y., Li, S., Wang, J., Luo, C., Zhao, S., Zheng, N., 2017.** Modulation of Intestinal Epithelial Permeability in Differentiated Caco-2 Cells Exposed to Aflatoxin M1 and Ochratoxin A Individually or Collectively. *Toxins* 10, 13.
- Garcia-Cantu, M.C., Hartmann, F.A., Brown, C.M., Darien, B.J., 2000.** Bordetella bronchiseptica and equine respiratory infections: a review of 30 cases. *Equine Veterinary Education* 12, 45-50.
- Garrod, D., Chidgey, M., 2008.** Desmosome structure, composition and function. *Biochimica et Biophysica Acta (BBA)-Biomembranes* 1778, 572-587.
- Geissmann, F., Manz, M.G., Jung, S., Sieweke, M.H., Merad, M., Ley, K., 2010.** Development of monocytes, macrophages, and dendritic cells. *Science (New York, N.Y.)* 327, 656-661.
- Geraghty, R.J., Krummenacher, C., Cohen, G.H., Eisenberg, R.J., Spear, P.G., 1998.** Entry of alphaherpesviruses mediated by poliovirus receptor-related protein 1 and poliovirus receptor. *Science (New York, N.Y.)* 280, 1618-1620.
- Gerber, H., 1970.** Clinical features, sequelae and epidemiology of equine influenza, *Proceedings 2nd int. Conf. Equine Infect. Dis., Paris, 1969.*, pp. 63-80.
- Gerez, J.R., Pinton, P., Callu, P., Grosjean, F., Oswald, I.P., Bracarense, A.P.F.L., 2015.** Deoxynivalenol alone or in combination with nivalenol and zearalenone induce systemic histological changes in pigs. *Experimental and Toxicologic Pathology* 67, 89-98.
- Gibson, J., Slater, J., Awan, A., Field, H., 1992.** Pathogenesis of equine herpesvirus-1 in specific pathogen-free foals: primary and secondary infections and reactivation. *Archives of virology* 123, 351-366.
- Gilkerson, J.R., Bailey, K.E., Diaz-Méndez, A., Hartley, C.A., 2015.** Update on Viral Diseases of the Equine Respiratory Tract. *Veterinary Clinics of North America: Equine Practice* 31, 91-104.
- Glorieux, S., Bachert, C., Favoreel, H.W., Vandekerckhove, A.P., Steukers, L., Rekecki, A., Van den Broeck, W., Goossens, J., Croubels, S., Clayton, R.F., 2011a.** Herpes simplex virus type 1 penetrates the basement membrane in human nasal respiratory mucosa. *PLoS One* 6, e22160.
- Glorieux, S., Favoreel, H.W., Steukers, L., Vandekerckhove, A.P., Nauwynck, H.J., 2011b.** A trypsin-like serine protease is involved in pseudorabies virus invasion through the basement membrane barrier of porcine nasal respiratory mucosa. *Vet Res* 42, 58.
- Glorieux, S., Van den Broeck, W., van der Meulen, K.M., Van Reeth, K., Favoreel, H.W., Nauwynck, H.J., 2007.** *In vitro* culture of porcine respiratory nasal mucosa explants for studying the interaction of porcine viruses with the respiratory tract. *Journal of virological methods* 142, 105-112.
- Goehring, L., Hussey, G.S., Ashton, L., Schenkel, A., Lunn, D., 2011.** Infection of central nervous system endothelial cells by cell-associated EHV-1. *Veterinary microbiology* 148, 389-395.
- Goehring, L.S., Winden, S.C., Maanen, C.v., Oldruitenborgh-Oosterbaan, M.M.S., 2006.** Equine Herpesvirus Type 1-Associated Myeloencephalopathy in The Netherlands: A Four-Year Retrospective Study (1999–2003). *Journal of veterinary internal medicine* 20, 601-607.

- Goldman, M.J., Anderson, G.M., Stolzenberg, E.D., Kari, U.P., Zasloff, M., Wilson, J.M., 1997.** Human β -defensin-1 is a salt-sensitive antibiotic in lung that is inactivated in cystic fibrosis. *Cell* 88, 553-560.
- González-Rábade, N., Badillo-Corona, J.A., Aranda-Barradas, J.S., del Carmen Oliver-Salvador, M., 2011.** Production of plant proteases *in vivo* and *in vitro* - a review. *Biotechnology Advances* 29, 983-996.
- Goodman, L.B., Loregian, A., Perkins, G.A., Nugent, J., Buckles, E.L., Mercorelli, B., Kydd, J.H., Palù, G., Smith, K.C., Osterrieder, N., 2007.** A point mutation in a herpesvirus polymerase determines neuropathogenicity. *PLoS pathogens* 3, e160.
- Granzow, H., Klupp, B.G., Fuchs, W., Veits, J., Osterrieder, N., Mettenleiter, T.C., 2001.** Egress of alphaherpesviruses: comparative ultrastructural study. *Journal of virology* 75, 3675-3684.
- Gray, W.L., Baumann, R.P., Robertson, A.T., Caughman, G.B., O'Callaghan, D.J., Staczek, J., 1987.** Regulation of equine herpesvirus type 1 gene expression: characterization of immediate early, early, and late transcription. *Virology* 158, 79-87.
- Grencis, R.K., Worthington, J.J., 2016.** Tuft Cells: A New Flavor in Innate Epithelial Immunity. *Trends Parasitol* 32, 583-585.
- Grevendonk, L., Janssen, B.G., Vanpoucke, C., Lefebvre, W., Hoxha, M., Bollati, V., Nawrot, T.S., 2016.** Mitochondrial oxidative DNA damage and exposure to particulate air pollution in mother-newborn pairs. *Environmental Health* 15, 10.
- Grinde, B., 2013.** Herpesviruses: latency and reactivation – viral strategies and host response. *Journal of Oral Microbiology* 5, 10.3402/jom.v3405i3400.22766.
- Gryspeerd, A., Chiers, K., Govaere, J., Vercauteren, G., Ducatelle, R., Van de Walle, G., Nauwynck, H., 2009.** Neonatal foal death due to infection with equine arteritis virus in Belgium. *Vlaams Diergeneeskundig Tijdschrift* 78, 189-193.
- Gryspeerd, A., Vandekerckhove, A., Van Doorselaere, J., Van de Walle, G., Nauwynck, H., 2011.** Description of an unusually large outbreak of nervous system disorders caused by equine herpesvirus 1 (EHV1) in 2009 in Belgium. *Vlaams Diergeneeskundig Tijdschrift* 80, 147-153.
- Gryspeerd, A.C., Vandekerckhove, A., Garré, B., Barbé, F., Van de Walle, G., Nauwynck, H., 2010.** Differences in replication kinetics and cell tropism between neurovirulent and non-neurovirulent EHV1 strains during the acute phase of infection in horses. *Veterinary microbiology* 142, 242-253.
- Gryspeerd, A.C., Vandekerckhove, A.P., Baghi, H.B., Van de Walle, G.R., Nauwynck, H.J., 2012.** Expression of late viral proteins is restricted in nasal mucosal leucocytes but not in epithelial cells during early-stage equine herpes virus-1 infection. *The Veterinary Journal* 193, 576-578.
- Gürtler, V., Seviour, R.J., 2010.** Systematics of members of the genus *Rhodococcus* (Zopf 1891) emend Goodfellow *et al.* 1998, *Biology of Rhodococcus*. Springer, pp. 1-28.
- Hamilton, A., Robinson, C., Sutcliffe, I.C., Slater, J., Maskell, D.J., Davis-Poynter, N., Smith, K., Waller, A., Harrington, D.J., 2006.** Mutation of the maturase lipoprotein attenuates the virulence of *Streptococcus equi* to a greater extent than does loss of general lipoprotein lipidation. *Infection and immunity* 74, 6907-6919.
- Hannant, D., Mumford, J.A., 1989.** Cell mediated immune responses in ponies following infection with equine influenza virus (H3N8): the influence of induction culture conditions on the properties of cytotoxic effector cells. *Veterinary immunology and immunopathology* 21, 327-337.
- Harder, J., Bartels, J., Christophers, E., Schröder, J.-M., 2001.** Isolation and characterization of human β -defensin-3, a novel human inducible peptide antibiotic. *Journal of Biological Chemistry* 276, 5707-5713.
- Harkema, J.R., Carey, S.A., Wagner, J.G., 2006.** The nose revisited: a brief review of the comparative structure, function, and toxicologic pathology of the nasal epithelium. *Toxicologic pathology* 34, 252-269.
- Harmon, M.W., Greenberg, S.B., Johnson, P.E., Couch, R., 1977.** Human nasal epithelial cell culture system: evaluation of response to human interferons. *Infection and immunity* 16, 480-485.
- Hart, K., Barton, M., Williams, K., Flaminio, M., Howerth, E., 2008.** Multinodular pulmonary fibrosis, pancytopenia and equine herpesvirus-5 infection in a Thoroughbred gelding. *Equine Veterinary Education* 20, 470-476.

- Hasebe, R., Sasaki, M., Sawa, H., Wada, R., Umemura, T., Kimura, T., 2009.** Infectious entry of equine herpesvirus-1 into host cells through different endocytic pathways. *Virology* 393, 198-209.
- Hazrati, E., Galen, B., Lu, W.Y., Wang, W., Yan, O.Y., Keller, M.J., Lehrer, R.I., Herold, B.C., 2006.** Human alpha- and beta-defensins block multiple steps in herpes simplex virus infection. *Journal of Immunology* 177, 8658-8666.
- Henninger, R.W., Reed, S.M., Saville, W.J., Allen, G.P., Hass, G.F., Kohn, C.W., Sofaly, C., 2007.** Outbreak of Neurologic Disease Caused by Equine Herpesvirus-1 at a University Equestrian Center. *Journal of Veterinary Internal Medicine* 21, 157-165.
- Herder, V., Barsnick, R., Walliser, U., Teifke, J.P., König, P., Czerwinski, G., Hansmann, F., Baumgärtner, W., Hewicker-Trautwein, M., 2012.** Equid herpesvirus 5-associated dermatitis in a horse - Resembling herpes-associated erythema multiforme. *Veterinary microbiology* 155, 420-424.
- Hervé, J.-C., Bourmeyster, N., Sarrouilhe, D., Duffy, H.S., 2007.** Gap junctional complexes: from partners to functions. *Progress in biophysics and molecular biology* 94, 29-65.
- Heussen, G., Alink, G., 1992.** Inhibition of gap-junctional intercellular communication by TPA and airborne particulate matter in primary cultures of rat alveolar type II cells. *Carcinogenesis* 13, 719-722.
- Hickman-Davis, J.M., Fang, F.C., Nathan, C., Shepherd, V.L., Voelker, D.R., Wright, J.R., 2001.** Lung surfactant and reactive oxygen-nitrogen species: antimicrobial activity and host-pathogen interactions. *American journal of physiology-lung cellular and molecular physiology* 281, L517-L523.
- Hines, M.T., 2007.** *Rhodococcus equi*. *Equine infectious diseases*, 281-295.
- Hoenerhoff, M.J., Janovitz, E.B., Richman, L.K., Murphy, D.A., Butler, T.C., Kiupel, M., 2006.** Fatal Herpesvirus Encephalitis in a Reticulated Giraffe (*Giraffa camelopardalis reticulata*). *Veterinary Pathology* 43, 769-772.
- Höllbacher, B., Schmitt, A.O., Hofer, H., Ferreira, F., Lackner, P., 2017.** Identification of proteases and protease inhibitors in allergenic and non-allergenic pollen. *International journal of molecular sciences* 18, 1199.
- Holyoak, G., Balasuriya, U., Broaddus, C., Timoney, P., 2008.** Equine viral arteritis: current status and prevention. *Theriogenology* 70, 403-414.
- Hoorn, B., 1964.** Respiratory viruses in model experiments. *Acta Oto-Laryngologica* 57, 138-144.
- Huang, S., Constant, S., Wiszniewski, L., Derouette, J.-P., 2008.** MucilAir: a novel human 3D airway epithelium model for acute or long term toxicity testing of chemicals. *ALTEX* 25, 30-31.
- Huang, T., Lehmann, M.J., Said, A., Ma, G.G., Osterrieder, N., 2014.** Major Histocompatibility Complex Class I Downregulation Induced by Equine Herpesvirus Type 1 pUL56 Is through Dynamin-Dependent Endocytosis. *Journal of Virology* 88, 12802-12815.
- Hue, E.S., Fortier, G.D., Fortier, C.I., Leon, A.M., Richard, E.A., Legrand, L.J., Pronost, S.L., 2014.** Detection and quantitation of equid gammaherpesviruses (EHV-2, EHV-5) in nasal swabs using an accredited standardised quantitative PCR method. *Journal of virological methods* 198, 18-25.
- Hullinger, P.J., Gardner, I.A., Hietala, S.K., Ferraro, G.L., MacLachlan, N.J., 2001.** Seroprevalence of antibodies against equine arteritis virus in horses residing in the United States and imported horses. *Journal of the American Veterinary Medical Association* 219, 946-949.
- Huseby, M.J., Kruse, A.C., Digre, J., Kohler, P.L., Vocke, J.A., Mann, E.E., Bayles, K.W., Bohach, G.A., Schlievert, P.M., Ohlendorf, D.H., 2010.** Beta toxin catalyzes formation of nucleoprotein matrix in staphylococcal biofilms. *Proceedings of the National Academy of Sciences* 107, 14407-14412.
- Huttner, K.M., Lambeth, M.R., Burkin, H.R., Burkin, D.J., Broad, T.E., 1998.** Localization and genomic organization of sheep antimicrobial peptide genes. *Gene* 206, 85-91.
- Ibrahim, E.S.M., Kinoh, M., Matsumura, T., Kennedy, M., Allen, G.P., Yamaguchi, T., Fukushi, H., 2007.** Genetic relatedness and pathogenicity of equine herpesvirus 1 isolated from onager, zebra and gazelle. *Archives of Virology* 152, 245-255.

- Jackson, A.D., Rayner, C., Dewar, A., Cole, P.J., Wilson, R., 1996.** A human respiratory-tissue organ culture incorporating an air interface. *American journal of respiratory and critical care medicine* 153, 1130-1135.
- Jackson, T., Kendrick, J., 1971.** Paralysis of horses associated with equine herpesvirus 1 infection. *Amer Vet Med Ass J*.
- Jackson, T., Osburn, B., Cordy, D., Kendrick, J., 1977.** Equine herpesvirus 1 infection of horses: studies on the experimentally induced neurologic disease. *American journal of veterinary research* 38, 709-719.
- Jeffery, P., Li, D., 1997.** Airway mucosa: secretory cells, mucus and mucin genes. *European Respiratory Journal* 10, 1655-1662.
- Judy, C., Chaffin, M., Cohen, N., 1999.** Empyema of the guttural pouch (auditory tube diverticulum) in horses: 91 cases (1977-1997). *Journal of the American Veterinary Medical Association* 215, 1666-1670.
- Karlin, S., Mocarski, E.S., Schachtel, G.A., 1994.** Molecular evolution of herpesviruses: genomic and protein sequence comparisons. *J Virol* 68, 1886-1902.
- Kawaoka, Y., Bean, W.J., Webster, R.G., 1989.** Evolution of the hemagglutinin of equine H3 influenza viruses. *Virology* 169, 283-292.
- King, M., 1980.** Viscoelastic properties of airway mucus. *Federation proceedings* 39, 3080-3085.
- King, M., 2005.** Mucus and its role in airway clearance and cytoprotection. *Physiologic Basis of Respiratory Disease*. BC Decker Inc: Hamilton, 409-416.
- Kleinsasser, N.H., Juchhoff, J., Wallner, B.C., Bergner, A., Harréus, U.A., Gamarra, F., Bührlen, M., Huber, R.M., Rettenmeier, A.W., 2004.** The use of mini-organ cultures of human upper aerodigestive tract epithelia in ecogenotoxicology. *Mutation Research/Genetic Toxicology and Environmental Mutagenesis* 561, 63-73.
- Klingeborn, B., Rockborn, G., Dinter, Z., 1980.** Significant antigenic drift within the influenza equi 2 subtype in Sweden. *Veterinary record* 106, 363-364.
- Knight, D.A., Holgate, S.T., 2003.** The airway epithelium: structural and functional properties in health and disease. *Respirology (Carlton, Vic.)* 8, 432-446.
- Knox, R., Suphioglu, C., Taylor, P., Desai, R., Watson, H.C., Peng, J.-L., Bursill, L.A., 1997.** Major grass pollen allergen Lol p 1 binds to diesel exhaust particles: implications for asthma and air pollution. *Clinical & Experimental Allergy* 27, 246-251.
- Knust, E., Bossinger, O., 2002.** Composition and formation of intercellular junctions in epithelial cells. *Science (New York, N.Y.)* 298, 1955-1959.
- Kondo, M., Finkbeiner, W., Widdicombe, J., 1993.** Cultures of bovine tracheal epithelium with differentiated ultrastructure and ion transport. *In Vitro Cellular & Developmental Biology-Animal* 29, 19-24.
- Koppers-Lalic, D., Verweij, M.C., Lipińska, A.D., Wang, Y., Quinten, E., Reits, E.A., Koch, J., Loch, S., Rezende, M.M., Daus, F., 2008.** Varicellovirus UL49. 5 proteins differentially affect the function of the transporter associated with antigen processing, TAP. *PLoS pathogens* 4, e1000080.
- Kraehenbuhl, J.P., Neutra, M.R., 1992.** Molecular and cellular basis of immune protection of mucosal surfaces. *Physiological reviews* 72, 853-879.
- Kumanomido, T., Akiyama, Y., 1975.** Immuno-effect of serum and nasal antibody against experimental inoculation with influenza A-Equi-2 virus. *Experimental Reports of Equine Health Laboratory* 1975, 44-52.
- Kurtz, B.M., Singletary, L.B., Kelly, S.D., Frampton, A.R., Jr., 2010.** Equus caballus major histocompatibility complex class I is an entry receptor for equine herpesvirus type 1. *J Virol* 84, 9027-9034.
- Kwak, Y.-K., Vikström, E., Magnusson, K.-E., Vécsey-Semjén, B., Colque-Navarro, P., Möllby, R., 2012.** The Staphylococcus aureus Alpha-Toxin Perturbs the Barrier Function in Caco-2 Epithelial Cell Monolayers by Altering Junctional Integrity. *Infection and Immunity* 80, 1670-1680.
- Kydd, J.H., Smith, K., Hannant, D., Livesay, G.J., Mumford, J.A., 1994.** Distribution of Equid herpesvirus-1 (EHV-1) in respiratory tract associated lymphoid tissue: implications for cellular immunity. *Equine Veterinary Journal* 26, 470-473.

- Laan, T.T., Bull, S., Pirie, R., Fink-Gremmels, J., 2006.** The role of alveolar macrophages in the pathogenesis of recurrent airway obstruction in horses. *J Vet Intern Med* 20, 167-174.
- Landolt, G.A., 2014.** Equine influenza virus. *Veterinary Clinics: Equine Practice* 30, 507-522.
- Larsen, L.E., Storgaard, T., Holm, E., 2001.** Phylogenetic characterisation of the GL sequences of equine arteritis virus isolated from semen of asymptomatic stallions and fatal cases of equine viral arteritis in Denmark. *Veterinary microbiology* 80, 339-346.
- Laval, K., 2016.** Equine CD172a⁺ Monocytic Cells, the ‘Trojan Horse’ for Equine Herpesvirus Type 1 (EHV-1) Dissemination in the Horse, Faculty of Veterinary Medicine. Ghent University, Merelbeke.
- Laval, K., Favoreel, H.W., Nauwynck, H.J., 2015a.** Equine herpesvirus type 1 replication is delayed in CD172a⁺ monocytic cells and controlled by histone deacetylases. *The Journal of general virology* 96, 118-130.
- Laval, K., Favoreel, H.W., Poelaert, K.C., Van Cleemput, J., Nauwynck, H.J., 2015b.** Equine herpesvirus type 1 enhances viral replication in CD172a⁺ monocytic cells upon adhesion to endothelial cells. *Journal of virology* 89, 10912-10923.
- Laval, K., Favoreel, H.W., Van Cleemput, J., Poelaert, K.C.K., Brown, I.K., Verhasselt, B., Nauwynck, H.J., 2016.** Entry of equid herpesvirus 1 into CD172a⁺ monocytic cells. *Journal of General Virology* 97, 733-746.
- Laval, K., Van Cleemput, J., Poelaert, K.C., Brown, I.K., Nauwynck, H.J., 2017.** Replication of neurovirulent equine herpesvirus type 1 (EHV-1) in CD172a⁺ monocytic cells. *Comparative immunology, microbiology and infectious diseases* 50, 58-62.
- Layman, Q.D., Rezabek, G.B., Ramachandran, A., Love, B.C., Confer, A.W., 2014.** A retrospective study of equine actinobacillosis cases: 1999–2011. *Journal of Veterinary Diagnostic Investigation* 26, 365-375.
- Leach, N.R., Roller, R.J., 2010.** Significance of host cell kinases in herpes simplex virus type 1 egress and lamin-associated protein disassembly from the nuclear lamina. *Virology* 406, 127-137.
- Leikina, E., Delanoe-Ayari, H., Melikov, K., Cho, M.-S., Chen, A., Waring, A.J., Wang, W., Xie, Y., Loo, J.A., Lehrer, R.I., 2005.** Carbohydrate-binding molecules inhibit viral fusion and entry by crosslinking membrane glycoproteins. *Nature immunology* 6, 995.
- Lekeux, P., Art, T., Hodgson, D.R., 2014.** Chapter 9 - The respiratory system: Anatomy, physiology, and adaptations to exercise and training, *The Athletic Horse (Second Edition)*. W.B. Saunders, pp. 125-154.
- Lepage, O.M., Perron, M.F., Cadore, J.L., 2004.** The mystery of fungal infection in the guttural pouches. *Veterinary journal (London, England : 1997)* 168, 60-64.
- Letek, M., Ocampo-Sosa, A.A., Sanders, M., Fogarty, U., Buckley, T., Leadon, D.P., González, P., Scortti, M., Meijer, W.G., Parkhill, J., 2008.** Evolution of the *Rhodococcus equi* vap pathogenicity island seen through comparison of host-associated vapA and vapB virulence plasmids. *Journal of bacteriology* 190, 5797-5805.
- Li, Y., Negussie, H., Qiu, Y., Reddy, V.R., Mateusen, B., Nauwynck, H.J., 2016.** Early events of canine herpesvirus 1 infections in canine respiratory and genital mucosae by the use of *ex vivo* models. *Research in veterinary science* 105, 205-208.
- Li, Y., Van Cleemput, J., Qiu, Y., Reddy, V.R., Mateusen, B., Nauwynck, H.J., 2015.** *Ex vivo* modeling of feline herpesvirus replication in ocular and respiratory mucosae, the primary targets of infection. *Virus research* 210, 227-231.
- Liesener, K., Curtui, V., Dietrich, R., Märtilbauer, E., Usleber, E., 2010.** Mycotoxins in horse feed. *Mycotoxin research* 26, 23-30.
- Lin, C., Holland Jr, R.E., Donofrio, J.C., McCoy, M.H., Tudor, L.R., Chambers, T.M., 2002.** Caspase activation in equine influenza virus induced apoptotic cell death. *Veterinary microbiology* 84, 357-365.
- Litjens, S.H., de Pereda, J.M., Sonnenberg, A., 2006.** Current insights into the formation and breakdown of hemidesmosomes. *Trends in cell biology* 16, 376-383.
- Livraghi, A., Randell, S.H., 2007.** Cystic Fibrosis and Other Respiratory Diseases of Impaired Mucus Clearance. *Toxicologic pathology* 35, 116-129.

- Longphre, M., Li, D., Gallup, M., Drori, E., Ordonez, C., Redman, T., Wenzel, S., Bice, D., Fahy, J., Basbaum, C., 1999.** Allergen-induced IL-9 directly stimulates mucin transcription in respiratory epithelial cells. *The Journal of clinical investigation* 104, 1375-1382.
- Ma, G., Feineis, S., Osterrieder, N., Van de Walle, G.R., 2012.** Identification and characterization of equine herpesvirus type 1 pUL56 and its role in virus-induced downregulation of major histocompatibility complex class I. *Journal of virology* 86, 3554-3563.
- Ma, J.Y., Ma, J.K., 2002.** The dual effect of the particulate and organic components of diesel exhaust particles on the alteration of pulmonary immune/inflammatory responses and metabolic enzymes. *Journal of Environmental Science and Health, Part C* 20, 117-147.
- Maanen, C.v., Oldruitenborgh-Oosterbaan, M.S., Damen, E., Derksen, A., 2001.** Neurological disease associated with EHV-1-infection in a riding school: clinical and virological characteristics. *Equine Veterinary Journal* 33, 191-196.
- Machida, N., Taniguchi, T., Nakamura, T., Kiryu, K., 1997.** Cardio-histopathological observations on aborted equine fetuses infected with equid herpesvirus 1 (EHV-1). *Journal of comparative pathology* 116, 379-385.
- MacLachlan, N., Balasuriya, U., Rossitto, P., Hullinger, P., Patton, J., Wilson, W., 1996.** Fatal experimental equine arteritis virus infection of a pregnant mare: immunohistochemical staining of viral antigens. *Journal of Veterinary Diagnostic Investigation* 8, 367-374.
- Mair, T.S., Batten, E.H., Stokes, C.R., Bourne, F.J., 1987.** The histological features of the immune system of the equine respiratory tract. *Journal of Comparative Pathology* 97, 575-586.
- Mair, T.S., Batten, E.H., Stokes, C.R., Bourne, F.J., 1988.** The distribution of mucosal lymphoid nodules in the equine respiratory tract. *Journal of Comparative Pathology* 99, 159-168.
- Mair, T.S., Derksen, F.J., 2000.** Chronic obstructive pulmonary disease: a review. *Equine Veterinary Education* 12, 35-44.
- Mair, T.S., Lane, J.G., 2005.** Diseases of the equine trachea. *Equine Veterinary Education* 17, 146-149.
- Marasas, W.F.O., Kellerman, T.S., Gelderblom, W.C., Thiel, P., Van der Lugt, J.J., Coetzer, J.A., 2014.** Leukoencephalomalacia in a horse induced by fumonisin B₁ isolated from *Fusarium moniliforme*.
- Marenzoni, M.L., Coppola, G., Maranesi, M., Passamonti, F., Cappelli, K., Capomaccio, S., Verini Supplizi, A., Thiry, E., Coletti, M., 2010.** Age-dependent prevalence of equid herpesvirus 5 infection. *Veterinary Research Communications* 34, 703-708.
- Marriott, C., 1990.** Mucus and mucociliary clearance in the respiratory tract. *Advanced Drug Delivery Reviews* 5, 19-35.
- Marshall, M., Bohach, G., Boehm, D., 2000.** Characterization of *Staphylococcus aureus* beta-toxin induced leukotoxicity. *Journal of natural toxins* 9, 125-138.
- Martella, V., Elia, G., Decaro, N., Di Trani, L., Lorusso, E., Campolo, M., Desario, C., Parisi, A., Cavaliere, N., Buonavoglia, C., 2007.** An outbreak of equine influenza virus in vaccinated horses in Italy is due to an H3N8 strain closely related to recent North American representatives of the Florida sub-lineage. *Veterinary microbiology* 121, 56-63.
- Matsumura, T., Kondo, T., Sugita, S., Damiani, A.M., O'Callaghan, D.J., Imagawa, H., 1998.** An equine herpesvirus type 1 recombinant with a deletion in the gE and gI genes is avirulent in young horses. *Virology* 242, 68-79.
- Matter, K., Balda, M.S., 2003.** Functional analysis of tight junctions. *Methods (San Diego, Calif.)* 30, 228-234.
- McCann, S., Mumford, J., Binns, M., 1995.** Development of PCR assays to detect genetic variation amongst equine herpesvirus-1 isolates as an aid to epidemiological investigation. *Journal of virological methods* 52, 183-194.
- McCollum, W., Prickett, M., Bryans, J., 1971.** Temporal distribution of equine arteritis virus in respiratory mucosa, tissues and body fluids of horses infected by inhalation. *Research in veterinary science* 12, 459.
- McGavin, M.D., Zachary, J.F., 2007.** *Pathological basis of veterinary disease*. Mosby Elsevier.
- McKenna, O.E., Posselt, G., Briza, P., Lackner, P., Schmitt, A.O., Gadermaier, G., Wessler, S., Ferreira, F., 2017.** Multi-Approach Analysis for the Identification of Proteases within Birch Pollen. *International journal of molecular sciences* 18, 1433.

- Mekuria, Z.H., El-Hage, C., Ficorilli, N.P., Washington, E.A., Gilkerson, J.R., Hartley, C.A., 2017.** Mapping B lymphocytes as major reservoirs of naturally occurring latent equine herpesvirus 5 infection. *Journal of General Virology* 98, 461-470.
- Meldrum, K., Gant, T.W., Leonard, M.O., 2017.** Diesel exhaust particulate associated chemicals attenuate expression of CXCL10 in human primary bronchial epithelial cells. *Toxicology in Vitro* 45, 409-416.
- Mohankumar, S., Senthilkumar, P., 2017.** Particulate matter formation and its control methodologies for diesel engine: A comprehensive review. *Renewable and Sustainable Energy Reviews* 80, 1227-1238.
- Monreal, L., Villatoro, A., Hooghuis, H., Ros, I., Timoney, P., 1995.** Clinical features of the 1992 outbreak of equine viral arteritis in Spain. *Equine veterinary journal* 27, 301-304.
- Moore, B.D., Balasuriya, U.B., Hedges, J.F., MacLachlan, N.J., 2002.** Growth characteristics of a highly virulent, a moderately virulent, and an avirulent strain of equine arteritis virus in primary equine endothelial cells are predictive of their virulence to horses. *Virology* 298, 39-44.
- Mora, A.L., Woods, C.R., Garcia, A., Xu, J., Rojas, M., Speck, S.H., Roman, J., Brigham, K.L., Stecenko, A.A., 2005.** Lung infection with γ -herpesvirus induces progressive pulmonary fibrosis in Th2-biased mice. *American Journal of Physiology-Lung Cellular and Molecular Physiology* 289, L711-L721.
- Mumford, J.A., Hannant, D., Jessett, D., O'Neil, T., Smith, K., Ostlund, E., 1994.** Abortigenic and neurological disease caused by experimental infection with equid herpesvirus-1.
- Murray, M.J., Piero, F., Jeffrey, S.C., Davis, M.S., Furr, M.O., Dubovi, E.J., Mayo, J.A., 1998.** Neonatal equine herpesvirus type 1 infection on a thoroughbred breeding farm. *Journal of Veterinary Internal Medicine* 12, 36-41.
- Myers, C., Wilson, W.D., 2006.** Equine influenza virus. *Clinical Techniques in Equine Practice* 5, 187-196.
- Negussie, H., Li, Y., Tessema, T.S., Nauwynck, H.J., 2016.** Replication characteristics of equine herpesvirus 1 and equine herpesvirus 3: comparative analysis using *ex vivo* tissue cultures. *Veterinary Research* 47, 19.
- Neu, S.M., Timoney, P.J., McCollum, W.H., 1988.** Persistent infection of the reproductive tract in stallions experimentally infected with equine arteritis virus, *Proceedings of the 5th Conf Equine Infec Dis*, pp. 149-154.
- Neubauer, A., Braun, B., Brandmuller, C., Kaaden, O.R., Osterrieder, N., 1997.** Analysis of the contributions of the equine herpesvirus 1 glycoprotein gB homolog to virus entry and direct cell-to-cell spread. *Virology* 227, 281-294.
- Neubauer, A., Osterrieder, N., 2004.** Equine herpesvirus type 1 (EHV-1) glycoprotein K is required for efficient cell-to-cell spread and virus egress. *Virology* 329, 18-32.
- Nevo, A., Weisman, Z., Sade, J., 1975.** Cell proliferation and cell differentiation in tissue cultures of adult muco-ciliary epithelia. *Differentiation* 3, 79-90.
- Newton, J., Wood, J., Castillo-Olivares, F., Mumford, J., 1999.** arteritis in the United Kingdom since the outbreak in 1993. *Veterinary record* 145, 511-516.
- Niesalla, H., Dale, A., Slater, J., Scholes, S., Archer, J., Maskell, D., Tucker, A., 2009.** Critical assessment of an *in vitro* bovine respiratory organ culture system: a model of bovine herpesvirus-1 infection. *Journal of virological methods* 158, 123-129.
- Niyonsaba, F., Kiatsurayanon, C., Ogawa, H., 2016.** The role of human β -defensins in allergic diseases. *Clinical & Experimental Allergy* 46, 1522-1530.
- Nugent, J., Birch-Machin, I., Smith, K., Mumford, J., Swann, Z., Newton, J., Bowden, R., Allen, G., Davis-Poynter, N., 2006.** Analysis of equid herpesvirus 1 strain variation reveals a point mutation of the DNA polymerase strongly associated with neuropathogenic versus nonneuropathogenic disease outbreaks. *Journal of virology* 80, 4047-4060.
- Ogunade, I., Martinez-Tuppi, C., Queiroz, O., Jiang, Y., Drouin, P., Wu, F., Vyas, D., Adesogan, A., 2018.** Silage review: Mycotoxins in silage: Occurrence, effects, prevention, and mitigation. *Journal of dairy science* 101, 4034-4059.
- Olson, L., Perkowski, S., Mason, D., 1989.** Isoproterenol-and salbutamol-induced relaxation of acetylcholine-and histamine-induced contraction of equine trachealis muscle *in vitro*. *American journal of veterinary research* 50, 1715-1719.

- Osterrieder, N., 1999.** Construction and characterization of an equine herpesvirus 1 glycoprotein C negative mutant. *Virus Res* 59, 165-177.
- Osterrieder, N., Neubauer, A., Brandmuller, C., Braun, B., Kaaden, O.R., Baines, J.D., 1996.** The equine herpesvirus 1 glycoprotein gp21/22a, the herpes simplex virus type 1 gM homolog, is involved in virus penetration and cell-to-cell spread of virions. *Journal of virology* 70, 4110-4115.
- Parillo, F., Arias, M.P., Supplizi, A.V., 2009.** Glycoprofile of the different cell types present in the mucosa of the horse guttural pouches. *Tissue and Cell* 41, 257-265.
- Park, S.K., Lee, W.J., Yang, Y.I., 2007.** Organ culture at the air-liquid interface maintains structural and functional integrities of inflammatory and fibrovascular cells of nasal polyps. *American journal of rhinology* 21, 402-407.
- Patel, J., Edington, N., Mumford, J., 1982.** Variation in cellular tropism between isolates of equine herpesvirus-1 in foals. *Archives of virology* 74, 41-51.
- Pazgier, M., Hoover, D., Yang, D., Lu, W., Lubkowski, J., 2006.** Human β -defensins. *Cellular and Molecular Life Sciences CMLS* 63, 1294-1313.
- Pelkonen, S., Lindahl, S.B., Suomala, P., Karhukorpi, J., Vuorinen, S., Koivula, I., Väisänen, T., Pentikäinen, J., Autio, T., Tuuminen, T., 2013.** Transmission of *Streptococcus equi* subspecies *zooepidemicus* infection from horses to humans. *Emerging infectious diseases* 19, 1041-1048.
- Perkins, G.A., Goodman, L.B., Tsujimura, K., Van de Walle, G.R., Kim, S.G., Dubovi, E.J., Osterrieder, N., 2009.** Investigation of the prevalence of neurologic equine herpes virus type 1 (EHV-1) in a 23-year retrospective analysis (1984-2007). *Veterinary microbiology* 139, 375-378.
- Piero, F.d., Wilkins, P.A., Lopez, J., Glaser, A.L., Dubovi, E., Schlafer, D., Lein, D., 1997.** Equine viral arteritis in newborn foals: clinical, pathological, serological, microbiological and immunohistochemical observations. *Equine veterinary journal* 29, 178-185.
- Plopper, C.G., Mariassy, A.T., Hill, L.H., 1980.** Ultrastructure of the nonciliated bronchiolar epithelial (Clara) cell of mammalian lung: II. A comparison of horse, steer, sheep, dog, and cat. *Experimental lung research* 1, 155-169.
- Pol, J.M., 1990.** Interferons affect the morphogenesis and virulence of pseudorabies virus. Interferons affect the morphogenesis and virulence of pseudorabies virus.
- Poth, T., Niedermaier, G., Hermanns, W., 2009.** Equine multinodular pulmonary fibrosis in association with an EHV-5 infection in 5 horses. *Wiener Tierärztliche Monatsschrift* 96, 203-208.
- Powell, D., Watkins, K., Li, P., Shortridge, K., 1995.** Outbreak of equine influenza among horses in Hong Kong during 1992. *Vet Rec* 136, 531-536.
- Pozzi, A., Yurchenco, P.D., Iozzo, R.V., 2017.** The nature and biology of basement membranes. *Matrix Biology* 57-58, 1-11.
- Prickett, M., 1970.** pathology of disease caused by equine herpesvirus 1, *Int Conf Equine Infec Dis Proc.*
- Proud, D., Sanders, S.P., Wiehler, S., 2004.** Human rhinovirus infection induces airway epithelial cell production of human beta-defensin 2 both *in vitro* and *in vivo*. *Journal of immunology (Baltimore, Md. : 1950)* 172, 4637-4645.
- Pusterla, N., Mapes, S., Akana, N., Barnett, C., MacKenzie, C., Gaughan, E., Craig, B., Chappell, D., Vaala, W., 2016.** Prevalence factors associated with equine herpesvirus type 1 infection in equids with upper respiratory tract infection and/or acute onset of neurological signs from 2008 to 2014. *Veterinary Record* 178, 70-70.
- Pusterla, N., Watson, J., Affolter, V., Magdesian, K., Wilson, W., Carlson, G., 2003.** Purpura haemorrhagica in 53 horses. *Vet Rec* 153, 118-121.
- Quinones-Mateu, M.E., Lederman, M.M., Feng, Z., Chakraborty, B., Weber, J., Rangel, H.R., Marotta, M.L., Mirza, M., Jiang, B., Kiser, P., Medvik, K., Sieg, S.F., Weinberg, A., 2003.** Human epithelial beta-defensins 2 and 3 inhibit HIV-1 replication. *AIDS (London, England)* 17, F39-48.
- Quintana, A.M., Landolt, G.A., Annis, K.M., Hussey, G.S., 2011.** Immunological characterization of the equine airway epithelium and of a primary equine airway epithelial cell culture model. *Veterinary Immunology and Immunopathology* 140, 226-236.
- Radlowski, M., 2005.** Proteolytic enzymes from generative organs of flowering plants (Angiospermae). *J Appl Genet* 46, 247-257.

- Randell, S.H., Boucher, R.C., 2006.** Effective mucus clearance is essential for respiratory health. *American journal of respiratory cell and molecular biology* 35, 20-28.
- Rappocciolo, G., Birch, J., Ellis, S.A., 2003.** Down-regulation of MHC class I expression by equine herpesvirus-1. *Journal of General Virology* 84, 293-300.
- Rawlings, N.D., Barrett, A.J., 1994.** Chapter 2 - Families of serine peptidases, *Methods in enzymology*. Elsevier, pp. 19-61.
- Reddy, V., Steukers, L., Li, Y., Fuchs, W., Vanderplasschen, A., Nauwynck, H., 2014.** The replication characteristics of infectious laryngotracheitis virus (ILTV) in the respiratory and conjunctival mucosa. *Avian Pathology: Journal of the WVPA* 21, 1-30.
- Reed, S.M., Toribio, R.E., 2004.** Equine herpesvirus 1 and 4. *Veterinary Clinics: Equine Practice* 20, 631-642.
- Reiner, S.L., 2007.** Development in motion: helper T cells at work. *Cell* 129, 33-36.
- Reis, H., Reis, C., Sharip, A., Reis, W., Zhao, Y., Sinclair, R., Beeson, L., 2018.** Diesel exhaust exposure, its multi-system effects, and the effect of new technology diesel exhaust. *Environment international* 114, 252-265.
- Ren, D., Daines, D.A., 2011.** Use of the EpiAirway model for characterizing long-term host-pathogen interactions. *Journal of visualized experiments: JoVE*.
- Reuss, S.M., Chaffin, M.K., Cohen, N.D., 2009.** Extrapulmonary disorders associated with *Rhodococcus equi* infection in foals: 150 cases (1987–2007). *Journal of the American Veterinary Medical Association* 235, 855-863.
- Rivedal, E., Witz, G., 2005.** Metabolites of benzene are potent inhibitors of gap-junction intercellular communication. *Archives of toxicology* 79, 303-311.
- Robinson, C., Kalsheker, N., Srinivasan, N., King, C., Garrod, D., Thompson, P., Stewart, G., 1997.** On the potential significance of the enzymatic activity of mite allergens to immunogenicity. Clues to structure and function revealed by molecular characterization. *Clinical & Experimental Allergy* 27, 10-21.
- Röhrl, J., Yang, D., Oppenheim, J.J., Hehlhans, T., 2010.** Human β -defensin 2 and 3 and their mouse orthologs induce chemotaxis through interaction with CCR2. *The Journal of Immunology* 184, 6688-6694.
- Roizman, B., Baines, J., 1991.** The diversity and unity of herpesviridae. *Comparative Immunology, Microbiology and Infectious Diseases* 14, 63-79.
- Roizmann, B., Desrosiers, R., Fleckenstein, B., Lopez, C., Minson, A., Studdert, M., 1992.** The family Herpesviridae: an update. *Archives of virology* 123, 425-449.
- Rowe, R.K., Brody, S.L., Pekosz, A., 2004.** Differentiated cultures of primary hamster tracheal airway epithelial cells. *In Vitro Cellular & Developmental Biology-Animal* 40, 303-311.
- Rudolph, J., Osterrieder, N., 2002.** Equine herpesvirus type 1 devoid of gM and gp2 is severely impaired in virus egress but not direct cell-to-cell spread. *Virology* 293, 356-367.
- Rudolph, J., Seyboldt, C., Granzow, H., Osterrieder, N., 2002.** The gene 10 (UL49. 5) product of equine herpesvirus 1 is necessary and sufficient for functional processing of glycoprotein M. *Journal of virology* 76, 2952-2963.
- Runswick, S., Mitchell, T., Davies, P., Robinson, C., Garrod, D.R., 2007.** Pollen proteolytic enzymes degrade tight junctions. *Respirology (Carlton, Vic.)* 12, 834-842.
- Rush, B., Mair, T., 2008.** *Equine respiratory diseases*. John Wiley & Sons.
- Saito, T., Kawaoka, Y., Webster, R.G., 1993.** Phylogenetic analysis of the N8 neuraminidase gene of influenza A viruses. *Virology* 193, 868-876.
- Sajjan, U., Wang, Q., Zhao, Y., Gruenert, D.C., Hershenson, M.B., 2008.** Rhinovirus disrupts the barrier function of polarized airway epithelial cells. *American journal of respiratory and critical care medicine* 178, 1271-1281.
- Salvi, A., Patki, G., Liu, H., Salim, S., 2017.** Psychological Impact of Vehicle Exhaust Exposure: Insights from an Animal Model. *Scientific reports* 7, 8306.
- Sang, Y., Ortega, M.T., Blecha, F., Prakash, O., Melgarejo, T., 2005.** Molecular cloning and characterization of three beta-defensins from canine testes. *Infect Immun* 73, 2611-2620.
- Sarkar, S., Balasuriya, U.B., Horohov, D.W., Chambers, T.M., 2015.** Equine herpesvirus-1 suppresses type-I interferon induction in equine endothelial cells. *Veterinary immunology and immunopathology* 167, 122-129.

- Sasaki, M., Hasebe, R., Makino, Y., Suzuki, T., Fukushi, H., Okamoto, M., Matsuda, K., Taniyama, H., Sawa, H., Kimura, T., 2011.** Equine major histocompatibility complex class I molecules act as entry receptors that bind to equine herpesvirus-1 glycoprotein D. *Genes to cells : devoted to molecular & cellular mechanisms* 16, 343-357.
- Sato, A., 2007.** Tuft cells. *Anatomical Science International* 82, 187-199.
- Saxegaard, F., 1966.** Isolation and identification of equine rhinopneumonitis virus (equine abortion virus) from cases of abortion and paralysis. *Nord. Vet. Med* 18, 504-512.
- Saxegaard, F., Teige Jr, J., Fjellheim, P., 1971.** Equine bronchopneumonia caused by *Bordetella bronchiseptica*. A case report. *Acta Veterinaria Scandinavica* 12, 114.
- Schierhorn, K., Brunnée, T., Paus, R., Schultz, K.-D., Niehus, J., Agha-Mir-Salim, P., Kunkel, G., 1995.** Gelatin sponge-supported histoculture of human nasal mucosa. *In Vitro Cellular & Developmental Biology-Animal* 31, 215-220.
- Schroeder, B.O., Wu, Z.H., Nuding, S., Groscurth, S., Marcinowski, M., Beisner, J., Buchner, J., Schaller, M., Stange, E.F., Wehkamp, J., 2011.** Reduction of disulphide bonds unmasks potent antimicrobial activity of human beta-defensin 1. *Nature* 469, 419.
- Schulzke, J., Gitter, A., Mankertz, J., Spiegel, S., Seidler, U., Amasheh, S., Saitou, M., Tsukita, S., Fromm, M., 2005.** Epithelial transport and barrier function in occludin-deficient mice. *Biochimica et biophysica acta (BBA)-Biomembranes* 1669, 34-42.
- Schumann, B., Winkler, J., Mickenautsch, N., Warnken, T., Dänicke, S., 2016.** Effects of deoxynivalenol (DON), zearalenone (ZEN), and related metabolites on equine peripheral blood mononuclear cells (PBMC) *in vitro* and background occurrence of these toxins in horses. *Mycotoxin research* 32, 153-161.
- Schwab, U.E., Fulcher, M.L., Randell, S.H., Flaminio, M.J., Russell, D.G., 2010.** Equine bronchial epithelial cells differentiate into ciliated and mucus producing cells *in vitro*. *In Vitro Cellular & Developmental Biology-Animal* 46, 102-106.
- Schweppe, R.E., Korch, C., 2018.** Challenges and Advances in the Development of Cell Lines and Xenografts. *Advances in Molecular Pathology* 1, 239-251.
- Scott, J.C., Dutta, S., Myrup, A., 1983.** *In vivo* harboring of equine herpesvirus-1 in leukocyte populations and subpopulations and their quantitation from experimentally infected ponies. *American journal of veterinary research* 44, 1344.
- Sekiguchi, R., Yamada, K.M., 2018.** Chapter Four - Basement Membranes in Development and Disease, in: Litscher, E.S., Wassarman, P.M. (Eds.), *Current Topics in Developmental Biology*. Academic Press, pp. 143-191.
- Selsted, M.E., Ouellette, A.J., 2005.** Mammalian defensins in the antimicrobial immune response. *Nature immunology* 6, 551-557.
- Shannon-Lowe, C., Rowe, M., 2011.** Epstein-Barr Virus Infection of Polarized Epithelial Cells via the Basolateral Surface by Memory B Cell-Mediated Transfer Infection. *PLoS Pathogens* 7, e1001338.
- Shapiro, L., Weis, W.I., 2009.** Structure and biochemistry of cadherins and catenins. *Cold Spring Harbor perspectives in biology* 1, a003053.
- Sheppard, D., 1998.** Airway epithelial integrins: why so many? *American journal of respiratory cell and molecular biology* 19, 349-351.
- Sieber, S., Gerber, V., Jandova, V., Rossano, A., Evison, J.M., Perreten, V., 2011.** Evolution of multidrug-resistant *Staphylococcus aureus* infections in horses and colonized personnel in an equine clinic between 2005 and 2010. *Microbial drug resistance* 17, 471-478.
- Sieczkarski, S.B., Brown, H.A., Whittaker, G.R., 2003.** Role of protein kinase C β II in influenza virus entry via late endosomes. *Journal of virology* 77, 460-469.
- Siedek, E., Whelan, M., Edington, N., Hamblin, A., 1999.** Equine herpesvirus type 1 infects dendritic cells *in vitro*: stimulation of T lymphocyte proliferation and cytotoxicity by infected dendritic cells. *Veterinary immunology and immunopathology* 67, 17-32.
- Skehel, J.J., Schild, G., 1971.** The polypeptide composition of influenza A viruses. *Virology* 44, 396-408.
- Slater, J., 2007.** Bacterial infections of the equine respiratory tract, *Equine Respiratory Medicine and Surgery*. Elsevier, pp. 327-353.

- Slater, J.D., Borchers, K., Thackray, A.M., Field, H.J., 1994.** The trigeminal ganglion is a location for equine herpesvirus 1 latency and reactivation in the horse. *The Journal of general virology* 75 (8), 2007-2016.
- Smith, D., Hamblin, A., Edington, N., 2002.** Equid herpesvirus 1 infection of endothelial cells requires activation of putative adhesion molecules: an *in vitro* model. *Clinical and Experimental Immunology* 129, 281-287.
- Smith, D.J., Hamblin, A.S., Edington, N., 2001.** Infection of endothelial cells with Equine herpesvirus-1 (EHV-1) occurs where there is activation of putative adhesion molecules: a mechanism for transfer of virus. *Equine Veterinary Journal* 33, 138-142.
- Smith, J.G., Nemerow, G.R., 2008.** Mechanism of adenovirus neutralization by human α -defensins. *Cell host & microbe* 3, 11-19.
- Smith, K., McGladdery, A., Binns, M., Mumford, J., 1997.** Use of transabdominal ultrasound-guided amniocentesis for detection of equid herpesvirus 1-induced foetal infection in utero. *American journal of veterinary research* 58, 997-1002.
- Smith, K., Whitwell, K.E., Mumford, J.A., Gower, S.M., Hannant, D., Tearle, J., 1993.** An immunohistological study of the uterus of mares following experimental infection by equid herpesvirus 1. *Equine Veterinary Journal* 25, 36-40.
- Smith, K.C., Mumford, J.A., Lakhani, K., 1996.** A comparison of equid herpesvirus-1 (EHV-1) vascular lesions in the early versus late pregnant equine uterus. *Journal of Comparative Pathology* 114, 231-247.
- Smith, P.M., Kahan, S.M., Rorex, C.B., von Einem, J., Osterrieder, N., O'Callaghan, D.J., 2005.** Expression of the full-length form of gp2 of equine herpesvirus 1 (EHV-1) completely restores respiratory virulence to the attenuated EHV-1 strain KyA in CBA mice. *Journal of virology* 79, 5105-5115.
- Song, J., Ye, S., 1997.** Effects of diesel exhaust particle on gap junction intercellular communication. *Wei sheng yan jiu= Journal of hygiene research* 26, 145-147.
- Sovinova, O., Tumova, B., Pouska, F., Nemeč, J., 1958.** Isolation of a virus causing respiratory disease in horses. *Acta virologica* 2, 52.
- Spießchaert, B., Goldenbogen, B., Taferner, S., Schade, M., Mahmoud, M., Klipp, E., Osterrieder, N., Azab, W., 2015.** Role of gB and pUS3 in equine herpesvirus 1 transfer between peripheral blood mononuclear cells and endothelial cells: a dynamic *in vitro* model. *Journal of virology* 89, 11899-11908.
- Spilman, M.S., Welbon, C., Nelson, E., Dokland, T., 2009.** Cryo-electron tomography of porcine reproductive and respiratory syndrome virus: organization of the nucleocapsid. *The Journal of general virology* 90, 527-535.
- Srinivasan, B., Kolli, A.R., Esch, M.B., Abaci, H.E., Shuler, M.L., Hickman, J.J., 2015.** TEER measurement techniques for *in vitro* barrier model systems. *Journal of laboratory automation* 20, 107-126.
- Staehein, L.A., 1974.** Structure and function of intercellular junctions. *International review of cytology* 39, 191-283.
- Stahl, G.H., Ellis, D.B., 1973.** Biosynthesis of respiratory-tract mucins. A comparison of canine epithelial goblet-cell and submucosal-gland secretions. *Biochemical Journal* 136, 845-850.
- Steukers, L., Vandekerckhove, A.P., Van den Broeck, W., Glorieux, S., Nauwynck, H.J., 2012.** Kinetics of BoHV-1 dissemination in an *in vitro* culture of bovine upper respiratory tract mucosa explants. *ILAR journal* 53, E43-54.
- Studdert, M., 1996.** Orthomyxoviridae. *Virus Infections of Equines*. Elsevier Science Publishers, Amsterdam, 281-284.
- Sutcliffe, I.C., Brown, A.K., Dover, L.G., 2010.** The rhodococcal cell envelope: composition, organisation and biosynthesis, *Biology of Rhodococcus*. Springer, pp. 29-71.
- Suzuki, Y., Ito, T., Suzuki, T., Holland, R.E., Chambers, T.M., Kiso, M., Ishida, H., Kawaoka, Y., 2000.** Sialic acid species as a determinant of the host range of influenza A viruses. *Journal of virology* 74, 11825-11831.
- Swanson, R., Edlund, A.F., Preuss, D., 2004.** Species specificity in pollen-pistil interactions. *Annual review of genetics* 38, 793-818.

- Sweeney, C.R., Timoney, J.F., Newton, J.R., Hines, M.T., 2005.** Streptococcus equi Infections in Horses: Guidelines for Treatment, Control, and Prevention of Strangles. *Journal of Veterinary Internal Medicine* 19, 123-134.
- Takahashi, T., Unuma, S., Kawagishi, S., Kurebayashi, Y., Takano, M., Yoshino, H., Minami, A., Yamanaka, T., Otsubo, T., Ikeda, K., 2016.** Substrate specificity of equine and human influenza A virus sialidase to molecular species of sialic acid. *Biological and Pharmaceutical Bulletin* 39, 1728-1733.
- Takai, Y., Nakanishi, H., 2003.** Nectin and afadin: novel organizers of intercellular junctions. *Journal of cell science* 116, 17-27.
- Taketomi, E.A., Sopelete, M.C., Moreira, P.F.d.S., Vieira, F.d.A.M., 2006.** Pollen allergic disease: pollens and its major allergens. *Revista Brasileira de Otorrinolaringologia* 72, 562-567.
- Telford, E., Studdert, M., Agius, C., Watson, M., Aird, H., Davison, A., 1993.** Equine herpesviruses 2 and 5 are γ -herpesviruses. *Virology* 195, 492-499.
- Telford, E.A., Watson, M.S., McBride, K., Davison, A.J., 1992.** The DNA sequence of equine herpesvirus-1. *Virology* 189, 304-316.
- Thormann, N., Van de Walle, G.R., Azab, W., Osterrieder, N., 2012.** The role of secreted glycoprotein G of equine herpesvirus type 1 and type 4 (EHV-1 and EHV-4) in immune modulation and virulence. *Virus research* 169, 203-211.
- Timoney, J., Kumar, P., 2008.** Early pathogenesis of equine Streptococcus equi infection (strangles). *Equine veterinary journal* 40, 637-642.
- Timoney, J.F., 1993.** Strangles. *Veterinary Clinics of North America: Equine Practice* 9, 365-374.
- Timoney, P., 1984.** Clinical, virological and epidemiological features of the 1984 outbreak of equine viral arteritis in the Thoroughbred population in Kentucky, USA, *Proceedings of the Grayson Foundation International Conference of Thoroughbred Breeders Organizations, Ireland*, pp. 24-33.
- Timoney, P.J., McCollum, W.H., 1987.** Equine viral arteritis. *The Canadian Veterinary Journal* 28, 693.
- Timoney, P.J., McCollum, W.H., 1993.** Equine viral arteritis. *Veterinary Clinics of North America: Equine Practice* 9, 295-309.
- Totlandsdal, A.I., Låg, M., Lilleaas, E., Cassee, F., Schwarze, P., 2015.** Differential proinflammatory responses induced by diesel exhaust particles with contrasting PAH and metal content. *Environmental toxicology* 30, 188-196.
- Turner, A.J., Studdert, M.J., 1970.** Equine herpesviruses. 3. Isolation and epizootiology of slowly cytopathic viruses and the serological incidence of equine rhinopneumonitis. *Australian veterinary journal* 46, 581-586.
- Vaid, R.K., Shanmugasundaram, K., Anand, T., Bera, B.C., Tigga, M., Dedar, R., Riyesh, T., Bardwaj, S., Virmani, N., Tripathi, B.N., 2018.** Characterization of isolates of Bordetella bronchiseptica from horses. *Journal of equine science* 29, 25-31.
- Vairo, S., Favoreel, H., Scagliarini, A., Nauwynck, H., 2013.** Identification of target cells of a European equine arteritis virus strain in experimentally infected ponies. *Veterinary microbiology* 167, 235-241.
- Vairo, S., Vandekerckhove, A., Steukers, L., Glorieux, S., Van den Broeck, W., Nauwynck, H., 2012.** Clinical and virological outcome of an infection with the Belgian equine arteritis virus strain 08P178. *Veterinary microbiology* 157, 333-344.
- Van de Walle, G.R., May, M.L., Sukhumavasi, W., von Einem, J., Osterrieder, N., 2007.** Herpesvirus chemokine-binding glycoprotein G (gG) efficiently inhibits neutrophil chemotaxis *in vitro* and *in vivo*. *Journal of Immunology* 179, 4161-4169.
- Van de Walle, G.R., Peters, S.T., VanderVen, B.C., O'Callaghan, D.J., Osterrieder, N., 2008a.** Equine herpesvirus 1 entry via endocytosis is facilitated by alphaV integrins and an RSD motif in glycoprotein D. *J Virol* 82, 11859-11868.
- Van de Walle, G.R., Sakamoto, K., Osterrieder, N., 2008b.** CCL3 and viral chemokine-binding protein gg modulate pulmonary inflammation and virus replication during equine herpesvirus 1 infection. *Journal of virology* 82, 1714-1722.

- Van De Walle, J., Sergent, T., Piront, N., Toussaint, O., Schneider, Y.-J., Larondelle, Y., 2010.** Deoxynivalenol affects *in vitro* intestinal epithelial cell barrier integrity through inhibition of protein synthesis. *Toxicology and Applied Pharmacology* 245, 291-298.
- van der Meulen, K., Caij, A., Naawynck, H., Pensaert, M., 2001.** An outbreak of equine viral arteritis abortion in Belgium. *Vlaams Diergeneeskundig Tijdschrift* 70, 221-222.
- van der Meulen, K., Caij, B., Pensaert, M., Nauwynck, H., 2006.** Absence of viral envelope proteins in equine herpesvirus 1-infected blood mononuclear cells during cell-associated viremia. *Veterinary microbiology* 113, 265-273.
- van der Meulen, K.M., Nauwynck, H.J., Buddaert, W., Pensaert, M.B., 2000.** Replication of equine herpesvirus type 1 in freshly isolated equine peripheral blood mononuclear cells and changes in susceptibility following mitogen stimulation. *Journal of General Virology* 81, 21-25.
- van der Meulen, K.M., Nauwynck, H.J., Pensaert, M.B., 2002.** Increased susceptibility of peripheral blood mononuclear cells to equine herpes virus type 1 infection upon mitogen stimulation: a role of the cell cycle and of cell-to-cell transmission of the virus. *Veterinary microbiology* 86, 157-163.
- van der Meulen, K.M., Nauwynck, H.J., Pensaert, M.B., 2003.** Absence of viral antigens on the surface of equine herpesvirus-1-infected peripheral blood mononuclear cells: a strategy to avoid complement-mediated lysis. *Journal of general virology* 84, 93-97.
- Van Itallie, C.M., Anderson, J.M., 2006.** Claudins and epithelial paracellular transport. *Annu. Rev. Physiol.* 68, 403-429.
- Van Maanen, C., 2002.** Equine herpesvirus 1 and 4 infections: an update. *Veterinary Quarterly* 24, 57-78.
- Vandekerckhove, A., Glorieux, S., Van den Broeck, W., Gryspeerdt, A., van der Meulen, K.M., Nauwynck, H.J., 2009.** *In vitro* culture of equine respiratory mucosa explants. *Veterinary Journal* 181, 280-287.
- Vandekerckhove, A.P., Glorieux, S., Gryspeerdt, A.C., Steukers, L., Duchateau, L., Osterrieder, N., Van de Walle, G.R., Nauwynck, H.J., 2010.** Replication kinetics of neurovirulent versus non-neurovirulent equine herpesvirus type 1 strains in equine nasal mucosal explants. *The Journal of general virology* 91, 2019-2028.
- Vandekerckhove, A.P., Glorieux, S., Gryspeerdt, A.C., Steukers, L., Van Doorselaere, J., Osterrieder, N., Van de Walle, G.R., Nauwynck, H.J., 2011.** Equine alphaherpesviruses (EHV-1 and EHV-4) differ in their efficiency to infect mononuclear cells during early steps of infection in nasal mucosal explants. *Veterinary microbiology* 152, 21-28.
- Vandenput, S., Istasse, L., Nicks, B., Lekeux, P., 1997.** Airborne dust and aeroallergen concentrations in different sources of feed and bedding for horses. *Veterinary Quarterly* 19, 154-158.
- Vinhas, R., Cortes, L., Cardoso, I., Mendes, V.M., Manadas, B., Todo-Bom, A., Pires, E., Verissimo, P., 2011.** Pollen proteases compromise the airway epithelial barrier through degradation of transmembrane adhesion proteins and lung bioactive peptides. *Allergy* 66, 1088-1098.
- Virmani, N., Bera, B., Singh, B., Shanmugasundaram, K., Gulati, B., Barua, S., Vaid, R., Gupta, A., Singh, R., 2010.** Equine influenza outbreak in India (2008-09): virus isolation, sero-epidemiology and phylogenetic analysis of HA gene. *Veterinary microbiology* 143, 224-237.
- Vivier, E., Tomasello, E., Baratin, M., Walzer, T., Ugolini, S., 2008.** Functions of natural killer cells. *Nature immunology* 9, 503.
- von Einem, J., Smith, P.M., Van de Walle, G.R., O'Callaghan, D.J., Osterrieder, N., 2007.** *In vitro* and *in vivo* characterization of equine herpesvirus type 1 (EHV-1) mutants devoid of the viral chemokine-binding glycoprotein G (gG). *Virology* 362, 151-162.
- Voynow, J.A., Rubin, B.K., 2009.** Mucins, mucus, and sputum. *Chest* 135, 505-512.
- Waddell, G., 1963.** A New Influenza Virus Associated with Equine Respiratory Disease. *J. Amer. vet. med. Assoc.* 143, 587-590.
- Walker, J.E., Wells, R.E., Jr., Merrill, E.W., 1961.** Heat and water exchange in the respiratory tract. *Am J Med* 30, 259-267.
- Wang, L., Raidal, S.L., Pizzirani, A., Wilcox, G.E., 2007.** Detection of respiratory herpesviruses in foals and adult horses determined by nested multiplex PCR. *Veterinary microbiology* 121, 18-28.

- Ward, C.L., Wood, J.L., Houghton, S.B., Mumford, J.A., Chanter, N., 1998.** Actinobacillus and Pasteurella species isolated from horses with lower airway disease. *Vet Rec* 143, 277-279.
- Webster, R., 1993.** Are equine 1 influenza viruses still present in horses? *Equine veterinary journal* 25, 537-538.
- Webster, R.G., Bean, W.J., Gorman, O.T., Chambers, T.M., Kawaoka, Y., 1992.** Evolution and ecology of influenza A viruses. *Microbiological reviews* 56, 152-179.
- Wellington, J., Lawrence, G., Love, D., Whalley, J., 1996.** Expression and characterization of equine herpesvirus 1 glycoprotein D in mammalian cell lines. *Archives of virology* 141, 1785-1793.
- Whitcutt, M.J., Adler, K.B., Wu, R., 1988.** A biphasic chamber system for maintaining polarity of differentiation of culture respiratory tract epithelial cells. *In vitro cellular & developmental biology* 24, 420-428.
- White, S.H., Wimley, W.C., Selsted, M.E., 1995.** Structure, function, and membrane integration of defensins. *Current opinion in structural biology* 5, 521-527.
- Widdicombe, J., Coleman, D., Finkbeiner, W., Tuet, I., 1985.** Electrical properties of monolayers cultured from cells of human tracheal mucosa. *Journal of Applied Physiology* 58, 1729-1735.
- Widmer, F., Hayes, P., Whittaker, R., Kumar, R., 2000.** Substrate preference profiles of proteases released by allergenic pollens. *Clinical and Experimental Allergy* 30, 571-576.
- Wieringa, R., de Vries, A.A., Raamsman, M.J., Rottier, P.J., 2002.** Characterization of two new structural glycoproteins, GP3 and GP4, of equine arteritis virus. *Journal of virology* 76, 10829-10840.
- Wieringa, R., de Vries, A.A., Rottier, P.J., 2003.** Formation of disulfide-linked complexes between the three minor envelope glycoproteins (GP2b, GP3, and GP4) of equine arteritis virus. *Journal of virology* 77, 6216-6226.
- Wilks, C.R., Studdert, M.J., 1974.** Equine herpesviruses. 5. Epizootiology of slowly cytopathic viruses in foals. *Australian veterinary journal* 50, 438-442.
- Williams, K., Maes, R., Del Piero, F., Lim, A., Wise, A., Bolin, D., Caswell, J., Jackson, C., Robinson, N., Derksen, F., 2007.** Equine multinodular pulmonary fibrosis: a newly recognized herpesvirus-associated fibrotic lung disease. *Veterinary Pathology* 44, 849-862.
- Williams, K.J., Robinson, N.E., Lim, A., Brandenberger, C., Maes, R., Behan, A., Bolin, S.R., 2013.** Experimental induction of pulmonary fibrosis in horses with the gammaherpesvirus equine herpesvirus 5. *PLoS One* 8, e77754.
- Willoughby, R., Ecker, G., McKee, S., Riddolls, L., Vernailen, C., Dubovi, E., Lein, D., Mahony, J., Chernesky, M., Nagy, E., 1992.** The effects of equine rhinovirus, influenza virus and herpesvirus infection on tracheal clearance rate in horses. *Canadian Journal of Veterinary Research* 56, 115.
- Wilson, S.S., Wiens, M.E., Smith, J.G., 2013.** Antiviral Mechanisms of Human Defensins. *Journal of Molecular Biology* 425, 4965-4980.
- Wilson, W.D., 1993.** Equine influenza. *Veterinary Clinics of North America: equine practice* 9, 257-282.
- Wilson, W.D., 1997.** Equine herpesvirus 1 myeloencephalopathy. *Veterinary Clinics: Equine Practice* 13, 53-72.
- Wong, D.M., Belgrave, R.L., Williams, K.J., Del Piero, F., Alcott, C.J., Bolin, S.R., Marr, C.M., Nolen-Walston, R., Myers, R.K., Wilkins, P.A., 2008.** Multinodular pulmonary fibrosis in five horses. *Journal of the American Veterinary Medical Association* 232, 898-905.
- Wood, J., Chanter, N., Newton, J., Burrell, M., Dugdale, D., Windsor, H., Windsor, G., Rosendal, S., Townsend, H., 1997.** An outbreak of respiratory disease in horses associated with *Mycoplasma felis* infection. *Vet Rec* 140, 388-391.
- Wood, J., Chirnside, E., Mumford, J., Higgins, A., 1995.** First recorded outbreak of equine viral arteritis in the United Kingdom. *Veterinary record* 136, 381-381.
- Woods, P.S., Robinson, N., Swanson, M., Reed, C., Broadstone, R., Derksen, F., 1993.** Airborne dust and aeroallergen concentration in a horse stable under two different management systems. *Equine Veterinary Journal* 25, 208-213.
- Wu, Z., Hoover, D.M., Yang, D., Boulegue, C., Santamaria, F., Oppenheim, J.J., Lubkowski, J., Lu, W., 2003.** Engineering disulfide bridges to dissect antimicrobial and chemotactic activities of human β -defensin 3. *Proceedings of the National Academy of Sciences* 100, 8880-8885.

- Xiao, C., Puddicombe, S.M., Field, S., Haywood, J., Broughton-Head, V., Puxeddu, I., Haitchi, H.M., Vernon-Wilson, E., Sammut, D., Bedke, N., Cremin, C., Sones, J., Djukanović, R., Howarth, P.H., Collins, J.E., Holgate, S.T., Monk, P., Davies, D.E., 2011.** Defective epithelial barrier function in asthma. *Journal of Allergy and Clinical Immunology* 128, 549-556.e512.
- Yamanaka, T., Niwa, H., Tsujimura, K., Kondo, T., Matsumura, T., 2008.** Epidemic of equine influenza among vaccinated racehorses in Japan in 2007. *Journal of Veterinary Medical Science* 70, 623-625.
- Yamanaka, T., Tsujimura, K., Kondo, T., Matsumura, T., Ishida, H., Kiso, M., Hidari, K.I., Suzuki, T., 2010.** Infectivity and pathogenicity of canine H3N8 influenza A virus in horses. *Influenza and other respiratory viruses* 4, 345-351.
- Yang, D., Chertov, O., Bykovskaia, S., Chen, Q., Buffo, M., Shogan, J., Anderson, M., Schröder, J., Wang, J., Howard, O., 1999.** β -Defensins: linking innate and adaptive immunity through dendritic and T cell CCR6. *Science (New York, N.Y.)* 286, 525-528.
- Yang, X., Forier, K., Steukers, L., Van Vlierberghe, S., Dubruel, P., Braeckmans, K., Glorieux, S., Nauwynck, H.J., 2012.** Immobilization of pseudorabies virus in porcine tracheal respiratory mucus revealed by single particle tracking. *PLoS One* 7, e51054.
- Yang, X.Y., Steukers, L., Forier, K., Xiong, R.H., Braeckmans, K., Van Reeth, K., Nauwynck, H., 2014.** A Beneficiary Role for Neuraminidase in Influenza Virus Penetration through the Respiratory Mucus. *Plos One* 9, 11.
- Zain, M.E., 2011.** Impact of mycotoxins on humans and animals. *Journal of Saudi Chemical Society* 15, 129-144.
- Zanin, M., Baviskar, P., Webster, R., Webby, R., 2016.** The Interaction between Respiratory Pathogens and Mucus. *Cell Host & Microbe* 19, 159-168.
- Zhang, G., Wu, H., Shi, J., Ganz, T., Ross, C.R., Blecha, F., 1998.** Molecular cloning and tissue expression of porcine beta-defensin-1. *FEBS letters* 424, 37-40.
- Zhao, H., Ma, J.K., Barger, M.W., Mercer, R.R., Millecchia, L., Schwegler-Berry, D., Castranova, V., Ma, J.Y., 2009.** Reactive oxygen species-and nitric oxide-mediated lung inflammation and mitochondrial dysfunction in wild-type and iNOS-deficient mice exposed to diesel exhaust particles. *Journal of Toxicology and Environmental Health, Part A* 72, 560-570.
- Zhao, J., Poelaert, K.C., Cleemput, J., Nauwynck, H.J., 2017.** CCL2 and CCL5 driven attraction of CD172a⁺ monocytic cells during an equine herpesvirus type 1 (EHV-1) infection in equine nasal mucosa and the impact of two migration inhibitors, rosiglitazone (RSG) and quinacrine (QC). *Veterinary research* 48, 14.
- Zink, M.C., Yager, J.A., Smart, N.L., 1986.** *Corynebacterium equi* infections in horses, 1958-1984: a review of 131 cases. *The Canadian Veterinary Journal* 27, 213.

Chapter 2.

Aims of the thesis

Respiratory disease is an important clinical manifestation in today's Westernized horses. Although they are often directly triggered upon pathogen infection, most problems affecting the conducting airways are of multifactorial origin. Horses nowadays are commonly kept and trained in poorly ventilated premises with high levels of dust and moulds. Increasing air pollution and plant pollination creates a constant or seasonal threat for pasture-kept horses. Besides, today's racing and competition requirements are an important physical and physiological stressor on the competing horse. The weekly recruitment of these stressed horses in one place for competition also facilitates the spread of respiratory pathogens. To counter these threats, the horses' respiratory tract is guarded with a repertoire of immune barriers, including mucus, firm intercellular junctions and the production of antimicrobial peptides such as β -defensins. Therefore, the majority of horses seems to cope with these constant threats very well and remains free of disease. Nonetheless, respiratory disease is one of the main causes of poor performance in competing horses and thus, has a serious economic impact on the horse industry worldwide. The aim of this thesis was to unravel the interplay between predominant pathogen-specific, host-specific and environmental factors that cause respiratory mucosal damage and trigger the onset of respiratory disease.

Both viral (EHV1, EHV5, EIV and EAV) and bacterial pathogens (*S. e. equi*, *S. e. zooepidemicus*, *S. aureus*, *A. equuli* and *B. bronchiseptica*) were examined in this PhD thesis, but we emphasized our work on equine herpesviruses. Equine herpesviruses, especially EHV1, are currently considered by many to represent the most important pathogens worldwide. Available vaccines fail to fully protect horses from infection or severe secondary symptoms and effective antiviral therapies are lacking. Besides, over 90% of the horse population is latently infected with one or more herpesviruses and foals cannot be efficiently protected from acquiring infection. The development of effective vaccines or antiviral therapies is impeded by the vast amount of immune-evading mechanisms herpesviruses have evolved during a long-term co-evolution with the horse. New insights in equine herpesvirus pathogenesis are urgently needed, starting with their primary replication at the level of the respiratory tract.

The specific research questions of the thesis are presented below.

- What is the importance of specific host immune barriers (i.e. mucus, intercellular junctions and β -defensins) against pathogen invasion, especially against infection by the host-adapted EHV1? The answers are formulated in Chapter 3 and 6.
- In Chapter 3, we found that the intercellular junctions form a major host barrier against EHV1 infection, as EHV1's main binding receptor is located basolaterally in the

respiratory epithelium. Therefore, we addressed the following question in Chapters 4 and 5: Which environmental factors (e.g. pollens, diesel exhaust and mycotoxins) could affect respiratory epithelial intercellular junctions and thereby facilitate a primary EHV1 infection?

- The final research question traced back roots on the pathogenesis of the emerging, yet ancient, pathogen EHV5 (Chapter 7): Could we unravel the first steps in EHV5 pathogenesis using *in vitro* and *ex vivo* equine models?

Chapter 3.

Access to a main alphaherpesvirus receptor, located basolaterally in the respiratory epithelium, is masked by intercellular junctions

Jolien Van Cleemput, Katrien C.K. Poelaert, Kathlyn Laval, Roger Maes, Gisela S. Hussey,
Wim Van den Broeck, Hans J. Nauwynck

Adapted from: Scientific Reports 2017; 7 (16656)

Summary

The respiratory epithelium of humans and animals is frequently exposed to alphaherpesviruses, originating from either external exposure or reactivation from latency. To date, the polarity of alphaherpesvirus infection in the respiratory epithelium and the role of respiratory epithelial integrity herein has not been studied. Equine herpesvirus type 1 (EHV1), a well-known member of the alphaherpesvirus family, was used to infect equine respiratory mucosal explants and primary equine respiratory epithelial cells (EREC), grown at the air-liquid interface. EHV1 binding to and infection of mucosal explants was greatly enhanced upon destruction of the respiratory epithelial integrity with EGTA or N-acetylcysteine. EHV1 preferentially bound to and entered EREC at basolateral cell surfaces. Restriction of infection via apical inoculation was overcome by disruption of intercellular junctions. Finally, basolateral, but not apical EHV1 infection of EREC was dependent on cellular N-linked glycans. Overall, our findings demonstrate that integrity of the respiratory epithelium is crucial in the host's innate defence against primary alphaherpesvirus infections. In addition, by targeting a basolaterally located receptor in the respiratory epithelium, alphaherpesviruses have generated a strategy to efficiently escape from host defence mechanisms during reactivation from latency.

Introduction

Alphaherpesviruses replicate in the mucosae of the upper respiratory and/or the genital tract of their specific host, which is essential for their efficient transmission. Primary replication in epithelial cells of the mucosa is followed by viral spread in neurons and/or lymphoid tissues and establishment of a lifelong latency (Grinde, 2013). Alphaherpesviruses can reactivate from latency sites when the immune system is compromised, such as during periods of stress. Reactivated virus travels back to respiratory or genital mucosae via anterograde axonal transport or via infected immune cells and efficiently replicates in the epithelium, which results in shedding of infectious virus in respiratory or genital secretions.

The long-term evolutionary relationship between alphaherpesviruses and their hosts has led to the development of several innate mucosal barriers in the latter. These barriers include the mucus layer, the mucociliary escalator, firm intercellular connections and the production of several antimicrobial peptides (Jacquot *et al.*, 1992). Mucus forms the first layer of defence against incoming pathogens. For example in swine, the mucus layer entraps pseudorabies virus (PRV) in the mucoprotein network by charge (Yang *et al.*, 2012). In respiratory mucosal explants, however, removing the mucus merely increases the number of plaques (unpublished data). We therefore hypothesize that alphaherpesviruses are somehow hindered in their primary replication in the respiratory mucosa by another specific barrier, the intercellular junctions (ICJ). The ciliated pseudo-stratified columnar epithelium has to carefully maintain its integrity and polarity by the action of ICJ. ICJ are specialized regions of contact between adjacent cells and form the morphological and functional barrier between apical and basolateral cell domains. In addition, they ensure resistance against mechanical forces (Staehein, 1974). Tight junctions (TJ) are the most apically located ICJ and function as a size and ion selective gate for the passage of molecules in between adjacent cells (Balda and Matter, 2016; Matter and Balda, 2003). In addition, they prevent diffusion of not only plasma membrane lipids and (glyco)proteins from the apical to the basolateral surface and vice versa, but also of incoming pathogens attached to apical surfaces. Adherent junctions (AJ) are located basally from the TJ and by connecting the cytoskeleton of neighbouring cells, they provide stability and uniformity to the epithelium (Baum and Georgiou, 2011).

Virus binding and subsequent entry may occur selectively at either the apical or basolateral domains of polarized cells, due to the specific sorting of cell surface receptors. Some viruses (e.g. simian virus 40, respiratory syncytial virus, hepatitis A virus, West Nile virus, chikungunya virus) preferentially infect polarized cells at the apical surfaces, while other

viruses (e.g. adenoviruses) prefer basolateral surfaces (Blank *et al.*, 2000; Chu and Ng, 2002; Clayson and Compans, 1988; Lim and Chu, 2014; Zabner *et al.*, 1997; Zhang *et al.*, 2002). *In vitro*, herpes simplex virus 1 (HSV1) entry in polarized human uterine (ECC-1), colonic (Caco-2), and retinal pigment (ARPE-19) epithelial cells occurs most efficiently from the apical surfaces, due to the presence of nectin-1. However, at basolateral surfaces, another putative receptor must function for HSV1 entry, since downregulation of nectin-1 does not influence infection at this site (Galen *et al.*, 2006). Moreover, basolateral surfaces of Madin-Darby canine kidney epithelial (MDCK) cells are infected more effectively by HSV1 than their apical surfaces (Marozin *et al.*, 2004; Topp *et al.*, 1997). In respiratory epithelial cells, the primary target cells of most alphaherpesviruses, polarity of infection and the importance of ICJ has not been studied to our knowledge. An experimental limitation in previous studies with continuous cell lines is that these do not really reflect the *in vivo* situation. Therefore, we used a respiratory mucosal explant model, which mimics *in vivo* conditions almost perfectly, to investigate the importance of ICJ for the infection of equine herpesvirus type 1 (EHV1), one member of the alphaherpesvirus family. In addition, we isolated primary equine respiratory epithelial cells (EREC) and cultivated them on transwells to examine the polarity of EHV1 binding and subsequent viral replication.

In horses and wild equids, EHV1 infection is widespread and economically very important and induces respiratory disorders, abortion and neurological symptoms (Allen and Bryans, 1986; Lunn *et al.*, 2009). The tissue tropism of EHV1 resembles that of the closely related varicella zoster virus (VZV) and HSV1, since these viruses all replicate well in upper respiratory epithelia and to a lesser extent in genital epithelia (Glorieux *et al.*, 2011; Negussie *et al.*, 2016; Steukers *et al.*, 2014; Zerboni *et al.*, 2014). Horses become infected by EHV1 after uptake of virus-containing secretions, which are transferred between horses through direct or indirect contact (Dayaram *et al.*, 2017; Gibson *et al.*, 1992). In contrast with HSV1, PRV and bovine herpesvirus type 1 (BoHV1), EHV1 is not able to directly cross the basement membrane or to infect respiratory mucosa-associated fibroblasts during primary replication in the respiratory epithelium (Glorieux *et al.*, 2011; Glorieux *et al.*, 2007; Steukers *et al.*, 2012; Vandekerckhove *et al.*, 2009; Vandekerckhove *et al.*, 2010). Instead, similar to VZV, EHV1 hijacks leukocytes to cause viremia, spread in the host and establish latency (Gibson *et al.*, 1992; Zerboni *et al.*, 2014). EHV1-infected leukocytes then transfer the virus to local vascular endothelial cells, where viral replication results in vasculitis, thrombosis and edema. In turn, these pathologies lead to severe symptoms such as abortion and nervous system disorders. Viral DNA has also been found in the trigeminal ganglia, suggesting that the virus also establishes latency in

neuronal tissues (Baxi *et al.*, 1995; Slater *et al.*, 1994). Because vaccines and antivirals are not fully effective, a complete understanding of EHV1 pathogenesis is needed, starting with its primary replication in the respiratory epithelium.

Material and methods

Virus

Two different Belgian EHV1 isolates were used in this study. The non-neurovirulent strain 97P70 was isolated in 1997 from the lungs of an aborted foetus (van der Meulen *et al.*, 2000). The neurovirulent strain 03P37 originates from the blood taken of a paralytic horse during an outbreak in 2003 (van der Meulen *et al.*, 2003a). Both virus stocks were sequenced in their ORF30 region to confirm the correct genotype and were used at their 6th passage (Vandekerckhove *et al.*, 2010).

EHV1 purification and Dio-labelling

Virus purification and subsequent Dio-labelling were performed as described previously (Laval *et al.*, 2016; Yang *et al.*, 2014). Briefly, culture fluids of EHV1-infected RK13 cells were clarified by centrifugation at 60,000 g for 2 h at 4°C. The virus pellet was pooled onto a discontinuous OptiPrep™ gradient (Sigma-Aldrich, St. Louis, MO, USA) containing 10-30% (w/v) of iodixanol and centrifuged at 100,000 g for 2.5 h at 4°C. After centrifugation, purified opalescent virus bands were harvested at the interface of the 15% and 20% layers. To ensure efficient virus lipophilic labelling, the buffer was exchanged to HNE buffer (5 mM HEPES, 150 mM NaCl, 0.1 mM EDTA, pH 7.4) by the use of a 50 K filter device (Millipore corporation, Bedford, MA, USA). While vortexing, 2 nM of 3,3'-Dioctadecyloxycarbocyanine perchlorate (Dio) dissolved in dimethyl sulfoxide (DMSO) (Molecular probes, Oregon, USA) was added to the virus. Subsequently, unbound Dio was removed by centrifugation onto a MicroSpin™ G-50 fine column (GE Healthcare, Buckinghamshire, UK). The degree of Dio-labelled virus purity (>90%) was evaluated by simultaneous immunofluorescent staining of EHV1 gB with mouse monoclonal antibody 3F6 (kindly provided by Prof. U. Balasuriya, University of Kentucky, USA) and quantitative analysis by confocal microscopy.

Tissue collection and processing

The nasal septa and tracheae from different healthy horses were collected at the slaughterhouse and transported in phosphate-buffered saline (PBS) with calcium and magnesium, supplemented with 0.1 mg/mL gentamicin (ThermoFisher Scientific, Waltham, MA, USA), 0.1 mg/mL kanamycin (Sigma-Aldrich), 100 U/mL penicillin, 0.1 mg/mL streptomycin (ThermoFisher Scientific) and 0.25 µg/mL amphotericin B (ThermoFisher Scientific). A physical examination of the selected horses (3 to 15 years of age) was performed before culling

to check the horses' overall health. Horses in bad condition or exhibiting ocular or nasal discharge were excluded from the selection process. Mock inoculations confirmed that selected horses were not experiencing an acute respiratory EHV1 infection at the time of slaughter. Nasal and tracheal explant supernatants tested negative for specific anti-EHV1 immunoglobulins A and G, ruling out the possibility that these antibodies, potentially mounted by the horse during a previous EHV1 infection or vaccination, interfered with our experimental set-up.

Respiratory mucosal explants

Nasal septum mucosal explants and tracheal mucosal explants were prepared as previously described (Vandekerckhove *et al.*, 2009). Briefly, the respiratory mucosa was stripped from the underlying cartilage and washed in PBS to remove excess blood. Tissues were cut into small square pieces (25 mm²), placed with the epithelial side facing upwards onto fine-meshed gauzes and cultured in a 37°C, 5% CO₂-humidified incubator for 24 h at the air-liquid interface in serum-free medium containing DMEM/RPMI (ThermoFisher Scientific), supplemented with 0.1 mg/mL gentamicin, 100 U/mL penicillin, 0.1 mg/mL streptomycin, and 0.25 µg/mL amphotericin B.

EREC

Primary equine respiratory epithelial cells (EREC) were isolated and cultured as described by Quintana *et al.* (2011). In summary, tracheae were trimmed upon arrival in the lab and washed in PBS to remove excess blood. Tissues were submerged into an enzyme mix of 1.4% pronase (Roche Diagnostics Corporation, Basel, Switzerland) and 0.01% deoxyribonuclease I (Sigma-Aldrich) in calcium- and magnesium-free PBS supplemented with 0.45% glucose (VWR International, Leuven, Belgium), 1% sodium pyruvate (ThermoFisher Scientific), 100 U/mL penicillin and 0.1 mg/mL streptomycin for 48 h at 4°C. Detached cells were then incubated in DMEM/F12 (ThermoFisher Scientific) containing 1% MEM non-essential amino-acids (ThermoFisher Scientific), 2.4 µg/mL insulin (Sigma-Aldrich), 100 U/mL penicillin and 0.1 mg/mL streptomycin in a plastic petri dish for 2 h to reduce fibroblast contamination by adherence. Isolated EREC were either seeded immediately or stored in liquid nitrogen at a density of 2×10⁶ cells per cryovial until further use. EREC were seeded at a concentration of 1.8×10⁶ cells/insert overnight into type IV collagen-coated (Sigma-Aldrich) 0.4 µm pore size transwell cell culture wells (Costar, Corning, Fisher Scientific, Fair Lawn, USA) in DMEM/F12 (ThermoFisher Scientific) supplemented with 5% non-heat inactivated foetal calf serum (FCS) (ThermoFisher Scientific), 1% MEM non-essential amino-acids, 100 U/mL penicillin, 1 mg/mL

streptomycin and 1.25 µg/mL amphotericin B. The next day, seeding medium was removed and the bottom platewells were filled with DMEM/F12, containing 2% Ultrosor G (Pall Life Sciences; Pall Corp., Cergy, France), 100 U/mL penicillin, 0.1 mg/mL streptomycin, and 1.25 µg/mL amphotericin B (EREC medium). The transwell, comprising the apical surface of the EREC, was left empty to mimic an air-liquid interface. EREC were incubated in a 37°C, 5% CO₂-humidified incubator and medium was changed every 1-2 days until full differentiation. After 5-7 days, the EREC attained a transepithelial electrical resistance (TEER) of ~500-700 Ω×cm⁻². TEER was measured using an epithelial voltohmmeter (Millipore). The net resistance was calculated by subtracting the background resistance and multiplying the resistance by the surface area of the membrane.

Disruption of intercellular junctions

Respiratory mucosal explants

Explants were cultured 24 h for adaptation before thoroughly washing and embedding them in agarose diluted in 2X MEM, to mimic *in vivo* conditions, as previously published (Vairo *et al.*, 2013). Next, the apical surface of the epithelium was exposed for 1 h at 37°C to 8 mM ethylene glycol tetra-acetic acid (EGTA) (VWR International, Leuven, Belgium), 500 mM N-acetylcysteine (NAC) (Sigma-Aldrich), 20 mM dithiotreitol (DTT) (Sigma-Aldrich) or 50 mM β-mercaptoethanol (ThermoFisher Scientific) in PBS. As a control, PBS supplemented with calcium and magnesium was used. Explants were removed from the agarose and washed three times in PBS and fixed in a phosphate-buffered 3.5% formaldehyde solution for 24 h, either immediately after the last wash or after an additional 24 h incubation on metal gauzes. Explants were then stored into 70% alcohol until further processing.

An automated system was used for paraffin embedding of the samples (Thermo Scientific™ STP 120 Spin Tissue Processor). Eight µm paraffin sections were first deparaffinised in xylene, then rehydrated in descending grades of alcohol, subsequently stained with haematoxylin-eosin, dehydrated in ascending grades of alcohol and xylene and finally mounted with DPX (Sigma-Aldrich). Ten pictures on five different sections per treated explant were taken with an Olympus IX50 light microscope fitted with 40X objective. The percentage of intercellular space in the epithelium was measured using ImageJ software (ImageJ, U.S. National Institutes of Health, Bethesda, Maryland, USA). The region of interest (ROI, i.e. the epithelium) was drawn manually for each picture in the 'ROI manager tool'. Next, the threshold value to distinguish blank spaces from cellular material was determined and the percentage of blank spaces between the cells (i.e. the intercellular space) was calculated.

To guarantee a sufficient viability (>90%) of the explants after treatment with different drugs, an In Situ Cell Death Detection Kit (Roche Diagnostics Corporation, Basel, Switzerland), based on terminal deoxynucleotidyl transferase dUTP nick end-labelling (TUNEL), was used.

EREC

Cells were grown to confluency and the transepithelial electrical resistance (TEER) was measured daily until a steady TEER of $\sim 500\text{-}700 \Omega \times \text{cm}^2$ was attained. TEER was measured prior to and following treatment with 8 mM EGTA in PBS or, as a control, PBS supplemented with calcium and magnesium. After 30 min, cells were washed three times in PBS. Control cells were incubated an additional 24 h to verify whether damage to the ICJ could be repaired. Viability of the cells was assessed by ethidium monoazide bromide (EMA) staining, ensuring that the treatment with EGTA did not cause a significant cell loss.

Infection assays

Respiratory mucosal explants

Explants were cultured at the air-liquid interface for 24 h, prior to extensive washing and embedment in agarose. Next, explants were treated with EGTA, NAC or PBS to dissociate ICJ, as described above. The apical surface of the epithelium was subsequently inoculated with $10^{6.5}$ TCID₅₀ of the neurovirulent 03P37 strain or the non-neurovirulent 97P70 strain for 1 h at 37°C. Explants were removed from the agarose and washed 3 times in PBS to remove unbound virus particles. Finally, explants were placed back onto their gauzes and serum-free medium was added. Twenty-four hours post-inoculation, explants were placed in methylcellulose-filled plastic tubes and frozen at -80°C until further processing.

EREC

Apical versus basolateral infection by HSV1 and 2 in a transwell system has already been described by Galen *et al.* (2006). EREC were grown to full differentiation in a transwell cell culture system and following disruption of ICJ, cells were exposed to 100 μL EHV1 neurovirulent 03P37 or non-neurovirulent 97P70 strain (MOI of 1) at either the apical or the inverted basolateral surface for 1 h at 37°C. Non-adsorbed virus particles were removed by washing the EREC three times with DMEM/F12. Fresh EREC-medium was added to the platewells and cells were further incubated at the air-liquid interface. Ten hours post-inoculation, cells were fixed in methanol for 20 min at -20°C and stored dry at -20°C until further processing.

Binding assays

To characterize the attachment of EHV1 to respiratory mucosal explants and EREC, direct virus-binding studies were carried out with Dio-labelled EHV1 particles. After disruption of the ICJ, cells or explants were chilled on ice for 5 min and washed 3 times with cold PBS. Respiratory mucosal explants were subsequently inoculated with Dio-labelled virus particles at a TCID₅₀ of 10^{6.5} for 1 h at 4°C. EREC were inoculated at a MOI of 10 with Dio-labelled virus particles at either the apical or inverted basolateral surfaces for 1 h at 4°C. Unbound virus was removed by washing the explants and cells 3 times with cold PBS. Explants were embedded in methylcellulose and frozen at -80°C until further processing. Cryosections were fixed for 15 min in 4% phosphate buffered paraformaldehyde (PFA) and cells were fixed for 10 min in 1% PFA. Nuclei were counterstained with Hoechst 33342 (10 µg/ml; ThermoFisher Scientific) for 10 min at room temperature and slides were mounted with glycerol-DABCO. Twenty cryosections of each explant were analysed and the total number of virus particles attached to the apical or basolateral surfaces was counted. The percentage of EREC with bound EHV1 particles was calculated based on the number of cells with viral particles bound on the plasma membrane of 300 randomly selected cells. The number of virus particles attached per cell was calculated based on the number of particles attached at the plasma membrane of 10 random EHV1-positive cells. For each cell, the entire plasma membrane was screened for the presence of virus particles by the use of confocal microscopy.

Enzymatic removal of cell surface N-linked glycans and sialic acids prior to EHV1 inoculation

To determine the role of different cellular N-linked glycan structures and sialic acids in EHV1 infection of EREC, basolateral and apical cell surfaces were pre-incubated with different enzymes (PNGase F and neuraminidase) or control PBS prior to inoculation with EHV1.

PNGase F (New England Biolabs, Ipswich, UK) removes complex, hybrid and oligomannose N-glycosylations and was applied onto apical or basolateral EREC surfaces for 12 h at a concentration of 25,000 U/mL, diluted in EREC medium, supplemented with 10% glycobuffer (New England Biolabs; Ipswich; UK). Neuraminidase from *Vibrio cholera* (Sigma-Aldrich) has a broad substrate spectrum for sialic acids and was used for 1 h at 50 mU/mL in PBS. The influenza A/Equine/Kentucky/98 (H3N8) strain served as a positive control during neuraminidase treatment of EREC. The virus was propagated in embryonated eggs and titrated onto Madin-Darby canine kidney (MDCK) cells. Influenza A strains can easily infect MDCK cells through interaction with cell-associated sialic acids, which can be removed with

neuraminidase (Stray *et al.*, 2000). Equine influenza virus (EIV) A nucleoprotein was stained with the mouse monoclonal antibody HB-65 (ATCC) and subsequently visualized with FITC[®]-labelled secondary goat anti-mouse IgG antibodies. Nuclei were counterstained with Hoechst 33342 and coverslips were mounted using glycerol-DABCO. The percentage of positive cells was calculated based on the total number of positive cells out of 300 randomly selected cells. Correct cleavage of the respective sialic acids was verified by immunofluorescent staining of EREC with biotinylated Maackia Amurensis lectin II (Vector laboratories). This complex was subsequently stained with Streptavidin-FITC[®] (ThermoFisher Scientific). Ten Z-stack confocal pictures were taken to distinguish apical from basolateral treatment. The means of the fluorescent apical or basolateral signals were compared with ImageJ software and dropped significantly after treatment with neuraminidase, compared to control. Following enzymatic treatment, cells were washed 3 times with DMEM/F12 and the inoculum was delivered on top of the respective surfaces for 1 h at 37°C. Concurrently, and as a positive control for enzymatic treatment, MDCK cells were treated with neuraminidase before inoculation with EIV. After 1 h inoculation, unbound virus particles were removed by washing and cells were incubated for 10 h before fixation in methanol, as described above.

Virus titration

Twenty-four hours after inoculation, explant supernatant was collected and stored at -80°C until titration. EHV1 titrations were conducted on RK13 cells, which were incubated at 37°C for 7 days. Titers were expressed as TCID₅₀.

Immunofluorescent staining and confocal microscopy

Respiratory mucosal explants

Explants were embedded in methylcellulose and frozen for subsequent cryosectioning. Cryosections were immunofluorescently stained to label late viral glycoproteins, the basement membrane, nuclei, heparan sulfate, chondroitin sulfate or sialic acids.

Sixteen µm thick cryosections were cut using a cryostat at -20°C and loaded onto 3-aminopropyltriethoxysilane-coated (Sigma-Aldrich) glass slides. Slides were then fixed in 4% PFA for 15 min and subsequently permeabilized in 0.1% Triton-X 100 diluted in PBS. Non-specific binding sites were blocked by 15 min incubation with avidin and biotin (ThermoFisher Scientific) at 37°C. To label late viral glycoproteins, a polyclonal biotinylated horse anti-EHV1 antibody was used for 1 h at 37°C (van der Meulen *et al.*, 2003b), followed by incubation with streptavidin-FITC[®] (ThermoFisher Scientific) for 1 h at 37°C. The basement

membrane of the tissues was stained with monoclonal mouse anti-collagen VII antibodies (Sigma-Aldrich), followed by secondary Texas Red[®]-labelled goat anti-mouse antibodies (ThermoFisher Scientific). Nuclei were detected by staining with Hoechst 33342 (ThermoFisher Scientific). Slides were mounted with glycerol-DABCO and analysed using a Leica (TCS SPE) confocal microscope. The total number of plaques was counted on 50 cryosections and plaque latitude was measured using the Leica confocal software package. Five cryosections per explant were completely photographed and the percentage of infection in the epithelium (i.e. ROI) was determined using ImageJ software. The ROI (i.e. the epithelium) was drawn manually for each picture in the 'ROI manager tool'. Next, the threshold value to distinguish the FITC[®]-positive signal from the background signal was determined and the percentage of FITC[®]-positive signal (i.e. infection) was calculated.

Cellular glycosaminoglycans, heparan sulfate, chondroitin sulfate A and B and sialic acids were respectively stained with a monoclonal mouse anti-heparan sulfate antibody (10E4; Ambsio, Abingdon, UK), a monoclonal mouse anti-chondroitin sulfate (CS-56; Bio-rad; Oxford; UK) or biotinylated Maackia Amurensis lectin II (Vector Laboratories; Peterborough; UK) followed by a goat anti-mouse FITC[®]-conjugated antibody or streptavidin-FITC[®].

EREC

Immunofluorescent staining to visualize EHV1 immediate early protein (IEP) and cell nuclei was performed directly in the transwells.

Antibodies were incubated directly in the transwells for 1 h at 37°C. Cells were first incubated with a 1:1,000 dilution of a polyclonal rabbit anti-IEP antibody, kindly provided by Dr. D. O'Callaghan, Louisiana State University, USA. The diluent used was PBS containing 10% negative goat serum. This was followed by incubation with a goat anti-rabbit IgG FITC[®]-conjugated antibody (ThermoFisher Scientific). Nuclei were counterstained with Hoechst 33342 for 10 min at 37°C. Transwell membranes were excised from the culture inserts and mounted on glass slides using glycerol-DABCO. Slides were examined using a Leica confocal microscope. The total number of plaques was counted on 5 random fields of approximately 3×10^4 cells per insert. Plaque latitude was measured on 10 individual plaques using the Leica confocal software package.

Statistical analyses

Significant differences ($P < 0.05$) between different treatments, different virus strains and different inoculation sites were identified by multiple-way analysis of variances (ANOVA) followed by Tukey's post-hoc test. If homoscedasticity of the variables was not met as assessed by the Levene's test, the data were log-transformed prior to ANOVA. Normality of the residuals was verified by the use of the Shapiro-Wilk test. If the variables remained heteroscedastic or normality was not met after log-transformation, a Kruskal-Wallis' test, followed by a Mann-Whitney's post-hoc test were performed. All analyses were conducted in IBM SPSS Statistics for Windows, version 23.0 (IBM Corp, Armonck, NY, USA).

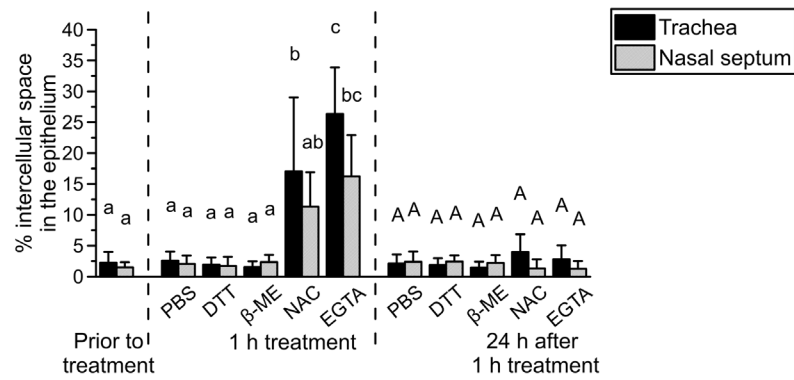
Results

EGTA and NAC, but not β -mercaptoethanol nor DTT reversibly disrupt respiratory epithelial intercellular junctions

Respiratory mucosal explants

As shown in Figure 1A, the percentage of intercellular space in the respiratory epithelium of both nasal and tracheal mucosal explants increased after treatment with 8 mM EGTA ($16 \pm 7\%$ and $26 \pm 8\%$) and 500 mM NAC ($11 \pm 6\%$ and $17 \pm 12\%$), but not after treatment with 20 mM DTT ($2 \pm 1\%$ and $2 \pm 1\%$), 50 mM β -mercaptoethanol ($2 \pm 1\%$ and $2 \pm 1\%$) or control PBS ($2 \pm 1\%$ and $2 \pm 1\%$). Representative haematoxylin-eosin images are shown in Figure 1B. The effect of NAC on intercellular bridges disappeared after decreasing its concentration by ten-fold. Increasing the concentration of DTT or β -mercaptoethanol by ten-fold did not alter the intercellular space, but did decrease cell viability, as assessed with TUNEL-staining (data not shown). Cell viability in the respiratory mucosal explants did not significantly drop after treatment with 8 mM EGTA or 500 mM NAC, compared to control PBS (Figure 2). Notably, the intercellular space are wider in tracheal mucosal explants, when compared to nasal mucosal explants after disruption with NAC and EGTA. Twenty-four hours after the 1 h treatment, samples were analysed to determine whether the respiratory epithelium was able to repair its ICJ. Indeed, the percentage of intercellular space in the respiratory epithelium of tracheal mucosal explants decreased back to $4 \pm 3\%$ 24 h after the 1 h treatment with NAC and to $3 \pm 2\%$ 24 h after the 1 h treatment with EGTA (Figure 1A). In nasal mucosal explants, a similar decrease in percentage of intercellular space was observed 24 h after the 1 h treatment with NAC and EGTA ($2 \pm 1\%$ and $2 \pm 1\%$, respectively).

A



B

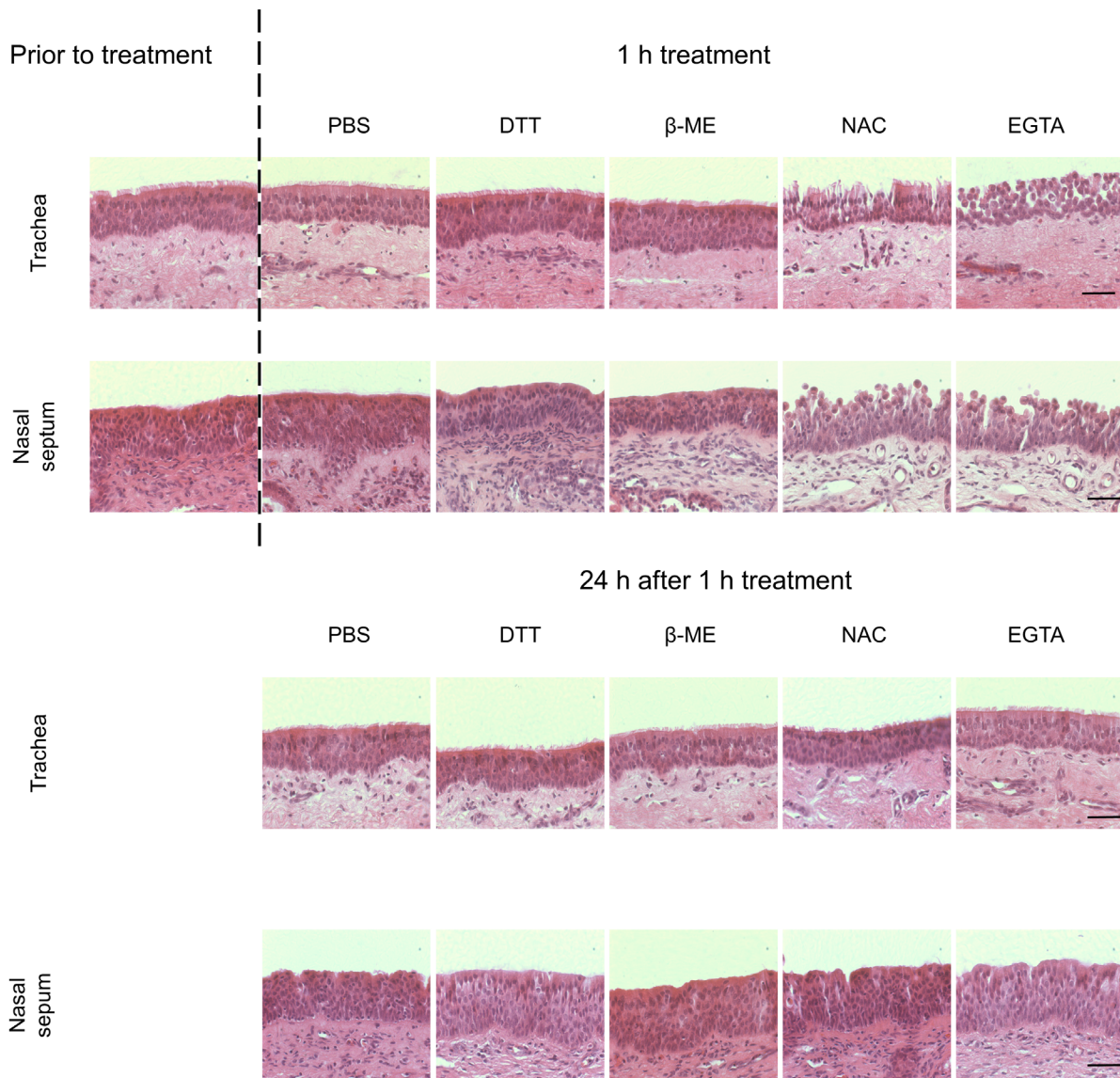


Figure 1. Disruption of ICJ in respiratory mucosal explants. (A) The percentage of intercellular space in equine respiratory mucosal explants after 1 h treatment with PBS (control), DTT, β -mercaptoethanol, NAC or EGTA (left) and 24 h after the 1 h treatment (right). Three independent experiments were performed and data are represented as means + SD, different lower case letters indicate significant ($P < 0.05$) differences after 1 h treatment, while different upper case letters indicate significant ($P < 0.05$) differences 24 h later. (B) Representative haematoxylin-cosin-stained images of the explants 1 h after treatment (up) and 24 h after the treatment (down). The scale bar represents 50 μ m.

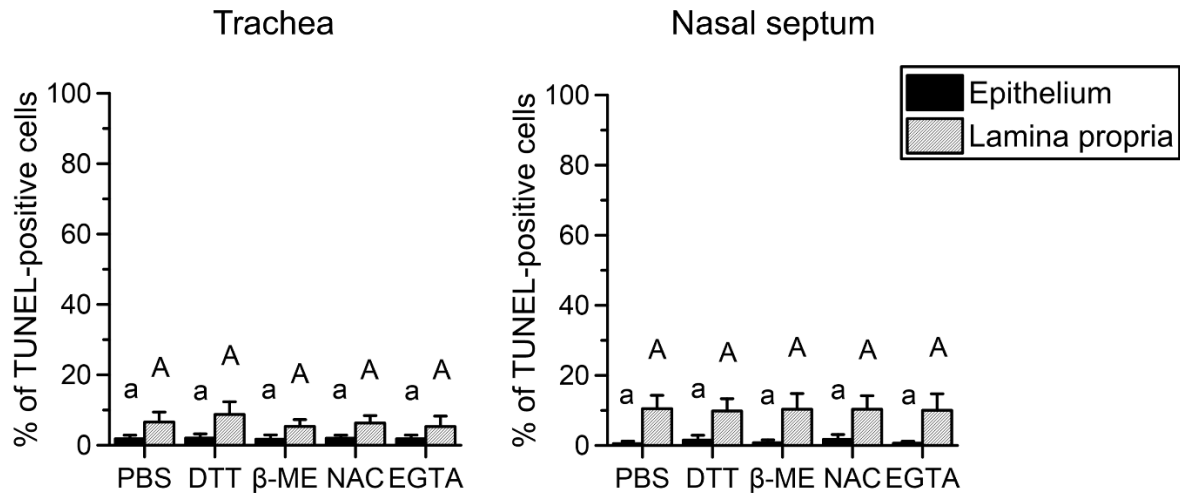


Figure 2. Cell viability in respiratory mucosal explants. TUNEL-staining data of tracheal (left) and nasal (right) mucosal explants after different treatments. Three independent experiments were performed and data are represented as means + SD. The lower case letters indicate significant ($P < 0.05$) differences in the epithelium, while the upper case letters indicate significant differences in the lamina propria.

EREC

EREC attained a steady transepithelial electrical resistance (TEER) of $\sim 500\text{-}700 \Omega \times \text{cm}^2$ after 5-7 days of incubation at the air-liquid interface in a transwell cell culture system. The TEER significantly dropped to baseline levels after treatment with EGTA, but not after treatment with PBS (Figure 3A). EGTA did not alter cell viability, as determined by EMA-staining (Figure 3B). Twenty-four hours after treatment, EREC regained a stable TEER of $500\text{-}700 \Omega \times \text{cm}^2$, indicating that EREC are able to restore their intercellular bridges efficiently.

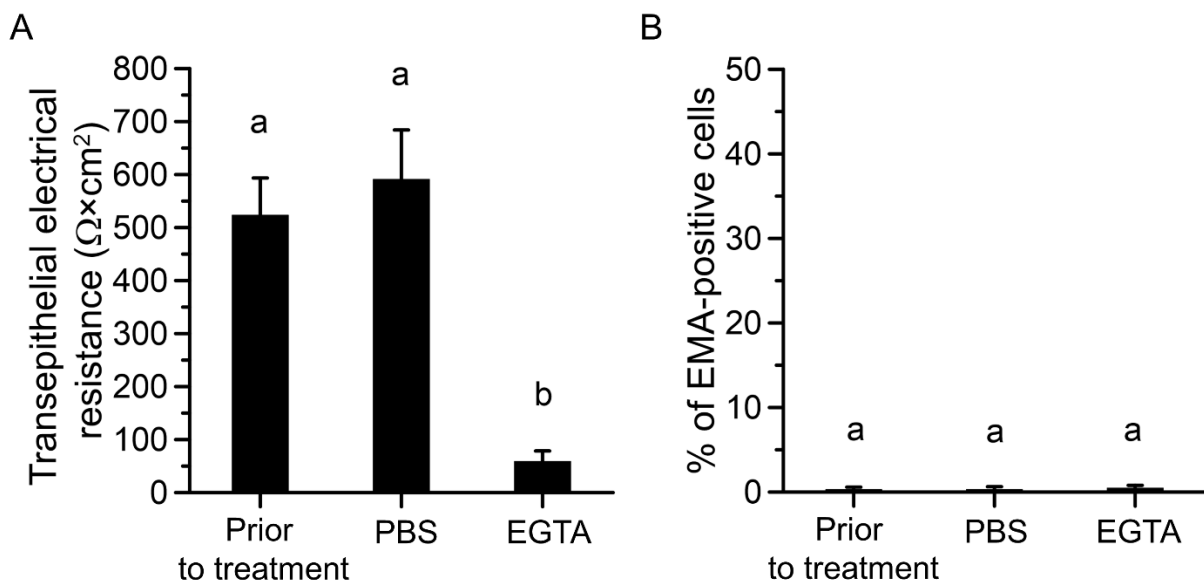


Figure 3. The disruption of intercellular bridges in EREC. (A) Transepithelial electrical resistance of EREC prior to treatment and after 30 min treatment with PBS (control) or EGTA. Three independent experiments were performed and the data are represented as means + SD. Different letters indicate significant ($P < 0.05$) differences. (B) EMA-staining confirmed no significant differences in cell viability after different treatments, when compared to cell viability prior to treatment. Three independent experiments were performed and data are represented as means + SD. Different letters indicate significant ($P < 0.05$) differences.

Intercellular junctions protect respiratory mucosal explants from EHV1 infection

Number of plaques - As shown in Figure 4A, upper left panel, the number of plaques per 50 cryosections increased from 23 ± 10 (03P37) and 30 ± 5 (97P70) in control-pretreated tracheal mucosal explants to 49 ± 11 (03P37) and 59 ± 16 (97P70) in NAC-treated tracheal mucosal explants and to 95 ± 24 (03P37) and 92 ± 26 (97P70) in EGTA-treated tracheal mucosal explants. Similarly, the number of plaques was significantly higher in nasal mucosal explants after NAC (50 ± 14 for 03P37 and 29 ± 15 for 97P70) and EGTA (8 ± 3 for 03P37 and 19 ± 17 for 97P70) pretreatment, compared to control pretreatment (1 ± 1 03P37 and 1 ± 1 97P70). In control-pretreated explants, the number of plaques in nasal mucosal explants was significantly lower compared to tracheal mucosal explants. After disruption of the ICJ by NAC however, the number of plaques in nasal mucosal explants did no longer significantly differ from NAC-pretreated tracheal mucosal explants. Remarkably, pretreatment with EGTA did not completely overcome this restriction in nasal mucosal explants.

Plaque latitude - The plaque latitude gives an indication about the ease of viral spread in the explant and is shown in Figure 4A, upper right panel. The average latitude of 03P37 strain plaques increased from $82 \pm 18 \mu\text{m}$ in control-pretreated tracheal mucosal explants to $106 \pm 32 \mu\text{m}$ and $157 \pm 38 \mu\text{m}$ after NAC and EGTA pretreatment, respectively. Similarly, the average latitude of the 97P70 strain plaques was significantly higher after NAC and EGTA pretreatment ($113 \pm 33 \mu\text{m}$ and $215 \pm 93 \mu\text{m}$ respectively), compared to control ($79 \pm 15 \mu\text{m}$). A similar pattern was observed in nasal mucosal explants.

Percentage of infection in the epithelium - In order to obtain a general view of EHV1 infection in explants, the percentage of infection in the epithelium (i.e. ROI) was calculated and is illustrated in Figure 4A, lower left panel. In control-pretreated tracheal mucosal explants, $1.38 \pm 0.21\%$ of the epithelium was infected by the 03P37 strain and $1.71 \pm 0.83\%$ by the 97P70 strain. Pretreatment of tracheal mucosal explants with NAC led to a significant increase of this percentage to $6.35 \pm 2.15\%$ (03P37) and $5.12 \pm 0.69\%$ (97P70) 24 hpi. Up to $19.57 \pm 10.49\%$ and $13.48 \pm 4.86\%$ of the epithelium got infected by the 03P37 strain and the 97P70 strain, respectively, after pretreatment with EGTA. A similar trend, although with lower values, was observed in nasal mucosal explants. In control-pretreated explants, only $0.23 \pm 0.17\%$ was infected with the 03P37 strain and $0.35 \pm 0.48\%$ with the 97P70 strain. This percentage increased significantly to $3.81 \pm 2.29\%$ (03P37), $4.24 \pm 1.24\%$ (97P70) and $1.93 \pm 0.24\%$ (03P37), $2.88 \pm 0.4\%$ (97P70) after NAC and EGTA pretreatment, respectively.

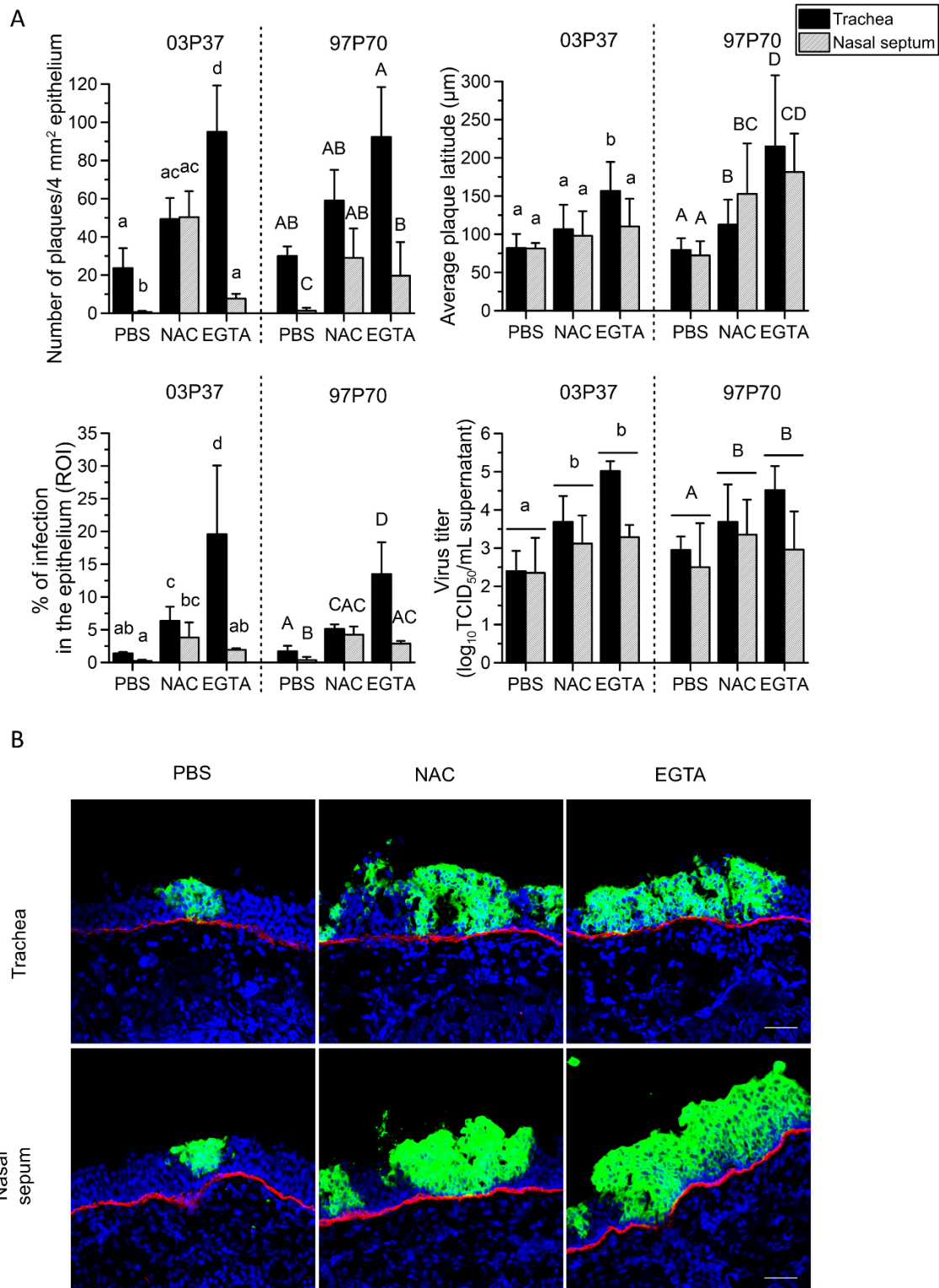


Figure 4. EHV1 infection of respiratory mucosal explants after disruption of ICJ with NAC or EGTA. (A) Respiratory mucosal explants were pre-incubated with NAC, EGTA or control PBS, prior to inoculation with EHV1 03P37 or 97P70 strain for 1 h at 37°C ($10^{6.5}$ TCID₅₀). Explants were frozen 24 hpi and cryosections were stained for late viral antigens. The total number of plaques was counted on 50 consecutive cryosections, the average plaque latitude was calculated based on a maximum of 10 individual plaques, the percentage of EHV1 infection in the epithelium was analysed on 5 random cryosections and the virus titer was determined in supernatant on RK13 cells. Data are represented as means + SD and different lower case numbers indicate significant ($P < 0.05$) differences in 03P37 strain infection, different upper case letters represent significant ($P < 0.05$) differences in 97P70 strain infection. Experiments were performed on 3 individual horses. (B) Representative confocal images of EHV1 plaques (green) in respiratory mucosal explants. The basement membrane is shown in red. Cell nuclei were counterstained with Hoechst (blue). The scale bar represents 50 μm

Virus titer - More efficient virus replication in the epithelium most likely results in the production of more extracellular virus particles. Indeed, virus titration on RK13 cells (Figure 4A, lower right panel) confirmed this hypothesis showing that EGTA-pretreated tracheal mucosal explant supernatant contained a 2 to 3 log higher (03P37) and 1 to 2 log higher (97P70) EHV1 titer than control-pretreated tracheal mucosal explants supernatant. NAC-pretreated tracheal mucosal explants supernatant was on average 1 log (03P37 and 97P70) higher than control supernatant. In general, the 03P37 and 97P70 titers of nasal mucosal explant supernatant were 0.5 to 1.5 log higher after pretreatment with NAC or EGTA, compared to controls.

Representative confocal images of EHV1 plaques in the respiratory mucosal explants are shown in Figure 4B.

EHV1 preferentially infects basolateral surfaces of respiratory epithelial cells

Number of plaques - To investigate whether EHV1 preferentially infects either apical or basolateral surfaces of EREC, we inoculated the cells by either route. On 3×10^4 EREC, we counted an average of 1 ± 1 viral plaques after apical inoculation with both the 03P37 and the 97P70 strain. Basolateral inoculation with the respective strains led to a 58 ± 30 -fold and 61 ± 14 -fold increase in the number of plaques on an area of 3×10^4 EREC, as shown in Figure 5A, left panel.

To determine whether ICJ also protect the basolateral surfaces of primary EREC from EHV1 infection, cells were treated with 8 mM EGTA before inoculation at the apical or inverted basolateral surfaces. Disruption of the ICJ increased EREC infection by 37 ± 20 -fold and 45 ± 21 -fold after inoculation at the apical surface with the 03P37 and 97P70 strain, respectively. Pretreatment with EGTA did not significantly change infection after inoculation at the basolateral surfaces with neither of the 2 strains.

Plaque latitude - No significant difference in EHV1 plaque latitude was found between different inoculation routes or between different pretreatments (Figure 5A, right panel).

Representative confocal images are shown in Figure 5B. Since no significant differences were observed between the two different strains, all further experiments were conducted with the 03P37 strain only.

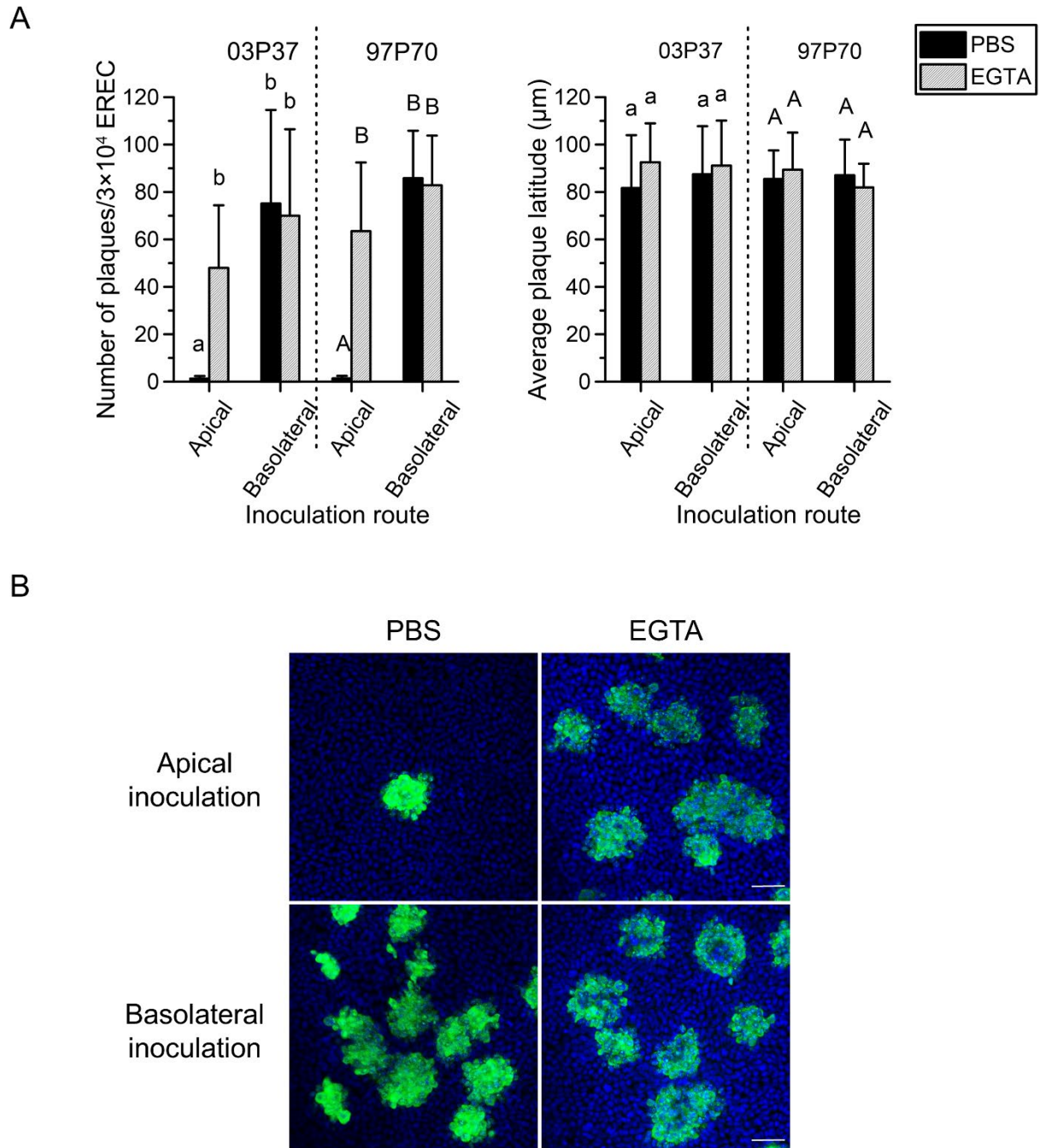


Figure 5. EHV1 preferentially infects the basolateral surface of EREC and disruption of ICJ overcomes the restriction to EHV1 infection at the apical surface. (A) To compare EREC susceptibility to EHV1, cells were exposed at either the apical surface or basolateral surface to EHV1 (MOI 1). Cells were fixed in methanol 10 hpi and stained for IEP. The total number of plaques was counted in five different fields of approximately 3×10^4 cells for each condition (left). Average plaque latitudes were measured on 10 individual plaques (right). Experiments were performed in triplicate on primary EREC of 3 different horses. Data are represented as means + SD and significant ($P < 0.05$) differences for 03P37 strain infection are indicated by lower case letters and for the 97P70 strain infection by upper case letters. (B) Representative confocal images of EHV1 IEP-positive plaques (green) in EREC monolayers, nuclei were detected with Hoechst (blue). The scale bar represents 50 μm

Increased epithelial cell susceptibility to EHV1 at the basolateral surfaces is correlated with the virus binding step

Here, we examined EHV1 binding to respiratory mucosal explants after control PBS, EGTA or NAC pretreatment and to EREC after control PBS or EGTA pretreatment.

Respiratory mucosal explants

The 03P37 strain was purified and Dio-labelled as previously described (Laval *et al.*, 2016). In PBS-pretreated tracheal mucosal explants and nasal mucosal explants, a respective total number of 320 ± 28 and 179 ± 61 virus particles was counted on the plasma membrane. This difference shows that the limited infection of nasal mucosal explants, compared to tracheal mucosal explants, can in part be related to a reduced viral attachment.

To more specifically evaluate the area of virus attachment, virus particles attached to either the apical surface or the basolateral surface were separately counted. As shown in Figure 6A, the difference in virus binding between both types of tissue was only found at the apical surface and not at the basolateral surfaces. Upon PBS pretreatment, 289 ± 28 EHV1 particles bound to the apical surface of tracheal mucosal explants, compared to 150 ± 52 EHV1 particles at the apical surface of nasal mucosal explants, whereas only 30 ± 1 and 30 ± 8 EHV1 particles were found at the basolateral surfaces of the respective mucosal explants.

Pretreatment with EGTA and subsequent disruption of ICJ integrity did not significantly increase the binding of EHV1 to the apical surfaces of both tracheal mucosal explants and nasal mucosal explants (203 ± 33 and 227 ± 32 , respectively). However, EHV1 binding to the basolateral surfaces increased to 322 ± 114 in tracheal mucosal explants and 216 ± 33 in nasal mucosal explants. Pretreatment of the explants with NAC, which was shown above to damage intercellular bridges and which is also being used as a mucolytic drug, did increase the number of viral particles attached to both the apical and basolateral surfaces of tracheal mucosal explants (1017 ± 378 and 830 ± 109) and nasal mucosal explants (654 ± 136 and 659 ± 155).

Representative confocal images are shown in Figure 6B.

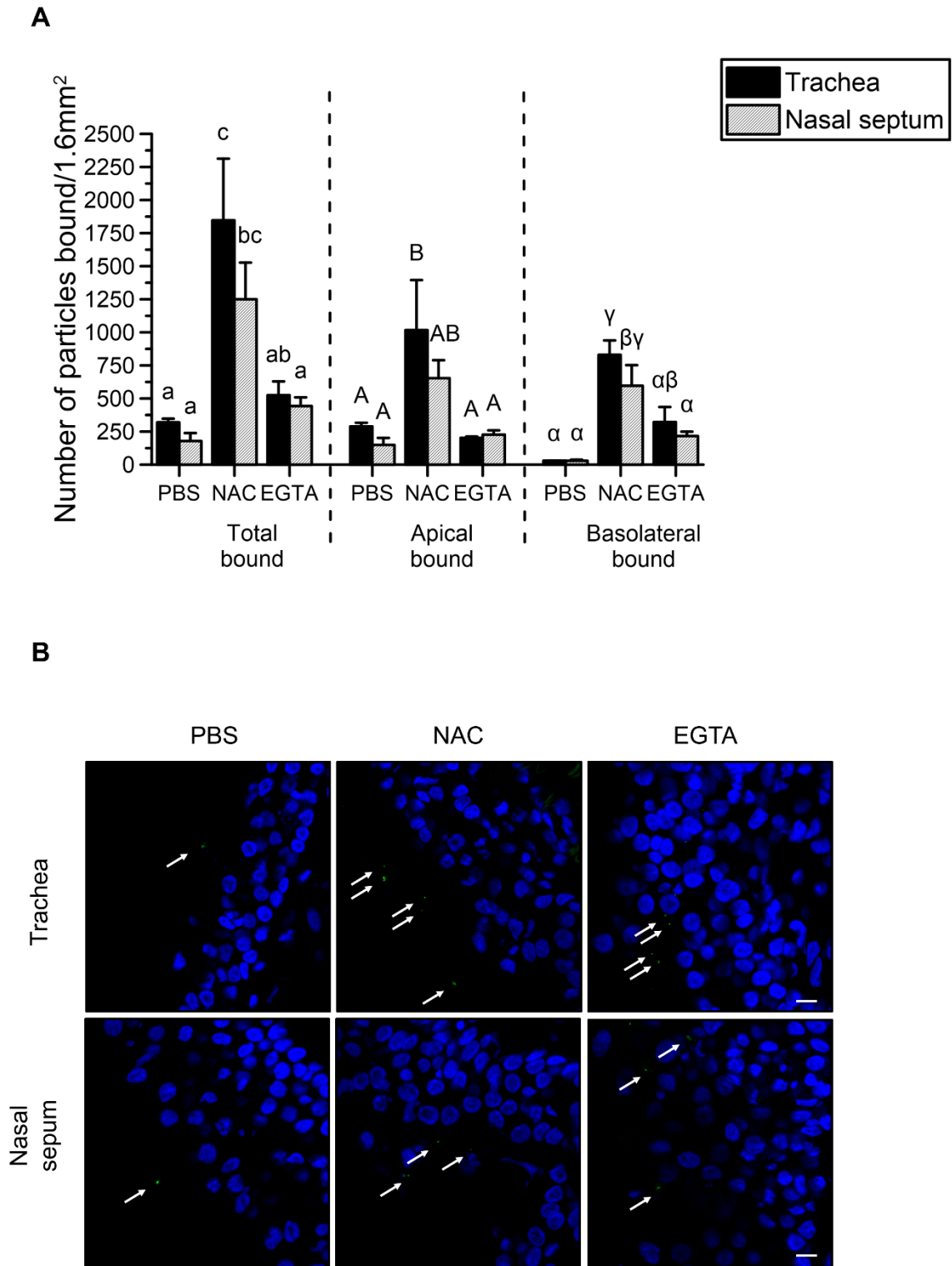


Figure 6. EHV1 attachment to equine respiratory mucosal explants is enhanced after disruption of intercellular junctions with NAC and EGTA. (A) Dio-labelled EHV1 particles ($10^{6.5}$ TCID₅₀) were added for 1 h at 4°C to the pretreated tracheal mucosal explants and nasal mucosal explants (PBS, NAC or EGTA). The total number, the number bound to the apical surfaces and to the basolateral surfaces were individually counted on 20 cryosections of 16 μ m. Three independent experiments were performed and data are represented as means + SD, different lower case letters represent significant ($P < 0.05$) differences in the total number of attached EHV1 particles. Significant ($P < 0.05$) differences in the number of EHV1 particles bound to the apical surfaces of explants are indicated by upper case letters. Different Greek letters indicate significant ($P < 0.05$) differences in the number of EHV1 particles bound to the epithelial basolateral surfaces of explants. (B) Representative confocal images of Dio-labelled EHV1 particles attached to tracheal mucosal explants and nasal mucosal explants upon different pretreatments (PBS, NAC or EGTA). The white arrows point at virus particles and the red dotted line represents the basement membrane. The scale bar measures 10 μ m.

EREC

These findings in explants were corroborated in EREC from three individual horses. As represented in Figure 7A, left panel, the percentage of EREC with bound EHV1 particles was significantly higher ($46 \pm 16\%$) after inoculation at the basolateral surfaces, compared to apical inoculation ($3 \pm 1\%$). Disruption of ICJ had a similar effect on EHV1 binding to EREC as in explants, where $25 \pm 8\%$ of the cells had virus particles attached to their plasma membrane upon apical inoculation. ICJ disruption in EREC had no effect on EHV1 binding upon basolateral inoculation ($45 \pm 9\%$), compared to control EREC with intact ICJ.

The number of virus particles bound to the plasma membrane of EHV1-positive EREC significantly increased after pretreatment with EGTA (3 ± 1), compared to PBS pretreatment (1 ± 1), upon apical inoculation (Figure 7A, right panel). Upon basolateral inoculation, the number of virus particles per EHV1-positive cell in either PBS- or EGTA-pretreated EREC was similar (2 ± 1 and 2 ± 1 , respectively). These results are visualized with confocal images in Figure 7B.

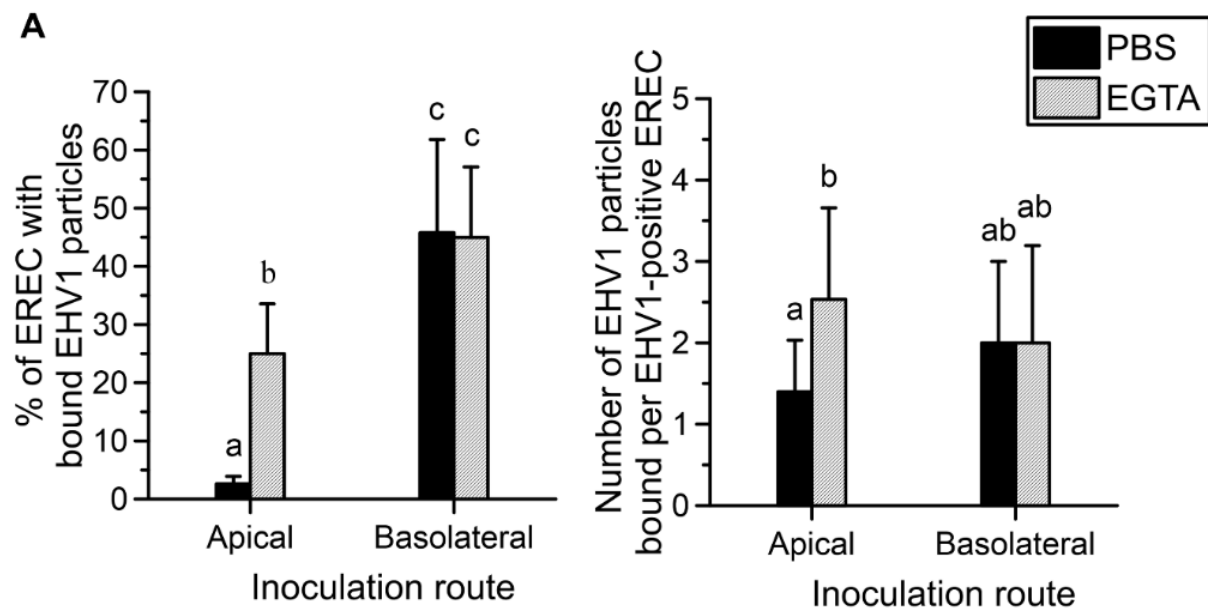


Figure 7. EHV1 binds up to 10-fold better at basolateral surfaces than at apical surfaces of EREC with intact intercellular junctions. (A) Cells were pre-incubated with PBS or EGTA and inoculated at 4°C for 1 h with Dio-labelled EHV1 particles (MOI 10). The percentage of cells with bound virus particles was calculated based on 5 random fields of 300 cells (left panel). The total number of particles per EHV1-positive cell was counted (right panel). Three independent experiments were performed and data are represented as means + SD, different letters indicate significant ($P < 0.05$) differences.

B

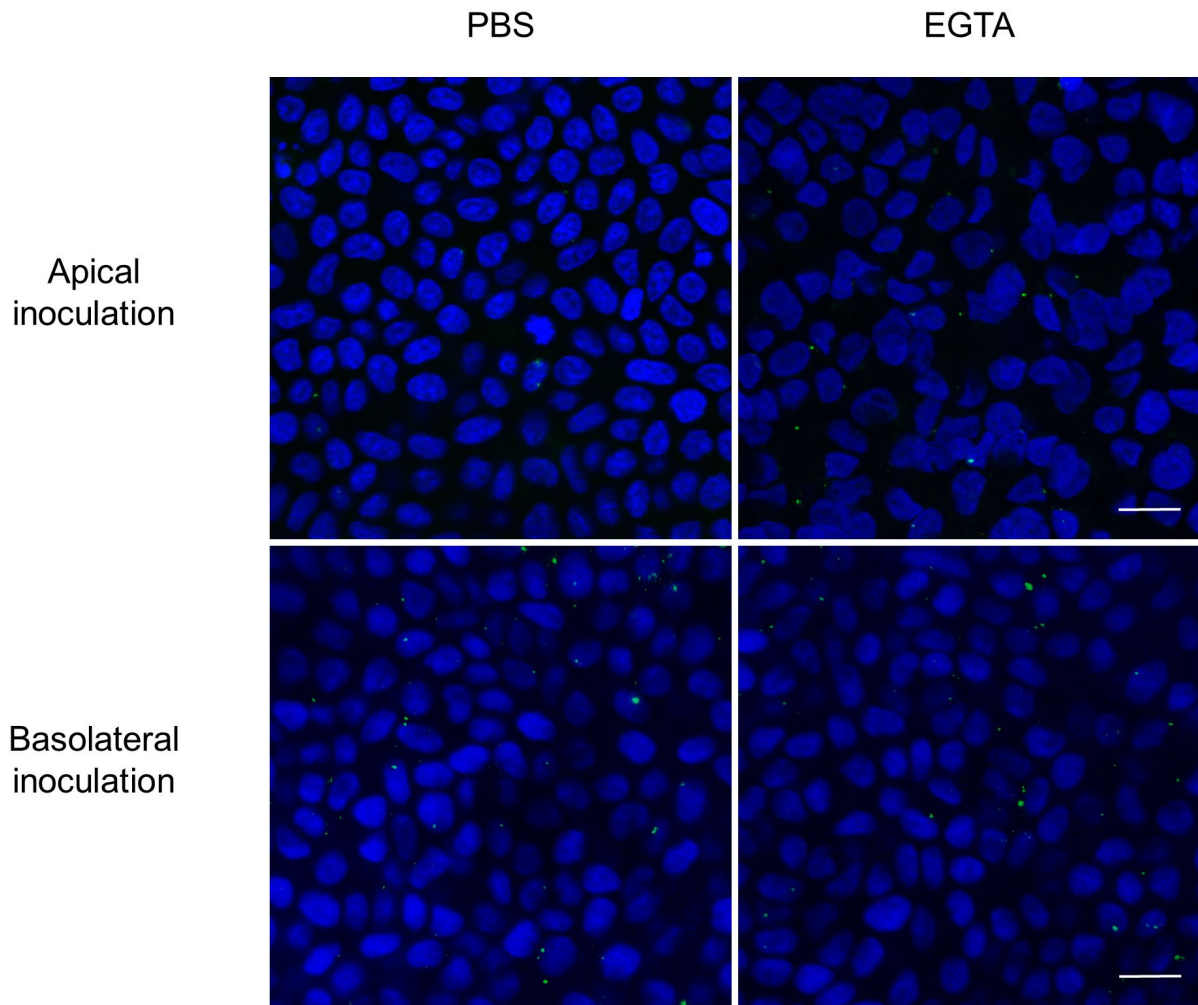


Figure 7. EHV1 binds up to 10-fold better at basolateral surfaces than at apical surfaces of EREC with intact intercellular junctions. (B) Representative confocal images of EREC with bound EHV1 particles (green), cell nuclei are stained in blue, the scale bar represents 10 μm .

N-glycans, but not heparan sulfate, chondroitin sulfate or sialic acids play a role in EHV1 infection of respiratory epithelial cells

Expression pattern in the respiratory epithelium - Cellular glycosaminoglycans and sialic acids are known to play a role in the attachment of several herpesviruses including HSV1, PRV, BoHV1 and EHV1 (Banfield *et al.*, 1995; Laval *et al.*, 2016; Osterrieder, 1999; Spear, 1993). The presence of these cellular glycosaminoglycans and sialic acids was first verified by immunofluorescent staining of respiratory mucosal explant cryosections. As shown in Figure 8, left panel, heparan sulfate is present solely at the basal site of the equine respiratory epithelium. A similar pattern was observed for the distribution of chondroitin sulfate in equine respiratory epithelium (Figure 8, middle panel). The lectin Maackia Amurensis lectin II binds α 2,3-linked sialic acids with high affinity, and not α 2,6-linked sialic acids. Sialic acids are distributed equally all over the plasma membrane of epithelial cells in respiratory mucosal explants, as shown in Figure 8, right panel. Isolation of primary cells might affect their glycosaminoglycan expression pattern and indeed, immunofluorescent staining of EREC turned out negative for heparan sulfate and chondroitin sulfate, but remained positive for sialic acids.

Role in EHV1 infection - To explore whether these sialic acids or, more generally, N-linked glycans, are involved in EHV1 infection, sialic acids or N-linked glycans were enzymatically cleaved by neuraminidase or PNGase F, respectively, from either the apical or basolateral cell surfaces prior to inoculation with EHV1 at the respective routes. As a positive control, MDCK cells were inoculated by an A/equine/Kentucky/98 influenza strain (H3N8) after neuraminidase pretreatment. Basolateral enzymatic removal of N-linked glycans rendered EREC 4-fold less susceptible to EHV1, compared to the control, as determined by counting the number of plaques on 3×10^4 EREC (Figure 9A). No significant difference in number of plaques could be detected between control PBS-pretreated cells and neuraminidase-pretreated cells, while equine influenza virus (EIV) infection of MDCK cells was significantly lower after enzymatic removal of sialic acids by neuraminidase (Figure 10 A). To further verify the correct cleavage of sialic acids on EREC surfaces, immunofluorescent staining was performed to compare the relative amount of sialic acids before and after enzymatic treatment by measuring the intensity of the fluorescent signal on 10 different Z-stacks. The enzyme could correctly remove sialic acids on either the apical or basolateral cell surfaces (Figure 10 B). Finally, plaque latitude did not significantly differ among different enzymatic pretreatments (Figure 9B). These findings demonstrate that EHV1 uses cellular N-linked glycans, but not heparan sulfate, nor chondroitin sulfate, nor sialic acids for initial infection of EREC.

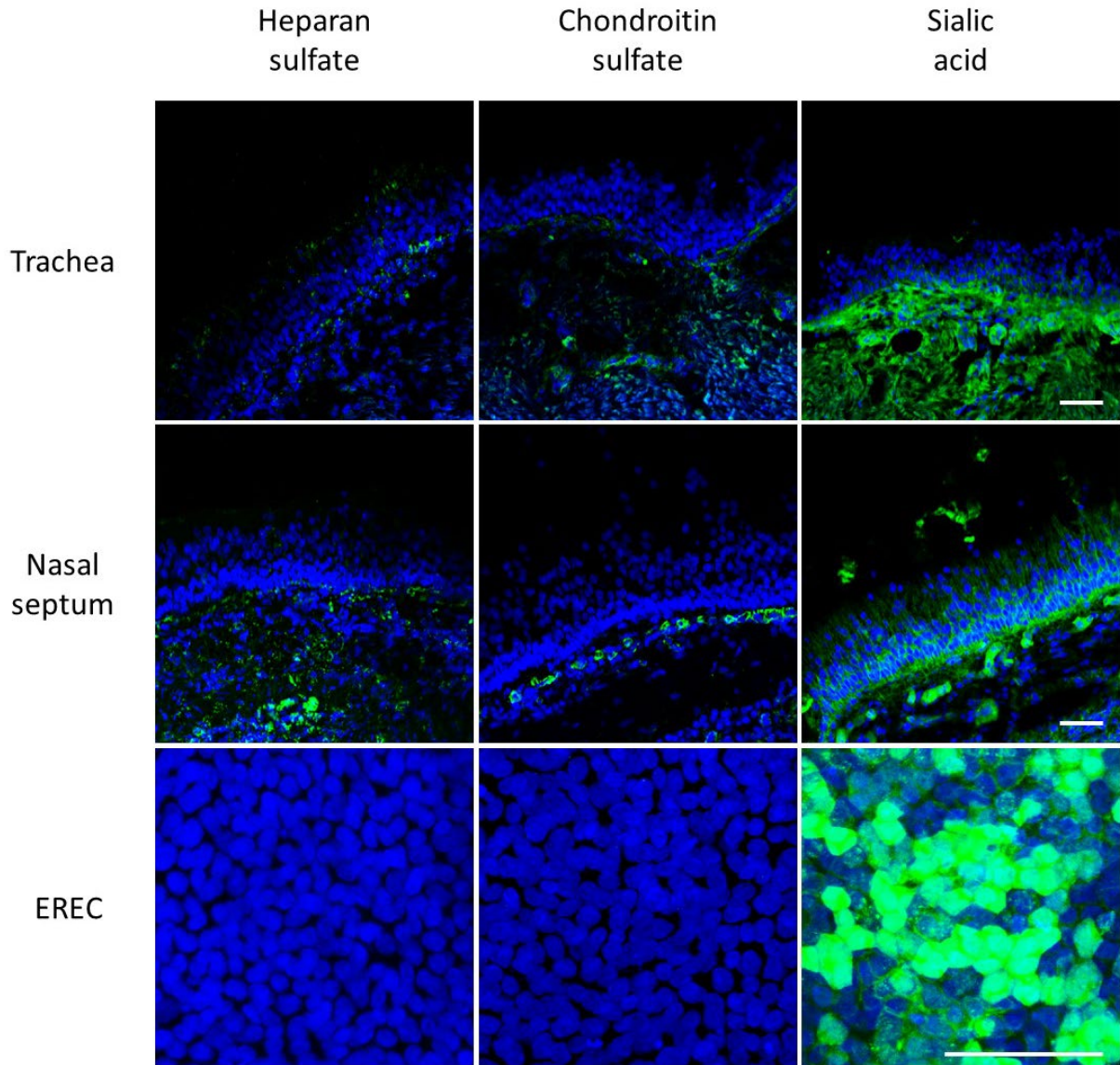


Figure 8. Localisation of heparan sulfate, chondroitin sulfate and α 2,3-linked sialic acid expression by confocal microscopy. Cryosections and cells were fixed in PFA before permeabilisation with Triton X-100. Heparan sulfate and chondroitin sulfate were visualized by labelling with monoclonal antibodies 10E4 and CS-56 (green), α 2,3-linked sialic acids were detected by biotinylated Maackia Amurensis lectin II (green). Hoechst stained cell nuclei blue. Respiratory mucosal explant epithelia express heparan sulfate and chondroitin sulfate at the basolateral membrane and α 2,3-linked sialic acids all over the plasma membrane (green) (upper and middle panel). Isolated EREC monolayers solely express α 2,3-linked sialic acids and not heparan sulfate, nor chondroitin sulfate (lower panel). The scale bar represents 50 μ m.

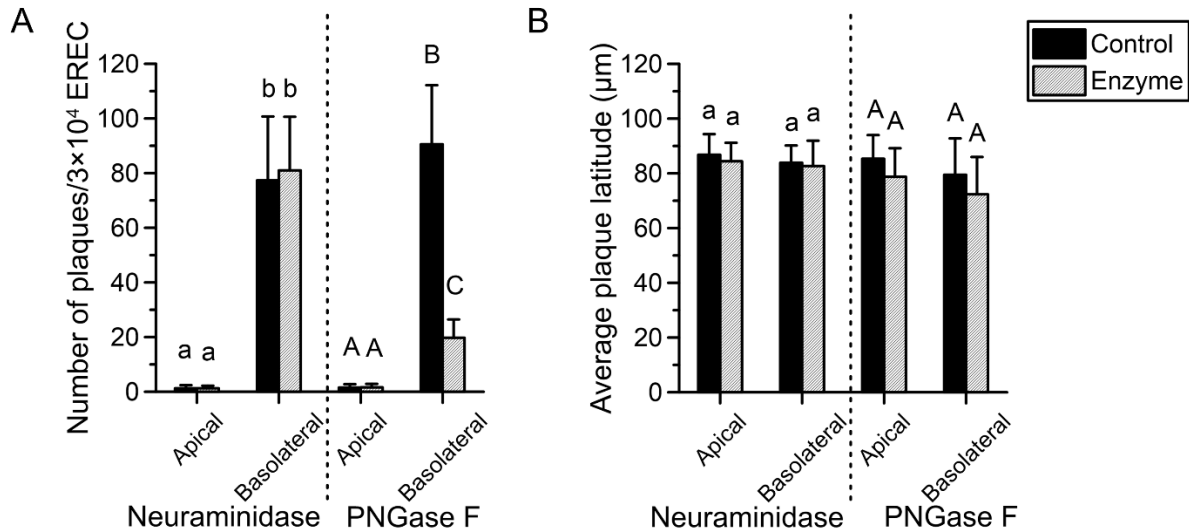


Figure 9. N-linked glycans, but not sialic acids play a role in EHV1 infection of EREC after basolateral inoculation. EREC were grown to confluency on transwells before enzymatic treatment with neuraminidase (1 h, 37°C) or PNGase F (12 h, 37°C) at either the apical or basolateral surface. Next, the same route was used for inoculation with EHV1 (MOI 1, 1 h, 37°C) and cells were fixed in methanol 10 hpi before IEP staining. The total number of plaques was counted in five different fields of approximately 3×10^4 cells for each condition (left). Average plaque latitudes were measured on 10 individual plaques (right). Experiments were performed in triplicate on primary EREC of 3 different horses. Data are represented as means + SD and significant ($P < 0.05$) differences are indicated by different letters.

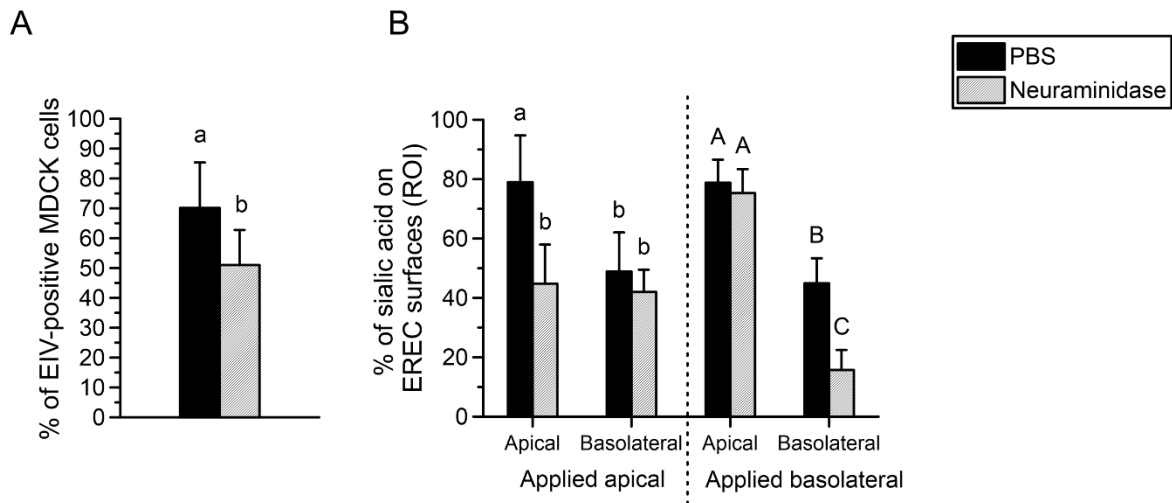


Figure 10. Validation neuraminidase assay. (A) During enzymatic treatment of EREC, MDCK cells were similarly pretreated with neuraminidase before inoculation with EIV. Cells were fixed at 6 hpi in methanol and EIV-positive cells were visualized using the monoclonal HB65 antibody. Five random fields of approximately 100 cells were screened to calculate the percentage of EIV-positive cells. Experiments were performed in triplicate. Data are represented as means + SD and different letters represent significant differences. (B) Correct sialic acid-cleavage from EREC surfaces was confirmed by confocal analysis of 10 different Z-stacks per treatment. EREC were grown to confluency on transwells and treated at either the apical surface (left) or basolateral surface (right) with neuraminidase or control PBS for 1 h at 37°C. Cells were then fixed in PFA and permeabilized in Triton X-100. Sialic acids were stained with biotinylated Maackia Amurensis lectin II and the percentage of fluorescent signal in either the apical or the basolateral domain of EREC was calculated. Data are represented as mean + SD. Significant differences after apical exposure are indicated by different lower case letters and after basolateral exposure by different upper case letters.

Discussion

The respiratory mucosa plays a vital role in the transmission of alphaherpesviruses. These viruses not only enter their host through infection of the respiratory tract, they also use the respiratory system to spread to new hosts later on in their life-cycle. Until now, the specific relationship between respiratory mucosa integrity and polarity on one hand and alphaherpesvirus infection on the other hand has not been studied. Previous studies examining polarity of alphaherpesvirus infections have been conducted in continuous cell lines, different from the *in vivo* replication sites. Here, we use an established equine respiratory mucosal explant model and to our knowledge, this study is the first to disrupt intercellular bridges in a mucosal explant system. In cell cultures, measuring the transepithelial electrical resistance or the leakage of labelled dextran or albumin across the apical and basolateral compartments of transwells is the standard method to verify epithelial permeability (Balda *et al.*, 1996; Galen *et al.*, 2006; Shasby and Shasby, 1986; Vinhas *et al.*, 2011; Wang *et al.*, 2000). *In vivo*, epithelial integrity could be assessed by measuring the transepithelial electrical voltage with an electrode, placed in the trachea (Wang *et al.*, 2000). However, none of these methods could be applied on mucosal explants and therefore, we set up a new protocol to verify ICJ integrity by examining the intercellular space in haematoxylin-eosin-stained paraffin coupes by means of image analysis. Equine tracheal and nasal mucosal explants were incubated with various metal-chelating and/or reducing drugs in order to disrupt epithelial integrity. Only the drugs affecting extra- and intracellular calcium levels (EGTA and NAC), and not the reducing agents affecting disulfide bonds in adhesion proteins (DTT or β -mercaptoethanol), were able to alter nasal and tracheal epithelial integrity. Calcium is the most important ion in regulating intercellular junction stability. Homophilic interactions between AJ directly depend on extracellular calcium availability (Baum and Georgiou, 2011). Alteration of intracellular calcium concentrations or depletion of extracellular calcium also mediates the redistribution of AJ and TJ proteins (Brown and Davis, 2002; Nilsson *et al.*, 1996). EGTA specifically sequesters extracellular calcium and adding it to cell culture medium of polarized epithelial cells rapidly results in splitting of their ICJ (Volberg *et al.*, 1986). NAC modulates intracellular calcium levels but until present, it was not proven to alter integrity of ICJ (Naziroglu *et al.*, 2014). Of these two drugs, EGTA most efficiently destroyed the ICJ, possibly due to its direct action in the destruction of ICJ protein interactions, compared to NAC, which indirectly modulates ICJ proteins. Notably, a rather high concentration of NAC was necessary to disrupt epithelial integrity in explants, which was toxic when applied directly on EREC. These findings

point out that care must be taken when using the mucolytic drug Lysomucil® to treat horses with chronic obstructive pulmonary disease or with severe pneumonia (Breuer and Becker, 1983; Mair and Derksen, 2000).

Although not significantly, destruction of epithelial integrity by both EGTA and NAC occurs more efficiently in tracheal mucosal explants, compared to nasal mucosal explants. Our observations complement those of previous *in vitro* and *ex vivo* studies, showing that the average transepithelial electrical resistance and subsequent ICJ integrity progressively decreases from proximal to distal airways (Ballard *et al.*, 1992; Boucher *et al.*, 1981; Lopez-Souza *et al.*, 2009). The resistance against incoming pathogens is also obvious after challenging the nasal septum with EHV1. In control-pretreated explants, EHV1 infection is significantly lower in nasal mucosal explants than in tracheal mucosal explants. This limited infection is presumably a direct consequence of impaired virus binding, considering the low number of EHV1 particles attached to nasal mucosal explants. As the primary air filter, the nasal septum is guarded with an overlying mucoprotein network, a specialized glycocalyx, a repertoire of antimicrobial peptides and firm intercellular contacts, which might entrap and neutralize incoming virus particles more efficiently (Fokkens and Scheeren, 2000). Disruption of ICJ with EGTA did not completely overcome the restriction to EHV1 infection of nasal mucosal explants. However, after pretreatment with NAC, infection was greatly enhanced to a similar level as in tracheal mucosal explants. It is known that NAC acts as a mucolytic by disrupting disulfide bonds in the mucoprotein network (Reas, 1963). Remarkably, using DTT and β -mercaptoethanol prior to EHV1 inoculation did not increase subsequent infection (data not shown). Thus in nasal mucosal explants, a similar destruction of the mucoprotein network and of ICJ is necessary in order for EHV1 to efficiently infect the epithelial cells. In addition, we observed a significant increase in EHV1 binding to apical surfaces of nasal and tracheal mucosal explants after NAC pretreatment, pointing out the relevance of the overlying mucoprotein network in both tissues. Disruption of intercellular contacts also results in greater virus binding to basolateral surfaces of the explants. First of all, virus particles are able to migrate in between neighbouring cells and get in direct contact with basolateral surfaces. Secondly, virus particles attached to transmembrane proteins in apical surfaces can freely move to the basolateral side of the plasma membrane, since cell polarity is lost (Mateo *et al.*, 2015). The results obtained with *ex vivo* respiratory mucosal explants most likely reflect what happens *in vivo* when epithelial integrity is lost. It has been shown that ICJ integrity is affected by several factors including pollens, mycotoxins, bacterial toxins, inflammatory cytokines (INF- γ , TNF- α and interleukins) and hormones (estradiol) (Capaldo and Nusrat, 2009; Gerez *et al.*, 2015;

Groten *et al.*, 2005; Kwak *et al.*, 2012; Runswick *et al.*, 2007; Van De Walle *et al.*, 2010; Vinhas *et al.*, 2011). Pollens exhibit proteolytic activities for efficient pollination, but when inhaled by humans or animals, these proteases can destruct TJ proteins (Runswick *et al.*, 2007; Vinhas *et al.*, 2011). Allergic reactions to pollens are linked to asthma and in humans, it is known that allergic patients tend to have a less firm epithelial barrier (Xiao *et al.*, 2011). Chronic allergies in pasture-kept horses are known as 'summer pasture recurrent airway obstruction' (SP-RAO) and are associated with inhaling pollens, moulds and mycotoxins (Costa *et al.*, 2006). It can be postulated that as a consequence, horses affected with SP-RAO might have a deficiency in epithelial integrity and therefore be more receptive for an EHV1 infection and shed EHV1 more easily towards other horses. Chronic airway inflammation is also linked to chronic microbial infections. Bacterial toxins and cellular cytokines produced upon viral and/or bacterial infections can directly alter ICJ protein redistribution and induce the development of asthma (Capaldo and Nusrat, 2009; Kwak *et al.*, 2012). Hormones such as estrogens are important for the regulation of the estrous cycle and the maintenance of pregnancy. In order to modulate their vascular functions (i.e. angiogenesis), estrogens need to disrupt cell-cell adhesions to allow the migration of endothelial cells (Groten *et al.*, 2005). In horses, fetoplacental estrogens slowly increase during pregnancy and blood concentrations peak at late term gestation. Remarkably, horses are most susceptible to EHV1 abortion during this period (Allen and Bryans, 1986). Smith *et al.* (2002) showed that 17β -oestradiol activates the expression of adhesion molecules on endothelial cells of the reproductive tract, which is a key step in transferring virus from infected leukocytes to endothelial cells. The precise role of 17β -oestradiol on the integrity of equine endothelial cells and subsequent transfer of EHV1 has not been studied. Destruction of endothelial integrity might facilitate the spread of EHV1 and furthermore, mares might be more sensitive for a respiratory re-infection when the intercellular bridges at the respiratory tract are damaged by estrogens. Indeed, it has been shown that the nasal respiratory epithelium is an estrogen target (Caruso *et al.*, 2003).

Since disruption of respiratory epithelial integrity leads to enhanced EHV1 binding, we hypothesized that its primary binding/entry receptor is located basolaterally. Therefore, we isolated EREC and inoculated them at either apical or basolateral surfaces. Indeed, we found that EHV1 preferentially binds to and infects EREC at basolateral surfaces. Along with EHV1, more respiratory viruses target a basolaterally located receptor, which is only exposed in a compromised epithelium. Adenoviruses bind to an integral TJ protein named 'coxsackievirus and adenovirus receptor', which is only accessible after disruption of epithelial integrity (Walters *et al.*, 2002). HSV1 most efficiently infects human epithelial cells from the apical

surface, due to the presence of nectin-1. However, downregulation of nectin-1 had no impact on basolateral infection, indicating that HSV1 can also use this putative basolaterally located receptor (Galen *et al.*, 2006).

It is known that EHV1 initially interacts with heparan sulfate on cell surfaces via gB and gC (Neubauer *et al.*, 1997; Osterrieder, 1999). The respiratory epithelium expressed heparan sulfate solely at the level of the basement membrane. This distribution pattern is in accordance with MDCK and murine mammary epithelial cells, which preferentially sort heparan sulfate to their basolateral domain (Caplan *et al.*, 1987; Rapraeger *et al.*, 1986). However, primary EREC lacked expression of heparan sulfate and in addition, pretreatment of EHV1 with heparin did not reduce subsequent EREC infection (unpublished data). Similar to heparan sulfate, chondroitin sulfate was present in the basolateral membrane of nasal and tracheal mucosal explant epithelia, but was absent in EREC. As assessed by immunofluorescent staining, sialic acids were ubiquitously expressed on EREC. Moreover, sialic acids are shown to play a role in EHV1 entry in monocytic CD172a⁺ cells (Laval *et al.*, 2016). Therefore, we specifically removed sialic acids with neuraminidase prior to EHV1 inoculation. However, no significant reduction in number of virus plaques was observed between neuraminidase- and control-pretreated EREC. These results indicate that other glycosaminoglycans play a role in EHV1 infection of EREC. Indeed, after non-specifically removing cellular N-linked glycans, subsequent EHV1 infection was impaired. Next, EHV1 glycoprotein gD binds to a cellular receptor to stabilise the binding and trigger entry into the cell (Csellner *et al.*, 2000). MHC I is shown to be a putative receptor for EHV1 gD in equine brain microvascular cells, dermal cells and PBMC (Kurtz *et al.*, 2010; Sasaki *et al.*, 2011). However, MHC I is ubiquitously expressed and therefore, does not correlate with EHV1 tissue tropism. EHV1 entry in PBMC is initiated by binding of gD to cellular integrins (Laval *et al.*, 2016; Van de Walle *et al.*, 2008). Integrins such as $\alpha_3\beta_1$, $\alpha_6\beta_4$ and $\alpha_v\beta_5$ are sorted to the basolateral domains of respiratory epithelial cells, allowing firm attachment to the extracellular matrix (Sheppard, 2003). The importance of these integrins in EHV1 infection of EREC is still unknown. Finally, nectins aid in calcium-independent cellular adhesion and are known to interact with several alphaherpesviruses, including HSV1 and 2, PRV and BoHV1 (Geraghty *et al.*, 1998). Nonetheless, EHV1 presumably does not depend on nectins, since CHO-K1 lack nectin-1 and -2 expression, although they are fully susceptible to EHV1 (Frampton *et al.*, 2005). Until present, the precise EREC binding/entry receptor for EHV1 remains unknown. Our observations point out that it is located at cellular basolateral surfaces and becomes apically accessible when intercellular adhesion is impaired.

We hypothesize that EHV1, among other alphaherpesviruses, exhibits a specific strategy for host invasion and subsequent spread. Upon inhalation, primary virus replication in respiratory epithelial cells is limited in order to avoid the onset of a strong immune response, but high enough to infect latency-inducible cells (leukocytes and neurons). Once present inside the host, the virus can invade the respiratory epithelium from its basolateral side upon reactivation. Spread can occur from infected leukocytes or from infected neurons through anterograde axonal transport. This is key for efficient secondary replication in the respiratory epithelium and shed of progeny virus to new hosts.

Taken together, our results shed new light on the pathogenesis of alphaherpesviruses in their specific target host cells, a significant aspect of medical research on herpesvirus-induced diseases.

Acknowledgements

The authors are grateful to Dr. O'Callaghan and Prof. Balasuriya for supplying the antibodies against EHV1 proteins. The authors also acknowledge Carine Boone, Chantal Vanmaercke, Ytse Noppe, Nele Dennequin and Lobke De Bels for their excellent technical support.

References

- Allen, G.P., Bryans, J.T., 1986.** Molecular epizootiology, pathogenesis, and prophylaxis of equine herpesvirus-1 infections. *Progress in veterinary microbiology and immunology* 2, 78-144.
- Balda, M.S., Matter, K., 2016.** Tight junctions as regulators of tissue remodelling. *Current Opinion in Cell Biology* 42, 94-101.
- Balda, M.S., Whitney, J.A., Flores, C., González, S., Cereijido, M., Matter, K., 1996.** Functional dissociation of paracellular permeability and transepithelial electrical resistance and disruption of the apical-basolateral intramembrane diffusion barrier by expression of a mutant tight junction membrane protein. *The Journal of cell biology* 134, 1031.
- Ballard, S.T., Schepens, S.M., Falcone, J.C., Meininger, G.A., Taylor, A.E., 1992.** Regional bioelectric properties of porcine airway epithelium. *Journal of applied physiology (Bethesda, Md. : 1985)* 73, 2021-2027.
- Banfield, B.W., Leduc, Y., Esford, L., Visalli, R.J., Brandt, C.R., Tufaro, F., 1995.** Evidence for an interaction of herpes simplex virus with chondroitin sulfate proteoglycans during infection. *Virology* 208, 531-539.
- Baum, B., Georgiou, M., 2011.** Dynamics of adherens junctions in epithelial establishment, maintenance, and remodeling. *The Journal of cell biology* 192, 907-917.
- Baxi, M.K., Efstathiou, S., Lawrence, G., Whalley, J.M., Slater, J.D., Field, H.J., 1995.** The detection of latency-associated transcripts of equine herpesvirus 1 in ganglionic neurons. *The Journal of general virology* 76(12), 3113-3118.
- Blank, C.A., Anderson, D.A., Beard, M., Lemon, S.M., 2000.** Infection of polarized cultures of human intestinal epithelial cells with hepatitis A virus: vectorial release of progeny virions through apical cellular membranes. *J Virol* 74, 6476-6484.
- Boucher, R.C., Stutts, M.J., Gatzky, J.T., 1981.** Regional differences in bioelectric properties and ion flow in excised canine airways. *Journal of applied physiology: respiratory, environmental and exercise physiology* 51, 706-714.
- Breuer, D., Becker, M., 1983.** Acetylcysteine (Fluimucil) in the treatment of COPD of the horse. *Tierärztliche Praxis* 11, 209-212.
- Brown, R.C., Davis, T.P., 2002.** Calcium modulation of adherens and tight junction function: a potential mechanism for blood-brain barrier disruption after stroke. *Stroke* 33, 1706-1711.
- Capaldo, C.T., Nusrat, A., 2009.** Cytokine regulation of tight junctions. *Biochimica et biophysica acta* 1788, 864-871.
- Caplan, M.J., Stow, J.L., Newman, A.P., Madri, J., Anderson, H.C., Farquhar, M.G., Palade, G.E., Jamieson, J.D., 1987.** Dependence on pH of polarized sorting of secreted proteins. *Nature* 329, 632-635.
- Caruso, S., Roccasalva, L., Di Fazio, E., Sapienza, G., Agnello, C., Ficarra, S., Di Mari, L., Serra, A., 2003.** Cytologic aspects of the nasal respiratory epithelium in postmenopausal women treated with hormone therapy. *Fertility and sterility* 79, 543-549.
- Chu, J.J., Ng, M.L., 2002.** Infection of polarized epithelial cells with flavivirus West Nile: polarized entry and egress of virus occur through the apical surface. *The Journal of general virology* 83, 2427-2435.
- Clayson, E.T., Compans, R.W., 1988.** Entry of simian virus 40 is restricted to apical surfaces of polarized epithelial cells. *Molecular and Cellular Biology* 8, 3391-3396.
- Costa, L.R., Johnson, J.R., Baur, M.E., Beadle, R.E., 2006.** Temporal clinical exacerbation of summer pasture-associated recurrent airway obstruction and relationship with climate and aeroallergens in horses. *American journal of veterinary research* 67, 1635-1642.
- Csellner, H., Walker, C., Wellington, J.E., McLure, L.E., Love, D.N., Whalley, J.M., 2000.** EHV-1 glycoprotein D (EHV-1 gD) is required for virus entry and cell-cell fusion, and an EHV-1 gD deletion mutant induces a protective immune response in mice. *Arch Virol* 145, 2371-2385.
- Dayaram, A., Franz, M., Schattschneider, A., Damiani, A.M., Bischofberger, S., Osterrieder, N., Greenwood, A.D., 2017.** Long term stability and infectivity of herpesviruses in water. *Scientific reports* 7, 46559.

- Fokkens, W.J., Scheeren, R.A., 2000.** Upper airway defence mechanisms. Paediatric respiratory reviews 1, 336-341.
- Frampton, A.R., Goins, W.F., Cohen, J.B., von Einem, J., Osterrieder, N., O'Callaghan, D.J., Glorioso, J.C., 2005.** Equine Herpesvirus 1 Utilizes a Novel Herpesvirus Entry Receptor. Journal of Virology 79, 3169-3173.
- Galen, B., Cheshenko, N., Tuyama, A., Ramratnam, B., Herold, B.C., 2006.** Access to nectin favors herpes simplex virus infection at the apical surface of polarized human epithelial cells. Journal of Virology 80, 12209-12218.
- Geraghty, R.J., Krummenacher, C., Cohen, G.H., Eisenberg, R.J., Spear, P.G., 1998.** Entry of alphaherpesviruses mediated by poliovirus receptor-related protein 1 and poliovirus receptor. Science (New York, N.Y.) 280, 1618-1620.
- Gerez, J.R., Pinton, P., Callu, P., Grosjean, F., Oswald, I.P., Bracarense, A.P.F.L., 2015.** Deoxynivalenol alone or in combination with nivalenol and zearalenone induce systemic histological changes in pigs. Experimental and Toxicologic Pathology 67, 89-98.
- Gibson, J.S., Slater, J.D., Awan, A.R., Field, H.J., 1992.** Pathogenesis of equine herpesvirus-1 in specific pathogen-free foals: primary and secondary infections and reactivation. Archives of Virology 123, 351-366.
- Glorieux, S., Bachert, C., Favoreel, H.W., Vandekerckhove, A.P., Steukers, L., Rekecki, A., Van den Broeck, W., Goossens, J., Croubels, S., Clayton, R.F., Nauwynck, H.J., 2011.** Herpes simplex virus type 1 penetrates the basement membrane in human nasal respiratory mucosa. PLoS One 6, e22160.
- Glorieux, S., Van den Broeck, W., van der Meulen, K.M., Van Reeth, K., Favoreel, H.W., Nauwynck, H.J., 2007.** *In vitro* culture of porcine respiratory nasal mucosa explants for studying the interaction of porcine viruses with the respiratory tract. Journal of virological methods 142, 105-112.
- Grinde, B., 2013.** Herpesviruses: latency and reactivation – viral strategies and host response. Journal of Oral Microbiology 5, 10.3402/jom.v3405i3400.22766.
- Groten, T., Pierce, A.A., Huen, A.C., Schnaper, H.W., 2005.** 17 beta-estradiol transiently disrupts adherens junctions in endothelial cells. FASEB journal: official publication of the Federation of American Societies for Experimental Biology 19, 1368-1370.
- Jacquot, J., Spilmont, C., de Bentzmann, S., Dupuit, F., Puchelle, E., 1992.** Structure and secretory functions of the respiratory epithelium. Archives internationales de physiologie, de biochimie et de biophysique 100, A41-46.
- Kurtz, B.M., Singletary, L.B., Kelly, S.D., Frampton, A.R., Jr., 2010.** Equus caballus major histocompatibility complex class I is an entry receptor for equine herpesvirus type 1. J Virol 84, 9027-9034.
- Kwak, Y.-K., Vikström, E., Magnusson, K.-E., Vécsey-Semjén, B., Colque-Navarro, P., Möllby, R., 2012.** The *Staphylococcus aureus* Alpha-Toxin Perturbs the Barrier Function in Caco-2 Epithelial Cell Monolayers by Altering Junctional Integrity. Infection and Immunity 80, 1670-1680.
- Laval, K., Favoreel, H.W., Van Cleemput, J., Poelaert, K.C.K., Brown, I.K., Verhasselt, B., Nauwynck, H.J., 2016.** Entry of equid herpesvirus 1 into CD172a⁺ monocytic cells. Journal of General Virology 97, 733-746.
- Lim, P.J., Chu, J.J.H., 2014.** A Polarized Cell Model for Chikungunya Virus Infection: Entry and Egress of Virus Occurs at the Apical Domain of Polarized Cells. PLoS Neglected Tropical Diseases 8, e2661.
- Lopez-Souza, N., Favoreto, S., Wong, H., Ward, T., Yagi, S., Schnurr, D., Finkbeiner, W.E., Dolganov, G.M., Widdicombe, J.H., Boushey, H.A., Avila, P.C., 2009.** *In vitro* susceptibility to rhinovirus infection is greater for bronchial than for nasal airway epithelial cells in human subjects. The Journal of allergy and clinical immunology 123, 1384-1390.e1382.
- Lunn, D.P., Davis-Poynter, N., Flaminio, M.J.B.F., Horohov, D.W., Osterrieder, K., Pusterla, N., Townsend, H.G.G., 2009.** Equine Herpesvirus-1 Consensus Statement. Journal of Veterinary Internal Medicine 23, 450-461.
- Mair, T.S., Derksen, F.J., 2000.** Chronic obstructive pulmonary disease: a review. Equine Veterinary Education 12, 35-44.

- Marozin, S., Prank, U., Sodeik, B., 2004.** Herpes simplex virus type 1 infection of polarized epithelial cells requires microtubules and access to receptors present at cell-cell contact sites. *The Journal of general virology* 85, 775-786.
- Mateo, M., Generous, A., Sinn, P.L., Cattaneo, R., 2015.** Connections matter – how viruses use cell–cell adhesion components. *Journal of Cell Science* 128, 431-439.
- Matter, K., Balda, M.S., 2003.** Functional analysis of tight junctions. *Methods (San Diego, CA)* 30, 228-234.
- Naziroglu, M., Senol, N., Ghazizadeh, V., Yuruker, V., 2014.** Neuroprotection induced by N-acetylcysteine and selenium against traumatic brain injury-induced apoptosis and calcium entry in hippocampus of rat. *Cellular and molecular neurobiology* 34, 895-903.
- Negussie, H., Li, Y., Tessema, T.S., Nauwynck, H.J., 2016.** Replication characteristics of equine herpesvirus 1 and equine herpesvirus 3: comparative analysis using *ex vivo* tissue cultures. *Veterinary Research* 47, 19.
- Neubauer, A., Braun, B., Brandmuller, C., Kaaden, O.R., Osterrieder, N., 1997.** Analysis of the contributions of the equine herpesvirus 1 glycoprotein gB homolog to virus entry and direct cell-to-cell spread. *Virology* 227, 281-294.
- Nilsson, M., Fagman, H., Ericson, L.E., 1996.** Ca²⁺-dependent and Ca²⁺-independent regulation of the thyroid epithelial junction complex by protein kinases. *Experimental cell research* 225, 1-11.
- Osterrieder, N., 1999.** Construction and characterization of an equine herpesvirus 1 glycoprotein C negative mutant. *Virus Res* 59, 165-177.
- Quintana, A.M., Landolt, G.A., Annis, K.M., Hussey, G.S., 2011.** Immunological characterization of the equine airway epithelium and of a primary equine airway epithelial cell culture model. *Veterinary Immunology and Immunopathology* 140, 226-236.
- Rapraeger, A., Jalkanen, M., Bernfield, M., 1986.** Cell surface proteoglycan associates with the cytoskeleton at the basolateral cell surface of mouse mammary epithelial cells. *The Journal of cell biology* 103, 2683-2696.
- Reas, H.W., 1963.** The effect of N-acetylcysteine on the viscosity of tracheobronchial secretions in cystic fibrosis of the pancreas. *The Journal of Pediatrics* 62, 31-35.
- Runswick, S., Mitchell, T., Davies, P., Robinson, C., Garrod, D.R., 2007.** Pollen proteolytic enzymes degrade tight junctions. *Respirology (Carlton, Vic.)* 12, 834-842.
- Sasaki, M., Hasebe, R., Makino, Y., Suzuki, T., Fukushi, H., Okamoto, M., Matsuda, K., Taniyama, H., Sawa, H., Kimura, T., 2011.** Equine major histocompatibility complex class I molecules act as entry receptors that bind to equine herpesvirus-1 glycoprotein D. *Genes to cells : devoted to molecular & cellular mechanisms* 16, 343-357.
- Shasby, D.M., Shasby, S.S., 1986.** Effects of calcium on transendothelial albumin transfer and electrical resistance. *Journal of applied physiology (Bethesda, Md. : 1985)* 60, 71-79.
- Sheppard, D., 2003.** Functions of pulmonary epithelial integrins: from development to disease. *Physiological reviews* 83, 673-686.
- Slater, J.D., Borchers, K., Thackray, A.M., Field, H.J., 1994.** The trigeminal ganglion is a location for equine herpesvirus 1 latency and reactivation in the horse. *The Journal of general virology* 75(8), 2007-2016.
- Smith, D., Hamblin, A., Edington, N., 2002.** Equid herpesvirus 1 infection of endothelial cells requires activation of putative adhesion molecules: an *in vitro* model. *Clinical and Experimental Immunology* 129, 281-287.
- Spear, P.G., 1993.** Entry of alphaherpesviruses into cells. *Seminars in Virology* 4, 167-180.
- Stachelin, L.A., 1974.** Structure and function of intercellular junctions. *International review of cytology* 39, 191-283.
- Steukers, L., Vandekerckhove, A.P., Van den Broeck, W., Glorieux, S., Nauwynck, H.J., 2012.** Kinetics of BoHV-1 dissemination in an *in vitro* culture of bovine upper respiratory tract mucosa explants. *ILAR journal* 53, E43-54.
- Steukers, L., Weyers, S., Yang, X., Vandekerckhove, A.P., Glorieux, S., Cornelissen, M., Van den Broeck, W., Temmerman, M., Nauwynck, H.J., 2014.** Mimicking herpes simplex virus 1 and herpes simplex virus 2 mucosal behavior in a well-characterized human genital organ culture. *The Journal of infectious diseases* 210, 209-213.

- Stray, S.J., Cummings, R.D., Air, G.M., 2000.** Influenza virus infection of desialylated cells. *Glycobiology* 10, 649-658.
- Topp, K.S., Rothman, A.L., Lavail, J.H., 1997.** Herpes virus infection of RPE and MDCK cells: polarity of infection. *Experimental eye research* 64, 343-354.
- Vairo, S., Van den Broeck, W., Favoreel, H., Scagliarini, A., Nauwynck, H., 2013.** Development and use of a polarized equine upper respiratory tract mucosal explant system to study the early phase of pathogenesis of a European strain of equine arteritis virus. *Veterinary Research* 44, 9.
- Van de Walle, G.R., Peters, S.T., VanderVen, B.C., O'Callaghan, D.J., Osterrieder, N., 2008.** Equine herpesvirus 1 entry via endocytosis is facilitated by alphaV integrins and an RSD motif in glycoprotein D. *J Virol* 82, 11859-11868.
- Van De Walle, J., Sargent, T., Piront, N., Toussaint, O., Schneider, Y.-J., Larondelle, Y., 2010.** Deoxynivalenol affects *in vitro* intestinal epithelial cell barrier integrity through inhibition of protein synthesis. *Toxicology and Applied Pharmacology* 245, 291-298.
- Van der Meulen, K., Vercauteren, G., Nauwynck, H., Pensaert, M., 2003a.** A local epidemic of equine herpesvirus 1-induced neurological disorders in Belgium. *Vlaams Diergeneeskundig Tijdschrift* 72, 366-372.
- Van der Meulen, K.M., Nauwynck, H.J., Buddaert, W., Pensaert, M.B., 2000.** Replication of equine herpesvirus type 1 in freshly isolated equine peripheral blood mononuclear cells and changes in susceptibility following mitogen stimulation. *Journal of General Virology* 81, 21-25.
- Van der Meulen, K.M., Nauwynck, H.J., Pensaert, M.B., 2003b.** Absence of viral antigens on the surface of equine herpesvirus-1-infected peripheral blood mononuclear cells: a strategy to avoid complement-mediated lysis. *Journal of general virology* 84, 93-97.
- Vandekerckhove, A., Glorieux, S., Van den Broeck, W., Gryspeerdt, A., van der Meulen, K.M., Nauwynck, H.J., 2009.** *In vitro* culture of equine respiratory mucosa explants. *Veterinary Journal* 181, 280-287.
- Vandekerckhove, A.P., Glorieux, S., Gryspeerdt, A.C., Steukers, L., Duchateau, L., Osterrieder, N., Van de Walle, G.R., Nauwynck, H.J., 2010.** Replication kinetics of neurovirulent versus non-neurovirulent equine herpesvirus type 1 strains in equine nasal mucosal explants. *The Journal of general virology* 91, 2019-2028.
- Vinhas, R., Cortes, L., Cardoso, I., Mendes, V.M., Manadas, B., Todo-Bom, A., Pires, E., Verissimo, P., 2011.** Pollen proteases compromise the airway epithelial barrier through degradation of transmembrane adhesion proteins and lung bioactive peptides. *Allergy* 66, 1088-1098.
- Volberg, T., Geiger, B., Kartenbeck, J., Franke, W.W., 1986.** Changes in membrane-microfilament interaction in intercellular adherens junctions upon removal of extracellular Ca²⁺ ions. *The Journal of cell biology* 102, 1832-1842.
- Walters, R.W., Freimuth, P., Moninger, T.O., Ganske, I., Zabner, J., Welsh, M.J., 2002.** Adenovirus fiber disrupts CAR-mediated intercellular adhesion allowing virus escape. *Cell* 110, 789-799.
- Wang, G., Zabner, J., Deering, C., Launspach, J., Shao, J., Bodner, M., Jolly, D.J., Davidson, B.L., McCray, P.B., Jr., 2000.** Increasing epithelial junction permeability enhances gene transfer to airway epithelia *In vivo*. *American journal of respiratory cell and molecular biology* 22, 129-138.
- Xiao, C., Puddicombe, S.M., Field, S., Haywood, J., Broughton-Head, V., Puxeddu, I., Haitchi, H.M., Vernon-Wilson, E., Sammut, D., Bedke, N., Cremin, C., Sones, J., Djukanović, R., Howarth, P.H., Collins, J.E., Holgate, S.T., Monk, P., Davies, D.E., 2011.** Defective epithelial barrier function in asthma. *Journal of Allergy and Clinical Immunology* 128, 549-556.e512.
- Yang, X., Forier, K., Steukers, L., Van Vlierberghe, S., Dubruel, P., Braeckmans, K., Glorieux, S., Nauwynck, H.J., 2012.** Immobilization of pseudorabies virus in porcine tracheal respiratory mucus revealed by single particle tracking. *PLoS One* 7, e51054.
- Yang, X.Y., Steukers, L., Forier, K., Xiong, R.H., Braeckmans, K., Van Reeth, K., Nauwynck, H., 2014.** A Beneficiary Role for Neuraminidase in Influenza Virus Penetration through the Respiratory Mucus. *Plos One* 9, 11.
- Zabner, J., Freimuth, P., Puga, A., Fabrega, A., Welsh, M.J., 1997.** Lack of high affinity fiber receptor activity explains the resistance of ciliated airway epithelia to adenovirus infection. *Journal of Clinical Investigation* 100, 1144-1149.

- Zerboni, L., Sen, N., Oliver, S.L., Arvin, A.M., 2014.** Molecular mechanisms of varicella zoster virus pathogenesis. *Nat Rev Micro* 12, 197-210.
- Zhang, L., Peeples, M.E., Boucher, R.C., Collins, P.L., Pickles, R.J., 2002.** Respiratory syncytial virus infection of human airway epithelial cells is polarized, specific to ciliated cells, and without obvious cytopathology. *J Virol* 76, 5654-5666.

Chapter 4.

Beyond allergy: how pollen proteases destroy respiratory epithelial cell anchors and drive alphaherpesvirus infection

Jolien Van Cleemput, Katrien C.K. Poelaert, Kathlyn Laval, Francis Impens, Wim Van den Broeck,
Kris Gevaert, Hans J. Nauwynck

Submitted to Scientific Reports

Summary

Pollens are well-known triggers of respiratory allergies and have been shown to disrupt the epithelial barrier in continuous cell lines. How pollens interact with the respiratory mucosa remains largely unknown due to lack of representative model systems. Following pollen inhalation, pollen protease-induced loss-of-barrier function might predispose the respiratory epithelium for alphaherpesvirus invasion, as these viruses target a basolaterally located receptor. We here demonstrate how pollen proteases of Kentucky bluegrass, white birch and hazel selectively destroy integrity of columnar respiratory epithelial cells, but not of basal cells, in both *ex vivo* equine respiratory mucosal explants and *in vitro* primary equine respiratory epithelial cells (EREC). In turn, this pollen protease-induced damage to respiratory epithelial cell anchorage resulted in increased infection by the host-specific and ancestral alphaherpesvirus equine herpesvirus type 1 (EHV1). Pollen proteases of all three plant species were characterized by zymography and those of white birch were fully identified for the first time as serine proteases of the subtilase-family and meiotic prophase aminopeptidase 1 using mass spectrometry-based proteomics. Together, our findings demonstrate that pollen proteases selectively and irreversibly damage anchorage of columnar respiratory epithelial cells. Alphaherpesviruses benefit from this partial loss-of-barrier function, resulting in increased infection of the respiratory epithelium.

Introduction

Alphaherpesviruses often colonize new hosts through the respiratory mucosae, where they initiate a primary replication in the respiratory epithelium. This primary replication is usually restricted in healthy hosts (Glorieux *et al.*, 2011; Glorieux *et al.*, 2009; Steukers *et al.*, 2012; Vandekerckhove *et al.*, 2010). We recently showed that the intercellular junctions (ICJ), formed by a network of close connections between adjacent cells, hinder alphaherpesvirus infection of the epithelium by masking access to a basolaterally located major viral binding receptor (Van Cleemput *et al.*, 2017). So far, airborne factors that predispose the respiratory epithelium for alphaherpesvirus infection remain unknown. Interestingly, respiratory allergies are associated with impaired barrier function by ICJ in the respiratory epithelium (Xiao *et al.*, 2011a). Plant pollens are well-known triggers of respiratory allergies and their proteases have been shown to affect the ICJ of continuous cell lines (Cortes *et al.*, 2006; Runswick *et al.*, 2007; Vinhas *et al.*, 2011). We hypothesized that this pollen protease-induced loss-of-barrier function might predispose the respiratory epithelium for alphaherpesvirus infection.

Pollen protease-induced disruption of epithelial integrity is believed to facilitate the delivery of pollen allergens to the subepithelial antigen-presenting cells and subsequent priming of T helper 2 (Th2) cells (Taketomi *et al.*, 2006; Xiao *et al.*, 2011b). In turn, the inflammatory reaction elicited by Th2 cell-specific cytokines (IL-4, IL-5 and IL-13) and failure of T regulatory cells to suppress these events further drives the immunopathology of allergies (Barnes, 2011; Batanero *et al.*, 2002; Grünig *et al.*, 1998). Pollen proteases are mainly localized at the pollen wall and assist in the assembly of a pollen tube within the flower pistil's transmission tract (Radlowski, 2005; Swanson *et al.*, 2004). However, they are easily liberated by hydration upon inhalation in the human and/or animal respiratory tract. Pollen proteases have already been characterized as serine, cysteine, threonine and metalloproteases in several plants including maize, white birch, pine, giant ragweed, rye and blue grass, easter lily and olive tree (González-Rábade *et al.*, 2011; Höllbacher *et al.*, 2017; Runswick *et al.*, 2007; Vinhas *et al.*, 2011; Widmer *et al.*, 2000). However, limited knowledge on plant genomics and proteomics hindered previous researchers from fully identifying these proteases.

Our study aimed at identifying specific plant proteases and depicting their impact on the respiratory epithelium and on subsequent alphaherpesvirus host invasion, using representative models. Previous studies examining pollen-induced loss-of-barrier function mainly used continuous cell lines. However, these continuous cell lines do not reflect the *in vivo* situation. Here, the horse (*Equus caballus*) and the horse-specific alphaherpesvirus equine herpesvirus

type 1 (EHV1) were used as our study system. Similarly to human pollen allergies, horses commonly suffer from summer pasture-associated recurrent airway obstruction (SP-RAO) during late winter-spring, as a result of peaking pollen concentrations in the ambient air. In addition, the horse has already been shown to act as a representative model to study allergies (Bullone and Lavoie, 2015). The horse-specific EHV1 is a well-known member of the alphaherpesvirus family and is closely related to other alphaherpesviruses (e.g. varicella-zoster virus, herpes simplex virus, pseudorabies and bovine herpesvirus type 1) (Davison, 2002; Karlin *et al.*, 1994). Interestingly, EHV1 even stood out as the most central one among all examined alphaherpesviruses (Karlin *et al.*, 1994). Thus, pollen-induced effects and host-specific alphaherpesvirus infections can optimally be studied using representative equine *ex vivo* and *in vitro* models, known to mimic *in vivo* conditions (Quintana *et al.*, 2011; Vandekerckhove *et al.*, 2009).

Material and methods

Preparation of pollen diffusates

Pollen diffusates were prepared as previously described (Runswick *et al.*, 2007). In summary, pollens from Kentucky bluegrass (KBG; *Poa pratensis*), white birch (WB; *Betula pendula*) and hazel (H; *Corylus americana*) were purchased from Stallergreens Greer (Cambridge, MA, USA). Pollens were shaken at a concentration of 100 mg/mL in phosphate buffered saline (PBS) for 2 h at 4°C prior to centrifugation at 10,000 g for 10 min at 4°C. The supernatant was harvested and filtered through 0.22 µm pore size filters (VWR International, Radnor, PA, USA). Finally, the protein concentration in the pollen diffusates was determined using the Bradford assay (ThermoFisher Scientific, Waltham, MA, USA) and a Nanodrop[®] spectrophotometer, following the manufacturer's instructions. All pollen diffusates were diluted with PBS to a final concentration of 5 mg/mL and either used immediately or frozen in aliquots at -20°C.

Gel electrophoresis

Pollen diffusates were diluted 1:1 in Laemmli sample buffer for 20 min at room temperature (RT) and loaded onto 10% SDS polyacrylamide (ThermoFisher Scientific) gels (Laemmli, 1970). The gels were run at 100 V for 110 min using a Mini Protean Tetra apparatus (Bio-Rad, Hercules, CA, USA). To assess the protein profile of the pollen diffusates, gels were stained for 1 h with Coomassie blue R-250 (Imperial[™] Protein Stain; ThermoFisher Scientific) and de-stained in H₂O overnight. White birch protein bands with corresponding enzymatic activity, as assessed by zymography, were excised from the gel, transferred to Eppendorf tubes, washed two times in H₂O and frozen at -20°C until further processing.

Proteomics sample preparation

Gel bands were washed with 500 µl H₂O, incubated for 15 min with 500 µl water/acetonitrile (1:1, v/v) and incubated for 15 min with 500 µl 100% acetonitrile before they were dried completely in a vacuum concentrator. 150 ng sequencing-grade trypsin (Promega) in 50 mM ammonium bicarbonate in water/acetonitrile (9:1, v/v) was added to the dried gel bands and proteins were digested overnight at 37°C. Peptides eluted from every gel band were dried completely in a vacuum concentrator and re-dissolved in 20 µl loading solvent A (0.1% TFA in water/acetonitrile (98:2, v/v)) for LC-MS/MS analysis.

LC-MS/MS and data analysis

From each gel band, 2 µl of re-dissolved peptides was injected for LC-MS/MS analysis on an Ultimate 3000 RSLCnano system in-line connected to an LTQ Orbitrap Elite mass spectrometer (ThermoFisher Scientific). Trapping was performed at 10 µl/min for 4 minutes in loading solvent A on a 20 mm trapping column (made in-house, 100 µm internal diameter [I.D.], 5 µm beads, C18 Reprosil-HD, Dr. Maisch, Germany) and the sample was loaded on a 200 mm analytical column (made in-house, 75 µm I.D., 1.9 µm beads C18 Reprosil-HD, Dr. Maisch). Peptides were eluted by a non-linear increase from 2 to 56% MS solvent B (0.1% FA in water/acetonitrile (2:8, v/v)) over 25 min at a constant flow rate of 250 nl/min, followed by a 10 min wash reaching 99% MS solvent B and re-equilibration with MS solvent A (0.1% FA in water/acetonitrile (2:8, v/v)). The mass spectrometer was operated in data-dependent mode, automatically switching between MS and MS/MS acquisition for the 20 most abundant ion peaks per MS spectrum. Full-scan MS spectra (300-2000 m/z) were acquired at a resolution of 60,000 in the orbitrap analyzer after accumulation to a target value of 3,000,000. The 20 most intense ions above a threshold value of 500 were isolated for fragmentation by CID at a normalized collision energy of 35% in the linear ion trap (LTQ), after filling the trap at a target value of 5,000 for maximum 20 ms (rapid scan rate mode).

Data analysis was performed with MaxQuant (version 1.6.1.0) using the Andromeda search engine with default search settings including a false discovery rate set at 1% on both the peptide and protein level. Spectra from all three gel bands were searched together against a database of *Betula Pendula* protein sequences reported by Salojarvi *et al.* (2017) (containing 29,919 protein sequences downloaded from <https://genomevolution.org> on March 27 2018). The mass tolerance for precursor and fragment ions was set to 4.5 and 20 ppm, respectively, during the main search. Enzyme specificity was set as C-terminal to arginine and lysine (trypsin), also allowing cleavage at arginine/lysine-proline bonds with a maximum of two missed cleavages. Oxidation of methionine residues (to sulfoxides), acetylation of protein N-termini and propionamide modification of cysteine residues were set as variable modifications. Identified proteins were reported from the proteinGroups.txt MaxQuant output files and putative proteases, glycosidases and lipases (Table 1) were manually selected based on the annotation of the orthologues Arabidopsis proteins provided by Salojarvi *et al.* (2017).

Zymography

Prior to gel electrophoresis, pollen diffusates were incubated with or without protease inhibitors for 2 h at 4°C under gentle agitation. The following protease inhibitors were used: (i) an

irreversible serine protease inhibitor 4-(2-Aminoethyl)benzenesulfonyl fluoride hydrochloride (AEBSF); 500 μM (Sigma-Aldrich; St. Louis, MO, USA), (ii) a metal chelator ethylene diamine tetra-acetic acid (EDTA); 2.5 μM (VWR), (iii) an irreversible cysteine protease inhibitor epoxide 64 (E-64); 15 μM (Sigma-Aldrich) and (iv) a reversible aspartic acid protease inhibitor pepstatin A; 10 μM (Sigma-Aldrich). Gels impregnated with 0.1% gelatine (from bovine skin; Sigma-Aldrich, St. Louis, MO, USA) were used and gel electrophoresis was performed as described above. Next, proteins were renatured by incubating the gels in 2.5% Triton-X 100 for 20 min at RT. Following a washing step in H_2O , the gels were transferred to a new tray containing development buffer (50 mM Tris-HCl pH 7.5, 200 mM NaCl, 5 mM CaCl_2 , 1 μM ZnCl_2 ; Sigma-Aldrich) supplemented with or without the above-described protease inhibitors. The gels were incubated overnight at 37°C and stained using Coomassie blue R-250, as described above. A ChemiDocMP Imaging System (Bio-Rad) was used to take pictures of the Coomassie blue-stained gels. RGB-pictures were converted to 8-bit grey-scaled images using ImageJ (ImageJ, U.S. National Institutes of Health, Bethesda, Maryland, USA). Finally, presence or absence of proteolytic bands was determined by plot-profiling the zymogram lanes in ImageJ.

Tissue collection and processing

The tracheae from different healthy horses were collected at the slaughterhouse and transported in PBS with calcium and magnesium, supplemented with 0.1 mg/mL gentamicin (ThermoFisher Scientific, Paisley, UK), 0.1 mg/mL kanamycin (Sigma-Aldrich), 100 U/mL penicillin, 0.1 mg/mL streptomycin (ThermoFisher Scientific) and 0.25 $\mu\text{g}/\text{mL}$ amphotericin B (ThermoFisher Scientific).

Respiratory mucosal explant isolation and cultivation

Tracheal mucosal explants were prepared as previously described (Van Cleemput *et al.*, 2017; Vandekerckhove *et al.*, 2009).

EREC isolation and cultivation

Primary equine respiratory epithelial cells (EREC) were isolated and cultured as described by Quintana *et al.* (2011) and Van Cleemput *et al.* (2017).

Pollen diffusate treatment of respiratory mucosal explants and EREC

Respiratory mucosal explants

Explants were cultured 24 h for adaptation before thoroughly washing and embedding them in agarose diluted in 2X MEM, to mimic *in vivo* conditions, as previously published (Vairo *et al.*, 2013; Van Cleemput *et al.*, 2017). Next, the apical surface of the epithelium was exposed for 12 h at 37°C to the pollen diffusates supplemented with or without the protease inhibitor mixture (PI) containing 500 µM AEBSF, 15 µM E-64 and 2.5 µM EDTA. As negative control, PBS with or without PI was used. One hour treatment with EGTA was included as positive control (Van Cleemput *et al.*, 2017). As negative control, PBS with or without protease inhibitors was used. Explants were removed from the agarose and washed three times in PBS and fixed in a phosphate-buffered 3.5% formaldehyde solution for 24 h, either immediately after the last wash or after an additional 24 h incubation on metal gauzes. Explants were then stored into 70% alcohol until further processing.

EREC

Cells were grown to confluency and the transepithelial electrical resistance (TEER) was measured daily until a steady TEER of ~500-700 $\Omega \times \text{cm}^{-2}$ was reached. The pollen diffusates with or without the above-described protease inhibitor mixture (PI) were added to the apical surface of the cells. EGTA was used as positive control and PBS with or without the PI was used as negative control. Cells were incubated for 12 h, while epithelial integrity and cell viability was assessed, as described below.

Assessment of epithelial integrity

Respiratory mucosal explants

Integrity of the intercellular junctions was verified by examining the intercellular space in haematoxylin-eosin-stained paraffin coupes, as previously described (Van Cleemput *et al.*, 2017). Briefly, explants were washed 3 times to remove excess pollen diffusates and fixed in phosphate-buffered 3.5% formaldehyde solution, either immediately or after an additional 24 h incubation. An automated system was used for paraffin embedding of the samples (Thermo Scientific™ STP 120 Spin Tissue Processor). Eight µm paraffin sections were first deparaffinised in xylene, then rehydrated in descending grades of alcohol, subsequently stained with haematoxylin-eosin, dehydrated in ascending grades of alcohol and xylene and finally mounted with DPX (Sigma-Aldrich). Pictures were taken with an Olympus IX50 light

microscope fitted with 40X objective. The percentage of intercellular space in the epithelium was measured using ImageJ software. The region of interest (ROI) was drawn manually for both the basal cell layer and the columnar cell layer in each picture using the 'ROI manager tool'. A schematic distinction between basal and columnar cells is given in the middle panel of Figure 3A. Next, the threshold value to distinguish blank spaces from cellular material was determined and the percentage of blank spaces between the cells (i.e. the intercellular space) was calculated. In addition, the thickness of the epithelium was measured 24 h after the 12 h treatment in five randomly chosen places per explant, using ImageJ software.

EREC

To assess epithelial integrity of the EREC, both the transepithelial electrical resistance (TEER) and the migration of rhodamine B isothiocyanate (RITC)-labelled Dextran 70S (Sigma-Aldrich) across the epithelium were determined. The TEER was measured using an epithelial voltohmmeter (Millipore corporation, Bedford, MA, USA) and the net resistance was calculated by subtracting the background resistance and multiplying the resistance by the surface area of the membrane. Following 2 h of incubation with the pollen diffusates, 50 μ L of 100 μ M RITC-labelled Dextran 70S was added to the apical compartment of the transwell for another 10 h. Next, 50 μ L of the basolateral compartment was transferred to a 96-well plate, suitable for fluorescent measurement (Greiner). Plates were measured at 530/590 nm, using a Flouroskan Ascent FL (ThermoFisher Scientific) plate reader. Finally, epithelial permeability was calculated as the percentage of RITC-dextran 70S in the basolateral chamber solution over that in the apical chamber solution.

Assessment of epithelial cell viability

Respiratory mucosal explants

Viability of the cells was determined on cryosections, using an In Situ Cell Death Detection Kit (Roche Diagnostics Corporation, Basel, Switzerland), based on terminal deoxynucleotidyl transferase dUTP nick end-labelling (TUNEL). The manufacturer's instructions were followed and slides were analysed using a Leica (TCS SPE) confocal microscope. The percentage of TUNEL-positive cells was calculated based on 300 randomly selected cells.

EREC

EREC viability was assessed by ethidium monoazide bromide (EMA) staining. Briefly, the apical surfaces of the cells were washed on ice for 5 min, prior to incubation with 50 μ g/mL EMA for 20 min on ice. Next, the cells were exposed to candescent light for 10 min, washed

and fixed in 1% paraformaldehyde (PFA) diluted in PBS for 10 min at RT. Nuclei were counterstained with Hoechst 33342 for 10 min at RT. Transwell membranes were excised from the culture inserts and mounted on glass slides using glycerol-DABCO. Slides were examined using a Leica (TCS SPE) confocal microscope. The percentage of EMA-positive cells was calculated based on 300 randomly selected cells. Finally, cell suspensions were cytopinned on glass slides and mounted using glycerol-DABCO.

Viral infection assays

Virus

A Belgian EHV1 isolate (03P37) was used in this study and originates from the blood taken of a paralytic horse during an outbreak in 2003 (van der Meulen *et al.*, 2003). The virus was propagated on rabbit kidney (RK13) cells and used at the 6th passage.

Respiratory mucosal explants

Explants were cultured at the air-liquid interface for 24 h, prior to extensive washing and embedment in agarose. Next, explants were exposed to the pollen diffusates or PBS with or without PI (negative control) for 12 h or to EGTA (positive control) for 1 h, as described above. Following a washing step, the apical surface of the epithelium was inoculated with $10^{6.5}$ TCID₅₀ of the 03P37 EHV1 strain for 1 h at 37°C. Explants were removed from the agarose and washed 3 times in PBS to remove non-adherent virus particles. Finally, explants were placed back onto their gauzes and serum-free medium was added. Twenty-four hpi, explants were placed into methylcellulose-filled plastic tubes and frozen at -80°C until further processing.

EREC

EREC were grown to full differentiation in a transwell cell culture system prior to treatment with the pollen diffusates with or without the protease inhibitor mixture, EGTA (positive control) or PBS with or without the protease inhibitor mixture (negative control). Following a thorough washing step, cells were exposed for 1 h to 100 µL EHV1 03P37 strain (MOI of 1) at the apical surface. Non-adsorbed virus particles were removed by washing the EREC three times with DMEM/F12. Fresh EREC-medium was added to the platewells and cells were further incubated at the air-liquid interface. Ten hours post-inoculation, cells were fixed in methanol for 20 min at -20°C and stored dry at -20°C until further processing.

Immunofluorescent staining and confocal microscopy

Respiratory mucosal explants.

Explants were embedded in methylcellulose and snap-frozen for subsequent cryosectioning. Sixteen μm thick cryosections were cut using a cryostat at -20°C and loaded onto 3-aminopropyltriethoxysilane-coated (Sigma-Aldrich) glass slides. Slides were then fixed in 4% paraformaldehyde for 15 min and subsequently permeabilized in 0.1% Triton-X 100 diluted in PBS. Non-specific binding sites were blocked by 15 min incubation with avidin and biotin (ThermoFisher Scientific) at 37°C . To label late viral glycoproteins, a polyclonal biotinylated horse anti-EHV1 was used for 1 h at 37°C (van der Meulen *et al.*, 2003), followed by incubation with streptavidin-FITC[®] (ThermoFisher Scientific) for 1 h at 37°C . The basement membrane of the tissues was stained with monoclonal mouse anti-collagen VII antibodies (Sigma-Aldrich), followed by secondary Texas Red[®]-labelled goat anti-mouse antibodies (ThermoFisher Scientific). Nuclei were detected by staining with Hoechst 33342 (ThermoFisher Scientific). Slides were mounted with glycerol-DABCO and analysed using a Leica (TCS SPE) confocal microscope. The total number of plaques was counted on 50 cryosections and plaque latitude was measured using the Leica confocal software package. Five cryosections per explant were completely photographed and the percentage of infection in the epithelium (i.e. region of interest or ROI) was determined using Image J software. The ROI (i.e. the epithelium) was drawn manually for each picture in the 'ROI manager tool'. Next, the threshold value to distinguish the FITC[®]-positive signal from the background signal was determined and the percentage of FITC[®]-positive signal (i.e. infection) was calculated.

EREC

Antibodies were incubated directly in the transwells for 1 h at 37°C . Cells were first incubated with a 1:1,000 dilution of a polyclonal rabbit anti-IEP antibody, kindly provided by Dr. D. O'Callaghan, Louisiana State University, USA. The diluent used was PBS containing 10% negative goat serum. This was followed by incubation with a goat anti-rabbit IgG FITC[®]-conjugated antibody (ThermoFisher Scientific). Nuclei were counterstained with Hoechst 33342 for 10 min at 37°C . Transwell membranes were excised from the culture inserts and mounted on glass slides using glycerol-DABCO. Slides were examined using a Leica confocal microscope. The total number of plaques was counted on 5 random fields of approximately 3×10^4 cells per insert. Plaque latitude was measured on 10 individual plaques using the Leica confocal software package.

Virus titration

Twenty-four hours after inoculation, explant supernatant was collected and stored at -80°C until titration. EHV1 titrations were conducted on RK13 cells, which were incubated at 37°C for 7 days. Titers were expressed as TCID₅₀.

Statistical analyses

Significant differences ($P < 0.05$) between different treatments were identified by one-way analysis of variances (ANOVA) followed by Tukey's post-hoc test. If homoscedasticity of the variables was not met as assessed by the Levene's test, the data were log-transformed prior to ANOVA. Normality of the residuals was verified by the use of the Shapiro-Wilk test. If the variables remained heteroscedastic or normality was not met after log-transformation, a Kruskal-Wallis' test, followed by a Mann-Whitney's post-hoc test was performed. All analyses were conducted in IBM SPSS Statistics for Windows, version 25.0 (IBM Corp, Armonck, NY, USA).

Results

Pollen grains of Kentucky bluegrass (KBG), white birch (WB) and hazel (H) release proteases with major metalloprotease and serine peptidase activities

Proteolytic activities of the pollen diffusates were first determined by gelatine zymography using specific protease inhibitors (Figure 1). Plot profiling of treated pollen diffusate lanes was performed by means of image analysis to determine the absence or presence of specific proteolytic bands. Following control treatment with PBS, all three pollen diffusates contained proteolytic bands with mobilities ranging from 70 kDa to over 250 kDa. In the KBG, WB and H lanes, one, three and two major proteolytic bands were identified, respectively. Sequestration of metal ions by EDTA inhibited metalloproteases as well as proteases that require metal ions for stabilisation and/or activation. This was sufficient to block merely all proteolytic bands in the three pollen diffusates, as designated by a drop in the respective plot profiles. Treatment of all three pollen diffusates with the serine protease inhibitor AEBSF clearly inhibited enzymatic activities in all proteolytic bands, except for two proteolytic bands in the WB lane, located slightly above 250 kDa and at 70 kDa. The former band was only efficiently blocked following sequestration of metal ions by EDTA, suggesting that it harboured a metalloprotease, while the latter band disappeared after inhibition of cysteine protease activity with E-64. Inhibiting aspartyl proteases with pepstatin A was not sufficient to block the proteolysis of gelatine in the proteolytic lanes of all pollen diffusates. Together, our zymography data indicate the presence of significant protease activity in plant pollen diffusates.

Protease identification in the pollen diffusate of white birch

The recent genomic sequencing of WB and accompanying annotation of its putative protein sequences (Salojärvi *et al.*, 2017) enabled us to reveal the identity of WB proteases using mass spectrometry (MS)-based proteomics. For this purpose, LC-MS/MS analysis was performed on three protein bands corresponding to different enzymatic bands on the zymograms (i.e. mobility at >250 kDa [1], 100-150 kDa [2] and 70 kDa [3]), which were excised following regular SDS-PAGE (Figure 2). The raw MS/MS data were searched against a database of *Betula Pendula* proteins for which functional annotation is available from orthologous proteins in *Arabidopsis thaliana*, a widely used model in molecular plant biology and an overview of identified proteases, glycosidases and lipases is given in Table 1. Further information on the *Arabidopsis thaliana* orthologous proteases can be found using their MEROPS accession number. MEROPS

is a peptidase database which groups proteases of similar evolutionary origins into (sub)clans and (sub)families.

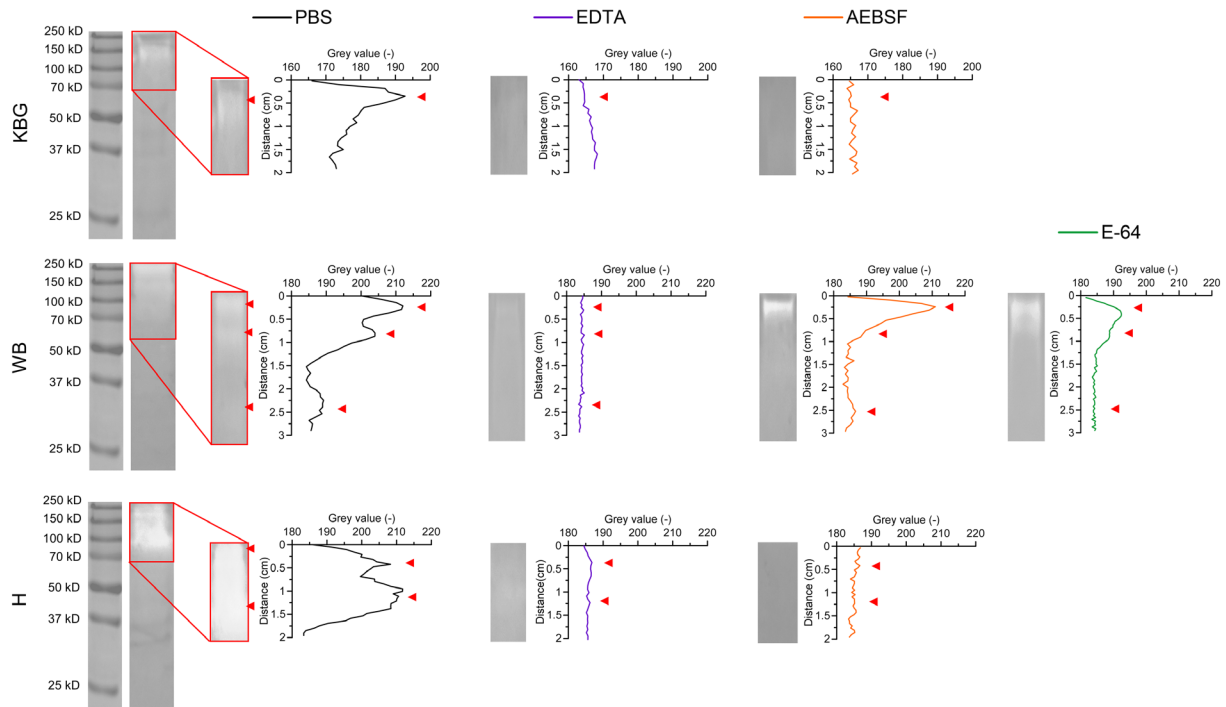


Figure 1. Pollen diffusates of Kentucky bluegrass (KBG; upper panel), white birch (WB; middle panel) and hazel (H; lower panel) contain proteolytically active compounds. Pollen diffusates were incubated with several protease inhibitors (2.5 μ M EDTA, 500 μ M AEBSF or 15 μ M E-64) prior to and during zymography on a gelatin substrate. Following overnight digestion at 37°C, Coomassie blue staining of the gelatin gels was performed. RGB-pictures were taken with a ChemiDocMP Imaging System (Bio-Rad) and converted to 8-bit grey-scaled images using ImageJ. A complete overview of the zymogram lanes of PBS-treated pollen diffusates is shown on the left. The red box designates the area that was used for plot profiling in ImageJ. Plot profiles and their corresponding zymogram lanes are shown in the right set of graphs. Proteolytic bands appear as white zones in the Coomassie blue-stained gelatin gel and are, together with their corresponding grey value peaks, designated by arrowheads.

In accordance with our zymography results, primarily serine proteases were identified in all three protein bands. In particular, the ‘subtilisin-like protease SBT1.7’ (Bpev01.c0015.g0096.m0001) was predominantly recovered from all three lanes, indicating that it exists in multiple forms. The identification of two additional subtilisin-like serine proteases (i.e. Bpev01.c1354.g0003.m0001 or ‘subtilisin-like protease SBT5.4’ and Bpev01.c0577.g0026.m0001 or ‘subtilisin-like serine protease’) in two out of three protein bands depicts a major presence of subtilases in the WB pollen diffusate. In addition, meiotic prophase aminopeptidase 1 (Bpev01.c0170.g0046.m0001), a metalloprotease with aminopeptidase activity was identified in the protein band with a size corresponding to 100-150 kDa. Besides these proteases, a repertoire of glycosidases and lipases were also found in different WB lanes (Table 1).

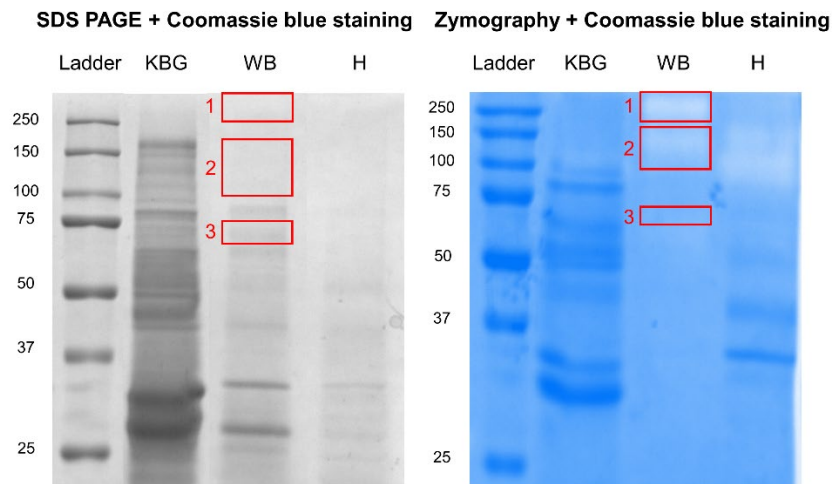


Figure 2. Protein (left) and proteolytic (right) profiles of pollen diffusates of Kentucky bluegrass (KBG), white birch (WB) and hazel (H). Three bands (1-3, left red boxes), corresponding to major proteolytic spots on zymography (1-3, right red boxes), were excised in the WB lane following SDS-PAGE and were subjected to LC-MS/MS analysis for protein identification.

Type (and MEROPS accession)	Protein ID	Corresponding Arabidopsis gene	Description	Lane (kD)	Sequence coverage %	Nr. of unique peptides
Serine protease (S08.112)	Bpev01.c0015.g0096.m0001	AT5G67360	Subtilisin-like protease SBT1.7	1	3.3	2
				2	14.6	10
				3	3	2
Serine protease (S08.A26)	Bpev01.c1354.g0003.m0001	AT5G59810	Subtilisin-like protease SBT5.4	2	1.2	1
				3	1.2	1
Serine protease (S08.A22)	Bpev01.c0577.g0026.m0001	AT1G20160	Subtilisin-like serine protease	2	1.8	1
Metalloprotease, aminopeptidase (M01.029)	Bpev01.c0170.g0046.m0001	AT1G63770	Meiotic prophase aminopeptidase 1	2	1.5	1
Glycosidase	Bpev01.c0504.g0008.m0001	AT4G20050	Polygalacturonase QRT3	1	8.4	4
				2	33.1	18
Glycosidase	Bpev01.c0298.g0032.m0001	AT3G48950	Endo-polygalacturonase-like protein	3	3.1	2
Glycosidase	Bpev01.c1877.g0001.m0001	AT5G64570	Beta-d-xylosidase	1	1.8	1
				2	5.8	4
Glycosidase	Bpev01.c0313.g0001.m0001	AT5G04885	Glycosyl hydrolase family protein	1	1.5	1
				2	6.3	1
Glycosidase	Bpev01.c0313.g0002.m0001	AT5G20950	Glycosyl hydrolase family protein	2	1.4	1
				3	3.3	1
				3	3.1	3
Glycosidase	Bpev01.c0031.g0026.m0001	AT5G12950	Putative glycosyl hydrolase of unknown function (DUF1680)	3	3.1	3
				1	1.7	1
				2	3.2	2
Lipase	Bpev01.c0547.g0017.m0001	AT4G13550	Triglyceride lipase	1	1.7	1
				2	3.2	2
				3	4.1	3

Table 1. Proteases, glycosidases and lipases identified via proteome analysis of three protein bands (>250 kDa [1], 100-150 kDa [2], and 70 kDa [3]) from the white birch pollen diffusate, corresponding to proteolytic spots on zymography (shown in Figure 2).

Pollen proteases selectively and irreversibly alter intercellular junctions of columnar equine respiratory epithelial cells

Respiratory mucosal explants

Pollen proteases of KBG and WB have been shown to affect epithelial integrity in Madin-Darby canine kidney (MDCK) cells and in human lung adenocarcinoma Calu-3 cells (Runswick *et al.*, 2007; Vinhas *et al.*, 2011). However, these continuous cell lines do not reflect the *in vivo* situation. Therefore, we examined the effect of pollen proteases on representative *ex vivo* respiratory mucosal explants, using our previously described protocol (Van Cleemput *et al.*, 2017).

As shown in the haematoxylin-eosin-stained images of Figure 3A, the intercellular space open up following treatment with all three pollen diffusates, compared to control treatment with PBS. There was no effect of any of the three pollen diffusates on epithelial integrity when protease inhibitors (PI; 500 μM AEBSF, 15 μM E-64 and 2.5 μM EDTA) were added, demonstrating that pollen proteases affect epithelial intercellular junctions (ICJ). Notably, basal cell ICJ were resistant to treatment with pollen proteases throughout the course of the experiment, as shown by the intact basal cell layer on haematoxylin-eosin-stained sections. Indeed, the intercellular space significantly ($P < 0.05$) increased in the columnar cell layer (left graph), but not in the basal cell layer (right graph). As a control, treatment with the Ca^{2+} -chelating agent EGTA efficiently disrupted the ICJ of both basal and columnar cells, as demonstrated by the significant increase ($P < 0.05$) in intercellular space in both cell layers. Viability of cells within the respiratory epithelium did not significantly drop after treatment with pollen diffusates, compared to control PBS (Figure 4A, left panel). However, desquamating cells did show signs of apoptosis, as shown in the right panel of Figure 4A (green signal).

In contrast to EGTA, the pollen diffusates irreversibly affected epithelial morphology, as assessed by measuring the thickness of the epithelium. Twenty-four hours after the 12 h pollen protease treatment, the height of the epithelium was significantly lower (KBG, $30 \pm 8 \mu\text{m}$; WB, $24 \pm 8 \mu\text{m}$; H, $28 \pm 8 \mu\text{m}$), compared to PBS or EGTA treatment ($62 \pm 15 \mu\text{m}$ and $60 \pm 12 \mu\text{m}$, respectively), as shown in Figure 3B. In addition, the ciliated appearance of the respiratory epithelium was lost upon incubation with the pollen diffusates. Again, these effects were attributed to the protease activities of all three pollen diffusates, as the addition of protease inhibitors prevented these changes in epithelial morphology. Representative haematoxylin-eosin images are given in the upper panel of Figure 3B.

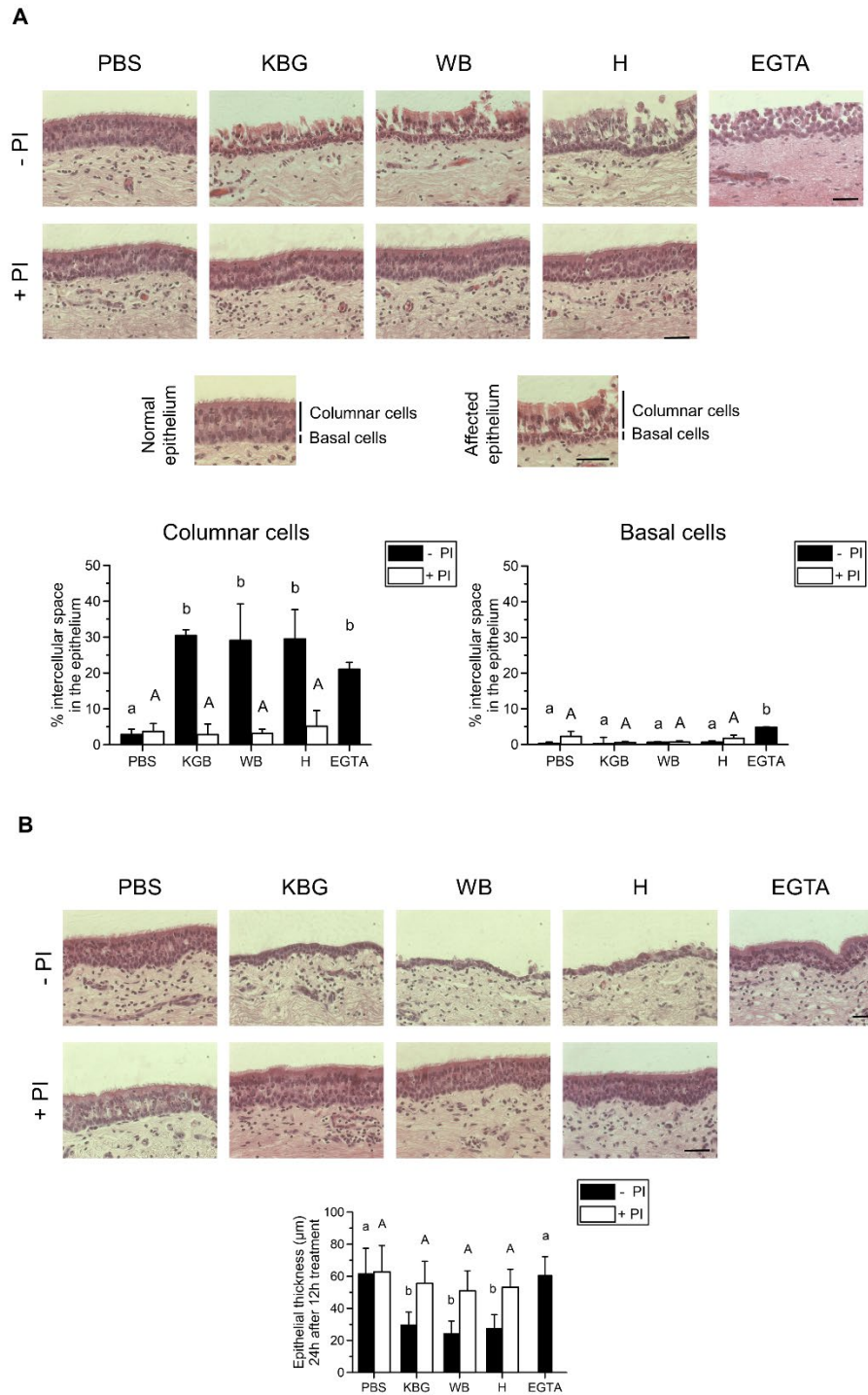


Figure 3. Pollen proteases selectively and irreversibly alter intercellular junctions of columnar equine respiratory epithelial cells in respiratory mucosal explants. Explants were treated with PBS (control), pollen diffusates (Kentucky bluegrass or KBG, white birch or WB and hazel or H) supplemented with or without protease inhibitors (PI) for 12 h or EGTA for 1 h. (A) Representative haematoxylin-eosin-stained images of the explants after treatment. The scale bar measures 50 µm (upper panel). Schematic representation of the columnar and basal layer of normal and pollen protease-affected respiratory epithelia (middle panel). The percentage of intercellular space in the columnar (left graph) and basal (right graph) cell layer of the respiratory epithelium after treatment (lower panels). Experiments were performed on explants from 3 individual horses and data are represented as means + SD. Different lower case letters indicate significant ($P < 0.05$) differences in treatments without PI, different upper case letters indicate significant ($P < 0.05$) differences in treatments with PI. (B) Representative haematoxylin-eosin-stained images of the explants 24 h after the treatment. The scale bar measures 50 µm (upper panel). The height of the epithelium was measured 24 h after the treatment (lower panel). Experiments were performed on explants from 3 individual horses and data are represented as means + SD. The lower case letters indicate significant ($P < 0.05$) differences in treatments without PI, different upper case letters indicate significant ($P < 0.05$) differences in treatments with PI.

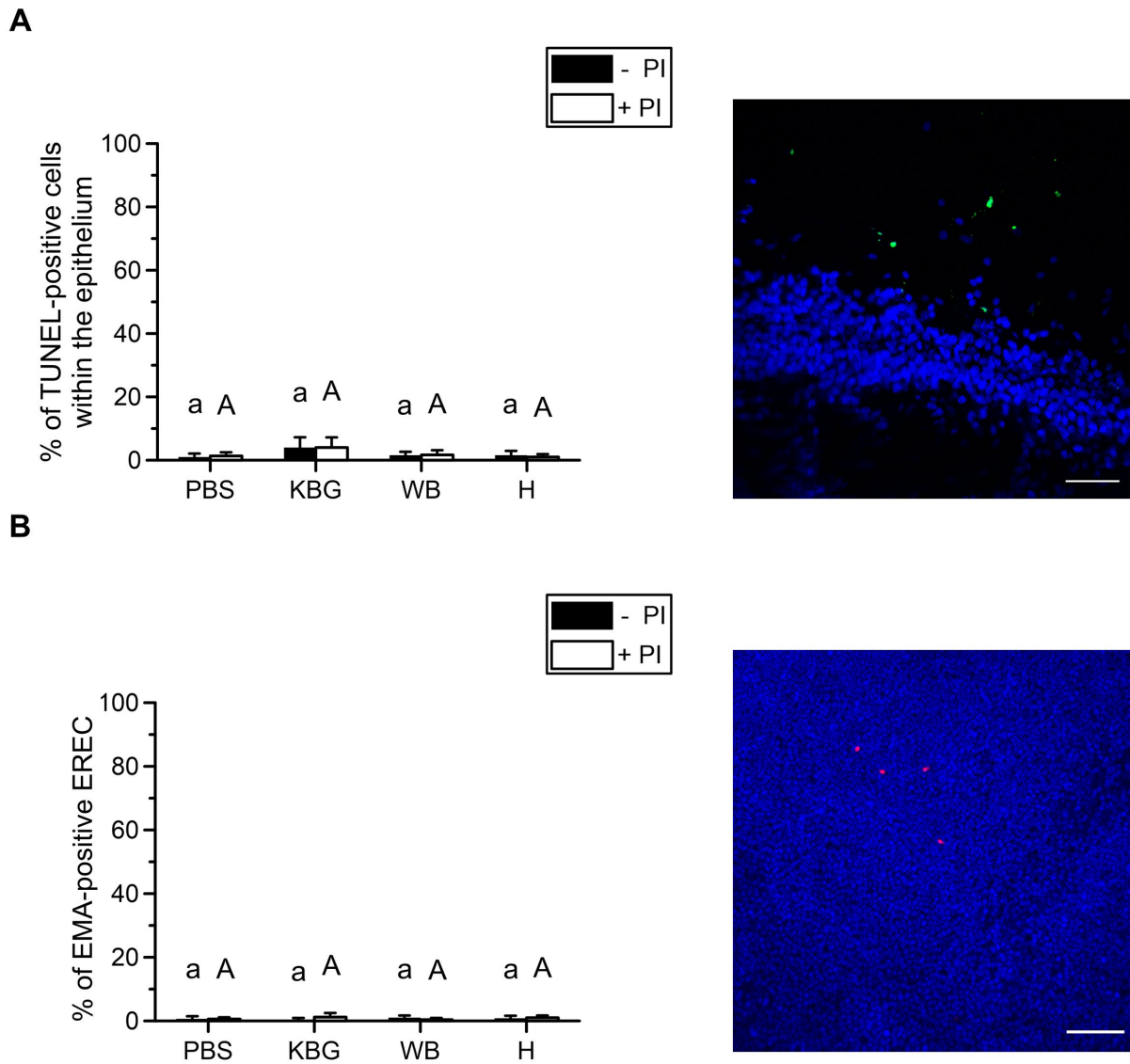


Figure 4. Cell viability of the cells within the epithelium was not affected upon treatment with pollen diffusates of Kentucky bluegrass (KBG), white birch (WB) or hazel (H), supplemented with or without protease inhibitors (PI). (A) TUNEL staining data of 12 h pollen diffusate-treated respiratory mucosal explants. Experiments were performed on explants from 3 individual horses and data are represented as means + SD. The lower case letters indicate significant ($P < 0.05$) differences in treatments without PI, different upper case letters indicate significant ($P < 0.05$) differences in treatments with PI (left). Representative confocal image of pollen protease-induced apoptosis (shown in green) in detaching epithelial cells (right). Cell nuclei are shown in blue. The scale bar represents 50 μm . (B) EMA staining confirmed no significant ($P < 0.05$) differences in viability of the EREC monolayer after different treatments. Three independent experiments were performed and data are represented as means + SD. The lower case letters indicate significant ($P < 0.05$) differences in treatments without PI, different upper case letters indicate significant ($P < 0.05$) differences in treatments with PI (left). Representative confocal image of pollen diffusate-treated EREC. Cell nuclei are shown in blue and a positive EMA-signal is shown in red. Scale bar measures 100 μm .

EREC

ICJ integrity of EREC was examined by measuring both the transepithelial electrical resistance (TEER) and transepithelial permeability to RITC-labelled dextran. EREC reached a steady TEER of $\sim 500\text{-}700 \Omega \times \text{cm}^{-2}$ after 5-7 days of incubation at the air-liquid interface in a transwell cell culture system. Starting from 30 min post addition, the TEER significantly dropped to baseline levels after treatment with EGTA (positive control), but not after treatment with PBS or with different pollen diffusates (Figure 5A). In contrast, the TEER increased in a time-dependent manner and reached values that were up to 2.5-fold higher at 12 h after exposure than at 0 h in both PBS- and pollen diffusate-treated EREC. The TEER of additional EREC that did not receive any treatment, i.e. had air-filled apical compartments, remained stable throughout the experiment (data not shown). TEER values did not significantly differ among PBS- and pollen diffusate-treated EREC. The pattern of TEER values was similar in EREC treated with pollen diffusates, supplemented with protease inhibitors, over time (data not shown). Similarly, the transepithelial permeability, as assessed by the percentage of migrated RITC-labelled dextran and shown in the right graph of Figure 5B, did not significantly differ between EREC exposed for 12 h to different pollen diffusates and control-treated EREC. Chelation of extracellular Ca^{2+} with EGTA, however, was able to significantly increase the percentage of migrated RITC-labelled dextran across the EREC up to 20%. Nonetheless, treatment with all three pollen diffusates, but not with PBS, EGTA or after supplementation of protease inhibitors, induced cell desquamation. Illustrative light microscopy pictures are given in Figure 5C. The loss of columnar cells upon pollen diffusate treatment was also apparent on the 3D reconstruction of 20 consecutive Z-stack confocal images of the EREC layer, shown in the left panels of Figure 5D and on haematoxylin-eosin-stained images of the EREC layer, shown in the right panels of Figure 5D. Viability of the EREC was not significantly affected upon treatment with pollen diffusates with or without protease inhibitors, as determined by EMA-staining (Figure 4B).

Together, these results show that integrity of the upper, i.e. columnar, respiratory epithelial cell layer is selectively disrupted by pollen proteases, while the basal cell layer somehow resists their damaging effect.

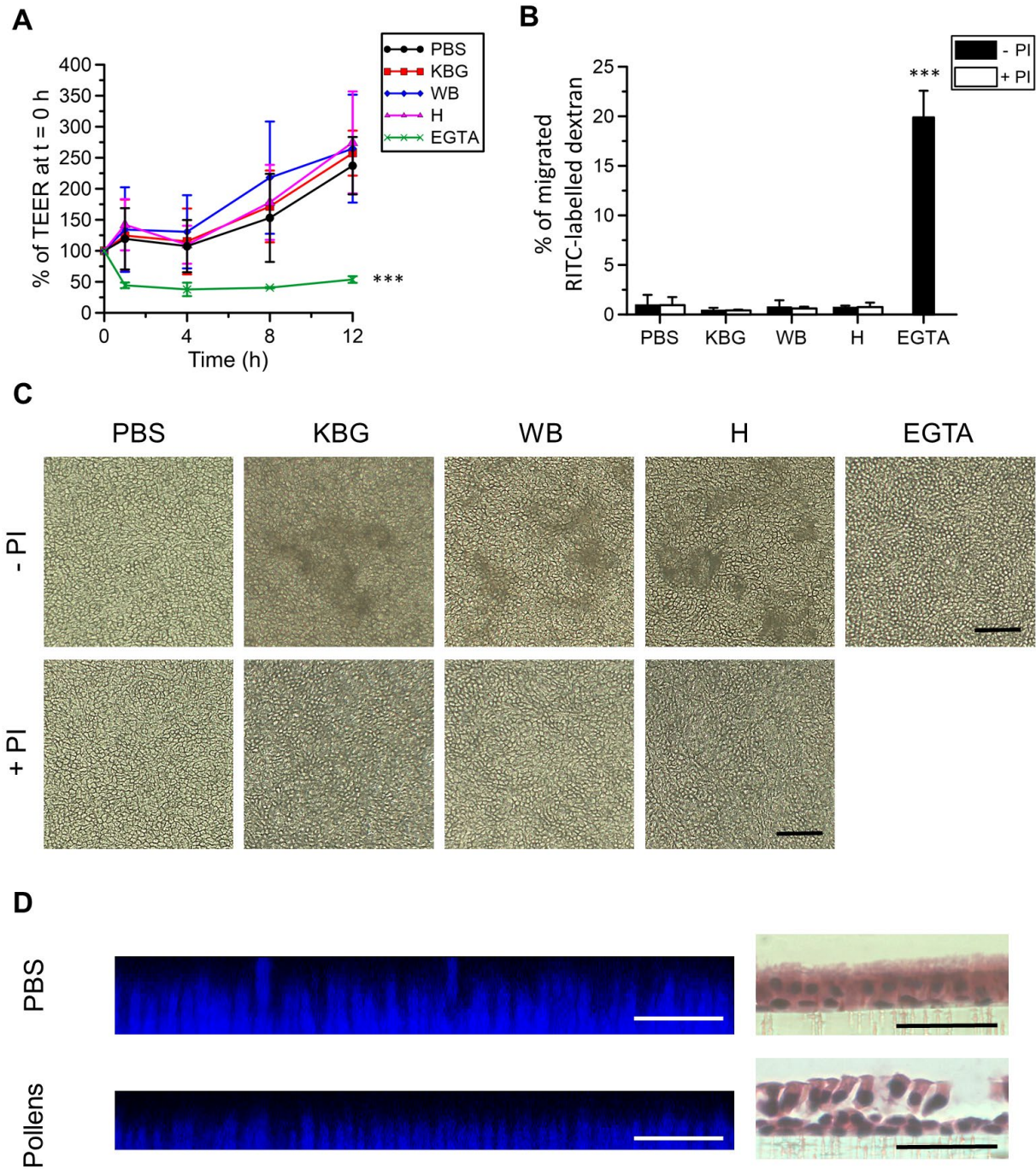


Figure 5. Pollen proteases selectively and irreversibly alter intercellular junctions of columnar primary equine respiratory epithelial cells (EREC). Polarized EREC were treated with PBS (control), pollen diffusates (Kentucky bluegrass or KBG, white birch or WB and hazel or H) or EGTA, supplemented with or without protease inhibitors (PI). (A) Transepithelial electrical resistance of EREC was measured over time and was normalized to time point 0 h. (B) Percentage of RITC-labelled dextran 70S in the basolateral chamber solution over that in the apical chamber solution. RITC-labelled dextran 70S was added 2 h after the initiation of the treatment and incubated for another 10 h (right panel). Three independent experiments were performed and the data are represented as means \pm SD. Asterisks indicate significant differences (***: $P < 0.001$). (C) Representative light microscopy pictures of EREC. Note the desquamating cells in EREC treated with pollen diffusates without PI (KBG, WB and H -PI). The scale bar measures 50 μ m. (D) Cross-section of the EREC layer from a 3D visualisation built up out of 20 consecutive confocal Z-stack images (left) or haematoxylin-eosin-stained paraffin coupes of the EREC layer (right) following treatment with PBS (control, upper panels) or pollens (lower panels). Cell nuclei are shown in blue (left) or purple (right) and the scale bar measures 50 μ m.

Pollen proteases predispose respiratory epithelial cells for efficient EHV1 infection

Respiratory mucosal explants

Number of plaques - As shown in Figure 6A, upper left panel, the number of plaques per 50 cryosections significantly ($P < 0.05$) increased from 12 ± 6 in PBS-pretreated explants (negative control) to 45 ± 9 (KBG), 51 ± 17 (WB) and 57 ± 16 (H) in pollen diffusate-pretreated explants. The number of plaques was significantly ($P < 0.05$) higher after EGTA pretreatment (positive control), compared to PBS pretreatment and did not significantly differ from the number of plaques in the pollen diffusate-pretreated explants. Inhibition of the proteases in the pollen diffusates with the protease inhibitors (PI) completely prevented the increase in subsequent EHV1 infection, as the number of plaques following pollen diffusate with PI pretreatment (6 ± 5 for KBG, 8 ± 7 for WB and 6 ± 6 for H) did not significantly differ from PBS pretreatment (with or without PI; 10 ± 6 and 12 ± 6 , respectively).

Plaque latitude - The plaque latitude gives an indication about the ease of viral spread in the explant epithelium and is shown in Figure 6A, upper right panel. The average latitude of EHV1 plaques increased significantly from $81 \pm 5 \mu\text{m}$ in PBS-pretreated explants to $127 \pm 22 \mu\text{m}$ (KBG), $126 \pm 5 \mu\text{m}$ (WB) and $114 \pm 8 \mu\text{m}$ (H) after pollen diffusate pretreatment. Similarly, the average EHV1 plaque latitude was higher after EGTA pretreatment ($157 \pm 38 \mu\text{m}$), compared to control. The average EHV1 plaque latitude in pollen diffusate with PI-pretreated explants ($92 \pm 31 \mu\text{m}$ for KBG, $88 \pm 27 \mu\text{m}$ for WB and $90 \pm 28 \mu\text{m}$ for H) was similar to PBS-pretreated explants (with or without PI; $89 \pm 32 \mu\text{m}$ and $81 \pm 5 \mu\text{m}$, respectively).

Percentage of infection in the epithelium - In order to obtain a general overview of EHV1 infection in explants, the percentage of infection in the epithelium (i.e. ROI) was calculated and is illustrated in Figure 6A, lower left panel. In PBS-pretreated explants, $2.20 \pm 1.78\%$ of the epithelium was infected by EHV1. Pretreatment of the explants with pollen diffusates led to a significant ($P < 0.05$) increase of this percentage to $12.83 \pm 6.63\%$ (KBG), $10.24 \pm 2.07\%$ (WB) and $12.19 \pm 3.61\%$ (H). Up to $22.90 \pm 6.70\%$ of the epithelium got infected by EHV1 after pretreatment with EGTA. A similar trend as in the number of plaques was observed for the percentage of infection in the epithelium of explants pretreated with PBS or pollen diffusates, supplemented with PI. Here, $1.41 \pm 0.37\%$ (PBS), $2.46 \pm 2.38\%$ (KBG), $3.38 \pm 1.01\%$ (WB) and $3.41 \pm 1.74\%$ (H) was infected with EHV1.

Virus titer - More efficient virus replication in the epithelium most likely results in the production of more extracellular virus particles. Indeed, virus titration (Figure 6A), lower right panel) confirmed this hypothesis showing that the supernatant of all pollen diffusate-pretreated

explants contained on average a 1 to 1.5 log₁₀ higher titer (4.74 ± 0.70 for KBG, 4.90 ± 0.36 for WB and 4.91 ± 0.92 for H) than control-pretreated explants (3.84 ± 0.2). EGTA-pretreated explant supernatant was on average 1.5 log₁₀ higher (5.02 ± 0.26) than control supernatant. Again, preventing protease activities by supplementing PI to the pollen diffusates resulted in a similar virus titer (4.06 ± 1.1 for KBG, 3.69 ± 0.78 for WB and 4.02 ± 0.96 for H), compared to control (3.72 ± 0.21). Representative confocal images of EHV1 plaques in the respiratory mucosal explants are shown in Figure 6B.

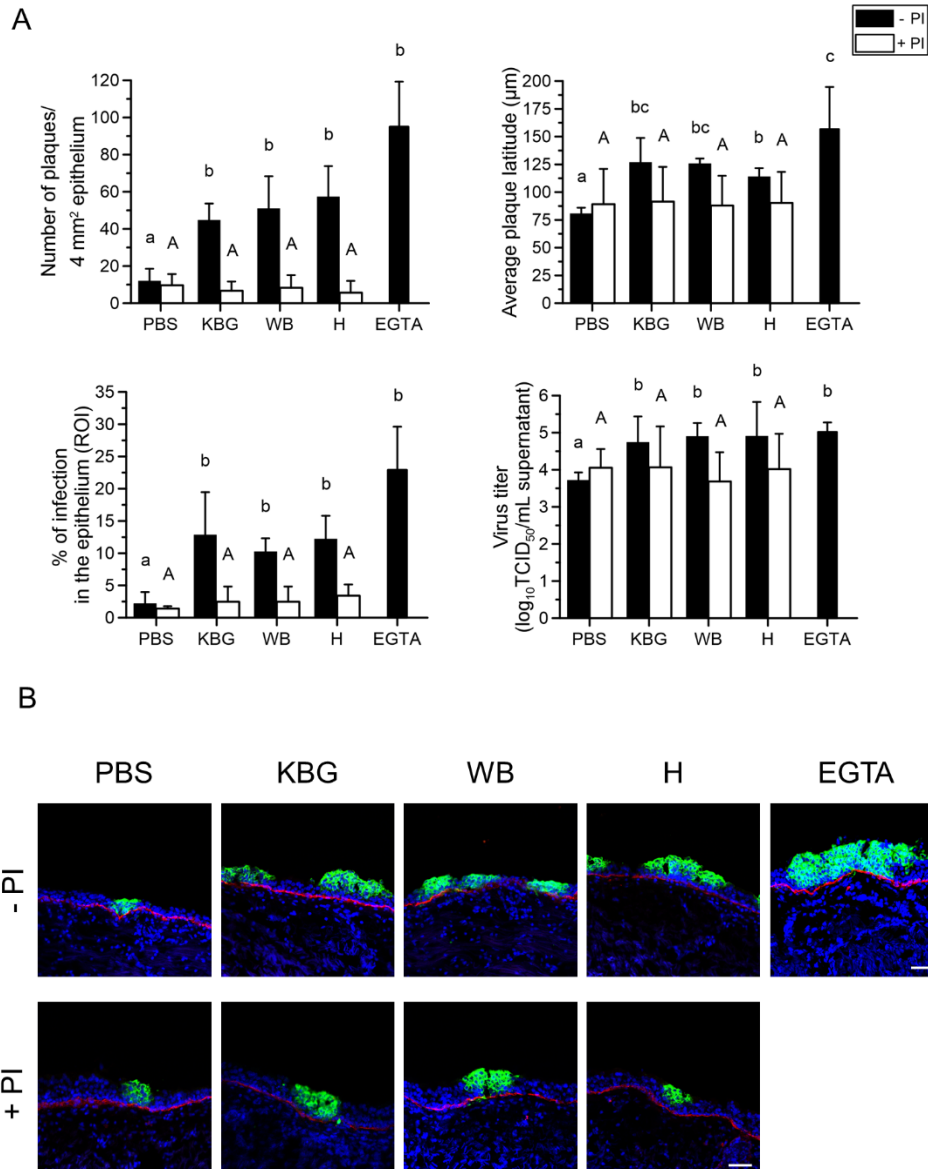


Figure 6. EHV1 infection of respiratory mucosal explants after pretreatment with PBS (control), pollen diffusates (Kentucky bluegrass or KBG, white birch or WB and hazel or H) or EGTA, supplemented with or without protease inhibitors (PI). Explants were frozen 24 hpi and cryosections were stained for late viral antigens. (A) The total number of plaques was counted on 50 consecutive cryosections (upper left panel), the average plaque latitude was calculated based on a maximum of 10 individual plaques (upper right panel), the percentage of EHV1 infection in the epithelium was analysed on 5 random cryosections (lower left panel) and the virus titer (lower right panel) was determined in supernatant on RK13 cells. Experiments were performed on explants from 3 individual horses and data are represented as means + SD. Different lower case letters indicate significant ($P < 0.05$) differences in pretreatments without PI, different upper case letters indicate significant ($P < 0.05$) differences in pretreatments with PI. (B) Representative confocal images of EHV1 plaques (green) in respiratory mucosal explants. The basement membrane is shown in red. Cell nuclei were counterstained with Hoechst (blue). The scale bar represents 50 μm .

EREC

Number of plaques - On 3×10^4 EREC, we counted an average of 6 ± 4 EHV1 plaques following PBS pretreatment of the cells. Disruption of columnar cell ICJ with proteases of KBG, WB and H increased the number of EHV1 plaques in 3×10^4 EREC to 8 ± 4 , 12 ± 3 and 11 ± 4 , respectively. Complete disruption of epithelial integrity with EGTA completely overcame the restriction upon apical inoculation, resulting in an average of 58 ± 10 EHV1 plaques per 3×10^4 EREC (Figure 7A, left panel). Addition of PI to the pollen diffusates during EREC pretreatment inhibited the increase in EHV1 infectivity.

Plaque latitude - No significant difference in EHV1 plaque latitude was found between different pretreatments (Figure 7A, right panel).

Representative confocal images of EHV1 plaques in EREC are shown in Figure 7B.

Taken together, the partial disruption of respiratory epithelial integrity by pollen proteases is sufficient to enhance subsequent EHV1 infection, but not to the same level as after a complete disruption of epithelial integrity with EGTA.

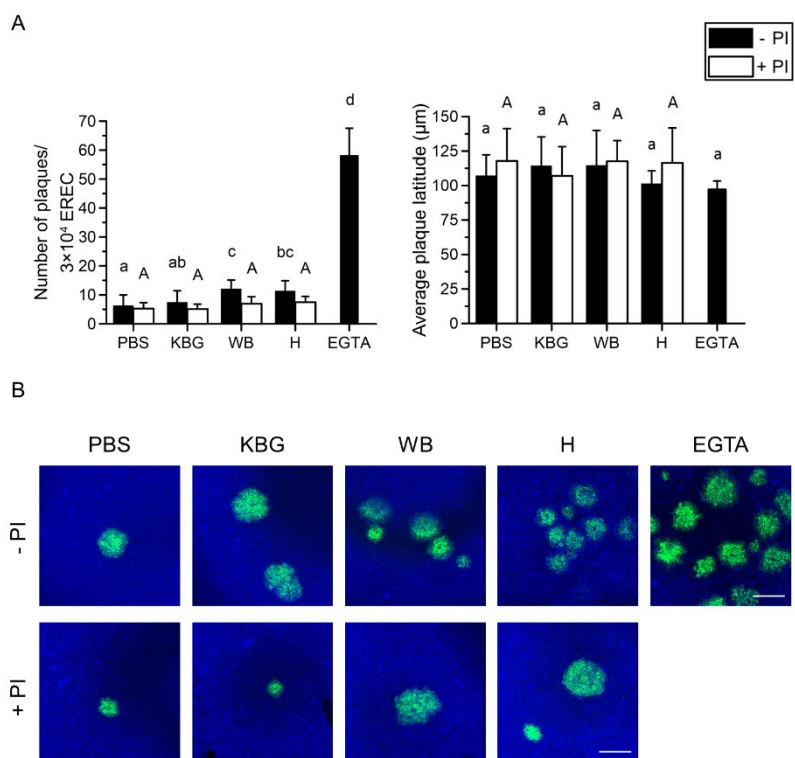


Figure 7. EHV1 infection of equine respiratory epithelial cells (EREC) after pretreatment with PBS (control), pollen diffusates (Kentucky bluegrass or KBG, white birch or WB and hazel or H) or EGTA, supplemented with or without protease inhibitors (PI). Cells were fixed 10 hpi and stained for immediate early protein (IEP). (A) The total number of plaques was counted in five different fields of approximately 3×10^4 cells for each condition (left). Average plaque latitudes were measured on 10 individual plaques (right). Experiments were performed in triplicate on primary EREC of 3 different horses. Data are represented as means + SD and different lower case letters indicate significant ($P < 0.05$) differences in pretreatments without PI, different upper case letters indicate significant ($P < 0.05$) differences in pretreatments with PI. (B) Representative confocal images of EHV1 IEP-positive plaques (green) in EREC monolayers, nuclei were detected with Hoechst (blue). The scale bar represents 100 μm .

Discussion

Alphaherpesviruses spread to new hosts through the respiratory tract, where they target a basolaterally located receptor in the epithelium (Van Cleemput *et al.*, 2017). In today's modern society, the human and animal respiratory tract is constantly exposed to respirable hazards, ranging from moulds and other airborne pathogens to air pollutants, dust and pollens. Pollen proteases were shown to affect epithelial barrier function in continuous cell lines and thus, might predispose the epithelium for alphaherpesvirus invasion (Cortes *et al.*, 2006; Runswick *et al.*, 2007; Vinhas *et al.*, 2011).

Consistent with previous studies, we observed that PBS-submerged pollens release high molecular weight proteases with major metalloprotease and serine peptidase activities (Cortes *et al.*, 2006; Runswick *et al.*, 2007; Vinhas *et al.*, 2011; Widmer *et al.*, 2000). These results were corroborated with our proteomics-derived data of the white birch (WB) pollen diffusate. Indeed, we mainly identified serine proteases of the subtilase family in all three WB proteolytic lanes, besides the metalloprotease meiotic prophase aminopeptidase 1 in the 100-150 kDa lane. The identified subtilases presumably occur in multiple forms, as some of them (e.g. Bpev01.c0015.g0096.m0001 or subtilisin-like serine protease 1.7) were derived from different proteolytic lanes following non-denaturing SDS-PAGE. Multiple other proteases were presumably present in the WB proteolytic lanes, as also EDTA and E-64 could efficiently block enzymatic activity on zymograms and the majority of MS/MS spectra could not be assigned to specific proteins by means of proteomics. For instance, our zymography results showed the presence of an additional major metalloprotease lacking serine protease activities in the >250 kDa band and a cysteine protease in the 70 kDa band of WB, but proteomics did not (yet) allow us to identify these proteases. Future knowledge on the complete protein database of WB should eventually unravel the identities of these putative proteases.

In line with previous studies in continuous cell lines, we found that pollen proteases disrupt epithelial integrity in *ex vivo* equine respiratory mucosal explants (Cortes *et al.*, 2006; Runswick *et al.*, 2007; Vinhas *et al.*, 2011). Remarkably, we found that only the intercellular junctions of columnar epithelial cells were affected by pollen proteases. This phenomenon was strikingly different from that observed after addition of the calcium-depleting agent EGTA, which rapidly caused splitting of both basal and columnar cell intercellular junctions (ICJ) (Van Cleemput *et al.*, 2017). As a result, the damage caused by pollens to the ICJ must have been independent of calcium concentration. First, the degradation of ICJ might be a direct consequence of proteolytic actions. The exposed domains of basal cell transmembrane proteins might be less

accessible to exogenous proteases, compared to those of columnar cells. A more tighter sealing in between basal cells would not be surprising, as loss of these cells would have detrimental effects on the epithelium. Basal cells not only function as progenitor cells, but also play a major role in fixation of the complete respiratory epithelium by expressing hemidesmosomal complexes (Boers *et al.*, 1998; Evans *et al.*, 1990). Second, activation of a protease-activated receptor (PAR) at the surface of epithelial cells could also induce a disruption of the epithelial integrity (Reed and Kita, 2004). PAR are G protein-coupled receptors that are activated after proteolytic cleavage of their N-terminus (Déry *et al.*, 1998). It was proposed by Vinhas *et al.* (2011) that the disruption of the epithelial barrier by pollen proteases could occur via the activation of a protease-activated receptor or PAR. Allergenic products of mites, moulds and the Japanese Cedar pollens have already been shown to activate PAR2, thereby initiating the disassembly of ICJ (Chiu *et al.*, 2007; Kato *et al.*, 2009; Kumamoto *et al.*, 2016). Interestingly, PAR1 and 2 are exclusively expressed by the columnar cells of the epithelium of the human respiratory tract and/or skin (Bocheva *et al.*, 2009; Knight *et al.*, 2001). It would be interesting to localize different PAR in the horse's respiratory epithelium to uncover their role in pollen protease-induced loss of epithelial integrity. Unfortunately, we were unable to visualize PAR2 in the horse's respiratory epithelium, as none of the commercially available antibodies against human PAR2 recognized equine PAR2 in immunofluorescent staining. Further support for a potential contribution of PAR2 in the pollen-induced loss of epithelial integrity comes from our zymography and proteomics results, as almost all proteolytic activities of the pollen diffusates were blocked with AEBSF. In addition, we mainly identified serine proteases of the subtilase family in the WB pollen diffusate using proteomics. Notably, PAR2 is selectively activated by serine proteases, through cleavage of its N-terminus (Cocks and Moffatt, 2001). We additionally identified a metalloprotease 'meiotic prophase aminopeptidase 1' in the WB pollen diffusate, together with a plethora of glycosidases and lipases. As described for matrix metalloprotease 9, meiotic prophase aminopeptidase 1 might also alter airway epithelial integrity (Vermeer *et al.*, 2009). Based on these findings, it seems reasonable to propose that pollen-derived glycosidases clear passage through the mucus blanket by destroying the mucoprotein network. This strategy not only allows for the delivery of pollen proteases and allergens, but also airborne pathogens to the respiratory epithelium.

Delivery of pollen-derived proteases to the respiratory epithelium clearly caused irreversible damage. Twenty-four hours after normalizing the medium, merely a thin layer of basal cells persisted in the explants upon treatment with pollen proteases. The normal ciliated appearance of the respiratory epithelium disappeared due to loss of desquamated and apoptotic epithelial

cells. *In vivo*, this reduced mucociliary clearance might even further promote the damaging effect of pollen substances, as the induced stasis might further concentrate them in one place. Cellular desquamation was also observed in the EREC upon exposure to pollen diffusates, which is in line with previous studies (Cortes *et al.*, 2006; Hassim *et al.*, 1998). However, in contrast with studies using continuous cell lines, we did not observe a decrease in transepithelial electrical resistance or an increase in transepithelial permeability across the EREC upon apical exposure to the pollen diffusates (Lee *et al.*, 2014; Vinhas *et al.*, 2011). This corroborates our observations in *ex vivo* respiratory mucosal explants, where integrity of the basal cells resisted treatment with pollen diffusates. Upon loss of their neighbouring epithelial cells, the basal cells may have rapidly flattened out and thereby covered the underlying surface, as they would do *in vivo* (Erjefalt *et al.*, 1995). Indeed, haematoxylin-eosin-stained paraffin coupes of the EREC layer confirmed that basal cells resisted pollen protease treatment, while covering the basement membrane. Surprisingly, coverage of the apical EREC surface with either PBS or pollen diffusates led to an increase of their TEER. As these results are consistent with those obtained from primary human bronchial epithelial cells after exposure to grass pollen extracts, we want to emphasize the importance of using appropriate representative models (Blume *et al.*, 2012). Here, the increase in epithelial integrity might have acted as a self-defence mechanism in a harmful environment (Lanaspa *et al.*, 2008). Indeed, respiratory epithelial cells generally thrive well at the air-liquid interface, but fail to maintain their differentiation level after full immersion in medium (Clark *et al.*, 1995; Grainger *et al.*, 2006; Whitcutt *et al.*, 1988).

We previously showed that upon destruction of epithelial integrity, infection of the respiratory epithelium with the alphaherpesvirus equine herpesvirus type 1 (EHV1) was greatly enhanced (Van Cleemput *et al.*, 2017). As this ancestral alphaherpesvirus targets a receptor located at the basolateral surface of epithelial cells, primary infections are limited and most often occur subclinically. Here, we demonstrated that the respiratory epithelium is more easily infected by EHV1 upon disruption of the ICJ by pollen proteases. Nonetheless, the increase in subsequent EHV1 infection was not to the same degree as following a complete destruction of epithelial integrity with EGTA. Indeed, the basal cells remained able to seal the epithelium upon exposure to pollen proteases, avoiding unlimited passage of virus particles. Nonetheless, the basolateral surface of (semi-)detaching columnar cells was still exposed to virus particles, enabling efficient infection. Especially in the more representative respiratory mucosal explants, EHV1 infection was predominantly enhanced upon pollen protease pretreatment, which was less obvious in EREC. Although the EREC, grown in optimal conditions, differentiate into a pseudo-stratified respiratory epithelium, they presumably cannot fully mimic the *in vivo*

differentiated respiratory epithelium of mucosal explants (Quintana *et al.*, 2011). Therefore, we hypothesize that EHV1 infection is only enhanced at certain islands within the EREC layer, where affected cells did not fully detach. Indeed, cells in the EREC layer more easily detached, compared to those embedded within the respiratory epithelium of mucosal explants. Loss of these cells in the EREC layer prevented EHV1 from infecting them which may explain why subsequent EHV1 infection was not as efficient as in the respiratory mucosal explants.

Our results are corroborated by the seasonally observed EHV1-associated symptoms (i.e. respiratory disease, central nervous system disorders and abortion), as these occur most often during late winter and spring, when pollen concentrations in the outdoor air peak (Goehring *et al.*, 2006; Sherman *et al.*, 1979; Wilson, 1997). Indeed, in Europe, hazel is the first to shed pollens in the air (December-April), followed by birch (March-April) and grasses (May-June) (D'amato *et al.*, 2007). In addition, climate change has already led to an earlier onset of biological spring and today's air pollution further amplifies and/or alters pollination (D'Amato *et al.*, 2001; Peñuelas and Filella, 2001). Nonetheless, other factors such as crowding of horses during winter and the seasonal breeding cycle of horses also contribute to these seasonally observed symptoms.

Vice versa, the enhanced replication of (alpha)herpesviruses in the respiratory epithelium might further promote the detrimental effects of pollens. First, the viral-induced destruction of epithelial cells leads to impaired mucociliary clearance, which may further concentrate pollen substances in one place (Houtmeyers *et al.*, 1999). Furthermore, epithelial damage will facilitate the delivery of these pollen substances to the underlying cells of the immune system to promote airway sensitization (Robinson *et al.*, 1997; Taketomi *et al.*, 2006; Xiao *et al.*, 2011b). Next, alphaherpesviruses might selectively activate T helper 2 cells or suppress T regulatory cells in certain individuals, which are both of key importance in the development of allergies. Indeed, T helper 2 responses have already been shown to exacerbate HSV1-induced keratitis in mice (Jayaraman *et al.*, 1993). However, further studies using appropriate host-specific models are required to uncover the role of alphaherpesviruses in T helper 2 cell priming.

Besides alphaherpesviruses, multiple other airborne pathogens might co-migrate along with pollen substances and benefit from this barrier dysfunction to enhance infection. For example, adenoviruses and reoviruses likewise preferentially infect the basolateral surface of respiratory epithelial cells (Excoffon *et al.*, 2008; Zabner *et al.*, 1997). In addition, damage to the ciliated epithelial cells by pollen proteases might favour subsequent attachment of and colonisation by respirable bacterial pathogens (e.g. *Streptococcus* species) (López and Martinson, 2017; Plotkowski *et al.*, 1986).

Taken together, we shed new light on the detrimental effects of pollens on the respiratory epithelium and their role in pathogen invasion. More precisely, we found that pollen proteases selectively and irreversibly disrupt intercellular junctions of columnar epithelial cells, while the indispensable basal cells are resistant and succeed in maintaining the epithelial barrier. Upon exposure to pollen proteases, the flattened basal cells can partly prevent the alphaherpesvirus EHV1 from reaching its binding receptor, located basolaterally in the epithelium. However, they cannot fully prevent infection of the respiratory epithelium, as EHV1 can still bind to the basolateral surface of semi-detaching epithelial cells. Furthermore, we hypothesize that a concurrent alphaherpesvirus invasion of the respiratory mucosa might further drive the onset and persistence of allergies through mechanisms yet to be elucidated.

Acknowledgements

The authors acknowledge Carine Boone, Chantal Vanmaercke, Nele Dennequin, Lobke De Bels and Jonathan Vandenberghe for their excellent technical support.

References

- Barnes, P.J., 2011.** Pathophysiology of allergic inflammation. *Immunological reviews* 242, 31-50.
- Batanero, E., Barral, P., Villalba, M., Rodríguez, R., 2002.** Sensitization of mice with olive pollen allergen Ole e 1 induces a Th2 response. *International archives of allergy and immunology* 127, 269-275.
- Blume, C., Swindle, E.J., Dennison, P., Jayasekera, N.P., Dudley, S., Monk, P., Behrendt, H., Schmidt-Weber, C.B., Holgate, S.T., Howarth, P.H., 2012.** Barrier responses of human bronchial epithelial cells to grass pollen exposure. *European Respiratory Journal*, erj00756-02012.
- Bocheva, G., Rattenholl, A., Kempkes, C., Goerge, T., Lin, C.Y., D'Andrea, M.R., Stander, S., Steinhoff, M., 2009.** Role of matriptase and proteinase-activated receptor-2 in nonmelanoma skin cancer. *The Journal of investigative dermatology* 129, 1816-1823.
- Boers, J.E., Ambergen, A.W., Thunnissen, F.B., 1998.** Number and proliferation of basal and parabasal cells in normal human airway epithelium. *American journal of respiratory and critical care medicine* 157, 2000-2006.
- Bullone, M., Lavoie, J.-P., 2015.** Asthma “of horses and men” - How can equine heaves help us better understand human asthma immunopathology and its functional consequences? *Molecular Immunology* 66, 97-105.
- Chiu, L.-L., Perng, D.-W., Yu, C.-H., Su, S.-N., Chow, L.-P., 2007.** Mold allergen, pen C 13, induces IL-8 expression in human airway epithelial cells by activating protease-activated receptor 1 and 2. *The Journal of Immunology* 178, 5237-5244.
- Clark, A.B., Randell, S.H., Nettesheim, P., Gray, T.E., Bagnell, B., Ostrowski, L.E., 1995.** Regulation of ciliated cell differentiation in cultures of rat tracheal epithelial cells. *American journal of respiratory cell and molecular biology* 12, 329-338.
- Cocks, T.M., Moffatt, J.D., 2001.** Protease-activated Receptor-2 (PAR2) in the Airways. *Pulmonary Pharmacology & Therapeutics* 14, 183-191.
- Cortes, L., Carvalho, A.L., Todo-Bom, A., Faro, C., Pires, E., Verissimo, P., 2006.** Purification of a novel aminopeptidase from the pollen of *Parietaria judaica* that alters epithelial integrity and degrades neuropeptides. *The Journal of allergy and clinical immunology* 118, 878-884.
- D'Amato, G., Liccardi, G., D'Amato, M., Cazzola, M., 2001.** The role of outdoor air pollution and climatic changes on the rising trends in respiratory allergy. *Respiratory Medicine* 95, 606-611.
- D'amato, G., Cecchi, L., Bonini, S., Nunes, C., Annesi-Maesano, I., Behrendt, H., Liccardi, G., Popov, T., Van Cauwenberge, P., 2007.** Allergenic pollen and pollen allergy in Europe. *Allergy* 62, 976-990.
- Davison, A.J., 2002.** Evolution of the herpesviruses. *Veterinary microbiology* 86, 69-88.
- Déry, O., Corvera, C.U., Steinhoff, M., Bunnett, N.W., 1998.** Proteinase-activated receptors: novel mechanisms of signaling by serine proteases. *American Journal of Physiology-Cell Physiology* 274, C1429-C1452.
- Erjefalt, J.S., Erjefalt, I., Sundler, F., Persson, C.G., 1995.** *In vivo* restitution of airway epithelium. *Cell and tissue research* 281, 305-316.
- Evans, M.J., Cox, R.A., Shami, S.G., Plopper, C.G., 1990.** Junctional adhesion mechanisms in airway basal cells. *American journal of respiratory cell and molecular biology* 3, 341-347.
- Excoffon, K.J.A., Guglielmi, K.M., Wetzal, J.D., Gansemer, N.D., Campbell, J.A., Dermody, T.S., Zabner, J., 2008.** Reovirus preferentially infects the basolateral surface and is released from the apical surface of polarized human respiratory epithelial cells. *The Journal of infectious diseases* 197, 1189-1197.
- Glorieux, S., Bachert, C., Favoreel, H.W., Vandekerckhove, A.P., Steukers, L., Rekecki, A., Van den Broeck, W., Goossens, J., Croubels, S., Clayton, R.F., 2011.** Herpes simplex virus type 1 penetrates the basement membrane in human nasal respiratory mucosa. *PLoS One* 6, e22160.
- Glorieux, S., Favoreel, H., Meesen, G., Van den Broeck, W., Nauwynck, H., 2009.** Different replication characteristics of historical pseudorabies virus strains in porcine respiratory nasal mucosa explants. *Veterinary microbiology* 136, 341-346.

- Goehring, L.S., Winden, S.C., Maanen, C.v., Oldruitenborgh-Oosterbaan, M.M.S., 2006.** Equine Herpesvirus Type 1-Associated Myeloencephalopathy in The Netherlands: A Four-Year Retrospective Study (1999–2003). *Journal of veterinary internal medicine* 20, 601-607.
- González-Rábade, N., Badillo-Corona, J.A., Aranda-Barradas, J.S., del Carmen Oliver-Salvador, M., 2011.** Production of plant proteases *in vivo* and *in vitro* - a review. *Biotechnology Advances* 29, 983-996.
- Grainger, C.I., Greenwell, L.L., Lockley, D.J., Martin, G.P., Forbes, B., 2006.** Culture of Calu-3 Cells at the Air Interface Provides a Representative Model of the Airway Epithelial Barrier. *Pharmaceutical Research* 23, 1482-1490.
- Grünig, G., Warnock, M., Wakil, A.E., Venkayya, R., Brombacher, F., Rennick, D.M., Sheppard, D., Mohrs, M., Donaldson, D.D., Locksley, R.M., 1998.** Requirement for IL-13 independently of IL-4 in experimental asthma. *Science (New York, N.Y.)* 282, 2261-2263.
- Hassim, Z., Maronese, S., Kumar, R., 1998.** Injury to murine airway epithelial cells by pollen enzymes. *Thorax* 53, 368-371.
- Höllbacher, B., Schmitt, A.O., Hofer, H., Ferreira, F., Lackner, P., 2017.** Identification of proteases and protease inhibitors in allergenic and non-allergenic pollen. *International journal of molecular sciences* 18, 1199.
- Houtmeyers, E., Gosselink, R., Gayan-Ramirez, G., Decramer, M., 1999.** Regulation of mucociliary clearance in health and disease. *European Respiratory Journal* 13, 1177-1188.
- Jayaraman, S., Heiligenhaus, A., Rodriguez, A., Soukiasian, S., Dorf, M., Foster, C., 1993.** Exacerbation of murine herpes simplex virus-mediated stromal keratitis by Th2 type T cells. *The Journal of Immunology* 151, 5777-5789.
- Karlin, S., Mocarski, E.S., Schachtel, G.A., 1994.** Molecular evolution of herpesviruses: genomic and protein sequence comparisons. *J Virol* 68, 1886-1902.
- Kato, T., Takai, T., Fujimura, T., Matsuoka, H., Ogawa, T., Murayama, K., Ishii, A., Ikeda, S., Okumura, K., Ogawa, H., 2009.** Mite serine protease activates protease-activated receptor-2 and induces cytokine release in human keratinocytes. *Allergy* 64, 1366-1374.
- Knight, D.A., Lim, S., Scaffidi, A.K., Roche, N., Chung, K.F., Stewart, G.A., Thompson, P.J., 2001.** Protease-activated receptors in human airways: Upregulation of PAR-2 in respiratory epithelium from patients with asthma. *Journal of Allergy and Clinical Immunology* 108, 797-803.
- Kumamoto, J., Tsutsumi, M., Goto, M., Nagayama, M., Denda, M., 2016.** Japanese Cedar (*Cryptomeria japonica*) pollen allergen induces elevation of intracellular calcium in human keratinocytes and impairs epidermal barrier function of human skin *ex vivo*. *Archives of dermatological research* 308, 49-54.
- Laemmli, U.K., 1970.** Cleavage of structural proteins during the assembly of the head of bacteriophage T4. *Nature* 227, 680.
- Lanaspa, M.A., Andres-Hernando, A., Rivard, C.J., Dai, Y., Berl, T., 2008.** Hypertonic stress increases claudin-4 expression and tight junction integrity in association with MUPP1 in IMCD3 cells. *Proceedings of the National Academy of Sciences* 105, 15797-15802.
- Lee, S.I., Pham, L.D., Shin, Y.S., Suh, D.H., Park, H.-S., 2014.** Environmental changes could enhance the biological effect of Hop J pollens on human airway epithelial cells. *Journal of Allergy and Clinical Immunology* 134, 470-472.e471.
- López, A., Martinson, S.A., 2017.** Chapter 9 - Respiratory System, Mediastinum, and Pleurae1, in: Zachary, J.F. (Ed.), *Pathologic Basis of Veterinary Disease (Sixth Edition)*. Mosby, pp. 471-560.e471.
- Peñuelas, J., Filella, I., 2001.** Responses to a warming world. *Science (New York, N.Y.)* 294, 793-795.
- Plotkowski, M.-C., Puchelle, E., Beck, G., Jacquot, J., Hannoun, C., 1986.** Adherence of type I *Streptococcus pneumoniae* to tracheal epithelium of mice infected with influenza A/PR8 virus. *American Review of Respiratory Disease* 134, 1040-1044.
- Quintana, A.M., Landolt, G.A., Annis, K.M., Hussey, G.S., 2011.** Immunological characterization of the equine airway epithelium and of a primary equine airway epithelial cell culture model. *Veterinary Immunology and Immunopathology* 140, 226-236.
- Radlowski, M., 2005.** Proteolytic enzymes from generative organs of flowering plants (Angiospermae). *J Appl Genet* 46, 247-257.

- Reed, C.E., Kita, H., 2004.** The role of protease activation of inflammation in allergic respiratory diseases. *Journal of Allergy and Clinical Immunology* 114, 997-1008.
- Robinson, C., Kalsheker, N., Srinivasan, N., King, C., Garrod, D., Thompson, P., Stewart, G., 1997.** On the potential significance of the enzymatic activity of mite allergens to immunogenicity. Clues to structure and function revealed by molecular characterization. *Clinical & Experimental Allergy* 27, 10-21.
- Runswick, S., Mitchell, T., Davies, P., Robinson, C., Garrod, D.R., 2007.** Pollen proteolytic enzymes degrade tight junctions. *Respirology (Carlton, Vic.)* 12, 834-842.
- Salojärvi, J., Smolander, O.-P., Nieminen, K., Rajaraman, S., Safronov, O., Safdari, P., Lamminmäki, A., Immanen, J., Lan, T., Tanskanen, J., 2017.** Genome sequencing and population genomic analyses provide insights into the adaptive landscape of silver birch. *Nature genetics* 49, 904.
- Sherman, J., Mitchell, W.R., Martin, S.W., Thorsen, J., Ingram, D.G., 1979.** Epidemiology of equine upper respiratory tract disease on standardbred racetracks. *Canadian Journal of Comparative Medicine* 43, 1-9.
- Steukers, L., Vandekerckhove, A.P., Van den Broeck, W., Glorieux, S., Nauwynck, H.J., 2012.** Kinetics of BoHV-1 dissemination in an *in vitro* culture of bovine upper respiratory tract mucosa explants. *ILAR journal* 53, E43-54.
- Swanson, R., Edlund, A.F., Preuss, D., 2004.** Species specificity in pollen-pistil interactions. *Annual review of genetics* 38, 793-818.
- Taketomi, E.A., Sopelete, M.C., Moreira, P.F.d.S., Vieira, F.d.A.M., 2006.** Pollen allergic disease: pollens and its major allergens. *Revista Brasileira de Otorrinolaringologia* 72, 562-567.
- Vairo, S., Van den Broeck, W., Favoreel, H., Scagliarini, A., Nauwynck, H., 2013.** Development and use of a polarized equine upper respiratory tract mucosal explant system to study the early phase of pathogenesis of a European strain of equine arteritis virus. *Veterinary Research* 44, 9.
- Van Cleemput, J., Poelaert, K.C.K., Laval, K., Maes, R., Hussey, G.S., Van den Broeck, W., Nauwynck, H.J., 2017.** Access to a main alphaherpesvirus receptor, located basolaterally in the respiratory epithelium, is masked by intercellular junctions. *Scientific reports* 7, 16656.
- van der Meulen, K., Vercauteren, G., Nauwynck, H., Pensaert, M., 2003.** A local epidemic of equine herpesvirus 1-induced neurological disorders in Belgium. *Vlaams Diergeneeskundig Tijdschrift* 72, 366-372.
- Vandekerckhove, A., Glorieux, S., Van den Broeck, W., Gryspeerdt, A., van der Meulen, K.M., Nauwynck, H.J., 2009.** *In vitro* culture of equine respiratory mucosa explants. *Veterinary Journal* 181, 280-287.
- Vandekerckhove, A.P., Glorieux, S., Gryspeerdt, A.C., Steukers, L., Duchateau, L., Osterrieder, N., Van de Walle, G.R., Nauwynck, H.J., 2010.** Replication kinetics of neurovirulent versus non-neurovirulent equine herpesvirus type 1 strains in equine nasal mucosal explants. *The Journal of general virology* 91, 2019-2028.
- Vermeer, P.D., Denker, J., Estin, M., Moninger, T.O., Keshavjee, S., Karp, P., Kline, J.N., Zabner, J., 2009.** MMP9 modulates tight junction integrity and cell viability in human airway epithelia. *American Journal of Physiology-Lung Cellular and Molecular Physiology* 296, L751-L762.
- Vinhas, R., Cortes, L., Cardoso, I., Mendes, V.M., Manadas, B., Todo-Bom, A., Pires, E., Verissimo, P., 2011.** Pollen proteases compromise the airway epithelial barrier through degradation of transmembrane adhesion proteins and lung bioactive peptides. *Allergy* 66, 1088-1098.
- Whitcutt, M.J., Adler, K.B., Wu, R., 1988.** A biphasic chamber system for maintaining polarity of differentiation of culture respiratory tract epithelial cells. *In vitro cellular & developmental biology* 24, 420-428.
- Widmer, F., Hayes, P., Whittaker, R., Kumar, R., 2000.** Substrate preference profiles of proteases released by allergenic pollens. *Clinical and Experimental Allergy* 30, 571-576.
- Wilson, W.D., 1997.** Equine herpesvirus 1 myeloencephalopathy. *Veterinary Clinics: Equine Practice* 13, 53-72.
- Xiao, C., Puddicombe, S.M., Field, S., Haywood, J., Broughton-Head, V., Puxeddu, I., Haitchi, H.M., Vernon-Wilson, E., Sammut, D., Bedke, N., 2011a.** Defective epithelial barrier function in asthma. *Journal of Allergy and Clinical immunology* 128, 549-556. e512.

- Xiao, C., Puddicombe, S.M., Field, S., Haywood, J., Broughton-Head, V., Puxeddu, I., Haitchi, H.M., Vernon-Wilson, E., Sammut, D., Bedke, N., Cremin, C., Sones, J., Djukanović, R., Howarth, P.H., Collins, J.E., Holgate, S.T., Monk, P., Davies, D.E., 2011b.** Defective epithelial barrier function in asthma. *Journal of Allergy and Clinical Immunology* 128, 549-556.e512.
- Zabner, J., Freimuth, P., Puga, A., Fabrega, A., Welsh, M.J., 1997.** Lack of high affinity fiber receptor activity explains the resistance of ciliated airway epithelia to adenovirus infection. *Journal of Clinical Investigation* 100, 1144-1149.

Chapter 5.

Deoxynivalenol, but not fumonisin B1, aflatoxin B1 or diesel exhaust particles disrupt the horse's respiratory epithelial barrier and predispose the respiratory epithelium for equine herpesvirus type 1 infection

Jolien Van Cleemput, Katrien C.K. Poelaert, Kathlyn Laval, Wim Van den Broeck, Hans J. Nauwynck

Manuscript in preparation

Summary

The horse's respiratory tract daily encounters a plethora of respirable hazards including air pollutants such as diesel exhaust and mycotoxins, toxic by-products of moulds. To date, their effect on respiratory epithelial integrity has not been studied. Diesel exhaust particles (DEP) and three major mycotoxins; deoxynivalenol (DON), aflatoxin B1 (AFB1) and fumonisin B1 (FB1) were applied to the apical surfaces of both *ex vivo* respiratory mucosal explants and *in vitro* primary equine respiratory epithelial cells (EREC), grown on transwells. DON, but not AFB1, FB1 or DEP affected epithelial intercellular junctions in both *ex vivo* and *in vitro* systems, as demonstrated by histological changes in respiratory epithelial morphology and a drop in transepithelial electrical resistance across the EREC monolayer, respectively. Since we previously showed that respiratory epithelial intercellular junctions form the main barrier against equine herpesvirus type 1 (EHV1) infection, we subsequently inoculated DON-pretreated mucosal explants and EREC with EHV1. Compared to control diluent and FB1-pretreated respiratory mucosal explants, DON-pretreated explants showed on average 6.5 ± 4.5 -fold more EHV1 plaques and produced on average 1 log₁₀ more extracellular virus particles, as assessed by confocal microscopy and virus titration, respectively. Similarly, EHV1 infection was greatly enhanced in EREC upon pretreatment with DON. Based on our findings, we propose that inhalation of DON from moulds predisposes horses for infections with EHV1, by affecting respiratory epithelial integrity.

Introduction

In modern equestrian society, the air breath by horses is inevitably filled with respirable hazards, ranging from dust and ammonia to mycotoxins, pollens and air pollutants. Despite this daily struggle, the well-armed respiratory tract of most horses seems to cope efficiently with these constant threats. Nonetheless, a vast amount of horses develops asthma or other chronic respiratory diseases during their life-span (Bracher *et al.*, 1991; Robinson *et al.*, 2006; Winder and Von Fellenberg, 1987; Wood *et al.*, 2005). In addition, (subclinical) respiratory disease is one of the mainly recognized causes of poor performance in competing horses and thus, has serious economic impacts on the horse industry worldwide (Allen *et al.*, 2006; Couetil and Denicola, 1999; Pirrone *et al.*, 2007). Besides imposing direct damage to the respiratory tract's mucosa, these threats are likely to predispose the horse for subsequent pathogen invasion. Indeed, we previously showed that pollen proteases disrupt integrity of the horse's respiratory epithelium and thereby enhance subsequent equine herpesvirus type 1 (EHV1) infection (Chapter 4). The precise effect of dust, ammonia, mycotoxins and air pollution on the horse's respiratory mucosa and its role in subsequent EHV1 infection still remains obscure. Since mycotoxins and air pollutants have been shown to alter epithelial intercellular junctions, this study examined their effect on the horse's respiratory epithelium using well-established *ex vivo* and *in vitro* equine models (Bracarense *et al.*, 2012; Gao *et al.*, 2017; Gerez *et al.*, 2015; Heussen and Alink, 1992; Lehmann *et al.*, 2009; Quintana *et al.*, 2011; Van Cleemput *et al.*, 2017; Van De Walle *et al.*, 2010; Vandekerckhove *et al.*, 2009).

Mycotoxins are toxic secondary metabolites produced by fungi mainly belonging to the genera *Fusarium*, *Aspergillus* and *Penicillium*. Aflatoxins, ochratoxins, fumonisins, trichothecenes (e.g. deoxynivalenol or DON) and zearalenone are five frequently encountered mycotoxins in equine feeds such as green forages, hays, silages and grains (Liesener *et al.*, 2010; Ogunade *et al.*, 2018). Upon inhalation in the horse's respiratory tract, these toxins or potentially toxin-producing moulds can cause acute respiratory disease, such as guttural pouch mycosis and/or a more chronic asthma-like syndrome, recurrent airway obstruction (RAO) (Laan *et al.*, 2006; Lepage *et al.*, 2004). Mycotoxins such as deoxynivalenol, alfatoxin and fumonisin have already been shown to alter epithelial integrity in intestinal epithelia *in vivo* and *in vitro* through inhibition of intercellular junction protein neosynthesis (Bracarense *et al.*, 2012; Gao *et al.*, 2017; Gerez *et al.*, 2015; Van De Walle *et al.*, 2010). Here, we investigated their role on respiratory epithelial integrity and subsequent infection with EHV1.

Since equestrian enterprises are mainly located in (sub)urban regions, horses are often exposed to air pollution. Air pollution majorly consists of diesel exhaust, a mixture of particulate matter, hydrocarbons (e.g. benzene), gases (e.g. nitrogen oxide or NO_x) and sulfur, produced during the combustion of diesel fuel in engines from vehicles, as well as industrial plants. Especially the particulate matter, mainly comprised of soot, contributes to the toxic effects of diesel exhaust, as these small particles (ranging from 0.1 µm to 10 µm) can easily reach the deeper structures of the respiratory tract upon inhalation (Mohankumar and Senthilkumar, 2017; Reis *et al.*, 2018). Diesel exhaust particles (DEP) are therefore commonly used to study the toxic effects of air pollution. Upon inhalation, these DEP cause oxidative stress with accompanying inflammatory processes and DNA damage (Grevendonk *et al.*, 2016; Ito *et al.*, 2000; Ma and Ma, 2002; Shukla *et al.*, 2000; Zhao *et al.*, 2009). High concentrations of DEP have been shown to alter tight junctions in 16 hBE cells, a human bronchial epithelial cell line (Lehmann *et al.*, 2009). By facilitating antigen delivery to subepithelial antigen-presenting cells, epithelial barrier dysfunction is involved in the initiation or progression of allergic diseases (Xiao *et al.*, 2011). Besides, diesel exhaust-induced inflammatory processes typically promote a T helper 2 immunologic response, stimulate mucus secretion and induce bronchial smooth muscle contractions (Meldrum *et al.*, 2017; Totlandsdal *et al.*, 2015; Zhao *et al.*, 2009). These symptoms are hallmark of the development of allergic diseases and asthma. In addition, tumorigenesis is promoted through the induction of DNA damage and the alteration of gap junction intercellular communication by diesel exhaust compounds (Heussen and Alink, 1992; Rivedal and Witz, 2005; Song and Ye, 1997). This study is the first to study the effect of these diesel compounds on the equine respiratory tract, more precisely on representative *ex vivo* respiratory mucosal explants and primary *in vitro* equine respiratory epithelial cells.

Material and methods

Reagents

Mycotoxins aflatoxin B1 (AFB1) from *Aspergillus flavus*, fumonisin B1 (FB1) from *Fusarium moniliforme* and deoxynivalenol (DON) were purchased from Sigma-Aldrich (St. Louis, MO, USA) and stock solutions were prepared in ethanol. Diesel exhaust particles (DEP; NIST[®] SRM[®] 2975) were purchased from Sigma-Aldrich and stock solutions were dissolved in dimethyl sulfoxide (DMSO).

Tissue collection and processing

The tracheae from different healthy horses were collected at the slaughterhouse and transported in phosphate-buffered saline (PBS) with calcium and magnesium, supplemented with 0.1 mg/mL gentamicin (ThermoFisher Scientific, Waltham, MA, USA), 0.1 mg/mL kanamycin (Sigma-Aldrich), 100 U/mL penicillin, 0.1 mg/mL streptomycin (ThermoFisher Scientific) and 0.25 µg/mL amphotericin B (ThermoFisher Scientific).

Respiratory mucosal explant isolation and cultivation

Tracheal mucosal explants were prepared as previously described (Van Cleemput *et al.*, 2017; Vandekerckhove *et al.*, 2009).

EREC isolation and cultivation

Primary equine respiratory epithelial cells (EREC) were isolated and cultured as described by Quintana *et al.* (2011) and Van Cleemput *et al.* (2017).

Mycotoxin treatment of respiratory mucosal explants and EREC

Respiratory mucosal explants

Explants were cultured 24 h for adaptation before thoroughly washing and embedding them in agarose diluted in 2X MEM, to mimic *in vivo* conditions, as previously published (Vairo *et al.*, 2013; Van Cleemput *et al.*, 2017). Next, the apical surface of the epithelium was exposed for 3 h at 37°C to 2 nM AFB1, 10 µM FB1, 50 µM DON or 1 µg/mL DEP, dissolved in serum-free medium (DMEM/RPMI [ThermoFisher Scientific], supplemented with 0.1 mg/mL gentamicin, 100 U/mL penicillin, 0.1 mg/mL streptomycin, and 0.25 µg/mL amphotericin B). An ethanol- and DMSO-based diluent was used as solvent control. Explants were removed from the agarose and washed three times in PBS and fixed in a phosphate-buffered 3.5% formaldehyde solution

for 24 h, either immediately after the last wash or after an additional 24 h incubation on metal gauzes. Explants were then stored into 70% alcohol until further processing.

EREC

Cells were grown to confluency and the transepithelial electrical resistance (TEER) was measured daily until a steady TEER of $\sim 500\text{-}700 \Omega \times \text{cm}^2$ was attained. Mycotoxins, DEP and control diluents were applied onto the apical EREC surfaces at the above-described concentrations. Cells were incubated for 3 h and cell viability was evaluated by means of ethidium monoazide bromide (EMA)-staining and was not significantly affected upon different treatments.

Assessment of epithelial integrity

Respiratory mucosal explants

Integrity of the intercellular junctions was verified by examining the intercellular space in haematoxylin-eosin-stained paraffin coupes, as previously described (Van Cleemput *et al.*, 2017).

EREC

To assess epithelial integrity of the EREC, the transepithelial electrical resistance (TEER) was measured using an epithelial voltohmmeter (Millipore corporation, Bedford, MA, USA). The net resistance was calculated by subtracting the background resistance and multiplying the resistance by the surface area of the membrane.

Viral infection assays

Virus

A Belgian EHV1 isolate (03P37) was used in this study and originates from the blood taken of a paralytic horse during an outbreak in 2003 (van der Meulen *et al.*, 2003a). The virus was propagated on rabbit kidney (RK13) cells and used at the 6th passage.

Respiratory mucosal explants

Explants were cultured at the air-liquid interface for 24 h, prior to extensive washing and embedment in agarose. Next, explants were exposed to the reagents or control diluents for 3 h, as described above. Following a washing step for removal of the reagents, the apical surface of the epithelium was inoculated with $10^{6.5}$ TCID₅₀ of the 03P37 EHV1 strain for 1 h at 37°C. Explants were removed from the agarose and washed 3 times in PBS to remove non-adherent

virus particles. Finally, explants were placed back onto their gauzes and serum-free medium was added. Twenty-four hours post-inoculation, explants were placed into methylcellulose-filled plastic tubes and frozen at -80°C until further processing.

EREC

EREC were fully grown in a transwell cell culture system prior to treatment with the reagents or control diluents. Following a thorough washing step, cells were exposed for 1 h to 100 µL EHV1 03P37 strain (MOI of 1) at the apical surface. Non-adsorbed virus particles were removed by washing the EREC three times with DMEM/F12. Fresh EREC medium (DMEM/F12, containing 2% Ultrosor G [Pall Life Sciences; Pall Corp., Cergy, France], 100 U/mL penicillin, 0.1 mg/mL streptomycin, and 1.25 µg/mL amphotericin B) was added to the platewells and cells were further incubated at the air-liquid interface. Ten hours post-inoculation, cells were fixed in methanol for 20 min at -20°C and stored dry at -20°C until further processing.

Immunofluorescent staining and confocal microscopy

Respiratory mucosal explants.

Explants were embedded in methylcellulose and snap-frozen for subsequent cryosectioning. Sixteen µm thick cryosections were cut using a cryostat at -20°C and loaded onto 3-aminopropyltriethoxysilane-coated (Sigma-Aldrich) glass slides. Slides were then fixed in 4% paraformaldehyde for 15 min and subsequently permeabilized in 0.1% Triton-X 100 diluted in PBS. Non-specific binding sites were blocked by 15 min incubation with avidin and biotin (ThermoFisher Scientific) at 37°C. To label late viral glycoproteins, a polyclonal biotinylated horse anti-EHV1 was used for 1 h at 37°C (van der Meulen *et al.*, 2003b), followed by incubation with streptavidin-FITC[®] (ThermoFisher Scientific) for 1 h at 37°C. The basement membrane of the tissues was stained with monoclonal mouse anti-collagen VII antibodies (Sigma-Aldrich), followed by secondary Texas Red[®]-labelled goat anti-mouse antibodies (ThermoFisher Scientific). Nuclei were detected by staining with Hoechst 33342 (ThermoFisher Scientific). Slides were mounted with glycerol-DABCO and analysed using a Leica (TCS SPE) confocal microscope. The total number of plaques was counted on 50 cryosections and plaque latitude was measured using the Leica confocal software package.

EREC

Antibodies were incubated directly in the transwells for 1 h at 37°C. Cells were first incubated with a 1:1,000 dilution of a polyclonal rabbit anti-IEP antibody, kindly provided by Dr. D.

O'Callaghan, Louisiana State University, USA. The diluent used was PBS containing 10% negative goat serum. This was followed by incubation with a goat anti-rabbit IgG FITC[®]-conjugated antibody (ThermoFisher Scientific). Nuclei were counterstained with Hoechst 33342 for 10 min at 37°C. Transwell membranes were excised from the culture inserts and mounted on glass slides using glycerol-DABCO. Slides were examined using a Leica confocal microscope. The total number of plaques was counted on 5 random fields of approximately 3×10^4 cells per insert. Plaque latitude was measured on 10 individual plaques using the Leica confocal software package.

Virus titration.

Twenty-four hours after inoculation, explant supernatant was collected and stored at -80°C until titration. EHV1 titrations were conducted on RK13 cells, which were incubated at 37°C for 7 days. Titers were expressed as TCID₅₀.

Statistical analyses

Significant differences ($P < 0.05$) between different treatments were identified by one-way analysis of variances (ANOVA) followed by Tukey's post-hoc test. If homoscedasticity of the variables was not met, as assessed by the Levene's test, the data were log-transformed prior to ANOVA. Normality of the residuals was verified by the use of the Shapiro-Wilk test. If the variables remained heteroscedastic or normality was not met after log-transformation, a Kruskal-Wallis' test, followed by a Mann-Whitney's post-hoc test were performed. All analyses were conducted in IBM SPSS Statistics for Windows, version 25.0 (IBM Corp, Armonck, NY, USA).

Results

Deoxynivalenol (DON), but not aflatoxin B1 (AFB1), fumonisin B1 (FB1) or diesel exhaust particles (DEP) disrupt respiratory epithelial intercellular junctions

Respiratory mucosal explants

Mycotoxins and diesel exhaust particles (DEP) have already been shown to alter the integrity of intestinal and lung epithelial cells, respectively (Bracarense *et al.*, 2012; Gao *et al.*, 2017; Gerez *et al.*, 2015; Lehmann *et al.*, 2009; Van De Walle *et al.*, 2010). Here, we examined for the first time their effect on the horse's respiratory epithelium using *ex vivo* respiratory mucosal explants and *in vitro* primary respiratory epithelial cells. The examined concentrations were based on data from the above-mentioned studies and most likely correspond to clinically relevant concentrations. For instance, diesel exhaust particle concentrations in the ambient air of urban regions go up to 25 $\mu\text{g}/\text{m}^3$ (Steiner *et al.*, 2016). In addition, a global mycotoxin survey found deoxynivalenol (DON) and fumonisin B1 (FB1) doses of up to 2-20 mg/kg in European roughage and cereal feeds (Biomim, 2016). Taking into account that the horse's nose is often in direct contact with these feeds, it seems reasonable to assume that inhaled mycotoxin concentrations range from several nanograms to even micrograms.

As shown in Figure 1A left panel, the percentage of intercellular space in the epithelium of respiratory mucosal explants was significantly ($P < 0.05$) higher after treatment with 50 μM DON ($10 \pm 2\%$), but not after treatment with 2 nM AFB1 ($3 \pm 1\%$), 10 μM FB1 ($2 \pm 1\%$), 1 $\mu\text{g}/\text{mL}$ DEP ($2 \pm 1\%$), compared to after treatment with control diluent ($2 \pm 1\%$). Increasing the concentration of AFB1, FB1 or DEP by ten-fold did not alter the intercellular space, but did decrease cell viability, as assessed by TUNEL staining (data not shown). Cell viability in the respiratory mucosal explants did not significantly drop after treatment with 50 μM DON or control diluent. Increasing the concentration of DON by 2-fold resulted in a significant drop in cell viability. Twenty-four hours after pretreatment, samples were analysed to determine whether the respiratory epithelium was able to repair its ICJ. Indeed, the percentage of intercellular space in the respiratory epithelium of the explants pretreated with DON decreased from $10 \pm 2\%$ to $3 \pm 1\%$ (Figure 1A, right panel). Figure 1B shows representative haematoxylin-eosin-stained images of explants fixed at 3 h post-treatment (upper panel) or 24 h after the treatment (lower panel).

EREC

EREC attained a steady transepithelial electrical resistance (TEER) of $\sim 500\text{-}700 \Omega \times \text{cm}^{-2}$ after 5-7 days of incubation at the air-liquid interface in a transwell cell culture system. The TEER significantly dropped to baseline levels after treatment with DON, but not after treatment with AFB1, FB1, DEP or control diluent (Figure 1C). DON did not alter cell viability, as determined by EMA-staining.

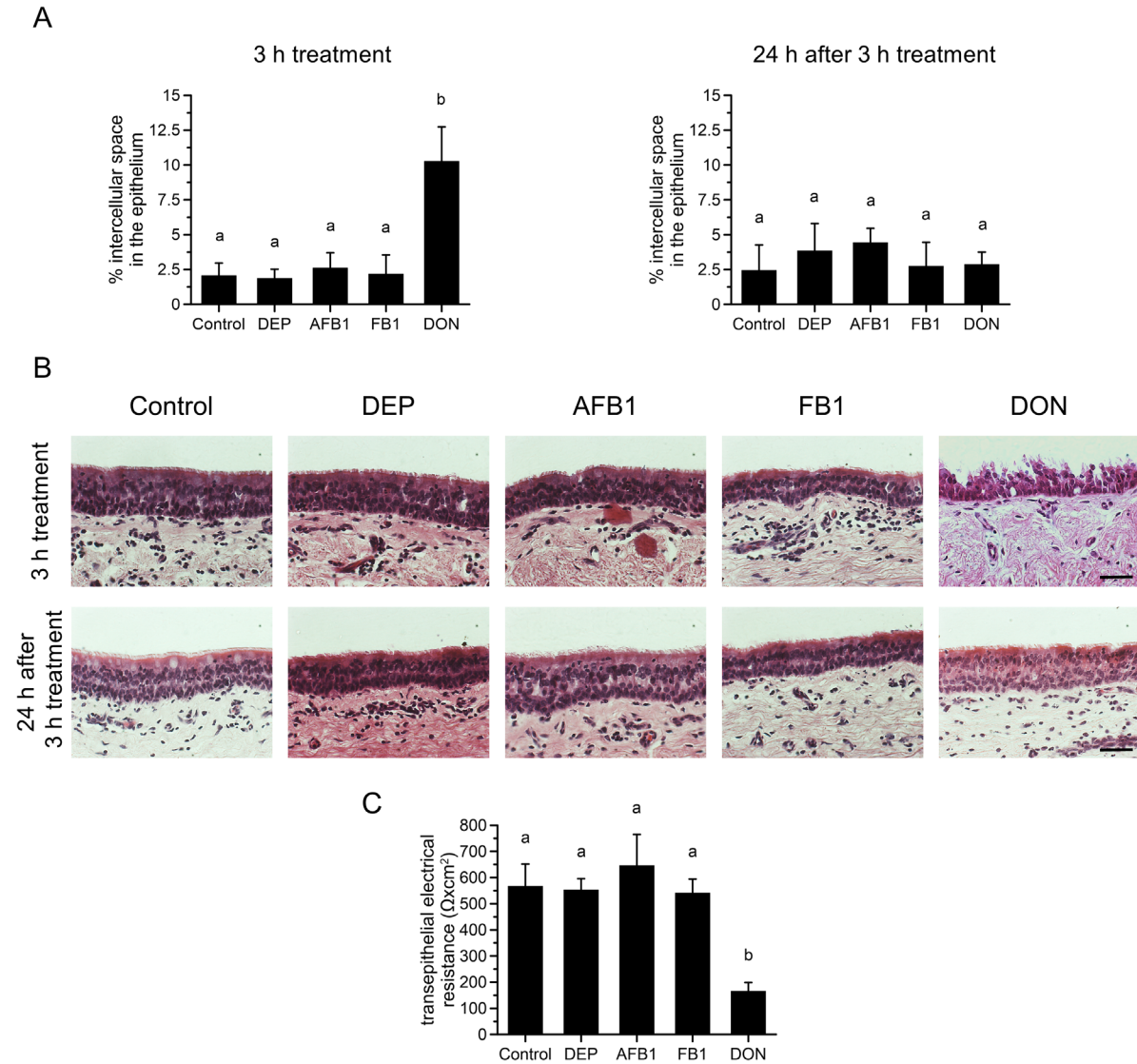


Figure 1. The effect of diesel exhaust particles (DEP) and mycotoxins (AFB1; aflatoxin B1, FB1; fumonisin B1 and DON; deoxynivalenol) on respiratory epithelial integrity. (A) The percentage of intercellular space in the respiratory epithelium of mucosal explants after 3 h treatment (left) and 24 h after the 3 h treatment (right). Experiments were performed on respiratory mucosal explants of 3 individual horses and data are represented as means + SD. Different letters indicate significant ($P < 0.05$) differences between different treatment. (B) Representative haematoxylin-eosin-stained images of respiratory mucosal explants 3 h after treatment (upper panel) and 24 h after the 3 h treatment (lower panel). The scale bar measures 50 μm . (C) The transepithelial electrical resistance of EREC 3 h after treatment. Experiments were performed on the EREC of 3 individual horses and data are represented as means + SD. Different letters indicate significant ($P < 0.05$) differences between different treatment.

DON predisposes respiratory epithelial cells for subsequent EHV1 infection

We previously showed that disruption of intercellular junctions predisposes respiratory epithelial cells for EHV1 infection (Van Cleemput *et al.*, 2017). Since DON affected epithelial integrity in both respiratory mucosal explants and in EREC, we analysed its effect on subsequent EHV1 infection. FB1 was included as an internal control, as this mycotoxin did not affect the ICJ of explants or EREC.

Respiratory mucosal explants

Number of plaques - As shown in Figure 2A left panel, the number of plaques per 50 cryosections significantly ($P < 0.05$) increased from 5 ± 5 in control diluent-pretreated explants to 32 ± 20 in DON-pretreated explants. The number of plaques following FB1 pretreatment (5 ± 2) did not significantly differ from the number of plaques in control diluent-pretreated explants.

Plaque latitude - The plaque latitude gives an indication about the ease of viral spread in the explant epithelium and is shown in Figure 2A, middle panel. The average latitude of EHV1 plaques increased significantly from $101 \pm 14 \mu\text{m}$ in control diluent-pretreated explants to $180 \pm 73 \mu\text{m}$ after DON pretreatment. The average EHV1 plaque latitude in FB1-pretreated explants ($103 \pm 41 \mu\text{m}$) was similar to control diluent-pretreated explants.

Virus titer - Increased viral replication in the epithelium most likely results in an increased production of extracellular infectious virus particles. Indeed, virus titrations (Figure 2A, right panel) showed that the supernatant of DON-pretreated explants contained on average a 1 \log_{10} higher virus titer (4.74 ± 1.18) than control- or FB1-pretreated explants (3.69 ± 0.34 and 3.52 ± 0.48). However, this increase was not significant ($P = 0.196$). Representative confocal images of EHV1 plaques in the respiratory mucosal explants are shown in Figure 2B.

EREC

Number of plaques - On 3×10^4 EREC, we counted an average of 4 ± 2 EHV1 plaques following control diluent pretreatment of the cells (Figure 3A, left panel). Following disruption of ICJ with DON, the number of EHV1 plaques in 3×10^4 EREC significantly ($P < 0.05$) increased to 16 ± 3 . Pretreatment of EREC with FB1 did not significantly increase the number of EHV1 plaques (3 ± 3 on 3×10^4 EREC), compared to control diluent pretreatment.

Plaque latitude - No significant difference in EHV1 plaque latitude was found between different pretreatments (Figure 3A, right panel). Representative confocal images of EHV1 plaques in EREC are shown in Figure 3B.

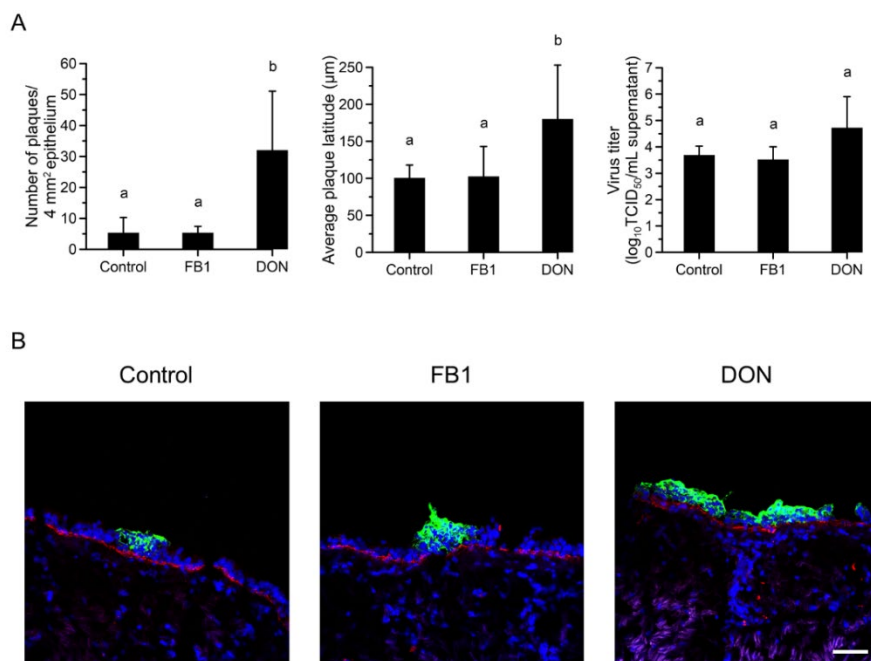


Figure 2. EHV1 infection of respiratory mucosal explants after pretreatment with PBS (control) or mycotoxines (FB1; fumonisin B1 and DON; deoxynivalenol). Explants were frozen 24 hpi and cryosections were stained for late viral antigens. (A) The total number of plaques was counted on 50 consecutive cryosections (left panel), the average plaque latitude was calculated based on a maximum of 10 individual plaques (middle panel) and the extracellular virus titer was determined by titration on RK13 cells (right panel). Experiments were performed on 3 individual horses and data are represented as means + SD. Different letters indicate significant ($P < 0.05$) differences in pretreatments. (B) Representative confocal images of EHV1 plaques (green) in respiratory mucosal explants. The basement membrane is shown in red. Cell nuclei were counterstained with Hoechst (blue). The scale bar represents 50 μm .

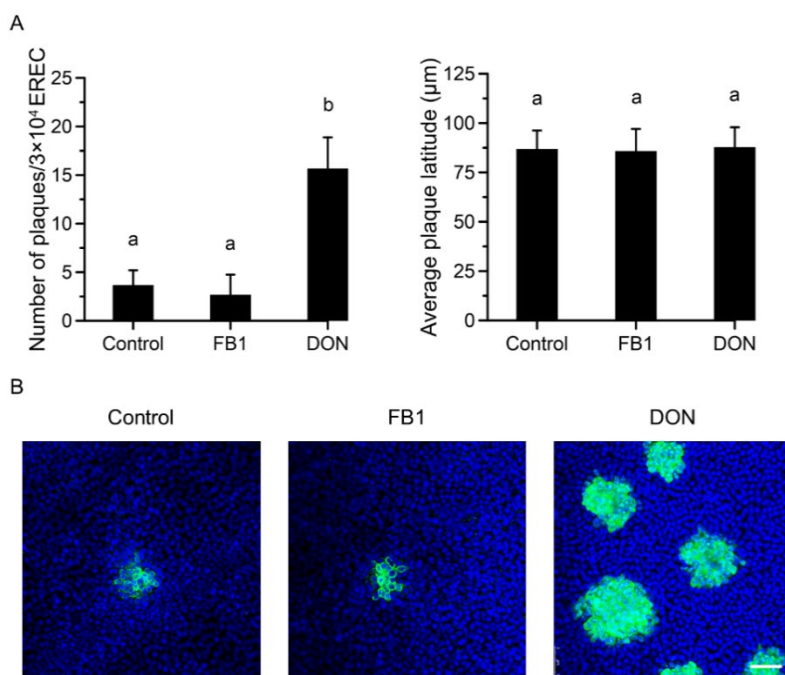


Figure 3. EHV1 infection of equine respiratory epithelial cells (EREC) after pretreatment with PBS (control) or mycotoxines (FB1; fumonisin B1 and DON; deoxynivalenol). Cells were fixed 10 hpi and stained for immediate early protein (IEP). (A) The total number of plaques was counted in five different fields of approximately 3×10^4 cells for each condition (left). Average plaque latitudes were measured on 10 individual plaques (right). Experiments were performed in triplicate on primary EREC of 3 different horses. Data are represented as means + SD and the different letters indicate significant ($P < 0.05$) differences between pretreatments. (B) Representative confocal images of EHV1 IEP-positive plaques (green) in EREC monolayers, nuclei were detected with Hoechst (blue). The scale bar represents 50 μm .

Discussion

With every breath, a number of potential respirable hazards enters the horse's respiratory tract. In today's equestrian world, these hazards range from air pollutants to dusts and mould. For example, horses kept in (sub)urban regions are constantly exposed to air pollution caused by traffic and industrial activities. Although Lehmann *et al.* (2009) reported that diesel exhaust particles (DEP) affected integrity of a human bronchial epithelial cell (16hBE) monolayer, we did not observe this in primary equine respiratory epithelial cells (EREC). The loss of specific differentiation markers during the immortalization process might have caused this discrepancy. Indeed, the formation of a tight and realistic intercellular network within a respiratory epithelial cell monolayer is one of the hallmarks of differentiation (Knust and Bossinger, 2002). Furthermore, the authors showed that by co-culturing 16 hBE cells with dendritic cells, the damaging effect of DEP on epithelial integrity was no longer observed. The authors proposed that by phagocytosing a major amount of deposited DEP, dendritic cells lowered the DEP burden on the epithelial cells. Similarly, dendritic cells might have phagocytosed DEP in our *ex vivo* respiratory mucosal explants. In our primary EREC culture system, residual dendritic cells could presumably also remove part of the DEP.

Moulds and their toxic secondary metabolites, i.e. mycotoxins, are ubiquitous contaminants in equine feeds such as green forages, hays, silages and grains (Liesener *et al.*, 2010; Ogunade *et al.*, 2018). While eating, especially from up-hanging hay racks, the horse's nose is in close contact with food and thus potentially breaths in a considerable amount of these toxic substances. The respiratory epithelium is the first barrier to encounter incoming hazards and could therefore be exposed to high doses of mycotoxins. Until now, the specific impact of these mycotoxins on the equine respiratory epithelium has not been studied. Previous studies examined the role of mycotoxins on epithelial integrity focussing on intestinal cells (Bracarense *et al.*, 2012; Gao *et al.*, 2017; Gerez *et al.*, 2015; Van De Walle *et al.*, 2010). Here, we used an established *ex vivo* equine respiratory mucosal explant model and *in vitro* primary equine respiratory epithelial cells, grown on transwells, to study the effect of mycotoxins.

DON, but not FB1 or AFB1 damaged epithelial integrity in both mucosal explants and EREC. Several other groups already reported that exposure to DON decreases the transepithelial electrical resistance (TEER) of intestinal epithelial cell monolayers (Kasuga *et al.*, 1998; Pinton *et al.*, 2009; Van De Walle *et al.*, 2010). This decrease in TEER was caused by a selective downregulation of claudin-4 and E-cadherin, but not of occludin or zonula occludens (ZO)1 protein expression upon DON exposure (Bracarense *et al.*, 2012; Pinton *et al.*, 2009; Van De

Walle *et al.*, 2010). It has already been described that tricothecenes (e.g. DON) inhibit protein neosynthesis by blocking the peptidyl transferase subunit of actively translating ribosomes (Feinberg *et al.*, 1989). Consequently, DON exposure of intestinal epithelial cells led to a significant decrease in the level of alkaline phosphatase and several nutrient transporters (Kasuga *et al.*, 1998; Maresca *et al.*, 2002; Turner *et al.*, 2008). Therefore, most authors concluded that the DON-induced downregulation of claudin-4 and E-cadherin was caused by a block in protein neosynthesis. It is not surprising that the expression of occludin was not affected upon exposure to DON, as this tight junction protein is recycled from and to the cell surface and thus, its formation depends less on protein neosynthesis (Morimoto *et al.*, 2005). In addition, blocking the ribosomal subunit by DON also induced the onset of an inflammatory cascade in both intestinal, as well as in immune cells. (Moon and Pestka, 2002; Moon *et al.*, 2007; Ouyang *et al.*, 1996; Sergent *et al.*, 2006; Van De Walle *et al.*, 2008; Zhou *et al.*, 2003). By impacting on protein synthesis and increasing inflammation, a thin line exists between a cytotoxic or non-cytotoxic outcome upon exposure to DON. Indeed, in our experiment, DON did not affect cell viability at the carefully chosen concentration and duration of exposure. However, increasing the concentration of DON by 2-fold or the duration time by 6-fold rapidly resulted in a significant loss of cell viability. Likewise, very low concentrations of AFB1 and FB1 were required in order to avoid the onset of apoptosis. These results complement those of others, reporting AFB1- and FB1-induced cytotoxicity at low concentrations (Du *et al.*, 2017; Wan *et al.*, 2013; Zhang *et al.*, 2015).

In contrast to previous studies examining the effects of chronic dietary mycotoxin exposure, we studied merely the acute effect on respiratory epithelial cells. As the nasal cavities filter out incoming debris, mycotoxin concentrations are likely to reach peak values in the surface-lining epithelium (Harkema *et al.*, 2006). Nonetheless, the mucociliary escalator and sneezing reflex rapidly remove incoming hazards upon inhalation, limiting the duration of exposure (Cohn and Reinero, 2007). Nonetheless, this acute exposure was sufficient to destroy epithelial integrity in both our respiratory mucosal explants and EREC.

Here, we demonstrated that the respiratory epithelium is more susceptible to EHV1 infection after complete disruption of the epithelial barrier by the mycotoxin DON. We previously demonstrated that EHV1 targets a receptor located at the basolateral surface of epithelial cells (Van Cleemput *et al.*, 2017). Consequently, this receptor becomes exposed upon disruption of epithelial integrity and subsequent loss of epithelial polarity. These data strongly suggest that feeding mouldy hay predisposes horses for a primary EHV1 infection. In addition, we previously showed that pollen proteases selectively affect the intercellular junctions of

columnar cells and therefore predispose them for EHV1 infection. In addition, multiple other airborne pathogens might benefit from this defective barrier. For instance, adenoviruses and reoviruses likewise preferentially infect the basolateral surface of respiratory epithelial cells (Excoffon *et al.*, 2008; Zabner *et al.*, 1997).

Taken together, our study is the first to show the detrimental effects of mycotoxins on the respiratory epithelium and the role of deoxynivalenol in invasion of the alphaherpesvirus equine herpesvirus type 1.

Acknowledgements

The authors acknowledge Carine Boone, Chantal Vanmaercke, Nele Dennequin, Lobke De Bels and Jonathan Vandenberghe for their excellent technical support.

References

- Allen, K., Tremaine, W., Franklin, S., 2006.** Prevalence of inflammatory airway disease in national hunt horses referred for investigation of poor athletic performance. *Equine Veterinary Journal* 38, 529-534.
- Biomn, 2016.** Mycotoxin Survey 2016 Third quarter (July to Sept, 2016).
- Bracarense, A.-P.F., Luciola, J., Grenier, B., Pacheco, G.D., Moll, W.-D., Schatzmayr, G., Oswald, I.P., 2012.** Chronic ingestion of deoxynivalenol and fumonisin, alone or in interaction, induces morphological and immunological changes in the intestine of piglets. *British Journal of Nutrition* 107, 1776-1786.
- Bracher, V., Von Fellenberg, R., Winder, C.N., Gruenig, G., Hermann, M., Kraehenmann, A., 1991.** An investigation of the incidence of chronic obstructive pulmonary disease (COPD) in random populations of Swiss horses. *Equine Veterinary Journal* 23, 136-141.
- Cohn, L.A., Reinero, C.R., 2007.** Respiratory Defenses in Health and Disease. *Veterinary Clinics of North America: Small Animal Practice* 37, 845-860.
- Couetil, L., Denicola, D., 1999.** Blood gas, plasma lactate and bronchoalveolar lavage cytology analyses in racehorses with respiratory disease. *Equine Veterinary Journal* 31, 77-82.
- Du, M., Liu, Y., Zhang, G., 2017.** Interaction of aflatoxin B1 and fumonisin B1 in HepG2 cell apoptosis. *Food Bioscience* 20, 131-140.
- Excoffon, K.J.A., Guglielmi, K.M., Wetzel, J.D., Gansemer, N.D., Campbell, J.A., Dermody, T.S., Zabner, J., 2008.** Reovirus preferentially infects the basolateral surface and is released from the apical surface of polarized human respiratory epithelial cells. *The Journal of infectious diseases* 197, 1189-1197.
- Feinberg, B., McLaughlin, C., Beasley, V., 1989.** Trichothecene mycotoxicosis: Pathophysiological effects.
- Gao, Y., Li, S., Wang, J., Luo, C., Zhao, S., Zheng, N., 2017.** Modulation of Intestinal Epithelial Permeability in Differentiated Caco-2 Cells Exposed to Aflatoxin M1 and Ochratoxin A Individually or Collectively. *Toxins* 10, 13.
- Gerez, J.R., Pinton, P., Callu, P., Grosjean, F., Oswald, I.P., Bracarense, A.P.F.L., 2015.** Deoxynivalenol alone or in combination with nivalenol and zearalenone induce systemic histological changes in pigs. *Experimental and Toxicologic Pathology* 67, 89-98.
- Grevendonk, L., Janssen, B.G., Vanpoucke, C., Lefebvre, W., Hoxha, M., Bollati, V., Nawrot, T.S., 2016.** Mitochondrial oxidative DNA damage and exposure to particulate air pollution in mother-newborn pairs. *Environmental Health* 15, 10.
- Harkema, J.R., Carey, S.A., Wagner, J.G., 2006.** The nose revisited: a brief review of the comparative structure, function, and toxicologic pathology of the nasal epithelium. *Toxicologic pathology* 34, 252-269.
- Heussen, G., Alink, G., 1992.** Inhibition of gap-junctional intercellular communication by TPA and airborne particulate matter in primary cultures of rat alveolar type II cells. *Carcinogenesis* 13, 719-722.
- Ito, T., Ikeda, M., Yamasaki, H., Sagai, M., Tomita, T., 2000.** Peroxynitrite formation by diesel exhaust particles in alveolar cells: Links to pulmonary inflammation. *Environmental Toxicology and Pharmacology* 9, 1-8.
- Kasuga, F., Hara-Kudo, Y., Saito, N., Kumagai, S., Sugita-Konishi, Y., 1998.** *In vitro* effect of deoxynivalenol on the differentiation of human colonic cell lines Caco-2 and T84. *Mycopathologia* 142, 161-167.
- Knust, E., Bossinger, O., 2002.** Composition and formation of intercellular junctions in epithelial cells. *Science (New York, N.Y.)* 298, 1955-1959.
- Laan, T.T., Bull, S., Pirie, R., Fink-Gremmels, J., 2006.** The role of alveolar macrophages in the pathogenesis of recurrent airway obstruction in horses. *J Vet Intern Med* 20, 167-174.
- Lehmann, A.D., Blank, F., Baum, O., Gehr, P., Rothen-Rutishauser, B.M., 2009.** Diesel exhaust particles modulate the tight junction protein occludin in lung cells *in vitro*. *Particle and fibre toxicology* 6, 26.

- Lepage, O.M., Perron, M.F., Cadore, J.L., 2004.** The mystery of fungal infection in the guttural pouches. *Veterinary journal* (London, England : 1997) 168, 60-64.
- Liesener, K., Curtui, V., Dietrich, R., Märtlbauer, E., Usleber, E., 2010.** Mycotoxins in horse feed. *Mycotoxin research* 26, 23-30.
- Ma, J.Y., Ma, J.K., 2002.** The dual effect of the particulate and organic components of diesel exhaust particles on the alteration of pulmonary immune/inflammatory responses and metabolic enzymes. *Journal of Environmental Science and Health, Part C* 20, 117-147.
- Maresca, M., Mahfoud, R., Garmy, N., Fantini, J., 2002.** The mycotoxin deoxynivalenol affects nutrient absorption in human intestinal epithelial cells. *The Journal of nutrition* 132, 2723-2731.
- Meldrum, K., Gant, T.W., Leonard, M.O., 2017.** Diesel exhaust particulate associated chemicals attenuate expression of CXCL10 in human primary bronchial epithelial cells. *Toxicology in Vitro* 45, 409-416.
- Mohankumar, S., Senthikumar, P., 2017.** Particulate matter formation and its control methodologies for diesel engine: A comprehensive review. *Renewable and Sustainable Energy Reviews* 80, 1227-1238.
- Moon, Y., Pestka, J.J., 2002.** Vomitoxin-induced cyclooxygenase-2 gene expression in macrophages mediated by activation of ERK and p38 but not JNK mitogen-activated protein kinases. *Toxicological Sciences* 69, 373-382.
- Moon, Y., Yang, H., Lee, S.H., 2007.** Modulation of early growth response gene 1 and interleukin-8 expression by ribotoxin deoxynivalenol (vomitoxin) via ERK1/2 in human epithelial intestine 407 cells. *Biochemical and biophysical research communications* 362, 256-262.
- Morimoto, S., Nishimura, N., Terai, T., Manabe, S., Yamamoto, Y., Shinahara, W., Miyake, H., Tashiro, S., Shimada, M., Sasaki, T., 2005.** Rab13 mediates the continuous endocytic recycling of occludin to the cell surface. *Journal of Biological Chemistry* 280, 2220-2228.
- Ogunade, I., Martinez-Tupia, C., Queiroz, O., Jiang, Y., Drouin, P., Wu, F., Vyas, D., Adesogan, A., 2018.** Silage review: Mycotoxins in silage: Occurrence, effects, prevention, and mitigation. *Journal of dairy science* 101, 4034-4059.
- Ouyang, Y.L., Li, S., Pestka, J.J., 1996.** Effects of vomitoxin (deoxynivalenol) on transcription factor NF- κ B/Rel binding activity in murine EL-4 thymoma and primary CD4⁺ T cells. *Toxicology and applied pharmacology* 140, 328-336.
- Pinton, P., Nougayrède, J.-P., Del Rio, J.-C., Moreno, C., Marin, D.E., Ferrier, L., Bracarense, A.-P., Kolf-Clauw, M., Oswald, I.P., 2009.** The food contaminant deoxynivalenol, decreases intestinal barrier permeability and reduces claudin expression. *Toxicology and applied pharmacology* 237, 41-48.
- Pirrone, F., Albertini, M., Clement, M.G., Lafortuna, C.L., 2007.** Respiratory mechanics in Standardbred horses with sub-clinical inflammatory airway disease and poor athletic performance. *The Veterinary Journal* 173, 144-150.
- Quintana, A.M., Landolt, G.A., Annis, K.M., Hussey, G.S., 2011.** Immunological characterization of the equine airway epithelium and of a primary equine airway epithelial cell culture model. *Veterinary Immunology and Immunopathology* 140, 226-236.
- Reis, H., Reis, C., Sharip, A., Reis, W., Zhao, Y., Sinclair, R., Beeson, L., 2018.** Diesel exhaust exposure, its multi-system effects, and the effect of new technology diesel exhaust. *Environment international* 114, 252-265.
- Rivedal, E., Witz, G., 2005.** Metabolites of benzene are potent inhibitors of gap-junction intercellular communication. *Archives of toxicology* 79, 303-311.
- Robinson, N., Karmaus, W., Holcombe, S., Carr, E., Derksen, F., 2006.** Airway inflammation in Michigan pleasure horses: prevalence and risk factors. *Equine veterinary journal* 38, 293-299.
- Sergeant, T., Parys, M., Garsou, S., Pussemier, L., Schneider, Y.-J., Larondelle, Y., 2006.** Deoxynivalenol transport across human intestinal Caco-2 cells and its effects on cellular metabolism at realistic intestinal concentrations. *Toxicology letters* 164, 167-176.
- Shukla, A., Timblin, C., BeruBe, K., Gordon, T., McKinney, W., Driscoll, K., Vacek, P., Mossman, B.T., 2000.** Inhaled particulate matter causes expression of nuclear factor (NF)- κ B-related genes and oxidant-dependent NF- κ B activation *In Vitro*. *American journal of respiratory cell and molecular biology* 23, 182-187.

- Song, J., Ye, S., 1997.** Effects of diesel exhaust particle on gap junction intercellular communication. *Journal of hygiene research* 26, 145-147.
- Steiner, S., Bisig, C., Petri-Fink, A., Rothen-Rutishauser, B., 2016.** Diesel exhaust: current knowledge of adverse effects and underlying cellular mechanisms. *Archives of Toxicology* 90, 1541-1553.
- Totlandsdal, A.I., Låg, M., Lilleaas, E., Cassee, F., Schwarze, P., 2015.** Differential proinflammatory responses induced by diesel exhaust particles with contrasting PAH and metal content. *Environmental toxicology* 30, 188-196.
- Turner, P., Wu, Q., Piekkola, S., Gratz, S., Mykkänen, H., El-Nezami, H., 2008.** Lactobacillus rhamnosus strain GG restores alkaline phosphatase activity in differentiating Caco-2 cells dosed with the potent mycotoxin deoxynivalenol. *Food and chemical toxicology* 46, 2118-2123.
- Vairo, S., Van den Broeck, W., Favoreel, H., Scagliarini, A., Nauwynck, H., 2013.** Development and use of a polarized equine upper respiratory tract mucosal explant system to study the early phase of pathogenesis of a European strain of equine arteritis virus. *Veterinary Research* 44, 9.
- Van Cleemput, J., Poelaert, K.C.K., Laval, K., Maes, R., Hussey, G.S., Van den Broeck, W., Nauwynck, H.J., 2017.** Access to a main alphaherpesvirus receptor, located basolaterally in the respiratory epithelium, is masked by intercellular junctions. *Scientific reports* 7, 16656.
- Van De Walle, J., Romier, B., Larondelle, Y., Schneider, Y.-J., 2008.** Influence of deoxynivalenol on NF- κ B activation and IL-8 secretion in human intestinal Caco-2 cells. *Toxicology letters* 177, 205-214.
- Van De Walle, J., Sergent, T., Piront, N., Toussaint, O., Schneider, Y.-J., Larondelle, Y., 2010.** Deoxynivalenol affects *in vitro* intestinal epithelial cell barrier integrity through inhibition of protein synthesis. *Toxicology and Applied Pharmacology* 245, 291-298.
- van der Meulen, K., Vercauteren, G., Nauwynck, H., Pensaert, M., 2003a.** A local epidemic of equine herpesvirus 1-induced neurological disorders in Belgium. *Vlaams Diergeneeskundig Tijdschrift* 72, 366-372.
- van der Meulen, K.M., Nauwynck, H.J., Pensaert, M.B., 2003b.** Absence of viral antigens on the surface of equine herpesvirus-1-infected peripheral blood mononuclear cells: a strategy to avoid complement-mediated lysis. *Journal of general virology* 84, 93-97.
- Vandekerckhove, A., Glorieux, S., Van den Broeck, W., Gryspeerdt, A., van der Meulen, K.M., Nauwynck, H.J., 2009.** *In vitro* culture of equine respiratory mucosa explants. *Veterinary Journal* 181, 280-287.
- Wan, L.Y.M., Turner, P.C., El-Nezami, H., 2013.** Individual and combined cytotoxic effects of Fusarium toxins (deoxynivalenol, nivalenol, zearalenone and fumonisins B1) on swine jejunal epithelial cells. *Food and Chemical Toxicology* 57, 276-283.
- Winder, N., Von Fellenberg, R., 1987.** Chronic small airway disease in horses slaughtered in Switzerland. *Schweizer Archiv für Tierheilkunde* 129, 585.
- Wood, J., Newton, J., Chanter, N., Mumford, J., 2005.** Inflammatory airway disease, nasal discharge and respiratory infections in young British racehorses. *Equine veterinary journal* 37, 236-242.
- Xiao, C., Puddicombe, S.M., Field, S., Haywood, J., Broughton-Head, V., Puxeddu, I., Haitchi, H.M., Vernon-Wilson, E., Sammut, D., Bedke, N., 2011.** Defective epithelial barrier function in asthma. *Journal of Allergy and Clinical immunology* 128, 549-556. e512.
- Zabner, J., Freimuth, P., Puga, A., Fabrega, A., Welsh, M.J., 1997.** Lack of high affinity fiber receptor activity explains the resistance of ciliated airway epithelia to adenovirus infection. *Journal of Clinical Investigation* 100, 1144-1149.
- Zhang, J., Zheng, N., Liu, J., Li, F.D., Li, S.L., Wang, J.Q., 2015.** Aflatoxin B1 and aflatoxin M1 induced cytotoxicity and DNA damage in differentiated and undifferentiated Caco-2 cells. *Food and Chemical Toxicology* 83, 54-60.
- Zhao, H., Ma, J.K., Barger, M.W., Mercer, R.R., Millecchia, L., Schwegler-Berry, D., Castranova, V., Ma, J.Y., 2009.** Reactive oxygen species-and nitric oxide-mediated lung inflammation and mitochondrial dysfunction in wild-type and iNOS-deficient mice exposed to diesel exhaust particles. *Journal of Toxicology and Environmental Health, Part A* 72, 560-570.
- Zhou, H.-R., Islam, Z., Pestka, J.J., 2003.** Rapid, sequential activation of mitogen-activated protein kinases and transcription factors precedes proinflammatory cytokine mRNA expression in spleens of mice exposed to the trichothecene vomitoxin. *Toxicological sciences* 72, 130-142.

Chapter 6.

Equine β -defensins: active against airborne bacteria and some viruses, but exploited by an ancestral host-specific alphaherpesvirus

Jolien Van Cleemput, Katrien C.K. Poelaert, Kathlyn Laval, Nathalie Vanderheijden,
Maarten Dhaenens, Frank Pasmans, Hans J. Nauwynck

Manuscript in preparation

Summary

The horse's respiratory tract needs to counter airborne pathogens on a daily base. As a result, the luminal-lining epithelium is guarded with a repertoire of immune barriers, including antimicrobial peptides such as β -defensins. The three main equine β -defensins (eBD1, 2 and 3) have not been fully characterized in horses. Especially at the level of the respiratory tract, their distribution profile and their role as antimicrobial and immunomodulatory peptide remains obscure. Therefore, this study aimed at unravelling the interplay between local eBDs and important equine airborne pathogens. The presence of eBD1-3 was first mapped in the horse's respiratory tract using RT-PCR and immunofluorescent staining. Minimal inhibitory concentration tests and synchronized virus plaque assays showed that eBD2 and especially eBD3 were active against several bacterial (*Streptococcus* sp., *Rhodococcus* sp., *Actinobacillus* sp. and *Bordetella* sp.) and viral (equine arteritis virus and equine influenza virus) field isolates through direct actions. Remarkably, infectivity of the ancient alphaherpesvirus equine herpesvirus type 1 (EHV1) in rabbit kidney epithelial cells (RK13) was enhanced upon virus pretreatment with eBD2 and 3. Binding assays using Dio-labelled EHV1 particles showed that these eBDs enhanced EHV1 attachment by concentrating virus particles as aggregates on the cell surface. Deletion of the multiple transmembrane-spanning viral envelope glycoprotein M, but not of the single transmembrane-spanning glycoprotein gp2, rendered EHV1 susceptible to the direct inhibitory actions of eBD2. Furthermore, all eBDs facilitated EHV1 binding to and entry in primary equine respiratory epithelial cells (EREC), grown at an air-liquid interface, through cell-mediated actions. Finally, EHV1 orchestrated EREC to synthesize eBDs, which in turn attracted blood leukocytes in a chemotaxis assay. As leukocytes disseminate EHV1 into the horse, eBD-induced chemotaxis may contribute to viral spread within the host. In conclusion, our results show that while bacteria and some viruses are susceptible to eBDs, the ancient alphaherpesvirus EHV1 resists eBDs by incorporating the membrane-stabilising glycoprotein M in the viral envelope. Moreover, we demonstrated that the virus exploits these eBDs to increase its infectivity and ensure spread within the host.

Introduction

The respiratory epithelium lining the majority of the respiratory tract is challenged by air turbulences and incoming pathogens on a daily basis. Among these pathogens, the orthomyxovirus equine influenza virus (EIV), the alphaherpesvirus equine herpesvirus type 1 (EHV1) and the arterivirus equine arteritis virus (EAV) are three major viral causes of respiratory infections in horses (Allen and Bryans, 1986; Timoney and McCollum, 1996; van Maanen and Cullinane, 2002). EIV is a widespread and highly contagious virus, capable of causing explosive outbreaks of respiratory disease in naive horse populations. Besides primary respiratory symptoms, EHV1 can cause abortion and central nervous system disorders following a cell-associated viremia. In contrast to EIV and EHV1, EAV does not display an epithelial cell tropism and rather directly targets immune cells for spread within the host. Nonetheless, the virus occasionally induces respiratory symptoms in horses, besides conjunctivitis, peripheral oedema and abortion. In addition to viruses, bacterial pathogens are constantly conveyed to the respiratory tract along with incoming air. Examples of bacteria naturally colonizing the equine airways are the Gram-positive *Staphylococcus aureus* and *Streptococcus equi* subspecies *zooepidemicus* (Lindahl *et al.*, 2013; Weese *et al.*, 2005). The Gram-positive *Streptococcus equi* subspecies *equi* causes upper respiratory tract catarrh in horses, which is often referred to as ‘strangles’ (Sweeney *et al.*, 2005; Timoney, 2004). The Gram-positive *Rhodococcus equi* resides in the equine intestinal tract but can cause severe pneumonia in foals upon inhalation (Takai, 1997). Although characteristically found as commensal organism in the intestinal mucosa of normal horses, *Actinobacillus equuli* is a potential pathogen, causing pneumonia and septicaemia in foals and sporadically in adult horses (Layman *et al.*, 2014; Ward *et al.*, 1998). Finally, Gram-negative *Bordetella bronchiseptica* is thought to be a non-commensal opportunistic pathogen in the horse and is occasionally isolated from horses with lower airway disease (Christley *et al.*, 2001; Garcia-Cantu *et al.*, 2000; Vaid *et al.*, 2018). To counter these tremendous threats, the respiratory epithelium is guarded with a repertoire of innate barriers and is able to efficiently recruit immune cells to mount an adaptive immune response. Therefore, most of these pathogens are overcome before the onset of respiratory disease.

One of first epithelial defence mechanisms against incoming pathogens is the production of antimicrobial peptides, such as β -defensins (BDs). BDs belong to the defensin family, small cationic peptides that exhibit a broad-spectrum antimicrobial activity against (myco)bacteria, fungi and viruses, as well immunomodulatory properties and have already extensively been

reviewed (Ganz, 2003; Pazgier *et al.*, 2006; Selsted and Ouellette, 2005; White *et al.*, 1995; Yang *et al.*, 2002). The hallmark of all defensins is the presence of three different intramolecular disulphide bonds, pairing three antiparallel β -strands. Based on disulphide connectivity, the defensin family is divided in two main subtypes, α and β -defensins. While α -defensins are mainly expressed in leukocytes and intestinal Paneth cells, β -defensins (BDs) are predominantly found in epithelia lining internal and external lumina, but can also be synthesized in leukocytes.

The first identified mammalian BD was extracted from bovine tracheal mucosa and was named 'tracheal antimicrobial peptide' (Diamond *et al.*, 1991). In the meantime, BDs have been described in several other species including humans, mice, pigs, dogs, sheep and horses (Bals *et al.*, 1999; Bensch *et al.*, 1995; Davis *et al.*, 2004; Huttner *et al.*, 1998; Sang *et al.*, 2005; Zhang *et al.*, 1998). Genes encoding BDs are usually clustered on the same chromosome, but vary in number and complexity among different species due to evolutionary diversification. However, regional similarities exist in the amino-acid sequence of individual BD members of different mammals. For example, human BD2 closely resembles the phylogenetically related porcine BD1, murine BD3 and equine BD1 (Bals *et al.*, 1999; Davis *et al.*, 2004; Zhang *et al.*, 1998). Unfortunately, nomenclature of defensins usually refers to the order in which defensins were discovered in each individual species, instead of to the similarity with other mammalian BD members. Therefore, we chose to name the herein-examined equine BDs (eBDs) according to their homologs in humans: eBD1, eBD2 and eBD3.

Unlike the α -defensins, BDs have only poorly been characterized in horses (Bruhn *et al.*, 2009). The first identified BD of the horse was denoted β -defensin 1 by Davis *et al.* (2004) (GenBank CAJ01797.1), but referring to its homology with human BD2, it was termed eBD2 in this study. Gene expression (mRNA) of the latter eBD has been detected in several equine tissues including liver, heart, spleen, kidney, small intestines, uterus, larynx, trachea and bronchus (Davis *et al.*, 2004; Marth *et al.*, 2015; Quintana *et al.*, 2011). EBD2 protein expression has immunohistochemically been visualized in the basal layers of the equine oesophagus, the apocrine ceruminous glands of the equine external auditory canal, the luminal and glandular epithelial cells of the equine endometrium and the apocrine glands of the equine scrotum (Hornickel *et al.*, 2011a, b; Schoniger *et al.*, 2013; Yasui *et al.*, 2007; Yasui *et al.*, 2005). Two years after the discovery of the first eBD, eBD2 and additional defensin genes, including eBD103, were mapped to a cluster on equine chromosome 27 following analysis of an equine BAC library (Looft *et al.*, 2006). Translation of eBD103-coding mRNA results in production of the equine β -defensin 103 (GenBank CAJ01801.1), which shows 79% similarity to human

BD3. Consequently, the latter eBD was denoted eBD3 in this study. It has already been shown that eBD3 is transcribed in the equine tongue and produced in the equine oesophagus (Bruhn *et al.*, 2011; Hornickel *et al.*, 2011a, b). Adjacent to the latter defensin cluster on chromosome 27, an additional cluster of defensin genes is present (EquCab3.0 genomic database). A repertoire of α -defensins, which have been studied by Bruhn *et al.* (2009), precedes the cluster-closing *DefB1* gene (NCBI Reference Sequence: XP_005606479.1). The product of this gene resembles human BD1 and was therefore named eBD1 in the present study. Until now, the existence of a BD1-homologue in horses has not been described.

The three main BDs (eBD1, 2 and 3) have not been fully characterized in horses. Especially at the level of the respiratory tract, their distribution profile and their role as antimicrobial and immunomodulatory peptide remain obscure. Defensins generally block infections, either by direct inactivation of the pathogen or by affecting the target cell (Ganz, 2003; Klotman and Chang, 2006; Wilson *et al.*, 2013). However, some defensins can also promote viral infections (Rapista *et al.*, 2011). It is currently unknown whether equine respiratory pathogens are sensitive or resistant to eBDs. Moreover, some pathogens may have developed defensin-exploiting strategies during co-evolution with their host. Understanding the impact of eBDs on equine pathogens and their role in host adaptive immunity could reveal new prevention and treatment strategies against important equine diseases. Therefore, this study aimed at unravelling the interplay between eBDs and equine airborne pathogens.

Material and methods

Tissue collection

The nasal septa, tracheae and lungs from 5 different healthy horses were collected at the slaughter house and transported in phosphate-buffered saline (PBS) with calcium and magnesium, supplemented with 0.1 mg/mL gentamicin (ThermoFisher Scientific, Waltham, MA, USA), 0.1 mg/mL kanamycin (Sigma-Aldrich, St. Louis, MO, USA), 100 U/mL penicillin, 0.1 mg/mL streptomycin (ThermoFisher Scientific) and 0.25 μ g/mL amphotericin B (ThermoFisher Scientific). The nasal and tracheal mucosa was stripped from the underlying cartilage and along with the lung tissues, cut into small square pieces (25 mm²). Tissue fragments for immunofluorescent staining were placed into methylcellulose-filled plastic tubes and tissue fragments for RT-PCR (0.3mg) were transferred into cryovials. All tissues were snap-frozen and stored at -80°C until further processing.

Immunofluorescent staining and confocal microscopy

Tissue fragments

Fifteen μ m thick cryosections were cut using a cryostat at -20°C and loaded onto 3-aminopropyltriethoxysilane-coated (Sigma-Aldrich) glass slides. Slides were then fixed in 4% paraformaldehyde (PFA) for 15 min and subsequently permeabilized in 0.1% Triton-X 100 diluted in PBS. To stain eBD1, eBD2 and eBD3, a rabbit polyclonal anti-human BD1 (ab115813, Abcam, Cambridge, UK), anti-human BD2 (ab183214, Abcam) and anti-human BD3 (ab19270, Abcam) diluted in PBS^{+Ca+Mg} with 10% negative goat serum (NGS), was used overnight at 4°C, followed by incubation with a goat anti-rabbit IgG FITC[®]-conjugated antibody (ThermoFisher Scientific) for 1 h at 37°C. Nuclei were detected by staining with Hoechst 33342 (ThermoFisher Scientific). Slides were mounted with glycerol-DABCO and pictures were taken using a Leica confocal microscope (TCS SPE, Leica Microsystems, Wetzlar, Germany). A rabbit polyclonal antibody against *Streptococcus suis* (Emelca Bioscience, Antwerp, Belgium) was used as an isotype control antibody. Anti-BD antibodies were chosen based on the homology between their immunogens and the respective eBD amino-acid sequences, published in the NCBI database. To ensure sensitivity of the antibodies for eBDs, electrophoresis and western blot of synthetically produced eBD1, 2 and 3 was performed, as described below. All antibodies could immunodetect the respective synthetic eBDs, as shown in Figure 2C.

EREC

Immunofluorescent staining was performed directly in the transwells and antibodies were incubated for 1 h at 37°C, unless stated otherwise. Cells were first incubated with a polyclonal biotinylated horse anti-EHV1 antibody (van der Meulen *et al.*, 2003b) or a mouse monoclonal anti-influenza A nucleoprotein antibody (HB-65, ATCC) diluted in PBS with 10% NGS, followed by incubation with streptavidin-FITC[®] (ThermoFisher Scientific) or a goat anti-mouse IgG FITC[®]-conjugated antibody (ThermoFisher Scientific), respectively. If indicated, cells were simultaneously stained for viral proteins and eBDs overnight at 4°C. For this, the transwells were incubated with the latter anti-EHV1 or anti-EIV antibodies, together with the rabbit polyclonal anti-BD1, 2, 3 or isotype control antibodies. EHV1 and EIV proteins were subsequently visualized with streptavidin-TexasRed[®] (ThermoFisher Scientific) or a TexasRed[®]-conjugated goat anti-mouse IgG antibody (ThermoFisher Scientific), while eBDs were detected with a goat anti-rabbit FITC[®]-conjugated antibody. Nuclei were counterstained with Hoechst 33342 for 10 min at 37°C. Transwell membranes were excised from the culture inserts and mounted on glass slides using glycerol-DABCO. Slides were examined using a Leica confocal microscope.

RT-PCR

Fragments from all tissues were disrupted in RTL-lysis buffer, supplied with the RNeasy Minikit (Qiagen, Hilden, Germany) and homogenized by passing the lysate several times through a blunt 20G needle. Total RNA was extracted from the lysate using the Qiagen RNeasy Minikit (Qiagen), following the manufacturer's instructions, and treated with 120 U deoxyribonuclease I (New England BioLabs, Ipswich, MA, USA) to eliminate genomic DNA contamination. RNA quantity and quality was assessed using a Nanodrop[®] spectrophotometer (ThermoFisher Scientific, Waltham, USA). Reverse transcriptase polymerase chain reaction (RT-PCR) of 1 μ g of RNA was performed in the Bio-Rad T100 thermal cycler using the Qiagen One-Step RT-PCR kit following the manufacturer's guidelines, with eBD-specific forward and reverse primers, shown in Table 1. Primers were designed based on published and predicted equine nucleotide sequences from the NCBI database, using the Integrated DNA Technologies (IDT) Primer Design tool, and were commercially synthesized (IDT, Coralville, IA, USA). All RT-PCR reactions included GAPDH (housekeeping gene) as a positive control. In addition, reactions without RNA functioned as negative controls. PCR products were run on a 1% agarose gel, subsequently stained with ethidium bromide and visualized with a Gel Doc 1000 imaging system (Bio-Rad). All PCR reaction products were purified for sequencing using the

PCR Clean-up Gel extraction kit (Macherey-Nagel, Düren, Germany) and sent to GATC Biotech (Constance, Germany) for Sanger sequencing. All sequenced PCR products were confirmed using MEGA software, version 6 (Molecular Evolutionary Genetics Analysis [MEGA], Philadelphia, PA, USA).

Gene	Foward primer (5'-3')	Reverse primer (5'-3')	NCBI accession number
GAPDH	AGGTCGGAGTAAACGGATTTG	CATAAGGTCCACCACCCTATTG	NM_001163856
eBD1	CCTCTGGAAGCCTCTGTCA	TTCCCGCCGTAACAAGTGC	XM_005606422
eBD2	CTTCCTCATTGTCTTCCTGTT	TAGCAGTTTCTGACTCCACATC	NM_001081887
eBD3	TCTTCGCATTGCTCTTTCT	GCTTCTATAAACTTCAAGGAGGCA	XM_003364245

Table 1. Primer design (5' to 3') for respective eBD1-3 and GAPDH. Primers were designed based on published and predicted equine nucleotide sequences from the NCBI database (right column).

Peptide synthesis, purification and oxidative folding

EBD1, 2 and 3 were chemically synthesized via in-house techniques at Biomatik (Cambridge, Canada) and subsequently high performance liquid chromatography (HPLC)-purified to >95%. The eBD molecular weights were verified by electrospray ionization mass spectrometry (ESI-MS). In the final step, toxic trifluoroacetic acid (TFA), essential during peptide synthesis, was exchanged for non-toxic HCl-salt in order to enable downstream cell experiments. All eBDs were stored as a lyophilized powder at -20°C until further processing. Lyophilized eBD2 and 3 were thawed and dissolved in 10 mM phosphate buffer (pH 7,7) at a concentration of 0.5 mg/mL. The folding reaction occurred through air-oxidation in open vessels, which were gently shaken overnight at room temperature. Oxidation of eBD1 was performed in 20% DMSO diluted in 0.1 M Tris buffer pH 6 for 2 h at room temperature (RT), essentially as described by Tam *et al.* (1991). Solutions were finally filtered sterile through 0.22 μ m pore size filters.

Electrophoresis and Western blot

Ten μ g of oxidized synthetic peptides was boiled in tricine sample buffer with or without β -mercaptoethanol (Sigma) and loaded onto 18% T, 6% C tricine-SDS polyacrylamide minigels (Jiang *et al.*, 2016; Schägger, 2006). The gels were run at 60 V for 1 h and 80 V for 3 h using a Mini Protean Tetra apparatus (Bio-Rad, Hercules, CA, USA) and transferred at 4°C for 50 min at 100 V onto 0.2 μ m pore size polyvinylidene difluoride (PVDF) membranes (Bio-Rad) in Towbin buffer. The blot membrane was dried and kept at -20°C. After briefly being soaked in methanol and rinsed in ultrapure water, aspecific binding sites were blocked by incubating the

membrane in PBS with 0.01% Tween 20 (PBST) and 5% non-fat milk for 1 h at RT. Peptides were immunodetected using the respective polyclonal rabbit anti-BD1, 2 and 3 antibodies, diluted 1:1,000 in PBST with 5% milk, followed by incubation of the membrane with a goat anti-rabbit IgG horseradish peroxidase (HRP)-conjugated antibody (Agilent, Santa Clara, CA, USA). The blot was developed with the Amersham ECL Prime detection kit (GE Healthcare Life Sciences, Pittsburgh, PA, USA). Following gel electrophoresis, additional gels were fixed and stained with Coomassie dye as described in Schagger (2006). Pictures were taken with the ChemiDocMP Imaging System (Bio-Rad).

Mass spectrometry

Protocol

Bottom-up analysis was performed in triplicate to confirm oxidation of the eBDs and quantify the relative abundance of disulphide bridges in the oxidized vs reduced forms. For this, lyophilized oxidized eBD1-3 was dissolved in triethylammonium bicarbonate (TEABC) buffer (Sigma-Aldrich) at a concentration of 50 $\mu\text{g}/\text{mL}$. One part was reduced by adding dithiothreitol (DTT) (Sigma-Aldrich) to a final concentration of 1 mM and another part was left oxidized for 1 h at 60°C. Next, free cysteine (C)-molecules were alkylated by adding methyl methanethiosulfonate (MMTS) (Sigma-Aldrich) to a final concentration of 10 mM for 10 min at RT. Acetonitrile (Sigma-Aldrich) was added to a final concentration of 5% to facilitate mass spectrometry (MS) analysis of the samples. Finally, trypsin (trypsin:protein ratio of 1:20; Promega) and 10 mM final concentration CaCl_2 were added for overnight digestion at 37°C. Peptides were then identified through LC-ESI-MS. LC was performed using a nano Acquity UPLC system (Waters, Zellik, Belgium). First, samples were delivered to a trap column (180 $\mu\text{m} \times 20 \text{ mm}$ nano Acquity UPLC 2G-V/MTrap 5 μm Symmetry C18, Waters) at a flow rate of 8 $\mu\text{L}/\text{min}$ for 2 min in 99.5% buffer A (0.1% formic acid). Subsequently, peptides were transferred to an analytical column (100 $\mu\text{m} \times 100 \text{ mm}$ nano Acquity UPLC 1.7 μm Peptide BEH, Waters) and separated at a flow rate of 300 nL/min using a gradient of 60 min going from 1% to 40% buffer B (0.1% formic acid in acetonitrile). MS data acquisition parameters were set according to Helm *et al.* (2014), with minor adaptations.

Data Analysis

Progenesis QI for Proteomics (Progenesis QIP 2.0, Nonlinear Dynamics, Waters) was used to process the raw LC-MS data of the triplicate measurements. Rank 3 MS/MS spectra of the MS precursors were exported as separate *.mgf peaklists. An error tolerant search against NCBI

Equus FASTA file (downloaded Februari 2018) supplemented with internal standards and the CRaP database was performed using a Mascot 2.5 in-house server (Matrix Science), with methylthio and ammonia-loss (KNQR) as variable modifications. Mass error tolerance for the precursor ions was set at 10 ppm and for the fragment ions at 50 ppm. Enzyme specificity was set to trypsin, allowing for up to two missed cleavages. These results were loaded back into Progenesis and the eBD peptides were flagged and exported with their ion intensities. Relative abundance of disulphide bridge formation was assessed by summing all methylthio peptide intensities and dividing them by the total sum of methylthio peptides in the reduced samples, i.e. 100%.

Bacteria and minimal inhibitory concentration assays

Clinical isolates were used in a minimal inhibitory concentration (MIC) assay to investigate the sensitivity of predominant bacterial pathogens from the equine respiratory tract to eBDs. Test organisms included Gram-positive *Streptococcus equi* subspecies *zooepidemicus* (4001), *Streptococcus equi* subspecies *equi* (3830), *Staphylococcus aureus* (3939), *Rhodococcus equi* (3851) and Gram-negative *Actinobacillus equuli* subspecies *equuli* (4005) and *Bordetella bronchiseptica* (3033). All organisms were grown on Oxoid™ sheep blood agar plus plates (ThermoFisher Scientific) overnight in a humidified incubator (5% CO₂) at 37°C. Inoculum was prepared by swabbing bacterial colonies from the plates, suspending them into PBS (turbidity equivalent to a 0.5 McFarland standard) and diluting this suspension 1:100 in Mueller Hinton II (MH) broth (BD biosciences, San Jose, CA, USA) achieving a final concentration of approximately 10⁶ colony forming units (CFU)/mL. EBD were serially 2-fold diluted in MH broth with concentrations ranging from 200 µg/mL to 0.02 µg/mL and pipetted into 96-well microtiter plates (Greiner Bio, Kremsmünster, Austria). Inoculum was added to eBD dilutions 1:1 and incubated in a humidified incubator (5% CO₂) at 37°C for 24 h. MIC values were determined as the lowest concentration of eBD at which there was no visible bacterial growth.

Cells

RK13 cells

Rabbit kidney (RK13) cells were purchased from the American Type Culture Collection (ATCC, Manassas, VA, USA) and maintained in minimal essential medium (MEM) (ThermoFisher Scientific) with 10% foetal calf serum (FCS) (ThermoFisher Scientific) and antibiotics. RK13 cells were used for propagating EHV1 and EAV virus stocks and for the respective antiviral assays.

MDCK cells - Madin-Darby canine kidney (MDCK) epithelial cells (ATCC) were seeded in MEM containing foetal calf serum (FCS) 10% FCS, 1 mg/mL lactalbumin (Sigma-Aldrich) and antibiotics. Cells were further maintained with identical medium without FCS. MDCK cells were used for EIV antiviral assays.

EREC

Primary equine respiratory epithelial cells (EREC) were isolated and cultured as described previously (Quintana *et al.*, 2011; Van Cleemput *et al.*, 2017).

Equine monocytes, T lymphocytes and polymorfonuclear cells

Equine peripheral blood mononuclear cells (PBMC) and polymorfonuclear (PMN) cells were isolated as described previously (Kuhns *et al.*, 2015; Laval *et al.*, 2015). Briefly, blood was collected on heparin (15 U/ml) (Leo, Ballerup, Denmark) by jugular venipuncture of three different healthy horses. The collection of blood was approved by the ethical committee of Ghent University (EC2017/118). Blood was diluted 1:1 in PBS and density centrifuged on Ficoll-Paque (GE Healthcare Life Sciences). The interphase band, containing the PBMC was collected before aspirating the remaining plasma together with the Ficoll-Paque medium, leaving the PMN cell- and erythrocyte-rich pellet. The latter pellet was diluted in PBS and mixed with an equal volume of 3% dextran, diluted in PBS (500.000 M, Sigma-Aldrich). Erythrocytes were allowed to sediment for 20 min at RT, before transferring the PMN-rich supernatant to a new tube. Following centrifugation at 300 g, remaining erythrocytes were lysed in ultrapure water for 30 s, followed by the quick addition of 10X PBS to restore isotonicity. PMN were further diluted in PBS and centrifuged at 300 g. Supernatant fluid was aspirated and the remaining PMN were re-suspended in RPMI, counted using a Bürker counting chamber and used immediately. After additional washing and centrifugation steps, PBMC were re-suspended in RPMI (ThermoFisher Scientific), supplemented with 1% MEM non-essential amino-acids, 1% sodium pyruvate (ThermoFisher Scientific), 4 U/mL interleukin-2 (202-IL, R&Dsystems, Minneapolis, Canada) and antibiotics. Ten hours post seeding, CD172a⁺ monocytic cells had adhered to the plastic (purity >90%, as assessed by flow cytometry) and non-adherent cells consisted of two dominant leukocyte populations: T and B lymphocytes. Following removal of non-adherent cells, CD172a⁺ monocytic cells were cultivated overnight in RPMI containing 1% MEM non-essential amino-acids, 1% sodium pyruvate, 1% bovine serum albumin (Sigma-Aldrich) and antibiotics. In the non-adherent cell population, equine T lymphocytes were separated from B lymphocytes by negative selection magnetic-activated cell sorting (MACS).

In summary, 5×10^7 cells were incubated with a mouse anti-horse pan B lymphocyte antibody (clone CVS36, Bio-Rad) diluted in PBS with 10% NGS for 1 h at 4°C. Cells were washed in ice-cold elution buffer (PBS + 2 mM EDTA + 2% FCS) and re-suspended in elution buffer containing 100 μ L rat anti-mouse IgG microbeads for 1 h at 4°C. Next, cells were washed in elution buffer before transferring them onto an LS column (MACS Miltenyi Biotech, Cologne, Germany). The cell-fraction that went through the column was collected and contained over 95% CD3⁺-positive T lymphocytes, as assessed by flow cytometry. Finally, equine T lymphocytes were seeded in RPMI supplemented with 1% MEM non-essential amino-acids, 1% sodium pyruvate, 4 U/mL interleukin-2 and antibiotics. The next day, CD172a⁺ monocytic cells were detached from the plastic by incubation with Accumax[®] (Sigma-Aldrich) for 30 min at 37°C, 5% CO₂. CD172a⁺ monocytic cells and T lymphocytes were washed in RPMI, centrifuged at 300 g, re-suspended in RPMI and counted using a Bürker counting chamber before further use.

Viruses, antiviral assays and virus binding assays

Viruses

Equine herpesvirus type 1 (EHV1), equine arteritis virus (EAV) and equine influenza virus (EIV) comprise the three most abundant viruses causing respiratory symptoms in the horse. A Belgian EHV1 isolate (03P37) was used in this study and originates from the blood taken of a paralytic horse during an outbreak in 2003 (van der Meulen *et al.*, 2003a). In addition, the virulent RacL11 EHV1 strain, isolated from an aborted foal, was used (Mayr *et al.*, 1968). Construction of the EHV1 RacL11 lacking gM or gp2 (RacL11 Δ gM and RacL11 Δ gp2, respectively) has already been reported (Osterrieder *et al.*, 1996; Rudolph *et al.*, 2002). To ensure that RacL11 Δ gM did not express gM, infected RK13 cells were immunofluorescently stained with the mouse monoclonal anti-EHV1 glycoprotein M antibody (12B2), kindly provided by prof. Balasuriya. All EHV1 strains were propagated in RK13 cells and used at the 7th passage. The Belgian EAV 08P178 strain was isolated from a neonatal foal suffering from respiratory distress (Vairo *et al.*, 2012). The virus was grown on RK13 cells and used at the 7th passage. The final passages of EHV1 and EAV on RK13 cells were propagated in FCS-deprived medium to obtain a serum-free virus stock. Stock solutions were titrated onto RK13 cells. The influenza A A/equine/Kentucky/98 influenza strain (H3N8) was propagated on eggs and titrated onto MDCK cells.

Purification and Dio-labelling of EHV1 for binding assays

Virus purification and subsequent Dio-labelling were performed as described previously (Laval *et al.*, 2016; Van Cleemput *et al.*, 2017).

Antiviral assay on RK13 and MCDK cells

Cells were grown to confluency in 24-well plates before thoroughly washing them with MEM to remove excess FCS. Serum contains several lectin-binding proteins, which are known to inactivate BDs (Maisetta *et al.*, 2008; Quinones-Mateu *et al.*, 2003). In a synchronized assay, the impact of eBD1-3 on different steps in the viral replication was evaluated. More specifically, in a first set of wells (i) direct virus inactivation was investigated by pre-incubating the 100X inoculum diluted in 10 mM phosphate buffer (PB) with eBD1-3 at concentrations ranging from 0 to 100 $\mu\text{g}/\text{mL}$ for 1 h at 37°C. Heparin treatment (100 U/mL; Leo) was included as a positive control for EHV1 binding inhibition. Inoculum was then diluted 1:100 in MEM in order to dilute remnant eBD in the inoculum. Cells were inoculated with pretreated inoculum at a final multiplicity of infection (MOI) of 0.001 for 2 h at 4°C. In a second set of wells, (ii) cells were pretreated with eBD1-3 (0-100 $\mu\text{g}/\text{mL}$) diluted in MEM for 1 h at 37°C, prior to inoculation, to examine whether eBDs protect cells from subsequent viral infection. Before inoculation (MOI 0.001, 2 h, 4°C), excess eBD1-3 was washed away with MEM. Virus binding occurs at 4°C and can be experimentally differentiated from viral entry, which depends on cellular mechanisms and therefore solely occurs after a temperature shift to 37°C. Following virus binding at 4°C, non-adherent virus particles were removed by washing all cells 3X on ice. In a third set of wells, (iii) eBD1-3 (0-100 $\mu\text{g}/\text{mL}$) diluted in MEM were added to the cells during virus entry at 37°C (1 h). Following the viral entry step at 37°C (1 h), all cells were briefly exposed to 40 mM citrate buffer (pH 3) to destroy any non-penetrated virus particles. Finally, all cells were covered with a solution containing 50% 2X MEM (ThermoFisher Scientific) and 50% 1.88% carboxymethylcellulose (Sigma-Aldrich). In a final set of wells, the latter solution was supplemented with eBD1-3 at concentrations ranging from 0 to 100 $\mu\text{g}/\text{mL}$ to evaluate their effect during (iv) post-entry. Ganciclovir (10 $\mu\text{g}/\text{mL}$; Cymevene[®], Roche), a herpetic kinase-activated nucleoside analogue terminating assembly of the viral DNA chain, was included as a positive control for the inhibition of EHV1 replication. Incubation of influenza virus-inoculated cells with N-acetylcysteine (NAC) has already been shown to inhibit viral replication and was therefore included as a positive control during EIV infection post-entry (Geiler *et al.*, 2010). EHV1 and EAV plaques were visualized 48 h after inoculation by fixing and staining the RK13 cell monolayers with a mixture of 0.5% crystal-violet (Sigma-Aldrich), 3% formaldehyde and

20% ethanol. The addition of trypsin to MDCK cell medium was omitted in this virus plaque assay to avoid destruction of the eBDs. Therefore, EIV was unable to induce viral plaques but merely infected single cells. MDCK cell monolayers were washed in PBS, air-dried at 37°C for 1 h and frozen at -20°C for a minimum of 2 h. After thawing, cell monolayers were fixed in 4% PFA at 4°C for 15 min. Aspecific binding sites were blocked by incubating the cells with a mixture of Tris-buffered saline (TBS), supplemented with 0.1% saponin and 5% NGS for 20 min at 37°C. EIV-positive cells were stained with the mouse monoclonal HB-65 antibody, diluted in TBS with 0.1% saponin and 2% NGS. After washing, a HRP-conjugated goat anti-mouse secondary antibody (Agilent, Santa Clara, CA, USA) was added in TBS with 0.1% saponin. For detection, a 5% aminoethyl carbazole (AEC) solution, supplemented with 0.025% H₂O₂ was added to the wells for 10 min at 37°C. The enzymatic reaction was stopped by washing the cells in PBS. With the use of an inverted light microscope, the total number of EHV1 and EAV plaques per well was counted, together with the total number of EIV-positive MDCK cells per well. Pictures were taken with the CTL ImmunoSpot F-419 (Cellular Technology Limited, Cleveland, OH, USA) and the latitude of EHV1 plaques was measured using ImageJ software (ImageJ, U.S. National Institutes of Health, Bethesda, MD, USA). Viability of the cells was assessed by ethidium monoazide bromide (EMA) staining, ensuring that the treatment with eBDs did not cause a significant cell loss.

Antiviral assay on EREC

Cells were grown to full differentiation in a transwell cell culture system prior to inoculation with EHV1 or EIV. EAV does not readily infect EREC and was therefore excluded from this experiment. Inocula were pretreated with 0 or 100 $\mu\text{g}/\text{mL}$ eBD1-3 in 10 mM PB for 1 h at 37°C and diluted 1:10 to obtain a final MOI of 0.2 (EHV1) or 2 (EIV) prior to inoculation (2 h, 4°C) of the cells at either the apical surfaces (EIV) or the inverted basolateral surfaces (EHV1). We previously showed that EHV1 preferentially infects EREC at their basolateral surfaces, compared to their apical surfaces (Van Cleemput *et al.*, 2017). On the contrary, more cells became infected with EIV following apical inoculation, compared to basolateral inoculation. In another set of wells, EREC were pretreated with 0 or 100 $\mu\text{g}/\text{mL}$ eBD1-3 in DMEM/F12 for 1 h at 37°C at either apical or basolateral surfaces, prior to inoculation (2 h, 4°C) with EIV (MOI 2) or EHV1 (MOI 0.2), respectively. Non-adsorbed virus particles were washed away on ice. In a third set of wells, EREC were treated with 0 or 100 $\mu\text{g}/\text{mL}$ eBD1-3 in DMEM/F12 during the virus entry step at 37°C (1 h). Next, cellular apical or basolateral surfaces were exposed to 40 mM citrate buffer (pH 3) to neutralize remnant non-penetrated virus particles (EIV or EHV1,

respectively). Fresh medium was added to the bottom wells and cells were further incubated at the air-liquid interface. In a last set of wells, 0 or 100 $\mu\text{g}/\text{mL}$ of eBD1-3 was supplemented in the medium to examine its antiviral effect during the viral post-entry step. Eighteen hours post-inoculation, cells were fixed in methanol for 20 min at -20°C and immunofluorescently stained for EIV or EHV1 proteins. Using confocal microscopy, the total number of EHV1 plaques was counted on 5 random fields of approximately 3×10^4 cells per insert. Plaque latitude was measured on 10 individual plaques using the Leica confocal software package. The total number of EIV-positive cells was counted on 5 random fields of approximately 1.5×10^4 cells per insert. Viability of the cells was assessed by EMA staining, ensuring that the treatment with eBD1-3 did not cause a significant cell loss.

EHV1 binding assay

To characterize the attachment of EHV1 to RK13 cells and EREC upon treatment with different eBDs, direct virus binding studies were carried out with Dio-labelled EHV1 particles. Following virus (100X inoculum) or basolateral EREC pretreatment with 0 or 100 $\mu\text{g}/\text{mL}$ eBD1-3 diluted in PB, cells were chilled on ice for 5 min and washed 3 times with cold PBS. Pretreated Dio-labelled virus particles were diluted 1:100 before inoculating RK13 cells at a MOI of 0.01 for 2 h at 4°C . Pretreated EREC were inoculated at the inverted basolateral surfaces with Dio-labelled EHV1 particles at a MOI of 0.2 for 2 h at 4°C . Non-adsorbed virus was removed by washing the cells 3 times with cold PBS. Cells were then fixed for 10 min in 1% PFA. Nuclei were counterstained with Hoechst 33342 (10 $\mu\text{g}/\text{ml}$; ThermoFisher Scientific) for 10 min at room temperature and slides were mounted with glycerol-DABCO. The percentage of cells with bound EHV1 particles was calculated based on the number of cells with viral particles bound on the plasma membrane of 300 randomly selected cells. The number of virus particles attached per cell was calculated based on the number of particles attached at the plasma membrane of 10 random EHV1-positive cells. For each cell, the entire plasma membrane was screened for the presence of virus particles by the use of confocal microscopy.

Chemotaxis assay

Chemotactic activity of eBD1-3 was determined using a 96-well Boyden chamber containing 5 μm pore size membranes (CytoSelect™, Cell Biolabs, San Diego, Ca, USA), following the manufacturer's instructions. Briefly, various concentrations of eBD1-3 (150 μL) were applied into the wells of the feeder tray before inserting the membrane tray. Equine polymorfonuclear cells, $\text{CD}172\text{a}^+$ monocytes and $\text{CD}3^+$ T lymphocytes were re-suspended in RPMI at a

concentration of 2×10^6 cells/mL and 100 μ L of each solution was added to the wells of the membrane tray. The chemotaxis chamber was transferred to a CO₂-humidified incubator for 5 h, before dislodging the cells from the underside of the membrane in the harvesting tray. In a clean 96-well plate, 75 μ L from the feeder tray and 75 μ L from the harvesting tray were mixed with 50 μ L of lysis buffer, containing CyQuant[®] GR dye. Finally, 150 μ L of the latter mixture was transferred to a 96-well plate, suitable for fluorescent measurement (Greiner). Cell migration values were reported as relative fluorescence units (RFU) measured at 480/520nm, using a Flouroskan Ascent FL (ThermoFisher Scientific) plate reader. Finally, background RFU from RPMI supplemented with eBD1-3, 10 mM PB (negative control) or 10% FCS (positive control) were subtracted from the respective cell migration values.

Induction of β -defensin expression in EREC in response to EHV1 and EIV infection

Primary equine respiratory epithelial cells (EREC) were grown on transwells and allowed to grow stable intercellular junctions, as assessed by transepithelial electrical resistance measurement. Mock or virus suspensions were applied at MOI 2 (EIV) or 0.2 (EHV1) to cellular apical or inverted basolateral surfaces, respectively for 1 h at 37°C. Unbound virus particles were then removed by washing the cell surfaces 3 times with PBS. Inserts were placed back into the platewells, fresh medium was added to the basolateral sides and cells were further incubated for 18 h. Cells were fixed in 1% PFA for 10 min, washed in PBS and simultaneously immunofluorescently stained for EIV or EHV1 proteins and eBD1-3.

The mean percentage of eBD fluorescent signal was calculated on 5 complete Z-stack confocal images using ImageJ. Finally, mean percentage of fluorescent signal (i.e eBD) from the mock-inoculated cells was compared to that of EHV1- or EIV-inoculated cells, the latter two groups containing infected as well as non-infected areas. More specifically, the threshold value to distinguish the FITC[®]-positive signal from the background signal was determined and the percentage of FITC[®]-positive signal (i.e. eBD) was calculated.

Statistical analyses

Significant differences ($P < 0.05$) between different treatments with or without eBDs and between mock-, EHV1- and EIV-inoculated cells were identified by analysis of variances (ANOVA) followed by a two-sided Dunnett's post-hoc test. If homoscedasticity of the variables was not met as assessed by the Levene's test, the data were log-transformed prior to ANOVA. Normality of the residuals was verified by using the Shapiro-Wilk test. If the variables remained

heteroscedastic or normality was not met after log-transformation, a Kruskal-Wallis' test, followed by a Mann-Whitney's post-hoc test were performed. All analyses were conducted in IBM SPSS Statistics for Windows, version 25.0 (IBM Corp, Armonck, USA).

Results

Distribution of eBDs across the equine respiratory tract

Respiratory tissue samples (nasal septum, trachea and lungs) were obtained from five different healthy horses in the slaughterhouse and immediately snap-frozen in liquid nitrogen. First, transcription of eBD-coding genes was verified by means of RT-PCR on total extracted RNA of different tissue samples. Second, the exact location of the three major eBDs was mapped to specific regions in the horse's respiratory tract by immunofluorescent staining of cryosections. As shown in Figure 1A, RNA specific for eBD1, 2, 3 and GAPDH (positive control) was expressed throughout all three respiratory tract locations (i.e. the nasal septum, the trachea and the lungs) of all five horses. RT-PCR products were Sanger-sequenced and identities were confirmed through comparison with the respective sequences, published in the NCBI-database. However, mRNA expression does not necessarily correlate with protein expression. By means of immunofluorescent staining, eBD1, 2 and 3 protein expression was detected in the nasal septum and in the trachea of all five horses, but not in the lungs (Figure 1B). More specifically, eBD1 was located within the cytoplasm of the nasal septum's secretory gland cells, but was rarely found in the epithelial cells lining the luminal surface. In tracheal tissues on the other hand, eBD1 was clearly visible in the cytoplasm of surface epithelial cells, especially at their apical side, as well as in that of the glandular cells. EBD2 was mainly expressed in the basal layers of both the surface epithelium and glands of the nasal septum and trachea. In addition, eBD2 appeared as a 'secreted smear' on top of the surface epithelia. EBD3 displayed a heterogeneous distribution pattern throughout the surface epithelium and an intense cytoplasmic immuno-positive staining was observed within the glandular cells. All antibodies were able to recognize synthetic eBD1, 2 and 3 following Western blot (Figure 2C).

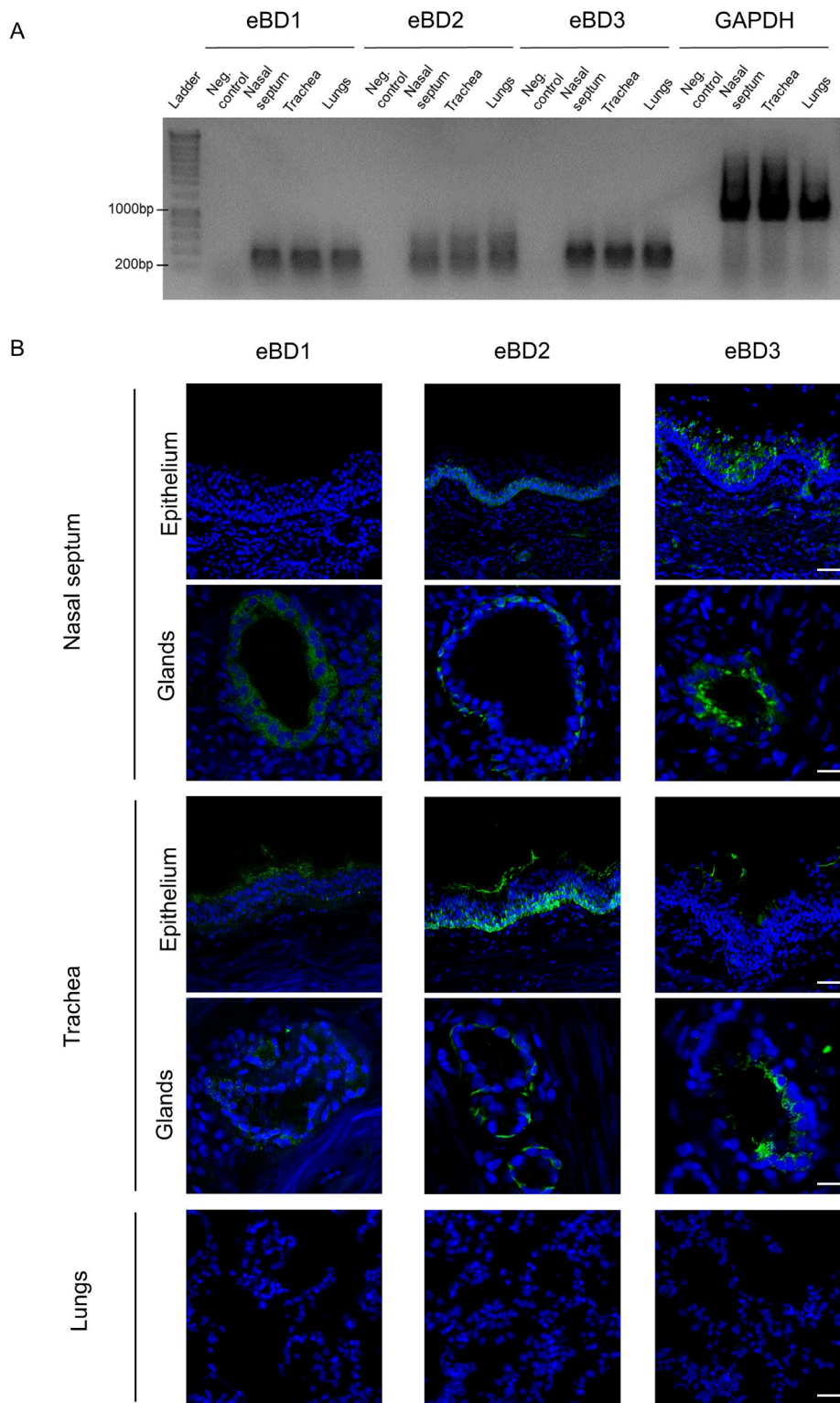


Figure 1. Distribution of eBD1-3 across the equine respiratory tract. (A) mRNA expression of eBD1-3 in the equine nasal septum, trachea and lungs. RT-PCR was performed on 1 μ g of total extracted RNA. PCR products were run on a 1% agarose gel and subsequently stained with ethidium bromide. GAPDH was the housekeeping gene used as an internal positive control. Reactions without RNA functioned as negative controls. (B) Representative confocal images of eBD1-3 protein expression (green) in the equine nasal septum, trachea and lungs. Cell nuclei were counterstained with Hoechst (blue). The scale bar represents 50 μ m.

Characterization of synthetic eBDs

Linear eBD1, 2 and 3 peptides, shown in Figure 2A, were commercially synthesized and oxidized in-house. Tricine SDS-PAGE and Coomassie blue staining of the reduced peptides revealed a step-wise pattern in eBD separation, where eBD1 showed the fastest migration, followed by eBD2 and eBD3 (Figure 2B). Inspection of both oxidized and reduced forms indicated that a major change had occurred during peptide oxidation. Oxidized forms migrated slower compared to reduced forms and this was especially true for eBD3. In addition, all eBDs oligomerized *in vitro* during oxidation. The eBD1 mixture contained an equal amount of monomer and dimer forms, while the eBD2 mixture was predominantly characterized by monomers. Similar to eBD1, eBD3 formed an equal amount of monomers and dimers. The reduced peptides were immunodetected by the use of the above-described antibodies against human BDs following Western blot, as shown in Figure 2C.

The fact that oxidation induced a major change in peptide conformation, is also visible in the LC-MS analysis. A schematic overview of the workflow used to investigate the efficiency of oxidation is given in Figure 2D. The *in vitro* oxidized peptides were either reduced by DTT or not, followed by MMTS treatment. Using this approach, the relative amount of cysteines that were complexed in a disulphide bridge, i.e. did not get modified by MMTS in the non-reduced form, could be estimated. Figure 2E shows the relative abundance of methylthio-carrying peptides, i.e. the relative decrease in open cysteines when the eBDs were oxidized. In line with the clear changes seen on gel electrophoresis, all eBDs thus showed a clear increase in oxidized cysteines. Especially in the oxidized eBD2 mixture, no cysteines were modified by MMTS, i.e. were unbound following oxidation. In addition, two precursor masses could be found in the oxidized eBD2 mixture with a charge state above 4+ that disappeared following reduction: 4327.039 (866.416 as 5+ and 1082.767 as 4+) and 4256.000 (852.207 as 5+) (Figure 2F). The first is the calculated mass of the amino-acid sequence (4336.12) minus 6 Da, i.e. three disulphide bridges formed. The latter is this sequence without the initial alanine (71.037 Da). This residual undigested precursor can be expected based on the fact that the folded form is less accessible to trypsin, resulting in a top down MS signal. Together, the MS data suggest that eBD2 is oxidized most efficiently and that eBD1 and eBD3 occur in more alternative forms, possibly comprising oligomers. In part, this could be due to the lyophilisation done after the peptides were oxidized and prior to MS analysis.

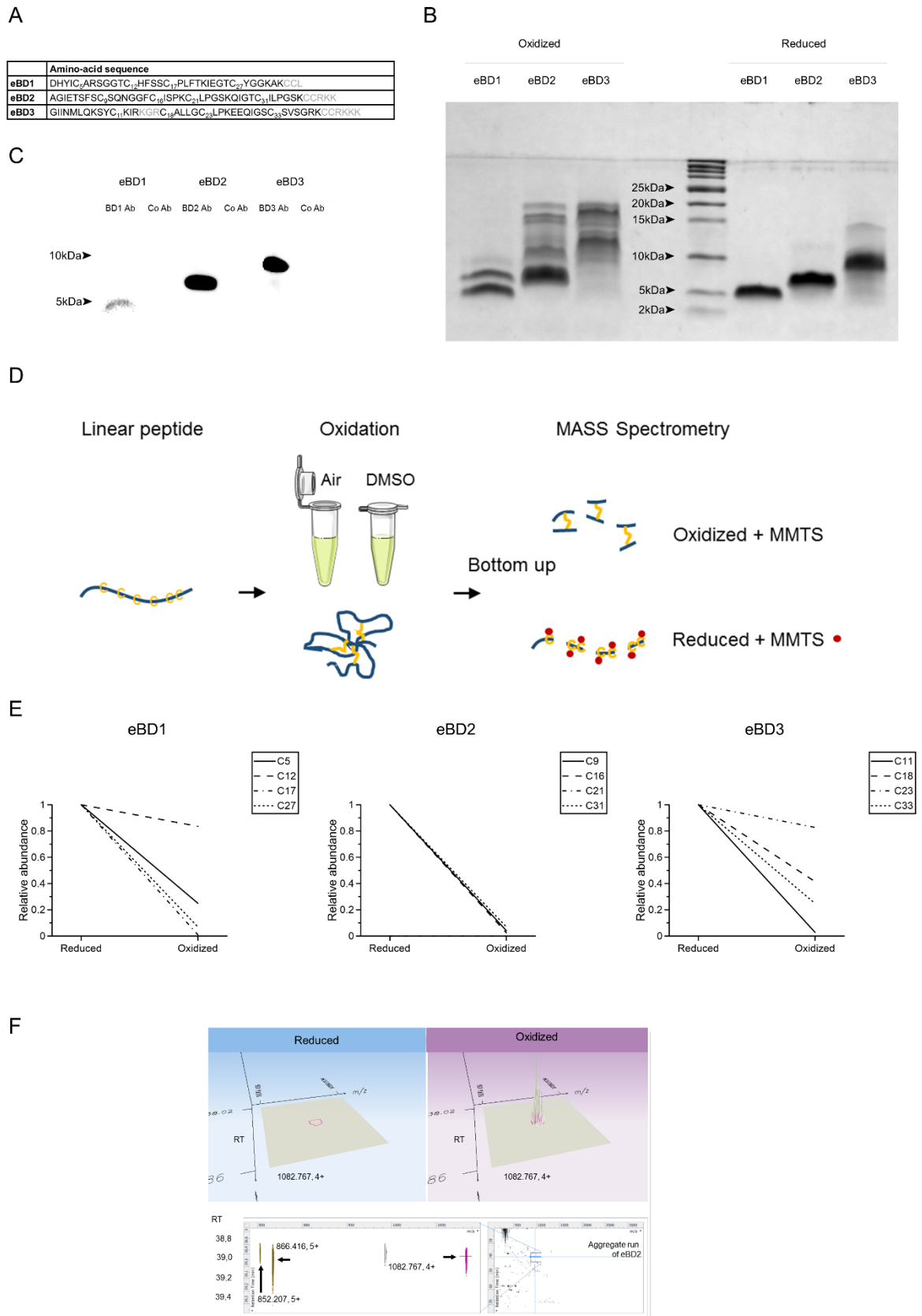


Figure 2. Characterisation of synthetic eBD1-3. (A) The amino-acid sequence of eBD1-3. Amino-acids indicated in grey were not covered in the MS bottom-up analysis described in D-F. (B) Tricine-SDS polyacrylamide (18%) gel electrophoresis of oxidized and reduced synthetic eBD1-3. Ten μ g of eBD1-3, diluted in tricine sample buffer with and without β -mercaptoethanol

was boiled for 5 min and loaded into the indicated lanes. The locations and sizes (kDa) of molecular weight markers are shown. (C) Western blot analysis of reduced eBD1-3. Synthetic peptides were run on tricine-SDS polyacrylamide gels (18%) and transferred onto PVDF membranes. EBD1-3 were immunodetected using the respective rabbit-anti human BD1-3 antibodies (BD1-3 Ab). A rabbit anti-*Streptococcus suis* functioned as isotype control antibody (Co Ab). The sizes (kDa) of molecular weight markers are shown. (D) Workflow used to investigate the efficiency of oxidation. Commercially synthesized eBD1-3 (shown in blue) were folded through air-oxidation (eBD2 and 3) or DMSO-oxidation (eBD1). Disulphide bonds between cysteine (C)-molecules are shown in yellow. Next, bottom-up analysis was performed in triplicate to confirm oxidation of the eBDs and quantify the relative abundance of disulphide bridges in the oxidized vs reduced forms. Free C-molecules (yellow) in the reduced and oxidized eBD1-3 mixtures were alkylated by adding methyl methanethiosulfonate (MMTS; red dots) prior to overnight digestion in trypsin. Peptides were then identified through LC-ESI-MS. (E) Relative abundance of disulphide bridge formation in the reduced and oxidized eBD1-3 mixture. Peptides were grouped by the methylthio-cysteine that they contain and the average abundance of the triplicate measurements of each of those forms was summed. By dividing these abundances by the summed abundance of the methylthio-cysteines in the DTT sample, the relative change in methylthio-cysteine can be estimated per location. It is clear that all eBDs were considerably oxidized, i.e. have reduced amounts of methylthio-cysteine compared to the DTT samples. In the case of eBD2, almost no methylthio-cysteine could be detected, implying full oxidation. (F) Detection of the undigested oxidized form of eBD2. Small region of interest of the aggregate run from the eBD2 analysis is shown in 3D, comprising m/z, retention time (RT) and intensity as dimensions. The signal of the 1082.767 (4+) is delineated in pink at RT 39.0 minutes (upper panel) in both reduced and oxidized form. In the lower panel, 2D representations (RT vs m/z) of extended regions of the LC-MS are shown. Left panel: the 4+ is highlighted in pink co-eluting with its 5+ form (866.416) and the 5+ minus alanine (852.207) form highlighted in brown. Right panel: complete overview of the aggregate LC-MS run (i.e. joint representation of the six runs on eBD2) with the region of interest depicted by the zoom box.

EBD2 and 3, but not eBD1 inhibit equine bacterial pathogens

Human defensins are able to destroy bacteria by permeabilizing the bacterial cell membrane (Lehrer *et al.*, 1989; White *et al.*, 1995). Whether bacterial pathogens are sensitive to eBD1-3 is currently unknown. Therefore, we performed a MIC test to determine bacterial growth inhibition by eBDs on a number of Gram-positive and Gram-negative bacteria, found in the equine respiratory tract. The examined concentration range of eBDs (0.1ng-100 μ g/mL) corresponds to clinically relevant concentrations found in mucus swabs, breast milk and bronchoalveolar lavages from humans (Ghosh *et al.*, 2007; Jia *et al.*, 2001).

The minimal concentrations of eBD1-3 inhibiting bacterial growth ranged from 25 to 100 μ g/mL and are represented in Table 2. While eBD1 (100 μ g/mL) shows no antibacterial activity and eBD2 solely inhibited growth of the Gram-negative bacteria (*Actinobacillus equuli* at 25 μ g/mL and *Bordetella bronchiseptica* at 100 μ g/mL), eBD3 exhibited a broad-spectrum activity against both Gram-negative and Gram-positive bacteria. In particular *Rhodococcus equi* and *Actinobacillus equuli* subsp. *equuli* showed high sensitivity for eBD3 at a concentration of 25 μ g/mL. Growth of *Bordetella bronchiseptica* and *Streptococcus equi* subsp. *equi* was both

inhibited at 100 $\mu\text{g}/\text{mL}$, while that of *Streptococcus equi* subsp. *zooepidemicus* and of *Staphylococcus aureus* was not affected.

Bacterium	Gram	MIC values ($\mu\text{g}/\text{mL}$)		
		eBD1	eBD2	eBD3
<i>Streptococcus equi</i> subsp. <i>equi</i> (3830)	+	> 100	> 100	100
<i>Streptococcus equi</i> subsp. <i>zooepidemicus</i> (4001)	+	> 100	> 100	> 100
<i>Staphylococcus aureus</i> (3939)	+	> 100	> 100	> 100
<i>Rhodococcus equi</i> (3851)	+	> 100	> 100	25
<i>Actinobacillus equuli</i> subsp. <i>equuli</i> (4005)	-	> 100	25	25
<i>Bordetella bronchiseptica</i> (3033)	-	> 100	100	100

Table 2. Activity of eBD1-3 on the growth of 4 Gram-positive and 2 Gram-negative equine bacterial isolates, commonly associated with respiratory disease. Bacteria were co-cultured with 0-100 $\mu\text{g}/\text{mL}$ eBD1, 2 or 3 for 24 h and MIC values were determined as the lowest concentration of eBD at which there was no visible bacterial growth.

While eBDs act against EIV and EAV, they enhance EHV1 infectivity

The temporal effects of eBD1-3 on different steps in the infection of RK13 cells (by EAV and EHV1), MDCK cells (by EIV) or EREC (by EIV and EHV1) were studied. To analyse viral infectivity, the total number of EHV1 and EAV plaques per well, as well as the total number of single EIV-positive cells were counted. In addition, EHV1 and EAV plaque latitudes were measured using image analysis. Incubation of the cells (RK13, MDCK, EREC) with the highest concentration of eBD1-3 (i.e. 100 $\mu\text{g}/\text{mL}$) did not cause a significant loss in cell viability, as assessed by EMA staining (data not shown).

Antiviral assay on RK13 and MDCK cells – (i) As shown in Figure 3A, virus pretreatment with 50 or 100 $\mu\text{g}/\text{mL}$ eBD2 and 3, but not with eBD1, significantly ($P < 0.01$ and $P < 0.001$, respectively) decreased the formation of EIV and EAV plaques in MDCK and RK13 cells, respectively, compared to 0 $\mu\text{g}/\text{mL}$. Especially eBD3 was particularly active against EIV, almost completely preventing infection at a concentration of 100 $\mu\text{g}/\text{mL}$. Remarkably, the same eBD2 and 3 (50 or 100 $\mu\text{g}/\text{mL}$) caused an average 3.5-fold increase ($P < 0.001$) in EHV1 infection of RK13 cells, observed both in the number of plaques and in plaque latitude (Figure 3A and Figure 4A upper panel, respectively). As expected, heparin pretreatment of EHV1 hindered the virus from subsequently binding to RK13 cells and significantly ($P < 0.001$) inhibited EHV1 plaque formation, but did not alter final plaque latitude. Representative images of EHV1 plaques are shown in Figure 4A (lower panel). (ii) Pretreatment of the cells with

eBD1-3 failed to protect them from subsequent EIV, EAV or EHV1 infection. In contrast, pretreatment of RK13 cells with 50 or 100 $\mu\text{g}/\text{mL}$ eBD3 significantly ($P < 0.001$) increased their susceptibility to EHV1 (number of plaques) by 1.5-fold (Figure 3B). Cell pretreatment with eBDs did not alter subsequent EHV1 plaque spread (data not shown). (iii) Supplementation of the medium with 50 or 100 $\mu\text{g}/\text{mL}$ eBD3 during the virus entry step significantly ($P < 0.01$) decreased EIV infectivity, but had no effect on EAV or EHV1 infectivity (Figure 3C). In addition, EHV1 plaque latitude was not affected by treating the RK13 cells with eBDs during virus entry (data not shown). (iv) As shown in Figure 3D, all eBDs failed to alter the number of plaques post virus penetration. However, the presence of eBD2 and 3 allowed EHV1 to spread faster to neighbouring cells in a dose-dependent manner, doubling the average viral plaque latitude at 100 $\mu\text{g}/\text{mL}$ compared to control ($P < 0.001$) (Figure 4B, upper panel). As expected, addition of the herpetic kinase-activated nucleoside analogue, ganciclovir, to RK13 cells almost completely blocked the formation and spread of EHV1 plaques ($P < 0.001$). The presence of 20 mM N-acetylcysteine in MDCK cell medium acted on the course of EIV infection, significantly reducing the final number of EIV-positive cells by 2.5-fold ($P < 0.001$). Representative images of EHV1 plaques are shown in Figure 4B, lower panel. Over the course of the experiment, EAV plaque latitude was never affected (data not shown).

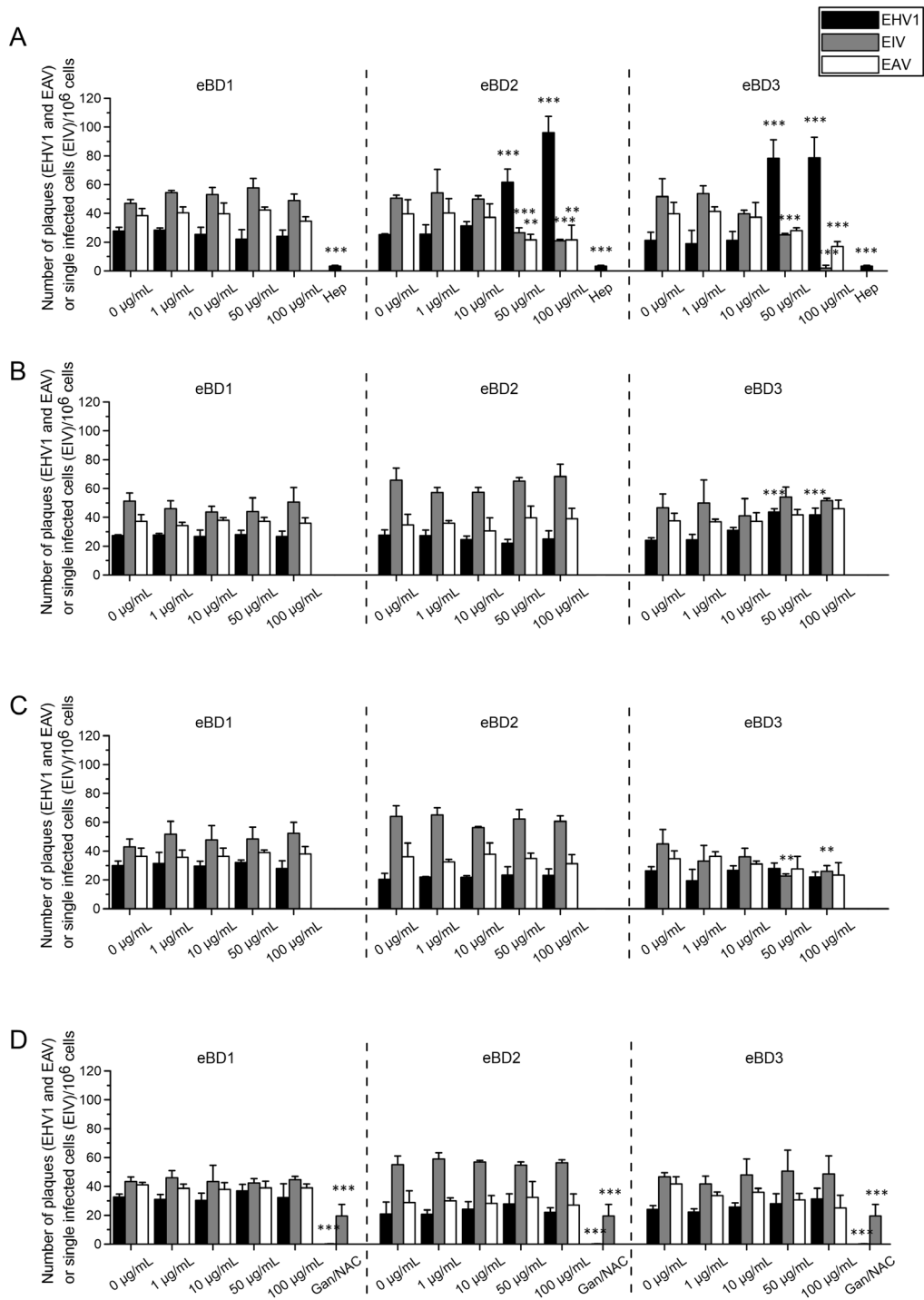


Figure 3. The impact of eBD1 (left graph panels), 2 (middle graph panels) and 3 (right graph panels) on different steps in the infection of continuous cell lines (RK13 cells for EHV1 and EAV or MDCK cells for EIV) with EHV1 (MOI 0.001; black bars), EIV (MOI 0.001; grey bars) and EAV (MOI 0.001; white bars). The total number of plaques (EHV1 and EVA) or individual infected cells (EIV) per well ($\pm 10^6$ cells) was counted and data are represented as means + SD. Experiments were performed in triplicate. Significant differences are indicated by asterisks: * $P \leq 0.05$; ** $P < 0.01$; *** $P < 0.001$. (A) Virus particles were pretreated with 0-100 $\mu\text{g/mL}$ eBD1-3 prior to inoculation for 2 h at 4°C . Heparin (Hep; 100 U/mL) was used as a positive internal control for blocking subsequent EHV1 binding. (B) Cells were pretreated with 0-100 $\mu\text{g/mL}$ eBD1-3 prior to virus inoculation for 2 h at 4°C . (C) EBD1-3 (0-100 $\mu\text{g/mL}$) were added during the virus entry step for 1 h at 37°C . (D) Following citrate treatment (pH 3), 0-100 $\mu\text{g/mL}$ eBD1-3 were added to the inoculated cells during the virus post-penetration step for 48 h. Ganciclovir (Gan; 10 $\mu\text{g/mL}$) or N-acetylcysteine (NAC; 20mM) were used as positive controls to block EHV1 or EIV replication, respectively.

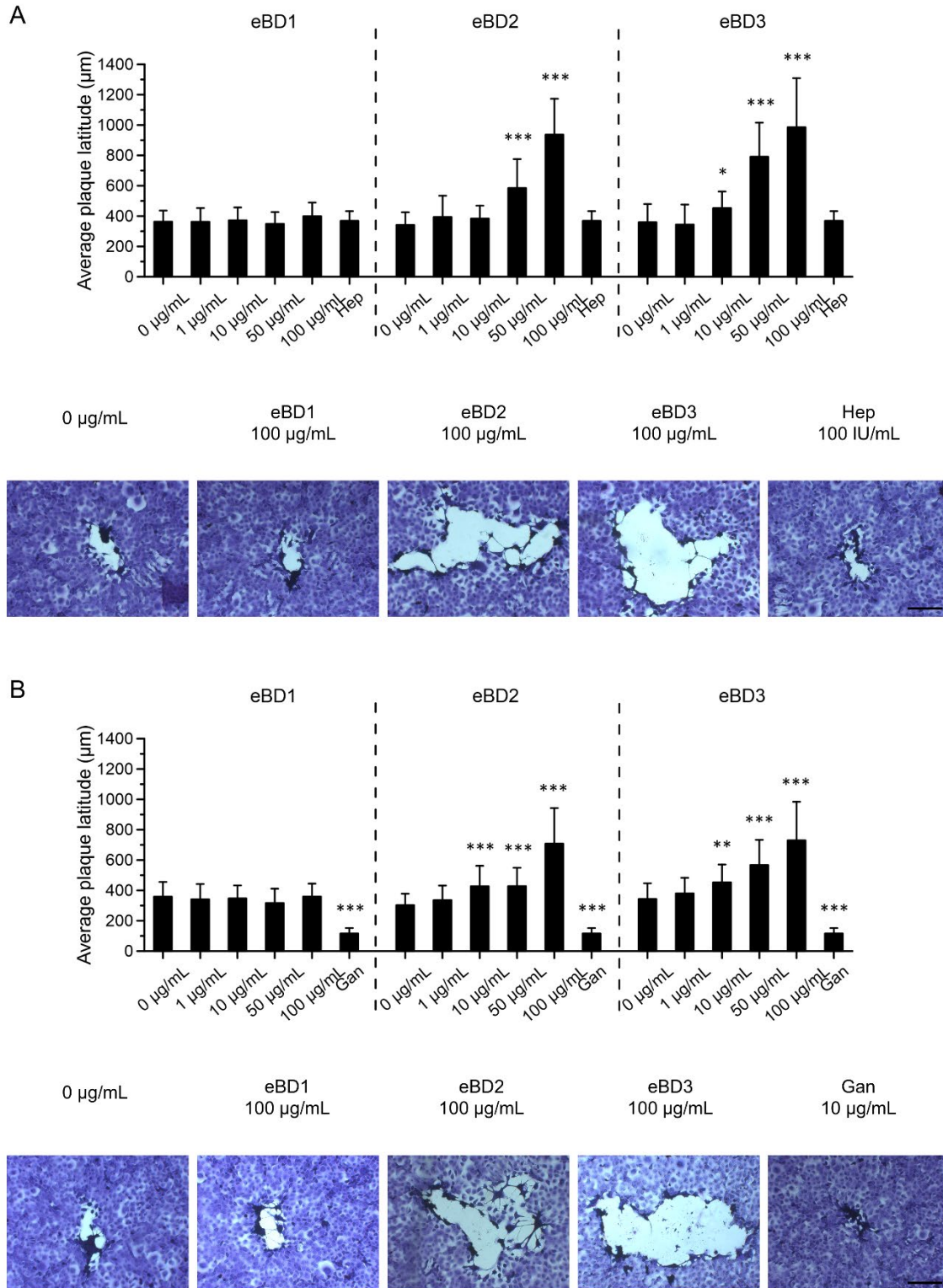


Figure 4. The effect of 0-100 $\mu\text{g/mL}$ eBD1 (left graph panels), eBD2 (middle graph panels) or eBD3 (right graph panels) on EHV1 spread in RK13 cells when added during (A) the virus pretreatment step or (B) the virus post-penetration step. The average plaque latitude was calculated based on 10 individual plaques. Experiments were performed in triplicate. Data are represented as means + SD (upper panels). Significant differences are indicated by asterisks: * $P \leq 0.05$; ** $P < 0.01$; *** $P < 0.001$. Heparin (Hep; 100 U/mL) was used as a positive internal control during virus pretreatment for blocking subsequent EHV1 binding. Representative images of EHV1 plaques in crystal-violet stained RK13 cell monolayers are shown in the lower panels. The scale bar represents 200 μm .

Antiviral assay on EREC - EREC were grown in transwells to full differentiation as assessed by measuring the transepithelial electrical resistance. Since EHV1 preferentially infects EREC at their basolateral surfaces and EIV more efficiently infects EREC at their apical surfaces, cells were inoculated via the respective preferential route with EHV1 or EIV (Van Cleemput *et al.*, 2017). EAV does not readily infect EREC and was therefore excluded from this experiment. (i) In accordance with what was observed in MDCK cells, eBD2 and 3 acted on EIV virions during virus pretreatment, significantly ($P < 0.05$ and $P < 0.001$, respectively) diminishing subsequent infection of EREC (Figure 5A). While eBD2- and 3-pretreated EHV1 virions more efficiently infected RK13 cells, they were not able to infect EREC more easily. (ii) Pretreatment of EREC with eBD1, 2 and 3 did not alter EIV infectivity, while they did render the cells more permissive for EHV1 infection, as demonstrated by the significant increase in number of plaques ($P < 0.01$ for eBD1 and $P < 0.001$ for eBD2 and 3). Results are shown in Figure 5B. (iii) As shown in Figure 5C, addition of the eBDs during virus entry enhanced subsequent EHV1 infection in EREC ($P < 0.001$ for eBD1, $P < 0.05$ for eBD2 and $P = 0.1$ for eBD3), while it did not affect EIV entry. (iv) None of the eBDs had an effect on viral infectivity after EHV1 or EIV entry was completed (Figure 5D). As expected, addition of the herpetic kinase-activated nucleoside analogue ganciclovir to EREC almost completely blocked the formation and spread of EHV1 plaques ($P < 0.001$). Remarkably, supplementation of the medium with NAC did not significantly inhibit EIV infection. Representative confocal images of EHV1- and EIV-infected EREC are shown in the right panels of Figure 5. EHV1 plaque latitude did not significantly change upon addition of eBDs in any of the examined viral infection steps (data not shown).

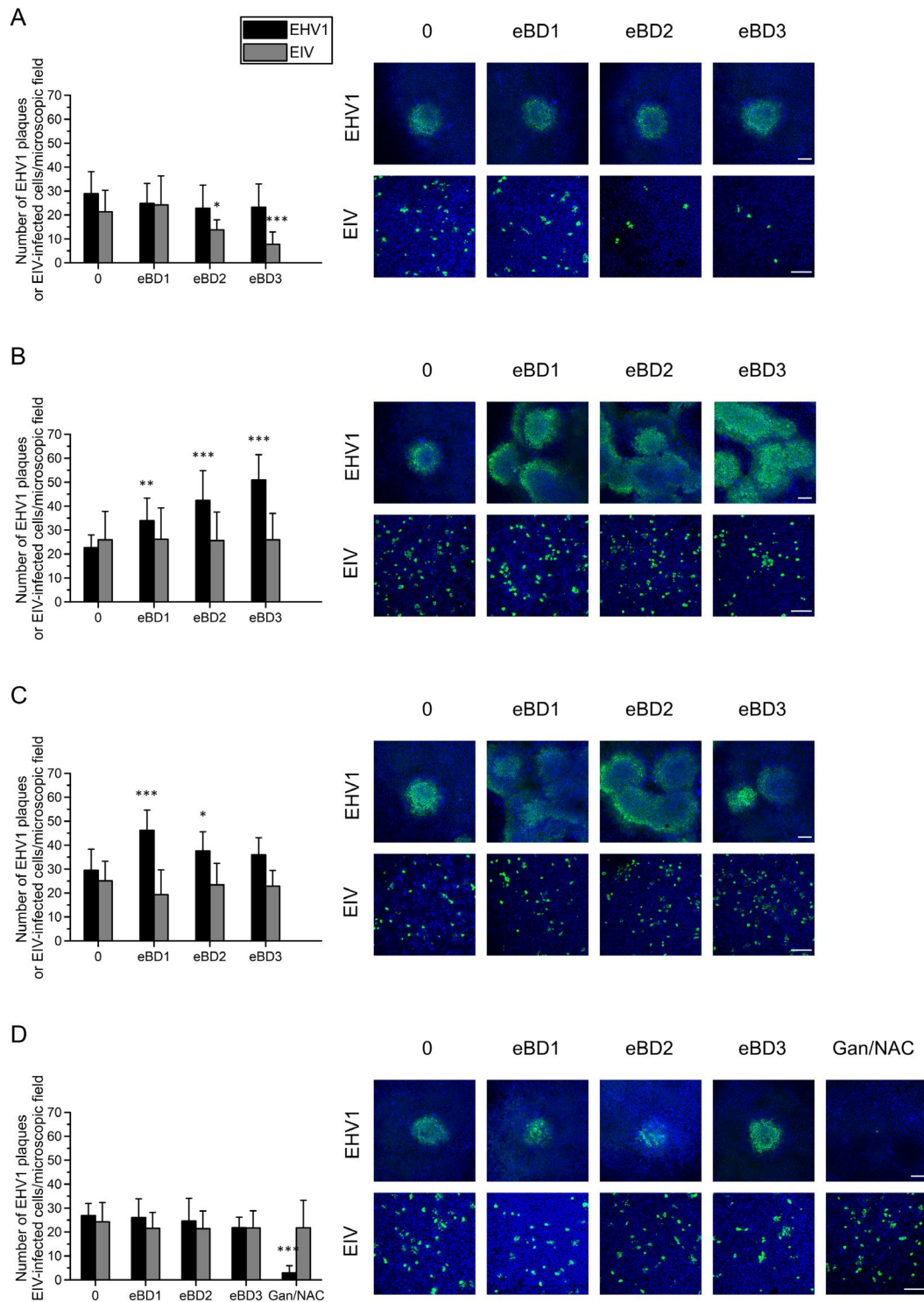


Figure 5. The impact of eBD1-3 on different steps in the infection of primary equine respiratory epithelial cells (EREC) with EHV1 (MOI 0.2; black bars) and EIV (MOI 2; grey bars). (A) Virus particles were pretreated with 0 or 100 $\mu\text{g}/\text{mL}$ eBD1-3 prior to inoculation for 2 h at 4°C. (B) Cells were pretreated with 0 or 100 $\mu\text{g}/\text{mL}$ eBD1-3 prior to virus inoculation for 2 h at 4°C. (C) EBD1-3 (0 or 100 $\mu\text{g}/\text{mL}$) were added during the virus entry step for 1 h at 37°C. (D) Following citrate treatment (pH 3), 0 or 100 $\mu\text{g}/\text{mL}$ eBD1-3 were added to the inoculated cells during the virus post-penetration step for 48 h. Ganciclovir (Gan; 10 $\mu\text{g}/\text{mL}$) or N-acetylcysteine (NAC 20 mU/mL) were used as a positive internal control to block EHV1 or EIV replication, respectively. The total number of plaques (EHV1) or individual infected cells (EIV) was counted on 5 microscopic fields ($\pm 3 \times 10^4$ cells for EHV1 and 1.5×10^4 cells for EIV) for each condition (left panels). Experiments were performed in triplicate on primary EREC of 3 different horses. Data are represented as means + SD and significant differences are indicated by asterisks: * $P \leq 0.05$; ** $P < 0.01$; *** $P < 0.001$. Representative confocal images of EHV1-positive plaques or EIV-positive individual cells (green) are shown in the right panels of each step. Cell nuclei were counterstained with Hoechst (blue). The scale bar represents 75 μm .

Envelope glycoprotein M renders EHV1 resistant to eBD2 - Glycoprotein M is a type III integral membrane protein, conserved throughout the herpesvirus family. As this glycoprotein spans the viral envelope multiple times, we hypothesized that it stabilizes and thereby protects the viral envelope from damage by the eBDs. Similarly as the 03P37 strain, infectivity of the parental RacL11 strain in RK13 cells was enhanced ($P < 0.05$) upon virus pretreatment with 100 $\mu\text{g}/\text{mL}$ eBD2, although to a lesser extent. In contrast, infectivity of the RacL11 strain deficient of glycoprotein M (RacL11 ΔgM) was significantly ($P < 0.05$) diminished upon incubation with 100 $\mu\text{g}/\text{mL}$ eBD2, compared to control (0 $\mu\text{g}/\text{mL}$) as shown in Figure 6A. The RacL11 strain deficient in glycoprotein 2 (RacL11 $\Delta\text{gp}2$) was included as an internal control and showed a similar significant ($P < 0.05$) increase in infectivity as the parental RacL11 strain upon virus pretreatment with eBD2. Representative images of the EHV1-infected RK13 cell monolayers, stained with crystal-violet, are shown in the upper and middle panel of Figure 6B. Immunofluorescent staining of RK13 cells infected with either the 03P37 strain, the RacL11 parental strain, the RacL11 $\Delta\text{gp}2$ strain or the RacL11 ΔgM strain confirmed that the latter does not express gM, while the former three strains do express gM (Figure 6B, lower panel).

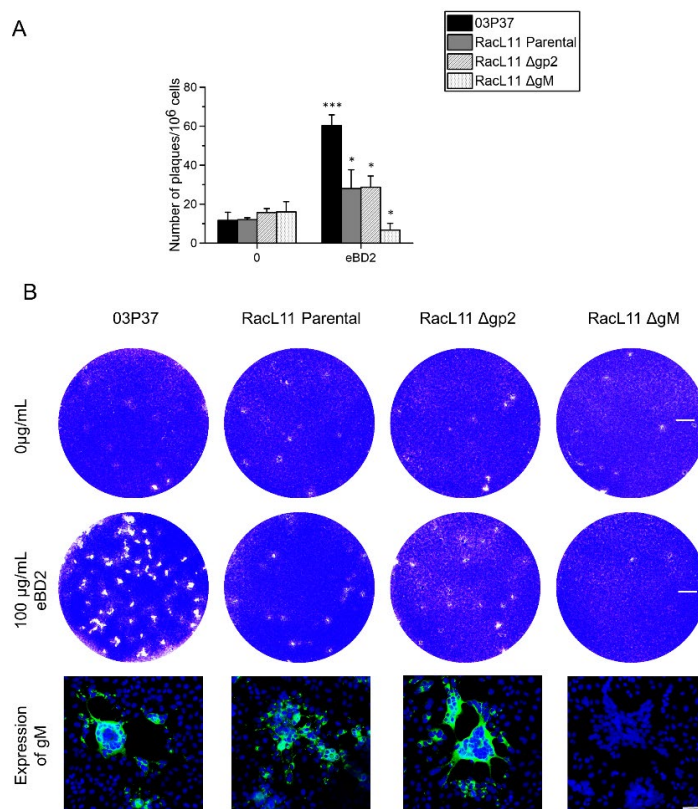


Figure 6. The role of glycoprotein M in EHV1 resistance against eBD2. (A) The EHV1 03P37 strain (black bars), parental RacL11 strain (grey bars), RacL11 strain lacking glycoprotein 2 (gp2) (striped bars) and RacL11 strain lacking glycoprotein M (gM) (dotted bars) were pretreated with 0 or 100 $\mu\text{g}/\text{mL}$ eBD2 prior to inoculation of RK13 cell monolayers. The total number of plaques per well ($\pm 10^6$ cells) was counted and experiments were performed in triplicate. Significant differences are indicated by asterisks: * $P \leq 0.05$; ** $P < 0.01$; *** $P < 0.001$. (B) Representative images of EHV1 plaques in crystal-violet stained RK13 cell monolayers (upper and middle panel). The scale bar represents 1 mm. Confocal images of EHV1 infected RK13 cells, stained with the mouse monoclonal anti-EHV1 gM antibody (12B2) (lower panel). The scale bar represents 50 μm .

EBDs enhance EHV1 infectivity by aggregating virions on the cell surface - To characterize the attachment of either eBD1-3-pretreated EHV1 particles to RK13 cells or untreated EHV1 particles to eBD1-3-pretreated EREC, a binding assay was carried out with purified and Dio-labelled EHV1 particles. As shown in the upper panel of Figure 7A, the percentage of RK13 cells with bound EHV1 particles was slightly, but not significantly higher after virus pretreatment with 100 $\mu\text{g}/\text{mL}$ eBD3 ($1,26 \pm 1,34$), compared to after eBD1 (100 $\mu\text{g}/\text{mL}$; $0,78 \pm 0,76\%$), eBD2 (100 $\mu\text{g}/\text{mL}$; $0,86 \pm 0,97\%$) or control (0 $\mu\text{g}/\text{mL}$; $0,92 \pm 0,92\%$) pretreatment. However, per positive cell up to 2-fold more virus particles were able to bind to the cell surfaces on average upon treatment with eBD2 and 3, compared to eBD1 or control treatment. As shown in representative confocal images, given in the lower panel of Figure 7A, EHV1 particles are concentrated to one specific area of the RK13 cell plasma membrane by eBD2 and 3. Conversely, EREC pretreatment with all eBDs (100 $\mu\text{g}/\text{mL}$) did significantly increase the percentage of EREC with bound EHV1 particles from $7 \pm 3\%$ to $17 \pm 6\%$, $17 \pm 5\%$ and $36 \pm 8\%$ upon treatment with eBD1, 2 and 3, respectively (Figure 7B upper panel). The number of EHV1 particles bound per EHV1 positive cell did not significantly differ between control-, eBD1- and eBD2-pretreated EREC. However, eBD3 pretreatment of EREC on average doubled the amount of bound EHV1 particles per positive cell. Representative confocal images are shown in the lower panel of Figure 7B.

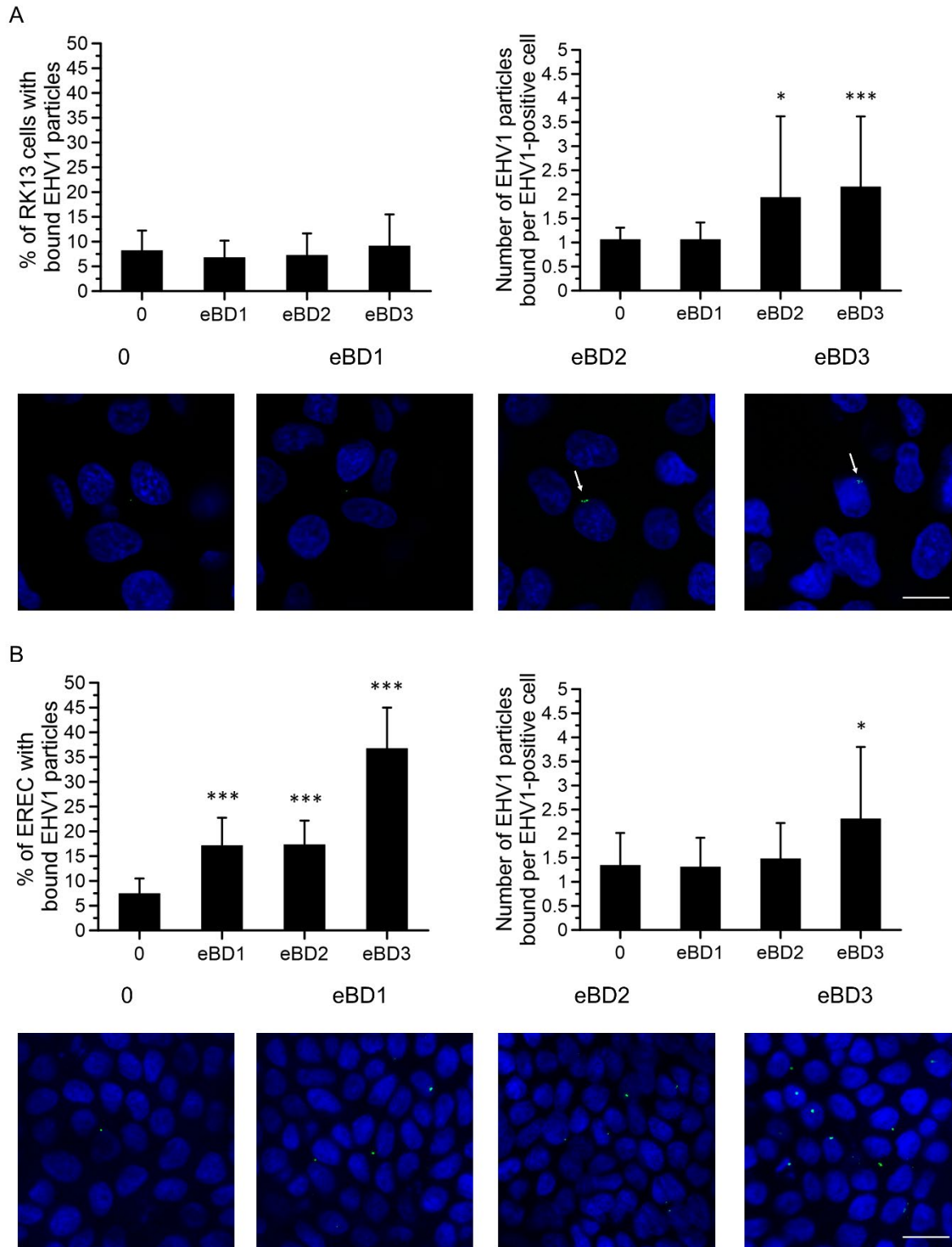


Figure 7. The role of eBD1-3 in the attachment of EHV1 to cells. (A) The binding of eBD1-3 (0 or 100 $\mu\text{g}/\text{mL}$)-pretreated and Dio-labelled EHV1 particles to RK13 cells. (B) The attachment of untreated and Dio-labelled EHV1 particles to eBD1-3 (0 or 100 $\mu\text{g}/\text{mL}$)-pretreated EREC. The percentage of cells with bound virus particles was calculated based on 5 random fields of 300 cells (upper left panels). The total number of particles per EHV1-positive cell was counted (upper right panels). Three independent experiments were performed with RK13 cells and EREC of three different horses were used. Data are represented as means + SD and significant differences are indicated by asterisks: * $P \leq 0.05$; ** $P < 0.01$; *** $P < 0.001$. The lower panels show representative confocal Z-stack images of (A) eBD1-3-pretreated and Dio-labelled EHV1 particles (green) attached to RK13 cells or (B) untreated and Dio-labelled EHV1 particles (green) bound to eBD1-3-pretreated EREC. Note the virus aggregates (arrows) bound to the RK13 cells upon virus pretreatment with eBD2 and 3. Cell nuclei were counterstained with Hoechst (blue). The scale bar represents 10 μm .

Viral infections induce eBD expression in EREC

Above, we demonstrated that eBDs are able to inhibit EIV, but enhance EHV1 infectivity. Here, we investigated whether these viruses elicit eBD expression at their target site of infection, EREC. This innate immune response would help the epithelium clear an EIV infection. Conversely, EHV1 would benefit from this response. Most studies in humans and mice examine the upregulation of cytokines or antimicrobial peptides by means of qRT-PCR. In horses, however, one of the main limiting factors to obtain a reliable outcome of qRT-PCR experiments, is the lack of good reference genes. Therefore, we chose to quantify the relative amount of eBD peptides in EIV-, EHV1- and mock-inoculated EREC by immunofluorescent staining of viral and eBD proteins, followed by confocal microscopy and image analysis with ImageJ. In EHV1- and EIV-inoculated cells, infected cells were distinguished from non-infected cells based on immunofluorescent staining of viral proteins. Representative images and results are shown in Figure 8A and B, respectively. EREC constitutively expressed a low amount of eBD1, which did not significantly differ among mock-inoculated cells ($0.92 \pm 0.41\%$), EHV1-inoculated cells ($1.05 \pm 0.84\%$) and EIV-inoculated cells ($1.12 \pm 0.89\%$). The mean percentage of eBD2-positive signal was significantly ($P < 0.001$) higher in EHV1-inoculated cells ($22.32 \pm 11.38\%$), compared to mock-inoculated cells ($7.49 \pm 2.67\%$). Especially infected cells within the EHV1-inoculated EREC monolayers showed a high percentage of eBD2-positive signal ($27.54 \pm 7.32\%$), while their non-infected neighbouring cells expressed only $17.68 \pm 12.67\%$ of eBD2. EIV-inoculated cells displayed a slight, but not significant increase in eBD2 expression ($8.92 \pm 6.21\%$). Among EIV-inoculated cells, infected cells did show statistically significant higher levels of eBD2-positive signal ($11.33 \pm 6.90\%$), when compared to neighbouring non-infected cells ($6.21 \pm 4.22\%$). Similarly to eBD2, eBD3 was significantly ($P < 0.001$) elevated in EHV1-inoculated cells ($13.94 \pm 8.00\%$), compared to mock-inoculated cells ($3.44 \pm 3.08\%$). Again, EHV1-infected cells expressed on average more eBD3 ($19.40 \pm 6.79\%$) than adjacent non-infected cells ($8.47 \pm 4.74\%$). EIV inoculation did not lead to a significant increase in eBD3 expression in EREC ($3.64 \pm 2.61\%$), compared to mock inoculation

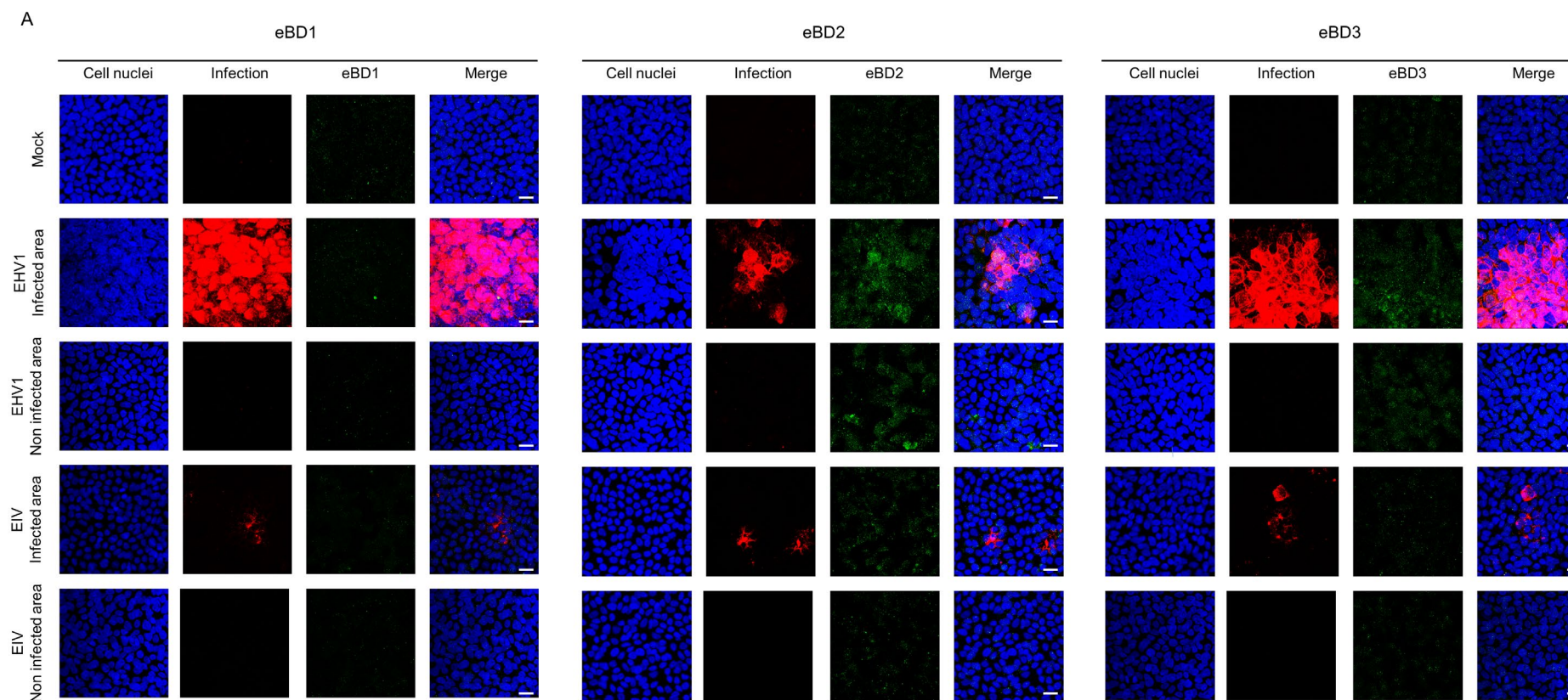


Figure 8. Viral infections elicit eBD2-3 protein expression in EREC. Cells were either mock-inoculated or inoculated with EHV1 (MOI 0.2) or EIV (MOI 2) for 18 h. (A) Representative confocal Z-stack images of eBD1-3 protein expression in mock-, EHV1- or EIV-inoculated EREC, the latter two groups containing infected as well as non-infected areas. EBD1-3 were visualized in green, while EHV1 late proteins and EIV nucleoprotein were simultaneously stained in red to distinguish infected from non-infected areas. Cell nuclei were counterstained with Hoechst (blue). The scale bar represents 10 μ m.

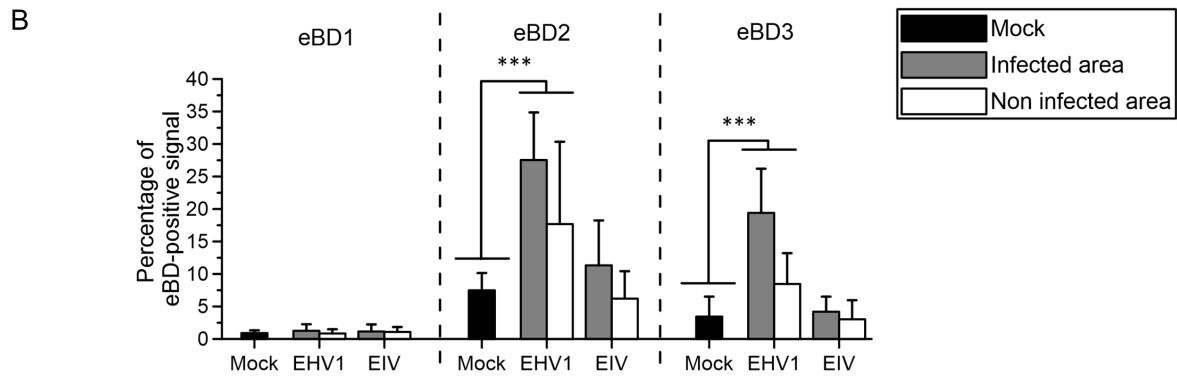


Figure 8. Viral infections elicit eBD2-3 protein expression in EREC. Cells were either mock-inoculated or inoculated with EHV1 (MOI 0.2) or EIV (MOI 2) for 18 h. (B) The mean percentage of eBD1 (left graph panel), eBD2 (middle graph panel) or eBD3 (right graph panel) fluorescent signal was calculated on 5 complete Z-stack confocal images using ImageJ. The mean fluorescent signal of the mock-inoculated cells (black bars) was compared to that of EHV1- or EIV-inoculated cells, the latter two groups containing infected (grey bars) as well as non-infected areas (white bars). Experiments were performed in triplicate on primary EREC of 3 different horses. Data are represented as means + SD and significant differences are indicated by asterisks: * $P \leq 0.05$; ** $P < 0.01$; *** $P < 0.001$.

EBDs are chemotactic for equine leukocytes

The upregulation of eBD production at sites of infection might be a key step in mounting the adaptive immune response by attracting resident and blood leukocytes. However, EHV1 might benefit from this chemotaxis, since the virus requires leukocytes for dissemination within the horse. In order to investigate chemotactic activity of eBD, CytoSelect™ cell migration assays were performed with equine polymorfonuclear (PMN) cells, CD172a⁺ mononuclear cells and CD3⁺ T lymphocytes, isolated from the blood taken from three different healthy donor horses. Results are shown in Figure 9 and reveal a dose-dependent migration of these blood leukocytes towards the different eBDs in a typical Gaussian manner. More specifically, eBD1 induced a dose-dependent migration of equine PMN cells and of equine T lymphocytes, with maximal migration at 1 ng/mL ($P < 0.01$) and 1 μ g/mL ($P = 0.08$), respectively. The chemotactic effect of eBD2 peaked between 1 ($P = 0.08$) and 10 ng/mL ($P < 0.05$) for equine PMN cells and at 1 μ g/mL ($P < 0.05$) for T lymphocytes. EBD3 induced migration of equine PMN cells, monocytic cells, T lymphocytes, reaching a maximum at a concentration of 1 ng/mL ($P < 0.01$), 1 μ g/mL ($P < 0.05$) and 1 μ g/mL ($P < 0.05$), respectively. While eBD1 and 2 failed to induce chemotaxis of equine monocytic cells, 1 μ g/mL of eBD3 was sufficient to induce monocytic cell migration. RPMI, supplemented with 10% FCS served as a positive control and efficiently ($P < 0.001$) induced chemotaxis of all cell types examined.

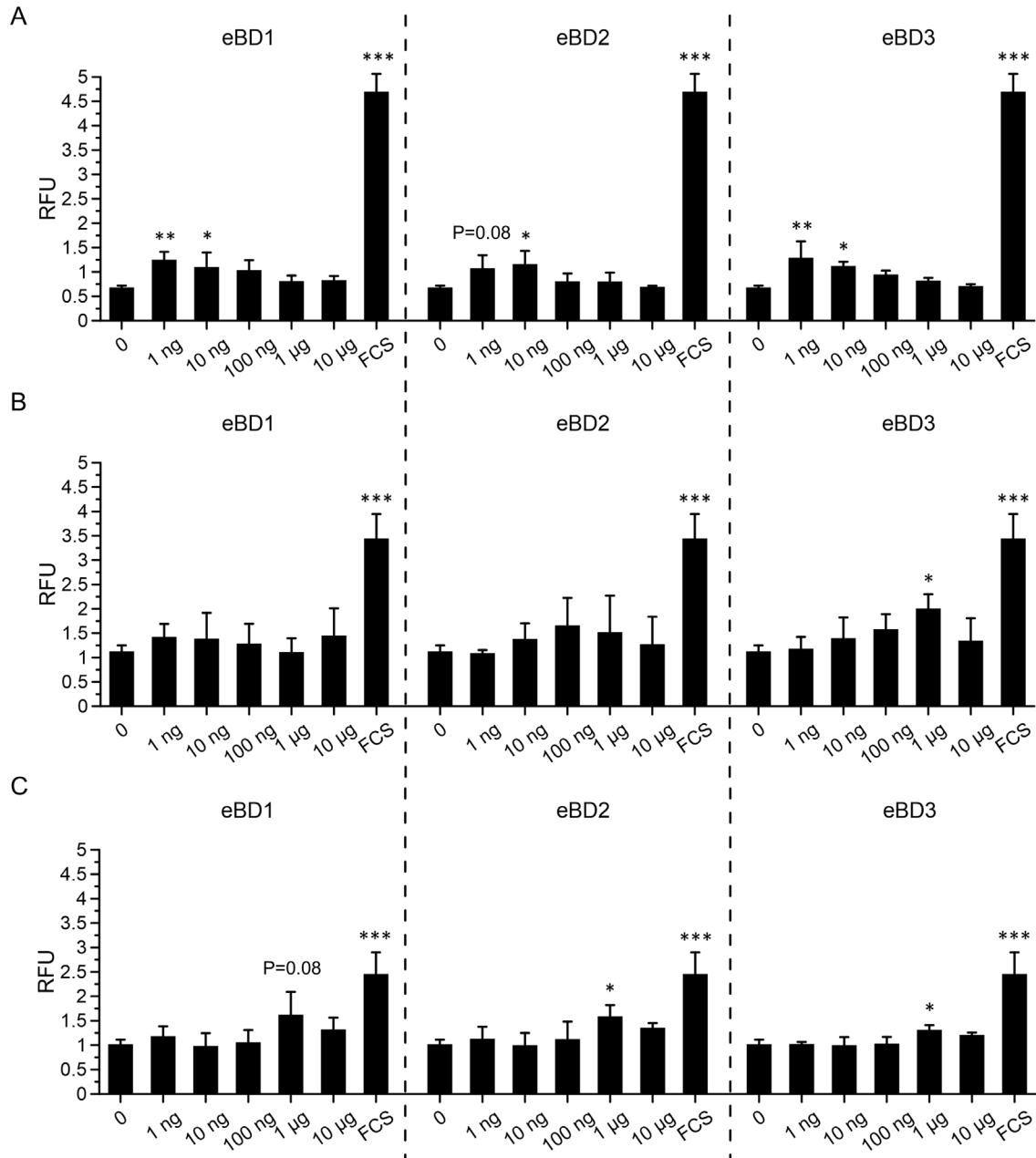


Figure 9. Chemotactic activity of eBD1-3 on equine blood leukocytes using a 96-well Boyden chamber. Migration of (A) polymorphonuclear cells, (B) CD172a⁺ monocytes and (C) CD3⁺ T lymphocytes induced by 0-10 μ g/mL eBD1 (left panels), eBD2 (middle panels) or eBD3 (right panels). Foetal calf serum (FCS) was used as an internal positive control. Experiments were performed in triplicate on blood leukocytes of three different healthy horse donors. Cell migration values are reported as relative fluorescence units (RFU) and represented as means + SD. Significant differences are indicated by asterisks: * $P \leq 0.05$; ** $P < 0.01$; *** $P < 0.001$.

Discussion

Beta defensins (BDs) are an essential protective component of respiratory epithelial cells and mucus, as they are not only able to directly kill incoming pathogens, but also modulate the onset of the host's adaptive immunity by recruiting immune cells (Ganz, 2003; Lehrer and Ganz, 2002; Selsted and Ouellette, 2005; Yang *et al.*, 2002). The equine variants have not been studied so far and although they resemble other phylogenetically related mammalian BDs, they clearly exhibit peculiarities of their own. First, we found that the three major eBDs were expressed in the upper respiratory tract of all five examined horses. In humans, solely BD1 is constitutively produced, while BD2 and 3 are only expressed at a low basal level or in response to microbial products and/or inflammatory cytokines (Harder *et al.*, 2001; Lee *et al.*, 2002; Singh *et al.*, 1998). In addition, we observed a marked difference in eBD1 expression between equine nasal and tracheal epithelial cells, which was low to absent in the former and present in the latter. The nasal cavities filter out most of the respirable debris and are colonized by a microbial flora, which in turn might silence eBD1 production in the luminal epithelial cells. Indeed, it has been shown that *Haemophilus influenzae* is capable of downregulating human BD1 release in bronchial epithelial cells (Tregidgo *et al.*, 2016). Since the expression of human BD2 and 3 is regulated in a distinct manner than that of BD1, it is not surprising that eBD1 expression and induction differed from that of 2 and 3 (Lee *et al.*, 2002; Starner *et al.*, 2005). The distribution patterns of eBD2 and 3 were similar between nasal and tracheal respiratory epithelia and showed vast homologies with previously reported expression profiles in the equine oesophagus, where eBD2 was mainly expressed in the basal layers and eBD3 expression extended from basal to more superficial layers (Hornickel *et al.*, 2011b). Correspondingly, mRNA for human BD2 and BD3 has been localized to epithelial and glandular cells in respiratory tissues from humans (Bals *et al.*, 1998; Harder *et al.*, 2001; Lee *et al.*, 2002; Singh *et al.*, 1998; Starner *et al.*, 2005). While these studies on human BD isolated BD2 and 3 from the lungs, we were unable to detect eBD protein expression in equine lung parenchym (Bals *et al.*, 1998; Ishimoto *et al.*, 2006; Singh *et al.*, 1998). This may be attributed to the fact that BDs from bronchoalveolar lavage or lung explants might arise from the epithelial cells lining the small bronchioles and not from the pneumocytes composing the alveoli. Indeed, BD3 protein was solely localized to human bronchial epithelial cells and was absent in the lung alveoli (Ishimoto *et al.*, 2006). Mammalian BDs have the capacity to inactivate bacterial and enveloped viral microorganisms by disrupting the microbial membrane (Bals *et al.*, 1998; Harder *et al.*, 2001; Schroeder *et al.*, 2011; Wilson *et al.*, 2013). Here, we investigated for the first time the exact antimicrobial

properties of the three eBDs. Similarly to its human homologue, oxidized eBD1 exhibited minimal antibacterial or antiviral effects (Doss *et al.*, 2009; Hazrati *et al.*, 2006; Howell *et al.*, 2004; Quinones-Mateu *et al.*, 2003; Singh *et al.*, 1998; Starner *et al.*, 2005). However, Schroeder *et al.* (2011) found that the human BD1's antimicrobial killing activity is revealed in reducing conditions (e.g. in the intestines). The human BD1 might even form bacteria-entrapping nets under these circumstances (Raschig *et al.*, 2017). Unfortunately, concentrations of DTT necessary for such reducing environments (i.e. the conversion of resaruzin to resorufin) affected bacterial and mammalian cell growth, making it impossible to examine the role of reduced eBD1. The existence of such an environment in the respiratory tract has not been shown so far, questioning the importance of eBD1 in *in vivo* innate respiratory mucosal immunity. Nonetheless, respiratory epithelial cell chaperones (e.g. thioredoxin) might shape eBD1 in a specific manner, unmasking bactericidal and/or virucidal actions (Jaeger *et al.*, 2013; Schroeder *et al.*, 2011). In addition, oxidized eBD1 is involved in the chemo-attraction of equine leukocytes, thereby aiding in the onset of adaptive immunity.

Oxidized eBD2 and especially eBD3 efficiently inhibited a range of equine bacterial and viral pathogens, primarily through direct actions on the pathogen. Gram-negative bacteria were generally more sensitive to eBDs, compared to Gram-positive bacteria, which is not surprising considering the outer cell structure of these microorganisms. In contrast to Gram-positive bacteria, which are protected by an outer peptidoglycan layer, Gram-negative bacteria are coated with an anionic lipopolysaccharide (LPS) exterior cell wall. Due to their polycationic and amphipatic nature, defensins can efficiently interact with and subsequently destroy this lipid bilayer (Dhople *et al.*, 2006; Lehrer *et al.*, 1989; White *et al.*, 1995). Similarly, EIV and EAV nucleocapsids are enclosed by a susceptible negatively charged phospholipid bilayer.

Although several strains of *Staphylococcus aureus* showed sensitivity towards human BD2 and especially 3, our field strain of *Staphylococcus aureus* resisted treatment with all eBDs (Harder *et al.*, 1997; Harder *et al.*, 2001; Sass *et al.*, 2010). Field strains might have acquired counter measurements against eBDs, such as the production of exoproteins (e.g. staphylokinase) which can bind and inactivate defensins (Jin *et al.*, 2004). Additionally, *Staphylococcus aureus* is able to reduce the charge of its membrane surface by modifying phosphatidylglycerol with l-lysine, thereby repulsing cationic defensins (Peschel *et al.*, 2001). Noteworthy, none of the eBDs inhibited *Streptococcus equi* subsp. *zooepidemicus* growth, while eBD3 did affect *Streptococcus equi* subsp. *equi*. This might be related to the fact that the former is a commensal pathogen in the horse, while the latter is not, suggesting that eBDs, like other antimicrobial proteins, shape the composition of microbiota at respiratory mucosal surfaces. Indeed, the two

resistant bacteria are known to reside in the horse's respiratory tract, while the sensitive bacteria are opportunistic pathogenic bacteria in the respiratory tract (Lindahl *et al.*, 2013; Sweeney *et al.*, 2005; Takai, 1997; Timoney, 2004; Weese *et al.*, 2005). Finally, *Rhodococcus equi* and *Actinobacillus equuli* were affected by eBD3 at relatively low concentrations. These bacteria are only rarely isolated from adult horses suffering from respiratory disease. On the contrary, these bacteria are amongst the major causes of pneumonia in foals up to 6 months of age. It has been documented that infants lack expression of human BD3, which might be extrapolated to foals and explain this peculiar age dependency of bacterial respiratory disease (Tugizov *et al.*, 2011).

It is not surprising that eBD3 was the most potent biocidal peptide out of all three eBDs, considering the fact that eBD3, followed by eBD2, has the highest content of cationic amino-acids, which are clustered as a 'functional unit' near the C-terminus of the peptide. This functional unit orchestrates the initial interaction of defensins with negatively charged phospholipids or glycoproteins. In addition, the mixture of oxidized eBD3 contained more dimeric forms, compared to eBD2. Following insertion of the amphipathic defensin through the lipid bilayer of a putative pathogen, defensins supposedly oligomerize to form a pore, which in turn is facilitated by dimer formation (Hill *et al.*, 1991). However, direct antibacterial activities of human BD2 and 3 were later shown to be independent of BD dimerization (Boniotto *et al.*, 2003; Hoover *et al.*, 2001). Nonetheless, dimer formation might still play an important role for eBDs in other biological (e.g. receptor-mediated) functions. Finally, human BD3 is a lectin, capable of interacting with glycoproteins or glycolipids that project through biological membranes (Hazrati *et al.*, 2006; Leikina *et al.*, 2005). As the majority of the eBD3 amino-acid sequence is homologous to that of human BD3, we can assume that eBD3 exhibits lectin-functions as well. Although such activity has not been reported for human BD2, eBD2 differs substantially from its human homologue and thus might display lectin properties as well. Indeed, following removal of N-linked glycans with the use of PNGase F on EHV1 surfaces, the pro-viral effect of eBD2 and 3 was nearly abolished (unpublished results). Lectin-binding is thought to be primarily of importance in the antiviral effects of BD3, by blocking receptors on either the viral envelope or the cell plasma membrane. It has already been shown that human BD3 blocks influenza virus fusion by forming a protective barricade of immobilized host cell glycoproteins (Leikina *et al.*, 2005). Although we saw a similar antiviral effect when adding eBD3 during viral entry in MDCK cells, we cannot exclude the fact that eBD3 merely inactivated surface-bound EIV particles prior to entry. Such direct anti-influenza effects have been reported for human BD1 and 2 (Doss *et al.*, 2009). Notably, we could not observe EIV

inhibition by pretreating MDCK or EREC cell surfaces prior to inoculation. In addition, eBD3 had no effect on EIV entry in EREC, suggesting that the virus was rapidly internalized by EREC and eBD3 lacked the time to inactivate infective surface-bound virions. Whether the direct inactivation (i.e. virus pretreatment) of EIV and EAV by eBD2 and 3 was a consequence of either direct viral envelope penetration or blocking/crosslinking viral binding/entry proteins remains speculative. It would be interesting to co-immunoprecipitate eBDs upon incubation with virus particles to determine glycoprotein interactions or perform electron microscopy studies to examine viral envelope structures.

Surprisingly, we demonstrated that eBD2 and 3 enhance EHV1 infectivity by concentrating virus particles on the RK13 cells, thereby promoting virion attachment. A similar pro-viral effect on human immunodeficiency virus (HIV) has been shown for the human α -defensins 5 and 6 (Rapista *et al.*, 2011). In addition, a recent study showed that human BD2-3 and human α -defensin 5 facilitated binding of HIV and human adenovirus (HAdV), respectively, to epithelial cells. Still, viral infectivity was diminished through co-internalisation of virus particles and defensins, which led to virus neutralization (Gounder *et al.*, 2012; Herrera *et al.*, 2016). This study is the first to reveal a pro-viral effect for BDs and moreover, we demonstrated that the viral ‘non-essential’ glycoprotein M (gM) renders EHV1 resistant to eBDs. Indeed, infectivity of the gM-lacking mutant was attenuated upon treatment with eBD2, while that of the parental and gp2-lacking strains remained enhanced. As gM harbours multiple transmembrane-spanning domains, we propose that it protects the virus from lipid bilayer-attacking eBDs by stabilizing the viral envelope (Osterrieder *et al.*, 1996; Pilling *et al.*, 1994). Further evidence of the role of gM in membrane-stabilization comes from the fact that gM of pseudorabies (PRV) and EHV1 inhibit the fusion induced by artificially optimized gB and gD (Klupp *et al.*, 2000). Nonetheless, other more glycosylated viral membrane proteins might facilitate eBD binding and subsequent EHV1 infectivity. More precisely, the highly cationic and possible lectin-like eBDs could aggregate negatively charged EHV1 particles through oligomerization and subsequent formation of high-order aggregates. The findings are consistent with our observation that eBDs have the tendency to self-associate in solution and with our binding experiments. In line with our observations, human α -defensins have been shown to aggregate virions of influenza virus, HAdV and BK virus (Doss *et al.*, 2009; Dugan *et al.*, 2008). Additionally, following removal of N-linked glycans with the use of PNGase F on EHV1 surfaces, the pro-viral effect of eBDs was diminished (unpublished results). The fact that we could not observe an increase in EHV1 infection upon inoculation of EREC, could be attributed to the pore size of the transwells. As EHV1 particles measure on average 150 nm, virus

aggregates may not efficiently reach the basolateral surface of EREC, grown on 400 nm pore size membranes. Unfortunately, membranes with larger pores did not support cell growth and apical inoculation of the cells did not yield a sufficient infection to test the eBDs (Van Cleemput *et al.*, 2017). Nonetheless, pretreatment of EREC with all eBDs increased subsequent EHV1 infectivity by facilitating virus binding and/or entry. Here, the effect was not attributed to the formation of aggregates, since we merely saw an increase in the number of EREC with bound EHV1 particles and did not observe virion aggregates. Since a similar pro-viral effect was observed when eBD1-3 were added during the viral entry step, we suggest that eBD1-3 directly bind to EHV1 binding/entry receptor(s) on the cell surface and thereby facilitate subsequent EHV1 binding to and entry in the cell. EBD1-3 might facilitate direct viral binding through neutralizing the net negative charge between the virion and cellular glycoproteins. Alternatively, by inducing a conformation change in EHV1's binding/entry receptor(s), subsequent EHV1 binding and entry might be enhanced. Finally, eBD1-3 might bind to other putative receptors on the cell surface, thereby inducing an upregulation and/or a conformational change of the EHV1 binding/entry receptor. It is not surprising that the effect of eBDs during cell pretreatment of RK13 cells was strongly attenuated, considering the fact that RK13 cells do not natively recognize foreign eBDs, while EREC are the natural target cells of eBDs. Finally, in RK13 cells but not in EREC, co-internalisation of these virus aggregates resulted in rapid cell-to-cell spread in the cell monolayer. The high crosslinkage of viral proteins to eBDs might have facilitated the formation of syncytia in these cells, since defensins have been shown to promote fusion of membranes (Fujii *et al.*, 1993). A similar enhancement of viral spread in RK13 cells was observed when eBDs were added post virus penetration. In EREC grown on transwells, EHV1 does not induce syncytia, corroborating our hypothesis that eBDs facilitate membrane-fusion and subsequent syncytia formation.

Our observations on EHV1 are strikingly different from those on the closely related human alphaherpesviruses herpes simplex virus 1 and 2, which were inactivated by human BD3 (Hazrati *et al.*, 2006). In evolution however, EHV1 most likely came into existence long before HSV, giving it a lead start in the development of immune evasion mechanisms, such as anti-defensin and even defensin-exploiting strategies (Karlin *et al.*, 1994).

EHV1 not only misuses these eBDs to infect EREC, but also upregulates the expression of eBD2 and 3 in EREC upon inoculation. This is presumably a direct consequence of EHV1 infection, followed by a paracrine signalling of neighbouring cells, since the expression is higher in infected cells than in adjacent non-infected cells. Epithelial BDs are often induced in response to viral infections in other species as well, e.g. in the respiratory tract of mice upon

influenza A infection, in human oral cavities upon challenge with HIV or in human bronchial epithelia infected with rhinovirus (Chong *et al.*, 2008; Proud *et al.*, 2004; Quinones-Mateu *et al.*, 2003). Similarly, EIV also induced eBD2 and 3 protein expression, but to a lesser extent than EHV1. The increase in eBD production attracted blood leukocytes, which are key in the clearance of infection. However, EHV1 depends on these leukocytes for viral spread within the horse and may cleverly take advantage of the induced increase in eBD expression during infection.

Taken together, we demonstrated that the horse's respiratory tract constitutively produces eBD1, 2 and 3, thereby potentially shaping the microbiota of the upper respiratory tract and protecting the lower respiratory tract from pathogen invasion. While the two less host-adapted equine viruses (EIV and EVA) are sensitive to eBDs, the ancestral alphaherpesvirus EHV1, a virus that has evolved with its host over long periods of time and is exquisitely well adapted to it, is resistant to eBDs (Davison, 2002). Moreover, the virus exploits these eBDs for enhancement of infectivity and attraction of potential virus-carrying leukocytes. These new insights into alphaherpesvirus host entry may be of great significance in medical research on herpesvirus-associated diseases.

Acknowledgements

The authors are grateful to Prof. Balasuriya for supplying the antibodies against EHV1 proteins. The authors also acknowledge Carine Boone, Marleen Foubert, Chantal Vanmaercke, Ytse Noppe, Nele Dennequin, Simon Daled and Jonathan Vandenbogaerde for their excellent technical support.

References

- Allen, G.P., Bryans, J.T., 1986. Molecular epizootiology, pathogenesis, and prophylaxis of equine herpesvirus-1 infections. *Progress in veterinary microbiology and immunology* 2, 78-144.
- Bals, R., Wang, X., Meegalla, R.L., Wattler, S., Weiner, D.J., Nehls, M.C., Wilson, J.M., 1999. Mouse beta-defensin 3 is an inducible antimicrobial peptide expressed in the epithelia of multiple organs. *Infect Immun* 67, 3542-3547.
- Bals, R., Wang, X., Wu, Z., Freeman, T., Bafna, V., Zasloff, M., Wilson, J.M., 1998. Human beta-defensin 2 is a salt-sensitive peptide antibiotic expressed in human lung. *The Journal of clinical investigation* 102, 874-880.
- Bensch, K.W., Raida, M., Magert, H.J., Schulz-Knappe, P., Forssmann, W.G., 1995. hBD-1: a novel beta-defensin from human plasma. *FEBS letters* 368, 331-335.
- Boniotto, M., Antcheva, N., Zelezetsky, I., Tossi, A., Palumbo, V., Falzacappa, M.V.V., Sgubin, S., Braida, L., Amoroso, A., Crovella, S., 2003. A study of host defence peptide β -defensin 3 in primates. *Biochemical Journal* 374, 707-714.
- Bruhn, O., Grotzinger, J., Cascorbi, I., Jung, S., 2011. Antimicrobial peptides and proteins of the horse--insights into a well-armed organism. *Vet Res* 42, 98.
- Bruhn, O., Paul, S., Tetens, J., Thaller, G., 2009. The repertoire of equine intestinal alpha-defensins. *BMC genomics* 10.
- Chong, K.T., Thangavel, R.R., Tang, X., 2008. Enhanced expression of murine beta-defensins (MBD-1, -2, -3, and -4) in upper and lower airway mucosa of influenza virus infected mice. *Virology* 380, 136-143.
- Christley, R.M., Hodgson, D.R., Rose, R.J., Wood, J.L.N., Reid, S.W.J., Whitear, K.G., Hodgson, J.L., 2001. A case-control study of respiratory disease in Thoroughbred racehorses in Sydney, Australia. *Equine Veterinary Journal* 33, 256-264.
- Davis, E.G., Sang, Y., Blecha, F., 2004. Equine beta-defensin-1: full-length cDNA sequence and tissue expression. *Vet Immunol Immunopathol* 99, 127-132.
- Davison, A.J., 2002. Evolution of the herpesviruses. *Veterinary microbiology* 86, 69-88.
- Dhople, V., Krukemeyer, A., Ramamoorthy, A., 2006. The human beta-defensin-3, an antibacterial peptide with multiple biological functions. *Biochimica et Biophysica Acta (BBA)-Biomembranes* 1758, 1499-1512.
- Diamond, G., Zasloff, M., Eck, H., Bresseur, M., Maloy, W.L., Bevins, C.L., 1991. Tracheal antimicrobial peptide, a cysteine-rich peptide from mammalian tracheal mucosa: peptide isolation and cloning of a cDNA. *Proceedings of the National Academy of Sciences of the United States of America* 88, 3952-3956.
- Doss, M., White, M.R., Teclé, T., Gantz, D., Crouch, E.C., Jung, G., Ruchala, P., Waring, A.J., Lehrer, R.I., Hartshorn, K.L., 2009. Interactions of α -, β -, and θ -defensins with influenza A virus and surfactant protein D. *The Journal of Immunology* 182, 7878-7887.
- Dugan, A.S., Maginnis, M.S., Jordan, J.A., Gasparovic, M.L., Manley, K., Page, R., Williams, G., Porter, E., O'Hara, B.A., Atwood, W.J., 2008. Human α -defensins inhibit BK virus infection by aggregating virions and blocking binding to host cells. *Journal of Biological Chemistry* 283, 31125-31132.
- Fujii, G., Eisenberg, D., Selsted, M.E., 1993. Defensins promote fusion and lysis of negatively charged membranes. *protein Science* 2, 1301-1312.
- Ganz, T., 2003. Defensins: antimicrobial peptides of innate immunity. *Nature reviews. Immunology* 3, 710-720.
- Garcia-Cantu, M.C., Hartmann, F.A., Brown, C.M., Darien, B.J., 2000. *Bordetella bronchiseptica* and equine respiratory infections: a review of 30 cases. *Equine Veterinary Education* 12, 45-50.
- Geiler, J., Michaelis, M., Naczek, P., Leutz, A., Langer, K., Doerr, H.-W., Cinatl, J., 2010. N-acetyl-l-cysteine (NAC) inhibits virus replication and expression of pro-inflammatory molecules in A549 cells infected with highly pathogenic H5N1 influenza A virus. *Biochemical Pharmacology* 79, 413-420.

- Ghosh, S.K., Gerken, T.A., Schneider, K.M., Feng, Z., McCormick, T.S., Weinberg, A., 2007.** Quantification of human beta-defensin-2 and -3 in body fluids: application for studies of innate immunity. *Clinical chemistry* 53, 757-765.
- Gounder, A.P., Wiens, M.E., Wilson, S.S., Lu, W., Smith, J.G., 2012.** Critical determinants of human alpha-defensin 5 activity against non-enveloped viruses. *Journal of Biological Chemistry*, jbc.M112. 354068.
- Harder, J., Bartels, J., Christophers, E., Schröder, J.-M., 1997.** A peptide antibiotic from human skin. *Nature* 387, 861.
- Harder, J., Bartels, J., Christophers, E., Schröder, J.-M., 2001.** Isolation and characterization of human β -defensin-3, a novel human inducible peptide antibiotic. *Journal of Biological Chemistry* 276, 5707-5713.
- Hazrati, E., Galen, B., Lu, W.Y., Wang, W., Yan, O.Y., Keller, M.J., Lehrer, R.I., Herold, B.C., 2006.** Human alpha- and beta-defensins block multiple steps in herpes simplex virus infection. *Journal of Immunology* 177, 8658-8666.
- Helm, D., Vissers, J.P.C., Hughes, C.J., Hahne, H., Ruprecht, B., Pachi, F., Grzyb, A., Richardson, K., Wildgoose, J., Maier, S.K., Marx, H., Wilhelm, M., Becher, I., Lemeer, S., Bantscheff, M., Langridge, J.I., Kuster, B., 2014.** Ion Mobility Tandem Mass Spectrometry Enhances Performance of Bottom-up Proteomics. *Molecular & Cellular Proteomics : MCP* 13, 3709-3715.
- Herrera, R., Morris, M., Rosbe, K., Feng, Z., Weinberg, A., Tugizov, S., 2016.** Human beta-defensins 2 and-3 cointernalize with human immunodeficiency virus via heparan sulfate proteoglycans and reduce infectivity of intracellular virions in tonsil epithelial cells. *Virology* 487, 172-187.
- Hill, C.P., Yee, J., Selsted, M.E., Eisenberg, D., 1991.** Crystal structure of defensin HNP-3, an amphiphilic dimer: mechanisms of membrane permeabilization. *Science (New York, N.Y.)* 251, 1481-1485.
- Hoover, D.M., Chertov, O., Lubkowski, J., 2001.** The Structure of human β -defensin-1 new insights into structural properties of β -defensins. *Journal of Biological Chemistry* 276, 39021-39026.
- Hornickel, I.N., Kacza, J., Schnapper, A., Beyerbach, M., Schoennagel, B., Seeger, J., Meyer, W., 2011a.** Demonstration of substances of innate immunity in the esophageal epithelium of domesticated mammals. Part I - Methods and evaluation of comparative fixation. *Acta Histochemica* 113, 163-174.
- Hornickel, I.N., Kacza, J., Schnapper, A., Beyerbach, M., Schoennagel, B., Seeger, J., Meyer, W., 2011b.** Demonstration of substances of innate immunity in the esophageal epithelium of domesticated mammals: Part II - Defence mechanisms, including species comparison. *Acta Histochemica* 113, 175-188.
- Howell, M.D., Jones, J.F., Kisich, K.O., Streib, J.E., Gallo, R.L., Leung, D.Y., 2004.** Selective killing of vaccinia virus by LL-37: implications for eczema vaccinatum. *The Journal of Immunology* 172, 1763-1767.
- Huttner, K.M., Lambeth, M.R., Burkin, H.R., Burkin, D.J., Broad, T.E., 1998.** Localization and genomic organization of sheep antimicrobial peptide genes. *Gene* 206, 85-91.
- Ishimoto, H., Mukae, H., Date, Y., Shimbara, T., Mondal, M., Ashitani, J., Hiratsuka, T., Kubo, S., Kohno, S., Nakazato, M., 2006.** Identification of hBD-3 in respiratory tract and serum: the increase in pneumonia. *European Respiratory Journal* 27, 253-260.
- Jaeger, S., Schroeder, B., Meyer-Hoffert, U., Courth, L., Fehr, S., Gersemann, M., Stange, E., Wehkamp, J., 2013.** Cell-mediated reduction of human β -defensin 1: a major role for mucosal thioredoxin. *Mucosal immunology* 6, 1179.
- Jia, H.P., Starner, T., Ackermann, M., Kirby, P., Tack, B.F., McCray, P.B., Jr., 2001.** Abundant human beta-defensin-1 expression in milk and mammary gland epithelium. *J Pediatr* 138, 109-112.
- Jiang, S., Liu, S., Zhao, C., Wu, C., 2016.** Developing protocols of tricine-SDS-PAGE for separation of polypeptides in the mass range 1-30 kDa with minigel electrophoresis system. *International Journal of Electrochemical Science* 11, 640-649.
- Jin, T., Bokarewa, M., Foster, T., Mitchell, J., Higgins, J., Tarkowski, A., 2004.** *Staphylococcus aureus* resists human defensins by production of staphylokinase, a novel bacterial evasion mechanism. *The Journal of Immunology* 172, 1169-1176.

- Karlin, S., Mocarski, E.S., Schachtel, G.A., 1994.** Molecular evolution of herpesviruses: genomic and protein sequence comparisons. *J Virol* 68, 1886-1902.
- Klotman, M.E., Chang, T.L., 2006.** Defensins in innate antiviral immunity. *Nature Reviews Immunology* 6, 447-456.
- Klupp, B.G., Nixdorf, R., Mettenleiter, T.C., 2000.** Pseudorabies Virus Glycoprotein M Inhibits Membrane Fusion. *Journal of Virology* 74, 6760.
- Kuhns, D.B., Long Priel, D.A., Chu, J., Zarembek, K.A., 2015.** Isolation and Functional Analysis of Human Neutrophils. *Current protocols in immunology*, edited by John E. Coligan *et al.* 111, 7.23.21-27.23.16.
- Laval, K., Favoreel, H.W., Nauwynck, H.J., 2015.** Equine herpesvirus type 1 replication is delayed in CD172a⁺ monocytic cells and controlled by histone deacetylases. *The Journal of general virology* 96, 118-130.
- Laval, K., Favoreel, H.W., Van Cleemput, J., Poelaert, K.C.K., Brown, I.K., Verhasselt, B., Nauwynck, H.J., 2016.** Entry of equid herpesvirus 1 into CD172a⁺ monocytic cells. *Journal of General Virology* 97, 733-746.
- Layman, Q.D., Rezabek, G.B., Ramachandran, A., Love, B.C., Confer, A.W., 2014.** A retrospective study of equine actinobacillosis cases: 1999–2011. *Journal of Veterinary Diagnostic Investigation* 26, 365-375.
- Lee, S.H., Kim, J.E., Lee, H.M., Lim, H.H., Choi, J.O., 2002.** Antimicrobial defensin peptides of the human nasal mucosa. *Annals of Otology, Rhinology & Laryngology* 111, 135-141.
- Lehrer, R., Barton, A., Daher, K.A., Harwig, S., Ganz, T., Selsted, M.E., 1989.** Interaction of human defensins with *Escherichia coli*. Mechanism of bactericidal activity. *The Journal of clinical investigation* 84, 553-561.
- Lehrer, R.I., Ganz, T., 2002.** Defensins of vertebrate animals. *Current Opinion in Immunology* 14, 96-102.
- Leikina, E., Delanoe-Ayari, H., Melikov, K., Cho, M.-S., Chen, A., Waring, A.J., Wang, W., Xie, Y., Loo, J.A., Lehrer, R.I., 2005.** Carbohydrate-binding molecules inhibit viral fusion and entry by crosslinking membrane glycoproteins. *Nature immunology* 6, 995.
- Lindahl, S.B., Aspán, A., Båverud, V., Paillot, R., Pringle, J., Rash, N.L., Söderlund, R., Waller, A.S., 2013.** Outbreak of upper respiratory disease in horses caused by *Streptococcus equi* subsp. *zooepidemicus* ST-24. *Veterinary microbiology* 166, 281-285.
- Looft, C., Paul, S., Philipp, U., Regenhart, P., Kuiper, H., Distl, O., Chowdhary, B.P., Leeb, T., 2006.** Sequence analysis of a 212 kb defensin gene cluster on ECA 27q17. *Gene* 376, 192-198.
- Maisetta, G., Di Luca, M., Esin, S., Florio, W., Brancatisano, F.L., Bottai, D., Campa, M., Batoni, G., 2008.** Evaluation of the inhibitory effects of human serum components on bactericidal activity of human beta defensin 3. *Peptides* 29, 1-6.
- Marth, C.D., Young, N.D., Glenton, L.Y., Noden, D.M., Browning, G.F., Krekeler, N., 2015.** Deep sequencing of the uterine immune response to bacteria during the equine oestrous cycle. *BMC genomics* 16, 934.
- Mayr, A., Pette, J., Petzoldt, K., Wagener, K., 1968.** Untersuchungen zur Entwicklung eines Lebendimpfstoffes gegen die Rhinopneumonitis (Stutenabort) der Pferde. *Zoonoses and Public Health* 15, 406-418.
- Osterrieder, N., Neubauer, A., Brandmuller, C., Braun, B., Kaaden, O.-R., Baines, J.D., 1996.** The equine herpesvirus 1 glycoprotein gp21/22a, the herpes simplex virus type 1 gM homolog, is involved in virus penetration and cell-to-cell spread of virions. *Journal of virology* 70, 4110-4115.
- Pazgier, M., Hoover, D., Yang, D., Lu, W., Lubkowski, J., 2006.** Human β -defensins. *Cellular and Molecular Life Sciences CMLS* 63, 1294-1313.
- Peschel, A., Jack, R.W., Otto, M., Collins, L.V., Staubitz, P., Nicholson, G., Kalbacher, H., Nieuwenhuizen, W.F., Jung, G., Tarkowski, A., 2001.** *Staphylococcus aureus* resistance to human defensins and evasion of neutrophil killing via the novel virulence factor MprF is based on modification of membrane lipids with l-lysine. *Journal of Experimental Medicine* 193, 1067-1076.
- Pilling, A., Davison, A.J., Telford, E.A., Meredith, D.M., 1994.** The equine herpesvirus type 1 glycoprotein homologous to herpes simplex virus type 1 glycoprotein M is a major constituent of the virus particle. *Journal of general virology* 75, 439-442.

- Proud, D., Sanders, S.P., Wiehler, S., 2004.** Human rhinovirus infection induces airway epithelial cell production of human beta-defensin 2 both *in vitro* and *in vivo*. *Journal of immunology* (Baltimore, Md. : 1950) 172, 4637-4645.
- Quinones-Mateu, M.E., Lederman, M.M., Feng, Z., Chakraborty, B., Weber, J., Rangel, H.R., Marotta, M.L., Mirza, M., Jiang, B., Kiser, P., Medvik, K., Sieg, S.F., Weinberg, A., 2003.** Human epithelial beta-defensins 2 and 3 inhibit HIV-1 replication. *AIDS* (London, England) 17, F39-48.
- Quintana, A.M., Landolt, G.A., Annis, K.M., Hussey, G.S., 2011.** Immunological characterization of the equine airway epithelium and of a primary equine airway epithelial cell culture model. *Veterinary Immunology and Immunopathology* 140, 226-236.
- Rapista, A., Ding, J., Benito, B., Lo, Y.-T., Neiditch, M.B., Lu, W., Chang, T.L., 2011.** Human defensins 5 and 6 enhance HIV-1 infectivity through promoting HIV attachment. *Retrovirology* 8, 45.
- Raschig, J., Mailänder-Sánchez, D., Berscheid, A., Berger, J., Strömstedt, A.A., Courth, L.F., Malek, N.P., Brötz-Oesterhelt, H., Wehkamp, J., 2017.** Ubiquitously expressed Human Beta Defensin 1 (hBD1) forms bacteria-entrapping nets in a redox dependent mode of action. *PLoS pathogens* 13, e1006261.
- Rudolph, J., O'Callaghan, D., Osterrieder, N., 2002.** Cloning of the Genomes of Equine Herpesvirus Type 1 (EHV-1) Strains KyA and RacL11 as Bacterial Artificial Chromosomes (BAC). *Zoonoses and Public Health* 49, 31-36.
- Sang, Y., Ortega, M.T., Blecha, F., Prakash, O., Melgarejo, T., 2005.** Molecular cloning and characterization of three beta-defensins from canine testes. *Infect Immun* 73, 2611-2620.
- Sass, V., Schneider, T., Wilmes, M., Körner, C., Tossi, A., Novikova, N., Shamova, O., Sahl, H.-G., 2010.** Human β -defensin 3 inhibits cell wall biosynthesis in Staphylococci. *Infection and immunity* 78, 2793-2800.
- Schägger, H., 2006.** Tricine-sds-page. *Nature protocols* 1, 16.
- Schoniger, S., Grafe, H., Schoon, H.A., 2013.** Beta-defensin is a component of the endometrial immune defence in the mare. *Pferdeheilkunde* 29, 335-346.
- Schroeder, B.O., Wu, Z.H., Nuding, S., Groscurth, S., Marcinowski, M., Beisner, J., Buchner, J., Schaller, M., Stange, E.F., Wehkamp, J., 2011.** Reduction of disulphide bonds unmasks potent antimicrobial activity of human beta-defensin 1. *Nature* 469, 419-+.
- Selsted, M.E., Ouellette, A.J., 2005.** Mammalian defensins in the antimicrobial immune response. *Nature immunology* 6, 551-557.
- Singh, P.K., Jia, H.P., Wiles, K., Hesselberth, J., Liu, L., Conway, B.-A.D., Greenberg, E.P., Valore, E.V., Welsh, M.J., Ganz, T., 1998.** Production of β -defensins by human airway epithelia. *Proceedings of the National Academy of Sciences* 95, 14961-14966.
- Starner, T.D., Agerberth, B., Gudmundsson, G.H., McCray, P.B., 2005.** Expression and activity of β -defensins and LL-37 in the developing human lung. *The Journal of Immunology* 174, 1608-1615.
- Sweeney, C.R., Timoney, J.F., Newton, J.R., Hines, M.T., 2005.** *Streptococcus equi* Infections in Horses: Guidelines for Treatment, Control, and Prevention of Strangles. *Journal of Veterinary Internal Medicine* 19, 123-134.
- Takai, S., 1997.** Epidemiology of *Rhodococcus equi* infections: A review. *Veterinary microbiology* 56, 167-176.
- Tam, J.P., Wu, C.R., Liu, W., Zhang, J.W., 1991.** Disulfide bond formation in peptides by dimethyl sulfoxide. Scope and applications. *Journal of the American Chemical Society* 113, 6657-6662.
- Timoney, J.F., 2004.** The pathogenic equine streptococci. *Vet. Res.* 35, 397-409.
- Timoney, P.J., McCollum, W.H., 1996.** Equine viral arteritis. *Equine Veterinary Education* 8, 32-35.
- Tregidgo, L., Cane, J., Bafadhel, M., 2016.** S103 Non-typeable haemophilus influenzae downregulates release of beta-defensin-1 from bronchial epithelial cells. *BMJ Publishing Group Ltd.*
- Tugizov, S.M., Herrera, R., Veluppillai, P., Greenspan, D., Soros, V., Greene, W.C., Levy, J.A., Palefsky, J.M., 2011.** HIV is inactivated after transepithelial migration via adult oral epithelial cells but not foetal epithelial cells. *Virology* 409, 211-222.
- Vaid, R.K., Shanmugasundaram, K., Anand, T., Bera, B.C., Tigga, M., Dedar, R., Riyesh, T., Bardwaj, S., Virmani, N., Tripathi, B.N., 2018.** Characterization of isolates of *Bordetella bronchiseptica* from horses. *Journal of equine science* 29, 25-31.

- Vairo, S., Vandekerckhove, A., Steukers, L., Glorieux, S., Van den Broeck, W., Nauwynck, H., 2012.** Clinical and virological outcome of an infection with the Belgian equine arteritis virus strain 08P178. *Veterinary microbiology* 157, 333-344.
- Van Cleemput, J., Poelaert, K.C.K., Laval, K., Maes, R., Hussey, G.S., Van den Broeck, W., Nauwynck, H.J., 2017.** Access to a main alphaherpesvirus receptor, located basolaterally in the respiratory epithelium, is masked by intercellular junctions. *Scientific reports* 7, 16656.
- Van der Meulen, K., Vercauteren, G., Nauwynck, H., Pensaert, M., 2003a.** A local epidemic of equine herpesvirus 1-induced neurological disorders in Belgium. *Vlaams Diergeneeskundig Tijdschrift* 72, 366-372.
- Van der Meulen, K.M., Nauwynck, H.J., Pensaert, M.B., 2003b.** Absence of viral antigens on the surface of equine herpesvirus-1-infected peripheral blood mononuclear cells: a strategy to avoid complement-mediated lysis. *Journal of general virology* 84, 93-97.
- Van Maanen, C., Cullinane, A., 2002.** Equine influenza virus infections: An update. *Veterinary Quarterly* 24, 79-94.
- Ward, C.L., Wood, J.L., Houghton, S.B., Mumford, J.A., Chanter, N., 1998.** Actinobacillus and Pasteurella species isolated from horses with lower airway disease. *Vet Rec* 143, 277-279.
- Weese, J.S., Archambault, M., B.M.Willey, Dick, H., Hearn, P., Kreiswirth, B.N., Said-Salim, B., McGeer, A., Likhoshvay, Y., Prescott, J.F., Low, D.E., 2005.** Methicillin-resistant Staphylococcus aureus in Horses and Horse Personnel, 2000–2002. *Emerging Infectious Diseases* 11, 430-435.
- White, S.H., Wimley, W.C., Selsted, M.E., 1995.** Structure, function, and membrane integration of defensins. *Current opinion in structural biology* 5, 521-527.
- Wilson, S.S., Wiens, M.E., Smith, J.G., 2013.** Antiviral Mechanisms of Human Defensins. *Journal of Molecular Biology* 425, 4965-4980.
- Yang, D., Biragyn, A., Kwak, L.W., Oppenheim, J.J., 2002.** Mammalian defensins in immunity: more than just microbicidal. *Trends in immunology* 23, 291-296.
- Yasui, T., Fukui, K., Nara, T., Habata, I., Meyer, W., Tsukise, A., 2007.** Immunocytochemical localization of lysozyme and beta-defensin in the apocrine glands of the equine scrotum. *Archives of dermatological research* 299, 393-397.
- Yasui, T., Tsukise, A., Fukui, K., Kuwahara, Y., Meyer, W., 2005.** Aspects of glycoconjugate production and lysozyme- and defensins-expression of the ceruminous glands of the horse (*Equus przewalskii* f. dom.). *European journal of morphology* 42, 127-134.
- Zhang, G., Wu, H., Shi, J., Ganz, T., Ross, C.R., Blecha, F., 1998.** Molecular cloning and tissue expression of porcine beta-defensin-1. *FEBS letters* 424, 37-40.

Chapter 7.

Unravelling the first key steps in equine herpesvirus type 5 (EHV5) pathogenesis using *ex vivo* and *in vitro* equine models

Jolien Van Cleemput, Katrien C.K. Poelaert, Kathlyn Laval, Hans J. Nauwynck

Submitted to Veterinary Research

Summary

Equine herpesvirus type 5 (EHV5) is an ubiquitous, yet obscure pathogen in the horse population and is commonly associated with fatal equine multinodular pulmonary fibrosis (EMPF). To date, little is known about the precise pathogenesis of EHV5. Here, we evaluated the dynamics of EHV5 infection in representative *ex vivo* and *in vitro* equine models, using immunofluorescent staining and virus titration. EHV5 was unable to infect epithelial cells lining the mucosa of nasal and tracheal explants. Similarly, primary equine respiratory epithelial cells (EREC) were not susceptible to EHV5 following inoculation at the apical or basolateral surfaces. Upon direct delivery of EHV5 particles to lung explants, few EHV5-positive cell clusters were observed at 72 hours post-inoculation (hpi). These EHV5-positive cells were identified as cytokeratin-positive alveolar cells. Next, we examined the potential of EHV5 to infect three distinct equine PBMC subpopulations (CD172a⁺ monocytes, CD3⁺ T lymphocytes and Ig light chain⁺ B lymphocytes). Monocytes did not support EHV5 replication. In contrast, up to 10% of inoculated equine T and B lymphocytes synthesized intracellular viral antigens 24 hpi and 72 hpi, respectively. Still, the production of mature virus particles was hampered, as we did not observe an increase in extracellular virus titer. After reaching a peak, the percentage of infected T and B lymphocytes decayed, which was partly due to the onset of apoptosis, but not necrosis. Based on these findings, we proposed a model for EHV5 pathogenesis in the horse. Uncovering EHV5 pathogenesis is the corner step to finally contain or even eradicate the virus.

Introduction

As a member of the *Gammaherpesvirus* subfamily, equine herpesvirus type 5 (EHV5) is optimally adapted to its natural host, meaning that infected horses are mainly asymptomatic (Davison *et al.*, 2009). EHV5 is endemic in the horse population and plenty of horses shed the virus in nasal secretions and/or carry the virus in peripheral blood mononuclear cells (PBMC) or lymphoid organs. Nonetheless, only a small fraction of them develop severe clinical symptoms (Akkutay *et al.*, 2014; Bell *et al.*, 2006b; Dunowska *et al.*, 1999; Dunowska *et al.*, 2002; Marenzoni *et al.*, 2010; Richter *et al.*, 2009; Torfason *et al.*, 2008; Wang *et al.*, 2007; Wong *et al.*, 2008). The virus typically causes upper respiratory tract disease (e.g. pharyngitis) or keratoconjunctivitis accompanied with clinical signs such as nasal and ocular discharge, tachypnea, coughing, fever, enlarged lymph nodes, anorexia, poor body condition and depression (Dunowska *et al.*, 2002; Franchini *et al.*, 1997; Hart *et al.*, 2008; Rushton *et al.*, 2013; Wong *et al.*, 2008). Single case reports linked EHV5 to B cell lymphomas, T cell leukemia and dermatitis (Herder *et al.*, 2012; Schwarz *et al.*, 2012; Vander Werf and Davis, 2013). However, the most dreadful complication of an EHV5 infection is the development of fatal equine multinodular pulmonary fibrosis (EMPF) (Williams *et al.*, 2007). EMPF is characterized by the presence of multiple fibrotic nodules throughout the lungs. Histologically, marked interstitial fibrosis with an ‘alveolar-like’ architecture, lined by cuboidal epithelial cells and thickening of the alveolar walls is visible (Poth *et al.*, 2009; Williams *et al.*, 2007; Wong *et al.*, 2008). The high correlation between the presence of EMPF and EHV5 DNA suggests that the virus is involved in the development of lung fibrosis. This is corroborated with the findings of a study on a closely related gammaherpesvirus murine herpesvirus type 4 (MuHV4). MuHV4 induces lung fibrosis in mice with a progressive deposition of interstitial collagen, increased transforming growth factor β and T helper 2 cytokine expression and hyperplasia of type II pneumocytes (Mora *et al.*, 2005). Similarly in humans, the development of idiopathic pulmonary fibrosis has been linked to the gammaherpesvirus Epstein Barr virus (EBV) (Egan *et al.*, 1995; Vergnon *et al.*, 1984). In addition, Williams *et al.* (2013) were able to experimentally induce lung fibrosis in horses upon direct delivery of virulent EHV5 strains into the lungs. However, the choice of viral strain, immunologic status of experimental animals and inoculation route may have favoured the outcome of disease. So far, the exact pathogenic role played by EHV5 in EMPF is unknown. The virus may be an etiologic agent or cofactor in the development of EMPF (Williams *et al.*, 2013; Wong *et al.*, 2008).

Despite the large number of epidemiological studies, little is known about the exact pathogenesis of EHV5 and many statements remain speculative. It is assumed that foals become infected through the upper respiratory tract around the age of 1 - 6 months (Bell *et al.*, 2006a). Closely related gammaherpesviruses, such as human herpesvirus type 8 (HHV8), bovine herpesvirus type 4 (BoHV4) and MuHV4 commonly spread through sexual contact or intrauterine transmission. Still, the presence of EHV5 in the equine reproductive tract has not been reported yet (Davison, 2011; Donofrio *et al.*, 2007; François *et al.*, 2013). Following primary infection, EHV5 establishes latency to persist in its host. Viral DNA is commonly isolated from blood-derived PBMC (mainly T and B lymphocytes) of healthy horses, indicating that these leukocyte subpopulations are the latency reservoirs of EHV5 (Bell *et al.*, 2006a; Mekuria *et al.*, 2017; Richter *et al.*, 2009; Torfason *et al.*, 2008). However, the exact mechanism used by EHV5 to reach and infect these cells is unknown. Besides blood- and lymph node-derived PBMC, also alveolar macrophages were found to harbour the virus (Poth *et al.*, 2009; Williams *et al.*, 2007; Williams *et al.*, 2013; Wong *et al.*, 2008). However, whether this observation was due to a direct viral infection or a consequence of phagocytosis remains speculative. In the lungs of horses suffering from EMPF, EHV5 antigens were additionally localized in alveolar pneumocytes and interstitial fibroblasts, indicating that the virus can infect these cell types (Williams *et al.*, 2013).

Although EHV5 is an old pathogen, it only recently attracted the attention of clinicians, horse-owners and researchers due to its association with EMPF. Effective therapies are lacking due to the limited knowledge on EHV5 pathogenesis in the horse. Therefore, our study aimed to uncover some of the first key steps herein.

Material and methods

Virus

The equine herpesvirus type 5 (EHV5) KB-P48 strain was kindly provided by dr. K. Borchers and originates from the blood taken of a captive Przewalski's wild horse. The horse had high immunoperoxidase monolayer assay (IPMA) and virus neutralizing (VN) anti-EHV5 antibody titers, but showed no clinical symptoms. The virus was propagated on rabbit kidney (RK13) cells and used at the 6th passage.

The alphaherpesvirus equine herpesvirus type 1 (EHV1) is known to infect both leukocytes (e.g. CD173a⁺ monocytic cells, T and B lymphocytes) and the respiratory epithelium of the horse (Gryspeerd *et al.*, 2010; Laval *et al.*, 2015; Vandekerckhove *et al.*, 2010). Therefore, the EHV1 strain 03P37 was used as a positive control during our viral infection assays. The 03P37 strain originates from the blood taken of a paralytic horse during an outbreak in 2003 (van der Meulen *et al.*, 2003a). The virus was propagated on rabbit kidney (RK13) cells and used at the 6th passage.

Tissue collection and processing

The nasal septa, tracheae and lungs from three different healthy horses were collected at the slaughterhouse and transported in PBS with calcium and magnesium (PBS^{+Ca+Mg}), supplemented with 0.1 mg/mL gentamicin (ThermoFisher Scientific, Waltham, MA, USA), 0.1 mg/mL kanamycin (Sigma-Aldrich), 100 U/mL penicillin, 0.1 mg/mL streptomycin (ThermoFisher Scientific) and 0.25 µg/mL amphotericin B (ThermoFisher Scientific).

Respiratory mucosal explant isolation and cultivation

Nasal and tracheal mucosal explants were prepared and cultivated as previously described (Van Cleemput *et al.*, 2017; Vandekerckhove *et al.*, 2009). Lung explants were obtained following a technique described for pigs with minor adaptations (Van Poucke *et al.*, 2010). Briefly, lung tissue was first cut up in cubes of approximately 1 cm x 1 cm x 5 cm (W x H x L). These cubes were then transferred to a 20 mL syringe containing 5 mL of 4% agarose (low temperature gelling; Sigma-Aldrich), diluted in PBS. After filling the syringe with 5 mL of additional agarose, it was transferred to 4°C until the agarose solidified (15 min). The tip of the syringe was cut off, before gently pushing the plunger and thereby moving the embedded lung tissue out of the barrel. Using a cryotome blade, thin lung tissues slices of 1 mm were cut and transferred to a petridish. Here, tissues were thoroughly washed to remove excess agarose and

finally trimmed to a surface of approximately 25 mm². Lung explants were transferred to 6 well plates, submerged in serum-free medium (DMEM/RPMI [ThermoFisher Scientific], supplemented with 0.1 mg/mL gentamicin, 100 U/mL penicillin, 0.1 mg/mL streptomycin, and 0.25 µg/mL amphotericin B) and cultivated at 37°C and 5% CO₂.

EREC isolation and cultivation

Primary equine respiratory epithelial cells (EREC) were isolated and cultured as described previously (Quintana *et al.*, 2011; Van Cleemput *et al.*, 2017).

Isolation of equine monocytes, T and B lymphocytes

Equine PBMC were isolated as described previously (Laval *et al.*, 2015). The collection of blood was approved by the ethical committee of Ghent University (EC2017/118). Ten hours post seeding, CD172a⁺ monocytic cells had adhered to the plastic (purity >90%, as assessed by flow cytometry (Laval *et al.*, 2015)) and non-adherent cells consisted of two dominant leukocyte populations: T and B lymphocytes. Following removal of non-adherent cells, equine CD172a⁺ monocytes were further maintained in RPMI supplemented with 5% FCS and antibiotics. Equine T lymphocytes were separated from B lymphocytes by negative selection magnetic-activated cell sorting (MACS). In summary, 5×10⁷ cells were incubated with a mouse anti-horse pan B lymphocyte antibody (clone CVS36, directed against the equine Ig light chains, Bio-Rad), diluted in PBS with 10% negative goat serum (NGS) for 1 h at 4°C. Cells were washed in ice-cold elution buffer (PBS + 2 mM EDTA + 2% FCS) and re-suspended in elution buffer, containing 100 µL rat anti-mouse IgG microbeads for 1 h at 4°C. Next, cells were washed in elution buffer before transferring them onto an LS column (MACS Miltenyi Biotech, Cologne, Germany). The cell-fraction that went through the column was collected and contained over 95% positive CD3⁺ T lymphocytes, as assessed by flow cytometry after indirect immunofluorescent staining with a mouse anti-equine CD3 monoclonal antibody (clone UC_F6G; California University, Davis, Figure 1A). The remaining cell-fraction contained the Ig light chain⁺ B lymphocytes, as assessed by flow cytometry after indirect immunofluorescent staining with a mouse anti-pan B lymphocyte antibody (clone CVS36; Figure 1B). Finally, equine T and B lymphocytes were counted using a Bürker counting chamber and were seeded in RPMI supplemented with 5% FCS, 1% MEM non-essential amino-acids, 1% sodium pyruvate, 4 U/mL interleukin-2 and antibiotics.

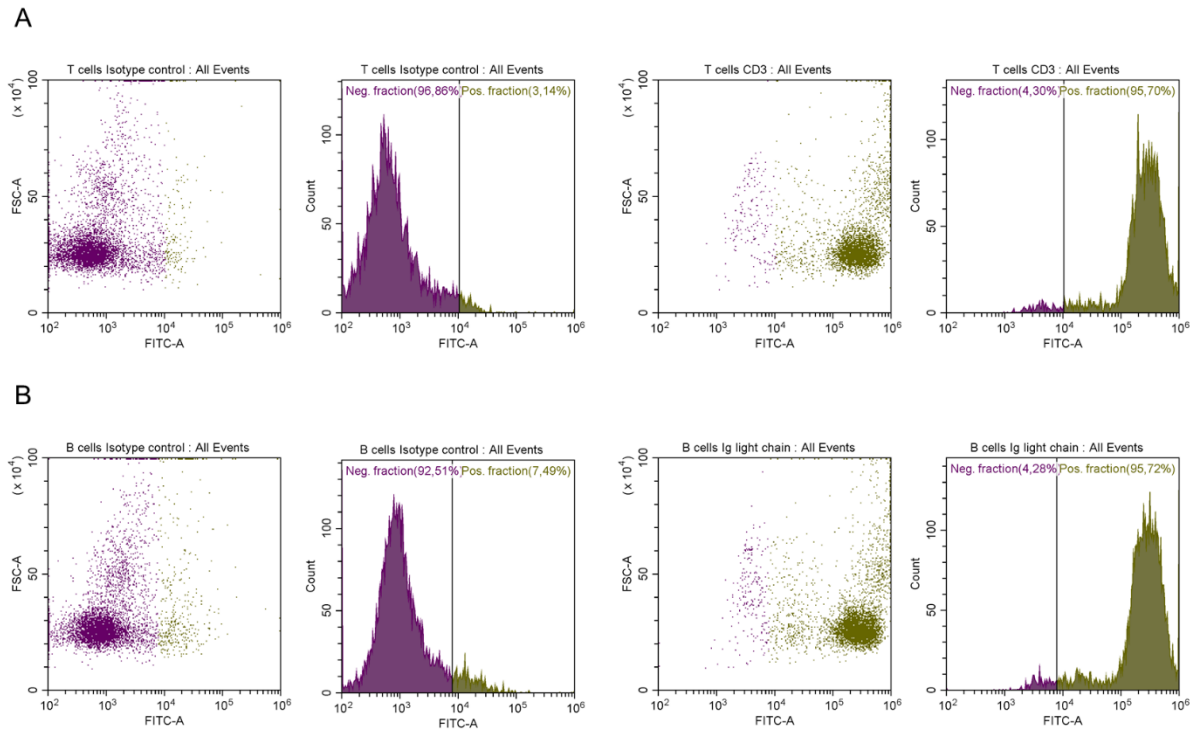


Figure 1. Flow cytometric analysis of the equine T and B lymphocyte populations' purity. Equine T and B lymphocytes were diluted in PBS, containing 10% NGS and antibodies (1:20) for 1 h at 4°C. Equine T and B lymphocytes were incubated with a mouse monoclonal anti-CD3 antibody (clone UC_F6G) or a mouse monoclonal anti-pan B lymphocyte antibody (clone CVS36), respectively. The mouse monoclonal anti-PCV2 antibody (A27) was used as isotype (IgG1) control antibody. After a centrifugation step, cells were incubated with a goat anti-mouse IgG FITC®-conjugated antibody for 1 h at 4°C. Finally, cells were analysed with a CytoFLEX flow cytometer (Beckman Coulter Life Sciences, Indianapolis, USA).

Viral infection assays

Respiratory mucosal explants

Explants were cultured 24 h for adaptation before thoroughly washing and transferring them to a clean 24-well plate, as previously published (Vandekerckhove *et al.*, 2009). While lung explants were left untreated, nasal and tracheal explants were incubated with 8 mM EGTA or PBS^{+Ca+Mg} (control) for 1 h at 37°C to dissociate intercellular junctions (Van Cleemput *et al.*, 2017). Following a thorough washing step, nasal, tracheal and lung explants were subsequently exposed to 10^{6.5} TCID₅₀ of the KB-P48 EHV5 strain or the 03P37 EHV1 strain (positive control) for 1 h at 37°C. Explants were then washed 3 times in PBS to remove unbound virus particles. Finally, explants were placed back onto their gauzes and serum-free medium was added. At corresponding time points, explants were placed into methylcellulose-filled plastic tubes and snap-frozen at -80°C until further processing.

EREC

We recently described a protocol for apical versus basolateral infection of EREC by EHV1 in a transwell system (Van Cleemput *et al.*, 2017). Cells were grown to confluency and the transepithelial electrical resistance (TEER) was measured daily until a steady TEER of ~500-700 $\Omega \times \text{cm}^{-2}$ was attained. The apical surface of EREC was then treated with 8 mM EGTA or $\text{PBS}^{+\text{Ca}+\text{Mg}}$ for 30 min at 37°C to dissociate the ICJ. Following a washing step in PBS, cells were exposed to 100 μL KB-P48 EHV5 strain (MOI of 1) or 03P37 EHV1 strain (MOI of 1) at either the apical or the inverted basolateral surface for 1 h at 37°C. Non-adsorbed virus particles were removed by washing the EREC three times with DMEM/F12. Fresh EREC medium was added to the platewells and cells were further incubated at the air-liquid interface. At corresponding time points, cells were fixed in methanol for 20 min at -20°C and stored dry at -20°C until further processing.

Equine monocytes, T and B lymphocytes

Monocytes, grown on cover slips, were mock-inoculated or inoculated with either EHV5 (MOI 1 or 10) or EHV1 (MOI 1; positive control) in 200 μl monocyte medium for 1 h at 37°C. Afterwards, the cells were gently washed twice to remove the inoculum and further incubated with fresh medium. At 6 h, 24 h, 48 h, 72 h and 96 hpi (hours post-inoculation), cell supernatant was collected and cells were fixed in methanol for 20 min at -20°C and stored dry at -20°C until further processing.

T and B lymphocytes were inoculated at a concentration of 2.5×10^6 cells/mL with EHV5 (MOI 1 or 10) or EHV1 (MOI 1) diluted in lymphocyte medium for 1 h at 37°C. The inoculum was removed by 2 centrifugation steps at 300 x g and cells were further incubated in 24-well plates with fresh medium. At 6 h, 24 h, 48 h, 72 h and 96 hpi, cells were pelleted by centrifugation at 300 g. The supernatant, containing free virus particles, was collected and cells were fixed in 1% paraformaldehyde (PFA) for 10 min at room temperature (RT) and finally stored in PBS at 4°C until further processing.

Polyclonal anti-EHV5 antibody

The polyclonal horse anti-EHV5 antibody originates from blood taken from a 9-year old Shetland pony stallion (Sultan) intended for routine diagnostic serological examination. The pony was kept in a premise, where one of the five horses (Haflinger breed) showed signs of nasal discharge and dullness and was diagnosed with EHV5 by PCR on a nasal swab. The affected horse was isolated from the herd and all horses (the Haflinger and four Shetland ponies)

were screened for the presence of EHV5-specific antibodies, regarding further isolation management. The amount of anti-EHV5 specific IPMA and VN antibodies was semi-quantitatively determined on RK13 cells using an IPMA (10^2 TCID₅₀ KB-P48) or a seroneutralization test, respectively. Antibodies against EHV5 were present in the sera of all five horses and the titer ranged from 2 to >256 (Sultan) for VN antibodies and from 2560 to 40960 (Sultan) for IPMA antibodies. The antibodies from Sultan's serum were then purified and biotinylated, similarly to the polyclonal horse anti-EHV1 antibody previously made in our lab (van der Meulen *et al.*, 2003b). As shown in Figure 2, left panels, the positive signal in EHV5-infected RK13 cells following both immunofluorescence (A) and immunocytological (B) staining with the biotinylated Sultan antibody (1:20) and subsequent incubation with streptavidin-FITC[®] or streptavidin-HRP, respectively, confirmed its suitability in further staining experiments. The biotinylated polyclonal horse anti-EHV1 antibody mixture did not contain anti-EHV5 antibodies and was used as a negative control (Figure 2).

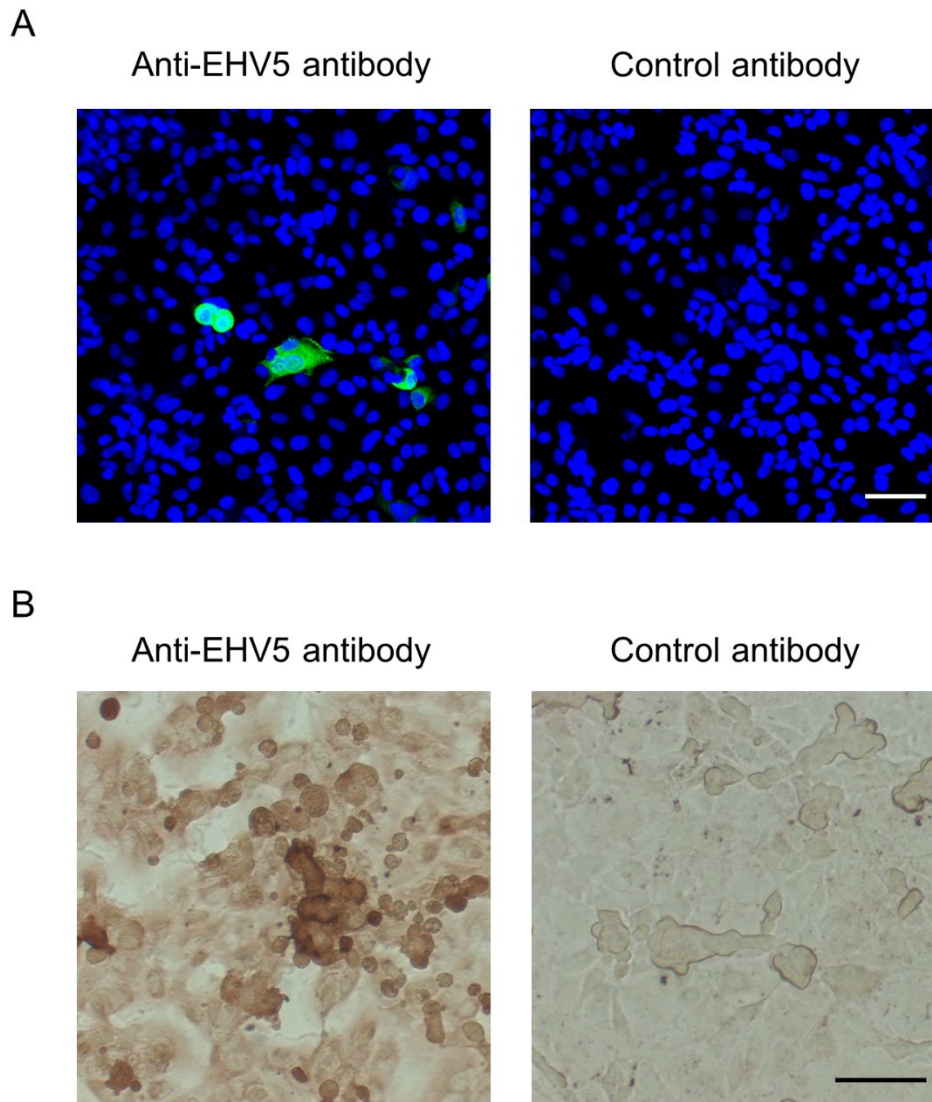


Figure 2. Validation of the polyclonal horse anti-EHV5 antibody (Sultan). The biotinylated polyclonal horse anti-EHV5 antibody (Sultan) recognizes EHV5 antigens in EHV5-infected RK13 cells 48 hpi in both (A) immunofluorescence and (B) immunocytological staining (left panels). The biotinylated polyclonal horse anti-EHV1 antibody was included as control antibody (right panels). The scale bar represents 50 μ m.

Immunofluorescent staining and confocal microscopy

Explants

Sixteen μ m thick cryosections of equine nasal, tracheal and lung explants were cut using a cryostat at -20°C and loaded onto 3-aminopropyltriethoxysilane-coated (Sigma-Aldrich) glass slides. Slides were then fixed in 4% PFA for 15 min and subsequently permeabilized in 0.1% Triton-X 100 diluted in PBS. Non-specific binding sites (e.g. equine IgG receptor) were first blocked by 45 min incubation with 10% negative horse serum, obtained during a previous *in vivo* study (Vairo *et al.*, 2012), diluted in PBS at 37°C . To label EHV5 and EHV1 proteins, the polyclonal biotinylated horse anti-EHV5 antibody (Sultan; 1:20) or polyclonal biotinylated

horse anti-EHV1 antibody, respectively, was used for 1 h at 37°C, followed by incubation with streptavidin-FITC[®] for 1 h at 37°C. Nuclei were detected by staining with Hoechst 33342 (ThermoFisher Scientific). Transwell membranes were excised from the culture inserts and mounted on glass slides using glycerol-DABCO. The number of viral plaques and/or single infected cells was evaluated on 100 consecutive cryosections, using confocal microscopy.

A double immunofluorescent staining of lung explant cryosections was performed to identify EHV5-positive cells as cytokeratin-positive. For this, cryosections were incubated for 1 h with the polyclonal biotinylated anti-EHV5 antibody (1:20), together with the monoclonal mouse anti-pan cytokeratin antibody (clone AE1/AE3; Agilent, Santa Clara, USA; 1:100). After a washing step, cryosections were incubated with streptavidin-FITC[®] and a goat anti-mouse IgG Texas Red[®]-conjugated antibody (ThermoFisher Scientific). Nuclei were detected by staining with Hoechst 33342.

EREC

Methanol-fixed EREC were directly stained in the transwells, as described above. The complete EREC monolayer was analysed using a Leica (TCS SPE) confocal microscope. As a negative control, mock-inoculated cells were stained following the above protocols. The polyclonal horse anti-EHV1 antibody was included as isotype control antibody (van der Meulen *et al.*, 2003b).

Equine monocytes, T and B lymphocytes

Methanol-fixed monocytes, grown on cover slips, were stained directly in the wells. PFA-fixed lymphocytes were cytopinned onto 3-aminopropyltriethoxysilane-coated (Sigma-Aldrich) glass slides and subsequently permeabilized in 0.1% Triton-X 100 diluted in PBS. Immunofluorescent staining further proceeded as described previously. Slides were mounted with glycerol-DABCO and analysed using confocal microscopy. The percentage of viral antigen-positive cells was calculated based on 300 cells counted in 5 distinct fields. In EHV5-infected lymphocytes, the percentage of cells showing DNA fragmentation due to EHV5 infection was additionally determined.

Cell death analysis

The percentage of mock- or EHV5-inoculated cells showing signs of apoptosis (annexin V-positive) or necrosis (propidium iodide positive) was determined 72 hpi, using the 'Dead Cell Apoptosis Kit' from ThermoFisher Scientific (V13241). Live cells were incubated with the appropriate reagents following the manufacturer's guidelines. Next, cells were fixed in 1% PFA

and stained for EHV5-antigens, as described above. The percentage of apoptotic or necrotic cells was calculated based on 300 cells counted in 5 distinct fields using confocal microscopy.

Virus titration

Cell and explant supernatants were collected at various time points and stored at -80°C until titration. EHV1 and EHV5 titrations were conducted on RK13 cells, which were incubated at 37°C for 7 days. EHV1 titers were determined based on cytopathogenic effect. EHV5 titers were determined based on EHV5-immunocytological staining. Briefly, RK13 cells were washed in PBS, air-dried at 37°C for 1 h and frozen at -20°C for a minimum of 2 h. After thawing, cells were fixed in 4% PFA at 4°C for 15 min. Aspecific binding sites were blocked by incubating the cells with a mixture of Tris-buffered saline (TBS), supplemented with 5% NGS for 20 min at 37°C. EHV5-positive cells were stained with the anti-EHV5 serum, diluted 1:1,000 in TBS with 2% NGS. After washing, a goat anti-horse IgG-peroxidase (Jackson ImmunoResearch, Cambridgeshire, UK) was added in TBS. For detection, a 5% aminoethyl carbazole (AEC) solution, supplemented with 0.025% H₂O₂ was added to the wells for 10 min at 37°C. The enzymatic reaction was stopped by washing the cells in PBS. All titers were expressed as TCID₅₀.

Statistical analyses

Significant differences ($P < 0.05$) between different time points or different MOI were identified by analysis of variances (ANOVA) followed by Tukey's post-hoc test. If homoscedasticity of the variables was not met as assessed by the Levene's test, the data were log-transformed prior to ANOVA. Normality of the residuals was verified by the use of the Shapiro-Wilk test. If the variables remained heteroscedastic or normality was not met after log-transformation, a Kruskal-Wallis' test, followed by a Mann-Whitney's post-hoc test were performed. Significant differences in the percentage of apoptotic cells between mock or EHV5 inoculations were identified by a Student's T test. All analyses were conducted in IBM SPSS Statistics for Windows, version 25.0 (IBM Corp, Armonck, NY, USA).

Results

EHV5 infects lung alveolar cells, but not the equine ciliated respiratory epithelium lining the nasal septum and trachea

To date, it is unclear how exactly EHV5 establishes a life-long infection in new hosts. The virus is delivered to the respiratory tract through inhalation and somehow finds its way to latency reservoirs (PBMC). Here, we examined whether EHV5 primarily infects equine respiratory epithelial cells using nasal and tracheal mucosal explant models and primary EREC. In addition, we examined whether EHV5 is able to infect cells within lung explants upon direct delivery.

Explants

Over the time course of the experiment, EHV5-infected cells were not detected in the respiratory epithelium of nasal and tracheal mucosal explants. In contrast, we counted an average of 3 ± 3 and 32 ± 15 EHV1 plaques in 8 mm^2 respiratory epithelium of nasal and tracheal mucosal explants, respectively. As EHV1 infection is known to be enhanced upon disruption of epithelial integrity (Van Cleemput *et al.*, 2017), nasal and tracheal mucosal explants were treated with EGTA prior to inoculation with EHV5. Despite the EGTA pretreatment, EHV5-infected cells were not found in the respiratory epithelium of these explants. Finally, EHV1-positive leukocytes were observed beneath the basement membrane 24 hpi. However, EHV5-positive leukocytes were absent in the EHV5-inoculated nasal and tracheal mucosal explants at all time points.

In lung explants on the other hand, a small amount (22 ± 9) of EHV5-infected cells was present in a volume of 8 mm^3 lung tissue at 72 hpi. EHV5-positive cells were usually found in a cell cluster of approximately 4 ± 2 EHV5-positive cells per cluster. Double immunofluorescent staining for cytokeratin confirmed that these infected cell clusters were of epithelial origins. Representative confocal images are given in Figure 3.

Nasal, tracheal and lung explants did not produce detectable progeny EHV5 particles 72 hpi, as viral titers in the supernatant remained below $1 \log_{10}\text{TCID}_{50}/\text{mL}$. The supernatant of nasal and tracheal mucosal explants contained an EHV1 titer of 2.4 ± 0.9 and $2.5 \pm 0.5 \log_{10}\text{TCID}_{50}/\text{mL}$, respectively.

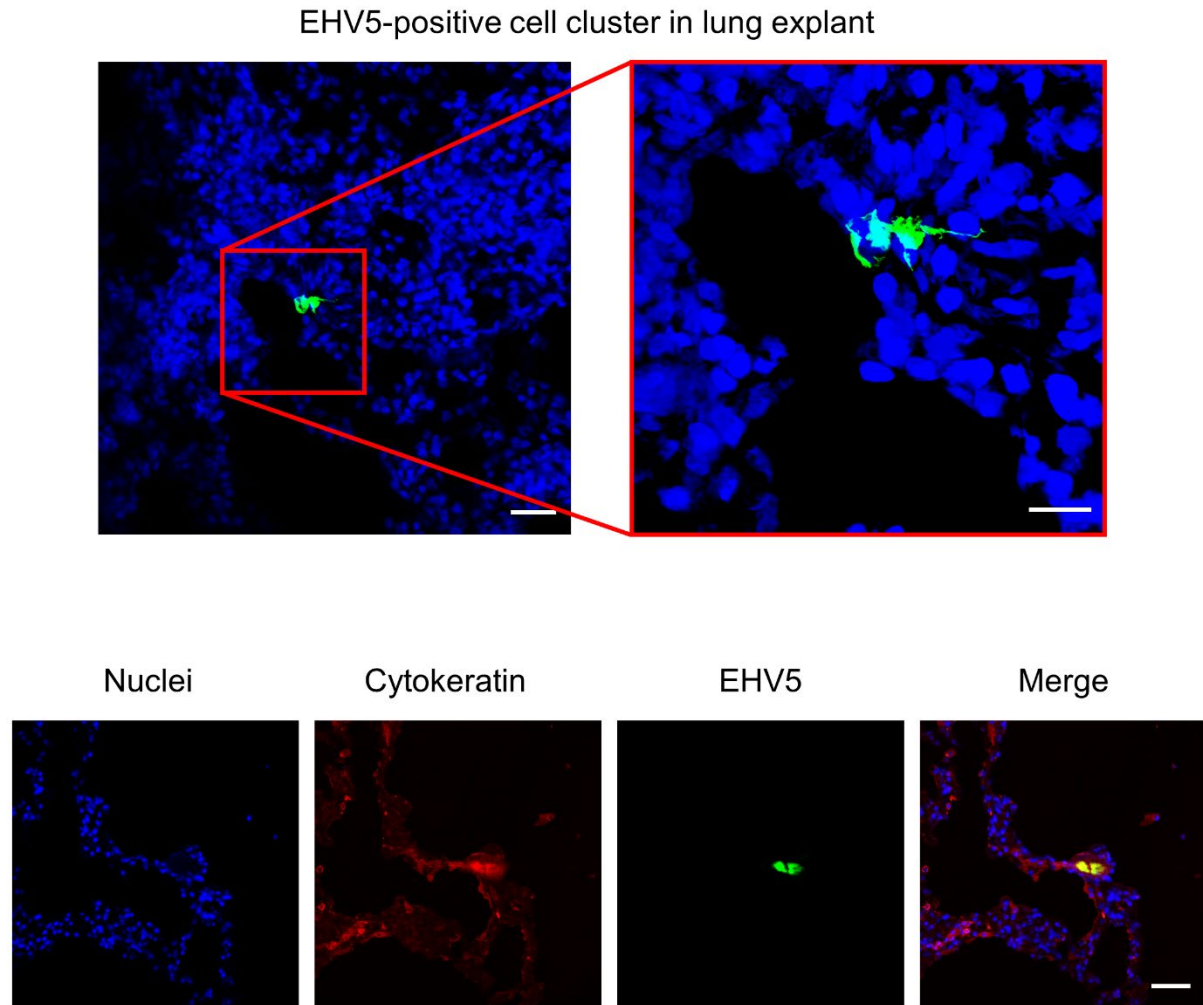


Figure 3. EHV5-antigen expression 72 hpi in localized cell clusters within EHV5-inoculated lung explants. In the upper panel, cryosections were stained for EHV5 antigens (Sultan; green) and cell nuclei (Hoechst; blue). In the lower panel, cryosections were simultaneously stained for EHV5 antigens (Sultan; green), cytoke­ratin (AE1/AE3; red) and cell nuclei (Hoechst; blue). The scale bar represents 50 μm .

EREC

EHV1 formed 1 ± 1 and 55 ± 26 viral plaques in 3×10^4 EREC following inoculation at the apical or basolateral surfaces, respectively. In contrast, none of the cells were EHV5-positive 96 h following inoculation at both surfaces. Similarly as observed in nasal and tracheal explants, disruption of EREC integrity with EGTA prior to inoculation did not overcome the restriction to EHV5 infection of the cells.

EHV5 does not replicate in equine monocytic cells, but induces a lytic infection in equine T and B lymphocytes *in vitro*

As the equine ciliated respiratory epithelium did not support EHV5 growth, we hypothesized that EHV5 directly infects PBMC. Therefore, we examined the ability of EHV5 to infect and replicate in equine PBMC. The kinetics of viral protein expression and virus production in equine CD3^+ T lymphocytes, Ig light chain⁺ B lymphocytes and CD172a^+ monocytes was

evaluated by confocal microscopy and virus titration of cell supernatant, respectively. Parallel mock inoculations confirmed the absence of EHV5-positive T lymphocytes, B lymphocytes and monocytes in the blood donor-derived PBMC.

T lymphocytes - In EHV5-inoculated T lymphocytes (MOI of 1), $1 \pm 1\%$ of the cells started to express viral proteins in the cytoplasm at 6 hpi, as shown in Figure 4, left graph. This percentage slightly, but not significantly increased over time to $2 \pm 2\%$ at 48 hpi and declined again to $1 \pm 1\%$ at 96 hpi. Increasing the MOI 10 times rapidly and significantly ($P < 0.05$) increased the percentage of infected cells to $6 \pm 3\%$ at 6 hpi and $9 \pm 4\%$ at 24 hpi. Starting from this time point, the percentage of EHV5-infected T lymphocytes declined gradually to $3 \pm 1.5\%$ at 96 hpi). Representative confocal images are shown in the upper panel of Figure 4. EHV1 antigens were visible in $1 \pm 0.3\%$ equine T lymphocytes 24 hpi.

No significant increase in extracellular EHV5 titer was observed over the course of the experiment (Figure 4, right graph).

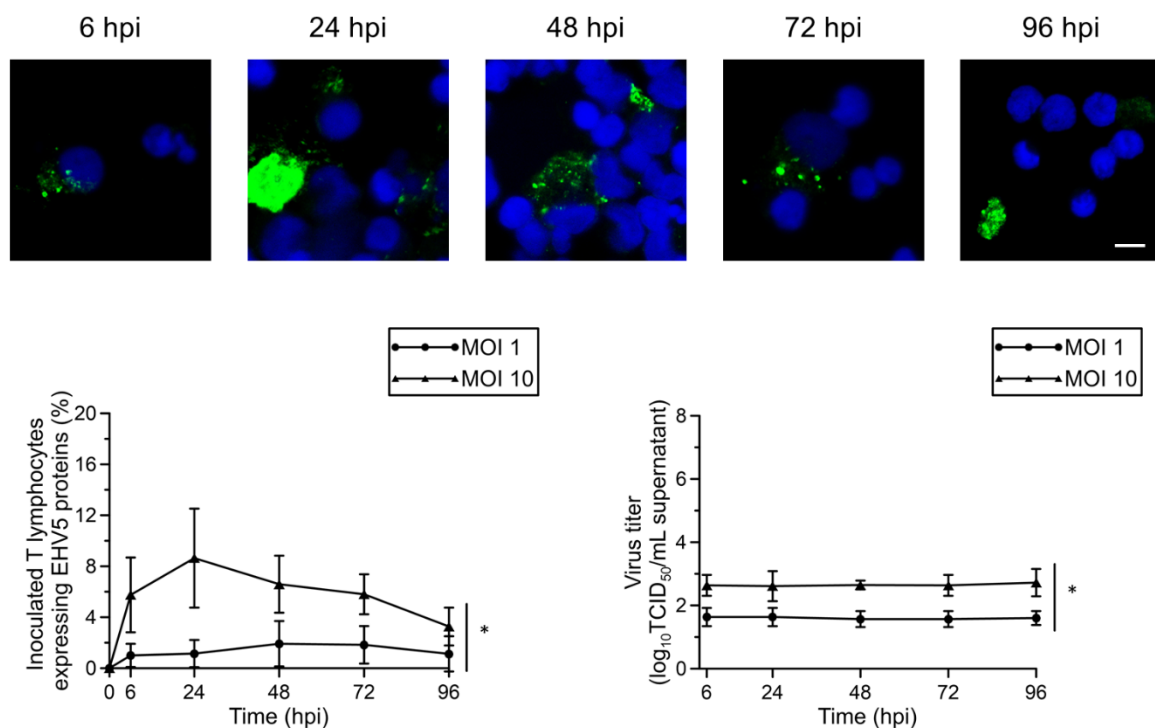


Figure 4. Expression of EHV5 antigens in EHV5-inoculated (MOI 1 or 10) T lymphocytes. At indicated time points, cells were fixed and immunofluorescently stained for EHV5 antigens. Upper panel; representative confocal images of EHV5 antigen expression (Sultan; green) in T lymphocytes. Cell nuclei were counterstained with Hoechst (blue). The scale bar represents 5 μ m (upper panel). Lower left panel; the percentage of EHV5-positive cells was calculated based on 300 cells counted in 5 distinct field. Lower right panel; the virus titer was determined in supernatant on RK13 cells. Data are represented as means \pm SD and asterisks indicate significant differences ($P < 0.05$) between MOI 1 and 10. Experiments were performed on 3 individual horses.

B lymphocytes - EHV5 inoculation of B lymphocytes at a MOI of 1 resulted in an average of $1 \pm 0.5\%$ EHV5-positive cells 6 hpi (Figure 5, left graph). This percentage significantly ($P < 0.05$) increased over time to a peak of $3.5 \pm 1\%$ at 72 hpi. At 96 hpi, only $2 \pm 1\%$ of the inoculated B lymphocytes remained EHV5-positive. Again, increasing the MOI to 10 resulted in a significant increase in cells expressing EHV5 antigens already at 6 hpi ($3 \pm 2\%$). This percentage further increased in a time-dependent manner to $10 \pm 4\%$ at 72 hpi. Similarly as to EHV5-inoculated T lymphocytes, the percentage of EHV5-positive inoculated B lymphocytes decreased again at 96 hpi ($5.5 \pm 2\%$). Representative confocal images are shown in the upper panel of Figure 5. We observed $0.5 \pm 0.2\%$ EHV1-positive equine B lymphocytes 24 hpi.

No significant increase in extracellular EHV5 titer was observed over the course of the experiment (Figure 5, right graph).

Monocytes - EHV5 antigens were not detected in EHV5-inoculated equine monocytes throughout the course of the experiment. In contrast, EHV1 antigens were expressed in $3.7 \pm 1.4\%$ of the inoculated monocytes 24 hpi.

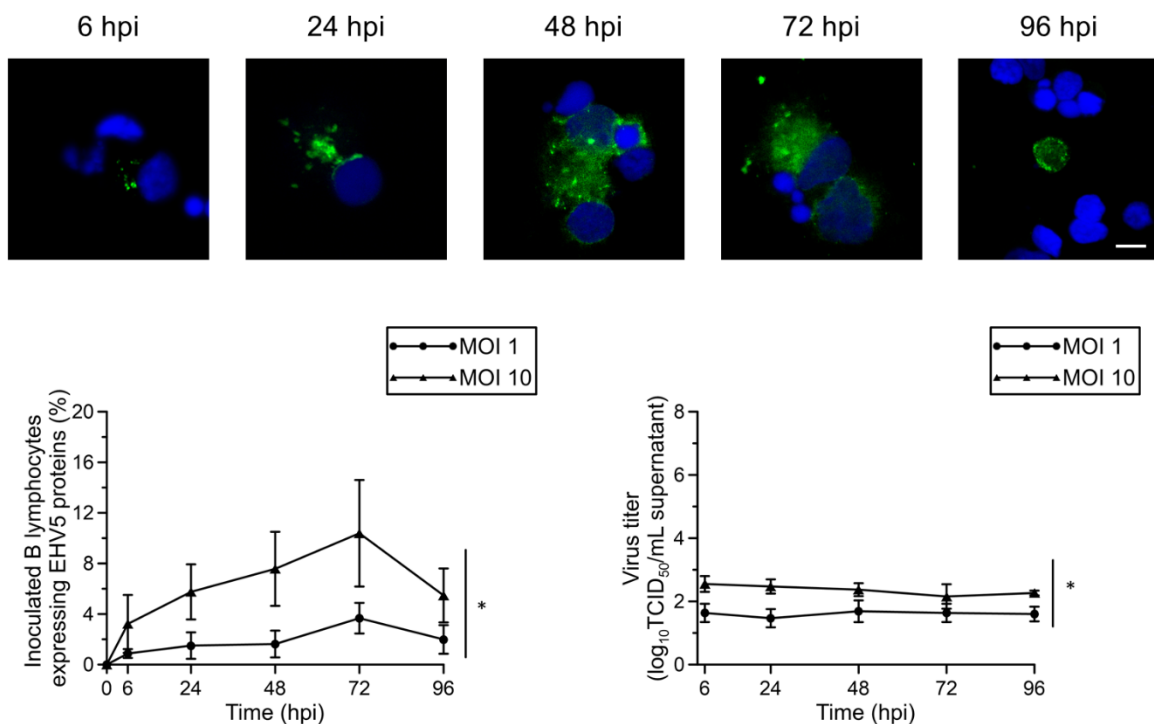


Figure 5. Expression of EHV5 antigens in EHV5-inoculated (MOI 1 or 10) B lymphocytes. At indicated time points, cells were fixed and immunofluorescently stained for EHV5 antigens. Representative confocal images of EHV5 antigen expression (Sultan; green) in B lymphocytes. Cell nuclei were counterstained with Hoechst 33342 (blue). The scale bar represents 5 μm (upper panel). The percentage of EHV5-positive cells was calculated based on 300 cells counted in 5 distinct fields (lower left panel). The virus titer was determined in supernatant on RK13 cells (right panel). Data are represented as means \pm SD and asterisks indicate significant differences ($P < 0.05$) between MOI 1 and 10. Experiments were performed on 3 individual horses.

EHV5 lytic infection causes nuclear fragmentation and apoptosis in equine T and B lymphocytes

It is known that the human gammaherpesvirus Epstein-Barr virus (EBV) induces DNA fragmentation during lytic infection of human B lymphoblasts (Kawanishi, 1993). This DNA fragmentation contributes to the cytopathic effect of EBV and eventually ends in cell death. As EHV5 was able to induce a lytic replication in equine T and B lymphocytes, we analysed whether cell nuclear morphology changed upon infection using Hoechst 33342. The fluorescent dye Hoechst 33342 binds to the minor groove of double-stranded DNA and can be used in immunofluorescent staining to identify chromatin condensation and nuclear fragmentation (Susin *et al.*, 1999). As nuclear fragmentation preludes cell death, we additionally analysed the percentage of cells showing signs of apoptosis (annexin V-positive) or necrosis (propidium iodide-positive) (Lincz, 1998). Apoptosis is a tightly regulated form of cell death and can be recognized by the binding of annexin V to phosphatidyl serine on the cell surface (Koopman *et al.*, 1994). In contrast, propidium iodide can penetrate the plasma membrane of necrotic cells and subsequently binds to nucleic acids.

Nuclear fragmentation - Starting from 6 hpi, we observed that EHV5 viral proteins co-localized with the nucleus of approximately $0.5 \pm 0.5\%$ of the EHV5-inoculated (MOI 10) T lymphocytes (Figure 6A) and $1 \pm 1\%$ of EHV5-inoculated (MOI 10) B lymphocytes (Figure 6B). Interestingly, all of these cells exhibited a translucent and/or punctuated Hoechst signal, as shown in the right panels of Figure 6A and B. The number of EHV5-positive T lymphocytes showing signs of nuclear fragmentation significantly ($P < 0.05$) increased to $3 \pm 1\%$ at 48 hpi and remained stable starting from this time point. The number of EHV5-positive B lymphocytes showing signs of nuclear fragmentation steadily increased in a time-dependent manner to $4.5 \pm 1.5\%$ at 96 hpi.

Cell death analysis - As shown in Figure 7, the percentage of apoptotic cells was significantly ($P < 0.001$) higher in EHV5-inoculated T lymphocytes ($6.5 \pm 1.5\%$) and B lymphocytes ($11.5 \pm 3\%$) 72 hpi, compared to mock-inoculated T lymphocytes ($4 \pm 1.5\%$) and B lymphocytes ($8 \pm 2\%$), respectively. Simultaneous staining of apoptosis (annexin V) and EHV5 antigens confirmed their co-localisation in both T and B lymphocytes, as illustrated in the right panels of Figure 7.

No significant difference was found in the percentage of necrotic cells between EHV5- and mock-inoculated T and B lymphocytes at 72 hpi.

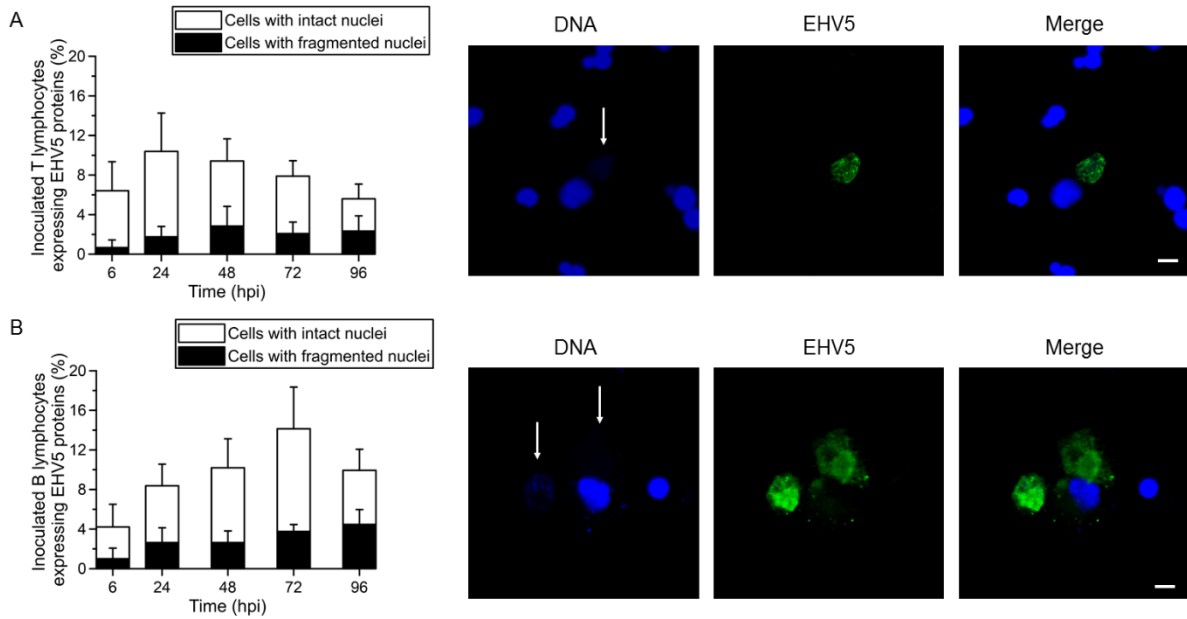


Figure 6. Induction of chromatin condensation and nuclear fragmentation in EHV5 antigen-expressing (A) T lymphocytes and (B) B lymphocytes following inoculation at a MOI of 10. Left panels; the percentage of EHV5-inoculated cells expressing both EHV5 antigens and nuclear fragmentation is indicated by black bars. White bars represent the percentage of inoculated cells that express EHV5 antigens but show no signs of nuclear fragmentation. Data are represented as mean + SD and were obtained from three individual horses. Right panels; representative confocal images of EHV5 expression (Sultan; green) in T and B lymphocytes. Cell nuclei were counterstained with Hoechst (blue). Note the translucent and/or compartmented appearance of cell nuclei (white arrows). The scale bar represents 5 μ m.

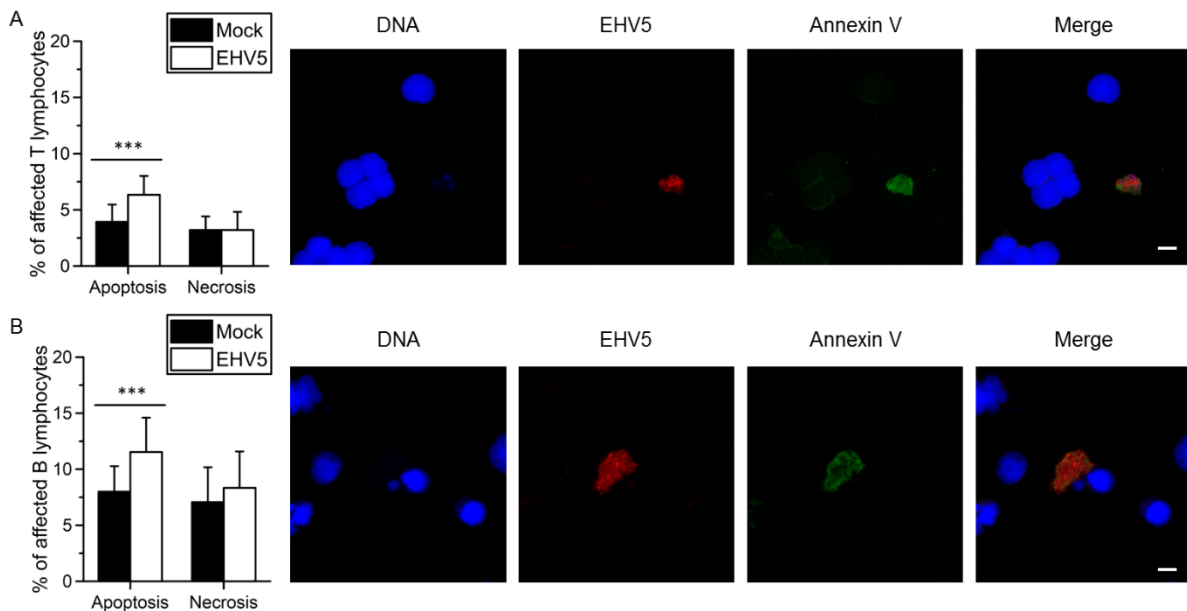


Figure 7. Induction of apoptosis in EHV5 antigen-expressing (A) T lymphocytes and (B) B lymphocytes following inoculation at a MOI of 10. Left panels: the percentage of mock- (black bars) or EHV5- (white bars) inoculated cells showing signs of apoptosis (left) or necrosis (right). Data are represented as means + SD and asterisks indicate significant differences (***) $P < 0.001$ between mock- and EHV5-inoculated cells. Experiments were performed on 3 individual horses. Cell death was analysed on living cells by the 'Dead Cell Apoptosis Kit' from ThermoFisher Scientific. Apoptosis was characterized by the binding of annexin V to cellular phosphatidyl serine and necrosis was identified by binding of propidium iodide to nucleic acids in the cell. Right panels: after incubation with annexin V-FITC® (green), cells were fixed and stained for EHV5 antigens (Sultan: red). Cell nuclei are counterstained in blue. The scale bar represents 5 μ m.

Discussion

The present study aimed at uncovering some of the first crucial steps in EHV5 pathogenesis, starting with the identification of susceptible target cells. For this, we first examined whether EHV5 can replicate in epithelial cells lining the horse's respiratory tract. Next, we evaluated EHV5 replication kinetics in different PBMC subpopulations, as PBMC are the presumable viral latency reservoirs.

Following direct delivery of EHV5 to equine nasal septum or tracheal mucosal explants, viral protein expression was not detected in respiratory epithelial cells or in single patrolling immune cells. These findings were corroborated in primary equine respiratory epithelial cells (EREC), in which no EHV5-positive cells were found following inoculation at both the apical or basolateral surface. In comparison, human epithelial cells are difficult to infect *in vitro* with the human gammaherpesvirus Epstein Barr virus (EBV) (Shannon-Lowe and Rowe, 2014). However, the virus is able to efficiently infect epithelial cells following EBV propagation in B lymphocytes (Borza and Hutt-Fletcher, 2002). On the contrary, epithelial-cell derived virus particles can infect B lymphocytes more efficiently. This state-of-the-art alternating cell tropism is facilitated through the degradation of viral gp42 by MHC II trafficking in B lymphocytes, thereby liberating gH/gL from the gp42/gH/gL complex. It was proposed that free gH/gL complexes are necessary for the interaction between the virion and epithelial cells. These observations may be in line with our data, as the epithelial cell-derived stock of EHV5 could efficiently infect equine T and B lymphocytes, but was unable to infect the ciliated respiratory epithelium. Interestingly, a few alveolar cells became EHV5-positive following inoculation of equine lung explants. In an *in vivo* study from Williams *et al.* (2013), EHV5 antigens were also detected in alveolar epithelial cells upon direct delivery of virus particles to the lungs. However, care must be taken by extrapolating these results to the real *in vivo* situation, as it is highly unlikely that free virus particles can directly access the lungs upon inhalation in healthy horses. Indeed, most viruses that overcome the nasal filter end up in the trachea and are disposed by the mucociliary escalator (Cohn and Reinero, 2007; Harkema *et al.*, 2006).

Next, we demonstrated that the percentage of positive T and B lymphocytes increased over time upon *in vitro* inoculation, reaching a peak at 24 hpi and 72 hpi, respectively, and then declined. This decay might indicate that infection was cleared. For example, apoptosis or controlled cell destruction can act as an innate response to counteract viral infection. Indeed, apoptosis prevents viral dissemination, as the cell is carefully disassembled and cleared by the host's immune system (Everett and McFadden, 1999). On the contrary, uncontrolled necrosis is

unfavourable for the host, as this results in the release of cytoplasmic material, including viral particles. In turn, these viral particles might spread in the host and infect new cells. Here, apoptosis, but not necrosis, was induced in up to 50% of the infected equine T and B lymphocytes. In comparison, EBV early proteins participate in the fragmentation of chromosomal DNA and the onset of apoptosis during lytic infection of human lymphoblasts *in vitro* (Kawanishi, 1993). However, the high MOI used in our and the latter experiment might have favoured the onset of apoptosis. Transcription and translation of a high number of viral DNA copies might have flooded the cellular endoplasmic reticulum with viral proteins destined for assembly. In turn, overload of the endoplasmic reticulum could have elicited a cascade of signal transduction pathways, eventually leading to apoptosis (Everett and McFadden, 1999). Indeed, it seems unlikely that a virus, so optimally adapted to its host, kills its host cell on purpose. On the contrary, multiple gammaherpesviruses (e.g. EBV, human herpesvirus type 8, BoHV4) have evolved mechanisms to induce latency and inhibit apoptosis, in order to prolong their survival in the host (Gregory *et al.*, 1991; Katano *et al.*, 2001; Okan *et al.*, 1995; Wang *et al.*, 1997). For example, in latently EBV-infected B lymphocytes, only a limited number of viral-coded proteins are expressed, including latent membrane protein 1 (LMP1). As this protein interacts with apoptotic signals, the virus cleverly guides the infected B lymphocyte towards a long-living (memory) state (Grimm *et al.*, 2005). The establishment of EHV5 latency in equine T and B lymphocytes could further explain the drop of EHV5-positive cells starting from 24 hpi and 72 hpi, respectively.

Although infected lymphocytes clearly produced viral proteins intracellularly, the extracellular virus titer did not increase throughout the course of the experiment. The low viral titers that were observed at all time points presumably reflect remnant inoculum-viral particles. In dying cells, viral proteins were contained through apoptosis. In live EHV5-infected cells, however, assembly of virus particles and/or release of cell-free progeny virions into surroundings must have been hampered. Indeed, herpesvirus infections are commonly non-productive in leukocytes and this strategy allows the virus to remain in its host, undetectable by the immune system (Gergely *et al.*, 1971; Laval *et al.*, 2015; Sarmiento and Kleinerman, 1990). Still, we frequently observed clustering of EHV5-positive T or B lymphocytes, indicating that the virus may spread via cell-cell transfer. Cell-to-cell transfer is a well-known strategy used by herpesviruses to bypass the hostile immune environment of the host, containing phagocytes, antibodies and complement (Imai *et al.*, 1998; Sattentau, 2008). Indeed, previous studies demonstrated that the efficiency of EBV transfer from B lymphocytes to epithelial cells was highly upregulated by cell-cell contact (Imai *et al.*, 1998; Shannon-Lowe *et al.*, 2006). Binding

of EBV gp350 with the B lymphocyte surface protein CD21 was proposed to unmask other putative viral glycoproteins, essential for epithelial cell binding. To investigate whether EHV5 could also be transferred from lymphocytes to EREC, we co-cultured infected lymphocytes at the apical surface of naïve EREC. Still, EHV5 was unable to infect and replicate in EREC (data not shown). It would be interesting to assess viral transfer from lymphocytes to the basolateral surface of EREC, as it would be the case *in vivo*. For example, EBV transfer infection of polarized epithelial cells is restricted to the basolateral surface, even though cell-cell contacts are also established at the apical surface (Shannon-Lowe and Rowe, 2011). The researchers suggested that putative EBV binding and entry receptors on the epithelial cells are similarly restricted to the basolateral surface. Unfortunately, we could not perform this experiment due to technical limitations. The small pore size of the transwells, necessary for EREC support, did not allow sufficient cell-cell contacts between the basolateral surface of EREC and equine lymphocytes (data not shown).

In our study, EHV5 did not replicate in equine monocytes *in vitro* and in fibroblasts of *ex vivo* mucosal explants. This is in contrast with a study from Williams *et al.* (2013), who found viral antigens in the alveolar macrophages and interstitial fibroblasts of the lungs *in vivo*. Differentiated macrophages are more specialized for phagocytosis than monocytes. Thus, the presence of viral antigens within alveolar macrophages of infected horses could merely be a consequence of phagocytosis. In addition, EHV5-positive fibroblasts were only found in a limited number of infected horses several weeks following initial challenge. In our short-living *ex vivo* explant system, EHV5 might not have been able to infect fibroblasts.

Based on this work, we suggest the following hypothetical model for EHV5 pathogenesis in the horse (Figure 8). Upon inhalation in a healthy horse, infectious EHV5 particles do not infect the ciliated respiratory epithelium, but are rather propelled by the mucociliary escalator towards the tonsillar crypts, embedded in the nasopharynx (Mair *et al.*, 1987, 1988; Mair and Lane, 2005). Lymphocytes reside in lymphoid follicles, just underneath the squamous epithelium of tonsillar crypts. As this epithelium contains gaps throughout the crypt surface, EHV5 possibly can directly access susceptible T and B lymphocytes. Following viral replication, virus particles are contained within these cells to protect them from the outer hostile environment. One part of these infected lymphocytes will eventually succumb due to apoptosis. The other part may be 'saved' by EHV5 to function as a life-long latency reservoir. Via periodic reactivation, a latently infected horse will recurrently shed progeny virus to the outer world. Indeed, viral DNA is frequently recovered from PBMC and nasal secretions of healthy horses (Bell *et al.*, 2006a; Mekuria *et al.*, 2017; Richter *et al.*, 2009; Torfason *et al.*, 2008). How exactly the virus escapes

from these lymphocytes to shed progeny virus in respiratory secretions is currently unknown. As for EBV, infected leukocytes might reroute to the respiratory tract and produce virions lacking gp42 (Imai *et al.*, 1998; Shannon-Lowe *et al.*, 2006). These virus particles might then be transferred to epithelial cells, which could amplify the infection and shed a high viral load in respiratory secretions to infect new hosts. Finally, epithelial cell-derived EHV5 particles are optimally designed, i.e. contain gp42, to infect lymphocytes. Regular patrolling within the mucosa-associated lymphoid tissue (MALT) of latently infected lymphocytes brings them to different sites of the respiratory mucosa, including the small bronchioli within the lungs. Here, free virus particles are able to infect alveolar cells and further spread to neighbouring cells using cell-cell transfer. Viral replication, together with host-specific predisposing factors (e.g. age and immunologic response) might eventually trigger the onset of fibrosis and EMPF (King Jr *et al.*, 2011). Overall, our findings established the foundations for future research, which will eventually elucidate the mechanisms regulating EHV5 disease and triggering the development of EMPF.

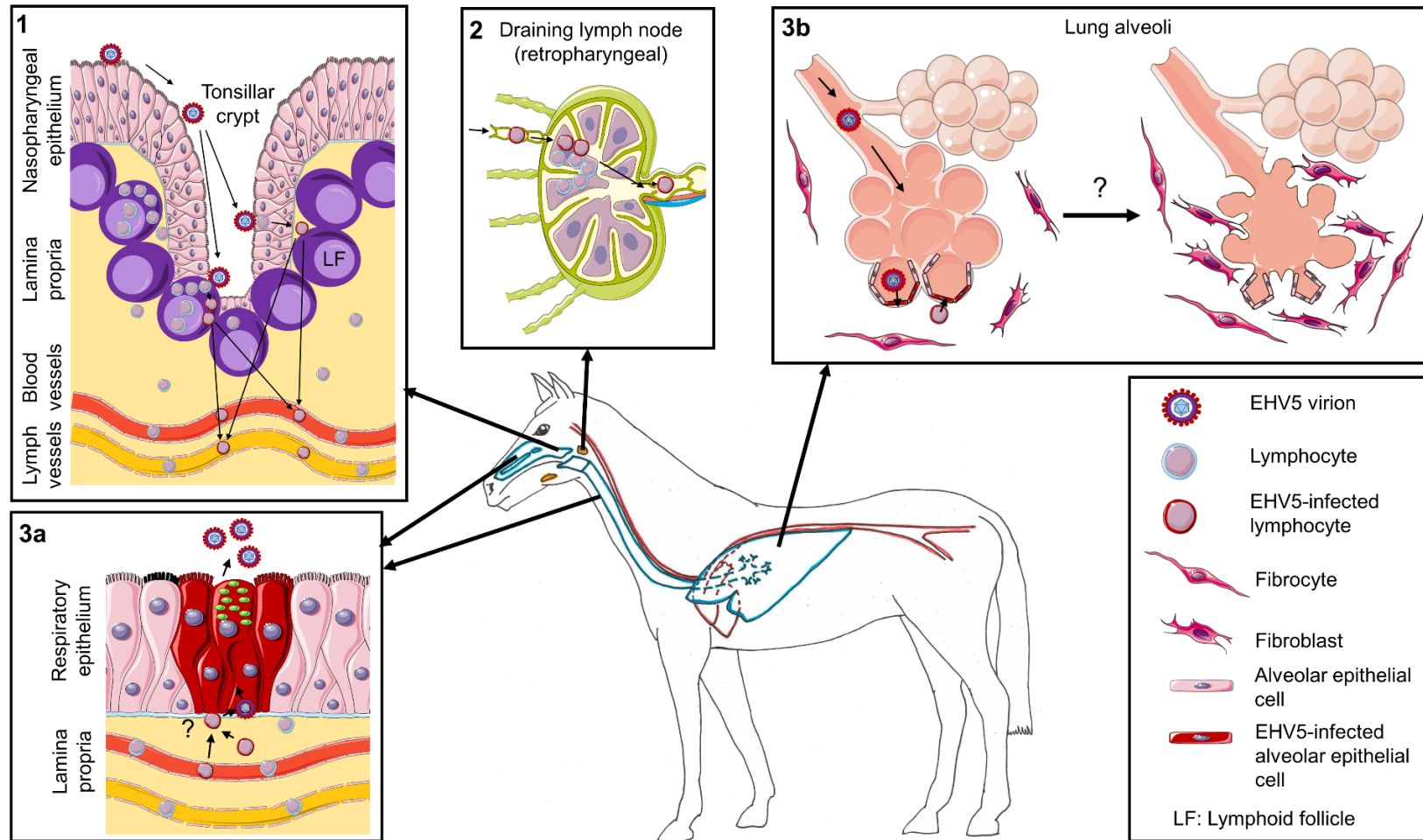


Figure 8. Hypothetical model of EHV5 pathogenesis in the horse. The horse's respiratory tract is designated in blue, the circulatory system in red and upper airway lymph nodes in orange. (1) EHV5 virions are propelled by the mucociliary escalator towards the tonsillar crypts, embedded in the nasopharynx. Here, EHV5 directly infects lymphocytes residing in lymphoid follicles (LF). Infected lymphocytes then transport the virus either directly to the bloodstream or via the lymph vessels and (2) the draining lymph nodes (especially the retropharyngeal lymph nodes) to the bloodstream. In lymphoid follicles or draining lymph nodes, EHV5 spreads to neighbouring lymphocytes via cell-cell transfer. EHV5-infected lymphocytes might either succumb due to apoptosis or survive and function as a life-long reservoir for EHV5. Via the bloodstream or via lymphocyte-homing, EHV5-infected lymphocytes (re)route to different parts of the respiratory tract, e.g. the nasal cavities or the trachea (3a) or the lungs (3b). (3a) EHV5-infected lymphocytes might transfer infection to epithelial cells, which could amplify the infection and shed a high viral load in respiratory secretions. (3b) EHV5 infects alveolar cells and spreads to neighbouring cells via cell-cell transfer. Viral replication, together with host-specific predisposing factors might eventually trigger the onset of fibrosis and EMPF due to yet unknown reasons. Drawings are based on Smart Servier medical art templates.

Acknowledgements

The authors are grateful to Dr. K. Borchers for supplying the EHV5 stock. The authors also acknowledge Carine Boone, Chantal Vanmaercke, Nele Dennequin and Jonathan Vandebogaerde for their excellent technical support. Finally, the authors want to thank the owner of the affected premise for supplying the diagnostic materials.

References

- Akkutay, A.Z., Osterrieder, N., Damiani, A., Tischer, B.K., Borchers, K., Alkan, F., 2014.** Prevalence of equine gammaherpesviruses on breeding farms in Turkey and development of a TaqMan MGB real-time PCR to detect equine herpesvirus 5 (EHV-5). *Archives of virology* 159, 2989-2995.
- Bell, S.A., Balasuriya, U.B., Gardner, I.A., Barry, P.A., Wilson, W.D., Ferraro, G.L., MacLachlan, N.J., 2006a.** Temporal detection of equine herpesvirus infections of a cohort of mares and their foals. *Veterinary microbiology* 116, 249-257.
- Bell, S.A., Balasuriya, U.B., Nordhausen, R.W., MacLachlan, N.J., 2006b.** Isolation of equine herpesvirus-5 from blood mononuclear cells of a gelding. *Journal of veterinary diagnostic investigation* 18, 472-475.
- Borza, C.M., Hutt-Fletcher, L.M., 2002.** Alternate replication in B cells and epithelial cells switches tropism of Epstein-Barr virus. *Nature medicine* 8, 594.
- Cohn, L.A., Reiner, C.R., 2007.** Respiratory Defenses in Health and Disease. *Veterinary Clinics of North America: Small Animal Practice* 37, 845-860.
- Davison, A.J., 2011.** Evolution of sexually transmitted and sexually transmissible human herpesviruses. *Annals of the New York Academy of Sciences* 1230.
- Davison, A.J., Eberle, R., Ehlers, B., Hayward, G.S., McGeoch, D.J., Minson, A.C., Pellett, P.E., Roizman, B., Studdert, M.J., Thiry, E., 2009.** The order herpesvirales. *Archives of virology* 154, 171-177.
- Donofrio, G., Herath, S., Sartori, C., Cavirani, S., Flammini, C.F., Sheldon, I.M., 2007.** Bovine herpesvirus 4 is tropic for bovine endometrial cells and modulates endocrine function. *Reproduction* 134, 183-197.
- Dunowska, M., Meers, J., Wilks, C., 1999.** Isolation of equine herpesvirus type 5 in New Zealand. *New Zealand Veterinary Journal* 47, 44-46.
- Dunowska, M., Wilks, C., Studdert, M., Meers, J., 2002.** Equine respiratory viruses in foals in New Zealand. *New Zealand Veterinary Journal* 50, 140-147.
- Egan, J.J., Stewart, J.P., Hasleton, P.S., Arrand, J.R., Carroll, K.B., Woodcock, A.A., 1995.** Epstein-Barr virus replication within pulmonary epithelial cells in cryptogenic fibrosing alveolitis. *Thorax* 50, 1234-1239.
- Everett, H., McFadden, G., 1999.** Apoptosis: an innate immune response to virus infection. *Trends in Microbiology* 7, 160-165.
- Franchini, M., Akens, M., Bracher, V., v Fellenberg, R., 1997.** Characterisation of gamma herpesviruses in the horse by PCR. *Virology* 238, 8-13.
- François, S., Vidick, S., Sarlet, M., Desmecht, D., Drion, P., Stevenson, P.G., Vanderplasschen, A., Gillet, L., 2013.** Illumination of murine gammaherpesvirus-68 cycle reveals a sexual transmission route from females to males in laboratory mice. *PLoS pathogens* 9, e1003292.
- Gergely, L., Klein, G., Ernberg, I., 1971.** Appearance of Epstein-Barr virus-associated antigens in infected Raji cells. *Virology* 45, 10-21.
- Gregory, C.D., Dive, C., Henderson, S., Smith, C.A., Williams, G.T., Gordon, J., Rickinson, A.B., 1991.** Activation of Epstein-Barr virus latent genes protects human B cells from death by apoptosis. *Nature* 349, 612.
- Grimm, T., Schneider, S., Naschberger, E., Huber, J., Guenzi, E., Kieser, A., Reitmeir, P., Schulz, T.F., Morris, C.A., Stürzl, M., 2005.** EBV latent membrane protein-1 protects B cells from apoptosis by inhibition of BAX. *Blood* 105, 3263-3269.
- Gryspeerd, A.C., Vandekerckhove, A., Garré, B., Barbé, F., Van de Walle, G., Nauwynck, H., 2010.** Differences in replication kinetics and cell tropism between neurovirulent and non-neurovirulent EHV1 strains during the acute phase of infection in horses. *Veterinary microbiology* 142, 242-253.
- Harkema, J.R., Carey, S.A., Wagner, J.G., 2006.** The nose revisited: a brief review of the comparative structure, function, and toxicologic pathology of the nasal epithelium. *Toxicologic pathology* 34, 252-269.

- Hart, K., Barton, M., Williams, K., Flaminio, M., Howerth, E., 2008.** Multinodular pulmonary fibrosis, pancytopenia and equine herpesvirus-5 infection in a Thoroughbred gelding. *Equine Veterinary Education* 20, 470-476.
- Herder, V., Barsnick, R., Walliser, U., Teifke, J.P., König, P., Czerwinski, G., Hansmann, F., Baumgärtner, W., Hewicker-Trautwein, M., 2012.** Equid herpesvirus 5-associated dermatitis in a horse—Resembling herpes-associated erythema multiforme. *Veterinary microbiology* 155, 420-424.
- Imai, S., Nishikawa, J., Takada, K., 1998.** Cell-to-cell contact as an efficient mode of Epstein-Barr virus infection of diverse human epithelial cells. *Journal of virology* 72, 4371-4378.
- Katano, H., Sato, Y., Sata, T., 2001.** Expression of p53 and human herpesvirus-8 (HHV-8)-encoded latency-associated nuclear antigen with inhibition of apoptosis in HHV-8-associated malignancies. *Cancer: Interdisciplinary International Journal of the American Cancer Society* 92, 3076-3084.
- Kawanishi, M., 1993.** Epstein-Barr virus induces fragmentation of chromosomal DNA during lytic infection. *J Virol* 67, 7654-7658.
- King Jr, T.E., Pardo, A., Selman, M., 2011.** Idiopathic pulmonary fibrosis. *The Lancet* 378, 1949-1961.
- Koopman, G., Reutelingsperger, C.P., Kuijten, G.A., Keehnen, R.M., Pals, S.T., van Oers, M.H., 1994.** Annexin V for flow cytometric detection of phosphatidylserine expression on B cells undergoing apoptosis. *Blood* 84, 1415-1420.
- Laval, K., Favoreel, H.W., Nauwynck, H.J., 2015.** Equine herpesvirus type 1 replication is delayed in CD172a⁺ monocytic cells and controlled by histone deacetylases. *The Journal of general virology* 96, 118-130.
- Lincz, L.F., 1998.** Deciphering the apoptotic pathway: all roads lead to death. *Immunology and cell biology* 76, 1-19.
- Mair, T.S., Batten, E.H., Stokes, C.R., Bourne, F.J., 1987.** The histological features of the immune system of the equine respiratory tract. *Journal of Comparative Pathology* 97, 575-586.
- Mair, T.S., Batten, E.H., Stokes, C.R., Bourne, F.J., 1988.** The distribution of mucosal lymphoid nodules in the equine respiratory tract. *Journal of Comparative Pathology* 99, 159-168.
- Mair, T.S., Lane, J.G., 2005.** Diseases of the equine trachea. *Equine Veterinary Education* 17, 146-149.
- Marenzoni, M.L., Coppola, G., Maranesi, M., Passamonti, F., Cappelli, K., Capomaccio, S., Verini Supplizi, A., Thiry, E., Coletti, M., 2010.** Age-dependent prevalence of equid herpesvirus 5 infection. *Veterinary Research Communications* 34, 703-708.
- Mekuria, Z.H., El-Hage, C., Ficorilli, N.P., Washington, E.A., Gilkerson, J.R., Hartley, C.A., 2017.** Mapping B lymphocytes as major reservoirs of naturally occurring latent equine herpesvirus 5 infection. *Journal of General Virology* 98, 461-470.
- Mora, A.L., Woods, C.R., Garcia, A., Xu, J., Rojas, M., Speck, S.H., Roman, J., Brigham, K.L., Stecenko, A.A., 2005.** Lung infection with γ -herpesvirus induces progressive pulmonary fibrosis in Th2-biased mice. *American Journal of Physiology-Lung Cellular and Molecular Physiology* 289, L711-L721.
- Okan, I., Wang, Y., Chen, F., Hu, L.-F., Imreh, S., Klein, G., Wiman, K.G., 1995.** The EBV-encoded LMP1 protein inhibits p53-triggered apoptosis but not growth arrest. *Oncogene* 11, 1027-1031.
- Poth, T., Niedermaier, G., Hermanns, W., 2009.** Equine multinodular pulmonary fibrosis in association with an EHV-5 infection in 5 horses. *Wiener Tierärztliche Monatsschrift* 96, 203-208.
- Quintana, A.M., Landolt, G.A., Annis, K.M., Hussey, G.S., 2011.** Immunological characterization of the equine airway epithelium and of a primary equine airway epithelial cell culture model. *Veterinary Immunology and Immunopathology* 140, 226-236.
- Richter, N., Ebert, M., Borchers, K., 2009.** Prevalence of EHV-2 and EHV-5 DNA in ocular and nasal swabs as well as peripheral blood mononuclear cells. *Pferdeheilkunde* 25, 38-44.
- Rushton, J.O., Kolodziejek, J., Tichy, A., Nell, B., Nowotny, N., 2013.** Detection of equid herpesviruses 2 and 5 in a herd of 266 Lipizzaners in association with ocular findings. *Veterinary microbiology* 164, 139-144.

- Sarmiento, M., Kleinerman, E.S., 1990.** Innate resistance to herpes simplex virus infection. Human lymphocyte and monocyte inhibition of viral replication. *The Journal of Immunology* 144, 1942-1953.
- Sattentau, Q., 2008.** Avoiding the void: cell-to-cell spread of human viruses. *Nature reviews. Microbiology* 6, 815-826.
- Schwarz, B., Gruber, A., Benetka, V., Rütgen, B., Schwendenwein, I., Leidinger, E., van den Hoven, R., 2012.** Concurrent T cell leukaemia and equine multinodular pulmonary fibrosis in a Hanoverian Warmblood mare. *Equine Veterinary Education* 24, 187-192.
- Shannon-Lowe, C., Neuhierl, B., Baldwin, G., Rickinson, A., Delecluse, H.-J., 2006.** Resting B cells as a transfer vehicle for Epstein-Barr virus infection of epithelial cells. *Proceedings of the National Academy of Sciences* 103, 7065-7070.
- Shannon-Lowe, C., Rowe, M., 2011.** Epstein-Barr Virus Infection of Polarized Epithelial Cells via the Basolateral Surface by Memory B Cell-Mediated Transfer Infection. *PLoS Pathogens* 7, e1001338.
- Shannon-Lowe, C., Rowe, M., 2014.** Epstein Barr virus entry; kissing and conjugation. *Current Opinion in Virology* 4, 78-84.
- Susin, S.A., Lorenzo, H.K., Zamzami, N., Marzo, I., Snow, B.E., Brothers, G.M., Mangion, J., Jacotot, E., Costantini, P., Loeffler, M., 1999.** Molecular characterization of mitochondrial apoptosis-inducing factor. *Nature* 397, 441.
- Torfason, E.G., Thorsteinsdottir, L., Torsteinsdóttir, S., Svansson, V., 2008.** Study of equid herpesviruses 2 and 5 in Iceland with a type-specific polymerase chain reaction. *Research in veterinary science* 85, 605-611.
- Vairo, S., Vandekerckhove, A., Steukers, L., Glorieux, S., Van den Broeck, W., Nauwynck, H., 2012.** Clinical and virological outcome of an infection with the Belgian equine arteritis virus strain 08P178. *Veterinary microbiology* 157, 333-344.
- Van Cleemput, J., Poelaert, K.C.K., Laval, K., Maes, R., Hussey, G.S., Van den Broeck, W., Nauwynck, H.J., 2017.** Access to a main alphaherpesvirus receptor, located basolaterally in the respiratory epithelium, is masked by intercellular junctions. *Scientific reports* 7, 16656.
- Van der Meulen, K., Vercauteren, G., Nauwynck, H., Pensaert, M., 2003a.** A local epidemic of equine herpesvirus 1-induced neurological disorders in Belgium. *Vlaams Diergeneeskundig Tijdschrift* 72, 366-372.
- Van der Meulen, K.M., Nauwynck, H.J., Pensaert, M.B., 2003b.** Absence of viral antigens on the surface of equine herpesvirus-1-infected peripheral blood mononuclear cells: a strategy to avoid complement-mediated lysis. *Journal of general virology* 84, 93-97.
- Van Poucke, S.G., Nicholls, J.M., Nauwynck, H.J., Van Reeth, K., 2010.** Replication of avian, human and swine influenza viruses in porcine respiratory explants and association with sialic acid distribution. *Virology journal* 7, 38.
- Vandekerckhove, A., Glorieux, S., Van den Broeck, W., Gryspeerdt, A., van der Meulen, K.M., Nauwynck, H.J., 2009.** *In vitro* culture of equine respiratory mucosa explants. *Veterinary Journal* 181, 280-287.
- Vandekerckhove, A.P., Glorieux, S., Gryspeerdt, A.C., Steukers, L., Duchateau, L., Osterrieder, N., Van de Walle, G.R., Nauwynck, H.J., 2010.** Replication kinetics of neurovirulent versus non-neurovirulent equine herpesvirus type 1 strains in equine nasal mucosal explants. *The Journal of general virology* 91, 2019-2028.
- Vander Werf, K., Davis, E., 2013.** Disease remission in a horse with EHV-5-associated lymphoma. *Journal of veterinary internal medicine* 27, 387-389.
- Vergnon, J., De The, G., Weynants, P., Vincent, M., Mornex, J., Brune, J., 1984.** Cryptogenic fibrosing alveolitis and Epstein-Barr virus: an association? *The Lancet* 324, 768-771.
- Wang, G.-H., Bertin, J., Wang, Y., Martin, D.A., Wang, J., Tomaselli, K.J., Armstrong, R.C., Cohen, J.I., 1997.** Bovine herpesvirus 4 BORFE2 protein inhibits Fas-and tumor necrosis factor receptor 1-induced apoptosis and contains death effector domains shared with other gamma-2 herpesviruses. *Journal of virology* 71, 8928-8932.
- Wang, L., Raidal, S.L., Pizzirani, A., Wilcox, G.E., 2007.** Detection of respiratory herpesviruses in foals and adult horses determined by nested multiplex PCR. *Veterinary microbiology* 121, 18-28.

- Williams, K., Maes, R., Del Piero, F., Lim, A., Wise, A., Bolin, D., Caswell, J., Jackson, C., Robinson, N., Derksen, F., 2007.** Equine multinodular pulmonary fibrosis: a newly recognized herpesvirus-associated fibrotic lung disease. *Veterinary Pathology* 44, 849-862.
- Williams, K.J., Robinson, N.E., Lim, A., Brandenberger, C., Maes, R., Behan, A., Bolin, S.R., 2013.** Experimental induction of pulmonary fibrosis in horses with the gammaherpesvirus equine herpesvirus 5. *PLoS One* 8, e77754.
- Wong, D.M., Belgrave, R.L., Williams, K.J., Del Piero, F., Alcott, C.J., Bolin, S.R., Marr, C.M., Nolen-Walston, R., Myers, R.K., Wilkins, P.A., 2008.** Multinodular pulmonary fibrosis in five horses. *Journal of the American Veterinary Medical Association* 232, 898-905.

Chapter 8.

General Discussion

A resting horse inhales and exhales about 60 liters of air per minute. During intensive exercise, equine athletes are able to breath in and out in less than half a second and thus, move over 1800 liters of air per minute. In addition, the horse is an obligate nasal airway breather, meaning that all this air needs to pass through the horse's extensive nasal cavities. Next, the air needs to cross the respiratory tract's bottleneck, the larynx, before it can flow towards the lungs. Although the respiratory tract has an overall smooth design, air turbulences and pressure fluctuations are inevitable during heavy breathing. Besides these physical stressors, a vast amount of airborne pathogens (e.g. bacteria, fungi and viruses) and respirable hazards (e.g. dust, ammonia, pollens, air pollution and even aerosol drugs) are conveyed into the horse's respiratory tract with each breath. In order to cope with these constant threats, the epithelium lining the conducting airways exhibits a plethora of physical barriers and innate and adaptive immune mechanisms. Still, respiratory disease is an important clinical manifestation in today's Westernized horses (Gilkerson *et al.*, 2015; Marr, 2016; Nagy *et al.*, 2017). This implies that airborne pathogens must have evolved mechanisms to circumvent these barriers and/or that other stressors might be at stake. In the horse population, respiratory disease commonly causes poor performance, a high morbidity and in some cases even death. Many viral and bacterial pathogens have been associated with respiratory disease, including herpesviruses, influenza viruses, equine arteritis virus, equine rhinoviruses, adenoviruses, *Streptococcus* sp., *Staphylococcus* sp., *Rhodococcus equi*, *Actinobacillus equuli*, *Mycoplasma* sp. and *Bordetella bronchiseptica*. Although the role of some of these pathogens as a primary causative agent can be speculative, they can all contribute to the development of a syndrome designated 'multifactorial respiratory disease complex'.

The evolutionary battle between host barriers and pathogens

The present thesis aimed to unravel the interplay between the horse's respiratory mucosa and important equine airborne pathogens and the impact of respirable hazards herein. The co-evolutionary interplay between pathogens and their host is commonly referred to as an 'evolutionary arms race' or the 'Red Queen hypothesis'. As herpesviruses exhibit a high level of host specificity, acquired through many years of co-evolution and are currently among the most important pathogens in the global horse industry, emphasis was put on equine herpesviruses in this thesis.

Herpesviruses already 'inhabited' the earth at the time of the dinosaurs, meaning that they are already evolving for over 150 million of years (McGeoch *et al.*, 1995). The further subdivision between alpha, beta and gammaherpesviruses presumably accelerated together with the

expansion of different mammalian species. The long-term co-evolution of herpesviruses and their hosts allowed these DNA viruses to steadily mutate and develop a repertoire of highly specialized strategies to persist in the host population. Therefore, it is not surprising that today's herpesviruses evade multiple steps of their host's immunity, for instance via the establishment of latency. It is not of interest for these viruses to severely harm their host, as that would impede further spread to new hosts.

Interestingly, EHV1 lies closest to the alphaherpesvirus consensus standard and therefore approximates the ancestral alphaherpesvirus, as it exhibited the most dominances in partial orderings among all examined alphaherpesviruses (HSV1 and 2, PRV and VZV) (Karlin *et al.*, 1994). In the equestrian world, EHV1 is probably the best-known and most dreadful herpesvirus. Nonetheless, EHV1 is highly prevalent in healthy horses worldwide without causing a lot of disease (Patel and Heldens, 2005). Still, in a small percentage of EHV1-infected horses, viral-induced symptoms, such as respiratory disorders, abortion and central nervous system disorders, do occur (Allen and Bryans, 1986; Lunn *et al.*, 2009). On the one hand, EHV1 directly causes these symptoms as a strategy to propagate and spread progeny virions. Indeed, viral load is often high in nasal swabs of EHV1-infected horses showing nasal discharge and exceeds peak values in aborted foetal and placental tissues (Edington *et al.*, 1986; Gardiner *et al.*, 2012; Gibson *et al.*, 1992; Gryspeerdt *et al.*, 2010). On the other hand, excessive viral activity and failure of the host's immune response to contain EHV1 infection might sometimes lead to unintended symptoms, such as central nervous system disorders (Edington *et al.*, 1986; Jackson and Kendrick, 1971; Wilson, 1997). Indeed, these symptoms tend to occur in elderly horses, which are thought to be immunocompromised (Goehring *et al.*, 2006; Henninger *et al.*, 2007). Despite numerous studies trying to develop antiviral therapies or effective vaccines, EHV1 still persists in the horse population. This points out that a better understanding of the interactions between EHV1 and its host are urgently needed, starting with those at the port of entry and exit: the horse's respiratory tract.

Previous *in vivo*, *ex vivo* and *in vitro* studies showed that primary EHV1 infection of the respiratory epithelium is restricted (Gryspeerdt *et al.*, 2010; Hussey *et al.*, 2014; Vandekerckhove *et al.*, 2010). We hypothesized that a specific host barrier, present in the respiratory mucosa, hinders incoming EHV1 particles from infecting the epithelium. One of the first barriers that EHV1, among other pathogens, needs to overcome in order to reach the surface-lining epithelial cells, is the mucus together with the mucociliary escalator. Both serve to entrap incoming pathogens and other particles and propel them towards the pharynx, where they are eventually discarded by swallowing. In addition, mucus contains a significant

concentration of secreted immunoglobulins A (sIgA). If the horse has previously mounted a mucosal immune response, these sIgA can specifically neutralize inhaled pathogens. The sticky mucus blanket has already been shown to entrap pseudorabies virus (PRV) particles, due to charge-charge interactions between the virion surface and mucins (Yang *et al.*, 2012). Surprisingly, we observed that the mucus layer on the respiratory epithelium did not majorly restrict EHV1 infection. Indeed, washing away the mucus in respiratory mucosal explants only marginally increased subsequent EHV1 infection of the respiratory epithelium. Therefore, we hypothesized that another physical barrier, such as firm intercellular junctions and/or antimicrobial peptides (e.g. β -defensins), act as major impeters of EHV1 infection.

The host mucoprotein network and intercellular junctions

A key piece in the horse's armour to combat EHV1

In the first part of the thesis, we found that the tight intercellular junction network between the cells of the respiratory epithelium forms a major barrier against EHV1 infection. Furthermore, we demonstrated that EHV1 targets a binding receptor that is located at the basolateral surface of respiratory epithelial cells.

The overlying and/or membrane-tethered mucoprotein network and ICJ both functioned as important barriers in the nasal septum. Indeed, the destruction of both mucoprotein network and intercellular junctions (ICJ) with N-acetylcysteine was required for EHV1 to efficiently infect epithelial cells of nasal mucosal explants. In contrast, we demonstrated that the EGTA-mediated destruction of ICJ of tracheal mucosal explants was sufficient for an efficient infection. It is not surprising that EHV1 infection is less efficient in the respiratory epithelium of nasal mucosal explants than in that of tracheal mucosal explants. Indeed, the cell composition of the respiratory epithelium in the nasal septum and the trachea is different and may explain these observations. More mucous cells reside in the respiratory epithelium of the nasal septum, compared to in that of the trachea, resulting in a thicker and more sophisticated membrane-tethered mucoprotein network (Harkema *et al.*, 2006). Furthermore, the ICJ of the respiratory epithelium lining the nasal septum are stronger than those of the respiratory epithelium lining the trachea (Ballard *et al.*, 1992; Boucher *et al.*, 1981; Lopez-Souza *et al.*, 2009). Thus, the (nasal) equine respiratory epithelium with its overlying mucoprotein network and firm ICJ became a valuable piece of armour for the horse during its evolutionary arms race with EHV1.

EHV1 takes advantage of the equine defences' weak points

Upon inhalation, EHV1 particles are dispersed over the surface epithelium of the nasal and tracheal mucosa, where they are primarily hindered from reaching their binding receptor by the horse's ICJ. When EHV1 hits the apical surface of respiratory epithelial cells, specific residues on gB and especially gC attach to putative cell surface-tethered sugar moieties. These sugar moieties are presumably not heparan sulphate, chondroitin sulphate or α 2,3-sialic acids, as these are not expressed at the apical surface of the horse's respiratory epithelium. This initial interaction between viral glycoproteins and cell surface glycans is usually unstable, allowing EHV1 to presumably detach again. Once specific viral ligands (e.g. gD) irreversibly adhere to a cellular receptor, EHV1 can trigger entry. As EHV1's main binding receptor is located basolaterally, we propose that EHV1 can hit its target only at certain 'lucky spots'. These lucky spots might not be so difficult to find in a healthy individual, since respiratory epithelial ICJ are constantly disassembled and reassembled in normal conditions. For instance, 'leukocyte patrolling' induces a selective and local redistribution of ICJ to allow cell passage (Edens and Parkos, 2000). Also, cell renewal requires a close balance between the shed of attrited cells and subsequent restitution by new cells to maintain epithelial permeability and polarity (Williams *et al.*, 2015). Upon (local) loss of this epithelial integrity, EHV1 could gain access to the paracellular compartment and find its basolaterally located receptor. In addition, this receptor might become exposed at the apical side of the plasma membrane due to impaired cell polarity. Alternatively, putative EHV1 binding receptors might be expressed inherently on the apical surface of polarized epithelial cells. For example, EHV1 has already been shown to interact with MHC I and specific integrins (e.g. α v β 3) to trigger binding and entry in equine brain microvascular endothelial cells and PBMC (Kurtz *et al.*, 2010; Laval *et al.*, 2016; Van de Walle *et al.*, 2008). These transmembrane proteins are also located in the plasma membrane of equine epithelial cells (Knight and Holgate, 2003). Still, EHV1 did not depend on these receptors to bind and enter equine respiratory epithelial cells (EREC), as blocking of these receptors did not significantly affect EHV1 infectivity in EREC. Similarly, blocking other herpesviral receptors on EREC, e.g. nectin-1, HVEM, integrin α 6 β 1, did not impair EHV1 infection (data not shown). Therefore, we hypothesize that this novel putative binding receptor is different from any known alphaherpesviral receptor. Nonetheless, other alphaherpesviruses presumably also use this putative basolaterally located receptor to infect epithelial cells. Indeed, Galen *et al.* (2006) found that herpes simplex virus type 1 (HSV1) is able to infect the basolateral surface of human epithelial cells via a putative receptor, different from nectin-1.

It may seem odd for EHV1 to go through all this trouble before infecting a cell. Still, hindering its primary replication is already a first clever step in deceiving its host. Indeed, a productive viral replication inevitably triggers a series of pathogen recognition receptors, including toll like receptors (TLR), which mediate an antiviral response via the activation of cell signalling pathways and the production of antiviral cytokines and chemokines (Xagorari and Chlichlia, 2008). An overload of these compounds is unfavourable for EHV1, as these can directly impair viral replication or modulate the onset of an adaptive immune response against EHV1. Thus, by minimizing the number of primary ‘infection spots’ in the horse’s respiratory tract, EHV1 may remain largely under the immunological radar while trying to get into its latency reservoirs, such as the trigeminal ganglion and CD8⁺ T lymphocytes. To do so, EHV1 elicits the production of specific chemokines, such as CCL2 and CCL5, in respiratory epithelial cells to attract CD172a⁺ monocytes, one of its main target cells (Gryspeerdt *et al.*, 2010; Zhao *et al.*, 2017). In addition, we showed in Chapter 6 that EHV1 induces a well-controlled chemotaxis of leukocytes towards the primary site of infection by upregulating the expression of β -defensins in EREC. Finally, epithelial brush cells are in direct contact with axons originating from the trigeminal nerve. Thus, only minor viral infection in EREC is required for EHV1 to transfer infection to these axons and subsequently to the cell bodies of the trigeminal ganglion via retrograde axonal transport (Sato, 2007).

We propose that the main advantage of targeting a basolaterally located receptor lies in the viral exit strategy. Upon reactivation of EHV1 in infected leukocytes or neurons, the virus travels back to the site of entry, the respiratory epithelium. Now, EHV1 is granted with direct access to its most optimal receptor, located basolaterally in the respiratory epithelium. Efficient viral binding and entry will result in an efficient secondary replication, with the shed of an extensive amount of progeny virions in respiratory secretions. Such vast burden of virus particles will increase the chances of infecting new hosts. Thus, during the evolutionary arms race between EHV1 and the horse, EHV1 seems to have found some pivotal gaps in the horse’s armour. An overview of how EHV1 might potentially access its main binding receptor is given in Figure 1A.

Respirable hazards assault the horse, making EHV1 surmount

Aerosol treatment with N-acetylcysteine

N-acetylcysteine (NAC) is a mucolytic agent, meaning that it can disrupt the extensively formed disulphide bonds in between mucins. In turn, this facilitates cilia propelling and disposal of the mucus (Reas, 1963). Therefore, pharmaceutical companies commercialized NAC as the acting

ingredient of Lysomucil® to treat patients with chronic obstructive pulmonary disease (COPD) and cystic fibrosis (Dauletbaev *et al.*, 2009; Decramer *et al.*, 2005). Lysomucil® is also used in veterinary medicine, and especially in the aerosol treatment of horses with recurrent airway obstruction (RAO; i.e. COPD) or severe pneumonia (Breuer and Becker, 1983; Mair and Derksen, 2000). Pharmaceutical companies even commercialized N-acetylcysteine as oral powder for horses (Equimucin®). However, no data on oral bioavailability of N-acetylcysteine in horses are available (Heads of Medicines Agencies, 2018). Furthermore, as a precursor of glutathione, NAC is also used to treat glutathione deficiency in humans, for example in acetaminophen intoxications or human immunodeficiency virus (HIV) infections (Atkuri *et al.*, 2007). Despite all these beneficial effects, current studies emphasize that care must be taken when using this drug in the treatment of respiratory diseases, especially in nebulizers. For the first time, we showed that NAC can destroy respiratory epithelial cell ICJ, most likely by modulating intracellular calcium levels (Brown and Davis, 2002; Nilsson *et al.*, 1996). The concentration we used in our experiments corresponds to the recommended dose for aerosol treatment in humans. Fortunately, most veterinarians dilute Lysomucil® at least by 3-fold to cover the complete horse's respiratory tract during nebulization. Nonetheless, local deposition of NAC might still act on epithelial integrity and predispose the horse for EHV1 infection.

Pollens

In Chapter 4, we demonstrated that by selectively disrupting epithelial integrity of columnar cells, pollens predispose the respiratory epithelium for EHV1 infection. The mechanism behind this selective destruction was inherently different from the calcium-modulating effects of EGTA and NAC. Indeed, the alteration of intra and extracellular calcium levels occurred throughout the complete respiratory epithelium, while proteases acted only on columnar cells. We proposed that pollen proteases might activate specific protease-activated receptors (PARs), localized only on the surface of columnar cells. Through the activation of several intracellular signalling pathways, PAR activation might eventually initiate the disassembly of ICJ (Chiu *et al.*, 2007; Kato *et al.*, 2009; Kumamoto *et al.*, 2016). Alternatively, the transmembrane domains of basal cell ICJ could be more concealed and protected from exogenous protease attacks.

Based on these results, it seems reasonable to propose that horses are at a higher risk for a primary EHV1 infection during pollen season. Damage to the epithelial barrier might increase their susceptibility to a primary EHV1 infection. Interestingly, EHV1-associated symptoms are frequently encountered during late winter and spring, when plant pollination proceeds (D'Amato *et al.*, 2001; Goehring *et al.*, 2006; Sherman *et al.*, 1979). Some horses, e.g. allergic

horses, might also be more sensitive for this pollen-induced damage to the epithelial barrier. Besides the direct degradation of ICJ, pollen-induced chronic airway inflammation might further impair epithelial integrity. Similarly in humans, allergic patients tend to have a less firm epithelial barrier (Xiao *et al.*, 2011). Although our results need to be verified with *in vivo* experiments in horses, based on our results, we would already suggest to carefully monitor allergic horses (i.e. exhibiting summer pasture-associated recurrent airway obstruction [SP-RAO]) with regard to EHV1 infections. These horses should be separated from ‘high risk virus shedding horses’ (e.g. yearlings and competing horses) and kept in small groups to minimize the chance for airborne EHV1 exposure, especially during pollen season. In addition, a daily check-up on the weather forecast could predict the exact peak of pollen concentrations in the outdoor air and help in taking preventive measures. For instance, we would encourage horse owners to keep the highly sensitive individuals indoors during these periods. Finally, as horses with SP-RAO could be at greater risk for a respiratory EHV1 infection, the chance that their mates are subsequently exposed to EHV1 is higher. Therefore, we would suggest to house pregnant mares separately from horses with SP-RAO during pollen season in order to minimize the chance of EHV1-induced abortions. Still, further extensive *in vivo* studies are required before these statements can be confirmed and generalized to the complete horse population. Taken together, we speculate that pollens present in the ambient air of horses work in favour of EHV1 by increasing the risk of infection and subsequent spread.

Mycotoxins

In Chapter 5, we demonstrated that exposure of the respiratory epithelium to the mycotoxin deoxynivalenol (DON) affects epithelial integrity and thereby increases the risk of an EHV1 infection. Here, destruction of the epithelial barrier most likely occurred through a third distinct mechanism. Similarly as in intestinal cells, we propose that respiratory epithelial cells fail to maintain a stable ICJ complex due to a mycotoxin-induced block in protein neosynthesis (Pinton *et al.*, 2009; Van De Walle *et al.*, 2010).

Based on these results, we want to emphasize the importance of monitoring the mycotoxin level in equine feeds and surroundings. According to Regulation (EC) No 882/2004, European member states should establish and implement multi-annual control programs for contaminants in animal feeds (van Egmond *et al.*, 2007). The frequency and thoroughness of these control programs should be based on food- and animal-specific risk assessments. In the veterinary field, this comes down to the fact that high priority is only given to grain-derived pig feeds but all other animals feeds are considered to be of ‘moderate’ or even ‘low risk’. In addition for horses,

an even higher risk to mycotoxin exposure arises from roughage such as straw, hay and grass silages (Ogunade *et al.*, 2018). Unfortunately, the mycotoxin load in these roughages is even less monitored than in commercial grain feeds. In this context, a global mycotoxin survey found DON doses of up to 2-20 mg/kg in European roughage and cereal feeds (Biomin, 2016). It seems reasonable to propose that these food-derived mycotoxins are inhaled and deposited on the horse's respiratory epithelium during feeding. For instance, roughage is often put in up-hanging hay racks or nets, forcing horses to feed with an upright head position. In this way, horses inevitably inhale the accompanying dust, moulds and mycotoxins. Future studies should measure the exact amount of mycotoxins in equine feeds. Next, the exact percentage of these food-derived mycotoxins that ends up in the horse's respiratory tract should be determined. Based on these results, new scientifically approved threshold levels of such mycotoxins in equine feeds could be implemented.

In line with what we previously described for pollen allergies, horses suffering from chronic allergies to dust and moulds, also known as RAO, should be carefully monitored to minimize the risk of EHV1 infection and subsequent spread. In contrast to horses suffering from SP-RAO, horses with RAO should better be kept in good pastures at all times, without hay or grass silage supplementation. If this is not feasible, a strict control of the horse's environment should be implemented to minimize the burden of dust, moulds and their toxic by-products in the ambient air. For example, hay should be steamed (preferably) or soaked for hours prior to feeding or replaced by complete pelleted diets, straw as bedding material should be replaced by wood shavings and the ventilation in the stable should be optimized (Earing *et al.*, 2013; Léguillette, 2003). As stated above, further *in vivo* studies are required before these statements can be confirmed and generalized to the complete horse population. In conclusion, we propose that mycotoxins present in equine feeds could work in favour of EHV1 by increasing the risk of infection and subsequent spread.

A novel drug as potential ally of the horse in the battle against EHV1

In this context, the use of drugs that strengthen respiratory epithelial ICJ may be an interesting strategy to modulate primary EHV1 infections. In order to quickly and specifically act on the respiratory epithelium, aerosol treatment would be the preferable administration method for such drug. To our knowledge, such ICJ-modulating drugs have not been reported yet. We propose that the development of the following formulation would be of high interest to grant further research. First of all, calcium should be added due to its indispensable role in ICJ stabilisation (Baum and Georgiou, 2011; Shasby and Shasby, 1986). Second, protease inhibitors

could be supplemented to act on foreign incoming proteases arising from pollens, but also from mites and other putative sources (Kato *et al.*, 2009). More precisely, we would advise to use AEBSF and E-64, as our results demonstrated that both compounds efficiently blocked the majority of the pollens' proteolytic activities. In addition, we found that the working concentrations of these protease inhibitors were not cytotoxic, in contrast to those of other tested protease inhibitors (e.g. bestatin and pepstatin). A third interesting compound might be mycotoxin-specific nanobodies[®] (e.g. against deoxynivalenol). Nanobodies[®] are therapeutic proteins derived from naturally occurring 'heavy-chain-only' immunoglobulin molecules in *Camelidae*. Nanobodies[®] are currently further developed as anti-thrombotics, as anti-virals and even as a potential candidate for cancer treatment (Van Bockstaele *et al.*, 2009; Vanlandschoot *et al.*, 2011). Therefore, it seems reasonable to propose that they can also be developed to bind and neutralize inhaled mycotoxins and other (bacterial-derived) toxins, potentially impairing ICJ stability. These nanobody-bound toxins could then be safely removed by the mucociliary escalator. Finally, regarding the importance of the mucoid network residing on top of the nasal septum, it could be of interest to add specific glycans, e.g. from mucins, to the drug formulation. Due to charge-charge differences and lectin-like functions, these components might help to immobilize EHV1 in the sticky gel layer and facilitate its disposal.

At this point, the efficacy of such aerosol therapy in the prophylaxis and treatment of EHV1 disease still remains highly speculative. The development of the proposed drug will be challenging, but no doubt rewarding. Indeed, compared to existing anti-EHV1 therapies (e.g. acyclovir and valacyclovir), the latter drug would be much more cost-efficient and thus be generally applicable for all horses, instead of merely the highly valued horses. Furthermore, preventing primary EHV1 infections in foals, together with strict quarantine measurements, could be the key step in the complete eradication of EHV1.

β-defensins

An example of 'Darwinian-evolved weapons' of the horse to shape the composition of the microbiota

Antimicrobial peptides are probably among the most ancient and efficient components of host defence and β-defensins (BDs) represent only a small part of this antimicrobial peptide plethora (Harwig *et al.*, 1994; Lehrer and Ganz, 2002). The general structure of BDs (i.e. cationic, 3 β-sheets and 3 disulphide bonds) is conserved within one species and between different species, but the amino-acid sequences broadly differ. In addition, BD genes are often located

in one or more clusters on the same chromosome (Hughes, 1999). These facts indicate that the complete repertoire of BD genes descended from a single ancestral gene by gene duplication and diversified as a result of 'positive Darwinian selection'. Not all of these BD genes are functional, as some of them contain premature stop codons. Thus, we could speculate that during evolution, some genes were selected over others and further diversified to combat microbial challenge.

In Chapter 6, we demonstrated that mRNA of eBD1-3 is constitutively expressed throughout the complete horse's respiratory tract and protein expression is localized to specific areas herein. In addition, we showed that equine β -defensin (eBD) 2 inhibits the growth of *Actinobacillus equuli* subsp. *equuli* and *Bordetella bronchiseptica* and eBD3 additionally inhibits that of *Streptococcus equi* subsp. *equi* and *Rhodococcus equi*. Although highly speculative, we propose that evolution favoured the existence and persistence of eBD2-3, as these aid in shaping a healthy microbiota at the respiratory mucosal surface. Namely, these eBDs are able to inhibit primary or non-commensal pathogens, i.e. pathogens that can directly cause disease upon entry and colonization of the host and thus, help the horse. For example, two eBD3-sensitive bacteria, *Streptococcus equi* subsp. *equi* and *Rhodococcus equi*, can cause purulent pharyngitis and/or pneumonia upon host colonization. On the contrary, commensal pathogens generally do not cause disease, unless other predisposing factors are at stake. These pathogens (e.g. *Staphylococcus aureus* and *Streptococcus equi* subsp. *zooepidemicus*) were not harmed by eBD1-3 and therefore have the opportunity to colonize different parts of the respiratory tract (e.g. the nasal cavities). In turn, these bacteria could work in favour of the horse by protecting it against unwanted invading microbes. Similarly in the horse's (hind)gut, a healthy microflora is indispensable for optimal functioning (Sanchez, 2018).

In the present thesis, we merely studied eBD1-3, as their human homologs represent the three central BD. However, considering the large genomic cluster of eBD genes on equine chromosome 27, multiple other eBDs might also be expressed at the horse's respiratory mucosal surfaces. Although we are only able to discuss about the role of eBD1-3 in the guardianship of the horse's respiratory mucosa, we believe that also other eBDs might be important in the modulation of a pathogen invasion and in the complete horse's immune surveillance. Future studies should try to uncover which genes are transcribed and how these products are assembled and function in the horse.

Weapons of the horse to conquer in the battle, but not in the war, against EIV and EAV

In Chapter 6, we showed that eBDs, especially eBD2 and 3, are potent antimicrobial peptides against enveloped viruses. Equine influenza virus (EIV), as well as equine arteritis virus (EAV) were efficiently neutralized after exposure to eBD2 and 3. As a mode of action, we propose that the highly cationic eBD2-3 first electrostatically bind to the negatively charged phospholipid bilayer of the viral envelope. Next, eBD2 and 3 can automatically impregnate themselves into this phospholipid bilayer due to their amphipathic characters. As eBD2 and 3 oligomerize *in vitro*, we propose that by assembling these oligomers in the viral envelope, eBD2 and 3 can create a transmembrane pore. Extensive damage of the viral envelope will eventually destroy the virion. Similarly, human BD2 has been proven to damage the envelope of respiratory syncytial virus (Kota *et al.*, 2008). Additionally, eBD2-3 might block important ligands on the viral surface (e.g. EIV haemagglutinin or EAV GP5), required for viral binding and/or entry. A similar mechanism has already been proposed for the neutralizing effect of several α -defensins and human BD3 on HIV, HSV1 and/or 2 virions (Hazrati *et al.*, 2006; Wang *et al.*, 2004).

In addition, we found that the horse's respiratory epithelium responds to an EIV infection by upregulating the expression of these two potent eBDs. In turn, these eBDs aid in the clearance of the infection. Despite its sensitivity to eBD2-3, EIV is still omnipresent in the horse population and regularly infects the respiratory epithelium. This indicates that EIV has evolved other distinct mechanisms to guarantee its survival in the host population. In contrast to host-specific viruses (e.g. EHV1), this segmented RNA-virus most likely relies on a fast and extensive viral replication together with regular antigenic drifts (and potentially shifts) to cause regular outbreaks in both naïve and vaccinated horses. In this context, EIV does not mind to take some collateral damage during its way into and out of the horse's respiratory tract. Indeed, at least some of the millions of produced EIV particles are likely to survive the impact of eBDs and putative other antiviral molecules during viral spread. Thus, it seems that during the evolutionary arms race between the horse and EIV, the horse evolved efficient weapons against EIV, but failed to eradicate the virus. Nonetheless, current horse riding organisations (e.g. Fédération Equestre Internationale or FEI and Koninklijke Belgische Ruitersport Federatie or KBRSF) try to aid the horse in the battle against EIV by imposing strict vaccination schemes for competing horses, thereby minimizing the chance for EIV infection and spread in the horse population.

EAV has a completely different strategy compared to EIV and EHV1, to spread and survive in the horse population. The virus can spread either via aerosol spread (respiratory route), sexual transmission (venereal route) or vertical spread (trans-placental route). We propose that upon entry, some EAV particles are damaged by the constitutively produced eBD2-3 but at least some virions get in contact with locally patrolling immune cells. By directly infecting these immune cells, EAV cleverly circumvents the viral-induced upregulation of eBD2 and 3 in epithelial cells. Finally, EAV is able to persist for longer periods of time in the ampullae of the vas deferens of adult stallions (Carossino *et al.*, 2017). This phenomenon is strikingly different from the explosive outbreaks caused by EIV infection or on the opposite, from the establishment of latency after primary EHV1 infection. Little *et al.* (1992) showed that the persistent infection of EAV is testosterone-dependent, as EAV persists in carrier stallions that are castrated and supplemented with testosterone, but is cleared from those that are not supplemented. Interestingly in macaques and rodents, the expression of a specific β -defensin gene cluster was mainly restricted to certain parts of the male reproductive tract and differentially regulated by androgens (Hu *et al.*, 2014; Jalkanen *et al.*, 2005; Radhakrishnan *et al.*, 2005). Similarly in horses, a novel β -defensin gene cluster was shown to be expressed in different parts of the male and female reproductive tract (Johnson *et al.*, 2015). Although highly speculative, the expression of eBDs in the reproductive tract of geldings and mares may differ from that of stallions due to differences in androgen levels. In turn, this differential expression pattern might be correlated with EAV clearance or persistence in the reproductive tract. Future studies should look deeper into the potential antiviral role of these eBDs and analyse their differential expression profiles in geldings, mares and stallions. In conclusion, the horse evolved efficient weapons against EAV during the evolutionary arms race between the horse and the virus. Still, evolution somehow enabled EAV to persist in carrier animals and survive in the present horse population.

EHV1 acts as a ‘sneak thief’

In Chapter 6, we showed that the envelope of EHV1 resists eBD1-3, through the incorporation of the type III transmembrane glycoprotein M. We propose that the multiple transmembrane-spanning domains (i.e. 8 in total) of glycoprotein M stabilize the viral envelope of EHV1 and thereby protect it from eBD permeabilization. These results complement those of an electron microscopy study by Daher *et al.* (1986), showing that morphology of the HSV1 envelope was not altered by incubation with human α -defensin 1. Further evidence of the role of gM in membrane-stabilization comes from the fact that gM of pseudorabies (PRV) and EHV1 inhibit

the fusion induced by artificially optimized gB and gD (Klupp *et al.*, 2000). To our knowledge, the capacity of other multiple transmembrane-spanning proteins to protect bilipidic layers from permeabilization has not been reported yet. This hypothesis would further add to the theory that eBDs are able to destroy EIV and EAV envelopes, due to their lack of multiple transmembrane-spanning proteins. Future studies should try to assemble artificial plasma membranes embedded with either multiple or single transmembrane-spanning proteins and evaluate their resistance against membrane-attacking proteins, e.g. defensins.

Furthermore, we demonstrated that EHV1 even misuses these eBDs in order to increase its infectivity through both viral- and cell-mediated mechanisms. As viral-mediated mode of action, we propose that the cationic eBD2-3 electrostatically bind to anionic residues on the viral envelope and/or transmembrane glycoproteins. Neutralizing the net negative virion charge may promote subsequent aggregation. Correspondingly, human adenovirus (HAdV) infections can be enhanced by coating them with poly-cations (Wang *et al.*, 2011). Due to the inherent ability of eBD2-3 to oligomerize, these aggregates could potentially expand even further. Plausible eBD2-3 target candidates on the surface of EHV1 are the highly glycosylated gC and gB. Further evidence on the role of gB herein comes from a previous study. With the use of surface plasmon resonance, Hazrati *et al.* (2006) showed that human BD3 could bind to gB of HSV1 and 2. However, instead of increasing subsequent HSV infectivity, human BD3 binding to gB inhibited subsequent HSV infectivity in human cervical epithelial cells. HSV gB is essential for viral fusion, as gB-free HSV virions are able to bind cells *in vitro*, but cannot infect them (Cai *et al.*, 1988). Remarkably, we observed that EHV1 gB was not essential for viral entry in RK13 cells. Indeed, RacL11ΔgB virions (passaged 6 times in a gB-complementing cell line and one time in RK13 cells) successfully infected single RK13 cells, as assessed with an immunocytological staining against IEP. Immunofluorescent staining of RacL11ΔgB-infected RK13 cells with the monoclonal mouse anti-gB antibody (3F6) confirmed the absence of gB in the RacL11ΔgB stock derived from RK13 cells. Still, EHV1 gB is presumably not (solely) involved in eBD-binding, as eBD2 was still able to enhance infection of gB-free EHV1 virions in RK13 cells. Similar results were obtained with gC-null EHV1 virions. Therefore, we propose that multiple negatively charged residues on different viral glycoproteins and on the viral envelop participate in eBD-binding and subsequent enhancement of infection. As cell-mediated mode of action, we suggest that eBD1-3 binding to receptors on the cell surface might neutralize the net negative charge of cellular glycans and promote viral attachment. Alternatively, eBDs might induce the upregulation and/or a conformational change of the EHV1 binding receptor. For instance, eBD binding to a putative transmembrane receptor might trigger an intracellular

signalling cascade. In turn, this might modulate the expression or modify the conformation of certain putative EHV1 receptors at the plasma membrane. In this context, human BD1-3 have been shown to activate cell signalling pathways through CCR6 binding (Diao *et al.*, 2014; Yang *et al.*, 1999). In addition, some studies reported the ability of human α -defensins to interfere with protein kinase C (Chang *et al.*, 2005; Salvatore *et al.*, 2007). In addition, cell surface expression of CXCR4 in PBMC can be modulated by human BD2-3 (Quinones-Mateu *et al.*, 2003). Alternatively, eBD2-3 might directly bind and modify these putative EHV1 receptors. Although one study reported the ability of human BD3 to crosslink host cell proteins, defensin-induced conformational changes in proteins have not been described yet (Leikina *et al.*, 2005). Future studies should try to elucidate the role of different EHV1 glycoproteins in the binding to eBD2-3.

Finally, we found that EHV1 infection elicited a higher production of eBD2-3 in respiratory epithelial cells compared to EIV infection. In addition, these eBDs were able to steadily attract monocytic cells and T lymphocytes, two EHV1-susceptible PBMC subpopulations (Gryspeerd *et al.*, 2010; Laval *et al.*, 2015). Chemotactic activities have similarly been reported for human α -defensins 1-3, human BD1-2 and mouse BD2 (Biragyn *et al.*, 2002; Territo *et al.*, 1989; Yang *et al.*, 2000; Yang *et al.*, 1999). In contrast, foetal calf serum (FCS)-induced chemotaxis was about 2-fold higher compared to eBD-induced chemotaxis. Therefore, we propose that EHV1 specifically orchestrates respiratory epithelial cells to synthesize eBD2-3 as a semi-potent chemoattractant for its target cells. Indeed, excessive chemotaxis and inflammation at the site of viral infection might be disadvantageous for EHV1 survival.

In conclusion, we believe that during the evolutionary arms race, EHV1 has evolved multiple mechanisms to resist and even exploit the host's eBDs. A hypothetical model of how EHV1 misuses these eBDs for viral spread in the horse, is given in Figure 1B.

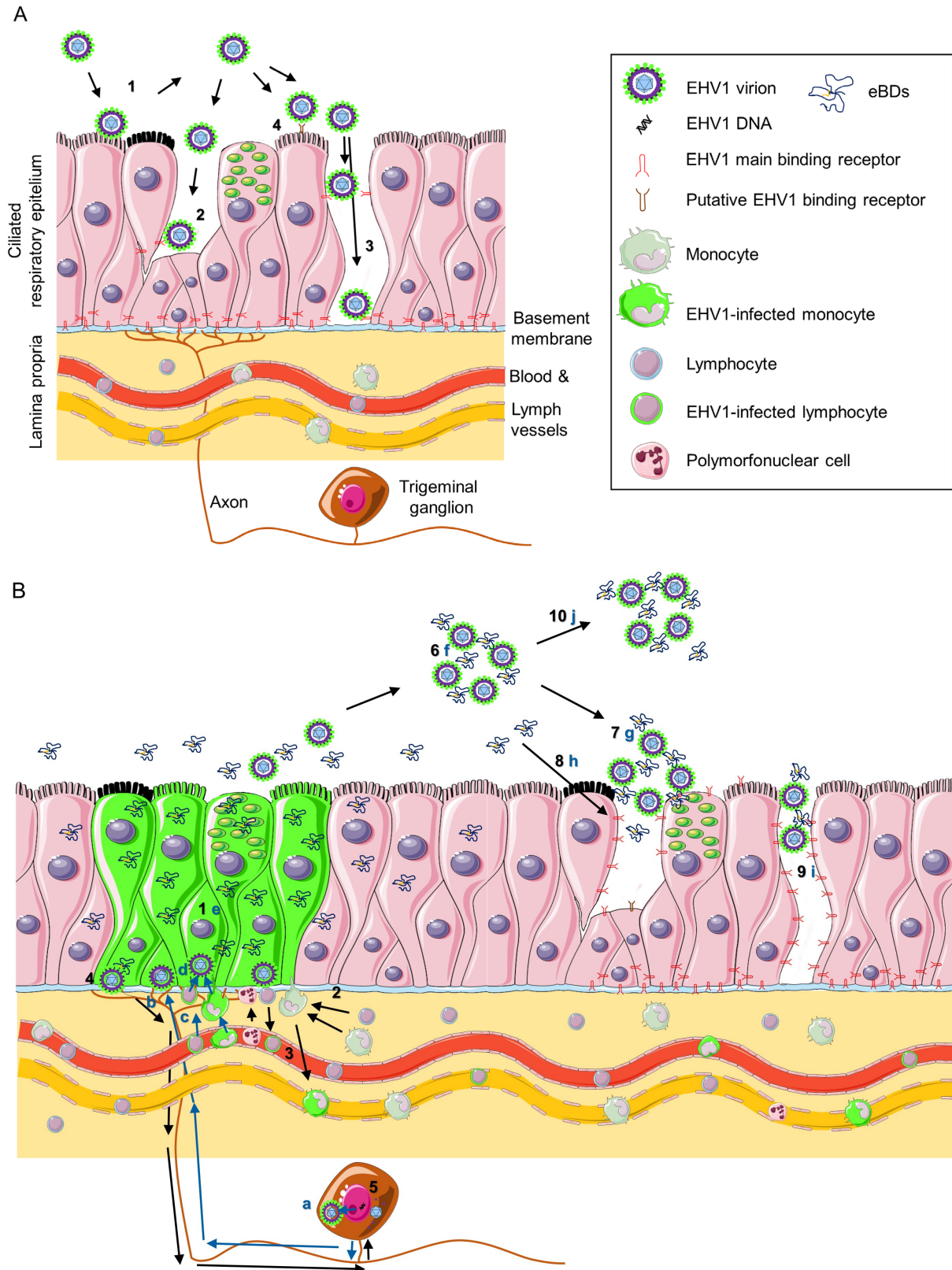


Figure 1. Hypothetical model of EHV1 primary infection in a new host (A and B, black arrows) and reactivation from a latently infected host (B, blue arrows). (A) (1) Inhaled EHV1 particles cannot stably bind to the apical surfaces of respiratory epithelial cells and detach again (1). At certain spots, epithelial integrity might be impaired by external or internal factors. Pollen proteases specifically disrupt epithelial integrity of columnar epithelial cells (2), while exposure to Lysomucil® and/or the mycotoxin deoxynivalenol completely disrupt the epithelial barrier (3). Cell turnover or lymphocyte diapedesis might (partly) impair integrity of both columnar and/or basal cells (2 or 3). Alternatively, EHV1 might bind to another putative apically located binding receptor (4). (B) EHV1 replicates in the respiratory epithelium in a plaque-wise manner (green). EHV1 orchestrates the respiratory epithelial cells to produce equine β -defensins (eBDs) (1). EBDs attract local and blood leukocytes (2), which in

turn might act as an EHV1 dissemination vessel to the bloodstream and/or a reservoir for EHV1 (3). In addition, EHV1 replication in e.g. brush cells grants the virus with direct access to the axons of the trigeminal ganglion (4). After retrograde axonal transport, EHV1 induces a state of latency in the trigeminal ganglion to persist in its host (5). The production of eBDs in the respiratory epithelium enhances further EHV1 infection through both viral- and cell-mediated actions. EBDs aggregate EHV1 virions (6) and thereby concentrate virus particles on the cell surface (7). EBDs act on respiratory epithelial cells, which might result in neutralisation of the net charge between an EHV1 virion and its putative main binding receptor and/or an upregulation and/or conformation change in EHV1's putative main binding receptor (8). Consequently, the chances of viral binding to cell surfaces will increase (9). Finally, EHV1-eBD aggregates might be spread in respiratory secretions to infect new hosts (10). In a latently infected host, EHV1 might reactivate and enter the productive cycle in neurons of the trigeminal ganglion (a). EHV1 travels back to the respiratory mucosa via anterograde axonal transport and can directly access its main binding receptor, located at basolateral respiratory epithelial cell surfaces (b). Similarly, EHV1-infected leukocytes might reroute to the respiratory mucosa (c) and transfer the virus to the basolateral surfaces of respiratory epithelial cells (d). Again, EHV1 replication results in the upregulation of eBD production by respiratory epithelial cells (e) which will lead to similar events as described above (f-j).

An alliance between modified β -defensins and the horse: is there a future?

Today's rise of multidrug-resistant pathogenic bacteria forced researchers to find alternatives to the traditional antibiotics. As an answer, multiple laboratories have screened a repertoire of defensin-like compounds for their potential use as an antimicrobial drug (Gordon *et al.*, 2005). Based on these results, pharmaceutical companies are currently developing new topical, as well as parenteral antimicrobial drugs that have a high likelihood of reaching commercialization. For instance, Plectasin NZ2114 is a chemically modified fungal defensin-like compound, active against *Streptococcus* sp., as well as *Staphylococcus* sp, and is presumably in a phase I clinical program at this moment (Li *et al.*, 2017; Zasloff, 2016). Next, Brilacidin (PMX30063) also shows extensive homologies with defensins and already advanced successfully through phase I and phase II clinical trials against acute *Staphylococcus aureus* skin or oral infections (Mensa *et al.*, 2014; Zasloff, 2016). So far, antimicrobial agents of this class have not yet been approved as drugs.

To test whether eBDs could be modified and developed as prophylactic or therapeutic antimicrobial drugs, the following considerations should be made. First of all, eBD2-3 seem to be valuable candidates, as they show distinct antimicrobial actions against bacteria, as well as viruses. In addition, they exhibit minimal cytotoxic activities and are thus considered to be safe. Therefore, the implementation of eBD2-3 in the aerosol therapy of horses suffering from respiratory infections could potentially work. However, given the fact that EHV1 benefits from eBD2-3 with an apparent increase in infection, these eBDs may not warrant further screening. Second, the previously proposed safety risk might be questioned if eBD2-3 would indeed activate specific (unwanted) signalling pathways. Nonetheless, we would encourage further development and trials with these eBDs. The implementation of these eBDs in the treatment of respiratory diseases in the horse will then, more than ever, highlight the need for proper diagnosis. Indeed, horses suffering from bacterial-, EIV- or EAV-induced respiratory disorders

could safely and potentially successfully be treated with these compounds. When nasal swabs test positive for EHV1, traditional therapies such as antibiotics and anti-inflammatory drugs should be preferred over eBDs. The same comment applies to the implementation of Lysomucil® in the aerosol treatment of horses with respiratory disorders.

EHV5: an obscure infiltrator in the global horse population

As a gammaherpesvirus, EHV5 is probably an older ancestor than the alphaherpesvirus EHV1 and thus, has experienced a longer co-evolution with its host (Karlin *et al.*, 1994). Perhaps this is the reason why the virus is highly present in the horse population. Indeed, EHV5 is frequently recovered from healthy horses and is only associated with disease in a handful of cases (Akkutay *et al.*, 2014; Bell *et al.*, 2006; Dunowska *et al.*, 1999; Dunowska *et al.*, 2002; Marenzoni *et al.*, 2010; Richter *et al.*, 2009; Torfason *et al.*, 2008; Wang *et al.*, 2007; Wong *et al.*, 2008).

In Chapter 7, we showed that an RK13 epithelial cell-derived EHV5 stock merely infected T and B lymphocytes, but was unable to replicate in the horse's ciliated respiratory epithelium. We speculate that this is an even more advanced strategy, compared to that of EHV1, to infiltrate the horse. Upon entry in a new host, EHV5 presumably directly infects its target latency reservoirs without initiating a primary replication in the respiratory epithelium. This strategy allows the virus to evade immunosurveillance. From the moment EHV5 successfully enters its target cells, it stays in. Even when EHV5-infected cells succumb due to infection, 'self-containing' apoptosis is induced rather than necrosis. Only when an opportunity rises (i.e. cell-cell contacts are established), EHV5 might transfer the infection. In some infected lymphocytes, EHV5 presumably establishes latency to survive over longer periods of time. Further evidence for this statement comes from the fact that EHV5 is often recovered from lymph nodes and blood of healthy horses (Bell *et al.*, 2006; Dunowska *et al.*, 1999; Richter *et al.*, 2009; Torfason *et al.*, 2008; Vander Werf *et al.*, 2014). At certain periods throughout the life-span of an EHV5-infected horse, the virus will exit through the horse's respiratory tract. Although highly speculative at this point, we propose that EHV5 transfers infection from infected lymphocytes to the basolateral surface of respiratory epithelial cells. A high amount of progeny virus particles are likely to be released in respiratory secretions and serve to infect new hosts. This may be accompanied by common respiratory disorders in the infected horse, such as nasal discharge, lymph node swelling, anorexia, depression and fever. Finally, EHV5 infection might induce the onset of more severe pathologies, such as fatal equine multinodular pulmonary fibrosis (EMPF), the development of lymphomas or leukaemia in a small number

of immunocompromised individuals (Schwarz *et al.*, 2012; Vander Werf and Davis, 2013; Williams *et al.*, 2007). Although we showed that EHV5 can directly infect lung alveolar cells, this does not provide any direct indication for the potency of EHV5 to induce fibrosis. Most likely, the onset of these malignancies is related to a (small) deviation in the balance between the horse's immune system and EHV5. Future studies should look at the precise mechanisms involved in the initiation and progress of these diseases. In conclusion, we could state that evolution granted EHV5 with several sophisticated immune-evasion mechanisms and current studies just discovered the 'tip of the iceberg'.

Afterword

This PhD thesis provides new insights in the dynamic and reciprocal interactions between the horse and equine airborne pathogens, presumably established during years of co-evolution. Natural selection led to adaptive changes in both the host and its pathogens, resulting in a heavily armoured horse and a repertoire of pathogen strategies. A summary of our findings on the interaction between EHV1 and the horse's respiratory mucosa is illustrated in Figure 1. It seems that no matter how many defence mechanisms the horse has developed during evolution, pathogens will always find a way to circumvent. It would be easy to conclude that the evolutionary arms race between pathogens and the horse cannot simply be won by the horse, due to its slow reproduction time and therefore slow evolution. Indeed, horses can produce one offspring every year, while viruses for instance, produce millions of progeny virions in a few hours only. In addition, evidence from this thesis strongly indicates that respirable hazards from today's modern society interrupt the thin host-pathogen balance by assaulting the horse. This does not mean that we should give up the battle. Today, science has already discovered a plethora of successful antimicrobial therapies and even eradication strategies. We would strongly encourage future research to act as an ally of the horse and expand our current knowledge on all of these important airborne pathogens, thereby focussing on the interplay between host barriers, airborne pathogens and modern society's respirable hazards.

References

- Akkutay, A.Z., Osterrieder, N., Damiani, A., Tischer, B.K., Borchers, K., Alkan, F., 2014.** Prevalence of equine gammaherpesviruses on breeding farms in Turkey and development of a TaqMan MGB real-time PCR to detect equine herpesvirus 5 (EHV-5). *Archives of virology* 159, 2989-2995.
- Allen, G.P., Bryans, J.T., 1986.** Molecular epizootiology, pathogenesis, and prophylaxis of equine herpesvirus-1 infections. *Progress in veterinary microbiology and immunology* 2, 78-144.
- Atkuri, K.R., Mantovani, J.J., Herzenberg, L.A., Herzenberg, L.A., 2007.** N-Acetylcysteine - a safe antidote for cysteine/glutathione deficiency. *Current Opinion in Pharmacology* 7, 355-359.
- Ballard, S.T., Schepens, S.M., Falcone, J.C., Meininger, G.A., Taylor, A.E., 1992.** Regional bioelectric properties of porcine airway epithelium. *Journal of applied physiology* (Bethesda, Md. : 1985) 73, 2021-2027.
- Baum, B., Georgiou, M., 2011.** Dynamics of adherens junctions in epithelial establishment, maintenance, and remodeling. *The Journal of cell biology* 192, 907-917.
- Bell, S.A., Balasuriya, U.B., Nordhausen, R.W., MacLachlan, N.J., 2006.** Isolation of equine herpesvirus-5 from blood mononuclear cells of a gelding. *Journal of veterinary diagnostic investigation* 18, 472-475.
- Biomin, 2016.** Mycotoxin Survey 2016 Third quarter (July to Sept, 2016). <https://nutricionanimal.info/wp-content/uploads/2016/11/Mycotoxin-Survey-Presentation-Q3-2016-1.pdf>
- Biragyn, A., Ruffini, P.A., Leifer, C.A., Klyushnenkova, E., Shakhov, A., Chertov, O., Shirakawa, A.K., Farber, J.M., Segal, D.M., Oppenheim, J.J., 2002.** Toll-like receptor 4-dependent activation of dendritic cells by β -defensin 2. *Science (New York, N.Y.)* 298, 1025-1029.
- Boucher, R.C., Stutts, M.J., Gatzky, J.T., 1981.** Regional differences in bioelectric properties and ion flow in excised canine airways. *Journal of applied physiology: respiratory, environmental and exercise physiology* 51, 706-714.
- Breuer, D., Becker, M., 1983.** Acetylcysteine (Fluimucil) in the treatment of COPD of the horse. *Tierärztliche Praxis* 11, 209-212.
- Brown, R.C., Davis, T.P., 2002.** Calcium modulation of adherens and tight junction function: a potential mechanism for blood-brain barrier disruption after stroke. *Stroke* 33, 1706-1711.
- Cai, W.H., Gu, B., Person, S., 1988.** Role of glycoprotein B of herpes simplex virus type 1 in viral entry and cell fusion. *Journal of Virology* 62, 2596-2604.
- Carossino, M., Loynachan, A.T., Canisso, I.F., Cook, R.F., Campos, J.R., Nam, B., Go, Y.Y., Squires, E.L., Troedsson, M.H., Swerczek, T., 2017.** Equine arteritis virus has specific tropism for stromal cells and CD8⁺ T and CD21⁺ B lymphocytes but not glandular epithelium at the primary site of persistent infection in the stallion reproductive tract. *Journal of virology, JVI*. 00418-00417.
- Chang, T.L., Vargas, J., DelPortillo, A., Klotman, M.E., 2005.** Dual role of α -defensin-1 in anti-HIV-1 innate immunity. *The Journal of clinical investigation* 115, 765-773.
- Chiu, L.-L., Perng, D.-W., Yu, C.-H., Su, S.-N., Chow, L.-P., 2007.** Mold allergen, pen C 13, induces IL-8 expression in human airway epithelial cells by activating protease-activated receptor 1 and 2. *The Journal of Immunology* 178, 5237-5244.
- D'Amato, G., Liccardi, G., D'Amato, M., Cazzola, M., 2001.** The role of outdoor air pollution and climatic changes on the rising trends in respiratory allergy. *Respiratory Medicine* 95, 606-611.
- Daher, K.A., Selsted, M.E., Lehrer, R.I., 1986.** Direct inactivation of viruses by human granulocyte defensins. *Journal of virology* 60, 1068-1074.
- Dauletbaev, N., Fischer, P., Aulbach, B., Gross, J., Kusche, W., Thyroff-Friesinger, U., Wagner, T., Bargon, J., 2009.** A phase II study on safety and efficacy of high-dose N-acetylcysteine in patients with cystic fibrosis. *European journal of medical research* 14, 352.
- Decramer, M., Rutten-van Mülken, M., Dekhuijzen, P.N.R., Troosters, T., van Herwaarden, C., Pellegrino, R., van Schayck, C.P.O., Olivieri, D., Del Donno, M., De Backer, W., Lankhorst, I., Ardia, A., 2005.** Effects of N-acetylcysteine on outcomes in chronic obstructive pulmonary disease (Bronchitis Randomized on NAC Cost-Utility Study, Bronchus): a randomised placebo-controlled trial. *The Lancet* 365, 1552-1560.

- Diao, R., Fok, K.L., Chen, H., Yu, M.K., Duan, Y., Chung, C.M., Li, Z., Wu, H., Li, Z., Zhang, H., 2014.** Deficient human β -defensin 1 underlies male infertility associated with poor sperm motility and genital tract infection. *Science translational medicine* 6, 249ra108-249ra108.
- Dunowska, M., Meers, J., Wilks, C., 1999.** Isolation of equine herpesvirus type 5 in New Zealand. *New Zealand Veterinary Journal* 47, 44-46.
- Dunowska, M., Wilks, C., Studdert, M., Meers, J., 2002.** Equine respiratory viruses in foals in New Zealand. *New Zealand Veterinary Journal* 50, 140-147.
- Earing, J.E., Hathaway, M.R., Sheaffer, C.C., Hetchler, B.P., Jacobson, L.D., Paulson, J.C., Martinson, K.L., 2013.** Effect of hay steaming on forage nutritive values and dry matter intake by horses. *Journal of animal science* 91, 5813-5820.
- Edens, H.A., Parkos, C.A., 2000.** Modulation of epithelial and endothelial paracellular permeability by leukocytes. *Advanced Drug Delivery Reviews* 41, 315-328.
- Edington, N., Bridges, C., Patel, J., 1986.** Endothelial cell infection and thrombosis in paralysis caused by equid herpesvirus-1: equine stroke. *Archives of virology* 90, 111-124.
- Galen, B., Cheshenko, N., Tuyama, A., Ramratnam, B., Herold, B.C., 2006.** Access to nectin favors herpes simplex virus infection at the apical surface of polarized human epithelial cells. *Journal of Virology* 80, 12209-12218.
- Gardiner, D.W., Lunn, D.P., Goehring, L.S., Chiang, Y.-W., Cook, C., Osterrieder, N., McCue, P., Del Piero, F., Hussey, S.B., Hussey, G.S., 2012.** Strain impact on equine herpesvirus type 1 (EHV-1) abortion models: Viral loads in foetal and placental tissues and foals. *Vaccine* 30, 6564-6572.
- Gibson, J., Slater, J., Awan, A., Field, H., 1992.** Pathogenesis of equine herpesvirus-1 in specific pathogen-free foals: primary and secondary infections and reactivation. *Archives of virology* 123, 351-366.
- Gilkerson, J.R., Bailey, K.E., Diaz-Méndez, A., Hartley, C.A., 2015.** Update on Viral Diseases of the Equine Respiratory Tract. *Veterinary Clinics of North America: Equine Practice* 31, 91-104.
- Goehring, L.S., Winden, S.C., Maanen, C.v., Oldruitenborgh-Oosterbaan, M.M.S., 2006.** Equine Herpesvirus Type 1-Associated Myeloencephalopathy in The Netherlands: A Four-Year Retrospective Study (1999-2003). *Journal of veterinary internal medicine* 20, 601-607.
- Gordon, Y.J., Romanowski, E.G., McDermott, A.M., 2005.** A review of antimicrobial peptides and their therapeutic potential as anti-infective drugs. *Current eye research* 30, 505-515.
- Gryspeerd, A.C., Vandekerckhove, A., Garré, B., Barbé, F., Van de Walle, G., Nauwynck, H., 2010.** Differences in replication kinetics and cell tropism between neurovirulent and non-neurovirulent EHV1 strains during the acute phase of infection in horses. *Veterinary microbiology* 142, 242-253.
- Harkema, J.R., Carey, S.A., Wagner, J.G., 2006.** The nose revisited: a brief review of the comparative structure, function, and toxicologic pathology of the nasal epithelium. *Toxicologic pathology* 34, 252-269.
- Harwig, S.S., Swiderek, K.M., Kokryakov, V.N., Tan, L., Lee, T.D., Panyutich, E.A., Aleshina, G.M., Shamova, O.V., Lehrer, R.I., 1994.** Gallinacins: cysteine-rich antimicrobial peptides of chicken leukocytes. *FEBS letters* 342, 281-285.
- Hazrati, E., Galen, B., Lu, W.Y., Wang, W., Yan, O.Y., Keller, M.J., Lehrer, R.I., Herold, B.C., 2006.** Human alpha- and beta-defensins block multiple steps in herpes simplex virus infection. *Journal of Immunology* 177, 8658-8666.
- Henninger, R.W., Reed, S.M., Saville, W.J., Allen, G.P., Hass, G.F., Kohn, C.W., Sofaly, C., 2007.** Outbreak of Neurologic Disease Caused by Equine Herpesvirus-1 at a University Equestrian Center. *Journal of Veterinary Internal Medicine* 21, 157-165.
- Heads of Medicines Agencies (2018).** Equimucin 2g, oral powder for horses. Summary of product characteristics. https://mri.cts-mrp.eu/Human/Downloads/DE_V_0108_001_FinalSPC.pdf
- Hu, S.-G., Zou, M., Yao, G.-X., Ma, W.-B., Zhu, Q.-L., Li, X.-Q., Chen, Z.-J., Sun, Y., 2014.** Androgenic regulation of beta-defensins in the mouse epididymis. *Reproductive Biology and Endocrinology* 12, 76.
- Hughes, A.L., 1999.** Evolutionary diversification of the mammalian defensins. *Cellular and Molecular Life Sciences CMLS* 56, 94-103.

- Hussey, G.S., Ashton, L.V., Quintana, A.M., Lunn, D.P., Goehring, L.S., Annis, K., Landolt, G., 2014. Innate immune responses of airway epithelial cells to infection with Equine herpesvirus-1. *Veterinary microbiology* 170, 28-38.
- Jackson, T., Kendrick, J., 1971. Paralysis of horses associated with equine herpesvirus 1 infection. *Amer Vet Med Ass J*.
- Jalkanen, J., Huhtaniemi, I., Poutanen, M., 2005. Discovery and characterization of new epididymis-specific beta-defensins in mice. *Biochimica et Biophysica Acta (BBA) - Gene Structure and Expression* 1730, 22-30.
- Johnson, G.P., Lloyd, A.T., O'Farrelly, C., Meade, K.G., Fair, S., 2015. Comparative genomic identification and expression profiling of a novel β -defensin gene cluster in the equine reproductive tract. *Reproduction, fertility, and development*.
- Karlin, S., Mocarski, E.S., Schachtel, G.A., 1994. Molecular evolution of herpesviruses: genomic and protein sequence comparisons. *J Virol* 68, 1886-1902.
- Kato, T., Takai, T., Fujimura, T., Matsuoka, H., Ogawa, T., Murayama, K., Ishii, A., Ikeda, S., Okumura, K., Ogawa, H., 2009. Mite serine protease activates protease-activated receptor-2 and induces cytokine release in human keratinocytes. *Allergy* 64, 1366-1374.
- Klupp, B.G., Nixdorf, R., Mettenleiter, T.C., 2000. Pseudorabies Virus Glycoprotein M Inhibits Membrane Fusion. *Journal of Virology* 74, 6760.
- Knight, D.A., Holgate, S.T., 2003. The airway epithelium: structural and functional properties in health and disease. *Respirology (Carlton, Vic.)* 8, 432-446.
- Kota, S., Sabbah, A., Harnack, R., Xiang, Y., Meng, X., Bose, S., 2008. Role of human beta defensin-2 during tumor necrosis factor- α /NF- κ B mediated innate anti-viral response against human respiratory syncytial virus. *Journal of Biological Chemistry*.
- Kumamoto, J., Tsutsumi, M., Goto, M., Nagayama, M., Denda, M., 2016. Japanese Cedar (*Cryptomeria japonica*) pollen allergen induces elevation of intracellular calcium in human keratinocytes and impairs epidermal barrier function of human skin *ex vivo*. *Archives of dermatological research* 308, 49-54.
- Kurtz, B.M., Singletary, L.B., Kelly, S.D., Frampton, A.R., Jr., 2010. Equus caballus major histocompatibility complex class I is an entry receptor for equine herpesvirus type 1. *J Virol* 84, 9027-9034.
- Laval, K., Favoreel, H.W., Nauwynck, H.J., 2015. Equine herpesvirus type 1 replication is delayed in CD172a⁺ monocytic cells and controlled by histone deacetylases. *The Journal of general virology* 96, 118-130.
- Laval, K., Favoreel, H.W., Van Cleemput, J., Poelaert, K.C.K., Brown, I.K., Verhasselt, B., Nauwynck, H.J., 2016. Entry of equid herpesvirus 1 into CD172a⁺ monocytic cells. *Journal of General Virology* 97, 733-746.
- Léguillette, R., 2003. Recurrent airway obstruction - heaves. *Veterinary Clinics: Equine Practice* 19, 63-86.
- Lehrer, R.I., Ganz, T., 2002. Defensins of vertebrate animals. *Current Opinion in Immunology* 14, 96-102.
- Leikina, E., Delanoe-Ayari, H., Melikov, K., Cho, M.-S., Chen, A., Waring, A.J., Wang, W., Xie, Y., Loo, J.A., Lehrer, R.I., 2005. Carbohydrate-binding molecules inhibit viral fusion and entry by crosslinking membrane glycoproteins. *Nature immunology* 6, 995.
- Li, Z., Wang, X., Wang, X., Teng, D., Mao, R., Hao, Y., Wang, J., 2017. Research advances on plectasin and its derivatives as new potential antimicrobial candidates. *Process Biochemistry* 56, 62-70.
- Little, T., Holyoak, G., McCollum, W., Timoney, P., 1992. Output of equine arteritis virus from persistently infected stallions is testosterone-dependent.
- Lopez-Souza, N., Favoreto, S., Wong, H., Ward, T., Yagi, S., Schnurr, D., Finkbeiner, W.E., Dolganov, G.M., Widdicombe, J.H., Boushey, H.A., Avila, P.C., 2009. *In vitro* susceptibility to rhinovirus infection is greater for bronchial than for nasal airway epithelial cells in human subjects. *The Journal of allergy and clinical immunology* 123, 1384-1390.e1382.
- Lunn, D.P., Davis-Poynter, N., Flaminio, M.J.B.F., Horohov, D.W., Osterrieder, K., Pusterla, N., Townsend, H.G.G., 2009. Equine Herpesvirus-1 Consensus Statement. *Journal of Veterinary Internal Medicine* 23, 450-461.

- Mair, T.S., Derksen, F.J., 2000.** Chronic obstructive pulmonary disease: a review. *Equine Veterinary Education* 12, 35-44.
- Marenzoni, M.L., Coppola, G., Maranesi, M., Passamonti, F., Cappelli, K., Capomaccio, S., Verini Supplizi, A., Thiry, E., Coletti, M., 2010.** Age-dependent prevalence of equid herpesvirus 5 infection. *Veterinary Research Communications* 34, 703-708.
- Marr, C.M., 2016.** Cardiac and Respiratory Disease in Aged Horses. *Veterinary Clinics of North America: Equine Practice* 32, 283-300.
- McGeoch, D.J., Cook, S., Dolan, A., Jamieson, F.E., Telford, E.A., 1995.** Molecular phylogeny and evolutionary timescale for the family of mammalian herpesviruses. *Journal of molecular biology* 247, 443-458.
- Mensa, B., Howell, G.L., Scott, R., DeGrado, W.F., 2014.** Comparative mechanistic studies of brilacidin, daptomycin and the antimicrobial peptide LL16. *Antimicrobial agents and chemotherapy*, AAC. 02955-02914.
- Nagy, A., Dyson, S.J., Murray, J.K., 2017.** Veterinary problems of endurance horses in England and Wales. *Preventive Veterinary Medicine* 140, 45-52.
- Nilsson, M., Fagman, H., Ericson, L.E., 1996.** Ca²⁺-dependent and Ca²⁺-independent regulation of the thyroid epithelial junction complex by protein kinases. *Experimental cell research* 225, 1-11.
- Ogunade, I., Martinez-Tuppi, C., Queiroz, O., Jiang, Y., Drouin, P., Wu, F., Vyas, D., Adesogan, A., 2018.** Silage review: Mycotoxins in silage: Occurrence, effects, prevention, and mitigation. *Journal of dairy science* 101, 4034-4059.
- Patel, J.R., Heldens, J., 2005.** Equine herpesviruses 1 (EHV-1) and 4 (EHV-4) – epidemiology, disease and immunoprophylaxis: A brief review. *The Veterinary Journal* 170, 14-23.
- Pinton, P., Nougayrède, J.-P., Del Rio, J.-C., Moreno, C., Marin, D.E., Ferrier, L., Bracarense, A.-P., Kolf-Clauw, M., Oswald, I.P., 2009.** The food contaminant deoxynivalenol, decreases intestinal barrier permeability and reduces claudin expression. *Toxicology and applied pharmacology* 237, 41-48.
- Quinones-Mateu, M.E., Lederman, M.M., Feng, Z., Chakraborty, B., Weber, J., Rangel, H.R., Marotta, M.L., Mirza, M., Jiang, B., Kiser, P., Medvik, K., Sieg, S.F., Weinberg, A., 2003.** Human epithelial beta-defensins 2 and 3 inhibit HIV-1 replication. *AIDS (London, England)* 17, F39-48.
- Radhakrishnan, Y., Hamil, K., Yenugu, S., Young, S., French, F., Hall, S., 2005.** Identification, characterization, and evolution of a primate β -defensin gene cluster. *Genes and immunity* 6, 203.
- Reas, H.W., 1963.** The effect of N-acetylcysteine on the viscosity of tracheobronchial secretions in cystic fibrosis of the pancreas. *The Journal of Pediatrics* 62, 31-35.
- Richter, N., Ebert, M., Borchers, K., 2009.** Prevalence of EHV-2 and EHV-5 DNA in ocular and nasal swabs as well as peripheral blood mononuclear cells. *Pferdeheilkunde* 25, 38-44.
- Salvatore, M., García-Sastre, A., Ruchala, P., Lehrer, R.I., Chang, T., Klotman, M.E., 2007.** β -defensin inhibits influenza virus replication by cell-mediated mechanism (s). *Journal of Infectious Diseases* 196, 835-843.
- Sanchez, L.C., 2018.** Chapter 12 - Disorders of the Gastrointestinal System, in: Reed, S.M., Bayly, W.M., Sellon, D.C. (Eds.), *Equine Internal Medicine (Fourth Edition)*. W.B. Saunders, pp. 709-842.
- Sato, A., 2007.** Tuft cells. *Anatomical Science International* 82, 187-199.
- Schwarz, B., Gruber, A., Benetka, V., Rütgen, B., Schwendenwein, I., Leidinger, E., van den Hoven, R., 2012.** Concurrent T cell leukaemia and equine multinodular pulmonary fibrosis in a Hanoverian Warmblood mare. *Equine Veterinary Education* 24, 187-192.
- Shasby, D.M., Shasby, S.S., 1986.** Effects of calcium on transendothelial albumin transfer and electrical resistance. *Journal of applied physiology (Bethesda, Md. : 1985)* 60, 71-79.
- Sherman, J., Mitchell, W.R., Martin, S.W., Thorsen, J., Ingram, D.G., 1979.** Epidemiology of equine upper respiratory tract disease on standardbred racetracks. *Canadian Journal of Comparative Medicine* 43, 1-9.
- Territo, M.C., Ganz, T., Selsted, M., Lehrer, R., 1989.** Monocyte-chemotactic activity of defensins from human neutrophils. *The Journal of clinical investigation* 84, 2017-2020.

- Torfason, E.G., Thorsteinsdottir, L., Torsteinsdóttir, S., Svansson, V., 2008.** Study of equid herpesviruses 2 and 5 in Iceland with a type-specific polymerase chain reaction. *Research in veterinary science* 85, 605-611.
- Van Bockstaele, F., Holz, J.-B., Revets, H., 2009.** The development of nanobodies for therapeutic applications. *Current opinion in investigational drugs (London, England: 2000)* 10, 1212-1224.
- Van de Walle, G.R., Peters, S.T., VanderVen, B.C., O'Callaghan, D.J., Osterrieder, N., 2008.** Equine herpesvirus 1 entry via endocytosis is facilitated by alphaV integrins and an RSD motif in glycoprotein D. *J Virol* 82, 11859-11868.
- Van De Walle, J., Sargent, T., Piront, N., Toussaint, O., Schneider, Y.-J., Larondelle, Y., 2010.** Deoxynivalenol affects *in vitro* intestinal epithelial cell barrier integrity through inhibition of protein synthesis. *Toxicology and Applied Pharmacology* 245, 291-298.
- van Egmond, H.P., Schothorst, R.C., Jonker, M.A., 2007.** Regulations relating to mycotoxins in food. *Analytical and bioanalytical chemistry* 389, 147-157.
- Vandekerkhove, A.P., Glorieux, S., Gryspeerdt, A.C., Steukers, L., Duchateau, L., Osterrieder, N., Van de Walle, G.R., Nauwynck, H.J., 2010.** Replication kinetics of neurovirulent versus non-neurovirulent equine herpesvirus type 1 strains in equine nasal mucosal explants. *The Journal of general virology* 91, 2019-2028.
- Vander Werf, K., Davis, E., 2013.** Disease remission in a horse with EHV-5-associated lymphoma. *Journal of veterinary internal medicine* 27, 387-389.
- Vander Werf, K.A., Davis, E.G., Janardhan, K., Bawa, B., Bolin, S., Almes, K., 2014.** Identification of Equine Herpesvirus 5 in Horses with Lymphoma. *Journal of Equine Veterinary Science* 34, 738-741.
- Vanlandschoot, P., Stortelers, C., Beirnaert, E., Ibañez, L.I., Schepens, B., Depla, E., Saelens, X., 2011.** Nanobodies[®]: New ammunition to battle viruses. *Antiviral Research* 92, 389-407.
- Wang, C.-H.K., Chan, L.W., Johnson, R.N., Chu, D.S.H., Shi, J., Schellinger, J.G., Lieber, A., Pun, S.H., 2011.** The transduction of Cocksackie and Adenovirus Receptor-negative cells and protection against neutralizing antibodies by HPMA-co-oligolysine copolymer-coated adenovirus. *Biomaterials* 32, 9536-9545.
- Wang, L., Raidal, S.L., Pizzirani, A., Wilcox, G.E., 2007.** Detection of respiratory herpesviruses in foals and adult horses determined by nested multiplex PCR. *Veterinary microbiology* 121, 18-28.
- Wang, W., Owen, S.M., Rudolph, D.L., Cole, A.M., Hong, T., Waring, A.J., Lal, R.B., Lehrer, R.I., 2004.** Activity of α - and θ -defensins against primary isolates of HIV-1. *The Journal of Immunology* 173, 515-520.
- Williams, J.M., Duckworth, C.A., Burkitt, M.D., Watson, A.J.M., Campbell, B.J., Pritchard, D.M., 2015.** Epithelial Cell Shedding and Barrier Function: A Matter of Life and Death at the Small Intestinal Villus Tip. *Veterinary Pathology* 52, 445-455.
- Williams, K., Maes, R., Del Piero, F., Lim, A., Wise, A., Bolin, D., Caswell, J., Jackson, C., Robinson, N., Derksen, F., 2007.** Equine multinodular pulmonary fibrosis: a newly recognized herpesvirus-associated fibrotic lung disease. *Veterinary Pathology* 44, 849-862.
- Wilson, W.D., 1997.** Equine herpesvirus 1 myeloencephalopathy. *Veterinary Clinics: Equine Practice* 13, 53-72.
- Wong, D.M., Belgrave, R.L., Williams, K.J., Del Piero, F., Alcott, C.J., Bolin, S.R., Marr, C.M., Nolen-Walston, R., Myers, R.K., Wilkins, P.A., 2008.** Multinodular pulmonary fibrosis in five horses. *Journal of the American Veterinary Medical Association* 232, 898-905.
- Xagorari, A., Chlichlia, K., 2008.** Toll-Like Receptors and Viruses: Induction of Innate Antiviral Immune Responses. *The Open Microbiology Journal* 2, 49-59.
- Xiao, C., Puddicombe, S.M., Field, S., Haywood, J., Broughton-Head, V., Puxeddu, I., Haitchi, H.M., Vernon-Wilson, E., Sammut, D., Bedke, N., 2011.** Defective epithelial barrier function in asthma. *Journal of Allergy and Clinical immunology* 128, 549-556. e512.
- Yang, D., Chen, Q., Chertov, O., Oppenheim, J.J., 2000.** Human neutrophil defensins selectively chemoattract naive T and immature dendritic cells. *Journal of Leukocyte Biology* 68, 9-14.
- Yang, D., Chertov, O., Bykovskaia, S., Chen, Q., Buffo, M., Shogan, J., Anderson, M., Schröder, J., Wang, J., Howard, O., 1999.** β -Defensins: linking innate and adaptive immunity through dendritic and T cell CCR6. *Science (New York, N.Y.)* 286, 525-528.

- Yang, X., Forier, K., Steukers, L., Van Vlierberghe, S., Dubruel, P., Braeckmans, K., Glorieux, S., Nauwynck, H.J., 2012.** Immobilization of pseudorabies virus in porcine tracheal respiratory mucus revealed by single particle tracking. *PLoS One* 7, e51054.
- Zasloff, M., 2016.** Antimicrobial peptides: do they have a future as therapeutics?, *Antimicrobial Peptides*. Springer, pp. 147-154.
- Zhao, J., Poelaert, K.C., Cleemput, J., Nauwynck, H.J., 2017.** CCL2 and CCL5 driven attraction of CD172a⁺ monocytic cells during an equine herpesvirus type 1 (EHV-1) infection in equine nasal mucosa and the impact of two migration inhibitors, rosiglitazone (RSG) and quinacrine (QC). *Veterinary research* 48, 14.

Chapter 9.

Summary - Samenvatting

Summary

Respiratory disease is one of the main clinical manifestations in horses and frequently results in poor performance, a high morbidity and in some cases even death. The origin of respiratory disease is usually multifactorial. To better understand the outcome of respiratory disease, it is of utmost importance to study not merely airborne pathogens, but also the interplay between these pathogens, the horse's physical and immune barriers and hazards present in the ambient air. These three factors have most likely influenced one another during the long-term co-evolution of pathogens with their host, and can therefore be considered as the 'archetypical trifecta of co-evolution'. As a result, today's airborne pathogens and horses exhibit a plethora of 'survival strategies', which already allowed them to adapt and persist for many years. The aim of this thesis was to unravel the interplay between predominant pathogen-specific and host-specific factors and how a misbalance between these factors might cause respiratory mucosal damage and trigger the onset of respiratory disease.

Among these airborne pathogens, herpesviruses are the 'gold standard' if it comes to host-specificity acquired through many years of co-evolution. In addition, herpesviruses are currently considered by many to be the most important pathogens in global horse industry. Therefore, this thesis put emphasis on equine herpesviruses. Equine herpesvirus type 1 and 5 (EHV1 and 5) are highly prevalent in healthy horses worldwide but infections are usually asymptomatic. Still, viral-induced symptoms do occur in a small percentage of infected horses for yet unknown reasons. The alphaherpesvirus EHV1 is probably the best-known and most dreaded virus in the horse industry, as the virus causes respiratory disorders, abortion, neonatal foal disease and central nervous system disorders. Despite numerous studies focussing on the development of antiviral therapies and/or effective vaccines, EHV1 still persists in the horse population. Therefore, this thesis first aimed to uncover more of the interactions between EHV1 and its host, starting with those at the port of entry and exit: the horse's respiratory tract.

In **Chapter 1**, an introduction about the three factors in the archetypical trifecta of co-evolution (i.e. the horse's respiratory mucosa, airborne pathogens and respirable hazards) is given.

In **Chapter 2**, the aims of this thesis were formulated.

Primary EHV1 infection of the respiratory epithelium is restricted in healthy horses, most likely due to specific host barriers. Therefore, in **Chapter 3**, the role of equine epithelial cell

intercellular junctions (ICJ) as a physical barrier in the protection against EHV1 infection was examined. In both nasal and tracheal mucosal explants, disruption of ICJ with the calcium-modulators N-acetylcysteine (Lysomucil®) and EGTA enhanced subsequent EHV1 binding and infection. The overlying mucoprotein network in nasal mucosal explants functioned as an additional important barrier, as a similar destruction of the mucoprotein network and of ICJ with the mucolytic and calcium-modulating drug N-acetylcysteine was necessary to completely overcome the restriction of EHV1 infection. EHV1 preferentially bound to and entered primary equine respiratory epithelial cells (EREC) at basolateral surfaces. Restriction of EHV1 infection in EREC via apical inoculation was overcome by disruption of ICJ. Finally, it was shown that basolateral but not apical EHV1 infection of EREC was dependent on cellular N-linked glycans.

In **Chapter 4**, we showed that pollen proteases of Kentucky bluegrass, white birch and hazel selectively affected ICJ integrity of respiratory columnar epithelial cells in both *ex vivo* respiratory mucosal explants and primary *in vitro* EREC. Proteomic analysis of the white birch pollen diffusate identified serine-proteases of the subtilase-family, followed by meiotic prophase aminopeptidase 1 and a repertoire of glycosidases and lipases. Following this pollen protease-induced partial loss of barrier function, EHV1 infection of both respiratory mucosal explants and primary EREC was enhanced.

In **Chapter 5**, it was demonstrated that the mycotoxin deoxynivalenol (DON), but not the mycotoxins fumonisin B1 and aflatoxin B1 and not diesel exhaust particles disrupt ICJ integrity in both equine respiratory mucosal explants and EREC. Consequently, exposure to DON resulted in an increased EHV1 infection of these respiratory epithelial cells.

Besides strictly maintaining a barrier function with tight ICJ, the respiratory epithelium constantly produces a vast amount of antimicrobial peptides, including β -defensins, to counter incoming pathogens. Therefore, in **Chapter 6**, we examined the antimicrobial role of equine β -defensins (eBDs) on important equine airborne pathogens, in addition to their chemotactic activities on different equine blood-derived leukocyte populations. The presence of eBD1-3 was first mapped in the horse's respiratory tract using RT-PCR and immunofluorescent staining. Minimal inhibitory concentration tests and synchronized virus plaques assays showed that eBD2 and especially eBD3 were active against several bacterial (*Streptococcus* sp., *Rhodococcus* sp., *Actinobacillus* sp. and *Bordetella* sp.) and enveloped viral (equine arteritis

virus or EAV and equine influenza virus or EIV) field isolates through direct actions. Remarkably, incorporation of the multiple transmembrane-spanning glycoprotein M in the viral envelope allowed EHV1 to resist the membrane-attacking eBDs. Moreover, eBD2-3 enhanced EHV1 attachment to and infectivity in rabbit kidney epithelial (RK13) cells by concentrating virus particles as aggregates on the cell surface. Furthermore, all eBDs facilitated EHV1 binding to and entry in primary EREC, through cell-mediated actions. Next, EIV, but especially EHV1 infection elicited the production of eBD2-3 in EREC. All eBDs were able to attract one or more subclasses of equine blood-derived leukocytes (i.e. polymorphonuclear cells, monocytes, T lymphocytes). Therefore, we stated that EHV1 specifically orchestrates EREC to synthesize eBDs for a well-controlled chemotaxis of equine leukocytes, essential vessels for viral dissemination and persistence in the horse.

The gammaherpesvirus EHV5 only recently gained more attention, due to its putative role in the development of equine multinodular pulmonary fibrosis (EMPF). As little is known about EHV5 pathogenesis in the horse, we used several equine *ex vivo* and *in vitro* models in **Chapter 7** to uncover the first key steps in EHV5 pathogenesis. We found that EHV5 was unable to infect epithelial cells lining the mucosa of nasal and tracheal explants. Similarly, primary EREC were not susceptible to EHV5 following inoculation at the apical or basolateral surfaces. Upon direct delivery of EHV5 particles to lung explants, EHV5 could infect a few alveolar epithelial cells, localized in cell clusters. While equine blood-derived monocytes did not support EHV5 replication, up to 10% of inoculated equine T and B lymphocytes synthesized intracellular viral antigens at 24 hpi and 72 hpi, respectively. Still, the production of mature virus particles was hampered, as we did not observe an increase in extracellular virus titer. After reaching a peak, the percentage of infected T and B lymphocytes decayed, which was partly due to the onset of apoptosis, but not necrosis. Based on these results, a hypothetical model of EHV5 pathogenesis in the horse is given in the discussion of Chapter 7.

In **Chapter 8**, the data obtained in this thesis were discussed with emphasis on ‘the co-evolutionary battle’ between equine pathogens (especially EHV1) and the horse.

The main conclusions drawn from this thesis are:

- EHV1 targets a basolaterally located receptor in the horse's respiratory epithelium for a specific viral strategy. Therefore, the horse's epithelial ICJ function as the main barrier against primary EHV1 infections.
- Respirable hazards, such as Lysomucil[®] nebulizing treatment and exposure to pollen proteases or the mycotoxin deoxynivalenol, disrupt epithelial ICJ integrity and therefore predispose the horse's respiratory epithelium for EHV1 infection.
- While bacteria and some viruses are susceptible to eBDs, the ancient alphaherpesvirus EHV1 resists eBDs by incorporating the membrane-stabilising glycoprotein M in the viral envelope. Moreover, we demonstrated that the virus exploits these eBDs to increase its infectivity and ensure spread within the host.
- The gammaherpesvirus EHV5 exhibits a completely distinct pathogenesis, compared to the alphaherpesvirus EHV1. EHV5 does not replicate in the equine ciliated respiratory epithelium, but directly interacts with equine T and B lymphocytes for viral spread and persistence in the horse. Finally, EHV5 can directly infect equine epithelial alveolar cells, but its role in the onset of EMPF remains obscure so far.

Samenvatting

Luchtweg- en ademhalingsproblemen zijn één van de belangrijkste klinische manifestaties bij paarden en geven frequent aanleiding tot het ‘poor performance syndroom’, een hoge morbiditeit en soms zelfs sterfte bij deze dieren. De oorzaak van deze luchtweg- en ademhalingsproblemen is vaak van multifactoriële aard. In het onderzoek naar luchtwegaandoeningen is het dus van groot belang om zich niet enkel te focussen op luchtwegpathogenen. Men moet eerder de wisselwerking bestuderen tussen deze pathogenen, de fysische en immunologische barrières ter hoogte van het ademhalingsstelsel van het paard en potentiële inhaleerbare gevaarlijke stoffen. Deze drie factoren hebben elkaar hoogstwaarschijnlijk beïnvloed tijdens de co-evolutie tussen pathogenen en het paard. Daarom kan de drie-eenheid van deze factoren beschouwd worden als het archetypische voorbeeld van co-evolutie. Het is dankzij deze co-evolutie dat vandaag de dag zowel paardenpathogenen als paarden zelf een waaier aan ‘overlevingsstrategieën’ hebben ontwikkeld. Het doel van deze thesis was dan ook om de wisselwerking tussen pathogeen-specifieke, gastheer-specifieke en omgevingsfactoren te onderzoeken en hoe deze factoren schade aan de luchtwegen kunnen toebrengen en zo het ontstaan van ademhalingsproblemen in gang zetten.

Van al deze luchtwegpathogenen zijn Herpesvirussen het schoolvoorbeeld van gastheerspecificiteit. Die gastheerspecificiteit hebben ze verkregen na jarenlange co-evolutie met het paard. Bovendien vormen herpesvirussen tegenwoordig één van de belangrijkste pathogenen wereldwijd in de paardenindustrie. Daarom werd in deze thesis de nadruk vooral gelegd op equine herpesvirussen. Equine herpesvirus type 1 en 5 (EHV1 en 5) zijn alom aanwezig in de paardenpopulatie maar infecties verlopen meestal asymptomatisch. Niettemin komen virus-geïnduceerde symptomen toch voor in een klein percentage van geïnfekteerde paarden. Het alfaherpesvirus EHV1 is waarschijnlijk het best gekende en meest gevreesde virus in de paardenindustrie, omdat het virus luchtwegproblemen, abortus, sterfte bij neonatale veulens en centrale zenuwstoornissen veroorzaakt. Ondanks het feit dat reeds vele studies geprobeerd hebben om antivirale therapieën en/of vaccins te ontwikkelen, is EHV1 nog steeds aanwezig in de globale paardenpopulatie. Om deze redenen was een belangrijke doelstelling van deze thesis om meer te weten te komen over de interacties tussen EHV1 en zijn gastheer, te beginnen bij de interacties ter hoogte van de intrede- en uittredepoort van het virus: het ademhalingsstelsel van het paard.

Hoofdstuk 1 bevat een algemene inleiding over de drie-eenheid van co-evolutie: de respiratoire mucosa van het paard, luchtwegpathogenen en inhaleerbare gevaarlijke stoffen.

De doelstellingen van deze thesis zijn verwoord in **Hoofdstuk 2**.

Primaire EHV1-infectie in het respiratoir epitheel is beperkt bij gezonde paarden. Dit komt hoogstwaarschijnlijk door de aanwezigheid van specifieke barrières in het respiratoir epitheel. In **Hoofdstuk 3** werd daarom de rol van cellulaire intercellulaire bruggen (ICJ) als fysieke barrière in de bescherming tegen een EHV1-infectie onderzocht. In zowel nasale als tracheale mucosale explanten resulteerde een destructie van de ICJ met calcium-modulerende producten (N-acetylcysteïne [Lysomucil[®]] en EGTA) tot een betere EHV1-binding en -infectie. De mucoproteïne laag op nasale mucosale explanten functioneerde als een bijkomende belangrijke barrière, aangezien hier een simultane destructie van dit mucoproteïne netwerk en van ICJ met het mucolytisch en calcium-modulerend agens N-acetylcysteïne nodig was om de restrictie in EHV1-infectie te op te heffen. EHV1 hechtte zich preferentieel vast aan de basolaterale zijde van equine respiratoire epitheelcellen (EREC) en infecteerde deze dan ook het beste langs deze weg. De restrictie in EHV1-infectie na inoculatie langs de apicale zijde van EREC viel weg wanneer de cellulaire ICJ aangetast waren. Tenslotte werd het nog aangetoond dat basolaterale maar niet apicale EHV1-infectie van EREC afhankelijk was van cellulaire N-gelinkte glycanen.

In **Hoofdstuk 4** werd aangetoond dat pollen proteasen van veldbeemdgras, witte berk en hazelaar selectief de ICJ integriteit van respiratoire columnaire epitheelcellen aantastten in zowel *ex vivo* respiratoire mucosale explanten als primaire *in vitro* EREC. Via proteomics werden een aantal serine proteasen van de subtilase familie geïdentificeerd, gevolgd door meiotische profase aminopeptidase 1 en een reeks van glycosidasen en lipasen. Als gevolg van deze pollen protease-geïnduceerde aantasting van cellulaire ICJ, was de EHV1-infectiegraad in zowel mucosale explanten als in primaire EREC verhoogd.

In **Hoofdstuk 5** werd gedemonstreerd dat het mycotoxine deoxynivalenol (DON), maar niet de mycotoxines fumonisin B1 en aflatoxin B1 en ook niet diesel uitstoot partikels de ICJ integriteit van zowel equine respiratoire mucosale explanten als van EREC aantasten. Vandaar dat een blootstelling van het respiratoir epitheel aan DON leidde tot een hogere EHV1-infectiegraad hierin.

Naast het behouden van een barrièrefunctie dankzij stevige ICJ, produceert het respiratoir epitheel ook een repertoire aan antimicrobiële peptiden, waaronder β -defensins, om inkomende pathogenen af te weren. In **Hoofdstuk 6** werd het belang van equine β -defensins (eBDs) als antimicrobiële peptiden tegen belangrijke luchtwegpathogenen van het paard onderzocht, tezamen met hun rol als chemo-attractant voor verschillende paardenbloed leukocytopopulaties. De aanwezigheid van eBD1-3 in de luchtwegen van het paard werd eerst in kaart gebracht met behulp van RT-PCR en immunofluorescentiekleuring. Door middel van minimale concentratie inhibitie testen en gesynchroniseerde virus plaque assays werd vervolgens aangetoond dat eBD2 en vooral eBD3 actief waren tegen verschillende bacteriële (*Streptococcus* sp., *Rhodococcus* sp., *Actinobacillus* sp. en *Bordetella* sp.) en virale (equine arteritis virus of EAV en equine influenza virus of EIV) pathogenen op een directe manier. Het was opmerkelijk dat incorporatie van het multiële membraan-overbruggende glycoproteïne M in de envelop van EHV1 het virus resistent maakte tegen de membraan-vernietigende eBDs. Daarenboven was de virale aanhechting aan en infectie van konijnenniercellen (RK13 cellen) zelfs verhoogd na pre-incubatie van EHV1 met eBD2-3. Deze eBDs concentreerden de viruspartikels als aggregaten op het celoppervlak van RK13 cellen. Verder vergemakkelijkten alle eBDs de virus binding aan en intrede in primaire EREC door op de cellen in te werken. Vervolgens werd aangetoond dat EIV- en vooral EHV1-infectie de productie van eBD2-3 opdreef in EREC. Alle eBDs waren in staat om één of meerdere subklassen van paardenbloed leukocyten (polymorfonucleaire cellen, monocyt en T lymphocyten) aan te trekken. Daaruit besloten we dat EHV1 specifiek EREC orkestreert om eBDs aan te maken, om zo een gecontroleerde chemotaxis van leukocyten te induceren. Deze leukocyten zijn dan ook het essentiële vervoersmiddel van EHV1 om zich te verspreiden en in stand te houden binnenin zijn gastheer.

Het gammaherpesvirus EHV5 won recent aan belang door zijn mogelijke rol in de ontwikkeling van equine multinodulaire pulmonaire fibrose (EMPF). Omdat er slechts weinig gekend is over de pathogenese van EHV5 in het paard, werd geprobeerd om enkele ‘sleutelstappen’ in deze pathogenese te achterhalen in **Hoofdstuk 7**. Hiervoor werden verschillende *ex vivo* en *in vitro* paardenmodellen gebruikt. EHV5 bleek niet in staat te zijn om epitheelcellen van nasale en tracheale mucosale explanten te infecteren. Zo ook waren primaire EREC niet gevoelig voor EHV5, niet na inoculatie langs de apicale zijde, noch langs de basolaterale zijde. Wanneer EHV5 partikels aangebracht werden op longexplanten, kon het virus wel enkele alveolaire epitheelcellen, gelokaliseerd in celclusters, infecteren. Terwijl er in paardenbloed monocyt geen EHV5 replicatie gezien werd, vertoonden tot wel 10% van de geïnoculeerde paardenbloed

T en B lymphocyten intracellulaire virale antigenen 24 en 72 uur na infectie, respectievelijk. Desondanks werd de productie van mature viruspartikels onderdrukt, aangezien geen stijging in extracellulaire virus titer kon worden waargenomen. Na het bereiken van een piek, nam het percentage van geïnfecteerde T en B lymphocyten weer af. Deze afname werd deels veroorzaakt door infectie-geïnduceerde apoptose, maar niet door necrose. In de discussie van Hoofdstuk 7 werd, gebaseerd op deze resultaten, een hypothetisch model opgesteld omtrent de pathogenese van EHV5 in het paard.

In **Hoofdstuk 8** werden op basis van de bekomen gegevens uit deze thesis een conclusie geformuleerd en nieuwe inzichten en hypothesen naar voor gebracht, met de nadruk op het ‘co-evolutionaire gevecht’ tussen paardenpathogenen (voornamelijk EHV1) en het paard.

De belangrijkste besluiten die uit deze thesis afgeleid kunnen worden zijn:

- EHV1 richt zich strategisch op een basolateraal-gelocaliseerde receptor in het respiratoir epitheel van het paard. Vandaar dat de epitheliale intercellulaire bruggen een belangrijke barrière vormen tegen een primaire EHV1-infectie.
- Inhaleerbare gevaren, zoals Lysomucil[®] nebulisatie en het inademen van pollen proteasen en/of van het mycotoxine deoxynivalenol, kunnen de epitheliale ICJ aantasten en zo het respiratoir epitheel van het paard vatbaarder maken voor een EHV1-infectie.
- Hoewel bacteriën en sommige virussen gevoelig zijn aan eBDs, is het aloude alfaherpesvirus EHV1 dat niet dankzij de aanwezigheid van glycoproteïne M, welke meerdere transmembranaire domeinen heeft, in de virale envelop. Bovendien hebben we aangetoond dat EHV1 deze eBDs misbruikt om zijn infectiegraad te verhogen en zijn spreiding in de gastheer te verzekeren.
- Het gammaherpesvirus EHV5 vertoont een compleet andere pathogenese in vergelijking met het alfaherpesvirus EHV1. In plaats van eerst te vermeerderen in het gecilieerd respiratoir epitheel, richt EHV5 zich meteen op T en B lymphocyten voor de virale spreiding en in stand houding binnenin de gastheer. EHV5 kan eveneens alveolaire epitheelcellen uit de long rechtstreeks infecteren. De rol van het virus in de ontwikkeling van EMPF blijft voorlopig onduidelijk.

Curriculum Vitae

Jolien Van Cleemput werd geboren in Sint-Niklaas op 17 mei 1990. In 2008 behaalde zij het getuigschrift van hoger secundair onderwijs aan de Onze-Lieve-Vrouw-Presentatie te Sint-Niklaas in de richting Grieks-Wiskunde. Datzelfde jaar startte zij de opleiding diergeneeskunde aan de Universiteit Gent en behaalde in 2014 het diploma “Master in de diergeneeskunde, afstudeerrichting paard” met grootste onderscheiding. Gedurende de bacheloropleiding werd ze uitgenodigd om verschillende onderzoeksprojecten mee te volgen in het ‘topstudentenprogramma’. Hierbij raakte ze geboeid door onderzoek en samen met haar passie voor paarden zorgde dit ervoor dat ze als masterproef koos voor een onderzoeksproject op equine herpesvirus type 1 (EHV1). Deze thesis werd in 2014 bekroond als ‘Beste masterproef van optie paard’ door de ‘Wetenschappelijke Vereniging voor de Gezondheid van het Paard’ en leidde in 2015 tot een publicatie in ‘Journal of General Virology’. Na het afstuderen als dierenarts, startte ze haar doctoraat op de pathogenese van EHV1 onder de supervisie van prof. dr. Nauwynck. Hiervoor kreeg ze de doctoraatsbeurs van het Fonds voor Wetenschappelijk Onderzoek (FWO) Vlaanderen. Tijdens haar doctoraat begeleidde ze verschillende masterstudenten en topstudenten tijdens hun thesis en organiseerde ze practica voor de studenten uit optie paard.

Publications in peer-reviewed international journals

- **Jolien Van Cleemput**, Katrien C.K. Poelaert, Kathlyn Laval, Roger Maes, Gisela S. Hussey, Wim Van den Broeck, Hans J. Nauwynck (2017). Access to a main alphaherpesvirus receptor, located basolaterally in the respiratory epithelium, is masked by intercellular junctions. *Scientific Reports* 7, 16656.
- **Jolien Van Cleemput**, Katrien C.K. Poelaert, Kathlyn Laval, Hans J. Nauwynck (2018). Unravelling the first key steps in equine herpesvirus type 5 (EHV5) pathogenesis using *ex vivo* and *in vitro* equine models. *Veterinary Research* (under review).
- **Jolien Van Cleemput**, Katrien C.K. Poelaert, Kathlyn Laval, Francis Impens, Wim Van den Broeck, Kris Gevaert, Hans J. Nauwynck (2018). Beyond allergy: how pollen proteases destroy respiratory epithelial cell anchors and drive alphaherpesvirus infection. *Scientific Reports* (submitted).
- Kathlyn Laval, Jonah Vernejoul, **Jolien Van Cleemput**, Orkide Koyuncu, Lynn Enquist (2018). Virulent PRV infection induces a specific and lethal systemic inflammatory response in mice. *Journal of Virology*, JVI-01614.
- Katrien C.K. Poelaert, **Jolien Van Cleemput**, Kathlyn Laval, Herman Favoreel, Roger Maes, Gisela S. Hussey, Hans J. Nauwynck (2018). Abortigenic but not neurotropic equine herpes virus 1 modulates the interferon antiviral defense. *Frontiers in Cellular and Infection Microbiology* 8 (312).

- Jing Zhao, Katrien C. K. Poelaert, **Jolien Van Cleemput**, Hans J. Nauwynck (2017). CCL2 and CCL5 driven attraction of CD172a⁺ monocytic cells during an equine herpesvirus type 1 (EHV-1) infection in equine nasal mucosa and the impact of two migration inhibitors, rosiglitazone (RSG) and quinacrine (QC). *Veterinary Research* 48(1).
- Marlien Schaeck, Felipe E. Reyes-Lopez, Eva Vallejos-Vidal, **Jolien Van Cleemput**, Luc Duchateau, Wim Van den Broeck, Lluís Tort, Annemie Decostere (2017). Cellular and transcriptomic response to treatment with the probiotic candidate *Vibrio lentus* in gnotobiotic sea bass (*Dicentrarchus labrax*) larvae. *Fish & Shellfish Immunology* 63.
- Kathlyn Laval, **Jolien Van Cleemput**, Katrien C. Poelaert, Ivy K. Brown, Hans J. Nauwynck (2016). Replication of neurovirulent equine herpesvirus type 1 (EHV-1) in CD172a⁺ monocytic cells. *Comparative Immunology, Microbiology and Infectious Diseases* 50.
- Kathlyn Laval, Herman W. Favoreel, **Jolien Van Cleemput**, Katrien C.K., Poelaert, Ivy K. Brown, Bruno Verhasselt, Hans J. Nauwynck (2015). Entry of equine herpesvirus 1 (EHV-1) into CD172a⁺ monocytic cells. *Journal of General Virology* 97(3).
- Kathlyn Laval, Herman W. Favoreel, Katrien C.K. Poelaert, **Jolien Van Cleemput**, Hans J. Nauwynck (2015). Equine herpesvirus type 1 (EHV-1) enhances viral replication in CD172a⁺ monocytic cells upon adhesion to endothelial cells. *Journal of Virology* 89(21).
- Yewei Li, **Jolien Van Cleemput**, Yu Qiu, Vishwanatha R.A.P. Reddy, Bart Mateusen, Hans J. Nauwynck (2015). *Ex vivo* modeling of feline herpesvirus replication in ocular and respiratory mucosae, the primary targets of infection. *Veterinary Research* 21(0).
- Katrien C.K. Poelaert, **Jolien Van Cleemput**, Kathlyn Laval, Herman Favoreel, Liesbeth Couck, Wim Van den Broeck, Hans J. Nauwynck (2018). Equine herpesvirus 1 bridges T-lymphocytes to reach its target organs. *Journal of Virology* (under review).
- Bo Yang, Jiexiong Xie, **Jolien Van Cleemput**, Ruifang Wei, Geert Opsomer, Hans J. Nauwynck (2018). Gammaherpesvirus BoHV-4 infects bovine respiratory epithelial cells mainly at the basolateral side. *Veterinary Research* (under review).

Selected oral presentations

- **Jolien Van Cleemput**, Katrien Poelaert, Kathlyn Laval, Gisela Hussey, Roger Maes, Wim Van den Broeck, Hans Nauwynck (2018). Aerogenic factors facilitating respiratory EHV1 infection. British Equine Veterinary Association (BEVA) congress.
- **Jolien Van Cleemput**, Katrien Poelaert, Kathlyn Laval, Gisela Hussey, Roger Maes, Wim Van den Broeck, Hans Nauwynck (2018). Access to a main EHV1 receptor, located basolaterally in the respiratory epithelium, is masked by intercellular junctions and revealed by pollen proteases. 11th International congress ESVV for veterinary virology.
- **Jolien Van Cleemput**, Katrien Poelaert, Kathlyn Laval, Nathalie Vanderheijden, Maarten Dhaenens, Hans Nauwynck (2018). The interplay between equine β -defensins and local viral pathogens in the horse's respiratory tract. 11th International congress ESVV for veterinary virology.

- **Jolien Van Cleemput**, Katrien Poelaert, Kathlyn Laval, Gisela Hussey, Roger Maes, Wim Van den Broeck, Hans Nauwynck (2018). Access to a main alphaherpesvirus receptor, basolaterally in the respiratory epithelium, is masked by intercellular junctions and revealed by pollens. 43nd International Herpesvirus Workshop.
- **Jolien Van Cleemput**, Katrien Poelaert, Kathlyn Laval, Gisela Hussey, Roger Maes, Wim Van den Broeck, Hans Nauwynck (2017). Access to a main alphaherpesvirus receptor, located basolaterally in the respiratory epithelium, is masked by intercellular junctions and revealed by pollen proteases. 5th Annual meeting of the Belgian Society for Virology.
- Katrien Poelaert, **Jolien Van Cleemput**, Kathlyn Laval, Herman Favoreel, Hans Nauwynck (2018). Equine herpesvirus 1 bridges T-lymphocytes to reach its target organs. 6th Annual meeting of the Belgian Society for Virology.
- Katrien Poelaert, **Jolien Van Cleemput**, Kathlyn Laval, Herman Favoreel, Hans Nauwynck (2018). Equine herpesvirus 1 bridges T-lymphocytes to reach its target organs. 11th International congress ESVV for veterinary virology.
- Katrien Poelaert, **Jolien Van Cleemput**, Kathlyn Laval, Herman Favoreel, Gisela Hussey, Roger Maes, Hans Nauwynck (2018). Abortigenic but not neurotropic equine herpesvirus 1 modulates the interferon antiviral defense. 11th International congress ESVV for veterinary virology.
- Katrien Poelaert, **Jolien Van Cleemput**, Kathlyn Laval, Herman Favoreel, Hans Nauwynck (2018). Equine herpesvirus 1 bridges T-lymphocytes to reach its target organs. 43nd International Herpesvirus Workshop.
- Katrien Poelaert, **Jolien Van Cleemput**, Kathlyn Laval, Herman Favoreel, Gisela Hussey, Roger Maes, Hans Nauwynck (2017). Type I interferon is crucial in host defence against equine herpesvirus type 1. 42nd International Herpesvirus Workshop.
- Katrien C.K. Poelaert, **Jolien Van Cleemput**, Kathlyn Laval, Herman W. Favoreel, Hans J. Nauwynck (2016). Type I interferon, crucial in host defence against EHV-1?. 4th Annual meeting of the Belgian Society for Virology.
- Kathlyn Laval, Herman W. Favoreel, Katrien C.K. Poelaert, **Jolien Van Cleemput**, Hans J. Nauwynck (2015). Equine herpesvirus type 1 (EHV-1) enhances viral replication in CD172a⁺ monocytic cells upon adhesion to endothelial cells. 40th International Herpesvirus Workshop.
- Kathlyn Laval, Herman W. Favoreel, Katrien C.K. Poelaert, **Jolien Van Cleemput**, Hans J. Nauwynck (2015). Equine herpesvirus type 1 (EHV-1) enhances viral replication in CD172a⁺ monocytic cells upon adhesion to endothelial cells. 10th International congress ESVV for veterinary virology.

Selected poster presentations

- **Jolien Van Cleemput**, Katrien Poelaert, Kathlyn Laval, Gisela Hussey, Roger Maes, Wim Van den Broeck, Hans Nauwynck (2018). Access to a main alphaherpesvirus receptor, basolaterally in the respiratory epithelium, is masked by intercellular junctions and revealed by pollens. 43nd International Herpesvirus Workshop.

- **Jolien Van Cleemput**, Katrien Poelaert, Kathlyn Laval, Nathalie Vanderheijden, Maarten Dhaenens, Hans Nauwynck (2018). Exploiting the host's epithelial β -defensins in multiple ways: a new immune evasive alphaherpesvirus strategy. 43nd International Herpesvirus Workshop.
- **Jolien Van Cleemput**, Katrien Poelaert, Kathlyn Laval, Gisela Hussey, Roger Maes, Wim Van den Broeck, Hans Nauwynck (2017). Respiratory cell intercellular junctions are an innate barrier against equine herpesvirus type 1 infection in horses. 5th International congress ESVV for veterinary virology.
- **Jolien Van Cleemput**, Katrien Poelaert, Kathlyn Laval, Gisela Hussey, Roger Maes, Wim Van den Broeck, Hans Nauwynck (2017). Respiratory cell intercellular junctions are an innate barrier against equine herpesvirus type 1 infection in horses. 42nd International Herpesvirus Workshop.
- Katrien Poelaert, **Jolien Van Cleemput**, Kathlyn Laval, Herman Favoreel, Hans Nauwynck (2018). Equine herpesvirus 1 bridges T-lymphocytes to reach its target organs. 43nd International Herpesvirus Workshop.
- Katrien Poelaert, **Jolien Van Cleemput**, Kathlyn Laval, Herman Favoreel, Gisela Hussey, Roger Maes, Hans Nauwynck (2017). Type I interferon is crucial in host defence against equine herpesvirus type 1. 5th International congress ESVV for veterinary virology.
- Katrien Poelaert, **Jolien Van Cleemput**, Kathlyn Laval, Herman Favoreel, Gisela Hussey, Roger Maes, Hans Nauwynck (2017). Type I interferon is crucial in host defence against equine herpesvirus type 1. 42nd International Herpesvirus Workshop.
- Kathlyn Laval, Herman W. Favoreel, Katrien C.K. Poelaert, **Jolien Van Cleemput**, Hans J. Nauwynck (2015). Equine herpesvirus type 1 (EHV-1) enhances viral replication in CD172a⁺ monocytic cells upon adhesion to endothelial cells. 40th International Herpesvirus Workshop.
- Kathlyn Laval, Herman W. Favoreel, Katrien C.K. Poelaert, **Jolien Van Cleemput**, Hans J. Nauwynck (2015). Equine herpesvirus type 1 (EHV-1) enhances viral replication in CD172a⁺ monocytic cells upon adhesion to endothelial cells. 10th International congress ESVV for veterinary virology.

Dankwoord

Na 4 jaar zwoegen ben ik nu bij het laatste hoofdstuk van mijn doctoraat beland: het dankwoord. 'Last, but not least' zoals ze zeggen, want een doctoraat maak je niet alleen en met dit dankwoord wil ik dan ook iedereen die zijn steentje bijgedragen heeft tot dit werk heel erg hard bedanken.

Eerst en vooral wil ik mijn promotor, prof. dr. Hans Nauwynck, bedanken om mij van bij het begin tot het einde te steunen. We dienden samen een voorstel in bij het FWO over de pathogenese van EHV1 in het paard. Vooral dat paard was zo belangrijk voor mij en jij deed alle moeite om mijn wensen in dat project te verweven. Maar hoe kan het ook anders, naarmate mijn doctoraat vorderde ben ik 'lichtelijk' afgeweken van ons originele plan. Desalniettemin ben ik supertrots op mijn doctoraat! Vele ideeën uit dit werk zijn voortgevloeid uit onze 'flitsende brainstormsessies'. Bedankt om elke dag weer je enthousiasme en passie voor onderzoek met mij te delen en om mij te doen inzien dat dierenartsen veel meer onderzoekscapaciteiten hebben dan dat ze zelf denken! Jij motiveerde me telkens weer opnieuw om uit die 'comfortzone' te stappen en nieuwe technieken te leren, nieuwe contacten te leggen, mijn grenzen te verleggen en andere oorden op te zoeken. Jij hebt mij (grotendeels) gemaakt tot de onderzoeker die ik vandaag geworden ben en hoop te blijven!

Next, I would like to thank my 'everlasting co-promotor' dr. Kathlyn Laval. This work would not have reached its present quality without your continuous support throughout my PhD. You were always eager to check my protocols, discuss about my results and correct my writings. I still remember the day I first met you and we discussed about my master thesis' subject. Already from that moment, I admired your enthusiasm for and deep knowledge on virology. During that period, you encouraged me to stay in research and I did not regret that so far! At the beginning of my PhD, we became real friends and by this time, you are one of my very best friends. Even with an ocean in between, we managed to stay in contact and support each other. Thank you so much for that! I will also never forget about the good times we had outside the lab (remember the plansjee ? ☺). I look forward to having you back as a colleague in 2019, when we will reunite at Princeton University!

Verder wil ik heel graag de leden van mijn begeleidingscommissie bedanken, prof. dr. Herman Favoreel en prof. dr. Piet Deprez, om heel dit werk op korte tijd te verbeteren! Herman, ook bedankt om tijdens mijn onderzoek altijd paraat te staan met wijze raad. Jouw suggesties konden me vaak weer verder op weg zetten! Bedankt ook aan de leden van de examencommissie, prof. dr. Laurent Gillet, prof. dr. Bruno Verhasselt, prof. dr. Frank Pasmans, dr. Tresemiek Picavet, ir. Brigitte Cay en dr. Kathlyn Laval om dit werk te willen verbeteren.

Prof. dr. Van den Broeck, bedankt voor al je raad omtrent histologische vragen. Prof. dr. Pasmans wil ik bedanken om mij met open armen te ontvangen in het labo bacteriologie en mij op weg te zetten met de MIC testen. Dankjewel, dr. Maarten Dhaenens, voor de 'proteomics

analyse' van de defensines. Prof. dr. Kris Gevaert en dr. Francis Impens, bedankt om zo snel en efficiënt de pollen proteasen te analyseren m.b.v. de mass spectrometer.

En nu is het aan jou, Katrien. In ons laatste masterjaar zijn we samen begonnen aan dit 'EHV1 avontuur' en naarmate ons doctoraat vorderde, werden we alsmaar betere vrienden. Vandaag kan ik je één van mijn allerbeste vrienden noemen en daar ben ik trots op! De afgelopen 5 jaar heb ik immens veel steun aan je gehad, zowel op het werk als daarbuiten. We waren onafscheidelijk (ik denk dat dat niet onopgemerkt bleef... ☺) en ik hoop dat dit ook mag blijven na ons doctoraat! Herinner je je de momenten dat we samen op bedrijfsbezoek gingen, naar het slachthuis reden, babbelden en lachten in onze bureau, naast elkaar aan de flow zwoegden, samen bij Hans zaten, samen reisden of op congres gingen naar Manchester, Parijs, New York, Vancouver en Wenen. Ik kan dan ook terecht zeggen dat dit alles maar half zo leuk geweest zou zijn zonder jou! Nu is het aan jou om de laatste eindspurt te nemen, maar ik weet dat je dit kan. Je hebt heel veel capaciteiten en je zal het nog ver schoppen! Katrien, ik ben zo blij dat wij dit samen hebben kunnen beleven en ik kijk al uit naar onze verdere avonturen! ☺

“Vele handen maken het werk lichter” wordt wel eens gezegd, maar dit geldt zeker ook voor mijn doctoraat. Hierbij wil ik graag alle fantastische laboranten en technische krachten bedanken die niet alleen het labo draaiende hielden, maar daarbij ook nog de moeite deden om mij te helpen met al mijn experimenten! Carine, ik heb heel erg genoten van de tijden dat we samen aan de flow zaten. Ik kon altijd met alles bij jou terecht, zowel werk-gerelateerd als daarbuiten. Je stond elke dag opnieuw paraat voor mij met een lach op je gezicht. Tijdens mijn doctoraat deed je ontelbare kleuringen en titraties voor mij, splitste je elke week opnieuw cellen en isoleerde je miljoenen PBMC's voor mij. Als er iets mislukte, zochten we samen naar oplossingen en je was altijd gemotiveerd om deze meteen uit te testen! Héél, héél, héél erg hard bedankt om mij zo te steunen! Ik wens je het allerbeste toe in je verdere leven met je man, je kinderen en al je kleinkinderen. Geniet ervan, je hebt het verdiend!

En dan is er Chantal, het 'boegbeeld' van het labo virologie. Bedankt om telkens opnieuw virusstocks te maken en mij te helpen waar het kon! Nele, ik heb erg genoten van onze babbels over de middag. Bedankt ook om telkens opnieuw antistoffen te biotinyleren en ook nog (even ;) bij de western blots te helpen! Melanie, ik kreeg elke dag opnieuw een vriendelijke goeiedag en je hielp me waar het kon, bedankt! Ytse, ook al ben je niet langer in het labo, ik wil je toch bedanken voor alle moeite die je deed toen je dat wel was. Je deed ellenlange viruspurificaties, western blots en PCR's voor mij met veel plezier, bedankt! Lieve, bedankt om mij in het begin allerlei technische kneepjes te leren! Verder is een bedankje voor de laboranten van het labo morfologie hier zeker op zijn plaats. Lobde, de coupes die jij voor mij met veel enthousiasme gemaakt en gekleurd hebt zijn eveneens ontelbaar, bedankt! Liesbeth, ook bedankt voor de leuke babbels en alle electronenmicroscopische tips en tricks! Marleen, mijn tijd in het labo bacteriologie was kort maar wel heel aangenaam en dat was mede dankzij jou! Bedankt om mij zo goed te helpen met al die MIC testen!

Dan is er het 'technisch team' dat altijd paraat stond voor vanalles en nog wat: Jonathan, Elody, Eleni en Zeger. Bedankt voor de vele ritjes naar het slachthuis, het coaten van ontelbare cryosectieglasjes en steriliseren van allerlei materiaal!

Ook een dikke merci aan het administratief team! Gertje, ik zal onze (grappige) gesprekken over de middag niet snel vergeten. Bedankt dat je altijd klaar stond voor mij! Marijke, bedankt om altijd alles supersnel in orde te brengen als ik iets nodig had! Ann, bedankt voor alle -altijd meteen geplaatste- bestellingen en om alles te regelen voor congressen! Dirk, bedankt dat ik altijd bij jou terecht kon voor computer-, layout- en poster-gerelateerde problemen!

En nu is het aan al mijn (ex-)collega's, te beginnen bij mijn bureaugenootjes. Fang, you came into the 'EHV1 office' about 2 years ago and I really appreciated your presence throughout my PhD. We had such a good time in Vienna, I liked your Chinese vibes! I am sure that you will have success in your life, you are a fantastic girl! Sarah, ook al ben je hier nog niet lang, ik denk dat ik je toch al een beetje ken. Je bent een hele lieve meid met veel enthousiasme voor onderzoek. Ik wens je veel succes toe met je superuitdagende project! Jing, our former EHV1 member, I enjoyed the talks we had (about EHV1 and more) and I wish you all the best in your future research career!

I especially want to thank Nathalie for all the advice on and help with molecular work on defensins and more! I had a good time with you in the lab and at congresses and meetings. I also enjoyed our numerous brainstorm sessions! Bas, bedankt om altijd klaar te staan met raad en daad als ik iets nodig had (met wat droge humor af en toe ☺)! Delphine, jou wil ik bedanken, niet alleen voor het delen van al je moleculaire kennis, maar ook voor de vele leuke (soms hilarische!) babbels die we hadden in en buiten het labo! Jason, Bo, Tingting, we started our PhD together in the lab, so we went through all the different phases of a PhD together. I enjoyed having you with me during the PhD and spending time together outside the lab! Gaëtan, Veerle, Robin and Dayoung, I appreciated our talks in the lab and I wish you all the best in your future research (and life ☺). Elien, Sharon and Wojciech, also known as the 'influenza team', thank you all for the good times during lunch and in the lab upstairs!

Also a special thanks to all former lab members, with whom I had the pleasure to work with during my PhD. Marilou, Wendy, Ivan, Garba, Pépé, Lowiese, Haile, Inge, Sebastiaan, Isaura, Vishi, Ilias, Kevin, Charlie, Hossein and Amy, thank you for all your advice and all the good times we had in and outside the lab!

Een warme dankuwel ook aan al mijn vrienden en familie die mee met mij dit doctoraat hebben gedragen. Lana, Nüşhja, Katrien en Sasha, oftewel de 'coolste dierenartsen', na 6 jaar studies gingen we elk onze eigen weg maar dat, en het feit dat we elk in een uithoek van Vlaanderen wonen, hield ons niet tegen om geregeld af te spreken. Daar ben ik heel blij om en ik heb ook heel erg had genoten van al die momenten samen! Bedankt om mij te steunen gedurende die 4 jaar. Kristof en Julie, ik kan mij geen betere 'schoonbroer' en 'schoonzus' wensen. Ik kijk met veel plezier terug op al onze uitgangsavonden, spelletjesavonden, etentjes, barbecues, nieuwjaarsavonden, enz. en ik hoop dat er nog vele van zulke mooie momenten samen mogen volgen! Bedankt om altijd klaar te staan voor Peter en mij! Ik wil jullie ook nog het allerbeste wensen voor jullie toekomst samen en een heel mooi huwelijk volgend jaar! ☺ Stany, Marieke, Stef en Lisa, jullie kwamen in mijn leven rond de tijd dat ik mijn doctoraat startte en sindsdien hebben we vele mooie, leuke en soms hilarische tijden beleefd samen! Stef, chapeau om zo snel je doctoraat af te werken, en dat tezamen met het plannen van een huwelijk! Stany en Marieke, ik wens jullie een heel goed doctoraat met vele artikels toe, maar vooral een mooie tijd

daarbuiten! Mathias, bedankt om (soms rechtstreeks, soms via Kathlyn) altijd klaar te staan met wijze raad. Slechts één opmerking of advies van jou kon voor mij een openbaring zijn! Ik heb genoten van onze etentjes samen en ik hoop om volgend jaar nog vele leuke momenten te beleven samen met jou en Kathlyn! Ivy, my American friend, you always made me smile! I am happy to look back at all the crazy parties and dancing evenings with you!

Verder wil ik ook mijn stalgenootjes, Morgan, Wendy, Katty, Els, Chari, Davy en Annick bedanken voor de leuke babbels en om een oogje in het zeil te houden bij Blitzzy tijdens de drukke perioden van mijn doctoraat! Ook bedankt aan Christ voor alle goede zorgen voor Blitzzy! Mieke, bedankt voor al je wijze (paarden)lessen en om mij één van de mooiste dingen uit mijn leven te brengen: Blitzzy! Yentl, bedankt voor alle leuke (paarden)babbels en je interesse in mijn doctoraat. Het hoofdstuk over EHV5 heb ik volledig aan jou en Sultan te danken! Ook heel erg had bedankt om zo goed voor Blitzzy te zorgen als ik er niet was!

Beatrise en Willy, ik ben wel met mijn gat in de boter gevallen zoals ze zeggen, met zo een fantastisch lieve ‘schoonouders’ als jullie! Bedankt om zo een warme thuis te bieden voor mij en Peter. Ik heb heel hard genoten van de familie-momenten samen en kijk uit naar meer! Bedankt om Peter en mij zo te steunen tijdens de drukke perioden van ons doctoraat! Ook bedankt voor de ritjes naar de luchthaven, voor de bezoeken bij ons thuis als wij het te druk hadden, om voor Blitzzy te zorgen als ik niet kon, enz.!

Mama, papa, er zijn geen woorden om te beschrijven hoe dankbaar ik jullie ben. Ik heb het geluk had om in zo een warm nest op te groeien en alle mogelijke kansen te krijgen! Dankzij jullie kon ik mijn droom om dierenarts te worden waar maken en kon ik dit doctoraat starten. Jullie stonden ALTIJD klaar als er iets was en jullie steunden mij in elke beslissing van mijn leven en daar ben ik jullie dankbaar voor. Mama, ook danku voor de huishoudhulp, papa, ook danku voor de hulp omtrent computerproblemen.

Meme, dankje voor alle leuke momenten samen, om mij zo te steunen en om mijn huisje af en toe te laten blinken! Ook bedankt aan tante Nancy, tante Annick, de ‘coiffeur’, Freya, Timo en Marco om zo een warme familie voor mij te zijn en mij altijd te steunen en te helpen waar kon!

En dan nu, mijn lieve Peter, 1000-maal dank aan jou! Mijn hele doctoraat heb jij ‘meegedragen’ en ik met trots het jouwe! We hebben al heel veel leuke momenten samen beleefd, waar ik met een lach op mijn gezicht aan terugdenk! Samen een doctoraat maken zorgde ervoor dat we ‘elkaars leed’ konden delen en dat hielp! Wat hebben we veel gezwoegd samen aan onze bureau ☺. Dankje om altijd voor mij klaar te staan voor vanalles en nog wat! Bedankt ook voor de vele brainstormsessies tot soms ’s avonds laat! Ik ben zo blij dat we ons doctoraat samen hebben kunnen beleven. Dit werk zou maar half zo goed geweest zijn zonder jouw steun! Ik ben heel erg fier op jou, je bent een fantastische wetenschapper en ik ben zeker dat je een schitterend doctoraat gaat afleggen en een mooie carrière tegemoet gaat! Op naar een mooie toekomst samen!

Jolien